Preclinical testing of a targeted TRAIL therapeutic for bone sarcoma

Zakareya Esame Khalil Gamie

Student number: S00078884

A thesis submitted in part requirement for the degree of Doctor of Philosophy from the Faculty of Medical Sciences at Newcastle University,

Newcastle upon Tyne, UK

Sarcoma research group

Northern Institute for Cancer Research

Sarcoma Research Group, Northern Institute for Cancer Research, Paul O' Gorman Building, Medical School, Framlington Place, University of Newcastle, Newcastle-upon-Tyne, NE2 4HH, UK.

November 2020

Acknowledgements

My parents Dr Esame Gamie and Laila Elbebawy, brother Dr Yehya Gamie and sister Emane Gamie

Newcastle University Supervisors:

Mr Kenneth Samora Rankin, Dr Anja Krippner-Heidenreich, Mr Craig Gerrand and Professor Kenneth Dalgarno

In vivo work:

Dr Helen Blair, Dr Emma Haagensen, Mankaran Singh, Christopher Huggins and Saimir Luli

Laboratory support:

Dr Emma Haagensen, Dr Massar Alsamraae, Dr Bharat Bhushan, Dr Daniel Frankel

Development of the targeted TRAIL therapeutic:

Professor Roland Kontermann and Dr Martin Siegemund, Universität Stuttgart, Germany

Academic mentors:

Professor Eleftherios Tsiridis MD, MSc, PhD, FACS, FRCS and Dr Eustathios Kenanidis MD, MSc, PhD, Academic Orthopaedic Unit, Aristotle University Medical School, Greece

Dr Nancy Redfern BSc, FRCA, Dip Clin Ed Hon, MRCP Hon, FRCS, Consultant Anaesthetist, Newcastle upon Tyne Hospitals NHS Foundation Trust, UK

Literature review co-authors:

Dr Konstantinos Kapriniotis, Dr Dimitra Papanikolaou, Dr Alexandros Stamatopoulos and Dr Theodosios Stamatopoulos, Academic Orthopaedic Unit, Aristotle University Medical School, Greece

Funding bodies:

Funding for this work was generously provided by

- Orthopaedic Research UK (ORUK). Charity Reg No: 111 1657.
- Dr William Edmund Harker Foundation
- Newcastle Healthcare Charity and Other Related Charities. Charity Reg No: 502 473.
- The JGW Patterson Foundation. Charity Reg No: 109 4086

I acknowledge the Newcastle University Flow Cytometry Core Facility (FCCF) for assistance with the generation of Flow Cytometry data

Also, HistoCyte Laboratories Ltd (Neon Building, Quorum Park, Newcastle upon Tyne, NE12 8BU provided contract services to process cells in accordance with their proprietary methods

Author's declaration

I hereby declare that no parts of the work referred to in this thesis have previously been submitted in support of an application for another degree or qualification of this or any other University.

Zakareya Gamie

November 2020

Abstract

Background: TNF-related apoptosis-inducing ligand (TRAIL) can induce cell death in cancer cells after binding to its TRAIL receptors [TRAILR, Death Receptor 4 (DR4) and Death Receptor 5 (DR5)] while sparing non-malignant cells. The application of TRAIL provides an approach that can potentially overcome drug resistance and toxicity associated with high doses of conventional therapies. It could be administered alone or in combination with conventional therapies and, therefore, may offer a promising new approach to bone sarcoma treatment. Enhancing the cytotoxic effect of TRAIL involves targeting a tumour associated antigen (TAA). Here, the aim was to characterise bone sarcoma cells for TRAILR expression and to assess the effectiveness, both *in vitro* and *in vivo* of a novel TRAIL construct, neural/glial antigen 2 (NG2) targeted TRAIL (ScFvNG2-Fc-scTRAIL).

Methods: Bone sarcoma cell lines were characterised for TRAILR and NG2 expression on RNA and protein level. Together with non-malignant cell lines, they were exposed to the novel TRAIL therapeutic (ScFvNG2-Fc-scTRAIL) in *vitro* and then tested *in vivo* in a newly developed xenograft model of dedifferentiated chondrosarcoma.

Results: Surface DR5 was expressed in all cell lines examined (very high: HT1080, MG63; moderate: SW153, U2OS, TC71). NG2 was also expressed (very high: SW1353, MG63; moderate: U2OS, HT1080). ScFvNG2-Fc-scTRAIL demonstrated enhanced cytotoxicity in DR5- and NG2-expressing cell lines (MG63>HT1080>U2OS), which increased with doxorubicin and was also found *in vivo* when engrafting a luciferase expressing HT1080 cell line in a dedifferentiated chondrosarcoma mouse model.

Conclusion: I demonstrate that a novel targeted TRAIL therapeutic, ScFvNG2-Fc-scTRAIL, has a selective and significant cytotoxic effect on cell lines expressing both cell surface DR5 and NG2, and these cytotoxic effects can be enhanced further with doxorubicin. Such combinations could minimise the risk of treatment failure due to drug resistance, a common problem of single agent approaches. Furthermore, these findings provide a framework for the clinical development of ScFvNG2-Fc-scTRAIL and could potentially be used in the neoadjuvant setting, which would be a shift from the usual convention of prioritising excision of the sarcoma.

Key words: Bone sarcoma, chondrosarcoma, TNF-related apoptosis-inducing ligand, apoptosis, death receptor, cancer therapy, scFv–TRAIL fusion proteins

Table of Contents

List of Tables

List of Figures

List of Equations

List of Abbreviations

Ab	Antibody
ADAs	Anti-drug-antibodies
Akt	Protein kinase B
BSA	Bovine serum albumin
Bcl-2	B-cell lymphoma 2
BMMSCs	Bone marrow-derived mesenchymal stem cells
cDNA	complementary DNA
cFLIP	FLICE-like inhibitory protein
cIAP	cellular Inhibitor of apoptosis protein
CRISPR	Clustered regularly interspaced short palindromic repeats
CSPG4	Chondroitin sulfate proteoglycan 4
DNA	Deoxyribonucleic acid
DcR1	Decoy Receptor 1
DcR2	Decoy Receptor 2
DMSO	Dimethyl sulfoxide
DR4	Death Receptor 4
DR5	Death Receptor 5
dsDNA	double stranded DNA
EDTA	Ethylenediaminetetraacetic acid
FBS	Fetal bovine serum

Fc	Fragment crystallizable region
FGF-B	Fibroblast growth factor-basic
HDAC	Histone deacetylase
HDACi	Histone deacetylase inhibitor
H-Ras	Harvey rat sarcoma viral oncogene homolog
HuEGF	Human epidermal growth factor
IHC	Immunohistochemistry
NEAA	Non-essential amino acids
NG2	Neuron-glial antigen 2
MCSP	Melanoma-associated chondroitin sulfate proteoglycan
MFI	Median fluorescence intensity
OPG	Osteoprotegerin
PI3K	Phosphatidylinositol-4,5-bisphosphate 3-kinase
PTEN	Phosphatase and tensin homolog
RANKL	Receptor activator of nuclear factor κB ligand
RIPK	Receptor-interacting serine/threonine-protein kinase
RT-PCR	Reverse transcription-polymerase chain reaction
RNA	Ribonucleic acid
ScFv	Single-chain variable fragment
SiRNA	Small interfering RNA
SKT	SuperKillerTRAIL

Smac	Second mitochondrial-derived activator of caspases
TRAIL	Tumour necrosis factor-related apoptosis-inducing ligand
TNF	Tumour necrosis factor
TNFLSF	Tumour necrosis factor ligand superfamily
Wst-8	(2-(2-methoxy-4-nitrophenyl)-3-(4-nitrophenyl)-5-(2,4-disulfophenyl)-2H-tetrazolium)
XIAP	X-linked Inhibitor of apoptosis protein

Chapter 1. Background and Introduction

Published in Cancer Letters as a Review Paper:

TNF-related apoptosis-inducing ligand (TRAIL) for bone sarcoma treatment: Pre-clinical and clinical data. **Gamie Z**, Kapriniotis K, Papanikolaou D, Haagensen E, Da Conceicao Ribeiro R, Dalgarno K, Krippner-Heidenreich A, Gerrand C, Tsiridis E, Rankin KS. Cancer Lett. 2017 Nov 28;409:66-80. doi: 10.1016/j.canlet.2017.08.036.

Introduction

Sarcomas are malignant tumours arising in tissues derived from the embryonic mesenchymal layer. They are rare, accounting for less than 1 % of all malignant tumours [1]. Although there are more than 50 sarcoma types, they are usually classified as soft tissue or bone sarcomas [2]. Bone sarcomas account for only 0.2 % of all neoplasms, approximately 1/10th the incidence of soft tissue sarcomas. The most common primary bone sarcomas are: (1) Osteosarcoma (35 %), occurring mostly in adolescence, with a second incidence peak in the elderly associated with Paget's disease or as a sequel to radiotherapy; (2) chondrosarcoma (25 %), most commonly seen after the age of 40; and (3) Ewing's sarcoma (16 %), presenting usually during the first two decades of life [3]. Patients with bone sarcoma have poor 5-year survival rates, close to 50 %, and survival has not improved over recent decades [4]. Survival is lower in those unresponsive to neoadjuvant treatment and in the 20-30 % of cases with detectable metastases at presentation, survival approaches 20 % [5]. Surgery is part of the multidisciplinary management of patients with primary bone sarcoma and is often complex, particularly in anatomical locations such as the pelvis. Depending on bone sarcoma type and location, chemotherapy and radiotherapy may be used as adjuncts alongside surgical treatment [6]. However, current therapies are limited by the development of drug resistance, toxicity associated with high dose therapies, non-selective tumour targeting and inaccessibility of tumour sites [7,8]. Recurrence sites include the lungs (60-85 %), the resection area (10-20 %) and the bones (10-20 %) [3].

Bone sarcoma genetics

Greater understanding of the molecular pathogenesis and the genetic aberrations occurring in bone sarcomas has been sought in the hope that novel therapeutic approaches may follow. Osteosarcoma is characterised by a wide range of mutations occurring in different sites of the genome, which leads to a wide range of intertumour genetic heterogeneity [9]. The most common aberrations reported include alterations in p53 and Rb pathways either via genetic mutations or at the epigenetic level (DNA methylation, histone modification, miRNA regulation) [10]. However, these aberrations have proven difficult to target *in vivo* and are related to resistance to conventional chemotherapy [11]. On the other hand, more than 90 % of Ewing's sarcoma cases are

characterised by a (11;22)(q24;q12) chromosomal translocation, which fuses the *EWS* gene on chromosome 22 with the *FLI1/ETS* gene on chromosome 11 and encodes the EWS/FLI-1 transcriptional factor [12,13]. This chimeric protein seems to play a crucial role in Ewing's sarcoma tumourigenesis affecting the expression of a variety of genes and interfering or working in parallel with other important oncogenic drivers such as the insulin-like growth factor (IGF) pathway, the sonic hedgehog (Shh) pathway and the over-expression of membrane type-1 matrix metalloproteinase, which facilitates invasion and metastasis [12-15]. Turning these findings into clinical outcomes remains a challenge, although some very promising clinical trials with factors targeting the IGF pathway have been published [16]. Interestingly, chondrosarcomas present a wide range of genetic aberrations mainly depending on the origin of the disease (central or peripheral chondrosarcoma) [17]. Central chondrosarcomas are characterised by a high frequency of somatic mutations in *IDH1* and *IDH2* genes, whereas these mutations are absent in peripheral chondrosarcomas [18]. In addition, chondrosarcomas presenting as part of syndromes are characterised by specific mutations, such as mutations in the *PTHR1* gene (Ollier's disease and Maffucci syndrome), *EXT1/2* genes (multiple osteochondromas) and the *P53* gene (Li-Fraumeni syndrome) [19]. Finally, structural and numerical chromosomal abnormalities are very frequent in high grade chondrosarcomas [20].

An alternative approach, that could overcome the existing limitations in treating bone sarcomas on a molecular basis, would be to trigger cancer cell death independently from genetic aberrations, by activating the caspase cascade extrinsically. One member of the tumour necrosis factor superfamily (TNFSF) is TNF-related apoptosis-inducing ligand (TRAIL) which can accomplish this expectation. TRAIL associated death receptors (DRs) are expressed at a high level in bone sarcomas but not in normal tissues and have emerged as an appealing molecular target for selective induction of apoptosis in bone sarcoma cells.

Inducing apoptosis via death receptors (DRs)

Apoptosis is considered the prominent process of programmed cell death, characterised by distinct morphological alterations. It is mainly driven by caspase cascade activation, which follows a wide range of cellular stimuli including defective DNA repair, cellular

stresses (heat damage, cytotoxic drugs, microorganisms, irradiation) and defective cellular signalling [21,22]. Apoptosis is principally activated via two distinct molecular pathways, the extrinsic and the intrinsic, although extensive communication between the two exists at different levels [22,23].

The intrinsic or mitochondrial apoptotic pathway is regulated by the fine balance between the pro- and anti- apoptotic arm of members of the Bcl-2 family [24,25]. It is characterised by an initial destabilisation of the mitochondrial membrane, which is followed by release of apoptogenic factors that form the apoptosome. Subsequently, the apoptosome triggers the caspase cascade, leading to cell death [26]. The *TP53* gene, acting as a cellular stress sensor, regulates among other genes the activation of the mitochondrial pathway [27]. This pathway is a principal target of many conventional chemotherapeutic agents, such as doxorubicin [28]. Most of these agents provoke mitochondrial membrane permeabilisation via different pathways including antiapoptotic Bcl-2 proteins inhibition, proapoptotic intracellular mediators up-regulation and direct toxic effect on the mitochondrial inner membrane [29]. *TP53* mutations, commonly reported in a high percentage of tumours, seem to moderate the effectiveness of these therapies, leading to tumour resistance [28,30].

In contrast, the extrinsic apoptotic pathway is triggered by the activation of DRs, a group of transmembrane receptors and members of the TNFSF containing a cytoplasmic death domain (DD). Currently, six types of DRs have been identified (TNF-R1, CD95, TRAIL-R1/DR4, TRAIL-R2/DR5, DR3, DR6), but the current thesis mainly focuses on death receptors binding TRAIL, known as DR4 (TRAIL-R1) and DR5 (TRAIL-R2) [23]. The DR4 and DR5 receptors are primarily expressed in cancer cells, but not in most non-transformed cells. Therefore, selective apoptosis can be triggered, without important tissue toxicities. Once TRAIL binds its receptors, a structural modification and/or oligomerisation of the receptor occurs, leading to its activation. Subsequently, the receptor's DD interacts with the adaptor molecule Fas-associated death domain (FADD) protein resulting in the formation of the death-inducing signalling complex (DISC). The DISC activates the initiator caspase 8, which then cleaves the effector caspases to mediate cell death [31,32]. There are two types of cells dependent on the intracellular signalling after DR activation. In type I cells, the amount of DISC and caspase 8 produced is adequate to trigger cell death, whereas in type II cells further amplification is needed.

Such amplification is succeeded through the activation of the intrinsic pathway [22,23,31,32]. The extrinsic pathway seems to be, at least partially, independent of p53 function [25]. As a result, it provides an alternative pathway to trigger tumour death in cancers refractory to conventional chemotherapy due to *TP53* mutations.

Regulation of DR expression and function has drawn the interest of many researchers, due to the potential unravelling of factors that can be targeted therapeutically. Studies of multiple myeloma cells and HeLa cells indicate that DR5 is, at least partially, regulated by p53 function. Particularly, downmodulation of p53 in myeloma cells led to decreased expression of DR5 and sensitivity to DR5 agonists, whereas p53 suppression with siRNA led to decreased expression of DR5 as well [33,34]. Other important DR5 transcriptional regulators include C/EBP-homologous protein (CHOP), NF-κB and the JNK pathway, whereas there is some evidence that androgen receptors may exert regulation as well [32,35]. At the translational level, a large number of miRNAs seem to interact with DR mRNAs thereby exerting multiple regulatory effects [32]. Furthermore, at the post-translational level, processes including glycosylation and palmitoylation play a crucial role in facilitating DR activity via the trafficking and anchorage of these receptors to the cellular membrane [36]. Not only O-glycosylation but N-glycosylation plays an important role in determining TRAIL sensitivity [37]. TRAIL-R2 is O-glycosylated and is required for receptor clustering, DISC formation and caspase 8 recruitment. Recent data, however, from Dufour *et al.,* (2017), suggests that TRAIL-R1 N-glycosylation can enhance its ability to trigger apoptosis and is important in modulating TRAIL mediated anti-viral responses and tumour immune surveillance. Significant changes in glycosylation occur in neoplastic cells and glycosylation status and the measurement of cellular expression levels of glycosylation enzymes (such as glucosyltransferases) could be used as potential biomarkers to predict the sensitivity of cancer cells to TRAIL [38]. Finally, the role of the ubiquitin-proteasome system (UBS) in the deconstruction of DRs after their activation is worth consideration. It is believed that a reduction in DR number due to UBS activation can lead to resistance to DR agonists mediated apoptosis [38].

TRAIL and the 'TRAIL receptors'

Like other members of the TNFSF, Kelly *et al*. state that 'TRAIL is a homotypic trimer that is expressed as a type II transmembrane protein and is cleaved proteolytically from the

cell surface and released in a soluble form' [31,39]. Five plasma membrane receptors can bind TRAIL. Upon binding of TRAIL to two receptors, TRAIL-R1 (also known as DR4, TNFRSF10a, CD261) and TRAIL-R2 (DR5, TNFRSF10b, CD262), the caspase cascade is activated which then causes apoptosis [31,40]. Other receptors include decoy receptors known as DcR1 (TRAIL-R3, TNFRSF10C, CD263) and DcR2 (TRAIL-R4, TNFRSF10D, CD264). Characteristics of these decoy receptors include that the DD is not present (DcR1), or the DD is truncated as well as being non-functional (DcR2) and because of this, upon binding of TRAIL, cell death is not directly initiated [40,41]. Finally, TRAIL binds to osteoprotegerin (OPG, TNFRSF11B), a soluble receptor that inhibits osteoclastogenesis by binding to RANKL (receptor activator of nuclear factor κB ligand) with high affinity and preventing association with its membrane receptor (RANK) [36,42,43]. OPG binds TRAIL with a lower affinity, implying a potential mechanism of cell death avoidance by preventing TRAIL/TRAIL-R interaction as it does with the RANKL/RANK system [42,43]. There is a debate as to whether TRAIL actually affects bone metabolism through interfering with osteoclastogenesis. In any case, both TRAIL overexpressing and TRAIL deficient mice achieve normal bone density, questioning the importance of such interaction *in vivo* [23,36].

The expression of TRAIL is mostly by immune cells such as natural killer cells, macrophages and T lymphocytes. Interferon-gamma is a cytokine that upregulates TRAIL expression and this suggests TRAIL has many roles in immune regulation [31,32,39]. TRAIL may play a role in T cell AICD (activation-induced cell death) in the thymus and peripheral blood [44,45]. Lamhamedi-Cheraddi *et al.* reported that TRAIL deficient mice had significantly impaired intrathymic negative selection, which led to excessive autoimmune responses [44]. However, other investigators did not manage to obtain similar results, questioning the importance of the TRAIL pathway in central immune tolerance [46,47]. Moreover, several studies proved the inhibitory function of TRAIL on the establishment of experimental autoimmune diseases. Song *et al.* reported that blockade of endogenous TRAIL with soluble DR5 (sDR5) was related to significant exacerbation of collagen-induced arthritis (experimental model of rheumatoid arthritis), whereas Hilliard *et al.* obtained similar results using sDR5 in experimental autoimmune encephalomyelitis (experimental model of multiple sclerosis) [48,49]. In contrast, Lub-de Hooge *et al.* reported that levels of sTRAIL in serum were higher in patients with

systemic lupus erythematosus comparing to healthy controls and patients with rheumatoid arthritis and Wegener's granulomatosis [50]. Therefore, further investigation is needed to clarify the precise role of TRAIL in immune regulation and immune tolerance. Finally, it seems that TRAIL may participate in allergic diseases, as well. Robertson *et al.* reported that TRAIL expression in bronchial biopsy samples and TRAIL concentration in bronchoalveolar lavage (BAL) fluid were significantly increased after antigen provocation in asthmatic patients compared to the normal controls [51].

Moreover, many studies suggest TRAIL has a role in tumour surveillance. Its antimetastatic action is clearly described in many studies [22,32,52]. Bos *et al.,* report that low levels of TRAIL expression in tumour samples correlate with an increased incidence of brain metastases in patients with breast cancer [53]. However, its role against primary tumours remains controversial [22,32,52]. In many cancer cells, apoptosis can be induced by TRAIL which is independent of the gene profile of *TP53*. However, in the majority of non-transformed cells, this does not occur [22,54]. The molecular basis of this selectivity remains quite unclear, although multiple factors have been described, such as the relative levels of TRAIL-R expression, the levels of DcR expression, intracellular inhibitors such as c-FLIP (FLICE inhibitory protein) and XIAP (X-linked inhibitor of apoptosis protein), and the type of intracellular signalling (I or II) following DR activation [31,40,55] (Figure 1). These differences between normal and tumour cells create an opportunity for therapeutic interventions that selectively target the apoptotic pathways in tumour cells, but to a lesser degree normal cells leading to fewer side effects.

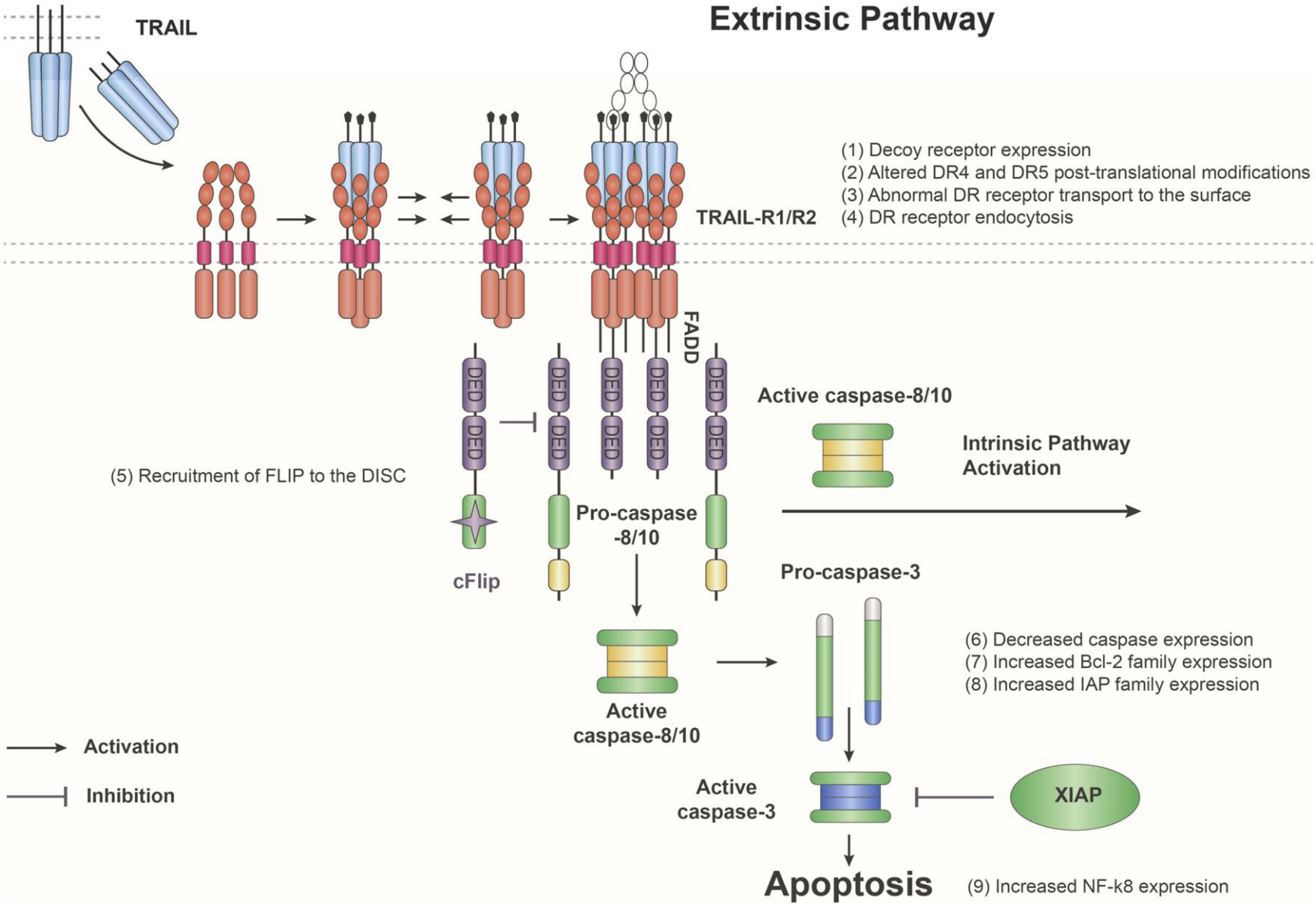
Extrinsic Pathway
TRAIL
TRAIL-R1/R2
(1) Decoy receptor expression
(2) Altered DR4 and DR5 post-translational modifications
(3) Abnormal DR receptor transport to the surface
(4) DR receptor endocytosis
FADD
DED
DED
DED
DED
DED
DED
DED
DED
DED
DED
(5) Recruitment of FLIP to the DISC
cFlip
Pro-caspase
-8/10
Active caspase-8/10
Intrinsic Pathway
Activation
Pro-caspase-3
Active
caspase-8/10
(6) Decreased caspase expression
(7) Increased Bcl-2 family expression
(8) Increased IAP family expression
Activation
Inhibition
Active
caspase-3
XIAP
Apoptosis
(9) Increased NF-k8 expression

Figure 1 - TRAIL activation of intrinsic and extrinsic apoptotic pathways. The intrinsic or mitochondrial pathway is regulated by the balance between the pro- and anti- apoptotic arm of the Bcl-2 family [24,25]. An initial destabilisation of the mitochondrial membrane is followed by release of apoptogenic factors that form the apoptosome and trigger the caspase cascade, leading to cell death. The extrinsic pathway is triggered by the activation of death receptors (DRs), a group of transmembrane receptors containing a cytoplasmic death domain (DD). The receptor's DD interacts with the adaptor molecule FADD (Fas-associated death domain protein) resulting in the formation of the death-inducing signalling complex (DISC). The DISC activates the initiator caspase 8, which then cleaves the effector caspases to mediate cell death. DED: death effector domains; c-FLIP: cellular FLICE-inhibitory protein; BAK: B cell lymphoma 2 (Bcl-2) homologous antagonist killer; BAX: Bcl-2-associated X; Bid: BH3-interacting domain death agonist; XIAP: X-linked inhibitor of apoptosis (IAP); Smac/DIABLO: Second mitochondria-derived activator of caspase/direct inhibitor of apoptosis-binding protein. Described resistance mechanisms are highlighted in bold.

Different TRAIL variants and TRAIL associated toxicity

Hepatic toxicity has been associated with Fas ligand and TNF administration. Concerns have been raised about TRAIL, particularly when administered as higher-order complexes (see below) [56]. A TRAIL-induced apoptotic response has been demonstrated in human hepatocytes in culture; however, studies have not raised the same concern *in vivo* in mice and non-human primates [57]. The variable effects found in different species remind us of the limitations of animal studies in predicting toxicity of chemotherapeutics on humans. Researchers have also used different forms of recombinant TRAIL. Some TRAIL versions are linked to amino-terminal tags to aid in isolation and purification, but can also enable the association of TRAIL trimers at higher concentrations. These tags include the polyhistidine tag (His-TRAIL), a Flag tag (that can aid in the crosslinking of TRAIL with concurrent use of M2 antibodies), a leucine-zipper or an isoleucine-zipper trimerisation domain (LZ-TRAIL, iz-TRAIL) [43]. TRAIL forms without extraneous amino acid residues (untagged) have been shown to be non-toxic in non-human primates [58].

Studies have shown that only aggregated forms of TRAIL, such as His-TRAIL or cross-linked Flag-TRAIL are capable of inducing cell death in primary human hepatocytes (PHH) at day 1 of *in vitro* culture. After some days of *in vitro* culture, PHH develop resistance to TRAIL. [56,59] Tagged TRAIL variants, like LZ-TRAIL, His-TRAIL are also toxic to proliferating human keratinocytes, as well as adult astrocytes [43]. While LZ-TRAIL and His-TRAIL display similar anti-tumour effects, LZ-TRAIL demonstrates much lower toxicity in normal cells than His-TRAIL [56]. In contrast, an unmodified soluble TRAIL consisting of 114-281 amino acids (Apo2L/TRAIL) has minimal toxic effects both on hepatocyte cell lines and after intravenous administration to cynomolgous monkeys [60]. Another study by Hao *et al.,* demonstrated the absence of DR4 and decreased levels of DR5 receptor expression in PHH, proposing a possible explanation for TRAIL resistance of normal liver cells. The authors also tested hepatotoxicity by injecting chimeric mice intraperitoneally and subcutaneously with non-tagged recombinant TRAIL (amino acids 114-281). There were no histopathological changes and no caspase-3 cleavage in the TRAIL-treated group hepatocytes [61]. TRAIL agonistic antibodies (e.g. Apomab), have been reported as safe *in vitro* and *in vivo* [62].

Although unmodified TRAIL has been reported to be safe for human hepatocytes *in vitro*, under some circumstances such as inflammation or cotreatment with chemotherapeutic agents, PHH can be sensitised to TRAIL-induced apoptosis [56]. Mundt *et al.,* demonstrated TRAIL overexpression at the protein level in hepatocytes from chronic hepatitis C virus (HCV) infected patients, as well as in the liver of mice after alcohol intake. Increased TRAIL expression led to steatosis and apoptosis of HCV infected cells, whereas it only caused steatosis without apoptosis in cells after alcohol intake. The authors concluded that hepatocyte steatosis and apoptosis are therefore regulated by separate molecular pathways [63]. Moreover, hepatitis B virus (HBV) was reported to lead to Bax overexpression and render liver cells sensitive to apoptosis through TRAIL [64]. Koschny *et al.,* reported that TRAIL cotreatment with low dose bortezomib, a proteasome inhibitor, had no toxic effect on PHHs, whereas the use of high concentrations of bortezomib led to TRAIL-mediated hepatocyte death. However, the threshold to sensitise liver cells was 40 times higher than that needed to induce apoptosis in cancer cells, thus opening a therapeutic window [65].

Soluble TRAIL can be genetically linked to a single-chain variable antibody fragment (scFv) and this is known as a fusion protein. This improves TRAIL selectivity as well as overcoming potential toxic effects. The scFv portion can be designed to bind to a pre-selected tumour specific target antigen (such as EpCam, CD7 and CD19) inducing the accumulation of TRAIL at the tumour site [52,66-68]. This causes the bystander effect which is where the therapy eliminates the cancer cells that express the target antigen [67], but the therapy also affects neighbouring cells that express or do not express the antigen [69] (Figure 2). In a bone fibrosarcoma cell line (HT1080), scFv:scTRAIL (engineered to recognize erb-b2) was found to be more effective than KillerTRAIL [52]. The scFv:scTRAIL has been found to have potent anti-tumour efficiency, with no severe side effects.

More recently, an anti-PD-L1:TRAIL fusion protein, which contains three PD-L1-blocking scFvs has been developed [70]. This has a multi-fold therapeutic effect, which includes targeted delivery of TRAIL in cells expressing PD-L1 and reactivation of antitumour T-cells by blocking the PD-1/PD-L1 interaction. In addition, suppressive immune cells such as monocyte/macrophages and dendritic cells are converted into pro-apoptotic cells and production of IFN-γ is increased thereby sensitising cells to TRAIL and upregulating PD-

L1 [70]. These encouraging data certainly ask for further investigation of fusion proteins containing TRAIL in the treatment of bone and soft tissue sarcoma.

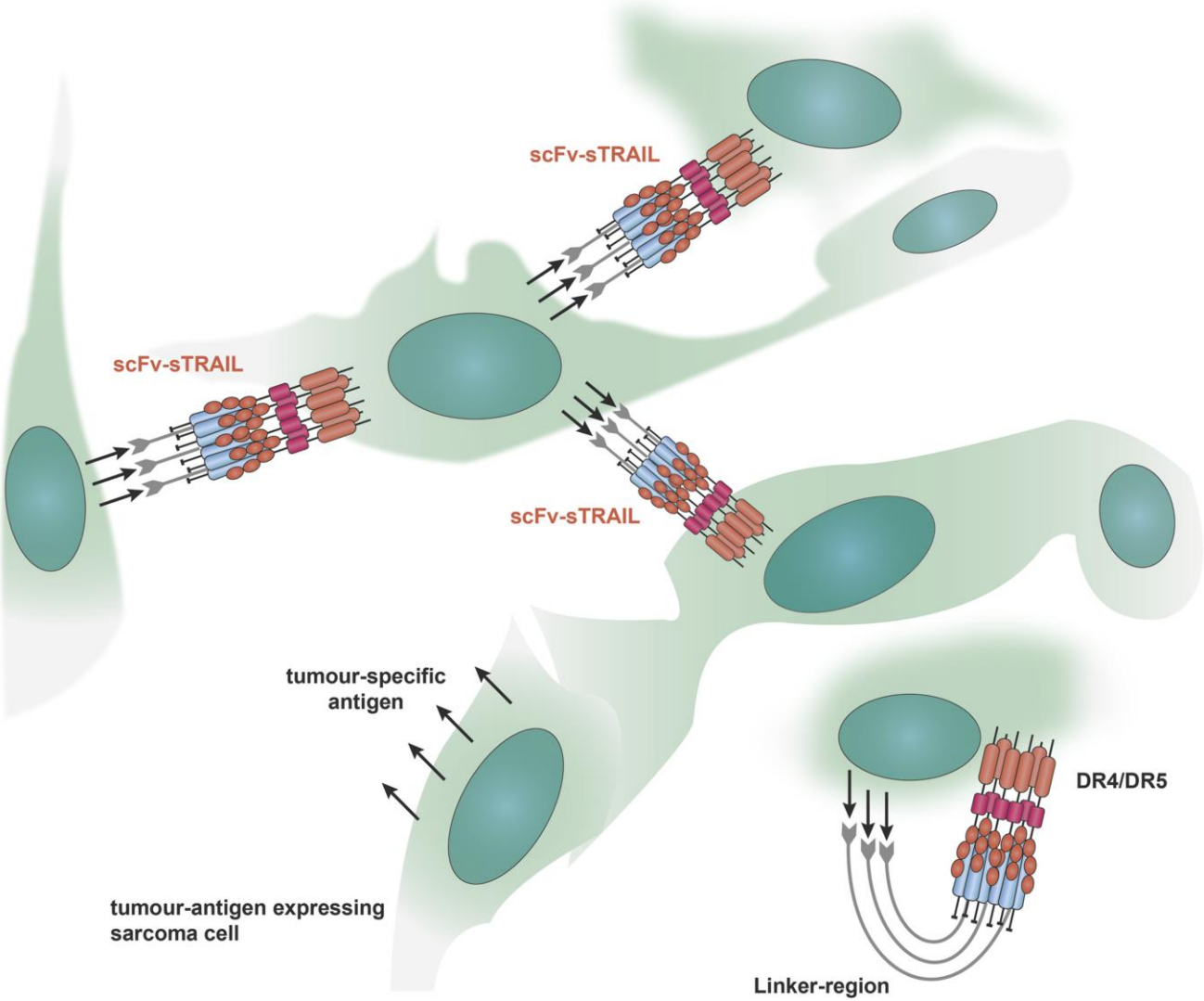
scFv-sTRAIL
scFv-sTRAIL
scFv-sTRAIL
tumour-specific
antigen
tumour-antigen expressing
sarcoma cell
DR4/DR5
Linker-region

Figure 2 - Use of ScFv:scTRAIL to target cancer cells. Soluble TRAIL can be genetically linked to a single-chain variable antibody fragment (scFv) and this is known as a fusion protein. The scFv portion can be designed to bind to a pre-selected tumour specific target antigen (such as EpCam, CD7 and CD19) and induce the accumulation of TRAIL at the tumour site. This causes the bystander effect which is where the therapy eliminates the cancer cell that expresses the target antigen but the therapy also affects neighbouring cells that express or do not express the antigen [67,69]. In a bone fibrosarcoma cell line (HT1080), scFv:scTRAIL (engineered to recognise erb-b2) was found to be more effective than a crosslinked from of TRAIL known as KillerTRAIL. In bone sarcoma, NG2, or neural/glial antigen 2, is an example of a tumour specific antigen expressed in chondrosarcoma cells that could potentially be targeted.

TRAIL and bone sarcomas

i) Preclinical studies

In vitro studies

Osteosarcoma cell lines have shown a wide range of sensitivities to TRAIL induced apoptosis. Generally, most cell lines are considered to be TRAIL resistant, although TRAIL sensitive lines have been described [55,71-73]. The molecular basis of TRAIL resistance remains unclear. The relative expression levels of death receptors, decoy receptors and osteoprotegerin (OPG) could be important determinants of TRAIL sensitivity; however, studies indicate an equal distribution in both sensitive and resistant cell lines [72,74,75]. Therefore, the key determinant of sensitivity is probably located downstream in the intracellular signalling pathways [74]. In any case, significant levels of DR expression are reported in all sensitive lines [72,73]. In addition, many conventional chemotherapeutic drugs sensitise resistant cell lines to TRAIL mediated apoptosis. The most prominent of them include doxorubicin, cisplatin and etoposide. Their mechanism of action includes up-regulation of DRs, down-regulation of anti-apoptotic proteins (c-FLIP), increase in caspase-8 expression and activation of the mitochondrial pathway [55,71,72,76,77]. Finally, other drugs reported to act synergistically with TRAIL in osteosarcoma include celecoxib and bisphosphonates. They enhance TRAIL potency mainly via down-regulation of antiapoptotic Bcl-2 protein and up-regulation of DR5 respectively [78,79].

Regarding Ewing's sarcoma, many cell lines exhibit high levels of sensitivity to TRAIL induced apoptosis [80-83]. Very high DR expression is reported in most cell lines and in tumour tissue. Mitsiades *et al.,* reported that 9/10 Ewing's sarcoma cell lines tested were TRAIL sensitive with both DR4 and DR5 protein expression detected in the sensitive cell lines by western blotting. On the contrary, the resistant line expressed only intracellular DR4 protein, but the death receptor was absent from the cell surface. In addition, this group investigated DR expression in Ewing's sarcoma biopsies by immunohistochemistry, reporting that 72 % of tissues tested expressed both DRs, whereas only 3 % expressed none [81]. Picarda *et al.,* attributed the resistance in some Ewing's sarcoma cell lines due to low levels of DR4 despite high expression of DR5 [84], whereas other studies suggest there is no significant difference in DR expression between sensitive and resistant cell lines [82]. In any case, it seems that the presence of

at least one functional DR is prerequisite for sensitivity to TRAIL-induced apoptosis [81]. In addition, caspase-8 expression levels seem to be an important determinant of Ewing's sarcoma sensitivity to TRAIL. Low levels of caspase-8 are associated with resistance phenomena both *in vitro* and *in vivo* [82,85,86]. Lissat *et al.,* reported that 24 % of tumour samples from Ewing's sarcoma biopsies express low levels of caspase-8, whereas intratumour heterogeneity of caspase-8 expression is reported as well, implying that there is a TRAIL resistant population of cells inside tumours due to a failure of the DR pathway to effectively induce apoptosis [86]. In addition, a number of studies indicate that IFN-γ restores both caspase-8 levels and TRAIL sensitivity of resistant lines *in vitro* [82,85,86]. Finally, proteasome inhibitors (e.g. bortezomib) and histone deacetylase inhibitors are found to exert synergistic effect when co-administered with TRAIL [87,88].

There is very little preclinical data for chondrosarcoma in the literature to date. Most of the chondrosarcoma cell lines are considered to be TRAIL resistant. However, combinational approaches with other drugs, such as doxorubicin, placlitaxel or the proteasome inhibitor MG132, seem to enhance TRAIL potency *in vitro* [89,90] (Table 1).

In vivo studies

A number of xenograft models have been used to evaluate TRAIL potency in the treatment of bone sarcomas *in vivo*. Picarda *et al.,* investigated the *in vivo* response of osteosarcoma and Ewing's sarcoma tumours to human TRAIL (hTRAIL) delivered by transduced plasmids, by inoculating *in vitro* sensitive cells of both sarcomas in a paraosseous location, closely to the metatarsus of the mice. TRAIL administration caused a significant decrease of both sarcoma incidence and tumour growth, prevented tumour-induced osteolysis and doubled animal survival 40 days after the inoculation. In addition, in an osteosarcoma metastatic model established by IV injection of *in vitro* sensitive osteosarcoma cells, TRAIL administration reduced lung dissemination significantly and increased animal survival more than three times, compared to the control group, 42 days after injection with cancer cells [73]. Moreover, Merchant *et al.,* (2004) reported that, although TRAIL seems quite potent *in vivo* against Ewing's sarcoma (4/21 animals with complete response, 9/21 animals with temporary response), its efficacy seems to be lower than expected from the *in vitro* experiments. Moreover,

Ewing's sarcoma cells that were TRAIL sensitive before inoculation, developed resistance when cultured after inoculation and *in vivo* development. Also, this resistance is correlated with down-regulation of death receptors. However, pretreatment with IFN-γ restores the initial sensitivity *in vitro* by up-regulating DR5 and caspase-8 expression. Finally, they investigated whether the combination of TRAIL and IFN-γ was superior to TRAIL alone *in vivo*. Surprisingly, both TRAIL alone or the combinational therapy had similar effects on the primary tumour. However, the combination therapy significantly decreased the metastatic rate and subsequently increased overall survival [85]. In conclusion, it seems that *in vivo* experiments using TRAIL against bone sarcomas show quite promising results. However, combination approaches with other factors seem essential to maximise the antitumour effect (Table 1).

ii) Clinical studies

Very few clinical trials evaluating TRAIL and other DR4/DR5 agonists in patients with primary bone sarcoma have been published to date. In addition, most published studies include a range of cancers other than sarcoma and therefore only limited data about sarcoma are available. Most trials indicate that TRAIL and other DR4/DR5 agonists (proapoptotic receptor agonists-PARAs) have a satisfactory safety profile, as serious adverse events rarely occur [91-94]. However, efficacy is moderate or low in contrast to more promising preclinical studies [91-97]. The best responses to date were reported by Herbst *et al.,* who described two patients with chondrosarcoma who experienced durable partial responses- as determined by response evaluation criteria in solid tumours (RECIST) - after treatment with recombinant human TRAIL (rhTRAIL) [80]. In addition, Camidge *et al.,* described a patient with chondrosarcoma who experienced a minor, non-evaluable by RECIST response (20 % reduction in measurable disease) after treatment with PRO95780 (Drozitumab; Genentech Inc., DR5 agonist) [95,96]. Merchant *et al.,* reported one progressive, treatment refractory osteosarcoma case that resulted in stabilisation, ongoing more than one year without any therapy, of the disease both clinically and on PET-scan after treatment with lexatumumab (HGS-ETR2; Human Genome Sciences Inc., DR5 agonist). A metastatic recurrent Ewing's sarcoma case was also reported in the same study with maintenance of regression following radiotherapy in the irradiated field for five months, while lexatumumab was being administered. Lesions, however, outside the field progressed [93]. Finally, as part of a study covering

wide range of solid carcinomas and sarcomas, Tabernero *et al.* reported five sarcoma cases with stable disease after treatment with conatumumab (AMG655; Amgen Inc., DR5 agonist) in combination with ganitumab (type I insulin-like growth factor receptor antagonist). Types of sarcomas investigated in the study included among others a 62-year-old woman with stage IV well-differentiated myxofibrosarcoma who had a partial response from the treatment, as determined by RECIST; a 38-year-old woman with stage IV synovial sarcoma and a 58-year-old man with stage IV leiomyosarcoma (both experiencing prolonged stable disease of 261 and 227 days respectively) [91]. In conclusion, it seems that the initial enthusiasm caused by *in vitro* studies has been moderated by clinical trial results. However, as described below, alternative TRAIL-based strategies, such as novel TRAIL delivery approaches, may be more effective (Table 2).

TRAIL resistance

Multiple factors contribute to a TRAIL-resistant phenotype, including death receptor DR4 and DR5 expression, their ability to initiate a signal, as well as the sensitivity threshold of tumour cells to the initiated signal. Other factors include loss of caspase-8 expression and the ability of tumour cells to mobilise to remote sites and survive hostile microenvironments [36]. The downregulation of DR4 and DR5 in chromosome 8p occurs in many cancer types through loss of heterozygosity or epigenetic changes such as promoter hypermethylation and leads to resistance. FLIPs (FLICE [Fas-associated death-domain-like IL-1β-converting enzyme]-inhibitory proteins) seem to regulate TRAIL-induced apoptosis in a complex manner [40]. They have similar structure to caspase-8 and -10 but lack proteolytic activity [98]. Overexpression of FLIPs has been linked to TRAIL resistance, but it has also been reported that cellular $FLIP_L$ (c-$FLIP_L$) can also act proapoptotically [98,99]. A study by Picarda *et al.,* of Ewing's sarcoma cell lines reported that 50 % of studied cell lines were resistant to TRAIL-induced apoptosis, [84] despite previous evidence of greater sensitivity [82,100]. The authors suggested a correlation between TRAIL resistance and reduced DR4 expression despite high DR5 levels. Using flow cytometry and caspase assays, they showed that TRAIL-resistant Ewing's sarcoma cells can be resensitised by inducing expression of a truncated but functional isoform of DR4 (bDR4), as well as by downregulating c-FLIP expression [84]. Another study by Mitsiades *et al.,* revealed no correlation between FLIP concentration or increased decoy

receptor expression and TRAIL resistance in Ewing's sarcoma cell lines; instead, the authors suggested that TRAIL resistance was due to decreased DR5 expression in the resistant cell line and found that when DR5 levels were restored, the resistant Ewing's sarcoma cells became TRAIL-sensitive [81]. A significant cause of resistance in some tumours including Ewing's sarcoma is loss of caspase expression attributed to caspase-8 downregulation due to hypermethylation of regulatory sequences in the caspase-8 gene. There is also *in vitro* data supporting that upregulation of endogenous caspase inhibitors such as XIAP, cIAP1, cIAP2 and survivin that block caspase-3,-7, 8 and -9 activation desensitises cells to TRAIL-induced apoptosis [101]. The transcription factor NF-κB, associated with oncogenetic mechanisms, upregulates antiapoptotic proteins such as IAPs, FLIP and Bcl-X_L, but there have been reports that NF-κB can act proapoptotically by regulating DR4, DR5 or TRAIL expression [21,102]. Proteasome inhibitors, such as bortezomib prevent IκBα protein degradation, thereby inhibiting the release of NF-κB. [88] Protein kinase C (PKC) activation was shown to inhibit TRAIL-induced apoptosis by preventing the recruitment of FADD to the DISC and the activation of NF-κB [103].

Enhancing TRAIL effectiveness

In order to overcome resistance, many studies have proposed agents that act synergistically with TRAIL and resensitise tumour cells to TRAIL-induced apoptosis (Table 3). Some agents that act synergistically are currently used as part of standard sarcoma chemotherapy. Doxorubicin acts effectively in combination with TRAIL in leukaemia, multiple myeloma and breast cancer cells by activating the intrinsic apoptotic pathway, while TRAIL activates the extrinsic pathway. Doxorubicin also upregulates TRAIL receptors DR4 and DR5 and inhibits the expression of extrinsic apoptosis inhibitor c-FLIP [36,104-106]. Other agents that cause increased DR4 and DR5 expression include etoposide, cisplatin, paclitaxel, tunicamycin, sulforaphane, proteasome inhibitor MG132 as well as treatment with irradiation [22,41,79]. Locklin *et al.,* reported that MG63 cells can also be sensitised to TRAIL with bisphosphonate treatment, via DR5 upregulation [75]. A study by Hotta *et al.,* reported that another chemotherapeutic drug, cis-diammine dichloroplatinum (CDDP) sensitises TRAIL-resistant osteosarcoma cell lines SAOS-2 and MG63 by promoting TRAIL-induced activation of procaspase-8 and procaspase-3, leading to increased caspase-8 activity. The authors demonstrated that

CDDP also downregulates c-FLIP and enhances TRAIL-induced decline in mitochondrial membrane potential [71]. Deng *et al.,* indicated that the combination of doxorubicin, IFNγ and TRAIL had an increased apoptotic effect in MG63 osteosarcoma cells compared to TRAIL monotherapy. Doxorubicin and IFNγ upregulate DR5 and promote caspase-8 activation [73,107]. Histone deacetylase inhibitors (HDIs) such as NAHA, NaB and MS275 also act synergistically with TRAIL by activating caspase-3 and caspase-9 [87]. Many cancer cells can be sensitised to TRAIL after treatment with proteasome inhibitors that block among others the NF-κB signalling pathway. This is of importance as non-canonical effects of TRAIL signalling can occur with recruitment of molecules such as TNF receptor-associated factor 2 (TRAF2) and receptor-interacting serine/threonine protein kinase 1 (RIPK1) resulting in NF-kB activation and upregulation of anti-apoptotic genes. This and the potential migration, invasion and proliferative effects of TRAIL signalling has been reviewed in detail recently by von Karstedt *et al.* [108]. A study by Lu *et al.,* in 2008 showed that bortezomib enhances TRAIL activity in Ewing's sarcoma cell lines [88]. Another way to promote TRAIL-induced apoptosis is by targeting inhibitors of apoptosis (IAPs) with pharmacological agents such as celecoxib, second mitochondria-derived activator of caspases (Smac) mimetics, as well as other antiapoptotic molecules like Bcl-2 inhibitors [78,109-111]. Guo *et al.,* demonstrated that Smac mimetics downregulate XIAP, cIAP1 and survivin in Jurkat cells, while Dai *et al.,* used a Smac mimetic, SH122, that enhances TRAIL activity in prostate cancer cells both by blocking XIAP and cIAP1 and by deactivating NF-kB [109,110]. Another study by Belz *et al.*, showed that a combination of a Smac mimetic (BV6) and dexamethasone promoted cIAP1, cIAP2 and XIAP degradation by the proteasome, thereby promoting the assembly of the ripoptosome (RIP-1/FADD/caspase-8 complex) [112]. Bcl-2 inhibitors have also been found to effectively promote cell death by inducing activation of caspase-8, Bid cleavage and therefore increase caspase-3 activity in prostate cancer cells [111]. Therefore, TRAIL combination therapies targeting either DR receptors and caspases or molecules that modulate TRAIL apoptotic pathways present a more promising therapeutic strategy than TRAIL monotherapy.

Another limitation for the use of sTRAIL in humans is its short *in vivo* half-life, which has been reported to be about 30 minutes [113,114]. Researchers have implemented various techniques in order to overcome this difficulty. One of the most common is the

binding of TRAIL to a tumour-specific single-chain variable antibody fragment (scFv), which results in a scFv:sTRAIL fusion protein with larger molecular weight, therefore reduced glomerulal excretion and extended circulation time [115]. Müller *et al.* genetically fused a modified variant of TRAIL, Flag-TNC-TRAIL, to human serum albumin (HSA) and showed that HSA-Flag-TNC-TRAIL has a serum half-life of 15 hours and enhanced *in vivo* anti-tumour activity [116]. Another strategy, reported by Kim *et al.*, is to use PEGylated TRAIL (PEG-TRAIL), which demonstrates higher stability, as well as an improved pharmacokinetic profile due to slower renal clearance [117,118]. The same authors linked PEGylated TRAIL to transferrin (Tf), creating Tf-PEG_{10K}-TRAIL. They showed that Tf-PEG_{10K}-TRAIL also has a prolonged half-life and is even more effective than PEG-TRAIL against tumours *in vivo*, due to transferrin's high affinity for Tf receptors [119]. Kim *et al.* also created poly (lactic-co-glycolic) acid (PLGA) microspheres that deliver PEG-TRAIL to tumour sites locally and continuously. The authors presented evidence that PEG-TRAIL microspheres have a sustained release profile (18 days) and are more effective in inhibiting tumour growth *in vivo.* This data indicates that they can be used as a long-term TRAIL delivery system with therapeutic advantages [120]. Using a similar strategy, the same team of authors designed nanoparticles (NPs) that deliver TRAIL by mixing PEGylated heparin (PEG-HE), poly-$_L$-lysine (PLL) and TRAIL. TRAIL-PEG-NPs demonstrated a 28.3 fold increase in half-life compared to TRAIL alone, as well as higher tumour suppression activity [121]. Although more *in vivo* studies are required, these encouraging results suggest that the above methods for TRAIL delivery could greatly improve its efficacy in a clinical setting.

TRAIL delivery through mesenchymal stem cells

Despite the initial enthusiasm following *in vivo* and *in vitro* studies and their conclusions characterising TRAIL as a selective and considerably safe anticancer therapy, limitations caused by its pharmacokinetic characteristics have moderated its application in clinical use [122,123]. A short half-life due to its rapid clearance requires frequent and high dose administration, which may lead to toxicity [122]. In addition, limited bioavailability in the tumour site, especially in metastatic regions, impairs its apoptosis inducing potency observed in preclinical models [114,123]. Approaches including cell delivery of TRAIL have been proposed and genetically modified mesenchymal stem cells (MSCs) expressing TRAIL seem to be a promising strategy for tackling rh-TRAIL limitations [124-

133]. Some useful features of MSCs render them effective carriers of specific agents such as TRAIL. First, they can be easily and effectively transduced usually either by lentiviral or adenoviral vectors and express high amounts of the desired agent [126,132,134-137]. In addition, MSCs are considered to be immune privileged due to low membrane expression of MHC and other immunopotent molecules [138,139]. Therefore, they manage to evade potential immune rejection and render allogeneic transplantation possible [131,140]. Moreover, MSCs seem to possess tumour tropism properties, migrating and being incorporated into the tumour site, especially the surrounding stroma. Many groups have published studies indicating that MSCs are gathered around a wide variety of tumours after IV administration, such as lung cancer, bone sarcomas and breast cancer [125,133,141]. A number of studies published during the last decade have demonstrated very satisfactory results regarding the apoptosis inducing potency of TRAIL expressing MSCs (Table 4) [124-133]. In fact, some studies indicate that MSCs expressing TRAIL induce higher rates of apoptosis compared to rh-TRAIL, and indeed some cancer types traditionally considered TRAIL resistant seem to be sensitised to MSC-expressed TRAIL [124-126,132]. Recent studies by Juan *et al.,* indicate that genetically modified MSCs express high amounts of membranous TRAIL via extracellular vesicles (EVs, cell-released membranous vesicles), which were mostly exosomes. These TRAIL-loaded EVs were very potent against all cancer cell lines tested, but showed no toxicity to normal cells [142]. As for the bone sarcomas, Grisendi *et al.,* transduced adipose derived MSCs via a retroviral vector and examined their apoptosis inducing potency in several bone sarcoma lines, as well as in a Ewing's sarcoma xenograft model. In this study, bone sarcoma lines were sensitive to MSC-expressed TRAIL with Ewing's sarcoma cell lines presenting the highest susceptibility (apoptosis rate approximately 71 %). The apoptosis induction was specifically associated with caspase 8 activation. Results from *in vivo* studies demonstrated a significant increase in apoptosis rates compared to the control group combined with a reported antiangiogenic function [125]. Similar results were reported by Guiho *et al.,* who used adipose-derived MSCs expressing TRAIL against Ewing's sarcoma both *in vitro* and *in vivo*. Significantly, some cell lines resistant to rh-TRAIL showed very satisfactory sensitivity to MSC-expressed TRAIL [124]. In conclusion, the use of MSCs in cancer therapy remains quite controversial. There are many conflicting studies supporting intrinsic tumour promoting or tumour suppressing properties of MSCs [143-145]. These differences may be attributed to experimental

conditions, MSC type and relevant concentrations, cancer type and the molecular microenvironment [146]. Undoubtedly, it seems that more studies are needed to clarify the safety of MSCs in cancer therapy.

Conclusion and future direction

Inducing apoptosis exclusively in cancer cells by stimulating DRs seems to be a promising therapeutic option for bone sarcomas, which still have a poor prognosis in many cases despite multi-modal therapy. TRAIL-mediated apoptosis is most effective in Ewing's sarcoma; however, osteosarcoma and chondrosarcoma are less TRAIL-sensitive. Whereas most studies *in vitro* and in non-human primates have indicated that TRAIL, especially non-oligomerised versions, are non-toxic to untransformed cells, more evidence is required to evaluate its safety to human tissues. In order to employ TRAIL-induced apoptosis in bone sarcoma cells in a clinical setting, overcoming resistance remains the main challenge. Multiple *in vitro* and *in vivo* studies have focused on enhancing TRAIL effectiveness by combining it with chemotherapeutic drugs that upregulate death receptors DR4 and DR5 and caspases 3 and 8, by targeting regulatory molecules in the TRAIL extrinsic pathway, or by designing new, more stable oligomerised variants of TRAIL.

Most primary bone tumours are treated with surgical resection of the tumour and subsequent reconstruction. Local delivery of tumouricidal agents may, therefore, be possible following surgery. Agents such as TRAIL may be eluted or delivered locally, possibly using cell-based strategies, into the tumour bed by biologically enhanced reconstructions. It may be possible to further increase TRAIL potency by using pre-activated mesenchymal stem cells (MSCs) to deliver TRAIL to the cancer site; however, the safety of this strategy requires careful evaluation. Other techniques have been reviewed for local delivery of antineoplastic agents into tumour sites, such as the use of surgical pastes and coating of implants [116]. Although *in vitro* promise has not been delivered in clinical studies for TRAIL agents, the anatomic location and present treatment paradigm mean that there is potential for these techniques. It is therefore essential that more preclinical and clinical studies are conducted to determine the detailed risks and benefits of this novel therapeutic strategy.

From *in vitro* studies, the potency of TRAIL along with other DR4/DR5 agonists have been assessed against bone sarcoma cell lines where in general, they were shown to be potent. The highest sensitivity was shown in Ewing's sarcoma cell lines, however cell lines that were less sensitive include the osteosarcoma and chondrosarcoma cell lines (Table 1). Satisfactory results are also shown from *in vivo* studies, especially in Ewing's sarcoma xenograft models. However, the very few clinical trials published so far indicate only low or moderate efficacy of soluble TRAIL in bone sarcoma cases (Table 2). Potentially, *in vivo* resistance can be overcome by strategies for example, co-administering soluble TRAIL with other drugs, fusion proteins and TRAIL cell delivery approaches, particularly through MSCs [110,130].

With regards to improving the efficacy of TRAIL, future investigation should build on the effectiveness of the use of fusion proteins of TRAIL targeting bone sarcoma- or soft tissue sarcoma-specific cell surface proteins to improve the selectivity of TRAIL and minimise side effects. Its success, however, depends on the expression of the target antigen by a significant fraction of the cancer cell population. One protein of interest in bone sarcoma is NG2, or neural/glial antigen 2, which is expressed highly on RNA level in chondrosarcoma [147] and moderately in osteosarcoma. Preliminary flow cytometry and western blotting data from our laboratory confirm this finding. Studies in melanoma have found increased half-life and enhanced activity with anti-MCSP/NG2-TRAIL *in vitro* and *in vivo,* [148] or by using a bispecific antibody directed at DR5 (anti-MCSP/NG2-DR5) [149], both worth pursuing further in bone sarcoma. Furthermore, technology such as RNA sequencing, whole genome and exome sequencing and single cell sequencing can help enable the better characterisation of cell and tissue samples to help gain more information about the potential susceptibility to TRAIL. This would be used to investigate levels of death receptor and decoy receptor expression, and factors that regulate the intrinsic and extrinsic apoptotic pathways. Recent PCR data from lung cancer samples has revealed increased levels of Akt, which contributes to TRAIL resistance [150]. Increased levels of XIAP, an inhibitor of apoptosis has also been found to contribute to TRAIL resistance among other factors such as NF-kB [151]. Further information is required regarding Akt, XIAP, NF-kB and other factors, which increase TRAIL resistance in bone and soft-tissue sarcoma at the genome and protein levels. This

would better inform the type of combination therapies such as the use of Smac mimetics, to be used for selected patients and personalise therapy.

Table 1. Important preclinical studies on the main bone sarcomas.

Authors	**Study Type**	**PARA Used**	**Cancer Studied**	**Study Purpose**	**Results**
Moon *et al.,* (2011) [79]	*In vitro*	TRAIL	Osteosarcoma	Proapoptotic effect of soluble TRAIL alone or combined with Bisphosphonate	sTRAIL alone efficacy: 6 % apoptotic rate TRAIL-Bisphosphonate efficacy: 46 % apoptotic rate
Cheong *et al.,* (2011) [89]	*In vitro*	TRAIL	Chondrosarcoma	Proapoptotic effect of TRAIL alone or in combination with proteasome inhibitor MG132	TRAIL alone efficacy: >80 % cell viability TRAIL-MG132 efficacy: <40 % cell viability
Picarda *et al.,* (2010) [73]	*In vitro* *In vivo*	TRAIL	Osteosarcoma Ewing's sarcoma	*In vitro* and *in vivo* efficacy of TRAIL on osteosarcoma and Ewing's sarcoma	*In vitro*: cell viability in both OS and EWS cell lines <20 % *In vivo*: significant decrease in

					tumour incidence, tumour growth, pulmonary metastatic rate and 2-fold increase in overall survival rates
Lissat *et al.,* (2007) [86]	*In vitro*	TRAIL	Ewing's sarcoma	Levels of caspase-8 expression in Ewing's sarcoma tissue samples IFN-γ effect on caspase-8 levels and sensitivity to TRAIL	24 % of tumour samples express low levels of caspase-8 IFN-γ increases caspase-8 expression levels and renders resistant cell lines sensitive
Sonnemann *et al.,* (2007) [87]	*In vitro*	TRAIL	Ewing's sarcoma	*In vitro* effect of TRAIL combined with histone deacetylase inhibitors (HDACi) in TRAIL resistant cell line	TRAIL alone efficacy: 17 % apoptotic rate TRAIL-HDI efficacy: 54 % apoptotic rate

Merchant *et al.,* (2004) [85]	*In vitro* *In vivo*	TRAIL DR5 agonist	Ewing's sarcoma	*In vitro* and *in vivo* efficacy of TRAIL and DR5 agonist on Ewing's sarcoma IFN-γ effect on *in vivo* reported TRAIL resistance	*In vitro*: 9/11 cell lines tested are equally sensitive to TRAIL and DR5 agonist *In vivo*: Complete response in 19 % and 9 %, temporary responses in 43 % and 61 % after treatment with TRAIL and DR5 agonist respectively IFN-γ restores *in vivo* acquired TRAIL resistance
Bouralexis *et al.,* (2004) [55]	*In vitro*	TRAIL	Osteosarcoma Soft tissue sarcoma Giant cell tumour	Proapoptotic effect of soluble TRAIL alone or combined with	The combination of sTRAIL with chemotherapeutic drugs (especially doxorubicin) significantly

				conventional chemotherapeutics	increased tumour cell death.
Tomek *et al.,* (2003) [90]	*In vitro*	TRAIL	Chondrosarcoma	Proapoptotic effect of TRAIL alone or in combination with conventional chemotherapeutics	TRAIL alone efficacy: Approx. 20 % apoptotic rate TRAIL-DOX: 90-95 % apoptotic rates
Hotta *et al.,* (2003) [71]	*In vitro*	TRAIL	Osteosarcoma	Proapoptotic effect of TRAIL alone or combined with conventional chemotherapeutics	TRAIL alone efficacy: 3.1 ± 2.3 % apoptotic rate (MG63 cell line) TRAIL-CDDP pretreatment: 24.2 ± 3.1 % apoptotic rate
Evdokiou *et al.,* (2002) [72]	*In vitro*	TRAIL	Osteosarcoma	Proapoptotic effect of TRAIL alone or combined with conventional chemotherapeutics	TRAIL alone efficacy: Considerable apoptotic rates (80 %) in 1/6 cell lines tested

					TRAIL-chemotherapeutics (DOX, CDDP, ETP) efficacy: Apoptotic rates >75 % in TRAIL resistant cell lines
Mitsiades *et al.,* (2001) [81]	*In vitro*	TRAIL	Ewing's sarcoma	Proapoptotic effect of TRAIL in EWS cell lines DR expression levels in EWS cell lines and tumour samples	TRAIL efficacy: 9/10 cell lines sensitive DR expression: 9/10 cell lines express both DR, 72 % of tumour samples express both DR, 25 % of tumour samples express 1 DR

Table 2. Important clinical studies in bone and soft tissue sarcomas.

Authors	**Study Type**	**PARA Used**	**Cancer Studied**	**Study Purpose**	**Results**
Tabernero *et al.,* (2015) [91]	Phase Ib/II Clinical Trial (NCT00819169)	Conatumumab (DR5 agonist; AMG655; Amgen Inc.)	Locally advanced or metastatic, treatment-refractory solid tumours (including sarcoma cases)	Phase Ib: Safety and tolerability of conatumumab (in combination with ganitumab- anti IGFR type 1) Phase II: Efficacy of conatumumab (in combination with ganitumab)	Dose Limiting Toxicities (as defined by the authors): 0/9 patients. Complete or partial response: 0/78 patients. Stable disease: 28/78 patients (5 sarcoma cases) (36 %)
Demetri *et al.,* (2012) [92]	Phase Ib/II Clinical Trial (NCT00626704)	Conatumumab (DR5 agonist; AMG655; Amgen Inc.)	Locally advanced or metastatic, unresectable soft tissue sarcomas	Phase Ib: Safety and tolerability of conatumumab (in combination with doxorubicin) Phase II: Progression-free survival (PFS) in conatumumab-doxorubicin group compared to placebo-	Safety: Treatment -related hematologic adverse events. Similar incidence in both groups. PFS: No significant difference between the conatumumab–doxorubicin

				doxorubicin group	group and placebo–doxorubicin group.
Merchant *et al.,* (2012) [93]	Phase I Clinical Trial (NCT00428272)	Lexatumumab (DR5 agonist; HGS-ETR2; Human Genome Sciences Inc.)	Ewing's Sarcoma Osteosarcoma Neuroblastoma Rhabdomyosarcoma	Safety, tolerability, pharmacokinetics, therapeutic efficacy of lexatumumab	DLTs (as defined by the authors): 1 /24 patients. Complete or partial response: 0/24 patients. Stable disease: 5/24 patients.
Subbiah *et al.,* (2012) [94]	Case study	Dulanermin (rhTRAIL; AMG951; Amgen Inc.)	Refractory chondrosarcoma	Efficacy of Dulanermin in a refractory chondrosarcoma case	Safety: No significant adverse events Efficacy: Partial response

Herbst *et al.,* (2010) [95]	Phase I Clinical Trial	Recombinant Human TRAIL (rhTRAIL)	Advanced cancer (including sarcoma cases)	Safety, tolerability, pharmacokinetics and antitumour activity of rhApo2L/TRAIL	Safety: 28 % of the patients with serious adverse events (as defined by the authors) Efficacy: 46 % of the patients with stable disease, 2 chondrosarcoma cases with partial response Ongoing with Phase 1 studies for osteosarcoma
Camidge *et al.,* (2010) [96]	Phase I Clinical Trial	PRO95780 (DR5 agonist; Drozitumab; Genentech Inc.)	Advanced malignancies (including sarcoma cases)	Safety, tolerability, pharmacokinetic, maximal tolerated dose (MTD) and antitumour activity of PRO95780	Safety: 10 % of the patients with DLTs (as defined by the authors) Efficacy: 3/50 patients with partial response (including one chondrosarcoma case)

Belch *et al.,* (2010) [97]	Phase II Clinical Trial (NCT00315757)	Mapatumumab (DR4 agonist; HGS-ETR1; Human Genome Sciences Inc.)	Relapsed/Refractory Multiple Myeloma	Efficacy and safety of mapatumumab-bortezomib compared to bortezomib alone	Safety: Similar incidence of adverse events in both groups Efficacy: Response rate, PFS and duration of response similar in both groups
Not published	Phase II Clinical Trial (NCT00543712)	PRO95780 (DR5 agonist; Drozitumab; Genentech Inc.)	Advanced chondrosarcomas	Efficacy and safety of PRO95780 when given as a single agent	Efficacy not evidenced for the study group

Table 3 - Agents that sensitise cells to TRAIL-induced apoptosis and their effects.

Agent	**Effect**	**Tumour Type**	**Reference**
Effects on DR4 and DR5			
Bisphosphonates	DR5 upregulation	Osteosarcoma MG63	[79]
Cisplatin	DR5 upregulation	Glioma	[41]
Doxorubicin	DR4 DR5 upregulation	Osteosarcoma MG63, leukaemia, multiple myeloma, breast, soft tissue sarcomas, prostate	[90,104,107]
Doxorubicin	c-FLIP downregulation	Leukaemia, multiple myeloma, breast, soft tissue sarcomas, prostate	[90,104]
Etoposide	DR5 upregulation	Colon, glioma, leukaemia	[41]
IFNγ	DR5 upregulation	Osteosarcoma MG63	[107]
Irradiation	DR4, DR5 upregulation	Leukaemia	[22,41]

Paclitaxel	DR4, DR5 upregulation	Prostate	[152]
Proteasome inhibitor MG132	DR5 upregulation	Soft tissue sarcomas	[89]
Sulphoraphane	DR5 upregulation	Hepatoma	[41]
Tunicamycin	DR5 upregulation	Prostate	[41]
Effects on caspases			
Bcl-2 inhibitors	Caspase-8 and Bid activation leading to caspase-3 activation	Prostate	[111]
CDDP	Caspase-8 activation, c-FLIP downregulation	Osteosarcoma SAOS-2 and MG63	[71]
Celecoxib	Survivin and Bcl-2 downregulation	Osteosarcoma MG63	[78]
Doxorubicin	Caspase-8 activation	Osteosarcoma MG63	[107]
HDIs (SAHA, NaB, MS275)	Caspase-3 and caspase-9 activation	Ewing's Sarcoma	[87]
IFNγ	Caspase-8 activation	Osteosarcoma MG63	[107]
Proteasome inhibitors e.g., bortezomib	Inhibition of NF-κB by preventing IκBα degradation	Ewing's sarcoma	[88]
Proteasome inhibitors e.g. exopomicin	Caspase-8, caspase-3 and caspase-9 activation	Osteosarcoma SAOS-2 and MG63	[77]
Smac mimetics	XIAP, cIAP1 and survivin downregulation, activation of caspase-3 and caspase-8,	Leukaemia, glioblastoma	[109]
Smac mimetics (BV6) and dexamethasone	Promotion of cIAP1, cIAP2 and XIAP degradation	Leukaemia	[112]
Smac mimetics (SH122)	XIAP and cIAP1 blocking by NF-κB inhibition	Prostate	[110]

Table 4 - Important studies of human mesenchymal stem cells expressing TRAIL.

Author	**Cancer type studied**	**Type of MSCs used**	**MSCs transduction**	***In vitro* results**	***In vivo* results**
Yuan *et al.*, (2017) [142]	Lung cancer (LC) Malignant pleural mesothelioma (MPM) Renal cancer (RC) Breast cancer (BC) Neuroblastoma (NB)	Bone Marrow-Derived MSCs	Lentiviral vector	MSCs express membranous TRAIL via extracellular vesicles (EVs), mostly exosomes Cancer cell lines: MSC TRAIL- EVs induce apoptosis in all cancer cell lines, even in those resistant to rhTRAIL	Not tested
Guiho *et al.,* (2016) [124]	Ewing's sarcoma (ES)	Adipose-Derived MSCs	MIGR1-TRAIL-GFP Vector	ES cell lines: High rates of apoptosis (>80 % in most lines) even in cell lines resistant to rhTRAIL	ES paratibial orthotopic model: Inhibition of tumour growth by 75 % and increase in

					survival rates by 60 %
Grisendi *et al.,* (2015) [125]	Osteosarcoma (OS) Ewing's Sarcoma (ES) Rhabdomyosarcoma (RD)	Adipose-Derived MSCs	pMIGR1 vector	Sarcoma cell lines: High rate of apoptosis (from 42 ± 0.6 % of RD to 71 ± 0.3 % of ES lines)	ES xenograft: Significant increase of apoptosis in comparison to controls (6.11 ± 0.98 % vs 0.27 ± 0.15 %)
Yuan *et al.,* (2015) [126]	Lung cancer (LC) Malignant pleural mesothelioma (MPM) Colon cancer (CC) Renal cancer (RC) Squamous Cell Carcinoma (SCC) Breast cancer (BC)	Bone Marrow-Derived MSCs	Lentiviral vector	BC and LC cell lines: MSCs expressing full length TRAIL and truncated soluble TRAIL both induce apoptosis. MSCs-flTRAIL induce higher rates of apoptosis than MSCs-sTRAIL in both cell lines (approx. 60 % vs 50 %).	Not tested

Yuan *et al.,* (2014) [127]	Lung cancer (LC)	Bone Marrow-Derived MSCs	Lentiviral vector	Lung cancer cell lines: Apoptosis rate ranges between 35–75 % (MSCs-flT)	Not tested
Lee *et al.,* (2013) [128]	Metastatic malignant fibrous histiocytoma (MFH)	Adipose-Derived MSCs	Adenoviral vector	MFH cells lines: High rate of apoptosis (89.1 ± 6.5 %)	MFH xenograft: Inhibition of local tumourigenesis, metastatic tumourigenesis and reduction of pre-established metastasis
Ciavarella *et al.,* (2012) [129]	Multiple myeloma (MM)	Adipose-Derived MSCs	MIGR1-TRAIL-GFP vector	MM cell lines: Significant rates of cell death (53.3 ± 3.6 % to 67.3 ± 2.5 %) when pretreated with bortezomib	Not tested
Barti Juhasz *et al.,* (2011)[130]	Rhabdomyosarcoma (RD)	Bone Marrow-Derived MSCs	pORF-h-TRAIL vector	RD cell culture: Significant inhibition (almost 85 %)	Not tested
Mohr *et al.,*	Pancreatic cancer (PC)	Bone Marrow-	Adenoviral vector	PC cell lines:	PC xenograft:

(2010) [131]		Derived MSCs		High rates of apoptosis (Panc1 line> 40 %, PancTu1 line> 50 %) when compared with XIAP silencing	Localised tumour: Tumour regression when MSC-TRAIL were combined with XIAP silencing Metastasis: 1/6 mice with lung metastasis in study group compared to 5/6 mice with lung metastasis in control group
Loebinger *et al.,* (2009) [133]	Lung cancer (LC) Breast cancer (BC) Squamous cell cancer (SCC) Cervical cancer (CC-HeLa)	Bone Marrow-Derived MSCs	Lentiviral vector (pRRL-cPPT-hPGK-mcs-WPRE)	Cancer cell lines: Significant increase in apoptosis: Lung cancer (19.6 % ± 0.8 %), breast cancer (37.7 % ± 6.5 %), squamous cell cancer (34.5 % ± 1.0 %) cervical cancer (36.1 % ± 3.5 %)	BC xenograft: Localised tumour: Reduction in tumour growth (0.12 ± 0.12 cm^3 vs 0.66 ± 0.69 cm^3) and weight (0.07 ± 0.06 g vs 0.33 ± 0.33 g) Metastasis: 3/8 mice tumour free in study group compared to 0/8 mice tumour free in controls in

				in combination with doxycycline	combination with doxycycline
Mohr *et al.,* (2008) [132]	Lung cancer (LC)	Bone Marrow-Derived MSCs	Adenoviral (type 5) vectors (Ad.EGFP, Ad.BGal, Ad.TR)	LC cell lines: Apoptosis rates of approx. 30 % vs <5 % in control lines	LC xenograft: Tumour increased by a factor of 1.25 in study group vs a factor of 3 in controls

MAIN AIMS OF THE PHD

- **Characterisation of a range of sarcoma cell lines for factors that contribute to TRAIL sensitivity.**
- **Study the effects of using 'pre-activated' bone marrow-derived mesenchymal stem cells (BMMSCs) expressing TRAIL on sarcoma cell lines.**
- **Screen sarcoma cell responses to enhanced forms of TRAIL.**
- **Study the effects of combining TRAIL with chemotherapy and novel sensitising agents *in vitro*.**
- **Study effects of using TRAIL in an *in vivo* mouse model of bone sarcoma.**
- **Study the effects of using 'pre-activated' bone marrow-derived mesenchymal stem cells (BMMSCs) expressing TRAIL on sarcoma cell lines.**

Chapter 2. General Materials and Methods

2.1 Mammalian cell culture

2.1.1 Bone sarcoma cell lines

A number of authenticated bone sarcoma cell lines representing osteosarcoma, chondrosarcoma and Ewing's sarcoma were used as part of this research. Sources include American Type Culture Collection (ATCC) and others, which are presented in Table 5.

Table 5 - Bone sarcoma cell lines utilised for experiments as part of the PhD.

Sarcoma cell line	**Sarcoma type**	**Patient**	**Source**
U2OS	Osteosarcoma	Derived from a moderately differentiated osteosarcoma from the tibia of a 15-year-old Caucasian female.	ATCC
SAOS-2	Osteosarcoma	Derived from an 11-year-old Caucasian female who was treated with RTG, methotrexate, adriamycin, vincristine, cytoxan, and aramycin-C. SAOS-2 is p53 deficient [153].	ATCC
MG63	Osteosarcoma	Derived from a 14-year-old Caucasian male. The MG63 cell line was kindly donated by Dr Neil Cross, senior lecturer in molecular and cellular biology at Sheffield Hallam University.	Sheffield Hallam University
SJSA-1	Osteosarcoma	The cell line was derived from a 19-year-old black male in 1982 from an osteosarcoma	ATCC

		of the femur. It is known to carry an amplification of the gene, which encodes the p53 associated protein MDM2. There is also a 15-fold amplification of the gli proto-oncogene.	
TC71	Ewing's sarcoma	Derived post chemotherapy from the humerus of 22-year-old male with Ewing's sarcoma with EWS/FLI1 translocation.	NICR catalogue
SW1353	Chondrosarcoma	Derived from a grade 2 chondrosarcoma of the right humerus in a 77-year-old Caucasian female.	ATCC
HT1080	Chondrosarcoma	Derived from a 35-year-old Caucasian male and is known to have activated N-ras oncogene. Originally described as a fibrosarcoma cell line, more recently IDH mutations detected in this cell line make it more characteristic of a dedifferentiated chondrosarcoma [154].	ATCC

2.1.2 Control cell lines

DR4 and DR5 positive control cell lines

As a DR4 positive cell line, I used a murine fibroblast cell line engineered to express DR4 (MF DR4-Fas). MF DR5-Fas was used as a DR5 positive cell line. These are TRAILR-Fas chimeras produced by replacing the intracellular portions of DR4 and DR5 contained the death domain (DD) with that of Fas [155]. I have demonstrated this using flow cytometry analysis (Figure 3).

(a)

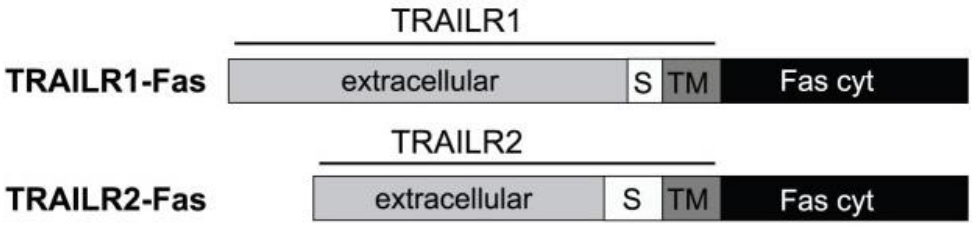

(b)

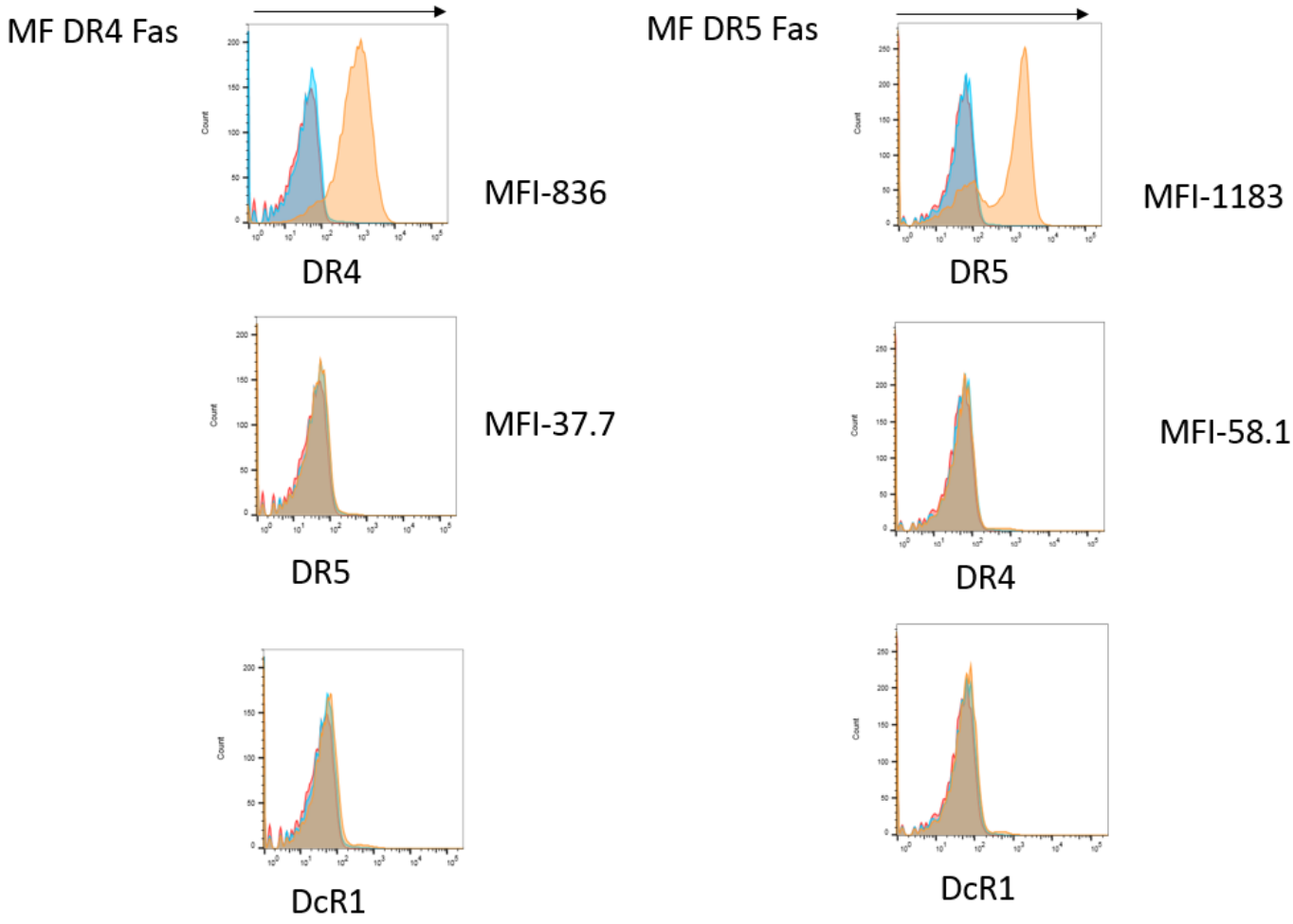

Figure 3 – (a) Schematic representation of TRAILR1-Fas (MF DR4-Fas) and TRAILR2-Fas (MF DR5-Fas) as presented by [155]. (b) MF DR4-Fas and MF DR5-Fas cells were used as positive control cell lines for DR4 and DR5 respectively. Methods and antibodies used are explained in Section 2.4. Background signal from isotype control was subtracted. MFI = median fluorescence intensity.

DR4 and DR5 negative control cell lines

The pharyngeal carcinoma (FaDu) cell line was used as a negative control for DR4. It has been reported to express a mutated form of DR4 [157], due to a homozygous mutation in the DR4 gene, which confers TRAIL resistance due to its lack of a death domain and has also been reported to be negative for DR5 [158]. A DR5 negative control cell line is the BJABLexR [155, 156], produced by exposing the Burkitt's lymphoma cell line to increasing doses of the TRAIL R2/DR5 agonistic antibody Lexatumumab and those surviving were harvested to yield a cell line with low DR5 levels [155]. Negative surface expression of DR4 in the FaDu cell line and DR5 in the $BJAB^{LexR}$ cell line was confirmed using flow cytometry (Figure 4).

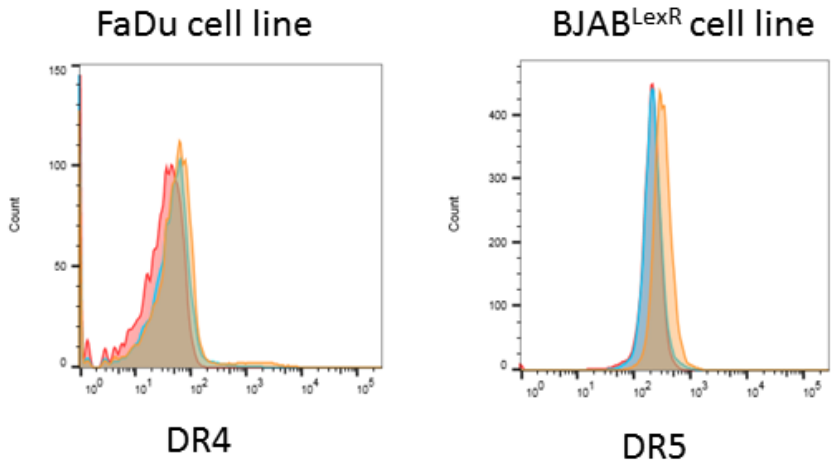

Figure 4 - The FaDu cell line is a DR4 negative control and the $BJAB^{LexR}$ cell line is a DR5 negative control.

Other control cell lines for death, decoy receptors and other relevant downstream proteins

Another DR5 positive control cell line is the HepG2 hepatocellular carcinoma cell line [156]. The MCF-7 breast carcinoma cell line is reported to be a positive control for DR4 [157], DcR2 [158] and PTEN [159]. The Mono Mac 6 cell line have characteristics of mature monocytes and have negative DR4 cell surface expression [160], and low TRAIL expression at the mRNA level [161]. As a positive control for decoy receptor 1 (DcR1), I used human umbilical vein endothelial cells (HUVECs) as described previously [162]. As

a positive control for decoy receptor 2 (DcR2), I used whole blood, specifically gating for the positive control peripheral blood granulocytes. I also used the 786-0 renal clear cell adenocarcinoma cell line from ATCC as a positive control for TRAIL [163] and H-Ras [164]. HeLa cells were also used as they have been described previously in the literature as a positive control for XIAP [165].

2.1.3 Non-malignant cell lines

As non-malignant cell lines, I used the normal human dermal fibroblast (NHDF) cell line derived from a neonatal male (ATCC); human bone marrow-derived mesenchymal stem cells (BMMSCs) obtained locally from the bone marrow of patients undergoing total hip arthroplasty (THA); human-derived osteoblasts (OBs); human vascular endothelial cells (HUVECs); a hepatocyte cell line (HHL5) and a ventricular cardiomyocyte cell line (AC10).

2.1.4 Cell culture

Tissue culture 6-well, 24-well and 96-well plates and 25cm^2, 75cm^2 and 125cm^2 vented cell culture flasks were obtained from Corning/Costar UK Ltd. (High Wycombe, UK) and were used to culture mammalian cell lines for experiments. For fluorescence assays, 96-well assay plates, clear bottom with lid were used (Corning/Costar UK Ltd). Mammalian cell lines were incubated at 37 ˚C in a humidified atmosphere of 5 % CO_2. The media and supplements used to maintain the cell lines are presented in Table 6. The passaging of cell lines was performed on a regular basis in a tissue culture hood every 2-3 days at a ratio of 1:5 to 1:20 once a confluence of 80-90 % was achieved.

Cells were detached from the plasticware by removing then washing off residual medium with phosphate-buffered saline (PBS; GIBCO-Invitrogen, Paisley, UK) before incubation at 37 °C with 1:10 Trypsin/ethylediaminetetraacetic acid 10x (EDTA; Sigma Aldrich) in PBS solution for about 3 minutes inside an incubator. Adding FBS-supplemented medium stopped the digestion process of surface proteins. Media was changed once every 72 hours.

Table 6 – Growth media and any additional supplements used to maintain cell lines used for the PhD project. FBS = fetal bovine serum, NEAA = non-essential amino acids, HuEGF = human epidermal growth factor, FGF = fibroblast growth factor.

Cell line	**Growth Media**	**Additional Supplements**
U2OS, SAOS-2, TC71, SJSA-1, MG63, SW1353, 786-0, Mono Mac 6, $BJAB^{LexR}$, MCF-7, HeLa	RPMI-1640	10 % FBS, 1 % Pen/Strep L-glutamine
HT1080, NHDF	DMEM	10 % FBS, 1 % Pen/Strep
HHL5	DMEM	10 % FBS, 1 % Pen/Strep, NEAA, L-glutamine
BMMSCs	DMEM	FGF-Basic (AA 1-155) Recombinant Human Protein (Thermo Fisher Scientific) 10 % FBS, 1 % Pen/Strep, L-glutamine
AC10	DMEM, F-12 Ham	10 % FBS, 1 % Pen/Strep, L-glutamine
HepG2	DMEM, F-12 Ham	10 % FBS, 1 % Pen/Strep, L-glutamine
HUVECs	Gibco™ Medium 200	Hydrocortisone 1 µg/ml, HuEGF (10 ng/ml), FGF-Basic (3 ng/ml), Heparin (10 µg/ml)
FaDu	MEM	10 % FBS, 1 % Pen/Strep

2.1.5 Cell counting

Cells were counted using an Improved Neubauer counting chamber (Hawksley, Lancing, UK). N cells were counted in one of the large squares (which contains 25 medium squares) and the concentration of the sample was calculated using the following equation: N x 10^4 cells/ml

2.1.6 Cryopreservation of cell lines

Cryopreservation medium	
FBS	20 %
DMSO	10 %
Culture media	10 ml

Cell lines were cryopreserved for storage. Cells were trypsinised and centrifuged at 300 x g for 3 minutes, then resuspended in 10 ml freeze media (80 % media, 20 % FBS, 10 % dimethyl sulfoxide (DMSO) at 2-5 x 10^6 cells/ml per cryovial. Cells were stored at -80 °C. For reculturing, cells were defrosted at 37 °C and transferred to a universal tube with 10 ml of media then centrifuged at 300 x g for 3 minutes. The supernatant was discarded and pellet resuspended in fresh media and transferred to a flask for continued culture.

2.2 TRAIL (Apo-2L; TNFSF10; CD253) ligands

Soluble (human) (rec.) SuperKillerTRAIL™ was obtained from Apidogen® life sciences (0.5 mg/ml). The extracellular domain of human TRAIL (aa 95-281) is fused at the N-terminus to a His-tag and a linker peptide. The active multimeric conformation is stabilised by an inserted mutation allowing an additional CC-bridge [166]. It demonstrates superior activity on human cell lines that require extensive cross-linking of TRAIL-Rs for killing (e.g. Jurkat cells) [167,168], which we have confirmed using Wst-8 assay (Figure 5a and b). FLAG-TRAIL and M2 antibody were obtained from Axxora LLC and Sigma Aldrich respectively. His-TRAIL was provided by Biolegend and recombinant human TNF (2 × 107 units/mg) was provided by Knoll AG (Ludwigshaven, Germany).

(a)

(b)

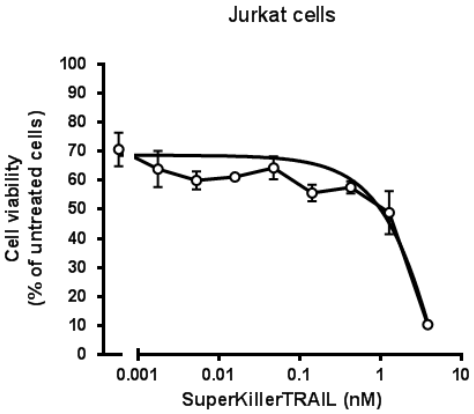

Figure 5 – Pictorial representation of the composition of (a) SuperKillerTRAIL™ (soluble) (human), (recombinant), ALX-201-115 and (b) Wst-8 assay demonstrating that when Jurkat cells are exposed to increasing concentrations of SuperKillerTRAIL there is a greater reduction in cell viability.

2.3 Reverse transcriptase-polymerase chain reaction (RT-PCR)

Background

SYBR green is a dye that binds in the minor groove of double-stranded DNA in a sequence independent way. Its fluorescence increases over 100-fold when it binds. The fluorescence can be detected online in real-time and the threshold cycle (Ct) of each sample can be recorded as a quantitative measure of the amount of PCR product in the sample [169]. The Ct value is defined as the fractional cycle number at which the

sample fluorescence signal passes a fixed threshold above baseline. Samples with a higher copy number initially, show high fluorescence earlier in the PCR process, resulting in a lower Ct value. Those with lower copy number have a higher Ct number. Quantitated transcript levels of the hypoxanthine phosphoribosyltransferase 1 (HPRT1) gene are used as the endogenous control and unknown samples are normalised to the HPRT1 content.

2.3.1.1 Molecular biology reagents

All RNA work was performed under RNase-free conditions using RNase-free reagents and materials. UltraPure™ DNase/RNase-Free Distilled Water (Thermo Fisher Scientific) was used for all work involving use of nucleic acids.

2.3.1.2 RNA extraction and cDNA synthesis

RNA was extracted from cell lines grown in T75 flasks using the Qiagen RNeasy extraction kit as per manufacturers' instructions [170].

Samples were first lysed and then homogenised. The lysate was then loaded into a spin column. Pure, concentrated RNA was eluted in 30–100 µl water.

2.3.1.3 RNA sample quality and concentration

Principle: Nucleic acid quality and quantification can be assessed by a number of methods, namely, UV spectrophotometry (Nanodrop), spectrophotofluorimetry (Qubit® Fluorometer), and microfluidic capillary electrophoresis (Bioanalyser). The use of each method has to be correlated with the downstream application. RNA quality and concentration in my samples was quantified using the NanoDrop® ND-1000 UV-Vis Spectrophotometer (Labtech, East Sussex, UK). Analysis time can be less than 30 seconds and there is no need for additional reagents or accessories. However, for low level nucleic acid samples it has poor sensitivity and specificity [171]. It should be used for quantities between 2 ng/µl – 3000 ng/µl. The ratio of the sample absorbance was measured at 260 nm and 280 nm. This is used to assess the purity of DNA and RNA. A ratio of about 1.8 is generally accepted as pure for DNA. A ratio of about 2 is generally accepted as pure for RNA. Absorbance measurement at 260 and 230 nm is a secondary measure for nucleic acid purity. They are normally higher than the 260/280 values and

are in the range of 1.8 - 2.2. An example of the concentrations and quality of RNA obtained from a range of cell lines is given below (Figure 6 and Figure 7).

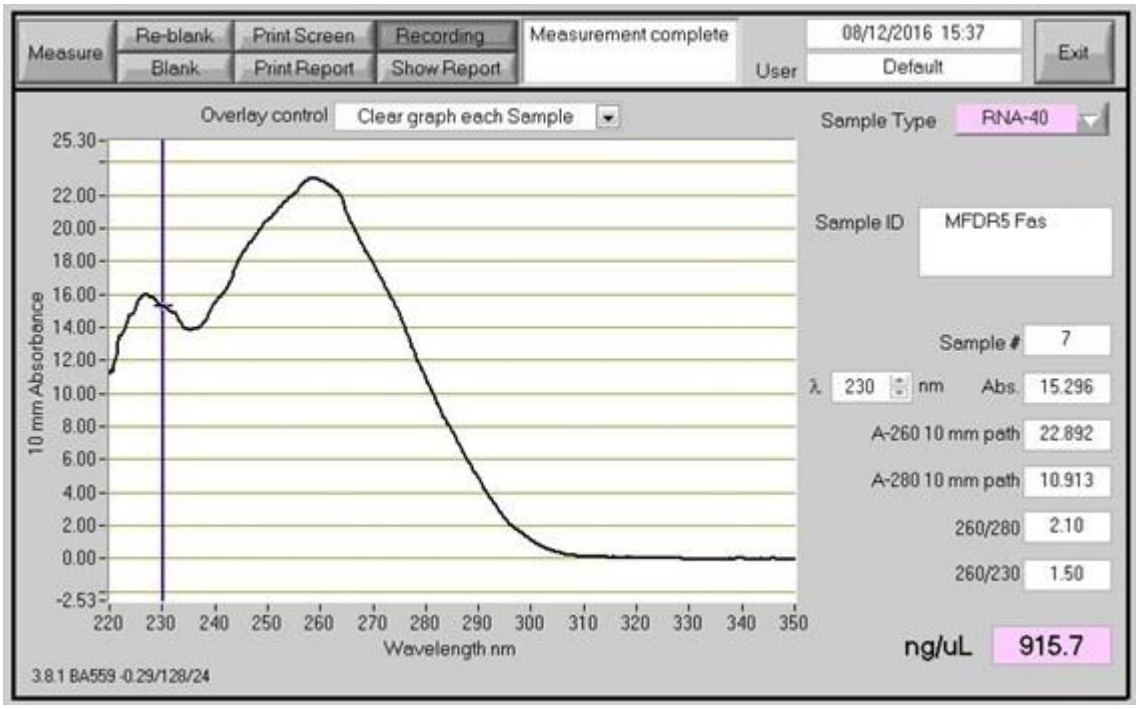

Figure 6 – Nanodrop readout for RNA extracted from a murine fibroblast cell line demonstrating acceptable quality 260/280 = 2.1, 260/230 = 1.5.

Sample ID	User ID	Date	Time	ng/ul	A260	A280	260/280	260/230	Constant	Cursor Pos.	Cursor abs.
NHDF RNA 6/3 ZG	Default	06/03/2017	11:35	433.35	10.834	5.437	1.99	2.27	40.00	230	4.763
HT1080 RNA 6/3 ZG	Default	06/03/2017	11:36	460.06	11.501	5.880	1.96	2.24	40.00	230	5.126
SJSA-1 RNA 6/3 ZG	Default	06/03/2017	11:38	312.62	7.815	3.830	2.04	2.10	40.00	230	3.718
SAOS-2 RNA 6/3 ZG	Default	06/03/2017	11:39	255.52	6.388	3.123	2.05	2.32	40.00	230	2.758
U2OS RNA 6/3 ZG	Default	06/03/2017	11:43	362.79	9.070	4.450	2.04	1.21	40.00	230	7.519

Figure 7 - Nanodrop report providing information about quality and concentration of the RNA obtained from bone sarcoma cell lines and the NHDF cell line.

2.3.1.4 cDNA conversion

The RNA harvested from the cell lines was converted to cDNA using an established laboratory protocol using the following components in the ratios below (Master Mix) (Table 7) added to the RNA harvested from the cell lines. Sterile tubes, pipette tips, gloves and nuclease-free reagents were used in all steps.

Table 7 - Mastermix components for cDNA synthesis.

Component	**Volume (µl) in 7.3 µl**
5x Reaction Buffer	4 µl (number of samples + 0.5 µl)
dNTP Mix (100 mM) (4 mM 1:25)	2 µl
Oligo $d(T)_{16}$ 1:5 dilution in RNase free water (DEPC)	1 µl
M-MLV Reverse Transcriptase (Promega GoScript™ Reverse Transcription System)	0.3 µl

1. Quality and concentration of RNA was measured using the nanodrop
2. 1000 ng/µl of RNA was taken from the sample and diethylpyrocarbonate (DEPC) water added to make up to a final volume of 12.7 µl
3. Sample was mixed gently and put in a heat block set at 65 ^{o}C for 5 minutes
4. 7.3 µl of the mastermix described above was added to the sample to make a final volume of 20 µl
5. Placed in heater at 37 ^{o}C for 1 hour
6. Then into heat block set at 100 ^{o}C for 10 minutes (to thermally inactivate the enzyme)
7. Sample diluted 1:3 by adding DEPC to final cDNA
8. cDNA sample quality and concentration was assessed using the nanodrop (Figure 8)
9. Stored at -20 ^{o}C

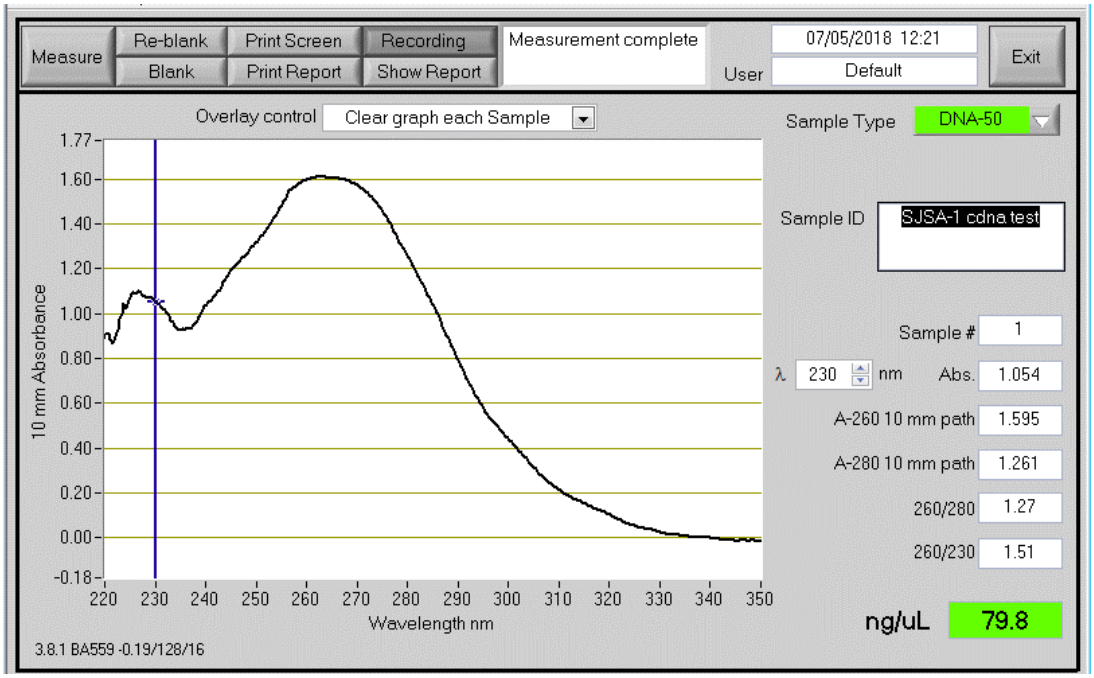

Figure 8 – Nanodrop readout for SJSA-1 cells demonstrating acceptable cDNA quality and concentration following conversion from RNA.

The mastermix consisted of forward and reverse primers, Platinum® SYBR® Green qPCR SuperMix-UDG with ROX (invitrogen™ by life technologies™) and sterile distilled water in a ratio of 0.4:0.4:5:2.2. Primer binding sites were checked using the SpliceCenter Website [172]. 2 µl of cDNA was mixed with 8 µl of the Mastermix in the wells of the PCR plate. Samples were in triplicates and experiments repeated up to 3 times. RT-PCR was performed using The Applied Biosystems™ QuantStudio™ 7 Flex Real-Time PCR System. All data was analysed using the QuantStudio™ Real-Time PCR Software version 1.2 (Applied Biosystems by Thermo Fisher Scientific).

2.3.1.5 Oligonucleotide primers

Primer check was used to display the splice variants and target location of PCR primer for my genes of interest were checked [(http://projects.insilico.us/SpliceCenter/PrimerCheck website (DR5 presented as an example in Figure 9)]

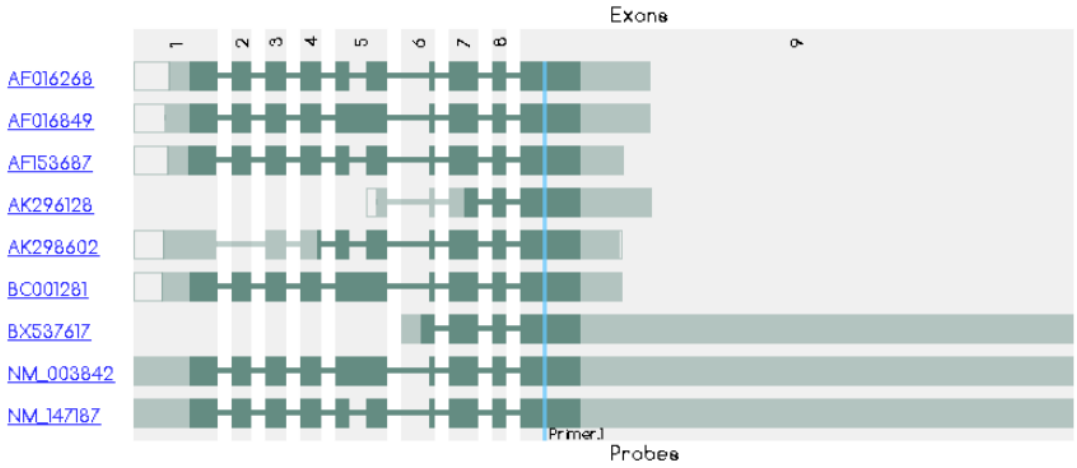

Figure 9 - DR5 primer binding site check. DR5 primers were selected to detect all DR5 splice variants. DR5 is also known as 'TNFRSF10B, CD262, DR5, KILLER, KILLER/DR5, TRAIL-R2, TRAILR2, TRICK2, TRICK2A, TRICK2B, TRICKB and ZTNFR9', gene located on chromosome 8, total exons = 9. **http://projects.insilico.us/SpliceCenter/PrimerCheck**

Primers were obtained from Sigma-Aldrich, as presented in Table 8.

Table 8 - Primers used to assess degree of transcript level expression for genes of interest.

Gene of interest	**Sense**	**Antisense**
DR4	5'-GCAGCTGGACCTCACGAAAA-3'	5'-CCTGGGCCTGCTGTACCA-3'
DR5	5'-GGCCACAGGGACACCTTGTA-3'	5'-TCGCCCGGTTTTGTTGA-3'
HPRT1	5'-TTGCTTTCCTTGGTCAGGCA-3'	5'-AGCTTGCGACCTTGACCATCT-3'
DcR1	5'-TCCCCAAGACCCTAAAGTTCG-3'	5'-CAGTGGTGGCAGAGTAAGC-3'
DcR2	5'-CTCCTACAAAGGGAAGCAGCC-3'	5'-CTAGGACCATTGGTAAGCTGCC-3'
TRAIL	5'-CAACTCCGTCAGCTCGTTAGAAAG-3'	5'-AGGAATGAATGCCCACTCCTT-3'
OPG	5'-TGCTGTTCCTACAAAGTTTAC-3'	5'-CTTTGAGTGCTTTAGTGCGTG-3'
XIAP	5'-TGGGACATGGATATACTCAGTTAACAA-3'	5'-GTTAGCCCTCCTCCACAGTGAA-3'

Akt	5’-CTTGCTTTCAGGGCTGCTCA-3’	5’-TACACGTGCTGCCACACGATAC-3’
PTEN	5’-AGTTCCCTCAGCCGTTACCT-3’	5’ATTTGACGGCTCCTCTACTG-3’
H-Ras	5’-CAGGAGACCCTGTAGGAGGA-3’	5’-TTTACTGTGATCCCATCTGTGC-3’
NG2	5’-CTGCAGGTCAGACTTGTTCTGG-3’	5’-CGACTGACAACGTGGCCC-3’
Cbfa1	5’-ATGTGTGTTTGTTTCAGCAGCA-3’	5’-TCCCTAAAGTCACTCGGTATGTGTA-3’
Osteopontin	5’-TTGCAGCCTTCTCAGCCAA-3’	5’-GGAGGCAAAAGCAAATCACTG-3’
Osteocalcin	5’-CGCCTGGGTCTCTTCACTAC-3’	5’-CTCACACTCCTCGCCCTATT-3’
$cFLIP_L$	5’-CCTAGGAATCTGCCTGATAATCGA-3’	5’-TGGGATATACCATGCATACTGAGATG-3’
cFLIPs	5’-GCAGCAATCCAAAAGAGTCTCA-3’	5’-ATTTCCAAGAATTTTCAGATCAGGA-3’

2.3.1.6 Run method

The run method set-up on The Applied Biosystems™ QuantStudio™ 7 Flex Real-Time PCR System is presented in Figure 10. Melt curve plots and standard curves are presented in Appendix Section 11.7.

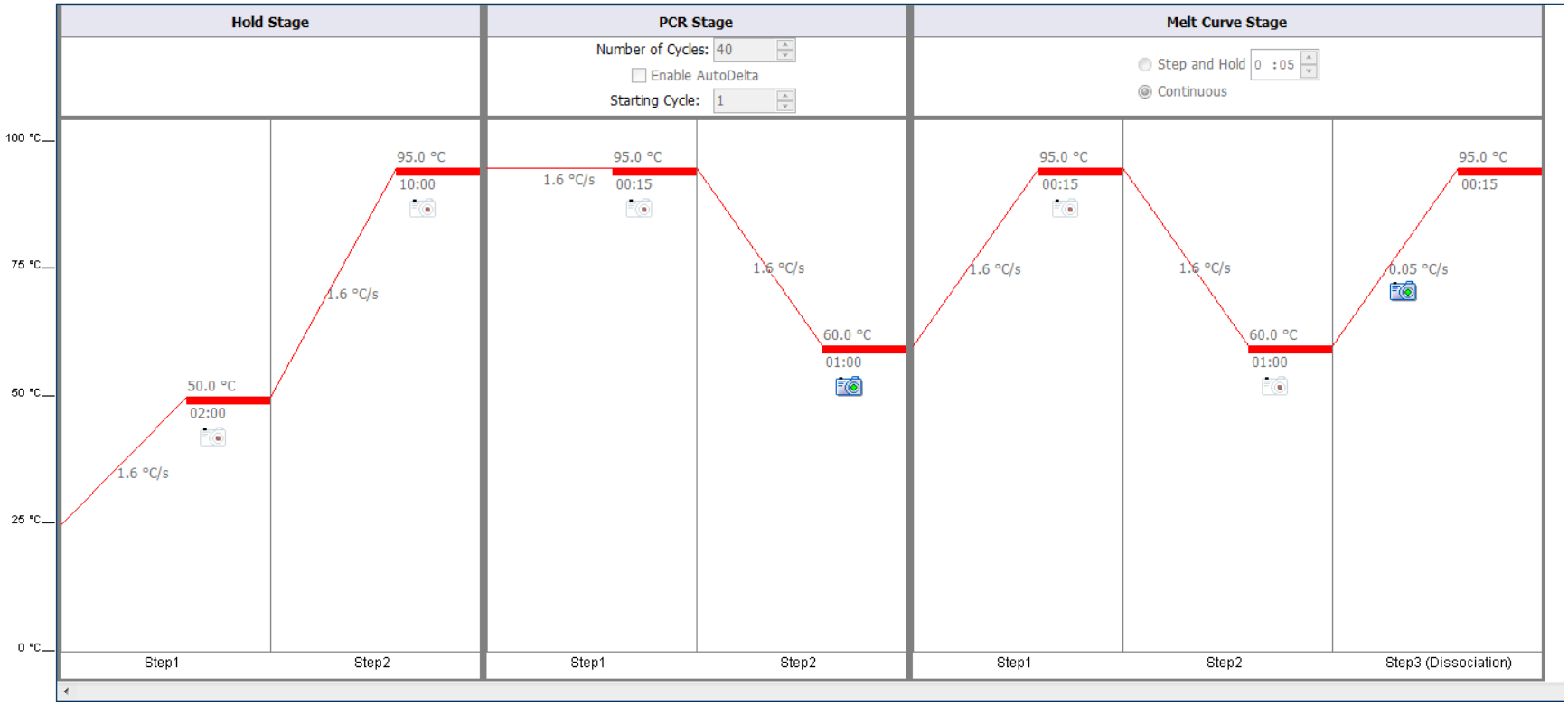

Figure 10 - Run method set-up on The Applied Biosystems™ QuantStudio™ 7 Flex Real-Time PCR System for the amplification of the target DNA sequence.

2.3.1.7 Quality assessment and quantitation of RNA transcript levels

To quantify cDNA levels, the relative standard curve and comparative Ct methods were used. The melt curve was used to assess efficiency of primer binding (Section 3.2). The Ct value from a serial dilution of a positive control was used to formulate the standard curve as a means to assess the efficiency of the PCR reaction. The standard curve for the housekeeping gene (HPRT1) was also produced and should be of similar quality. I have presented figures of the melt curves of the standard and unknown samples (showing only one peak at equivalent temperature for all samples), amplification plots and standard curves in the Appendix (Chapter 11). This is demonstrated for all the genes investigated in all the bone sarcoma cell lines. Ct values were calculated using the equation below (Equation 1). Data was normalised to the housekeeping gene (HPRT1).

$$\Delta CT = Ct(\text{reference gene HPRT1}) - Ct(\text{gene of interest})$$

$$\text{Fold change} = 2^{\Delta CT}$$

Equation 1 – Calculation of ΔCT. Each experiment had 3 technical repeats and experiments were repeated up to 3 times. Results are presented as Mean +/- SEM.

2.4 Flow cytometry

Principle: Flow cytometry measures single cells passing in a stream through a detector system. It is able to distinguish differences in cell size (forward scatter – FSC) and internal complexity (side scatter – SSC) based on angle of light emitted from the analysed cell. Furthermore, cells can be stained with fluorescently labelled antibodies, which can be used to identify cell surface and cytoplasmic antigens. The fluorescent chemical bound to the antibody is known as a fluorophore and it absorbs the laser energy of specific wavelength produced in the flow cytometer and subsequently releases it at a specified wavelength, which is detected by a bandpass filter [173,174].

2.4.1 Cell preparation and staining for flow cytometry

Flow buffer:
500 ml phosphate buffered saline (PBS)
BSA - 0.025 %
EDTA - 2.5 ml of 0.2 mM
Na-Azide - 0.05 %

Cells were harvested using flow buffer, pelleted at 400 g for 7 minutes and resuspended in 50 µl/ [1x10^6 cells in total] in polystyrene round-bottom flow cytometry tubes (5 ml, BD Falcon™). Samples were incubated with 10 µg/ml of human IgG (HuIgG, Native Human IgG, BIO-RAD, 5 mg/ml) for 15-20 minutes for blocking to reduce the degree of non-specific binding. This was followed by staining with a fluorochrome-conjugated primary antibody (Table 9) and incubation for 1 hour in the dark. Cells were then washed, centrifuged and made up in 500 µl of flow buffer for analysis using the BD FACSCanto™ flow cytometry system. A titration was undertaken for each antibody to determine the optimal concentration for staining the desired surface protein. A comparison was carried out between using fixed then stained, stained then fixed or unfixed cells kept on ice. In all conditions tested very similar DR5 surface expressions were obtained for both the TC71 and HT1080 cell line (Section 2.4.1.1). A decision was made to use unfixed cells kept for all following experiments. Isotype controls were used to assess the degree of non-specific binding and to optimise the concentration of human IgG to be used for blocking [175,176]. Using 10 µg/ml of human IgG was found to sufficiently block unspecific antibody binding (Figure

13). Whole blood was taken from healthy volunteers and red cell lysis buffer (BD Pharm Lyse™, Lysing Buffer) was used to lyse red blood cells before staining cells for decoy receptor 2 (DcR2) and also gating on granulocytes, which are DcR2 positive control cells. The LIVE/DEAD™ Fixable Aqua Dead Cell Stain (405 nm excitation) (Thermo Fisher Scientific) was used to help identify dead cells and select the live cells for analysis.

Table 9 – Fluorochrome-conjugated antibodies used in flow cytometry analysis. PE = Phycoerythrin. APC = Allophycocyanin.

Antibody	**Clone**	**Stock concentration**	**Final concentration**	**Fluorochrome**	**Source**
Anti-DR5 (CD262)	DJR2-4(7-8)	200 µg/ml	12 µg/ml	PE	BioLegend
Anti-DR5 (CD262)	DJR2-4(7-8)	200 µg/ml	12 µg/ml	APC	BioLegend
Anti-DR5 isotype control IgG1k	MOPC-21	200 µg/ml	12 µg/ml	PE	BioLegend
Anti-DR4 (CD261)	DJR3	200 µg/ml	12 µg/ml	PE	BioLegend
Anti-DR4 (CD261)	DJR3	200 µg/ml	12 µg/ml	APC	BioLegend
Anti-DR4 isotype control IgG1k	MOPC-21	200 µg/ml	12 µg/ml	PE	BioLegend
Anti-DcR1	DJR3	200 µg/ml	12 µg/ml	PE	BioLegend
Anti-DcR1 isotype control	MOPC-21	200 µg/ml	12 µg/ml	PE	BioLegend
Anti-DcR2	104918	25 µg/ml	1.5 µg/ml	PE	R&D systems
Anti-DcR2 isotype	11711	25 µg/ml	1.5 µg/ml	PE	R&D systems

control IgGk1					
Anti-NG2	LHM-2	10 µg/ml	0.6 µg/ml	APC	R&D systems
Anti-NG2 isotype control	11711	10 µg/ml	0.6 µg/ml	APC	R&D systems
Anti-CD3	UCHT1	50 µg/ml	3 µg/ml	APC	BD Bioscience /Pharmingen
Anti-CD73	AD2	100 µg/ml	6 µg/ml	APC	BioLegend
Anti-CD90	5E10	25 µg/ml	1.5 µg/ml	APC	BioLegend

2.4.1.1 Gating strategy

A gating strategy was employed to select for single cells (i.e., excluding doublets) in the stained bone sarcoma cell population and used consistently throughout the project (Figure 11 and Appendix Section 11.1).

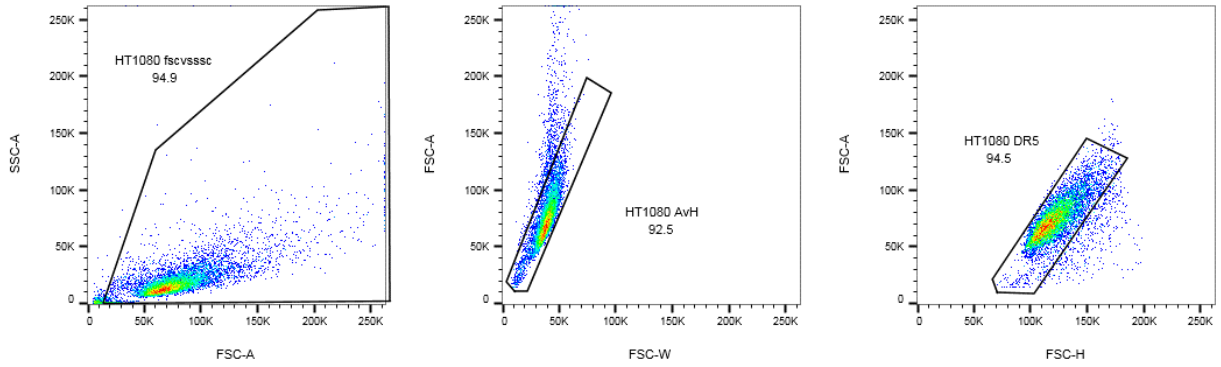

Figure 11- Example of the gating strategy used to select for single cells and exclude the doublets in the HT1080 dedifferentiated chondrosarcoma cells stained for DR5. The following axes were used FSC-A vs SSC-A, FSC-W vs FSC-A (AvH) and FSC-H vs FSC-A (AvW).

2.4.1.2 Use of live cells

An assessment was made using flow cytometry if using live cells or stained then fixed cells produced a different result. Both strategies demonstrated a similar degree of median fluorescence intensity (MFI) histogram shift when gating on the live cells (Figure 12). A decision was made to use unfixed live cells kept on ice and analyse on the same day, or stain then fix the cells if the analysis was going to be delayed (Appendix Section 11.1).

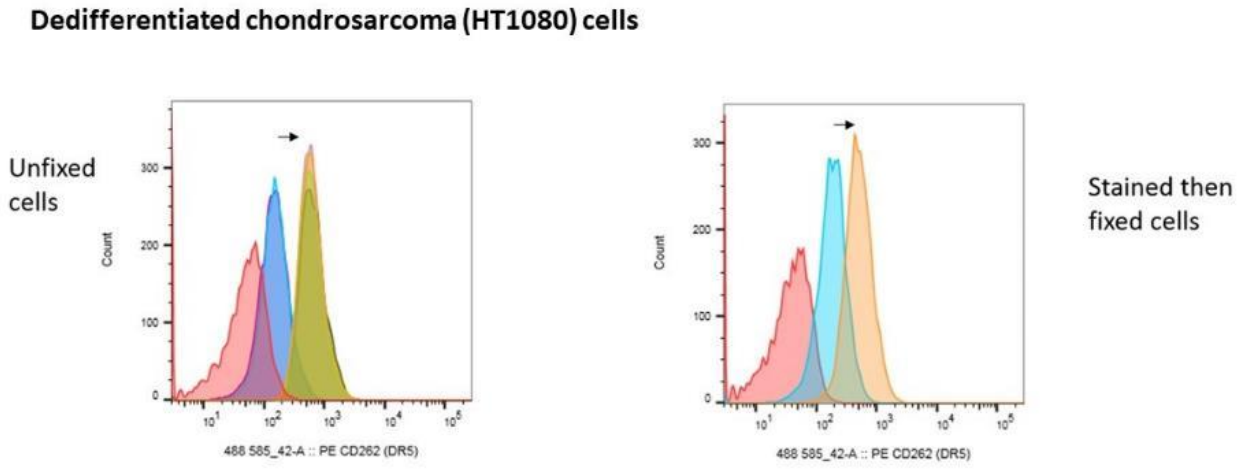

Figure 12 – Flow cytometry assessment of unfixed stained live HT1080 cells vs stained then fixed HT1080 cells. In the presence of 10 µg/ml huIgG. Both methods demonstrate a similar degree of MFI histogram shift in DR5 expression compared to the isotype control. HT1080 = dedifferentiated chondrosarcoma cell line.

2.4.2 Reducing non-specific binding

Use of human IgG blocking agent

An assessment was made using flow cytometry to determine if 10 µg/ml of huIgG would be optimal to reduced non-specific bonding of the primary antibody. The non-specific binding was reduced (and isotype control histogram was found to superimpose the unstained histogram) when a concentration of 10 µg/ml of huIgG blocking agent was used (duration about 15 minutes before staining with primary antibody) and was used for any subsequent experiments (Figure 13). The findings supported the use of isotype control antibody to assess the degree of non-specific binding and the quality of blocking [175,176].

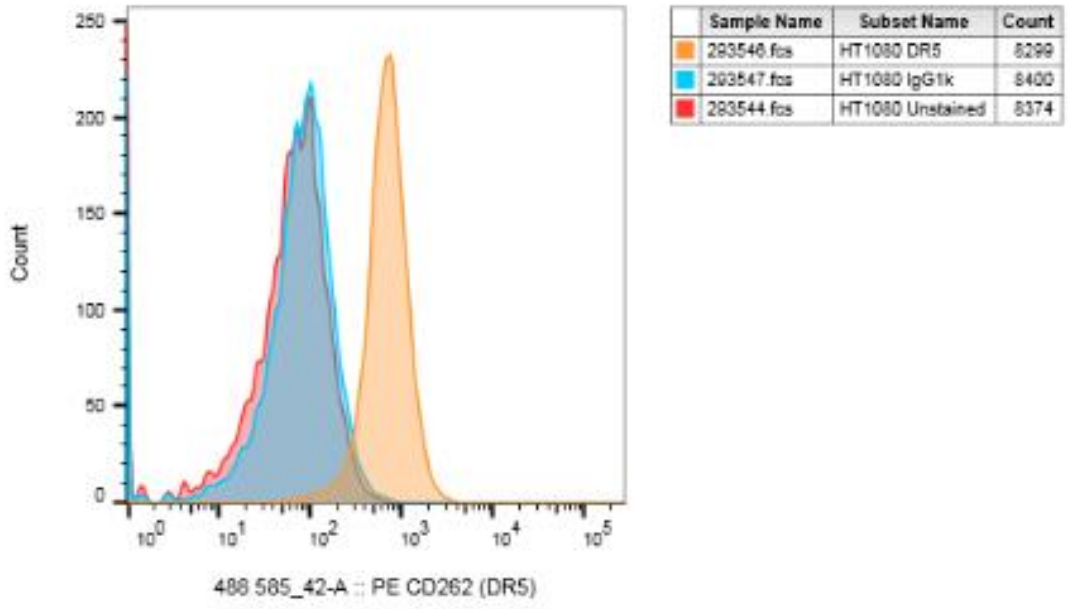

Figure 13 - Flow cytometry assessment of the use of human IgG blocking agent. Non-specific binding was reduced (isotype control histogram BLUE superimposed the unstained histogram RED) when using the concentration of 10 µg/ml of human IgG blocking agent (applied for 15 minutes before staining with the primary antibody) reduced the non-specific binding.

FcR blocking

Non-specific binding to any Fc receptors present can cause erroneous results [175]. An experiment was carried out to compare the degree of flow cytometry histogram shift with or without using an FcR blocking agent (not in the presence of 10 µg/ml huIgG).

Inclusion of FcR blocking (human FcR blocking reagent, Miltenyi Biotec, 20 µl per 10^7 cells) did not influence the degree of non-specific binding when comparing the degree of MFI histogram shift of the isotype control with or without the presence of the FcR blocking agent (Figure 14) indicating that the use of the FcR blocking agent is not necessary and use of huIgG is sufficient.

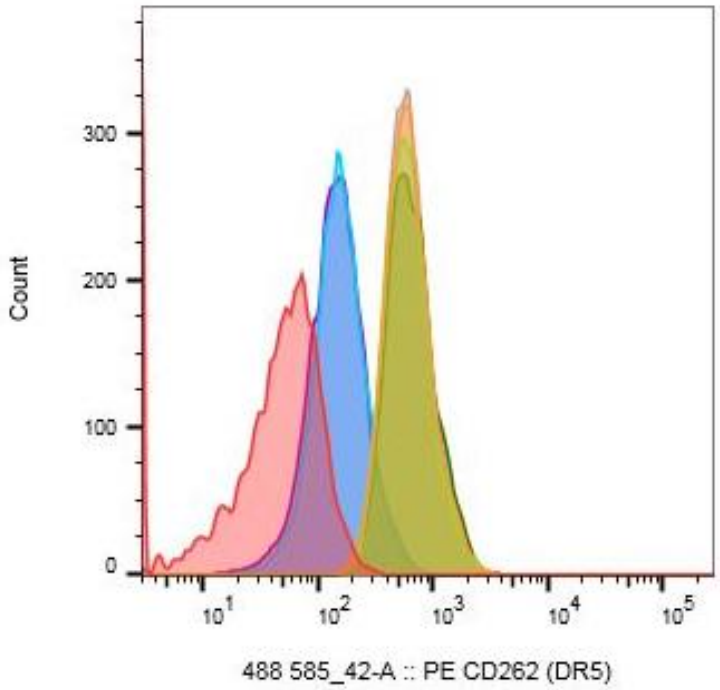

	Sample Name	Subset Name	Count
	264603.fcs	HT1080 cells unblocked and unstained AvW	8540
	264608.fcs	Stained HT1080 cells(1) AvW	8053
	264609.fcs	Stained HT1080 cells(2) AvW	7599
	264610.fcs	Stained HT1080 cells(3) AvW	7451
	264620.fcs	Stained HT1080 cells + FcRb AvW	8002
	264605.fcs	ITC DR5 HT1080 cells AvW	7711
	264607.fcs	ITC + FcRb DR5 HT1080 cells AvW	8141

Figure 14 – Flow cytometry assessment of the use of FcR blocking. Inclusion of FcR blocking (human FcR blocking reagent, Miltenyi Biotec, 20 µl per 10^7 cells) did not decrease the degree of non-specific binding. The isotype control (ITC) histograms in the presence of FcR blocking agent (purple histogram) superimposes the histogram of the isotype control without the presence of the FcR blocking agent (light blue histogram).

Antibody fluorochrome non-specific binding

There may be a preference for the binding of particular fluorochromes (conjugated to an antibody) to antigen receptors or other receptors or interaction partners [177]. Both PE and APC produced similar results and reduced my suspicion that there may be a preferential affinity of the APC or PE fluorochrome with DR5 in the bone sarcoma cell lines (Figure 15).

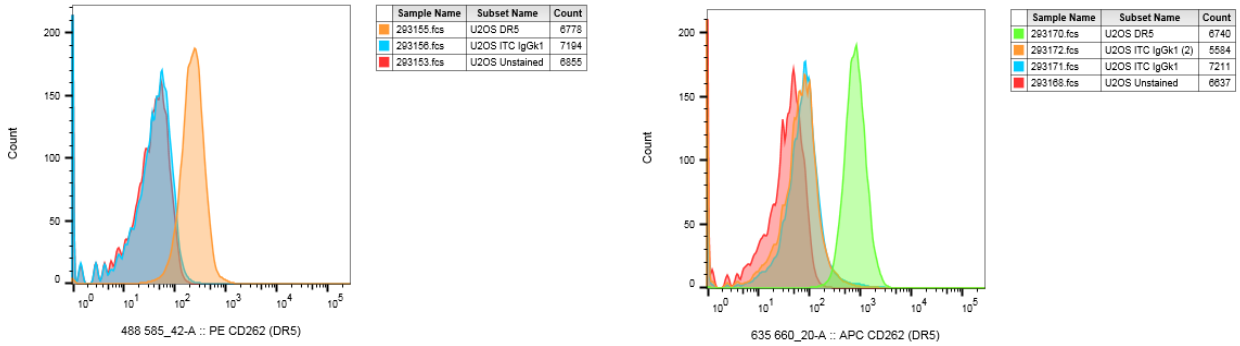

Figure 15 – Flow cytometry assessment of the use of different fluorochromes. A similar degree of shift relative to the isotype control in DR5 surface expression in the U2OS osteosarcoma cell line was demonstrated when using an anti-DR5 antibody either conjugated to the PE or APC fluorophore.

2.4.3 Antibody concentration optimisation for DR4 and DR5 specific antibodies

An assessment was made using flow cytometry of the optimal antibody concentration to use. The degree of shift was similar when using the highest (20 µg/ml) or lowest (4 µg/ml) anti-DR5 primary antibody concentration on the positive control mouse MF DR5-Fas cell line, which expresses human DR5. The antibody used is specific for human DR5 (Figure 16) and does not bind to DR4 (Figure 17).

This was repeated for other positive control cell lines (see below, MF DR4-Fas for DR4, HUVECS for DcR1 and granulocytes for DcR2). For example, 12 µg/ml of anti-DR5 antibody and 10 µg/ml of huIgG for blocking in 50 µl flow buffer was consistently used in experiments.

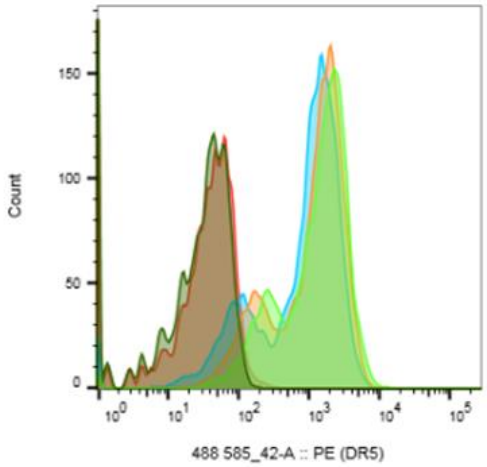

	Sample Name	Subset Name	Count
	257097.fcs	ITC Blocked H+M(5) stained	2134
	257095.fcs	H+M blocked(5) stained(5) MF DR5 Fas cells alive	2615
	257093.fcs	H+M blocked(5) stained(3) MF DR5 Fas cells alive	5641
	257091.fcs	H+M blocked(5) stained(1) MF DR5 Fas cells alive	5912
	257034.fcs	Unstained and unblocked AvW	4816

Figure 16 – Flow cytometry assessment of DR5 positive control cell line and the optimal antibody concentration to use. Titration of the anti-DR5 primary antibody [20 µg/ml (5 = 5 µl in 50 µl flow buffer) vs 12 µg/ml (3 = 3 µl in 50 µl flow buffer) vs 4 µg/ml (1 = 1 µl in 50 µl flow buffer)] used to stain for DR5 in the positive control MF DR5-Fas cell line resulted in similar degrees of histogram shift in the flow cytometry plot. Non-specific binding was reduced when IgG blocking agent [both Human, H and Mouse, M used at 10 µg/ml (5 = 5 µl in 50 µl flow buffer)] as no shift in the Isotype Control (ITC) was observed relative to the unstained control.

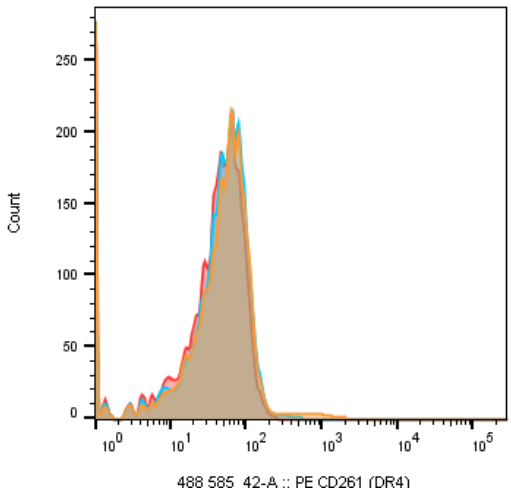

	Sample Name	Subset Name	Count	Median : 488 585_42-A
	294167.fcs	DR4 stained MF DR5 Fas cells AvW	8077	51.8
	294169.fcs	ITC IgG1k MF DR5 Fas cells AvW	8018	48.9
	294166.fcs	MF DR5 Fas cells unstained AvW	7630	43.2

Figure 17 - Flow cytometry assessment of DR5 positive control cell line. The mouse MF DR5-Fas cell line is negative for human DR4 [using anti-DR4 (12 µg/ml)].

Death receptor 4 (DR4)

The MF DR4-Fas cell line was used as the positive control cell line for DR4 using the same staining protocol described above and that the antibody used is specific for DR4 (Figure 18) and does not bind to DR5 (Figure 19).

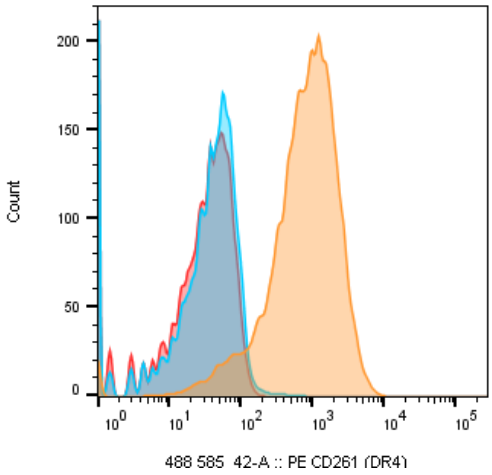

	Sample Name	Subset Name	Count	Median : 488 585_42-A
	294710.fcs	DR4 stained MFDR4 Fas cells AvW	6697	836
	294712.fcs	IgG1k stained MFDR4 Fas cells AvW	7024	34.8
	294709.fcs	Unstained MFDR4 Fas cells AvW	7037	27.6

Figure 18 – Flow cytometry assessment of DR4 positive control cell line. The mouse MF DR4-Fas cell line, which expresses human DR4 is positive for DR4 [using anti-DR4 (12 µg/ml)].

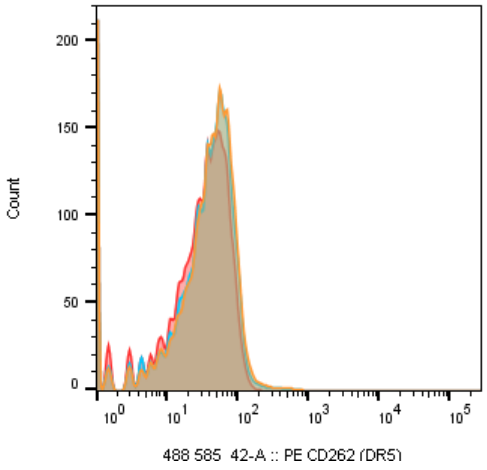

	Sample Name	Subset Name	Count	Median : 488 585_42-A
	294711.fcs	DR5 stained MFDR4 Fas cells AvW	6930	37.7
	294712.fcs	IgG1k stained MFDR4 Fas cells AvW	7024	34.8
	294709.fcs	Unstained MFDR4 Fas cells AvW	7037	27.6

Figure 19 - Flow cytometry assessment of DR4 positive control cell line. The mouse MF DR4-Fas cell line negative for human DR5 [using anti-DR5 (12 µg/ml)].

Decoy receptor 1 (DcR1)

Human umbilical vein endothelial cells (HUVECs) were utilised as the positive control cell line for DcR1 detection [162] and was confirmed that the antibody was specific for DcR1 (Figure 20).

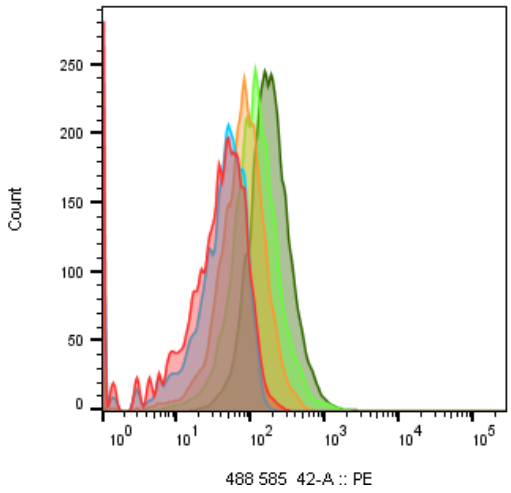

	Sample Name	Subset Name	Count	Median : 488 585_42-A
	311925.fcs	Unstained HUVECs AvW	7331	31.6
	311927.fcs	ITC DcR1 HUVECs AvW	3430	40.4
	311923.fcs	3ul DcR1 HUVECs AvW	4346	76.3
	311914.fcs	5ul DcR1 HUVECs AvW	6696	111
	311915.fcs	10ul DcR1 HUVECs AvW	7739	173

Figure 20 – Flow cytometry assessment of DcR1 positive control cell line. Human umbilical vein endothelial cells (HUVECs) were utilised for this purpose. An increased shift to the right was found with increasing concentration of the anti-DcR1 antibody (3 µl, 5 µl and 10 µl). 3 µl refers to a concentration of 12 µg/ml of anti-DcR1 antibody.

Decoy receptor 2 (DcR2)

The granulocyte fraction of whole blood was utilised as positive control cells for decoy receptor 2 (DcR2) detection (Figure 21). The lymphocyte fraction was utilised as the negative control. The two populations were separated based on the expression of CD3 (Figure 22). The MCF-7 cell breast cancer cell line was a cell line used also as negative control for both DcR1 and DcR2 (Figure 23).

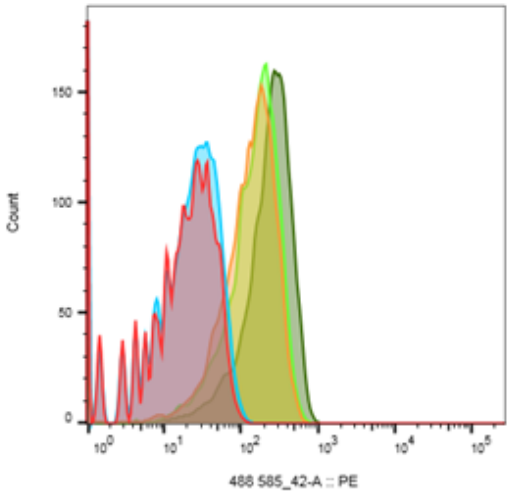

	Sample Name	Subset Name	Count
	309054.fcs	Unstained Granulocyes AvW	10481
	309055.fcs	Isotype control stained Granulocyes AvW	5108
	309056.fcs	3uL DcR2 stained Granulocyes AvW	4879
	309057.fcs	5uL DcR2 stained Granulocyes AvW	5005
	309058.fcs	10uL DcR2 stained Granulocyes AvW	4824

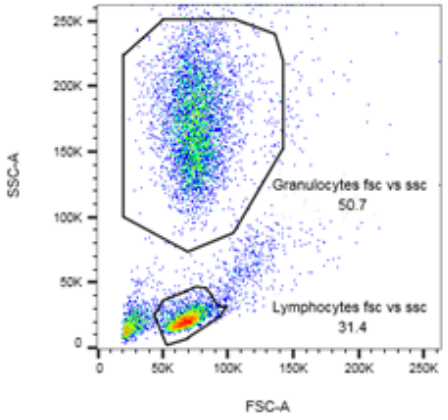

309057.fcs
Ungated
10000

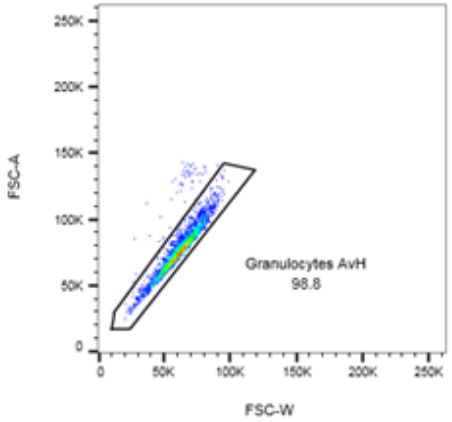

309057.fcs
Granulocytes fsc vs ssc
5075

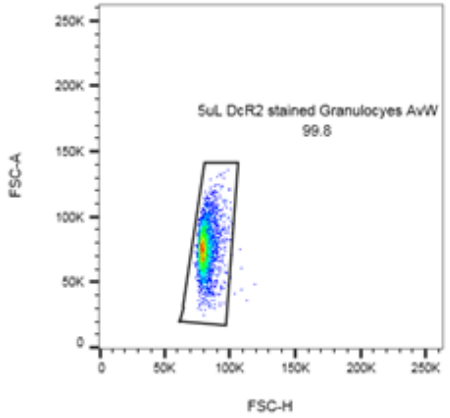

309057.fcs
Granulocytes AvH
5013

Figure 21- Flow cytometry assessment of DcR2 positive control cell line. Granulocytes staining positive for DcR2 (at three different concentrations of DcR2 antibody 0.5 µg/ml, 1.5 µg/ml and 2.5 µg/ml) and lymphocytes staining negative (at the highest concentration of 5 µg/ml).

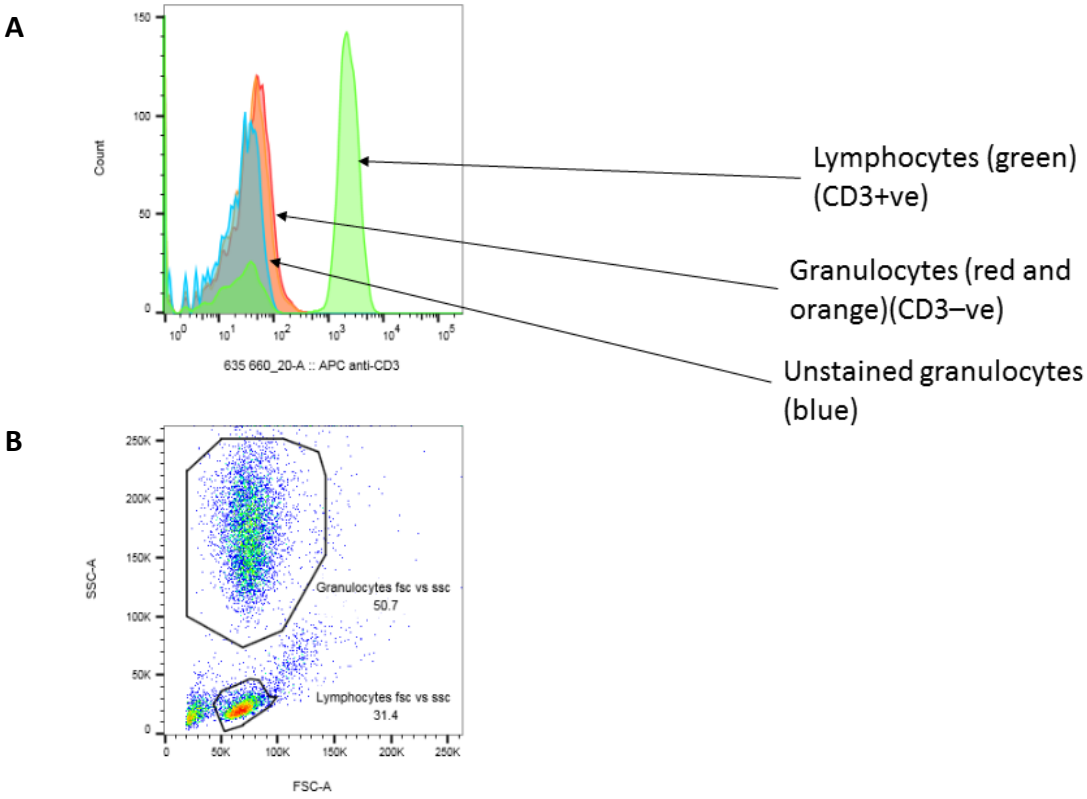

Figure 22 – Flow cytometry gating strategy to separate lymphocyte fraction and granulocyte fraction based on the expression of CD3: (A) The lymphocyte population (green in histogram) was identified by using anti-CD3 Ab. Granulocytes stained negative for CD3 (red and orange in histogram) [Anti-CD3 used at 3 µg/ml]. Unstained granulocytes (blue in histogram). (B) Example of gating strategy for granulocytes in the blood samples analysed.

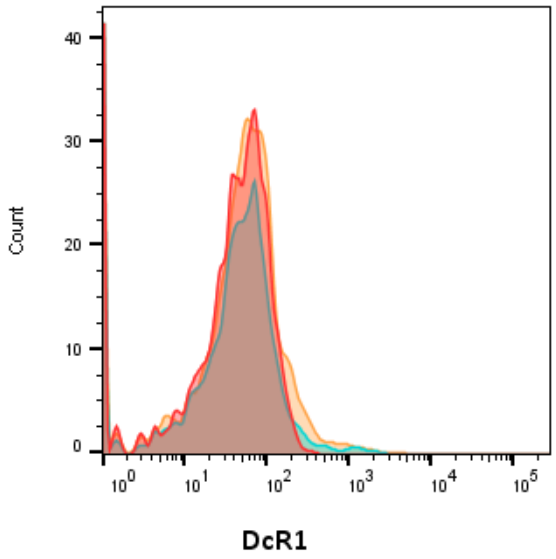

	Sample Name	Subset Name	Count	Median : 488 585_42-A
	302321.fcs	MCF-7 Unstained	3416	42.0
	302324.fcs	IgG1k MCF-7	1765	42.0
	302325.fcs	DcR1 MCF-7	1500	50.7

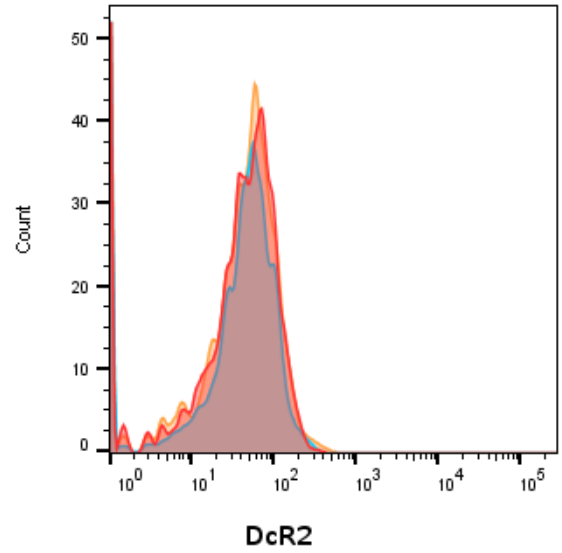

	Sample Name	Subset Name	Count	Median : 488 585_42-A
	302321.fcs	MCF-7 Unstained	3416	42.0
	302328.fcs	IgG1k MCF-7	1132	43.6
	302331.fcs	DcR2 MCF-7	1792	42.0

Figure 23 – Flow cytometry assessment of DcR1 and DcR2 negative control MCF-7 cell line. Flow cytometry demonstrated no significant surface expression of DcR1 or DcR2 in the breast adenocarcinoma MCF-7 cell line. Anti-DcR2 antibody used at 1.5 µg/ml. Anti-DcR1 antibody used at 12 µg/ml.

2.5 ImageStream® analysis

The ImageStream® multispectral imaging flow cytometer was used as a method to visualise the surface protein expression in selected sarcoma cell lines to help support findings from flow cytometry. Samples were prepared as described in Section 2.4.1. Data was analysed using the IDEAS® analysis software package. Image Display Mapping was consistent for all cell lines and set at the following: (X Range Min = 70, Max = 382; Midpoint x = 220, y = 127) and x-axis scale was set at (Min = 65, Max = 387).

2.6 Immunohistochemistry

Cell line blocks were created courtesy of HistoCyte Laboratories Ltd (Neon Building, Quorum Park, Newcastle upon Tyne, NE12 8BU provided contract services to process cells in accordance with their proprietary methods), which contained a number of sarcoma cell lines (Table 10). The cell numbers were processed to make 1 block of 15 multicores. The position of each cell line core within the block is demonstrated below (Figure 24). Slides were prepared from this block and they were stained for DR5 (Monoclonal rabbit anti-DR5, D4E9, Cell Signaling Technology, Cat# 8074, 1:100) using established protocols with aid of Ventana system. Cells were fixed for 2 hours in 10 % neutral buffered formalin and ultimately processed into wax by standard tissue processing protocol. Processing was carried out by cellular pathology at the Royal Victoria Infirmary, Newcastle Hospitals.

Table 10 - Cell lines and numbers for immunohistochemistry. The cell numbers were processed to make 1 block of 15 cores.

Cell Line	**Cell Number**
FADU	~1.5x10^8
MCF7	~1.2x10^8
U2OS	~3.75x10^8

TC71	~1.2x10^8
SW1353	~1.5x10^8
BJAB Lex R	~4.6x10^7
HEP G2	~1.2x10^8
SJSA	~1.35x10^8

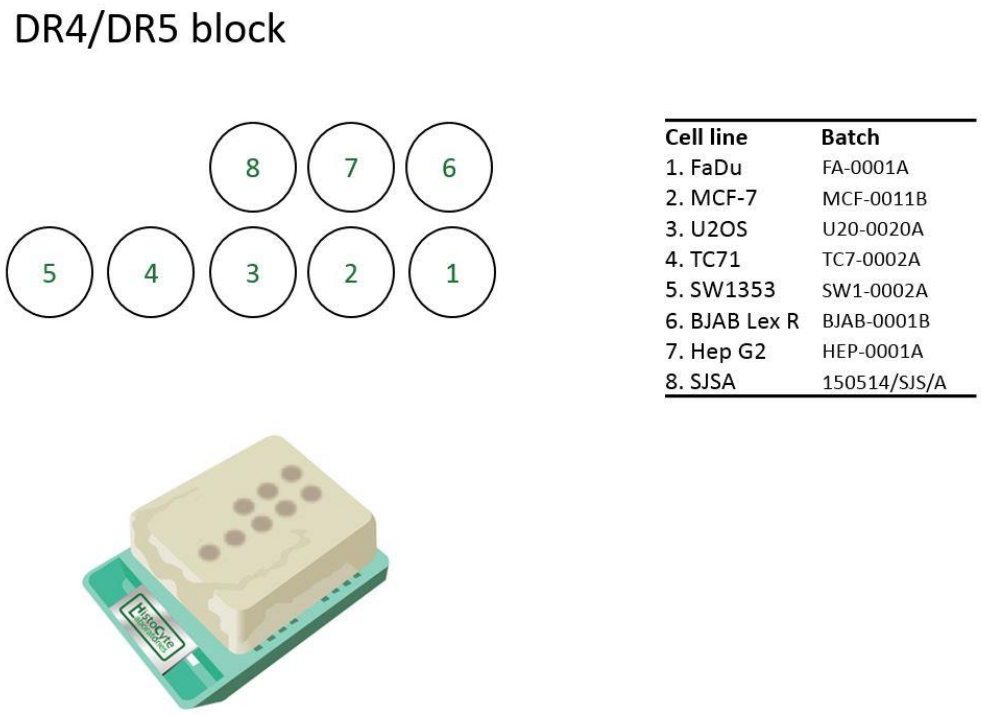

Figure 24 – Example of cell line block created embedded with bone sarcoma cell lines for Immunohistochemistry (IHC) analysis. All cell lines were stained at the same time. Batch numbers are an internal coding method to be able to trace the work that has been performed.

2.7 Western blotting

Principle: This is an important technique in molecular biology which distinguishes a specific protein from a mixture of proteins extracted from cells. Essentially it involves: (1) separation of the proteins by size, (2) transfer to solid membrane, (3) marking the protein of interest using primary and secondary antibodies to visualise the size, degree of expression and number of isoforms on the membrane [178].

2.7.1 Sample preparation

Cell lines grown in 125 mm^2 dishes were harvested by removing media and washing with PBS and then adding 1 ml radioimmunoprecipitation assay (RIPA) buffer (Thermo Fisher Scientific) containing 10 µl Halt™ Protease Inhibitor Cocktail (100X) (Thermo Fisher Scientific). Cells were scraped off and cell lysate collected in an Eppendorf tube on ice. Samples were sonicated using the MSE Soniprep 150 benchtop ultrasonic disintegrator (amplitude 10.0, once for 10 seconds). The samples were then centrifuged (10 minutes at 14000 rpm at 4 °C), the supernatant transferred into a fresh sample tube and used for western blot analysis or stored at -80 °C until analysis.

2.7.2 Subcellular fractionation

This was performed using the Subcellular Protein Fractionation Kit for Cultured Cells from Thermo Fisher Scientific as per protocol (Subcellular Protein Fractionation Kit for Cultured Cells, Cat number:78840). Regent volumes were used according to cell pellet volume. Cytoplasmic (CEB), membrane (MEB) and nuclear (NEB) extraction buffers were used maintaining the volume ratio of CEB:MEB:NEB reagents at 200:200:100 µl, respectively for 20 µl pellet. Briefly, after adding CEB to the cell pellet, samples were incubated at 4 °C for 10 minutes with gentle mixing using a rotator disk. Samples were centrifuged at 500 × g for 5 minutes and supernatant transferred to a tube that was pre-chilled on ice according to the manufacturer's instructions.

To obtain the membrane protein fraction ice-cold MEB containing protease inhibitors were added to the pellets. The tube was then vortexed for 5 seconds on the highest setting and then incubated at 4 °C for 10 minutes with gentle mixing using a rotator

disk. The sample was then centrifuged at 3000 × g for 5 minutes. The supernatant was transferred (membrane extract) to a clean pre-chilled tube on ice.

Finally, to enrich for nuclear proteins, upon addition of protease inhibitors (that contained NEB and were ice-cold) to the pellet, this was then vortexed for 15 seconds at the highest setting according to the manufacturer's instructions. The tube was then incubated at 4 °C for 30 minutes with gentle mixing using a rotator disk. Then centrifuged at 5000 × g for 5 minutes. The supernatant (soluble nuclear extract) fraction was transferred to a clean pre-chilled tube on ice.

2.7.3 BCA protein assay

Principle: Protein concentrations can be evaluated based upon the formation of a colorimetric complex.

Methods: The Pierce™ BCA Protein Assay Kit (Thermo Fisher Scientific) was used to help quantify the concentration of protein in cell lysates. Bovine serum albumin (BSA) standard vial supplied with the kit was used to produce standard curves (20-2000 µg/ml. The BCA working reagent (WR) was prepared as per protocol. 10 µl each of the BSA protein standard dilutions and 10 µl each of RIPA containing samples of unknown concentration (generated as described in 2.7.1 and diluted 1:10 in PBS) were used. The samples were applied in duplicates to a 96-well plate. 200 µl of the WR was added to each well (sample to WR ratio = 1:20), the plate was mixed thoroughly, then covered and incubated at 37 °C for 30 minutes. With the spectrophotometer set to 562 nm, I subsequently measured the absorbance of all the samples within 10 minutes. A standard curve was generated and used to quantify the concentration of the unknown samples (example shown in the Appendix- Chapter 11, Figure 194).

2.7.4 Sodium dodecyl sulphate-polyacrylamide gel electrophoresis (SDS-PAGE)

Principle: SDS-PAGE is an electrophoresis method in which SDS binds to the proteins and makes them all uniformly negatively charged and allows protein separation by mass when they migrate towards the gel towards the positively charged electrode.

Method: Approximately 40 µg of protein was mixed with a tracking dye (Bolt™ LDS Sample Buffer (4X), Life technologies) and a reducing agent (Bolt™ Sample Reducing

Agent (10X) 500 mM dithiothreitol (DTT), Life technologies) according to the manufacturer's instructions. The samples were heated at 100 °C for 10 minutes. Denatured protein samples were separated by electrophoresis. Up to 40 µg of total cell lysate proteins were run on a SDS-PAGE using precast Criterion™ XT Precast Gels/Extended Shelf Life, 4-12 % Bis-Tris or 4–20 % Criterion™ TGX™ Precast Midi Protein Gel, 18 well (BIO-RAD) at 100V (BIO-RAD PowerPac™ Basic Power Supply) with either Bolt™ MES SDS Running Buffer or Tris-Glycine SDS Running buffer respectively (Novex® by life technologies) until they reached the bottom and then electrophoretically transferred to a nitrocellulose membrane 0.45 µm (BIO-RAD). Prestained protein marker was utilised (BIO-RAD Precision plus™ Kaeidoscope™).

2.7.5 Protein transfer and antibody incubations

Proteins were transferred onto a nitrocellulose membrane using the BIO-RAD Blot module with aid of Criterion™ blotter filter paper (BIO-RAD) and Tris-Glycine buffer (BIO-RAD).

Membranes were then blocked for 1 hour at room temperature using 5 % dry milk (Marvel Dried Milk) in Tris-buffered saline (TBS). After the blocking step, the membranes were incubated overnight at 4 °C with primary antibodies diluted in TBS, 0.1 % tween (TWEEN®20, Sigma Aldrich) and 5 % BSA (or according to specific manufacturer's instructions).

The membranes were washed with TBS with 0.1 % tween (TBST) three times for 5 minutes each at room temperature and incubated with secondary antibodies, which were diluted in 5 % milk blocking buffer (1 in 1000) for 1 hour at room temperature. After secondary antibody incubation, the membranes were washed with TBST three times and developed using the Clarity™ Western ECL Substrate (BIO-RAD). Membranes were analysed using the BIO-RAD ChemiDoc™ MP Imaging System.

2.7.6 Antibodies

The antibodies utilised are presented (Table 11). Further details on the antibodies used and rationale is given in Appendix Section 11.2.

Table 11 - Primary and secondary antibodies used for western blotting. Abbreviations, aa = amino acid.

Antibodies	Clone	Source	Dilution	Identifier	Immunogen
Primary					
Monoclonal rabbit anti-DR5	EPR1659(2)	Abcam Recombinant Antibodies	1:10000 to 1:50000	Cat# ab181846	aa 426 to 440
Monoclonal rabbit anti-DR5	D4E9	Cell Signaling Technology	1:1000	Cat# 8074	residues surrounding Arg260
Monoclonal mouse anti-DR4	32A242	Abcam	1:500	Cat# ab13890	aa 1-20
Monoclonal rabbit anti-DR4	D9S1R	Cell Signaling Technology	1:1000	Cat# 42533	carboxy terminal, cytoplasmic domain of human DR4
Polyclonal rabbit anti-DR5	N/A	Abcam	1:500	Cat# ab8416	aa 388-407
Polyclonal rabbit anti-DR4	N/A	Abcam	1:500 to 1:1000	Cat# ab8414	aa 450-468
Monoclonal rabbit anti- human TRAIL	C92B9	Cell Signaling Technology	1:1000	Cat# 3219	residues surrounding Lys60
Monoclonal rabbit anti-GAPDH	D16H11	Cell Signaling Technology	1:1000	Cat# 5174	residues near the carboxy terminus of human GAPDH
Monoclonal mouse anti-GAPDH	D4C6R	Cell Signaling Technology	1:1000	Cat# 97166	residues near the amino terminus of human GAPDH
Monoclonal mouse anti-lamin A/C	4C11	Cell Signaling Technology	1:2000	Cat# 4777	Immunisation of a recombinant fragment of human lamin A protein
Secondary					
Polyclonal Goat Anti-Mouse Immunoglobulins/ HRP	N/A	Agilent Dako	1:1000	Ref: P0447	-
Polyclonal Goat Anti-Rabbit Immunoglobulins/ HRP	N/A	Agilent Dako	1:1000	Ref: P0448	-

2.7.7 Stripping of membranes

Stripping buffer was used (Restore™ PLUS Western Blot Stripping Buffer, Thermo Fisher Scientific) to strip most high-affinity antigen-antibody interactions and enable reuse of the membranes to stain for other proteins of interest. Membranes were incubated in the stripping buffer for 15 minutes at room temperature, thoroughly washed with TBS with 0.1 % tween (TBST) and then blocked for 1 hour using 5 % dry milk (Marvel Dried Milk) in Tris-buffered saline (TBS) and incubation with another primary antibody of interest.

2.8 Cell proliferation assays

2.8.1 CKK-8 cell proliferation assay

Principle: Resazurin-based and tetrazolium-based assays use the reducing power of living cells to measure the cell proliferation. However, proliferation assay sensitivities can differ with regards to the cell numbers present and this is evaluated further (see Appendix 11.3).

Method: The Wst-8 tetrazolium-based assay, Cell Counting Kit-8 (CCK-8) (Dojindo EU GmbH), was used to assess the cytotoxic effects of TRAIL ligands on bone sarcoma cell lines. It is reduced by dehydrogenase activity in cells to give a yellow coloured formazan appearance, which can be measured using a spectrophotometer. The benefits of Wst-8 include less toxicity, efficiently reduced by dehydrogenases, highly sensitive and that it shows faster colour development compared to comparable salts [179].

The BMG Labtech FLUOstar® Omega plate reader was used to measure absorbance at 488 nm and the survival rate (%) was calculated using the values as per manufacturer's instructions [180] according to Equation 2:

$$\text{Survival rate (\%)} = \frac{A_{\text{sample}} - A_b}{A_c - A_b} \times 100$$

Equation 2 - A_{sample} = absorbance sample A_b = absorbance blank, A_c = absorbance negative control.

2.8.2 Analysis of assay efficiency

A Z'-factor score [(1 – AVR (assay variability ratio)] can be calculated to determine the efficiency of an assay [181] [182]. Also described here: https://www.graphpad.com/support/faq/calculating-a-z-factor-to-assess-the-quality-of-a-screening-assay/[183].

Z'-factor is calculated as follows:

$$Z'factor = 1 - \frac{3 \times (\sigma_p + \sigma_n)}{|\mu_p - \mu_n|}$$

Equation 3 – Z' factor equation

Where:

σ_p is the standard deviation of the positive control (staurosporine treated cells)

σ_n is the standard deviation of the negative controls (untreated cells or vehicle only)

μ_p is the mean of the positive control (staurosporine treated cells)

μ_n is the mean of the negative control (untreated cells or vehicle only)

The value should be above 0.5

Table 12 from Iverson *et al.,* 2006 [181] provides further details about the interpretation of the value:

Table 12 – Z'-factor interpretation

Z-factor	Interpretation
1.0	Ideal. Z-factors can never exceed 1.
between 0.5 and 1.0	An excellent assay.
between 0 and 0.5	A marginal assay.
less than 0	There is too much overlap between the positive and negative controls for the assay to be useful.

Assays were undertaken in a 96-well plate. All wells on the periphery were filled with PBS. The position of the plate in the incubator can also influence the results obtained due to differing effects on samples that are placed in the periphery. As a test, 6 wells with staurosporine treated cells and 6 with untreated cells at contralateral sides was used to examine for this. A graph was plotted to assess for differences in results between the positive and negative controls in the peripheral wells for the position in the incubator chosen and no significant differences were observed (Figure 25).

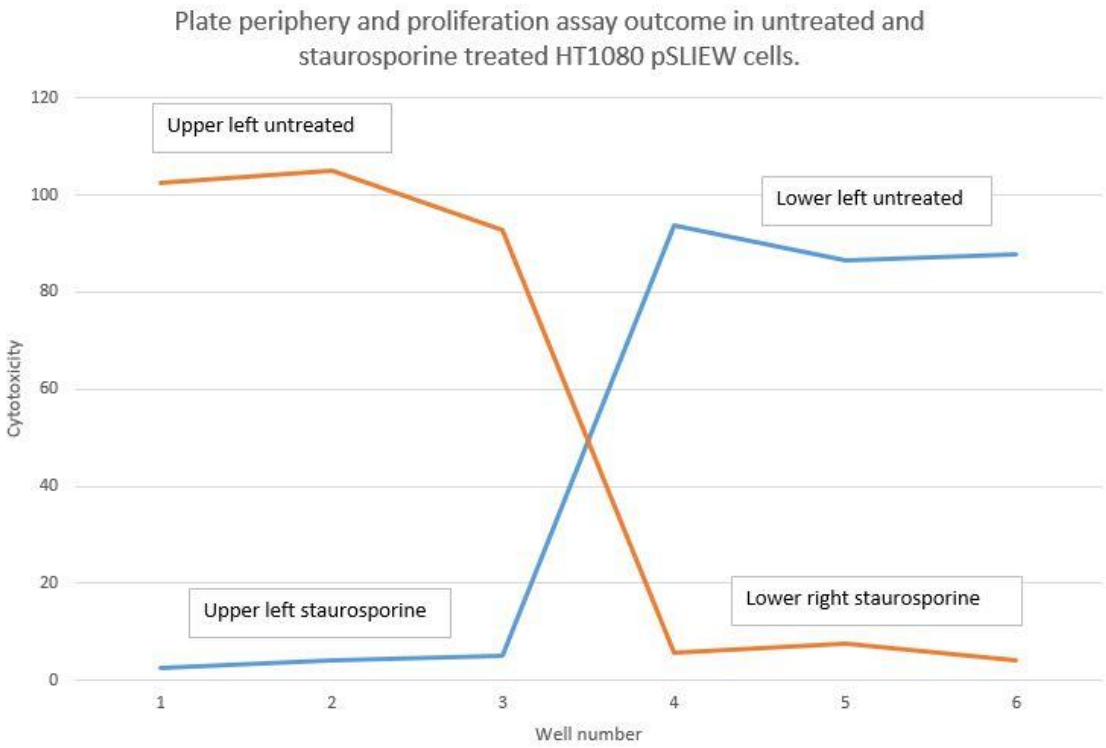

Figure 25 – Proliferation assay outcome [cytotoxicity (%)] for untreated and staurosporine treated HT1080 cells in the periphery of the 96-well plate at location of plate chosen within the incubator.

2.8.3 Assessment of the quality and performance of screening of cytotoxicity assays for crosslinked vs non-crosslinked forms of TRAIL and other agents

Throughout the PhD project, cells were seeded into 96-well plates and treated with different forms of TRAIL and other chemotherapeutic or sensitising agents. An example 96-well plate setup and example absorbance values for HT1080 cell line is demonstrated (Figure 26) followed by a Z' factor calculation (Equation 4):

0.04	0.06	0.07	0.06	0.06	0.06	0.05	0.05	0.18	0.18	0.18	0.09
0.09	1.59	1.75	1.85	1.90	1.79	1.77	1.71	1.54	1.52	1.21	0.05
0.08	1.28	1.51	1.51	1.51	0.27	0.25	0.23	0.23	0.22	0.19	0.03
0.06	1.31	1.46	1.53	1.51	1.48	1.52	1.59	1.43	1.51	1.09	0.05
0.10	1.33	1.42	1.49	1.40	1.45	1.37	1.41	1.36	1.25	1.17	0.04
0.08	1.43	1.56	1.56	1.58	1.53	1.60	1.67	1.58	1.28	0.84	0.04
0.14	1.37	1.55	1.61	1.63	1.60	1.47	1.54	1.52	1.36	0.87	0.05
0.10	0.09	0.08	0.07	0.07	0.06	0.06	0.05	0.05	0.05	0.05	0.04

Background - No cells

Yellow – PBS filled wells

Light blue – Untreated samples

Red – Staurosporine treated (1 µM)

Blue – FLAG TRAIL with M2 antibody (0.5 µg/ml) (x 2 technical repeats - highest concentration on the right)

Olive – SuperKillerTRAIL (x 2 technical repeats - highest concentration on the right)

Purple – His TRAIL (x 2 technical repeats - highest concentration at the top)

Turquoise – FLAG TRAIL without M2 antibody (x 2 technical repeats - highest concentration at the top)

Figure 26 – Example 96-well plate setup with TRAIL treated, staurosporine treated and untreated columns. The numbers indicate absorbance values.

Z' factor calculation using the values from Figure 26

Mean Untreated (negative control) = 1.6 Standard deviation Untreated = 0.22

Mean Staurosporine (positive control) = 0.26 Standard deviation Staurosporine = 0.03

$$Z'factor = 1 - \frac{3 \times (\sigma_p + \sigma_n)}{|\mu_p - \mu_n|}$$

Equation 4 – Z' factor calculation: AVR (Assay Variance Ratio) = 0.6 therefore 1-AVR (Z-factor) = 0.4 using the absorbance values in Figure 26.

Calculation of survival rate from absorbance values

Survival rate was calculated by using Equation 5 as per cck-8 proliferation protocol - values in percentage %) (Figure 27) [180]:

$$\text{Survival rate (\%)} = \frac{A_{\text{sample}} - A_b}{A_c - A_b} \times 100$$

Equation 5 – Calculation of survival rate using absorbance values

A_b = absorbance background

A_c = absorbance control

	100	111	119	108	92	95	100	89	94	64	
	78	94	94	84	90	84	87	83	76	70	
	80	91	96	83	95	100	106	99	78	47	
	81	88	93	76	100	91	96	95	84	49	

Figure 27 – Example of survival rate (%) in each well calculated using the values from Figure 74.

2.8.4 Analysis of the mechanism of cell death

Caspase-3 activity was assessed using the NucView 488 Caspase-3 Assay Kit for Live Cells (Biotium).

Principle: NucView® 488 Caspase-3 substrate enters the cell and is cleaved by caspase-3 to from a dye that binds DNA and stains the nucleus bright green.

Nucview: NucView® 488 Caspase-3 substrate, 0.2 mM in DMSO (125 µl) was diluted in 5 ml media and 50 µl was added to each well of 96-well plate containing bone sarcoma TRAIL treated cells.

Effects of caspase inhibition were studied using the cell permeable and irreversible pan caspase inhibitor z-Val-Ala-Asp-fluoromethylketone (Z-VAD-FMK) (BioVision) and the reversible caspase-3 inhibitor Ac-DEVD-CHO contained within the NucView® 488 Caspase-3 Assay Kit (Biotium). Necrostatin (RIP1 Inhibitor II, NecS1, Calbiochem) was used to study the effects of inhibiting necroptosis.

2.8.5 IncuCyte® live-cell imaging

Principle: This system allows real-time assessment of confluency and performance of cytotoxicity assays within an incubator. This was used to assess cell proliferation over a time course and the cytotoxic effects of different forms of TRAIL with or without other agents on the cell lines. IncuCyte images and measurements can be performed several times as specified in a 24-hour period and data extracted and analysed using the IncuCyte® Zoom software (Essen BioScience®).

The cell number allowing optimal cell growth over at least 4 days was evaluated and revealed that cell numbers less than 2000 cells per well in each well of a 96-well to be sufficient to be able to evaluate the effects of therapy on the exponential phase of cell growth for an osteosarcoma cell line (U2OS), Ewing's sarcoma cell line (TC71), chondrosarcoma cell line (SW1353) and a dedifferentiated chondrosarcoma cell line (HT1080). It also appeared that the rate of growth of the TC71 cells was the greatest, with about 20 % increase in confluence by 80 hours compared to 10 % for the U2OS and SW1353 cell lines. The well confluency percentage was normalised to the confluency at time point zero when assessing data obtained (please see Appendix Section 11.4).

2.8.6 Graph production and statistics

Graphs were produced with the aid of Microsoft® Excel® 2016 and GraphPad Prism 7 - for Windows. Statistics and calculation of IC50 values were carried out using GraphPad Prism 7 - for Windows and IBM SPSS Statistics®.

2.8.7 siRNA knockdown of DR4, DR5, DcR2 and NG2

Principle: Double stranded siRNAs are unwounded into single strands when introduced (the leading and the lagging strands) the lagging strand is degraded; however, the leading strand binds to a protein complex known as the RNA-induced silencing complex (RISC). When the RNA loaded RISC comes into contact with its complementary strand (target gene mRNA transcript), base pairing occurs which activates a cleavage mechanism catalysed by a member of the Argonaute protein family. The cleavage of the target mRNA transcript renders it untranslatable and the particular protein synthesis is downregulated [184,185].

Methods: The siRNA sequences (sense and antisense) (Sigma Aldrich) used to knockdown the transcripts of my gene of interest are presented (Table 13). They have been used and validated before and the target location and the siRNA-targeted isoforms were all checked using http://projects.insilico.us/SpliceCenter/PrimerCheck to check that the isoforms of interest were targeted. Bone sarcoma cells were cultured in a 6-well plate to approximately 60-70 % confluency in 1750 µl of cell culture medium. 250 µl of cell culture medium with no FBS (basal medium) was used with 2 µl of Lipofectamine® RNAiMAX Transfection Reagent (Thermo Fisher Scientific) and siRNA to achieve a final concentration of 100 nM of siRNA. Time course experiments revealed that 72 hours is an optimal time period to achieve knockdown in the cell lines investigated. The degree of surface protein knockdown was evaluated using flow cytometry, as used in previous studies for the assessment of the efficacy of siRNA [186].

Table 13 -siRNA sequences to achieve knockdown of selected targets.

Gene of interest	**Sense/complimentary**	**Antisense/reverse complimentary**
DR4	5’-CAGGAACUUUCCGGAAUGACA-3’	5’-UGUCAUUCCGGAAAGUUCCUG-3’

DR5	5’-GCAAGUCUUUACUGUGGAA-3’	5’- UUCCACAGUAAAGACUUGC -3’
DcR2	5’-GGAUGGUCAAGGUCAGUAA-3’	5’UUACUGACCUUGACCAUCC-3’
NG2	5’-GUGGACCAGUACCCUACGG-3’	5’- CCGUAGGGUACUGGUCCAC-3’
Scrambled/non-targeting	5’-CCTACCAGGGAATTTAAGAGTGTAT-3’	5’- AUACACUCUUAAAUUCCCUGGUAGG-3’

Greater than 70 % DR5 knockdown (KD) could be successfully achieved in the SJSA-1 and U2OS osteosarcoma cell lines. Greater than 70 % DR4 KD could be achieved in the TC71 Ewing’s sarcoma cell line. Greater than 70 % DcR2 KD in the SJSA-1 osteosarcoma cell line. Greater than 70 % NG2 KD was achieved in both the U2OS osteosarcoma and SW1353 chondrosarcoma cell lines (Sections 5.2 and 7.7).

2.8.8 Clustered regularly interspaced short palindromic repeats (CRISPR) knockout of DR5 in HT1080 dedifferentiated chondrosarcoma and SW1353 chondrosarcoma cell lines

Principle: As stated by Ran *et al*. (2013) genome engineering technologies ‘include zinc-finger nucleases (ZFNs), transcription activator-like effector nucleases (TALENs) and the RNA-guided CRISPR-Cas nuclease system’. CRIPSR-Cas is utilised by bacteria to cleave foreign genetic elements. Cas9 is a nuclease guided by small RNAs via base pairing with the target DNA. Cas9 stimulates a double strand break (DSB) at the target locus and the repair process can either be ‘through non-homologous end joining (NHEJ), or homologous directed repair (HDR)’ as stated in a protocol by Ran *et al*. (2013). NHEJ can mediate gene knockouts via indels that occur within the coding exon resulting in frameshift mutations and premature stop codons. HDR occurs at lower frequency and can be used to generate a defined modification in the presence of a repair template [187].

The Cas9 can either be delivered as gRNA or protein. The guide RNA (gRNA) directs the Cas9 to the desired site in the genome for editing. I selected gRNAs to enable knockout of the DR5 gene. Selection of gRNA was carried out using the Thermo Fisher GeneArt

CRISPR Search and Design Tool (https://www.thermofisher.com/uk/en/home/life-science/genome-editing/geneart-crispr/geneart-crispr-search-and-design-tool.html) (Figure 28).

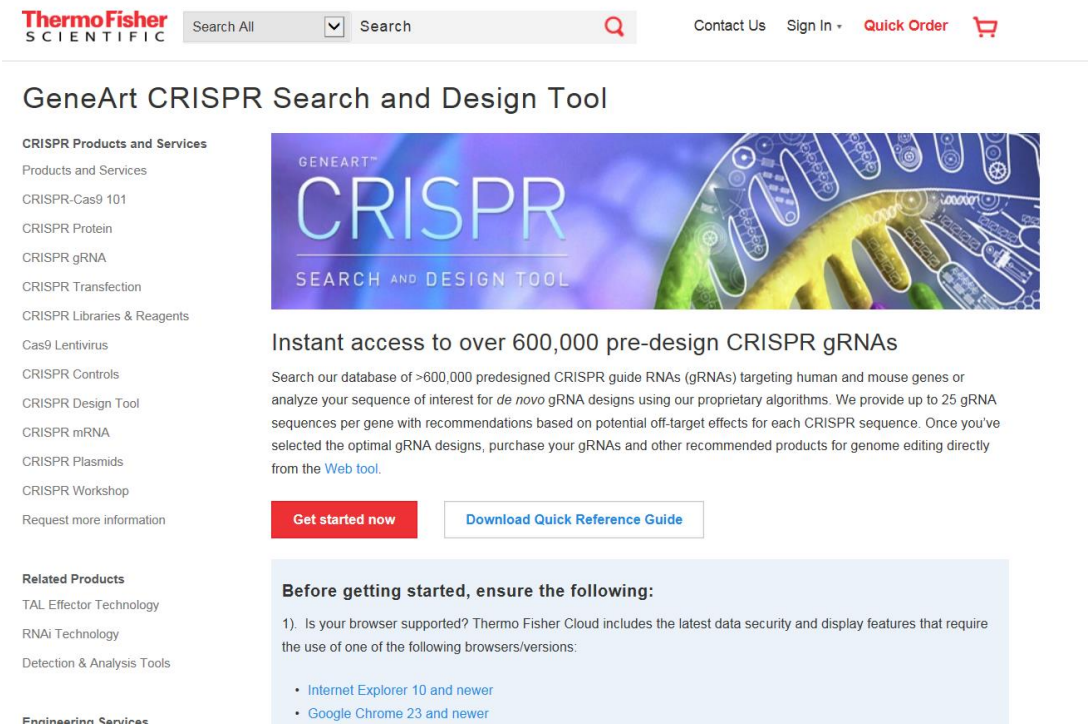

Figure 28 – Thermo Fisher GeneArt CRISPR Search and Design Tool (https://www.thermofisher.com/uk/en/home/life-science/genome-editing/geneart-crispr/geneart-crispr-search-and-design-tool.html).

The following reagents, primers and equipment were utilised as part of the CRISPR workflow to knockout human DR5. Human HPRT1 was used as a control:

In vitro transcription (IVT) primers:

IVT-TNFRSF10B-gRNA-T1-fwd
TAATACGACTCACTATAGGACAACGAGCACAAGG
IVT-TNFRSF10B-gRNA-T1-rev
TTCTAGCTCTAAAACAGACCCTTGTGCTCGTTGT

Genome cleavage detection (GCD) kit primers:

GCD-Set1-TNFRSF10B-gRNA-T1-fwd

AAGGAAGGGAGGGAAAGAAAGG

GCD-Set1-TNFRSF10B-gRNA-T1-rev

TACACCGACGATGCCCGAT

GeneArt™ Platinum™ Cas9 Nuclease (1 µg/µl); GeneArt™ CRISPR Nuclease mRNA (15 µg). Lipofectamine™ CRISPRMAX™ Cas9 Transfection Reagent; GeneArt™ Precision gRNA Synthesis Kit; Lipofectamine™ MessengerMAX™; Opti-MEM™, Reduced Serum Medium; E-Gel™ iBase™ and E-Gel™ Safe Imager™ Combo Kit (UK only) to be used with E-GEL EX GELS; 2 %. Qubit™ RNA BR Assay Kit; RNA Century(TM)-Plus Markers; RNA Loading Dye; E-GEL 1 KB Plus DNA Ladder.

The GeneArt™ Genome Cleavage Detection (GCD) kit (Thermo Fisher Scientific) is a semi-quantitative DNA mismatch detection assay. The kit is used to detect heterozygous mutations and determine the efficiency of the editing process and works on the following principles:

1. gDNA extraction (depends on product used) and PCR-amplification of the target region
2. Denature dsDNA amplicons
3. Re-annealing, with mutant and wild-type duplex formation
4. Enzymatic cleavage of heteroduplex dsDNA
5. DNA electrophoresis
6. Band densitometry to measure efficiency

gRNA synthesis

Procedure:

Part 1 – PCR Assembly of *In vitro* Transcription Template (1 hour)

Prepare a 0.3 µM solution of PCR primers for each gene target and the positive control as listed below (Table 14).

Table 14 – Primers used to produce gRNA to target desired gene.

Component	**Kit Positive Control (HPRT1)**	**Target 1 TNFRSF10B (DR5)**
10 µM Target-specific Oligo mix, Fwd + Rev Primers	3.3 µl	3.3 µl
Nuclease-free water	96.7 µl	96.7 µl
Total	**100 µl**	**100 µl**

Transfection procedure

The following protocol presented gives information on transfection procedure and plate setup with use of appropriate controls.

1. Remove old media & add 0.5 ml fresh media from the individual wells in a 24-well plate. Cells were seeded at 1x10^5. Cell confluency was 60-70 % at time of transfection.
2. Obtain 7 sterile Eppendorf tubes, the specific gRNA, Opti-MEM I Medium, Cas9 mRNA, and Lipofectamine MessengerMAX reagent.
3. To the first tube, add Opti MEM I medium and Lipofectamine MessengerMAX Reagent as indicated in the table below (Table 15).

Table 15 - Lipofectamine and basal media quantity for transfection of **Cas9 mRNA–gRNA complex or Cas9 protein–gRNA complex**. Cas9 mRNA was used for KO of DR5.

	Tube 1 Lipid Dilution	**Tube 2** Lipid Dilution
Lipofectamine MessengerMAX reagent (for mRNA)	13.2 µl	0
Lipofectamine CRISPRMAX (for protein)	0	6.6 µl
Opti-MEM medium	220 µl	110 µl

4. After adding both components, mix well by vortexing and incubate at room temperature for at least 5 minutes.
5. In the other 5 sterile tubes, prepare the dilutions of each reagent in Opti-MEM I medium as listed in the table below (Table 16).

Table 16 - Constituents of tubes for Cas9 mRNA or Cas9 protein with gRNA to form the **Cas9 mRNA–gRNA complex or Cas9 protein–gRNA complex** respectively for individual wells including use of appropriate control samples.

Volumes are for 4/2/2/2/2 reactions	**Tube 1** Cas9 (mRNA) + gRNA1	**Tube 2** gRNA1 Only Control	**Tube 3** Cas9 mRNA Only Ctrl
Opti-MEM I	100 µl	50 µl	50 µl
Cas9 Nuclease mRNA	2 µl (1 µg)	0	1 µl (1 µg)
Cas9 Nuclease protein	0	0	0
gRNA	2.5 µl (250 ng)	1.25 µl (250 ng)	0
Plus reagent (for protein)	0	0	0

6. After mixing together the above components, vortex each tube briefly to mix.
7. Add diluted MessengerMAX Reagent from Tube 1 to each of the other vials as listed below (Table 17).

Table 17 - Combination of Cas9 **mRNA–gRNA complex or Cas9 protein–gRNA complex** with transfection reagent.

*** Volumes are for 4/4/2/2 reactions**	**Tube 1** Cas9 (mRNA) + gRNA1	**Tube 2** gRNA1 Only Control	**Tube 3** Cas9 mRNA Only Ctrl
Tube 1, Diluted Lipofectamine MessengerMAX reagent	100 µl	50 µl	50 µl
Tube 2, Diluted Lipofectamine CRISPRMAX reagent	0	0	0

8. Mix gently by pipetting up and down or tapping the tube with your finger. Vortexing not recommended here.
9. Incubate all tubes at room temperature for 10–15 minutes. The CRISPR/lipid complexes form in this step.
10. Add 50 µl from the appropriate tube to each well of the 24-well plate already containing 0.5 ml media. After each addition, swirl the media very gently over the cells to mix.
11. Incubate the cells in a humidified 37 °C, 5 % CO2 incubator for 40-48 hours.

Genome cleavage detection assay

Genome cleavage detection (GCD) assay assessment of DR5 gRNA editing efficiency

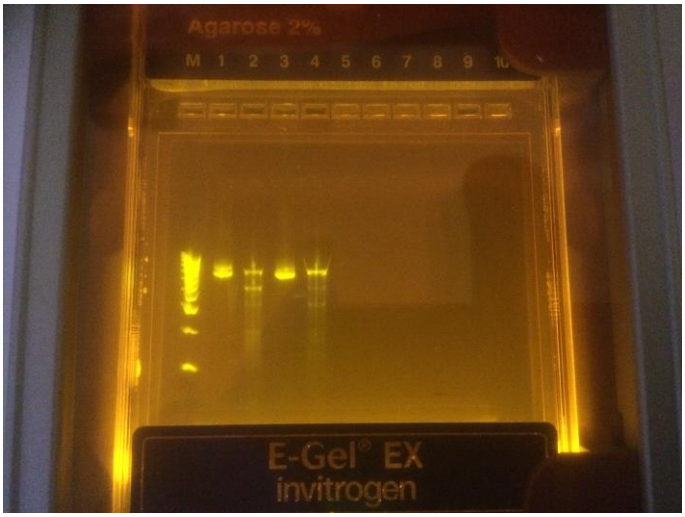

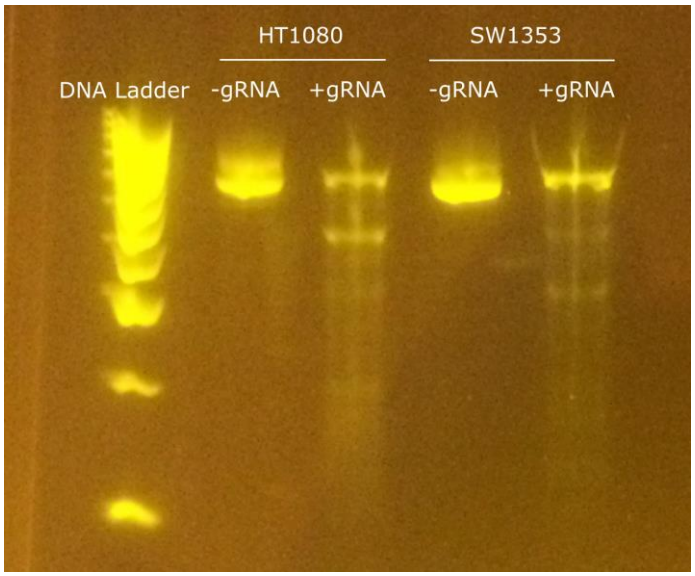

Figure 29 – GCD assay and DNA electrophoresis (using E-Gel® EX Invitrogen system, 2 % agarose) to confirm presence of cleaved DNA products and degree of efficiency of editing in cell lines with an indel created by CRISPR Cas9. (a) DNA ladder, (b) HT1080 no gRNA (-gRNA), (b) HT1080 plus gRNA (+gRNA), (c) SW1353 no gRNA (-gRNA), (d) SW1353 plus gRNA (+gRNA). On inspection, there is about 50 % efficiency indicated by the top band in lanes (c) and (e) in relation to the bands in (b) and (d) respectively.

SW1353 DR5 CRISPR KO negative population selection using FACS

The DR5-ve SW1353 population of interest was defined and sorted using fluorescence-activated cell sorting (FACS) (Figure 30). The cells were seeded into a 6-well plate and cultured further.

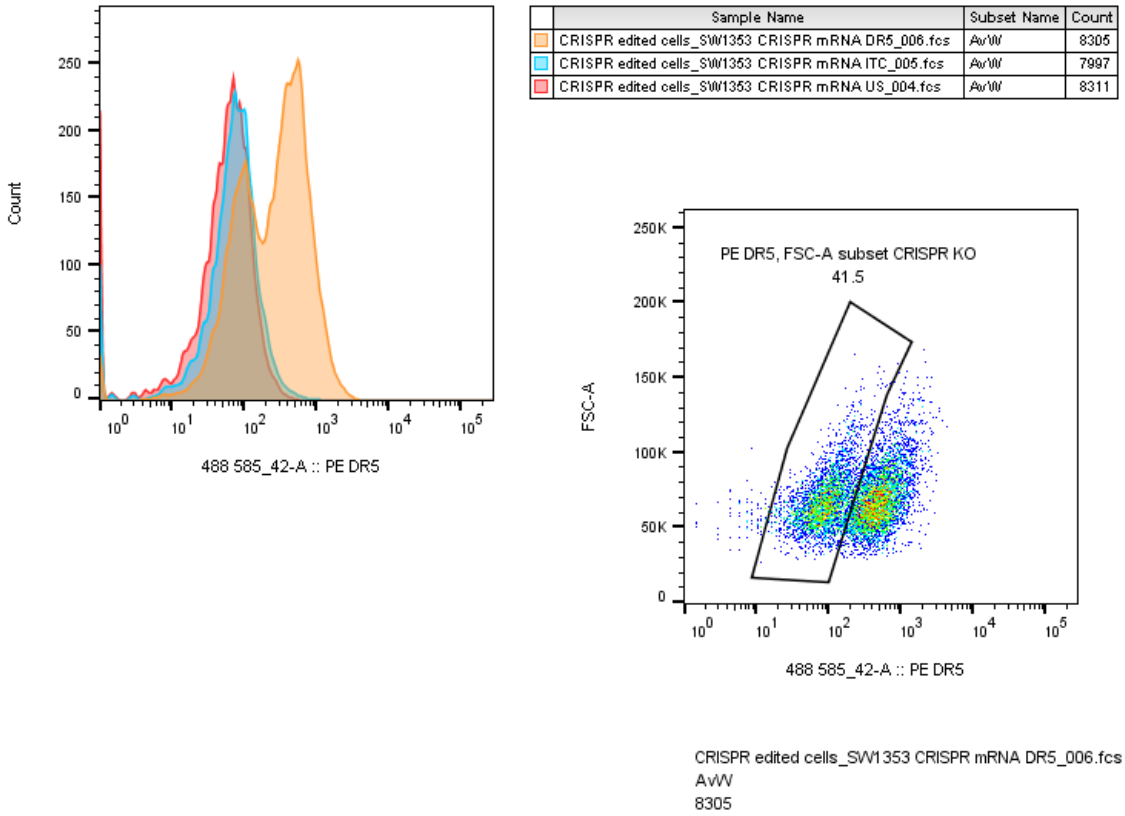

Figure 30 - Two populations (SW1353 DR5 positive and negative subsets) could be observed using FACS and the negative cells (approx. 42 %) were sorted into a 6-well plate.

After cell sorting, SW1353 cells were again stained with anti-DR5 and the negative population confirmed using flow cytometry (Figure 31).

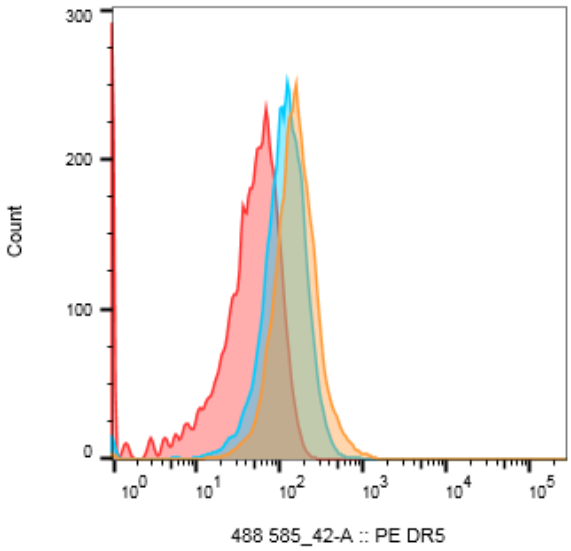

Figure 31 – DR5 negative SW1353 population (orange), isotype control (blue), unstained (red).

Cells were then sorted into single cell clones in a 96-well plate, with few clones selected and then grown in culture and frozen to be used when required.

HT1080 DR5 CRISPR KO negative population selection using FACS

The DR5-ve HT1080 population of interest was defined and sorted using FACS (Figure 32). The cells were seeded into a 6-well plate and cultured further.

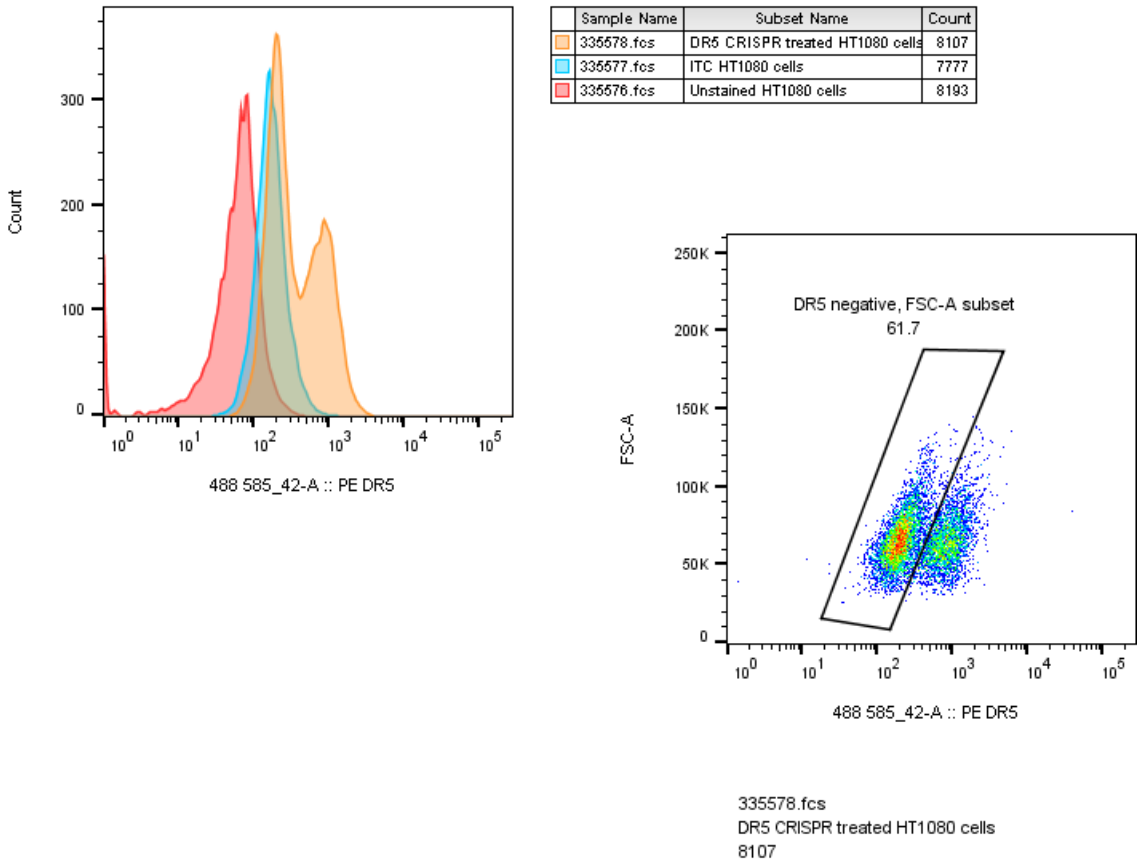

Figure 32 – Two populations (HT1080 DR5 positive and negative subsets) could be observed using FACS and the negative cells (approx. 62 %) were sorted into a 6-well plate.

After cell sorting, HT1080 cells were again stained with anti-DR5 and the negative population confirmed using flow cytometry (Figure 33). Cells were then sorted into single cell clones in a 96-well plate.

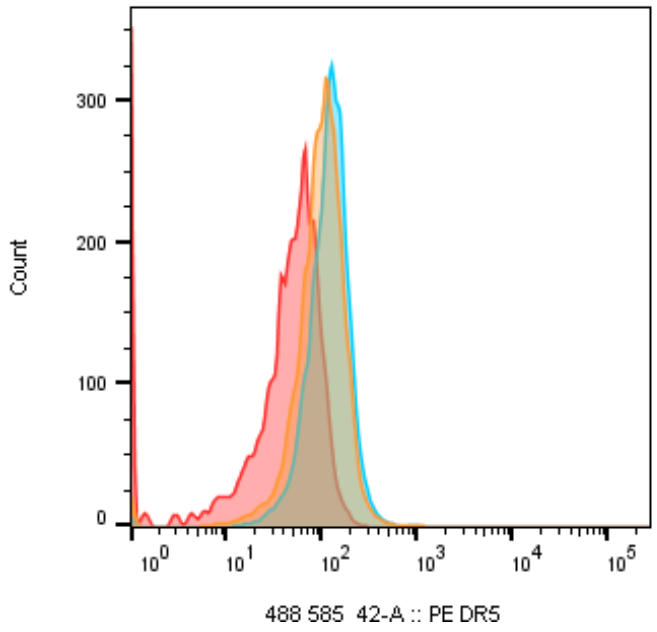

Figure 33 – DR5 negative HT1080 population (orange), isotype control (blue), unstained (red).

2.9 Harvesting of human bone marrow-derived mesenchymal stem cells (BMMSCs)

Human bone marrow-derived mesenchymal stem cells (BMMSCs) were derived from patients undergoing total hip arthroplasty (THA) using the protocol below. Ethical approval was obtained for this process.

Reagents

DMEM (1000 mg/ml glucose) – Sigma D5546

bFGF – Millipore GF003 10 µg/ml – used at 8 ng/ml

Batch tested FBS – Sigma (Birch -20 ^{o}C)

Ficoll-Paque (1.077 g/ml; GE Healthcare 17-5442-02)

Dulbecco's PBS containing Pen/Strep (100 U/ml and 100 µg/ml respectively)

MSC Wash Buffer – 5 mM EDTA /0.2 % BSA/Pen/Strep/D-PBS

MSC Culture medium – DMEM (1000 mg/ml glucose)/ 20 % FCS/Pen/Strep/Glutamine

Method – Isolating MSCs from femoral heads

1. Working in a Class II tissue culture hood, thoroughly clean bone pliers with 70 % ethanol, or sterilise by baking.
2. Place the femoral head on a large sterile petri dish.
3. Wearing protective steel mesh gloves (blue glove/steel glove/blue glove), use the bone pliers to dissect out the trabecular bone fragments from the medullary cavity.
4. Mince the fragments thoroughly, and place in a 25 ml universal tube containing 10 ml of D-PBS/Pen/Strep.
5. Pass this mixture through a 100 µm cell strainer into a 50 ml Falcon tube. Discard the solid material left in the strainer.

6. Add 10 ml of Ficoll to a 50 ml Falcon tube.

7. By ‘kissing’ the tubes, carefully layer the cell mixture over the Ficoll.

8. Centrifuge at 800 x g, 40 minutes, room temp (or 895 x g, 30 minutes).

9. Mononuclear cells are isolated at the gradient interface as a buffy coat.

10. Fat may collect on top of the gradient – carefully remove this with a 1 ml Gilson.

11. Carefully remove the buffy coat (with a 1 ml Gilson) into 10 ml MSC wash buffer.

12. Collect cells by centrifugation (200 x g, 10 minutes, room temp).

13. Resuspend the cell pellet in MSC wash buffer and collect cells as before.

14. Resuspend the cell pellet in 4-5 ml of MSC medium, and culture in a T25 flask as normal. Since this suspension contains a heterogeneous mix of cells, we do not routinely perform a cell count. Published densities are in the range of 0.5 - 2 x 10^5/cm^2.

15. MSCs will adhere within 24 hours. Macrophages and HSCs should remain in suspension.

16. After 24-36 hours, remove and discard the suspended cells. Since the MSCs attach to the flask very firmly, you can wash the flask to remove any loosely attached macrophages by blasting the flask surface with MSC medium.

17. Add fresh medium to the flask, with 8 ng/ml bFGF. Replace the medium every 72 hours, adding bFGF each time.

18. Although the flask may initially look completely empty, a T25 flask should be 70 % confluent within 10-14 days. The cells can then be passaged with trypsin-EDTA and expanded/frozen as normal.

19. MSCs will remain multipotent until approximately passage 8-10.

2.10 *In vivo* studies

2.10.1 Introduction and justification of use

The complex microenvironment and vasculature found in mammalian species can have a profound effect on the activity of tumour cells and interacting compounds (therapeutics) and cannot be extensively modelled in laboratory cell culture. Therefore prior to translating a therapeutic into phase one trials in humans, *in vivo* evidence of efficacy is required. We have precedent in the published data from our German collaborators showing the therapeutic potential of targeted TRAIL therapeutics in other colorectal models [188,189] and therefore, the utilisation of the orthotopic mouse model of bone sarcoma at our institution, which has been validated using bone sarcoma cell lines [190] is an obvious step forward. A key feature of our model is the use of bone sarcoma cells transduced to express luciferase. This allows us to monitor tumour growth using the *in vivo* imaging system (IVIS) in order to obtain real time information on response to therapy and to avoid tumours reaching an excessive size. The mouse strain used is the immunodeficient NSG (Jax® mice strain name: NOD.Cg-*Prkdc*^{scid} *Il2rg*^{tm1wjl}/SzJ) and mean age of implantation into the distal femur was 12 weeks. In summary, the mouse model was necessary to help validate the use of targeted TRAIL therapeutics as a treatment modality for bone sarcoma.

2.10.2 Ethics for animal experiments

All animal studies were carried out in accordance with the UK Home Office Animals (Scientific Procedures) Act (ASPA) 1986 for the use of animals in scientific procedures and will be performed by personnel who have completed approved Home Office training and hold current personal licences under the Animals (Scientific Procedures) Act 1986. Our laboratory has a current Home Office project licence (P74687DB5), which expires in November 2023 and incorporates a harm-benefit analysis. Our laboratory implemented the 3Rs principles and best practice in our *in vivo* procedures. Studies are continually reviewed by the Newcastle University animal welfare and ethical review body (AWERB).

Animals were kept under specific pathogen free conditions, and all experimental manipulations with mice were performed under sterile conditions in a laminar flow hood except imaging. Intrafemoral injections and all imaging procedures were performed on anaesthetised mice and all efforts made to minimise suffering. All of my work

incorporates the principles of Animals in Research: Reporting *In Vivo* Experiments (ARRIVE) guidelines [191].

2.10.3 Methodology and pilot data

2.10.3.1 Establishment of xenografts using the DR5 and NG2 positive HT1080 dedifferentiated chondrosarcoma cell line

I carried out an engraftment study to assess if the HT1080 cell line would engraft into bone and successfully achieved 100 % engraftment of the HT1080 cell line into the femora of 6 NSG mice, following intrafemoral injection. CT imaging of the mice demonstrated destruction of the femur consistent with engraftment (Figure 34).

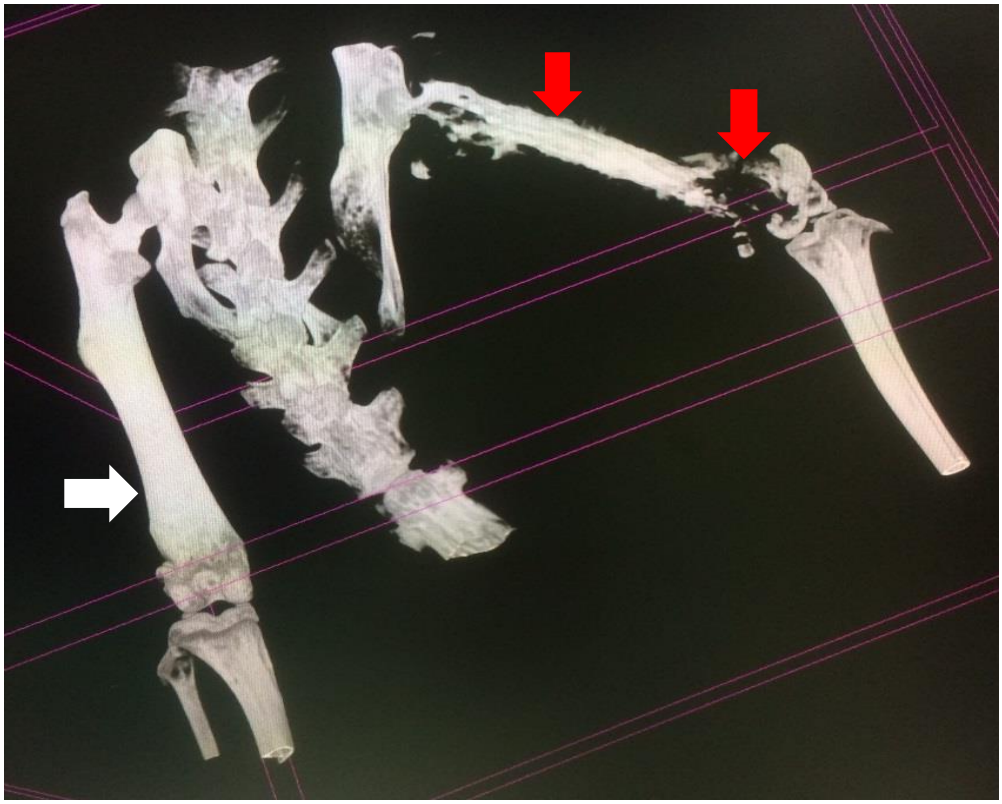

Figure 34 - Micro CT demonstrating bony destruction and thinning of the right femur 6 weeks following intrafemoral injection of HT1080 cell line (red arrows) compared to the normal/noninjected bone of the left femur (white arrow).

The *in vivo* imaging system (IVIS) was used to monitor tumour growth in the engrafted HT1080 cells transduced to express luciferase (HT1080 pSLIEW) using the same method described to transduce leukaemic cells with pSLIEW [192]. Flow cytometry analysis

demonstrated satisfactory levels of expression prior to engraftment (Figure 35). Alongside traditional tumour size measurements using calipers, the IVIS indicates the tumour volume doubling time and, therefore, the optimal time for administration of therapeutics followed by precise monitoring of the response. I found reliable engraftment and a quantifiable signal from 2 weeks onwards (Figure 36). The degree of signal was quantified as total flux in photons per second (p/s) using the Living Image® 3.2 software.

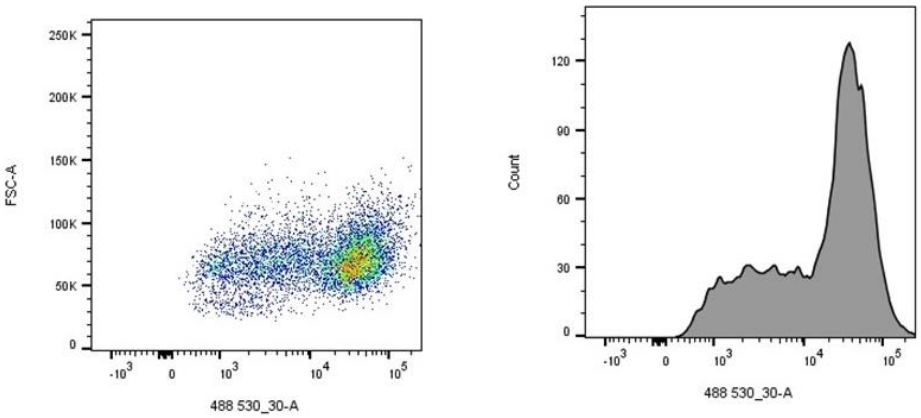

Figure 35 – Flow cytometry analysis cells of HT1080 bone sarcoma cells transduced to express luciferase (HT1080 pSLIEW) demonstrating majority of cell population contains

pSLIEW vector, which carries the luciferase and GFP gene allowing the cells to express GFP (detected by 488 530_30-A bandpass filter).

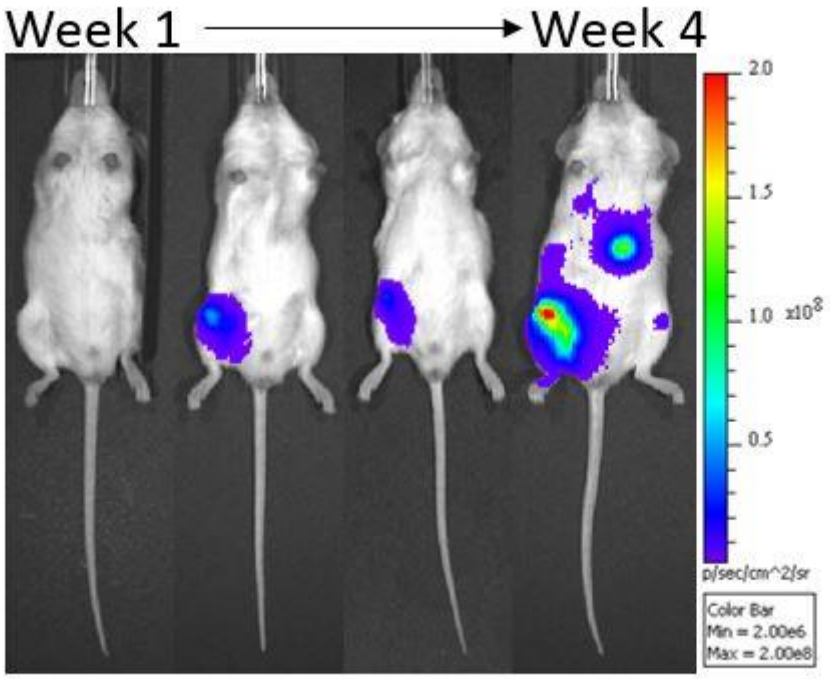

Figure 36 - Mouse with HT1080 pSLIEW cells engrafted into the femur demonstrating a stable, quantifiable IVIS signal in the region of engraftment from week 2 post implantation.

This will allow me to administer and monitor the effectiveness of the NG2 targeted TRAIL versus controls, which will include non-targeted TRAIL and vehicle only (phosphate buffered saline). Six to eight mice were used in each study arm and randomisation was performed as per ARRIVE guidelines. Maximum tumour size allowed was 1 cm at the primary site before administration of the therapeutics. Optimal timing of administration was at 2 weeks from implantation according to my pilot study. Tumour size could be monitored by caliper measurements, IVIS and CT imaging (1-2 weekly) for up to 30 days. Mice were euthanised by the schedule 1 method.

Chapter 3. Characterisation of bone sarcoma cell lines for death receptor (DR) and decoy receptor (DcR) expression

3.1 Introduction

Bone sarcoma cells have been found to express death receptors (DRs) and recombinant human TRAIL (rhTRAIL) and DR4/DR5 agonists have been used in clinical studies for sarcoma to induce cell death; however, promising *in vitro* and *in vivo* findings have not translated clinically, and clinical trials have not progressed beyond phase 2. In addition to DR expression, other factors that can confer resistance to TRAIL therapy include decoy receptor (DcR) expression and upregulation of the inhibitor of apoptosis proteins (IAPs). More recent studies have described resistance mechanisms to TRAIL in bone sarcoma and other malignancies through upregulation of c-myc, NF-kB, H-Ras and Akt as discussed in the introductory chapter.

Furthermore, correlation of the expression status of DRs with clinical parameters revealed predominantly DR5 and occasionally also DR4 are negative prognostic markers [156]. This has been described more recently in non-small cell lung cancer (NSCLC) [193]. Nuclear localisation of DR5 has also been observed in TRAIL-resistant tumour cells such as the human hepatocellular carcinoma cell line HepG2 [156,194]. Stimulation of DR5 is generally thought to induce apoptosis; however, the exact role of DR5 at the tumour site is unclear. Furthermore, the function of decoy receptors (DcRs) has been debated in the literature; however, they are generally thought to reduce the efficacy of TRAIL binding to the DRs.

The aims of this chapter are to:

1. Examine death receptor (DR) and decoy receptor (DcR) transcriptomic differences in bone sarcoma and non-malignant cell lines.

2. Investigate the death receptor 4 and 5 (DR4 and DR5) total protein and surface expression levels in bone sarcoma and non-malignant cell lines.

3. Examine decoy receptor (DcR) surface expression.

3.2 Quantification of TRAIL receptors DR4 and DR5 on mRNA level using quantitative Real-Time Polymerase Chain Reaction (qRT-PCR)

3.2.1 mRNA expression levels of DR4 and DR5 level in various bone sarcoma cell lines

Various bone sarcoma cell lines were analysed for their mRNA expression by RT-qPCR. Osteosarcoma (U2OS, SJSA-1 SAOS-2, MG63), Ewing's sarcoma (TC71), chondrosarcoma (SW1353) and dedifferentiated chondrosarcoma (HT10180). Primer selection and quantitative real-time polymerase chain reaction (qRT-PCR) settings are detailed in the methods (Section 2.3). Positive and negative control cell lines used are detailed in Section 2.1.2. High DR4 transcript levels were found in osteosarcoma (MG63 and SAOS-2) cell lines and Ewing's sarcoma (TC71) cell line. High DR5 mRNA transcript levels were found in the osteosarcoma (MG63 and SJSA-1) cell lines and dedifferentiated chondrosarcoma (HT1080) cell line. Overall DR4 is expressed less than DR5 levels (Figure 37).

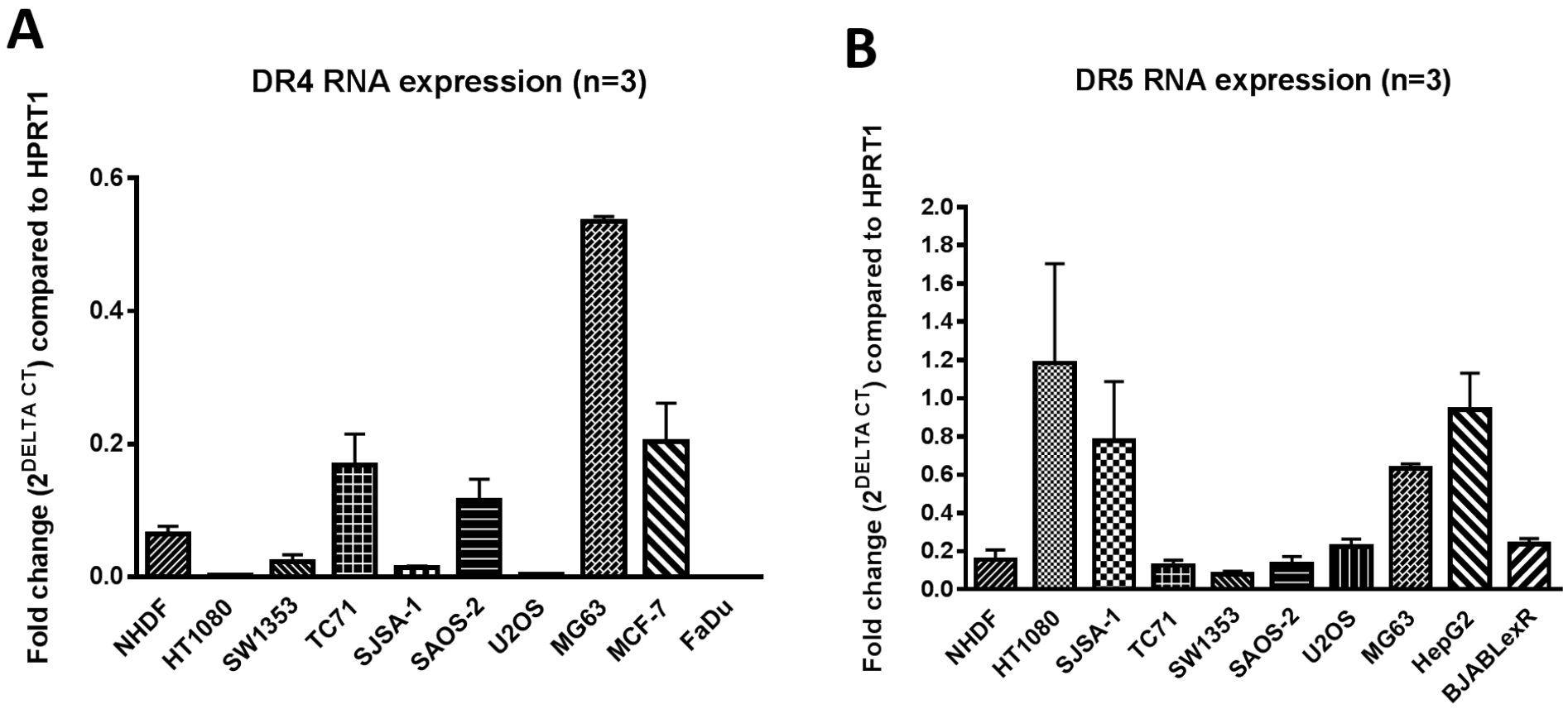

Figure 37 – qRT-PCR used to determine DR4 and DR5 mRNA transcript levels in bone sarcoma cell lines and normal human dermal fibroblast (NHDF) cell line. (A) For DR4 mRNA transcript levels, the MCF-7 breast carcinoma cell line was used as a positive control. The FaDu pharyngeal carcinoma cell line was used as a negative control. (N = 3). (B) For DR5 mRNA transcript levels, the human hepatocellular carcinoma HepG2 cell line was used as a positive control. The Burkitt's lymphoma BJABLexR cell line was used as a negative control. (N = 3).

3.2.2 Decoy receptor (DcR) 1 and 2 mRNA levels in various bone sarcoma cell lines

The RT-qPCR data in this study revealed the DcR1 levels to be highest in the U2OS cell line. The SJSA-1 osteosarcoma cell line expressed the greatest DcR2 mRNA levels (Figure 38). This correlated to the elevated surface levels found using flow cytometry (see Section 3.3.3.3). The SJSA-1 cell line has also been quite TRAIL resistant and increased DcR2 could be a potential mechanism for resistance. The cell line, however, is also known to have elevated MDM2 – an inhibitor of p53. There was less of a correlation between DcR1 transcript levels and surface protein levels. Further investigation of protein expression levels would include performing western blotting.

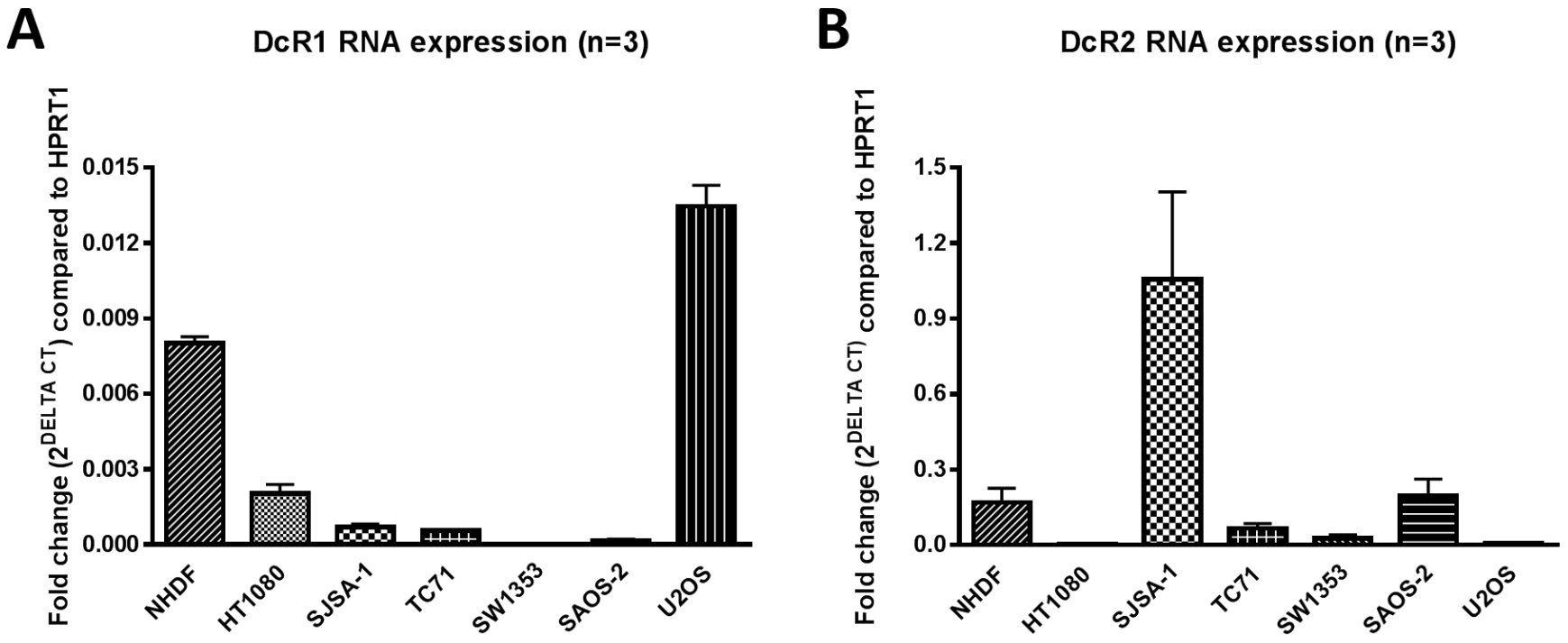

Figure 38 – qRT-PCR used to determine decoy receptor 1 (DcR1) and decoy receptor 2 (DcR2) mRNA transcript levels in bone sarcoma cell lines and normal human dermal fibroblast (NHDF) cell line. (A) Decoy receptor 1 (DcR1) mRNA transcript levels were elevated in the U2OS osteosarcoma cell line and the normal human dermal fibroblast (NHDF) cell line. (B) Decoy receptor 2 (DcR2) mRNA transcript levels were most elevated in the SJSA-1 osteosarcoma cell line.

3.2.2.1 Osteoprotegerin (OPG)

OPG levels have been investigated as a resistance mechanism to TRAIL therapy [195]. However, the levels of OPG required to stop signalling is unclear. Cell lines more resistant to TRAIL therapy have included the NHDF cell line and the SW1353 chondrosarcoma, SJSA-1 osteosarcoma and SAOS-2 osteosarcoma cell lines (Chapter 4). High OPG transcript levels were found in a non-malignant cell line of mesenchymal origin (NHDF) (Figure 39) and supports a previous study reporting high levels in other non-malignant cells such as BMMSCs [195] and a potential role in conferring resistance; however, further studies would be required to assess cell surface and shedded OPG protein levels.

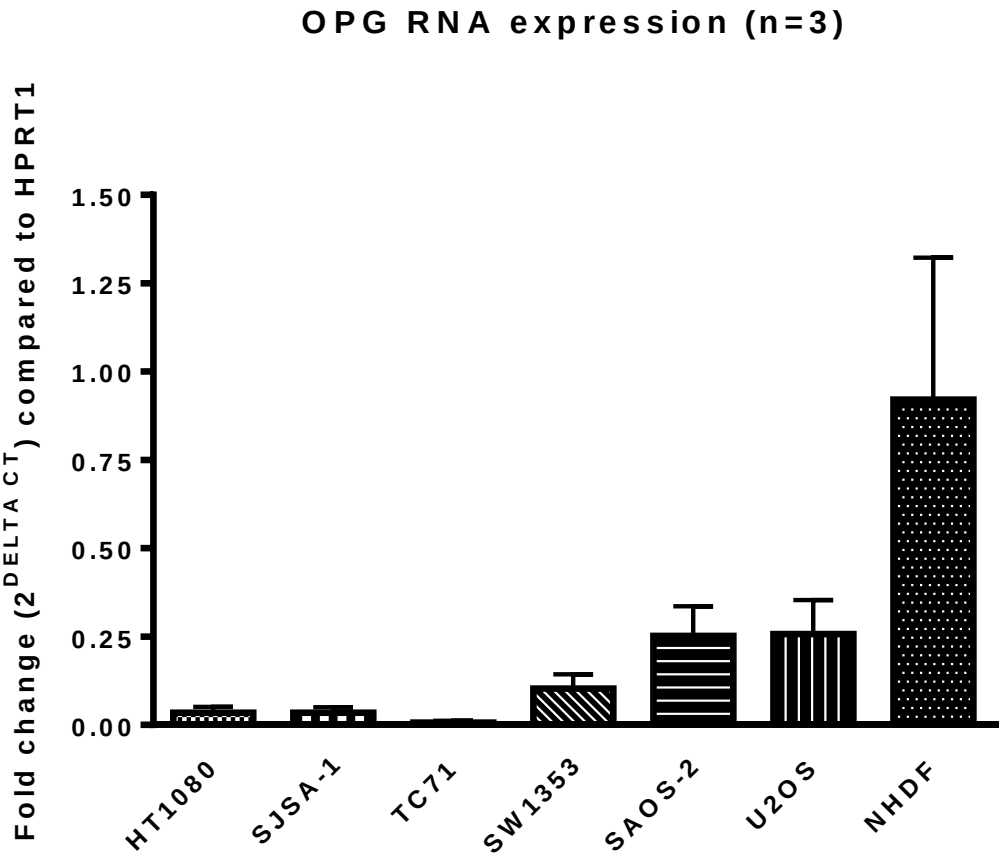

Figure 39 – qRT-PCR used to determine OPG mRNA transcript levels. Elevated levels were found in the normal human dermal fibroblast (NHDF) cell line in comparison to bone sarcoma cell lines.

3.3 Quantification at the protein level using western blotting and flow cytometry

3.3.1 Western blotting

3.3.1.1 Death receptor 4 (DR4) is present in bone sarcoma and non-malignant cell lines

DR4 total protein levels were assessed by western blotting. Death receptor 4 (DR4) expression was strongly expressed in the TC71 Ewing's sarcoma cell line followed by the MG63 and SAOS-2 osteosarcoma cell lines cell lines (Figure 40 and Figure 41).

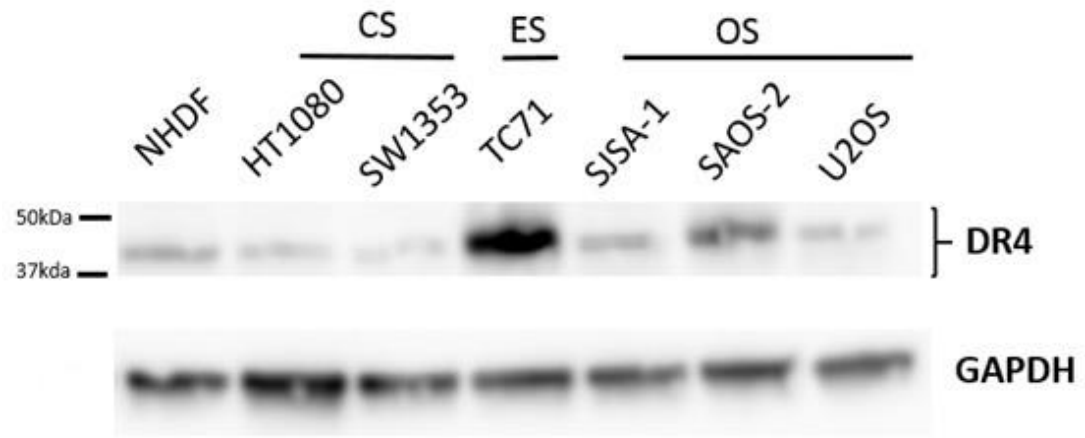

Figure 40 - Western blot analysis of DR4 receptor expression in bone sarcoma cell lines (DR4 predicted size: between 50-60 kDa). 40 µg of total cell lysate loaded. Mouse anti-human DR4 primary antibody, Abcam [32A242] (ab13890). High expression is found in the TC71 Ewing's sarcoma cell line followed by the SAOS-2 osteosarcoma cell line. CS = chondrosarcoma, ES = Ewing's sarcoma, OS = osteosarcoma.

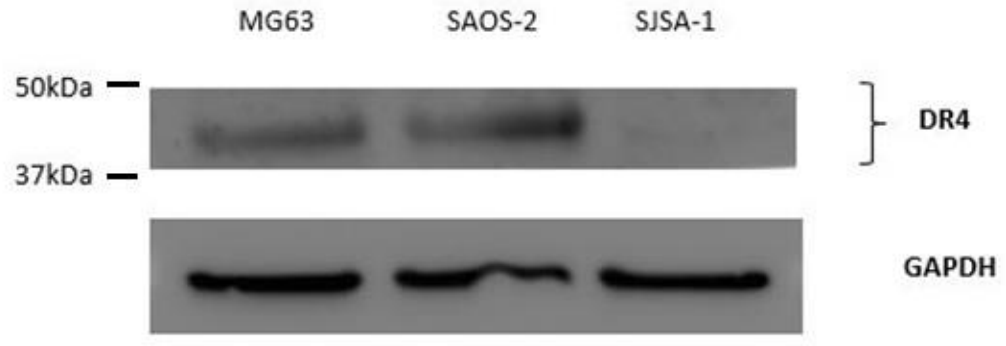

Figure 41 - Western blot analysis of DR4 receptor expression in bone sarcoma cell lines. High DR4 receptor expression found in the MG63 and SAOS-2 osteosarcoma cell lines compared to the SJSA-1 osteosarcoma cell line. 40 µg of total cell lysate loaded. Mouse anti-human DR4 primary antibody, Abcam [32A242] (ab13890).

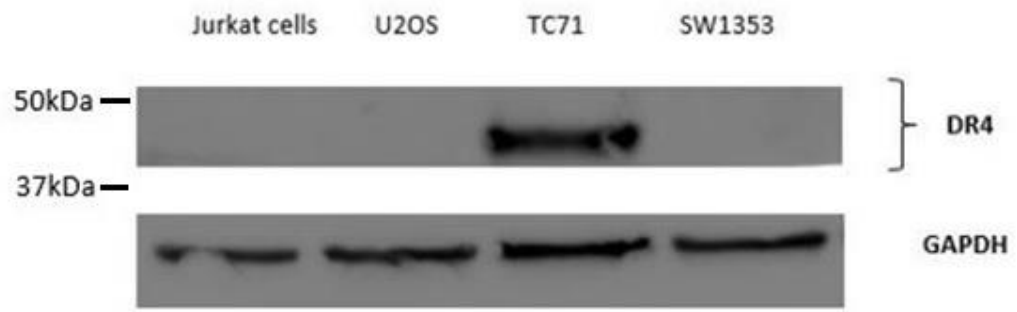

Figure 42 - Western blot analysis of DR4 receptor expression in bone sarcoma cell lines. High DR4 receptor expression in the Ewing's sarcoma TC71 cell line compared to the U2OS osteosarcoma cell line, SW1353 chondrosarcoma cell line and Jurkat cells [167,168] (an immortalised human T lymphocyte cell line reported to be negative for DR4) [196,197]. 40 µg of total cell lysate loaded. Mouse anti-human DR4 primary antibody, Abcam [32A242] (ab13890).

3.3.1.2 Death receptor 5 (DR5) is present in bone sarcoma and non-malignant cell lines

Death receptor 5 (DR5) is expressed as long and short isoforms in bone sarcoma and non-malignant cell lines (potential function of the isoforms is further discussed in Section 3.4). The MG63 osteosarcoma cell line and HT1080 dedifferentiated chondrosarcoma cell line expressed the greatest levels of DR5 (Figure 43 to Figure 47).

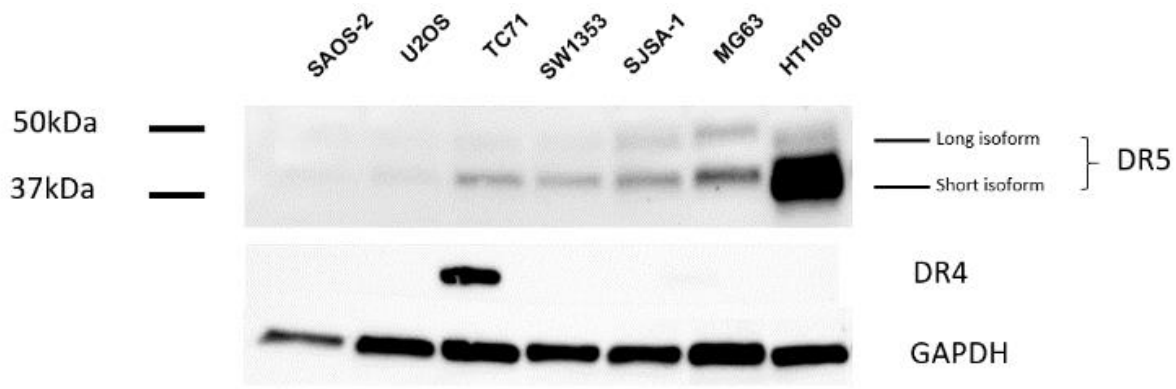

Figure 43 – Western blot analysis of DR5 receptor expression in bone sarcoma cell lines. The HT1080 dedifferentiated chondrosarcoma cell line expresses the greatest quantities of DR5, particularly the short isoform in comparison to the other bone sarcoma cell lines. The TC71 Ewing's sarcoma cell line also expresses DR4. 40 µg of total cell lysate loaded. Rabbit anti-human DR5 monoclonal antibody, Cell Signaling Technology (CST) (D4EP) XP® Rabbit mAb.

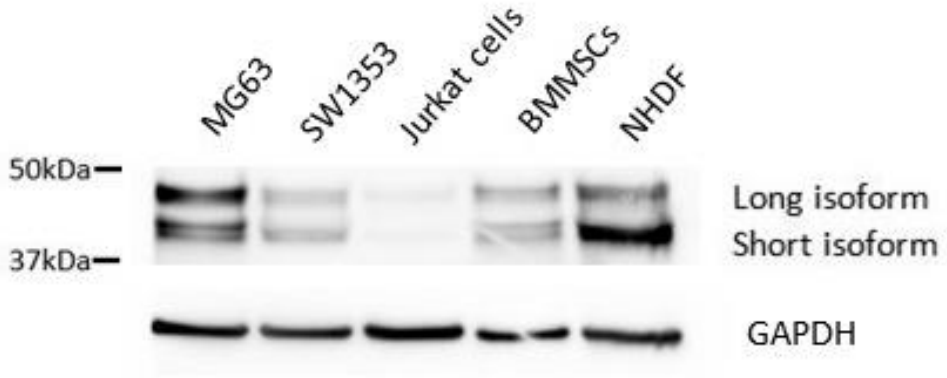

Figure 44 - Western blot analysis of DR5 receptor expression in bone sarcoma cell lines. Long and short isoforms of DR5. The MG63 osteosarcoma cell line and the normal human dermal fibroblast (NHDF) cell line express a high level of DR5. The NHDF cell line also expresses a high quantity of the short isoform compared to the long. SW1353 = chondrosarcoma cell line; BMMSCs = bone marrow-derived stem cells; Jurkat cells were used as a control for the short and long isoforms of DR5. 40 µg of

total cell lysate loaded. Rabbit anti-human DR5 monoclonal antibody, Cell Signaling Technology (CST) (D4EP) XP® Rabbit mAb.

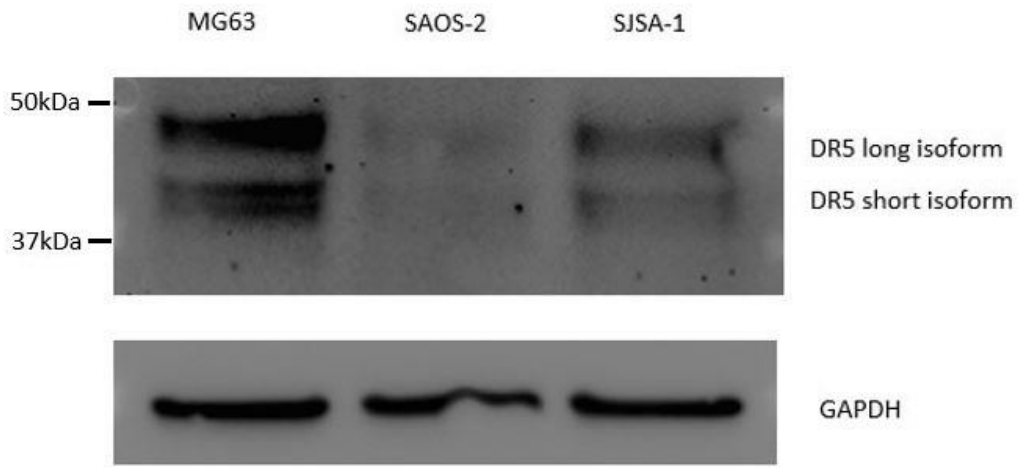

Figure 45 - Western blot analysis of DR5 receptor expression in three osteosarcoma cell lines (MG63, SAOS-2 and SJSA-1). Two isoforms can be observed (long and short) in all cell lines with strongest expression in the MG63 cell line. They can be pre-processed or processed forms of DR5. 40 µg of total cell lysate loaded. Rabbit anti-human DR5 monoclonal antibody, Cell Signaling Technology (CST) (D4EP) XP® Rabbit mAb.

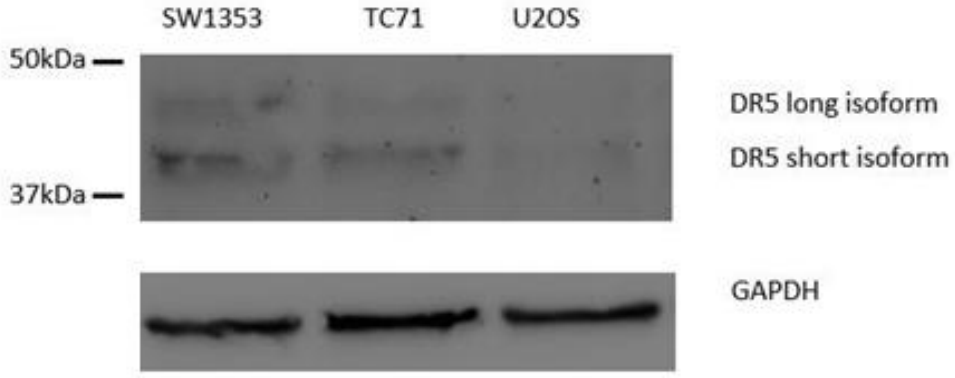

Figure 46 - Western blot analysis of DR5 receptor expression in bone sarcoma cell lines. Strong expression can be seen in the SW1353 chondrosarcoma and TC71 Ewing's sarcoma cell lines compared to the U2OS osteosarcoma cell line. Both isoforms are present; however, the shorter isoform appears to be more prominent. 40 µg of total cell lysate loaded. Rabbit anti-human DR5 monoclonal antibody, Cell Signaling Technology (CST) (D4EP) XP® Rabbit mAb.

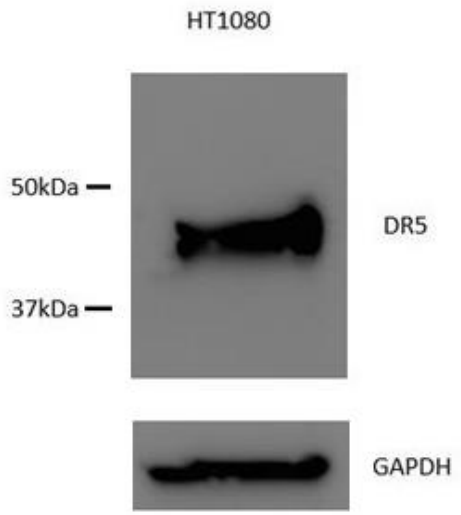

Figure 47 – Western blot analysis of DR5 receptor expression in the HT1080 dedifferentiated chondrosarcoma cell line. Very strong expression of DR5 in the dedifferentiated chondrosarcoma HT1080 cell line. 40 µg of total cell lysate loaded. Rabbit anti-human DR5 monoclonal antibody, Cell Signaling Technology (CST) (D4EP) XP® Rabbit mAb.

3.3.2 High DR5 expression in HT1080 dedifferentiated chondrosarcoma cell line in all compartments

Protein expression was analysed using western blotting in the cell membrane, cytoplasm and nuclear fractions.

3.3.2.1 Death receptor 5 (DR5) in membrane subfraction

Membrane DR5 receptor expression was strongest in the dedifferentiated chondrosarcoma HT1080 cell line followed by the NHDF and SJSA-1 cell lines (Figure 48).

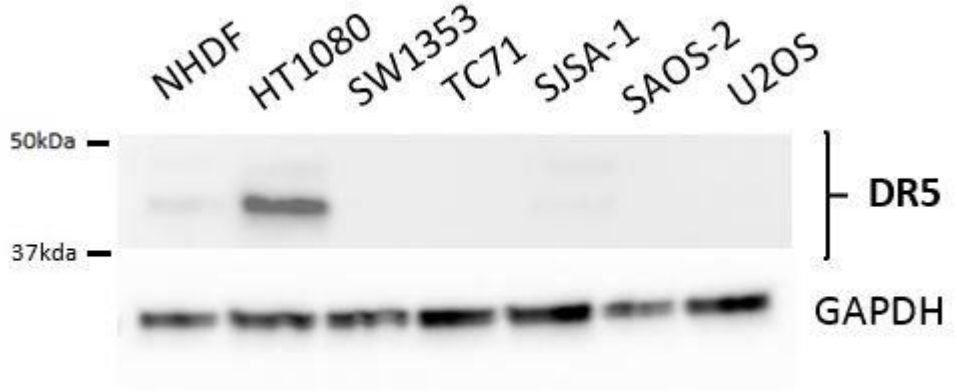

Figure 48 - Western blot analysis of DR5 receptor expression in bone sarcoma cell lines Membrane portion of subfractionation demonstrated membrane DR5 receptor expression is strongest in the dedifferentiated chondrosarcoma HT1080 cell line. Two bands were visible and this is likely to represent the two isoforms (short and long) of DR5 described, with greater expression of the short in the HT1080 cell line. Both are slightly apparent for the NHDF and SJSA-1 cell lines. 20 µg of total cell lysate loaded DR5 monoclonal antibody rabbit, anti-human, Abcam® Recombinant Antibodies, [EPR1659(2)] (ab181846).

3.3.2.2 Death receptor 5 (DR5) in nuclear subfraction

In the nuclear subfraction, DR5 was mainly seen in the HT1080 cell line (Figure 49). Lamin A/C was used as the housekeeping protein for this fraction. Increased levels of nuclear DR5 has been related to increased aggressiveness via the inhibition of microRNA maturation [194].

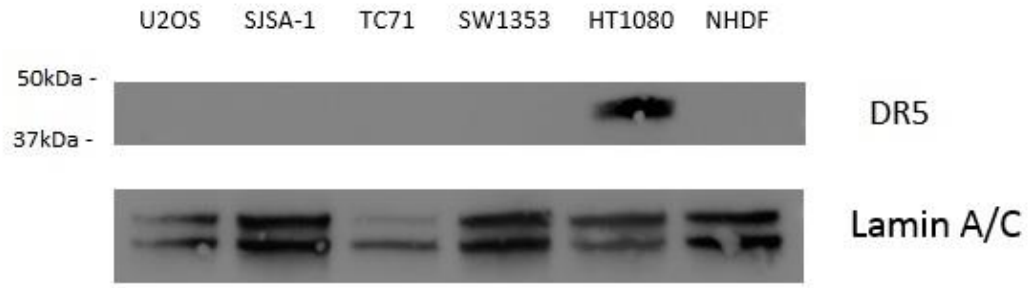

Figure 49 - DR5 expression is elevated in the dedifferentiated chondrosarcoma HT1080 cell line compared to the other bone sarcoma cell lines in the nuclear subfraction. 20 µg of total cell lysate loaded DR5 monoclonal antibody rabbit, anti-human, Abcam® Recombinant Antibodies, [EPR1659(2)] (ab181846).

3.3.2.3 Death receptor 5 (DR5) in cytoplasmic subfraction

In the cytoplasmic subfraction, elevation in the expression of DR5 could again be seen in the HT1080 dedifferentiated chondrosarcoma cell line compared to the osteosarcoma (U2OS) cell line and Ewing's sarcoma (TC71) cell lines (Figure 50).

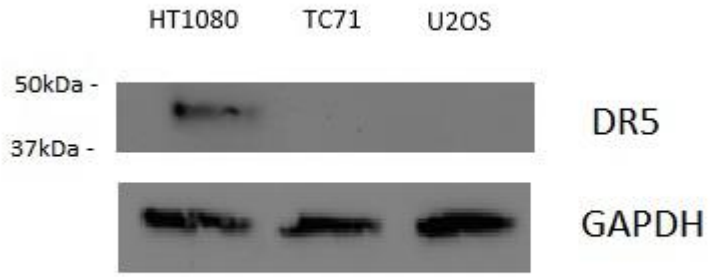

Figure 50 - In the cytoplasmic subfraction elevation in the expression of DR5 could again be seen in the HT1080 dedifferentiated chondrosarcoma cell line compared to the osteosarcoma (U2OS) cell line and Ewing's sarcoma (TC71) cell lines. 20 µg of total cell lysate loaded DR5 monoclonal antibody rabbit, anti-human, Abcam® Recombinant Antibodies, [EPR1659(2)] (ab181846).

3.3.3 Surface expression of death receptor 4 and 5 (DR4 and DR5) and decoy receptors 1 and 2 (DcR1 and DcR2)

Flow cytometry was used to detect surface levels of DR4, DR5, decoy receptor 1 (DcR1) and decoy receptor 2 (DcR2) in sarcoma and non-malignant cell lines. Examples of the gating strategies used to exclude the doublets and dead cells are described in Section 2.4. The degree of DR or DcR surface protein expression on bone sarcoma cell lines was visualised and presented pictorially using histogram plots. The median fluorescence intensity (MFI) for surface receptor expression was calculated using FlowJo™ software (BD, Becton, Dickinson & Company), and the MFI for the isotype control was subtracted from this as a measure of degree of expression [MFI(S)-MFI(Isotype control)]. Examples of this are demonstrated in our DR4 and DR5 positive control cell lines (Section 2.1.1) and the TC71 Ewing's sarcoma cell line (Figure 51).

Bone sarcoma cell lines

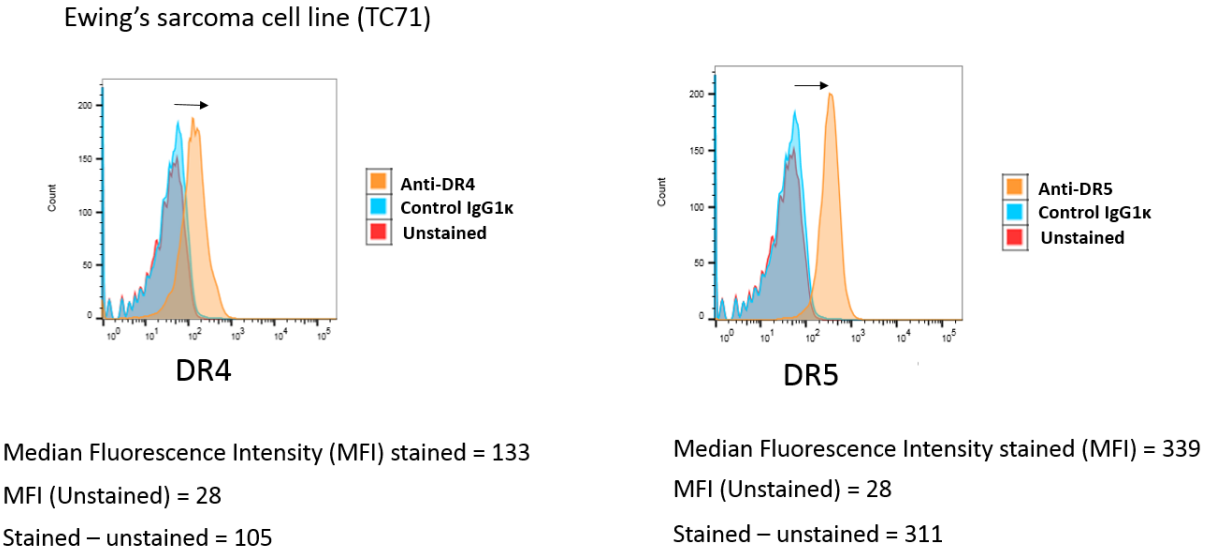

Figure 51 – Flow cytometry analysis for surface expression of DR4 and DR5 in the TC71 Ewing's sarcoma cell line. Degree of expression presented as histogram plots and quantified using MFI. After subtracting background fluorescence, DR5 is expressed to a greater extent (311) than DR4 (105).

3.3.3.1 Surface expression of DR4 and DR5

Surface DR4 is present in all bone sarcoma cell lines and was found to be the greatest in the TC71 Ewing's sarcoma cell line. Surface DR5 is greatest in the HT1080 dedifferentiated chondrosarcoma cell line, followed by the MG63 and SJSA-1 osteosarcoma cell lines (Figure 52).

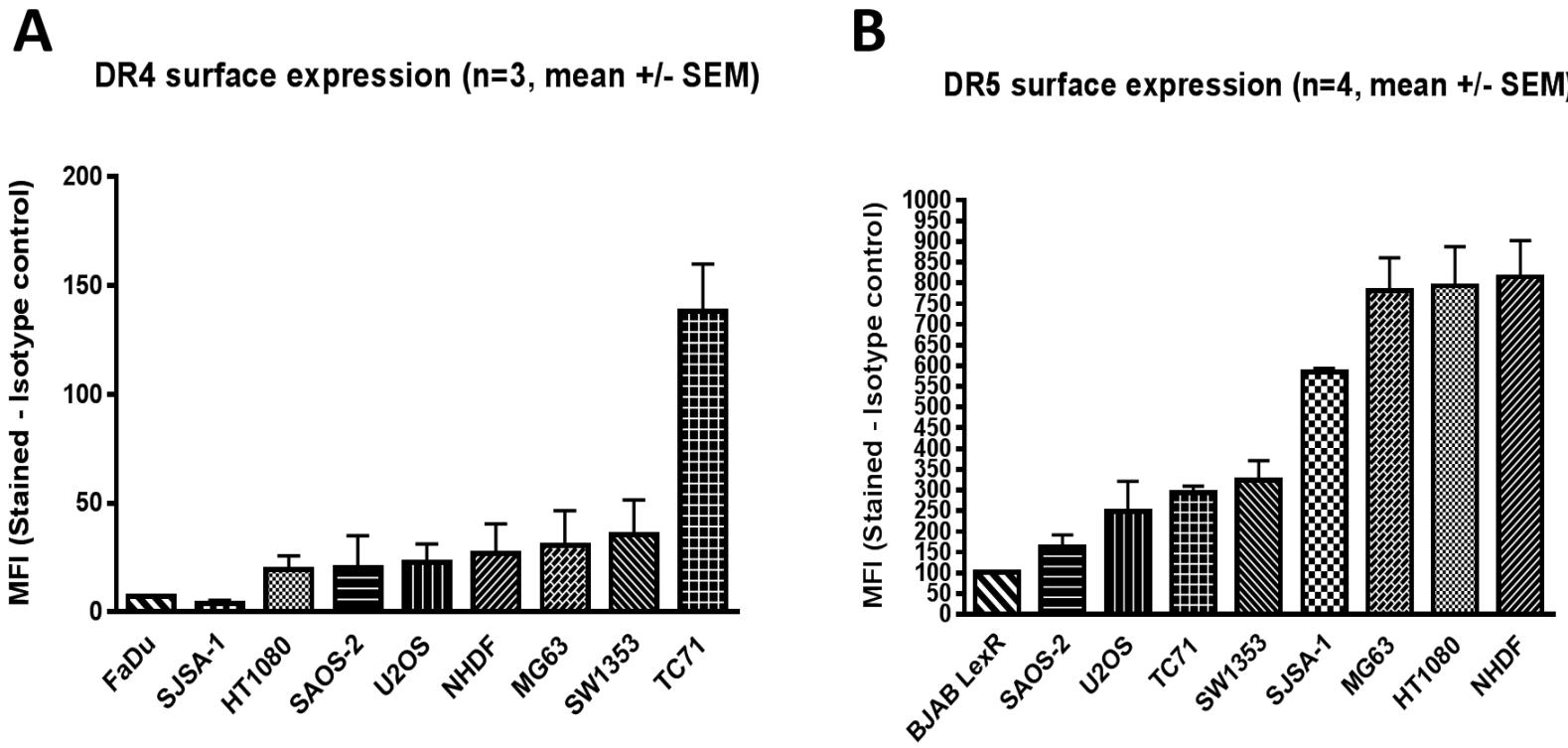

Figure 52 – DR4 and DR5 surface expression levels determined using flow cytometry. (A) For DR4, FaDu = pharyngeal carcinoma cell line, which is the negative control. Normal human dermal fibroblast (NHDF) is the non-malignant cell line (N = 3). (B) For DR5 surface expression levels (mean +/-SEM; n = 4). Burkitt's lymphoma cell line (BJAB LexR) was used as a negative control. Normal human dermal fibroblast (NHDF) is the non-malignant cell line (N = 4).

3.3.3.2 Surface expression of DR4 and DR5 in non-malignant cell lines

Surface expression of DR4 and DR5 was evident in non-malignant cell lines. DR5 surface levels were expressed at a higher level than DR4 (Figure 53).

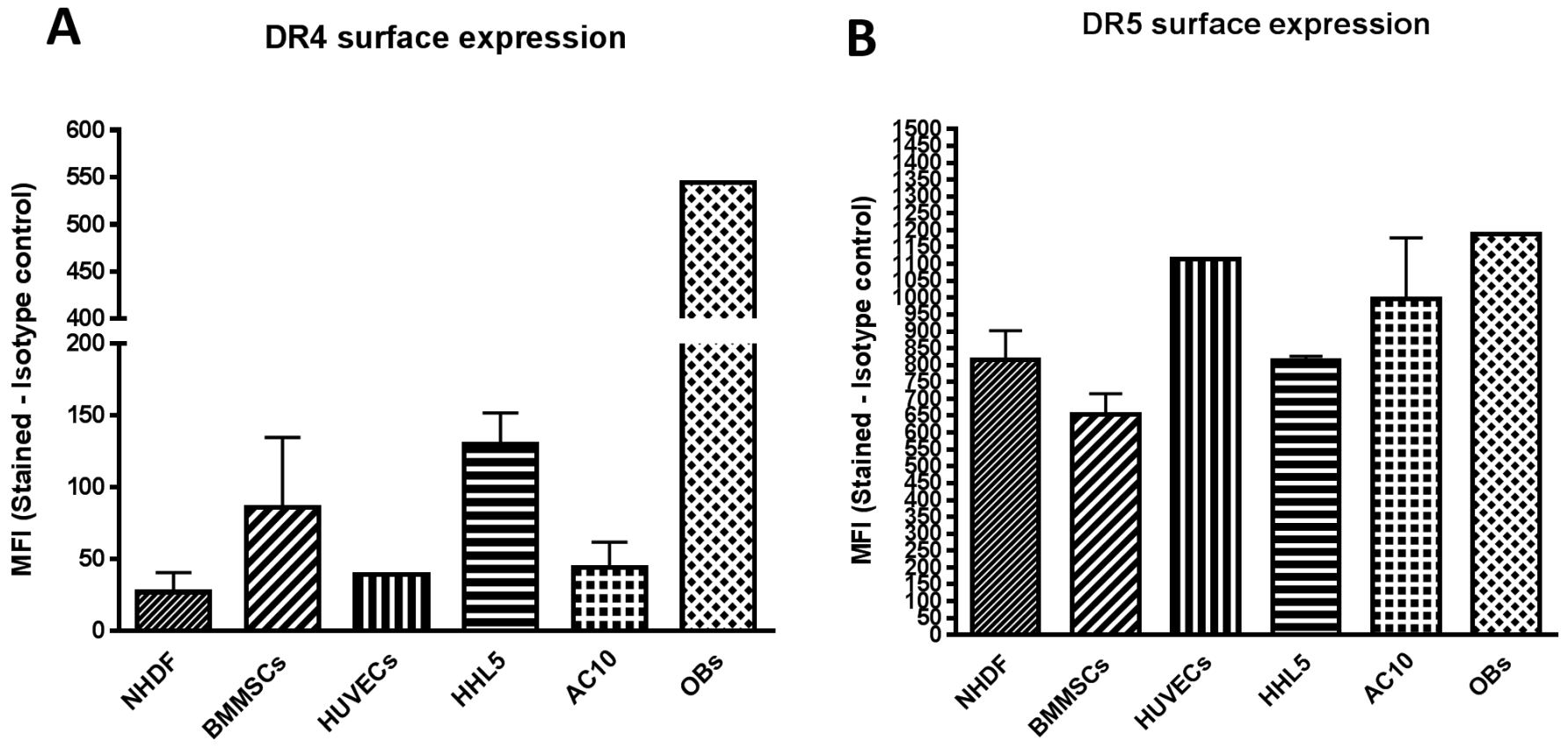

Figure 53 - DR4 and DR5 surface expression levels in non-malignant cell lines determined using flow cytometry. OBs and HUVECs (n = 1). NHDF = normal human dermal fibroblasts, BMMSCs = bone marrow-derived mesenchymal stem cells. HUVECs = human umbilical vein cells, HHL5 = human hepatocytes, AC10 – ventricular cardiomyocytes, OBs = human osteoblasts.

3.3.3.3 Decoy receptor (DcR) expression

In the following section, surface DcR expression levels were assessed using flow cytometry. Positive control cell lines, HUVECs and peripheral blood granulocytes, were used as positive controls for DcR1 and DcR2 respectively (Section 2.4).

Bone sarcoma cell lines

The SAOS-2 osteosarcoma cell line expressed the greatest level of DcR1. The SJSA-1 osteosarcoma and TC71 Ewing's sarcoma cell lines were found to have increased levels of surface DcR2 as shown by flow cytometry data when compared to the other bone sarcoma cell lines (Figure 54).

Non-malignant cell lines

DcR1 and DcR2 expression was greatest in the human-derived osteoblasts (OBs) (Figure 55).

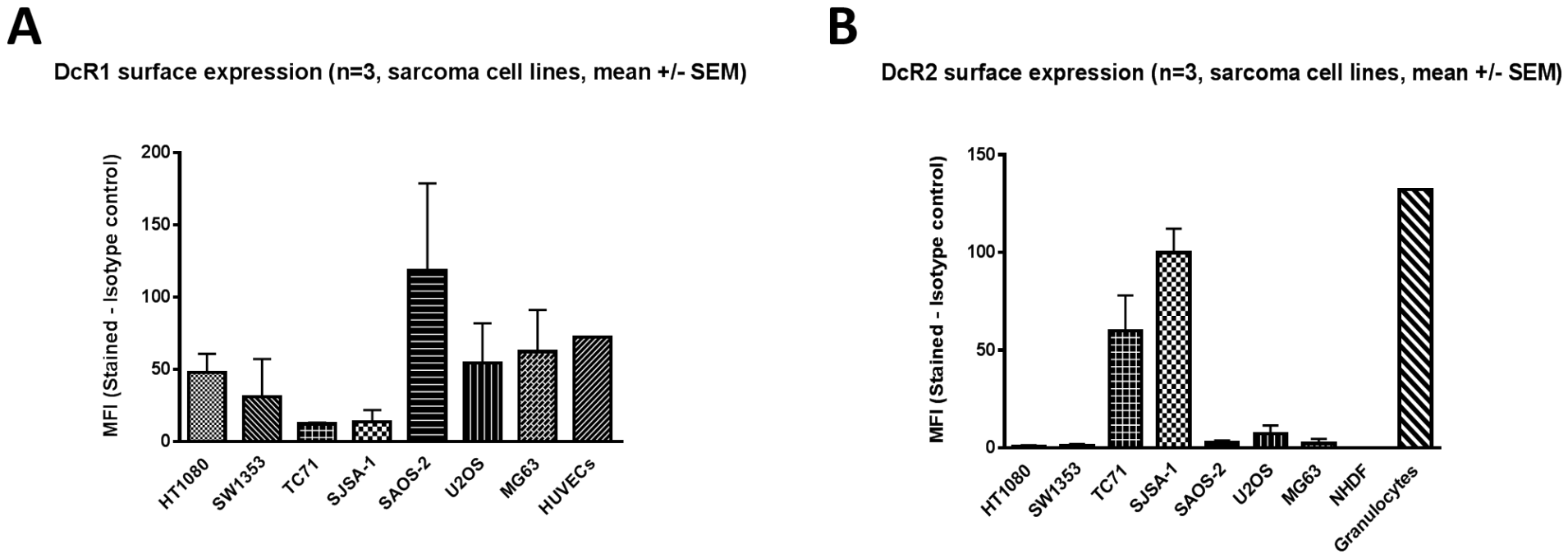

Figure 54 – DcR expression levels in bone sarcoma cell lines assessed using flow cytometry. (A) The SAOS-2 osteosarcoma cell line expressed the greatest level of DcR1. Human umbilical vein cells (HUVECs) were used as a positive control (N = 3). (B) The SJSA-1 osteosarcoma cell line and TC71 Ewing's sarcoma cell line express high levels of decoy receptor 2 (DcR2) in comparison to the other cell lines. Granulocytes derived from human blood were used as a positive control (N = 3).

Non-malignant cell lines

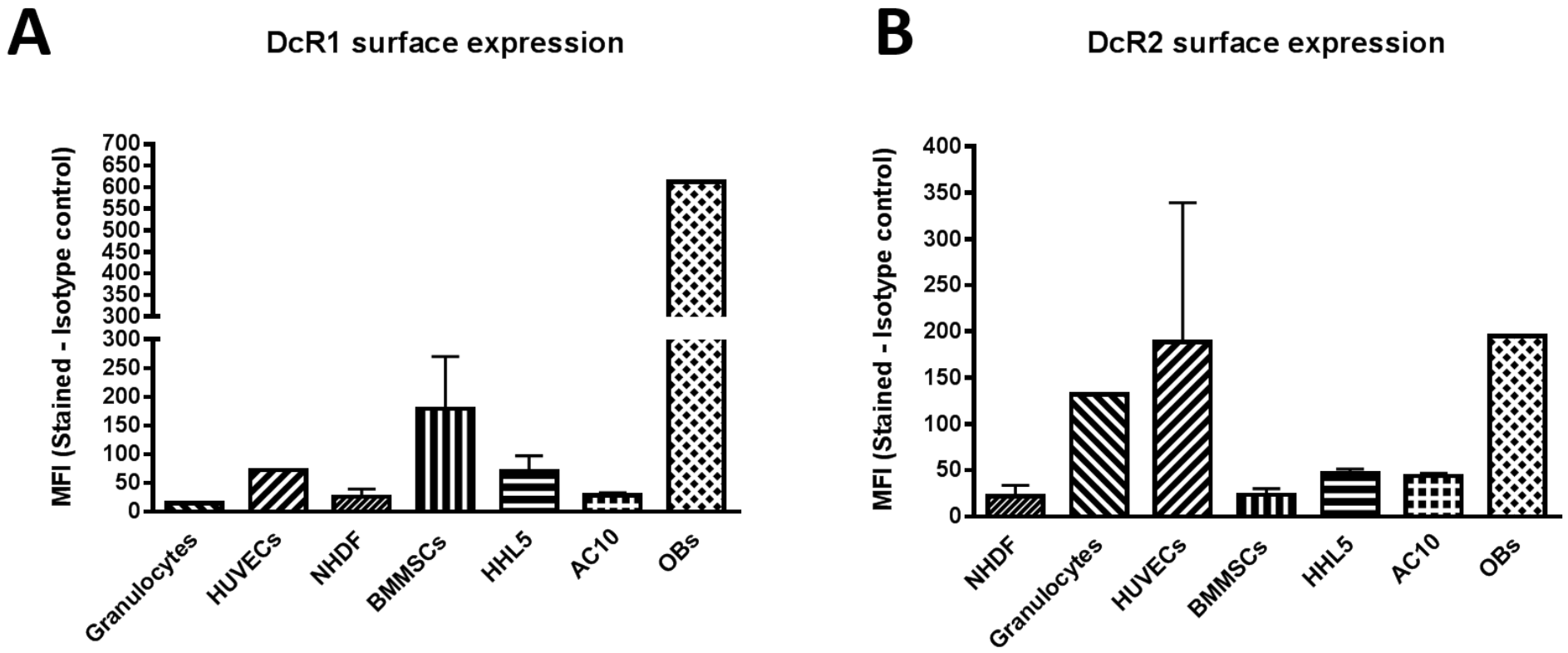

Figure 55 – DcR expression levels in non-malignant cell lines assessed using flow cytometry. (A) DcR1 expression was greatest in the human-derived osteoblasts (OBs) (MFI = 613). OBs and HUVECS (n = 1). (B) DcR2 expression is elevated in granulocytes, HUVECs and human-derived osteoblasts (OBs). OBs (n = 1) and HUVECS (n = 2).

3.3.3.4 TNF-related apoptosis-inducing ligand (TRAIL)

TRAIL expression in the bone sarcoma cell lines was explored as part of the project as its degree of expression maybe related to tumour aggressiveness (discussed further in Section 3.4). TRAIL expression was not visible on western blotting compared to the positive control 786-0 renal clear cell adenocarcinoma cell line (Figure 56) and no shift was evident on the TC71 Ewing's sarcoma cell line flow cytometry histogram (Figure 57).

Western blotting

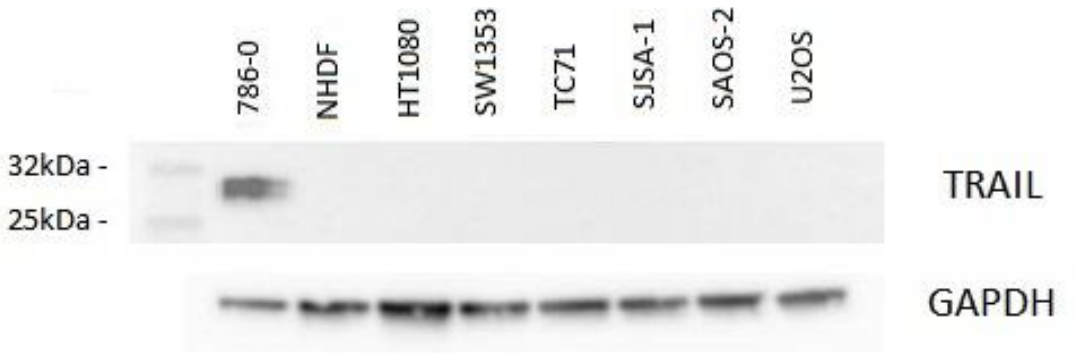

Figure 56 - TRAIL expression in bone sarcoma cell lines in comparison to the positive control 786-0 human renal carcinoma cell line. TRAIL was not found to be significantly expressed in any of our bone sarcoma cell lines. 40 µg of total cell lysate loaded. TRAIL (C922B9) rabbit anti-human monoclonal antibody, Cell Signaling Technology (CST).

Flow cytometry (TRAIL)

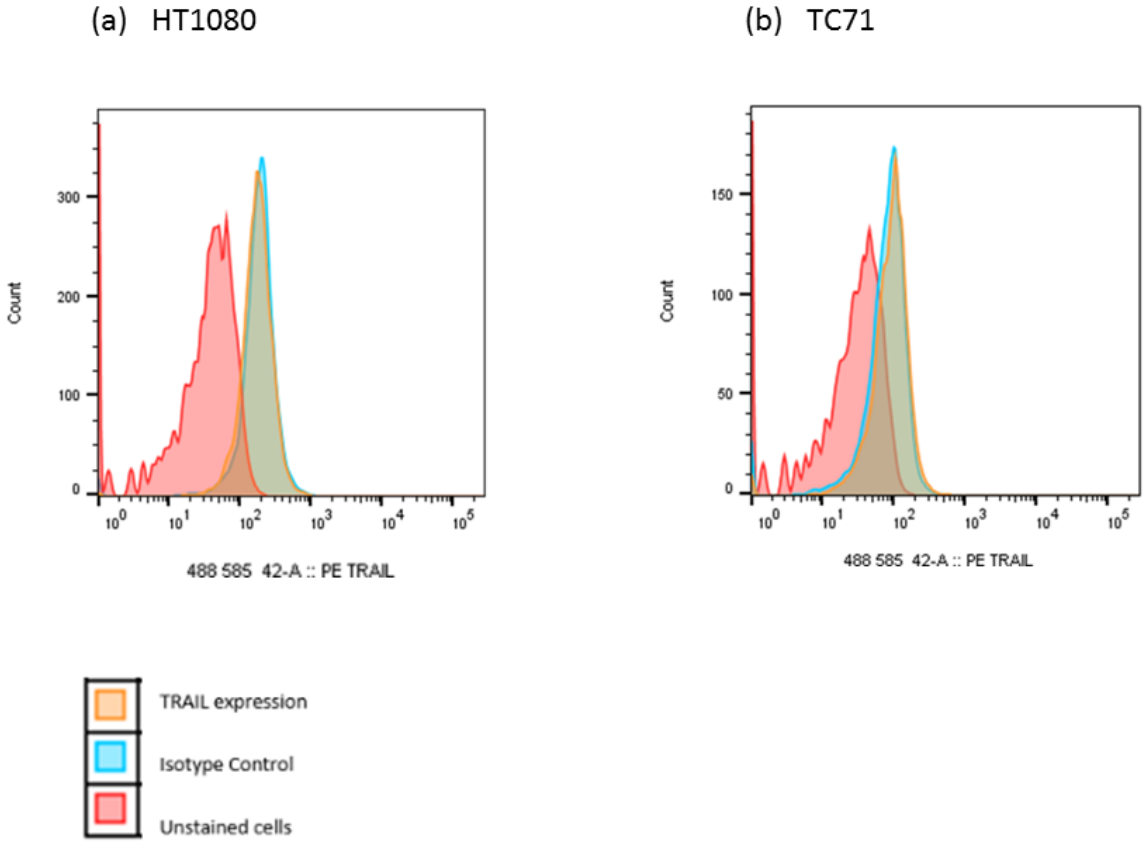

Figure 57 - Flow cytometry data demonstrating no significant surface level expression of TRAIL in the (a) HT1080 dedifferentiated chondrosarcoma cell line or the (b) TC71 Ewing's sarcoma cell line.

3.3.4 Immunohistochemistry (IHC)

A cell line block was created and used to prepare sections of slides for Immunohistochemistry (IHC) staining (Figure 58). DR5 immunohistochemistry testing was tested on a range of cell lines embedded in a paraffin block. Anti-DR5 monoclonal antibody from Cell Signaling Technology (CST) (Section 2.6) was tested at twofold dilutions at 1:50-1:200. The ideal concentration was found to be 1 in 100; less background positivity could be observed in negative control cell lines. Examples of staining of sections of the cell line blocks are demonstrated. There was strong staining in dedifferentiated chondrosarcoma HT1080 cells (a). Moderate staining is demonstrated in SJSA-1 osteosarcoma cells (b). There is absent staining in MCF-7 breast carcinoma cells (c) and the negative control BJAB Burkitt's lymphoma cells (d) (Figure 59).

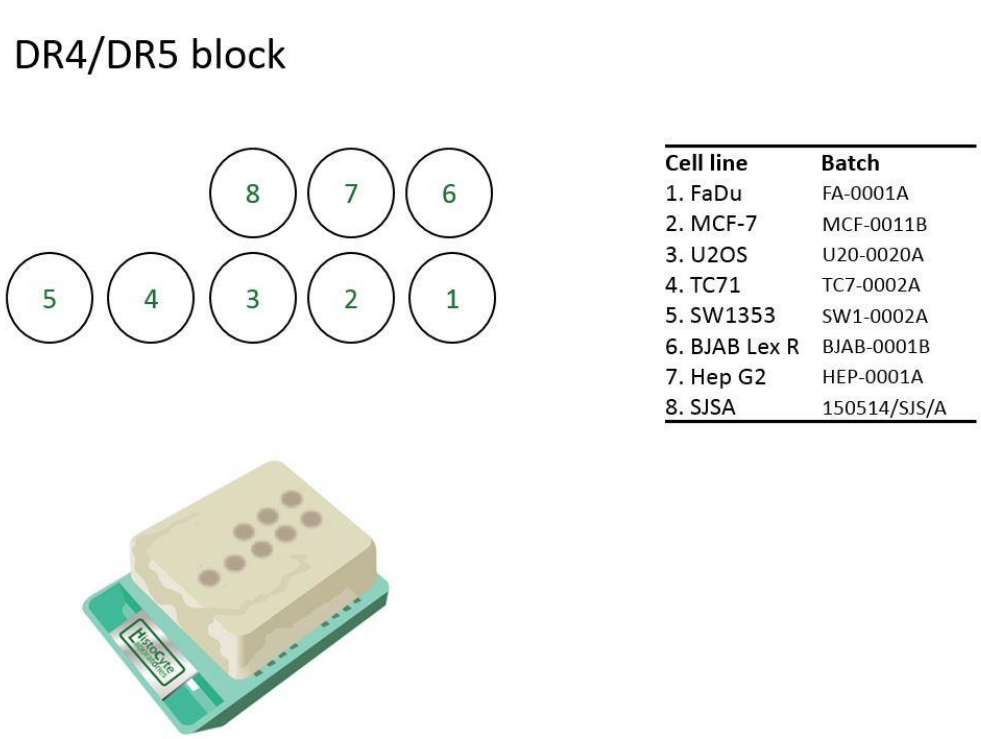

Figure 58– Cell line block with a range of cell lines used for Immunohistochemistry (IHC) staining. All cell lines were stained at the same time. Batch numbers are an internal coding method to be able to trace the work that has been performed.

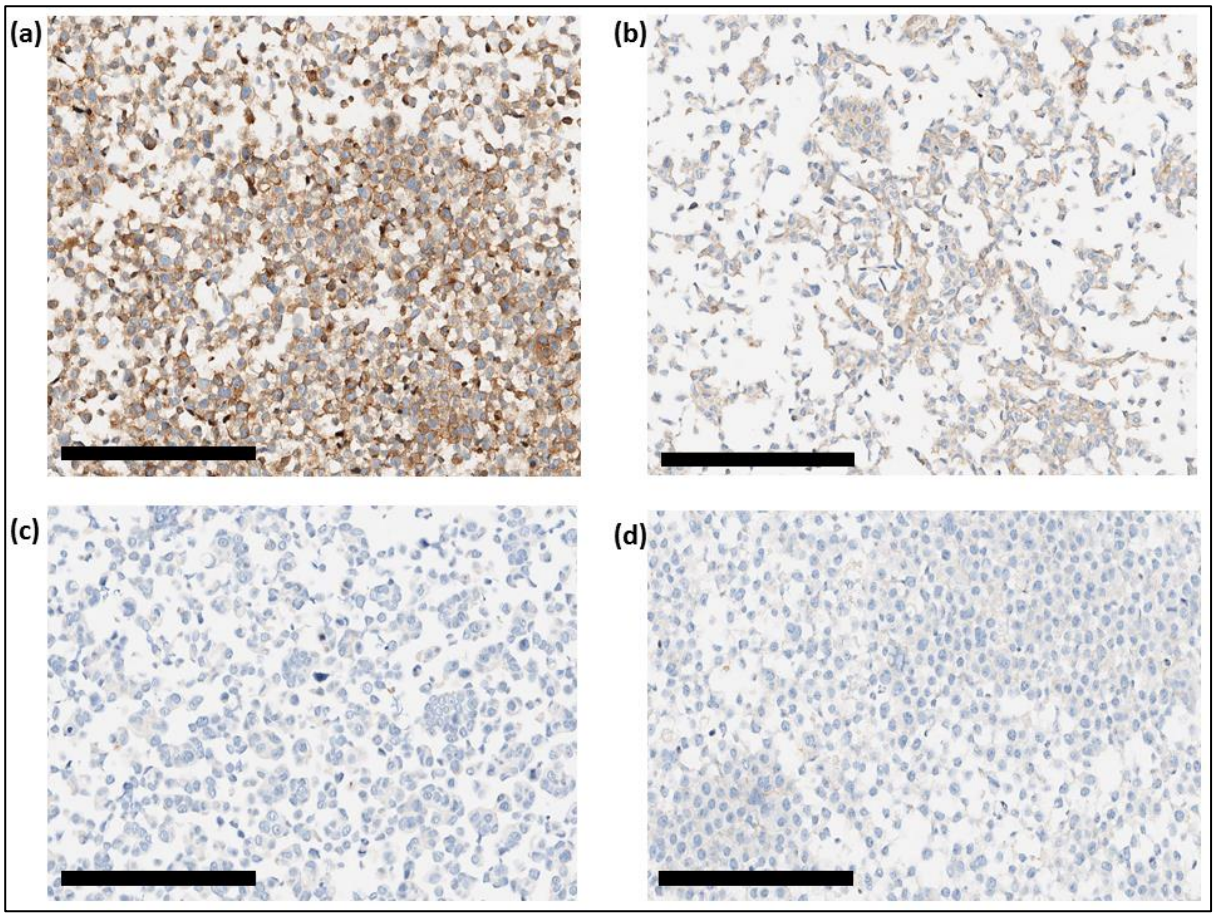

Figure 59 - Selected cell lines from the cell line block at higher magnification. Antibody used at a concentration of 1 in 100. Scale bars = 200 µM. There is strong staining in dedifferentiated chondrosarcoma HT1080 cells (a). Moderate staining is demonstrated in SJSA-1 osteosarcoma cells (b). There is absent staining in MCF-7 breast carcinoma cells (c) and the negative control BJAB Burkitt's lymphoma cells ($BJAB^{LexR}$) (d).

3.4 Discussion and future direction

There are two classes of human TRAIL receptors: The full-length intracellular death domain containing receptors, death receptor 4 (DR4) and death receptor 5 (DR5). They can induce apoptosis and are most widely expressed. The non-death domain containing receptors are decoy receptor 1 (DcR1), decoy receptor 2 (DcR2) and osteoprotegerin (OPG), which also functions as soluble receptor activator of NF-kB ligand (RANKL) also known as TNFRSF-11. At the plasma membrane, a GPI (glycosylphosphatidylinositol) anchor attaches decoy receptor 1 which lacks an intracellular domain. Decoy receptor 2 (DcR2) contains a cytoplasmic domain that is reported to induce NF-kB activation but not apoptosis as it had caused only a truncated death domain as discussed in the DcR section below.

Death receptor expression

In summary, all bone sarcoma cell lines were found to express death receptor 5 (DR5) also known as TRAIL-R2, particularly the HT1080 dedifferentiated chondrosarcoma cell line and the SJSA-1 and MG63 osteosarcoma cell lines at both RNA and protein levels. The Ewing's sarcoma TC71 cell line also expresses DR4 (TRAIL-R1). The TC71 and SJSA-1 osteosarcoma cell line expressed decoy receptor 2 (DcR2).

DR expression can be in a mature processed form (signal peptide cleaved) or as a non-processed form. Post-translational modification can occur and for example, glycosylated and non-glycosylated forms usually exist. For DR4 as well as DR5, the theoretical molecular weight for the processed, mature form is approximately 42 kDa. So, for some samples at a certain differentiation stage or cancer grade, only the precursor form may be present, the mature form or both forms together. Western blotting data demonstrated DR4/DR5 receptor mature form expression in all the bone sarcoma cell lines. Band intensity from western blotting did not always reflect, however, the MFI in flow cytometry and transcript level abundance in the qRT-PCR data obtained.

DR5 expression was visible on western blotting for most cell lines. The strongest expression was in the HT1080 cell line. The weakest in the SAOS-2 cell line. The findings correlated to cell surface expression flow cytometry. The membrane,

cytoplasm and nuclear subfractionation portions also demonstrated the high level of DR5 surface expression in the HT1080 cell line. Interestingly the very high surface and total protein expression of DR5 in the non-malignant NHDF cell line was not found at the transcriptional level unlike for the sarcoma cell lines (HT1080, MG63 and SJSA-1) and is probably due to a different post-transcriptional process in malignant and non-malignant cells. For DR4 there was similarities between transcript levels and protein levels but only the TC71 cell line had high surface levels contrary to other sarcoma cells cell lines (MG63 and SAOS-2) having demonstrable levels on PCR and western blotting but not at the surface. This could be due to different processes occurring at the membrane level (discussed further in Chapter 4).

Death receptor isoforms

Evidence of more than one DR5 isoform could also be seen on western blotting in U2OS, TC71, SJSA-1, MG63, SAOS-2, HT1080, BMMSC cell lines and the positive control Jurkat cell line [167,168,198,199]. Isoform function requires further investigation; however, the short isoform (DR5-S) has been postulated to have a greater role in the activation of caspase 8 compared to the long isoform (DR5-L). The short isoform has a predicted molecular mass of 40 kDa and the long isoform 43 kDa. They are generated by alternative pre-mRNA splicing and differ by a 29 AA extension in the extracellular domain [200,201]. Further recent investigations reveal that this soluble extracellular domain in the long isoform of DR5 has a function in inhibiting the interactions between DR5 to DR5 through disruption of receptor oligomerisation required for activation of TRAIL-R. This has proven interest due to the fact that the short or long isoforms are present which could be used as a viable predictive biomarker for TRAIL therapy. The literature states that DR5 exists in monomeric (M), dimeric (D), trimeric (T), and oligomeric (O) forms, which can be visualised when protein samples are run in non-reduced form [167].

I have also found in my study that DR5 in bone sarcoma cell lines has a short and long isoform (Figure 44). In terms of the function of these isoforms, it is unclear; however, in the induction of apoptosis, the short isoform may have a more important role. In order to investigate the isoform expression in bone sarcoma cell lines, I used the Jurkat cell line as a control because the long isoform of DR5 is highly expressed in this cell line

[167,168]. In my project the long isoform band appeared of similar intensity to the short isoform in bone sarcoma cell lines on western blotting. BMMSCs contained both isoforms; however, NHDF cells appeared to express greater quantities of the short isoform. Recently, it is thought that because the long isoform is present, this could confer resistance to apoptosis [167]. In the SJSA-1 the larger long isoform appears slightly stronger; however, this requires further investigation.

There are different isoforms for DR4 including the complete or short isoform (bDR4), and their involvement in TRAIL sensitivity requires further investigation. The bDR4 isoform has been found in TC71 and the A673 Ewing's sarcoma cell lines [202]. This is a band found on western blots at lower molecular weight compared to the one DR4 band detected in my western blot. The bDR4 isoform requires a specific antibody for detection [202]. Interestingly when DR4 has been knocked down using shRNA, the cells were no longer sensitive to TRAIL despite the presence of DR5. The same study found high relative gene expression of DR4 compared to DR5 (in the TC71 cell line) a trend also found in my PCR results (Figure 37); however, they also found elevated levels of DcR1 which was not observed in my study. There is a correlation between the level of expression of DR4 and sensitivity of TRAIL in Ewing's sarcoma cell lines [202]. This particular study found a more pivotal role for DR4 in TRAIL sensitivity through DISC formation, procaspase 8 and c-FLIP recruitment [202]. This is consistent with previous reports that have investigated DR4 in the MCF-7 breast cancer cell line [203,204]. Reports also suggest that DR4 is the more important death receptor in pancreatic cancer despite the presence of DR5 and targeting DR4 is more efficacious than the use of 'wild-type' TRAIL, which can target both receptors if pre-oligomerised [205]. I have investigated this in bone sarcoma cell lines in Chapter 5.

Function of the death receptors

At 37 ^{o}C TRAIL binds to DR5 with higher affinity than the other membrane expressed TRAIL receptors. It is likely that under physiological conditions, binding to DR5 would be favoured especially when endogenous TRAIL is limited. I have found in the current investigation that the surface presence of DR5 reflects that found in cell lines derived from pancreatic cancer, chronic lymphocytic leukaemia, or mantle cell lymphoma described in the literature [206]; however, these cells have been found to use only DR4

for apoptosis induction by TRAIL. In addition, apoptosis induction via DR5 requires cross-linking of the untagged soluble TRAIL implying that the DR5 requires higher apoptotic threshold than DR4 [206].

However, some leukaemia and lymphoma cell lines undergo antibody-mediated DR5 triggering, which is sufficient to produce apoptosis without additional crosslinking. Data from a previous study has highlighted that DR4 and DR5 fulfill partially overlapping but distinct functions, many of which remain to be discerned [206]. In this study, I have also found that DR5 in bone sarcoma cell lines has a short and long isoform. The role of these isoforms is unclear; however, some reports suggest that the short isoform may be more important for the induction of apoptosis. The Jurkat cell line is known to express the long isoform of DR5 to a greater degree and was used as a control cell line to investigate the isoform expression in bone sarcoma cell lines [167,168]. In my project the long isoform band appeared of similar intensity to the short isoform in bone sarcoma cell lines on western blotting. BMMSCs contained both isoforms; however, NHDF cells appeared to express greater quantities of the short isoform. It has been postulated recently that presence of the long isoform could confer resistance to apoptosis [167]. In the SJSA-1 the larger long isoform appears slightly stronger; however, this requires further investigation.

There are reports of non-canonical effects when TRAIL binds to DRs, as reviewed by Von Karstedt *et al.,* (2017) [206]. Non-canonical signalling triggers the formation of a secondary cytosolic complex retaining FADD, TRAF2 and NF-kB essential modifier (NEMO). Both this complex and the DISC activates NF-kB, p38, JUN N-terminal kinase (JNK) and ERK. RIPK1, is also associated with DRs when caspase-8 is inhibited and is required for TRAIL-induced Src and STAT3 activation and promotion of migration. LUBAC is present in both complex one and complex two and TRAIL signalling limiting caspase-8 activation enabling recruitment of inhibitor of kB (IkB) kinase (IKK) complex resulting in NF-kB activation [206].

Potential differing function based on cellular location

It has become evident that the subcellular localisation of TRAIL and the DRs could regulate specific functions and therefore play a role in pro-apoptotic and pro-survival

signalling. The pattern of staining in primary tissue should be evaluated to analyse any correlation with tumour growth and response to TRAIL based therapeutics.

Nuclear DR5 has been shown to inhibit microRNA maturation and thus enhances the malignancy of tumours [194]. High cytoplasmic levels in bladder cancer patients have been correlated with improved recurrence free rates [207]. The differential distribution of DRs in the cellular compartments could be a reason for the discrepancy between receptor expression and prognosis. It has also been postulated that the DcRs can also occur in intracellular compartments, and however act in a largely undefined manner [208,209].

DR5 which is normally expressed at the plasma membrane, has also been found in the nucleus where it promotes proliferation by interacting with accessory proteins of the microprocessor complex leading to impaired maturation of microRNA let-7 which is known to be a negative regulator of KRAS mRNA [208]. It, therefore, appears that the sub-cellular compartmentalisation of DR5 may determine distinct DR5 signalling.

I attempted sub-fractionation followed by western blotting of the fractions and found that in the H1080 dedifferentiated chondrosarcoma cell line there appears to be strong expression in all compartments: Nuclear, cytoplasm, and plasma membrane.

HUVECs cells express both DR4 and DR5 on the surface and are known to be capable of inducing NF-kB activation upon ligation. HUVECs cells are known to express DcR1/TRAIL-R3, a factor for resistance to TRAIL-induced apoptosis. As reported by others, the removal of this receptor can result in sensitivity to TRAIL-induced apoptosis [210]. Consistent with the theory that location may determine function, DcR1 could be found in the cytoplasmic organelles in the HUVEC cell line. Whereas in a different cell line (MRC-5 fibroblasts), DcR1 was predominantly localised in the nucleus, suggesting that the post-translational mechanisms that direct newly synthesised protein to different compartments may play a role in determining where the DcR is deployed on the cell surface and have a protective role from TRAIL-induced apoptosis on the cell surface. The significance for nuclear localisation of DcR1 is currently unknown but it has been of interest that DcR1 has sequences compatible with those needed to bind to the nuclear export factor exporting 1, as reviewed by Don Zhang *et al.,* (2000)[162].

Effect of death receptor expression in the tumour microenvironment

In addition to pro-apoptotic effects of TRAIL binding to DR4 and DR5 and non-canonical effects, there are also potential tumour suppressive roles of TRAIL such as binding to DRs on tumour supportive immune cells inducing apoptosis in those cells. Also, TRAIL can kill immune cells that express PD-L1 or PD-L2. These immune cells can inhibit the cytotoxic T-cell activity on the cancer cells through binding to PD-1 on T-cells. T-cells are liberated and are able to perform their function when the PD-L1/ PD-L2 and PD-1 interaction is disrupted. The pro-tumourigenic role is thought to arise as TRAIL can bind to the DRs on the cancer cells, which thereby release cytokines and stimulate tumour associated macrophages [206]. The actions of TRAIL in cancer have, therefore, been described as a double-edged sword.

Significance of decoy receptor expression

Three decoy receptors (DcRs) are known to interfere with TRAIL signalling and have been investigated in the literature: DcR1 (TRAIL-R3), DcR2 (TRAIL-R4) and OPG. The main mechanism of interference with DR signalling is via the reduction of signalling-competent receptor complexes. However, there is also data to suggest that the expression of DcR2 (TRAIL-R4) is related to induction of survival pathways such as induction of NF-kB and Akt as another mechanism that contributes to its inhibitory effect [211,212]. Inhibitory effects have been found to be reversed on inhibition of Akt [212]. Decoy receptor 1 (DcR1), TRAIL-R3, was not found to be expressed at significant levels on all of the bone sarcoma cell lines.

DcR2 is considered to be a p53 target gene, which regulates its expression via an intronic p53 binding site. DcR2 can be higher in malignant cells compared to non-malignant cells and has been related to a decreased survival in patients with prostate carcinoma. The combination of SiRNA targeting DcR2 and overexpressing full-length TRAIL in the PC3 cells using an adenoviral vector (Ad5hTRAIL) decreased PC3 colony number percentage [213]. It has also been postulated that the DcR may have shifting functions depending on subcellular location and internalisation upon TRAIL ligand stimulus but this requires further study [208,209,214]. There are situations whereby the decoy mechanism may be expected to play an important role such as when there are high levels of the DcRs or at very low ligand concentrations (Neumann et al., 2014).

DcR1 and DcR2 have been postulated to function as oncogenes and they are also reported to inhibit tumourigenesis. The reason that they may inhibit tumourigenesis is that they can reduce NF-kB activity indirectly by reducing signalling through DR4 and DR5. This is believed to play an anti-apoptotic role and is part of the pathogenesis of several human cancers.

DcRs can also block the NF-kB activation via DR4 and DR5 in response to TRAIL [215]. More recently, it has been thought that the DcRs can interfere with DR signalling-competent receptor complexes, as they are arranged in a heteromeric ligand receptor cluster driven by PLAD (pre-ligand assembly domains) -mediated receptor and ligand receptor interactions. However, it is thought that DcR2, can signal to activate NF-kB and Akt, which is suggested as an additional mechanism contributing to the inhibitory effect of this decoy receptor. The activation of NF-kB and Akt is mediated by its truncated death domain, which is incapable of inducing apoptosis as it cannot form the death-inducing signalling complex (DISC).

Interestingly, there is conflicting information about the function of the truncated death domain, and it is thought that it does not play a role in the inhibitory function of the receptor. However, data by Degli-Esposti *et al.,* 1997 [216], suggested that the activation of NF-kB via its cytoplasmic domain is through a unknown molecular mechanism and it may well be that other anti-apoptotic proteins are also involved in the DcR2-mediated resistance against TRAIL.

Interestingly, DR4 can mediate the phosphorylation of IkB-alpha, an inhibitor of p65 NF-kB, which is a central step in the activation of the classical NF-kB pathway. This was inhibited by over-expression of functional and cytoplasmic DcR2. Interestingly, I have found in TC71 cell Ewing's Sarcoma cell line, expression of both DR4 and DcR2 on the cell surface, and this mechanism may have a role in this cell line. DcR1 and OPG levels, however, were found to be low at RNA and surface protein levels.

Overall, however, TRAIL is not thought to be a potent inducer of NF-kB activation and may be controlled in a cell-specific manner. Also, most investigations have studied apoptotic and non-apoptotic TRAIL receptors and the interference between them at the membrane level. However, it is clearer now that the DcRs, can also be carried by

intracellular compartments and may act in an undefined manner thus far; relocalisation may possibly shift their function.

Another DcR which has been of interest in the literature is osteoprotegerin (OPG). It is thought that bone marrow-derived stem cells, and the MG63 osteosarcoma cell line can produce a quantity of OPG that can inhibit apoptosis. This was reviewed by Picarda *et al,* 2012 [217]. The biological importance of the interactions has been of interest because of findings that at physiological conditions, OPG combined TRAIL with an affinity similar to that of RANKL, and also breast and prostate cancer cell lines are quoted to 'produce sufficient OPG to protect them against TRAIL-induced apoptosis'. OPG can also be produced by bone marrow-derived stem cells which have been derived from breast or prostate cancer patients. They have been found to produce sufficient levels of OPG to protect tumour cells from TRAIL-induced apoptosis. The bone-derived OPG can promote the survival of the tumour cell types within the bone microenvironment [217].

Investigators have also found that stem cells, fibroblasts and endothelial cells can abundantly release OPG. When TRAIL is administered, they found that the spontaneous release decreased upon recombinant TRAIL therapy through a decrease of photophosphorylation levels of P38/MAPK, suggesting this is a pathway involved in stabilisation of OPG mRNA [218]. I found elevated expression of OPG at the RNA level in the normal human dermal fibroblast (NHDF) cell line in comparison to bone sarcoma cell lines.

In summary, with regards to DcRs, there are three main possible mechanisms they are thought to act by: (1) Classical decoy mechanism of binding TRAIL more than the unbound TRAIL to the death receptors. This is known as classical decoy mechanism but has not been shown to have a major role in experimental conditions. (2) Formation of signalling-incompetent receptor complexes via PLAD interactions. (3) Activation of DcR-mediated survival pathways in certain circumstances.

Death receptor gene methylation

The four DRs I have focussed on are located in tandem fashion at chromosome location 8p21-22. Methylation is known to initiate at one or more chromosomal CPG

sites in a promoter region and spread to adjacent sites along the DNA strand until it meets a contracting force in the form of open and active chromatin.

Methylation and the resulting silencing have been thought to occur to silence proapoptotic effects of DR4 and DR5 genes and may also result in silencing of the adjacent DcR1 and DcR2 receptor genes. It has been postulated that this methylation may not be of clinical importance of DcRs and that it may be just a secondary effect. However, it has been found that the methylation of DcRs can occur independently of each other and of DR4 and DR5. DcR1 and DcR2 are thought to function as oncogenes because of postulated antiapoptotic effects. The silencing of DcRs could favour tumourigenesis.

So, it is likely that that methylation of DcRs is not a secondary event and may play a role in tumour pathogenesis. This is of interest as DRs can activate the NF-kB pathway as initially described by Masters SA *et al*., (1997) and DcRs can lack ability to activate the NF-kB pathway [219]. However, more recently, DcR2 has been related to increasing NF-kB prosurvival signalling [158] and downregulation using siRNA has been found to sensitise cancer cell lines including breast and colorectal to TRAIL and chemotherapeutic agents [158,220].

So, in this regard, DcRs may block the NF-kB activation by DR4 and DR5. This is because DRs can activate NF-kB and in turn activate proliferation and survival signals in cell types and other circumstances which are under investigation. The DcRs may block this and methylation and suppression of their transcription and translation may contribute to reduced proapoptotic signalling via NF-kB.

If DcRs can block proliferative potential, then down regulating these receptors is a hypothesis that is consistent with potential increased progression of the tumour and low DcR expression. I have found that, on the surface level, the majority of sarcoma cell lines do not express DcR1; however, there are two bone sarcoma cell lines, the SJSA1 osteosarcoma cell line and the TC71 Ewing's sarcoma cell line that express DcR2 and would be of interest to study further to clarify the DcR mechanism (explored in Chapter 5).

TRAIL

It has been suggested that in some cell lines such as the prostate carcinoma cell line (PC3), that expression of TRAIL can reduce tumourigenic potential [221]. However, it has also been highlighted as a prognostic marker in patients newly diagnosed with acute myeloid or acute lymphoblastic leukaemia as they express significantly lower levels of TRAIL in the serum compared to the control [222,223]. After start of therapy, increased TRAIL levels were found to be predictive of better patient survival [223]. Higher expression has been associated with low tumour grade and better progression free survival in ovarian and renal cancer patients [224,225]. Loss of expression has been correlated with malignant progression [226,227].

Cancerous cells may evade apoptosis upon downregulation of TRAIL. However, it has also been associated with tumour progression and shorter survival in patients with renal and colorectal cancers [228,229] by protecting tumour cells from the immune system and promoting metastases. Other studies, however, have shown no correlation or no prognostic value [230-232].

In vitro investigations were performed as part of this project to investigate the TRAIL expression in cancer cells using western blotting and flow cytometry and found no evidence of significant TRAIL expression at the protein level in bone sarcoma cells. My conclusion here is that there is reduced TRAIL expression thereby less of a tumour suppressive role in the tumour microenvironment, which highlights the aggressiveness of bone sarcoma. Also, the lack of DcR expression may signify that TRAIL signalling, when present, is less inhibited in these cell types thereby indicating more of a non-canonical activity of the TRAIL binding to DRs and more stimulation of proliferation.

Chapter 4. Exploration of factors that reduce the susceptibility to TRAIL therapy using real-time polymerase chain reaction (RT-PCR)

4.1 Introduction

The resistance of tumour cells to TRAIL has been postulated to rely on a single mechanism. This is different to the mechanism of resistance in non-transformed cells, which can be due to multiple pathways. Van Dijk *et al.,* (2013) found that factors such as cFLIP, also known as 'cellular FLICE-like inhibitory protein, anti-apoptotic B cell lymphoma two (Bcl-2) proteins, and X-linked inhibitor of apoptosis protein (XIAP)', were independently able to confer resistance to TRAIL [233]. Inhibition or removal of the single anti-apoptotic 'pivotal' block could be sufficient to restore sensitivity. In contrast however, the deficiency of only one of these proteins was not sufficient to elicit TRAIL sensitivity in non-malignant cells.

Proliferation and survival involves signalling through Ras and Akt pathways, which are interconnected [234]. Akt is normally activated by a growth factor binding to a receptor tyrosine kinase (RTK) but can also be activated by mutations downstream such as PIK3CA or loss of inhibitor PTEN reported in myxoid/round cell liposarcoma and aggressive leiomyosarcoma respectively. The Ras pathway is involved in differentiation, proliferation, survival and invasion and may cross-activate the Akt pathway via PI3K [234]. The molecular pathways involved in sarcomagenesis and potential targets have been summarised in a diagram by Demicco *et al.,* (2012) (Figure 60).

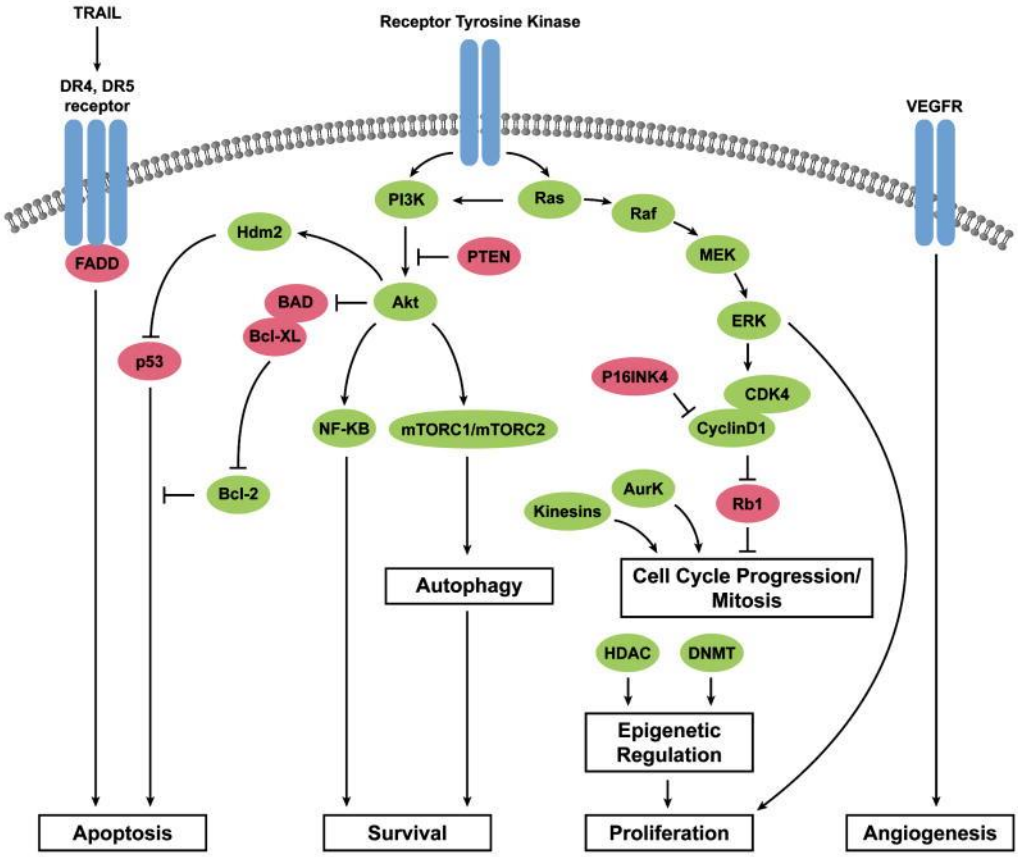

Figure 60 – Molecular pathways involved in sarcomagenesis. Green = Protumourigenic factors activated or overexpressed in sarcoma. Red = Tumour suppressors that may be inactivated in sarcoma. Adapted from [234].

The main aims of this chapter are to:

1. Examine transcriptomic differences in single factors that may confer TRAIL resistance in bone sarcoma cell lines (and compare to non-malignant cells), which if targeted may increase sensitivity to TRAIL.

2. Provide a foundation for further investigation at the protein level and use of specific sensitising agents to be used alone or combined with TRAIL.

4.2 Inhibitors of apoptosis

Cellular FLICE-inhibitory protein (c-FLIP)

$cFLIP_L$ transcript levels were found to be the greatest in the HT1080 dedifferentiated chondrosarcoma, the U2OS osteosarcoma and the TC71 Ewing's sarcoma cell lines (Figure 61).

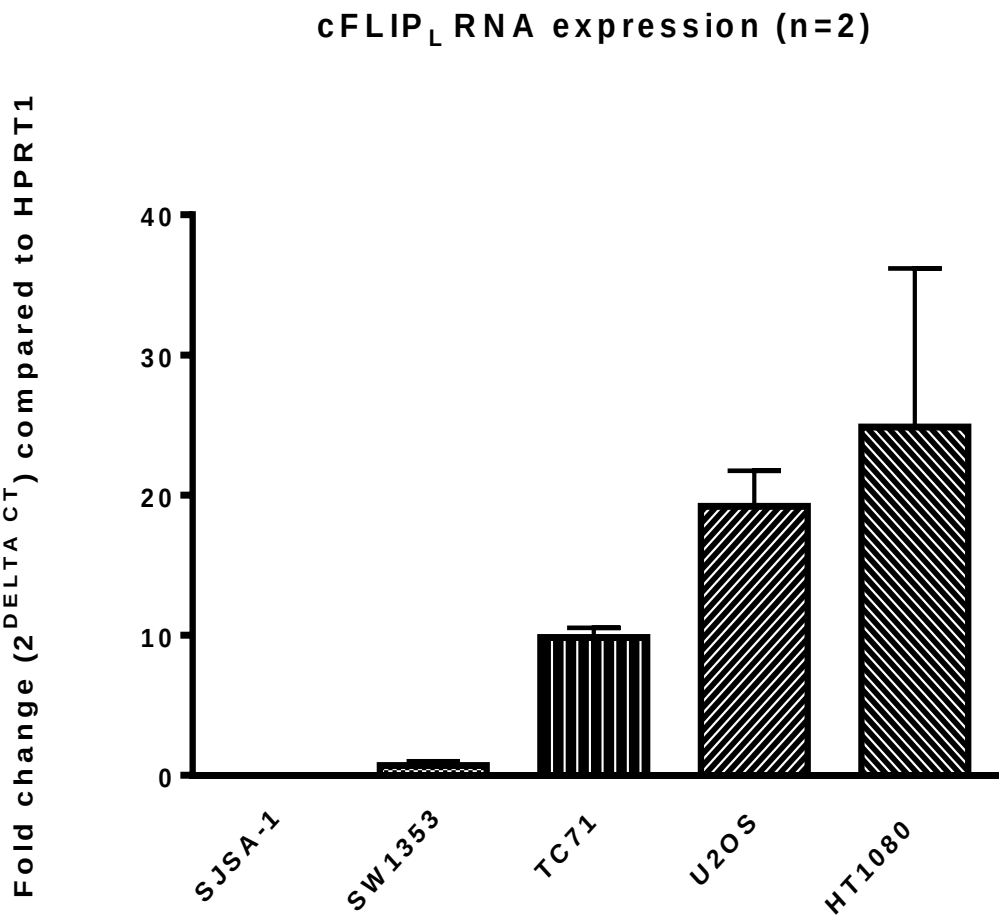

Figure 61 – qRT-PCR used to determine $cFLIP_L$ mRNA expression levels in bone sarcoma cell lines (mean +/-SEM, n = 2). $cFLIP_L$ was found to be elevated in the HT1080 dedifferentiated chondrosarcoma, the U2OS osteosarcoma and the TC71 Ewing's sarcoma cell lines.

X-linked inhibitor of apoptosis protein (XIAP)

The highest transcript levels of X-linked inhibitor of apoptosis protein (XIAP) were found in the SAOS-2 osteosarcoma cell line (Figure 62).

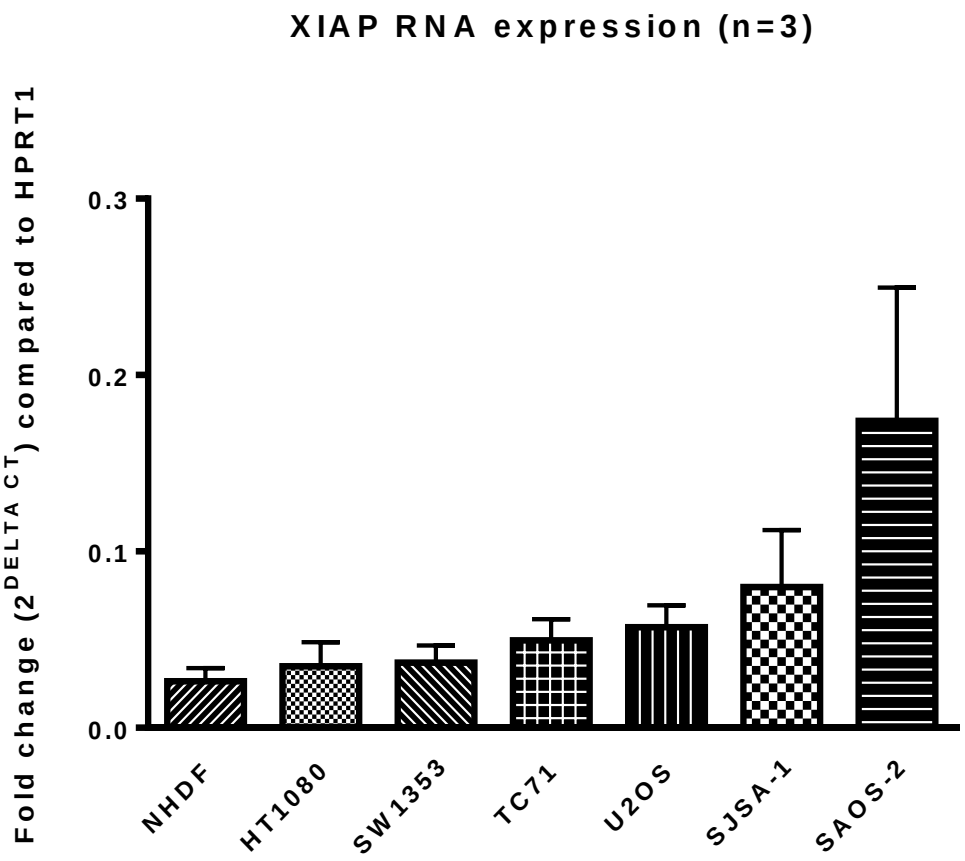

Figure 62 – qRT-PCR used to determine XIAP mRNA expression levels in bone sarcoma cell lines (mean +/-SEM, n = 3). Highest levels were found in the SAOS-2 cell line. Elevated XIAP levels is a factor thought to confer resistance to TRAIL.

4.3 Proliferation and survival

Akt

In the SAOS-2 osteosarcoma cell line and HT1080 dedifferentiated chondrosarcoma cell line, elevated Akt mRNA levels could be observed; however, elevated levels were also present in normal human dermal fibroblast cell line (NHDF) and MSCs (Figure 63).

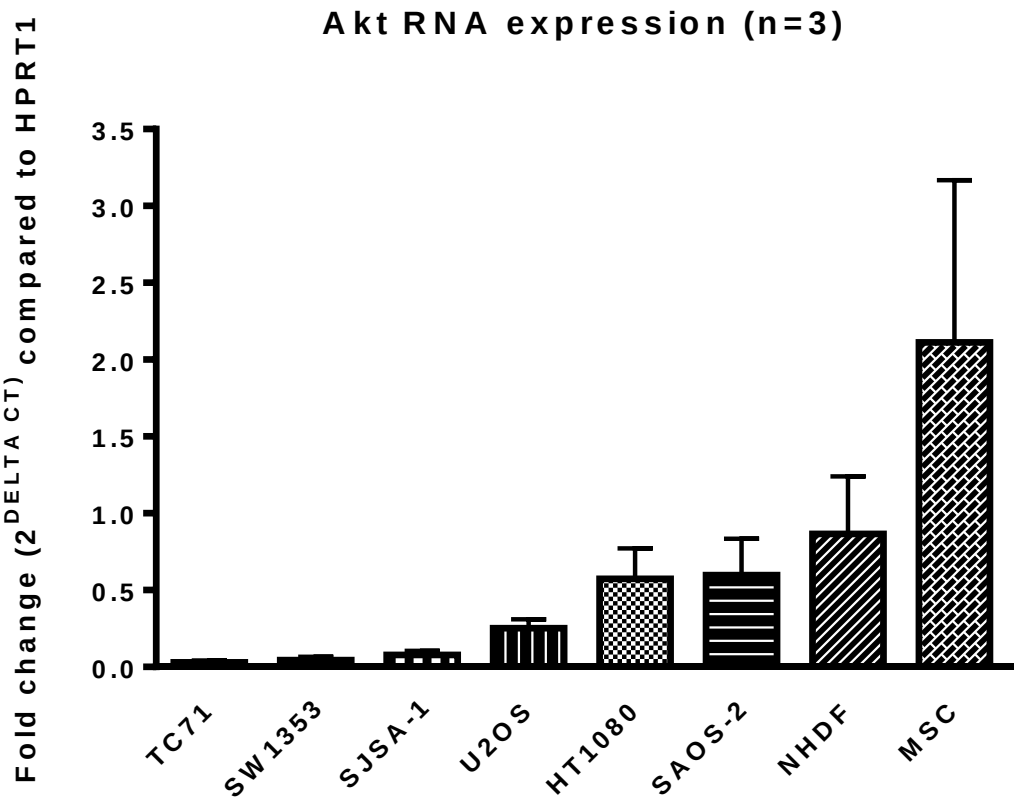

Figure 63 – qRT-PCR used to determine Akt mRNA expression levels in bone sarcoma cell lines (mean +/-SEM, n = 3). Akt was expressed at the greatest level in the human bone marrow-derived mesenchymal stem cells (MSCs).

H-Ras

The SAOS-2 osteosarcoma cell line has also increased H-Ras transcript levels compared to the other bone sarcoma cell lines. The MSCs also have significantly elevated levels (Figure 64).

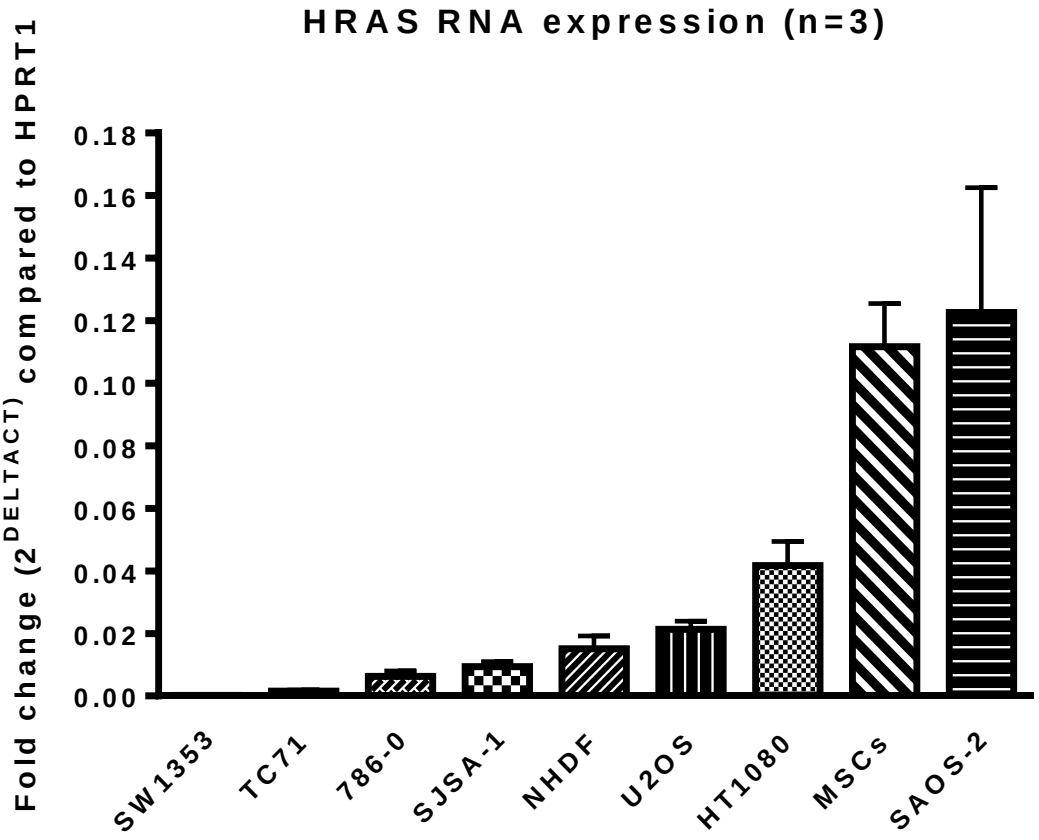

Figure 64 - qRT-PCR used to determine H-Ras mRNA expression levels in bone sarcoma cell lines (mean +/-SEM, n = 3). H-Ras expression in bone sarcoma cell lines (mean +/-SEM, n = 3), normal human dermal fibroblast (NHDF) cell line, mesenchymal stem cells (MSCs) and the 786-0 renal clear cell adenocarcinoma cell line. Elevated H-Ras levels has been one of the factors thought to confer resistance to TRAIL.

Phosphatase and tensin homolog (PTEN)

Phosphatase and tensin homolog (PTEN) expression was found to be elevated in U2OS osteosarcoma and SW1353 chondrosarcoma cell lines and also in MSCs (Figure 65).

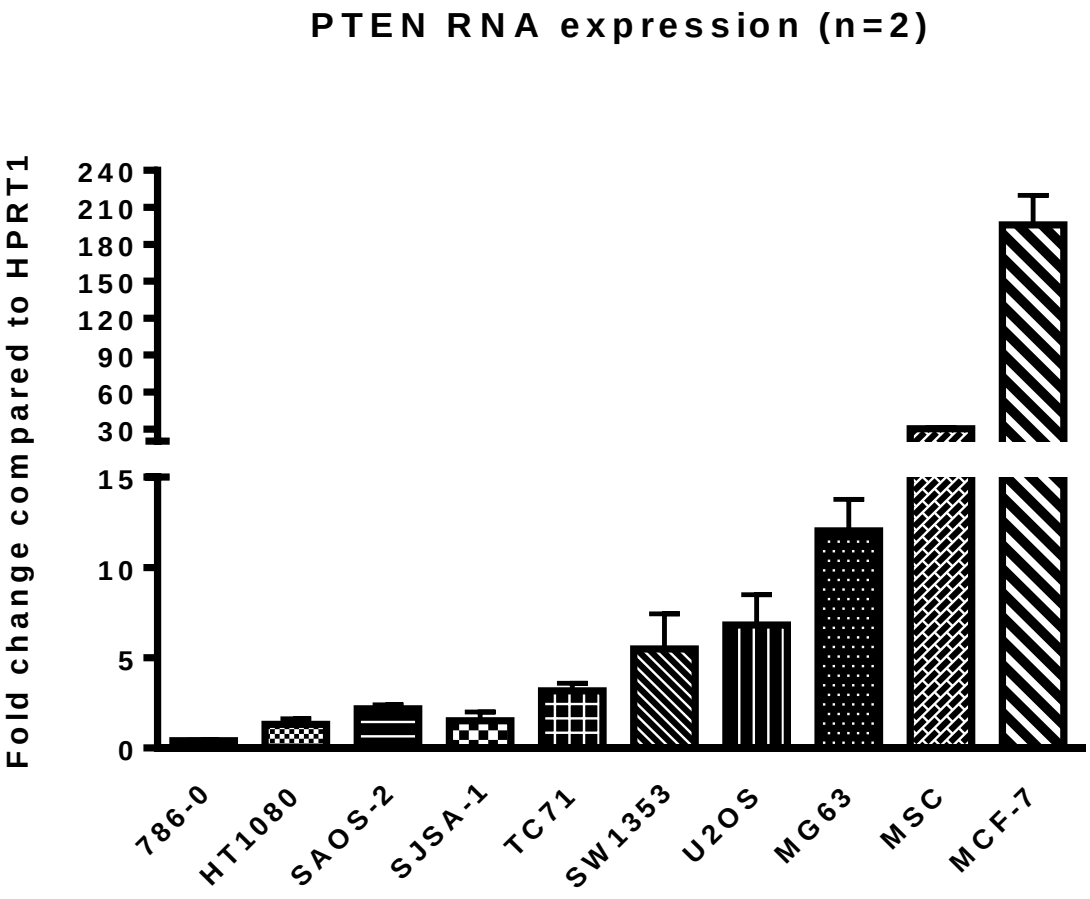

Figure 65 – qRT-PCR used to determine PTEN mRNA expression levels in bone sarcoma cell lines (mean +/-SEM, n = 2). PTEN mRNA transcript levels (mean +/-SEM, n = 2). The MCF-7 breast carcinoma cell line was used as the positive control as described previously [159] (Fold change = 196). MSCs PTEN transcript levels were also elevated (Fold change = 30). 786-0 renal adenocarcinoma cells were included as negative control as recently described [235].

4.4 TNF-related apoptosis-inducing ligand (TRAIL)

The SJSA-1 and SAOS-2 osteosarcoma cell lines were found have elevated TRAIL transcript levels compared to other cell lines; however, it was much lower than the positive control 786-0 cell line (Figure 66).

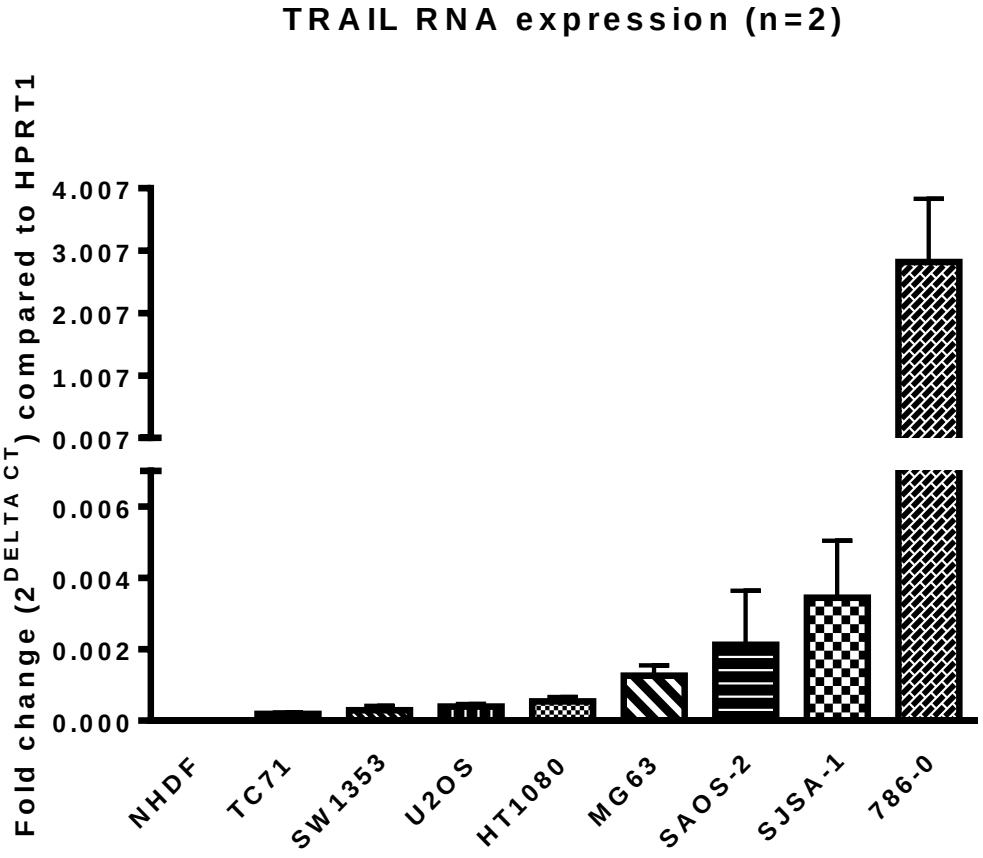

Figure 66 – qRT-PCR used to determine TRAIL mRNA expression levels in bone sarcoma cell lines (mean +/-SEM, n = 2). Low levels in bone sarcoma cell lines and the NHDF cell line in comparison to the positive control cell line renal clear cell carcinoma (786-0) cell line. The SJSA-1 osteosarcoma cell line appears to express the highest TRAIL transcript levels in comparison to other bone sarcoma cell lines.

4.5 Chondroitin sulfate proteoglycan 4 (CSPG4), also known as melanoma-associated chondroitin sulfate proteoglycan (MCSP) or neuron-glial antigen 2 (NG2)

RT-PCR data revealed high NG2 expression in MG63 osteosarcoma and SW1353 chondrosarcoma cell lines (Figure 67).

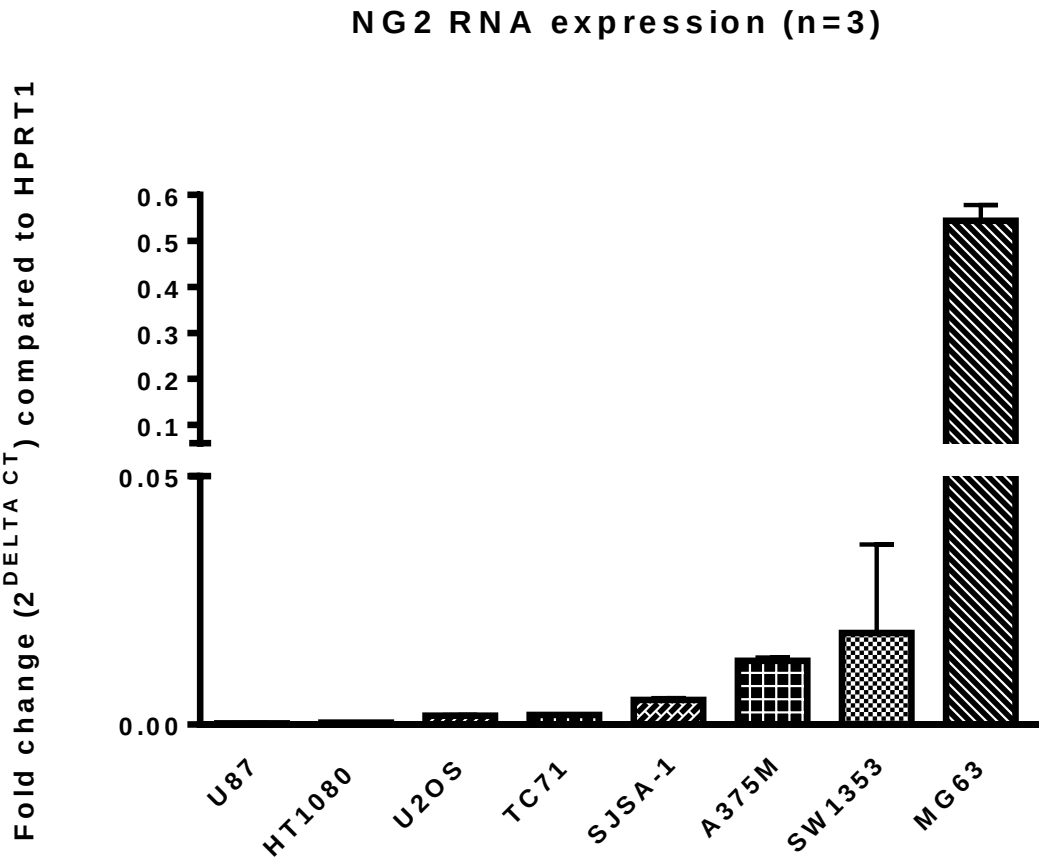

Figure 67 – qRT-PCR used to determine NG2 mRNA expression levels in bone sarcoma cell lines (mean +/-SEM, n = 3). NG2 expression in bone sarcoma cell lines (mean +/-SEM, n = 3). NG2 levels were greatest in the MG63 osteosarcoma cell line. The A375M melanoma cell line was included as the positive control.

4.6 Discussion and future direction

c-FLIP

cFLIP has been thought to be a key regulator of receptor mediated apoptosis in cancer. The three splice variance identified, $cFLIP_L$, $cFLIP_S$ and $cFLIP_R$, all function as apoptosis inhibitors involved in the modulation of caspase-8 and 10 activity, both in physiologic and pathologic contexts [236,237]. A cell type specific pro-apoptotic role, depending on caspase-8 to cFLIP ratio has also been described for the long isoform [237]. The long isoform has been thought to be a 'critical factor in determining the balance between apoptotic and pro-survival signalling', as stated by Bagnoli *et al*. (2010). Dysregulation of the levels of $cFLIP_L$ is frequently found in tumours, where $cFLIP_L$ behaves as a potent inhibitor of DR dependent apoptosis [237].

Downregulation of cFLIP may represent an alternative novel therapeutic approach whose efficacy remains cell and tissue type dependent. Intracellular expression of $cFLIP_L$ and $cFLIP_S$ can be regulated at multiple levels and transcription of cFLIP has been shown to be modulated by NF-kB, c-myc and more recently direct regulation of cFLIP promoter by p63 in the epidermis [238]. cFLIP proteins have a short half-life in normal cells and their expression and turnover is controlled by the ubiquitin protein system. The proteasomal degradation is a critical point in determining the balance between cell death and prosurvival signalling dependent upon DR triggering [237].

Suppression of both isoforms using siRNA can enhance the sensitivity of the U2OS osteosarcoma cell line to TRAIL [239]. Other investigations suggest the long isoform c-$FLIP_L$ is the more important isoform to target. I have found that the HT1080 cell line expresses high levels of the $cFLIP_L$ transcript cFLIP inhibitory protein can be elevated in a number of Ewing's sarcoma cell lines [240], and is abundantly expressed in 18 of 18 patients. Caspase-8 was also expressed, but there was more inter- and intratumoural variation. In Burkitt's lymphoma, cFLIP expression correlates with chemoresistant disease and the expression of cFLIP in solid tumour cell lines can protect against chemotherapy induced apoptosis *in vitro*. De Hooge *et al.,* 2007, demonstrated that despite cFLIP expression in the Ewing's sarcoma cell lines, there was no relation between cFLIP expression and resistance to DR pathway immediate apoptosis. There

have been therapeutic strategies aimed at inhibiting cFLIP, by using siRNA, or small molecule inhibitors. However, this small molecule inhibition of cFLIP recruitment to the DISC is hampered by high homology among the DED-containing proteins [237].

Other strategies include combining TRAIL with chemotherapeutic agents that have been found to downregulate cFLIP expression and synergise with TRAIL in inducing cell death [237]. These include conventional drugs like doxorubicin, cisplatin, 5-fluorouracil, irinotecan, and the taxanes. Other agents which may be effective in regulating cFLIP expression include proteasome inhibitors and HDAC inhibitors. However, the overall cFLIP expression level can be cell and tissue type dependent [241].

Despite inconsistent results with regards to identifying cells that may be resistant, there does appear to be a clinical correlation between cFLIP expression and adverse prognosis in colon and endometrial cancer, Burkitt's lymphoma, and ovarian cancer. This may be useful in identifying patients at higher risk of cancer related death and who may benefit from alternate therapeutic modalities.

XIAP

There are many inhibitor of apoptosis proteins (IAPs) described in the literature. There are eight members of the mammalian IAP family:

Neuronal IAP, cellular IAP one (cIAP1), cellular IAP (cIAP2) two, X-chromosome-linked IAP (XIAP), survivin, ubiquitin-conjugating BIR domain enzyme Apollon, melanoma IAP and IAP-like protein two. Playing a direct role in apoptosis regulation are the following proteins, XIAP, cIAP1, cIAP2 and ML-IAP [242].

Targeting XIAP using siRNA has been found to suppress tumour growth in combination with TRAIL in preclinical models of pancreatic cancer [243]. Small molecule inhibitors of XIAP together with TRAIL have also been found to reduce leukaemic burden in a mouse model of acute lymphoblastic leukaemia (ALL) [244]. Smac mimetics have also been developed and act by blocking IAP proteins, as naturally occurs with the endogenous antagonist Smac Diablo molecule. The proteins XIAP, cIAP1 and cIAP2 are

antagonised by Smac which has been used clinically to induce or facilitate the induction of apoptosis.

I have found elevated XIAP transcript levels in the SAOS-2 and SJSA-1 osteosarcoma cell lines and further study should investigate expression at the protein level; however, significant susceptibility to Smac mimetics was not found when coadministered with SuperKillerTRAIL (SKT) (explored in Section 6.4).

H-Ras

H-Ras has been implicated in conferring resistance to TRAIL in cell lines such as A549, HT29, and 786-0 and the inhibition of H-Ras can sensitise cells to TRAIL [164]. This is in comparison to the more marginal effects observed when K-Ras is inhibited. It has been shown that H-Ras is involved in the transport of DR4 and/or DR5 to the cell membrane as inhibition of H-Ras in cell lines with low surface levels restored the surface expression of DRs. Total protein was not altered, therefore it has been concluded that the increase in cell surface expression is due to the redistribution of receptors from the intracellular compartments to the cell membrane, through lipid-raft dependent events occurring at the post-translational level [157]. Other events of importance occurring at the cell membrane, which can confer resistance include constitutive endocytosis, which has been reported in breast cancer cells such as the MCF-7 cell line [157]. I have found that the surface expression of DR5 and DR4 in SAOS-2 is lower when compared to other sarcoma cells lines (discussed under flow cytometry), which is in keeping with this theory. However, the HT1080 and SJSA-1 cell lines have the highest levels of surface DR5. The TC71 cell line expressed both surface DR4 and DR5. Further investigation of this theory would include assessing the levels of H-Ras at the protein level and the use of H-Ras inhibitors to assess whether there is an increase in surface DR4 or DR5 in the SAOS-2 cell line.

Akt

Levels of Akt and DR5 at the mRNA level correlate with NSCLC (non-small cell lung cancer) staging, differentiation and lymph node metastasis [193]. Levels of Akt were much higher in NSCLC tissues of late stage, poorly differentiated and with lymph node metastasis, suggesting exertion of its function through transcriptional regulation. This

was also the case with DR5 expression levels. Akt phosphorylation has been related to resistance to TRAIL in NSCLC [193]. I decided to investigate Akt mRNA levels in the sarcoma cell lines. In the HT1080 cell line, elevated Akt mRNA levels could be seen in the PCR data; however elevated levels are also present in normal fibroblast cell line, in contrast to other studies [193] in which lower levels were found in normal tissues adjacent to NSCLC tissues. However, Akt isoforms (my primers were designed to detect all isoforms) can be similar in normal and malignant tissues [245]. Increased level of DcR1 mRNA can be found in normal tissues, similar to our DcR1 findings in the NHDF cell line in comparison to the bone sarcoma cell lines (except for the U2OS cell line) this was not reflected, however, in the surface DcR1 receptor data using flow cytometry.

Inhibition of Akt can sensitise cells (human umbilical vein endothelial cells) to TRAIL induced apoptosis. Agents that can inhibit Akt such as perifosine and triciribine sensitise AML and prostate cancer cells to TRAIL induced apoptosis respectively. Interestingly novel agents are being developed to enhance DR4 expression and downregulate Akt via siRNA [246].

PTEN

Phosphatase and tensin homolog (PTEN) limits the proliferation of cells and has an inhibitory effect on the PI3K/AKT pathway. Reduction in PTEN mRNA levels and lower staining of PTEN on IHC has been observed in osteosarcoma tissues compared to normal adjacent tissues. Similarly, this has been found for NF-kB and has been correlated to poorer survival [247]. The influence of microRNAs on PTEN is thought to promote anti-apoptotic effects, proliferation and invasion in Ewing's sarcoma and osteosarcoma [248,249].

TRAIL

More recently, it has been postulated that TNF-related apoptosis-inducing ligand (TRAIL) may promote cancer through the stimulation of the secretion of factors from tumour cells that induce immune cell death [206], which raises the question that this could be a potential mechanism that promotes progression and/or resistance. There are also recent reports to suggest that TRAIL can stimulate cytokine release and the

attraction of certain immune cells that can help the tumour growth and also that signalling through DR5 may promote cell proliferation [206]. It is known that TRAIL can be expressed on immune cells such as activated NK cells and cytotoxic cells in response to factors such as interferon secreted from virus infected cells as a mechanism to kill those infected cells [250]. However, the degree of TRAIL expression in cancer and sarcoma cells is unclear and if so, what the role is; however, this has been explored in a recent review [206] and may be cancer suppressive through apoptosis of tumour supportive immune cells or cancer promoting via the apoptosis of cytotoxic T-cells that would kill cancer cells. Furthermore, the role of DR5 receptor expression in the tumour cell is unclear and has been postulated to be due to an increase in apoptosis at the tumour site or may promote the migration and invasion of cells either through the receptor signalling on the surface [206] or via intra nuclear roles [194].

TRAIL signalling not only activates apoptotic signalling pathways but can also activate non-apoptotic signalling pathways such as NF-kB and Akt [206]. DcR2 has also been reported to activate NF-kB and confer resistance [158]. NF-kB inhibitors have been found to sensitise pancreatic and myeloma cell TRAIL induced apoptosis [251,252]. However, NF-kB has also been reported to positively regulate DR5 expression involving Histone Deacetylase 1 [253]. HDAC inhibition (explored in Chapter 6) can activate NF-kB [253] and has been found to strongly enhance apoptosis activity in haematological and solid tumours [254,255]. The SJSA-1 has demonstrated high levels of DcR2 and TRAIL transcript levels and it would be of interest to further investigate the levels of NF-kB in the SJSA-1 cell line.

NG2/CSPG4/MCSP

Neuron glial antigen 2 (NG2), is also known as chondroitin sulphate proteoglycan 4, (CSPG4) or melanoma-associated chondroitin sulfate proteoglycan (MCSP). This has been of interest as it has been associated with the pathology of multiple types of cancer such as melanoma, breast cancer, squamous cell carcinoma and adult and paediatric sarcomas. NG2 has a role in growth and survival, as well as, spreading and metastases of tumour cells and resistance to chemotherapeutic agents. High NG2 levels have been correlated to aggressive forms of soft tissue sarcoma such as liposarcoma. Flow cytometry data revealed very high surface expression of NG2 in the

MG63 osteosarcoma cell line (Chapter 7), also reflected in the PCR data (4.5). NG2 is reported to promote chemoresistance by activation of integrin-dependent PI3K/Akt signalling [256]. However, there was no obvious correlation between Akt and NG2 in the bone sarcoma cell lines.

Chapter 5. Investigating the cytotoxic effects of non-crosslinked and crosslinked forms of TRAIL on bone sarcoma cell lines

5.1 Introduction

Soluble recombinant human TRAIL has not yielded the clinical results expected from its promising preclinical findings possibly due to factors such as its short half-life and bivalent structure which does not mimic the trimeric true form of TRAIL. Phase 2 studies (which have included DR4 and DR5 agonists) have not supported progression of clinical studies of TRAIL in sarcoma to phase 3 [257]. Studies have suggested that soluble human recombinant TRAIL and DR agonists are not as effective as crosslinked forms of TRAIL at inducing cell death particularly through DR5. For the osteosarcoma U2OS cell line a minimum of 1 μg/ml concentration of the recombinant soluble form of TRAIL is required to induce cell death [258]. However, there has also been a concern that crosslinked forms of TRAIL are more toxic to normal cells particularly hepatocytes.

The aims of this chapter are to:

1. Investigate the cytotoxic effects of crosslinked and non-crosslinked forms of TRAIL in the bone sarcoma cell lines and determine IC50 values.

2. Investigate cytotoxic effects of crosslinked and non-crosslinked forms of TRAIL in non-malignant cells.

3. The effect of death receptor (DR) and decoy receptor (DcR) knockdown and response to TRAIL.

4. To explore CRISPR knockout of DR5 and response to TRAIL.

5.1.1 Crosslinked forms of TRAIL versus non-crosslinked forms of TRAIL on MF DR4-Fas, MF DR5-Fas and bone sarcoma cell lines

Non-crosslinked and crosslinked forms of TRAIL were initially tested on positive control cell lines known to express DR4 and DR5, MF DR4-Fas and MF DR5-Fas, respectively. It was found that the crosslinked SuperKillerTRAIL (SKT) was more effective than non-crosslinked FLAG TRAIL in these control cell lines. The HT1080 dedifferentiated chondrosarcoma cell line may be sensitive to crosslinked forms of TRAIL (KillerTRAIL) [259], which was confirmed in this study (Figure 68). Crosslinked and non-crosslinked forms were then tested on an osteosarcoma cell line (U2OS), Ewing's sarcoma cell line (TC71) and chondrosarcoma cell line (SW1353). Assessments were made using Wst-8 (CCK-8) cytotoxicity assays and the IncuCyte® live-cell analysis system (Figure 69 to Figure 78, Table 18). Generally, it was found that the crosslinked forms (SKT and FLAG TRAIL with M2 antibody) were more effective than the non-crosslinked forms (FLAG TRAIL alone or His TRAIL). Furthermore, the SW1353 chondrosarcoma cell line and the NHDF cell line were resistant despite expressing DR5 (Chapter 3). There was also evidence of stimulatory effects in the U2OS and TC71 cell lines when FLAG TRAIL alone was administered.

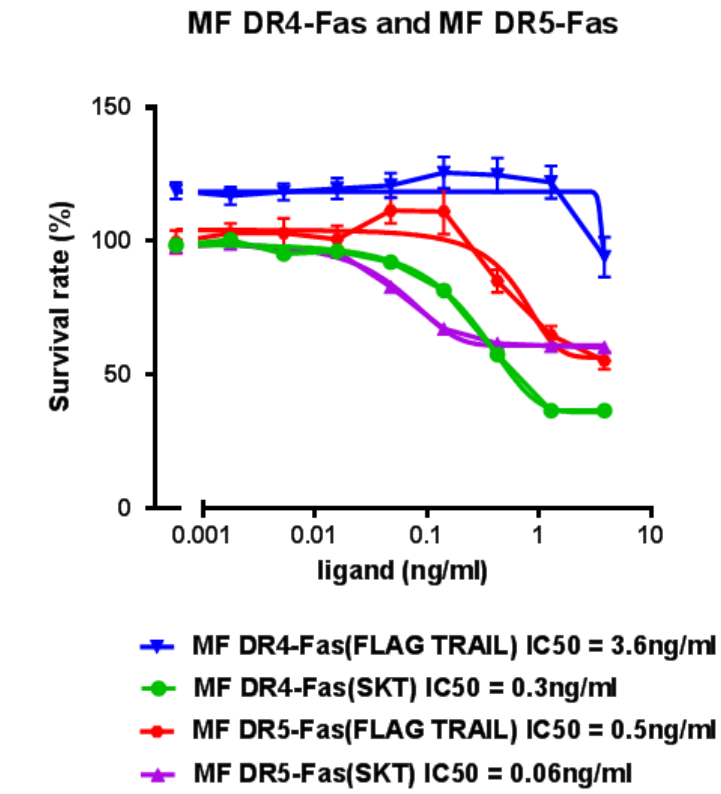
MF DR4-Fas and MF DR5-Fas
Survival rate (%)
150
100
50
0
0.001
0.01
0.1
1
10
ligand (ng/ml)
MF DR4-Fas(FLAG TRAIL) IC50 = 3.6ng/ml
MF DR4-Fas(SKT) IC50 = 0.3ng/ml
MF DR5-Fas(FLAG TRAIL) IC50 = 0.5ng/ml
MF DR5-Fas(SKT) IC50 = 0.06ng/ml

a

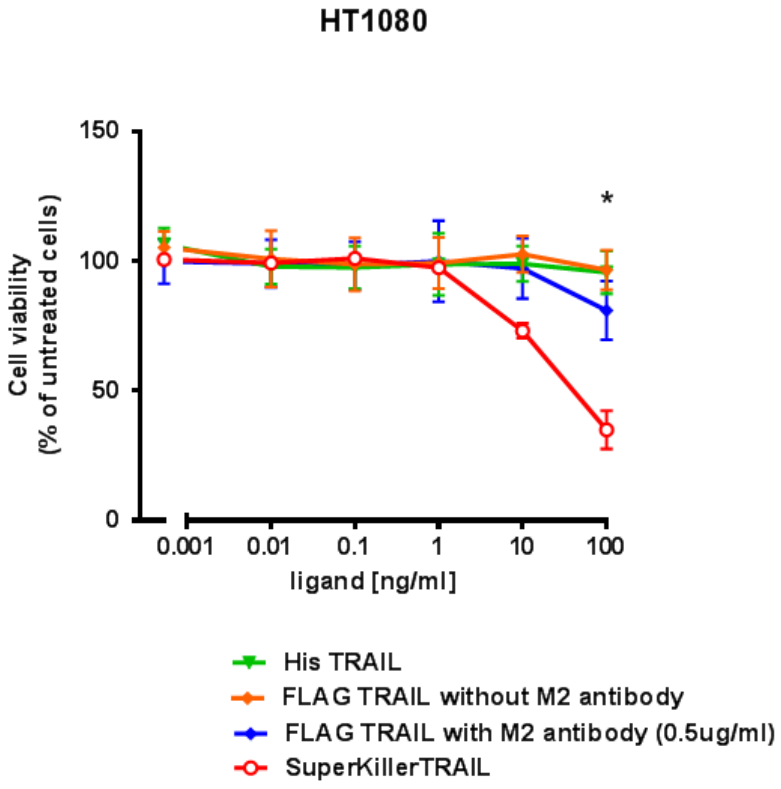
HT1080
Cell viability
(% of untreated cells)
150
100
50
0
*
0.001
0.01
0.1
1
10
100
ligand [ng/ml]
His TRAIL
FLAG TRAIL without M2 antibody
FLAG TRAIL with M2 antibody (0.5ug/ml)
SuperKillerTRAIL

b

Figure 68 – Wst-8 cytotoxicity assays on control cell lines (a) Crosslinked SuperKillerTRAIL (SKT) has a greater effect on the positive control cell lines (MF DR4-Fas and MF DR5-Fas) than non-crosslinked FLAG TRAIL. (b) SuperKillerTRAIL has a greater effect compared to non-crosslinked FLAG TRAIL or His TRAIL on HT1080 dedifferentiated chondrosarcoma cell line cell line (n = 4; mean +/-SEM,* = p<0.05, unpaired t-test).

5.1.2 IncuCyte and Wst-8 data (crosslinked vs non-crosslinked TRAIL)

U2OS osteosarcoma cell line

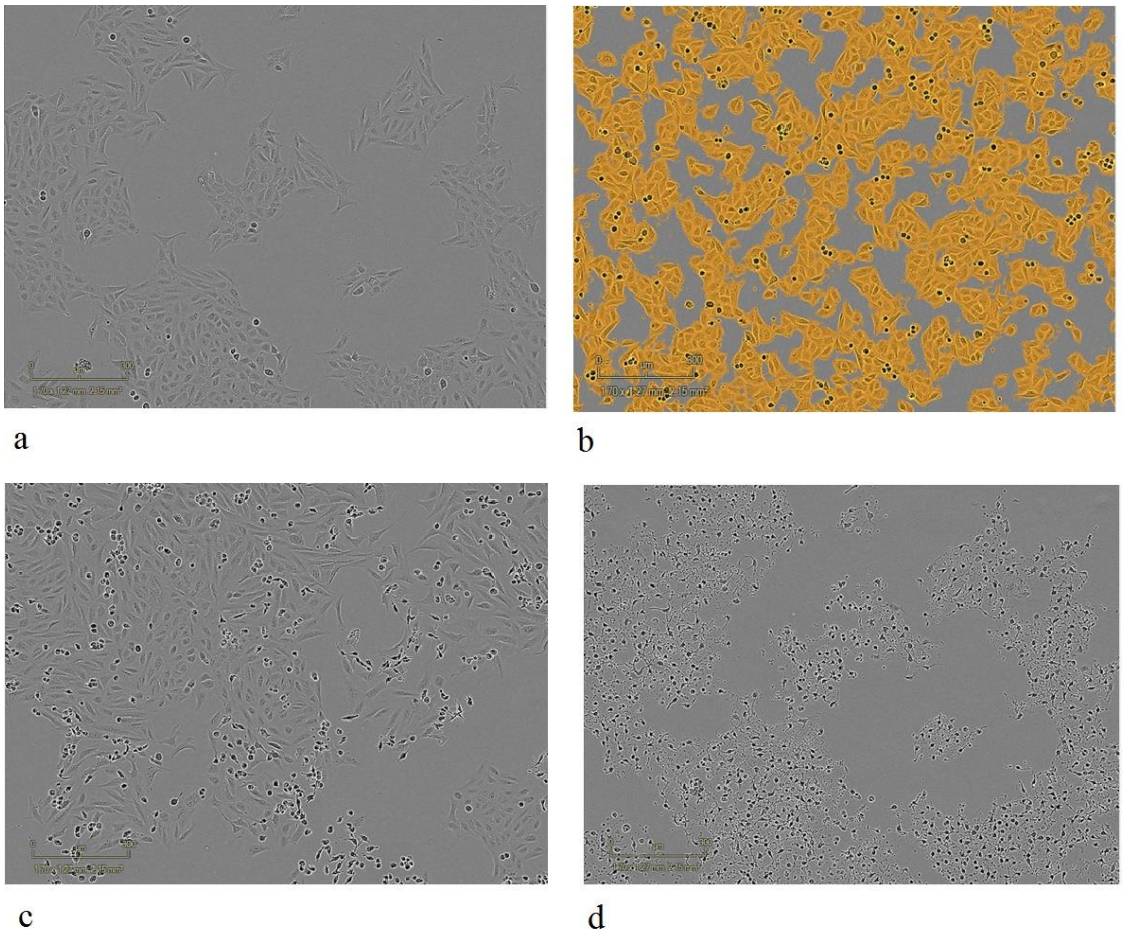

Figure 69 – IncuCyte® live-cell analysis images for U2OS cell line before and at 24 hours after treatment with 100 ng/ml SuperKillerTRAIL. (a) Example of a view of the cells in a well using the IncuCyte® live-cell imaging system. Before treatment with 100 ng/ml SKT. (b) Example of the application of a confluency mask to assess percentage of confluency in one well of 96-well plate. (c) After 24 hours of treatment with 100 ng/ml

SKT rounded body apoptotic cells are visible along with intact cells. (d) After 24 hours of treatment with staurosporine all the cells are dead.

U2OS osteosarcoma cell line (n=3)

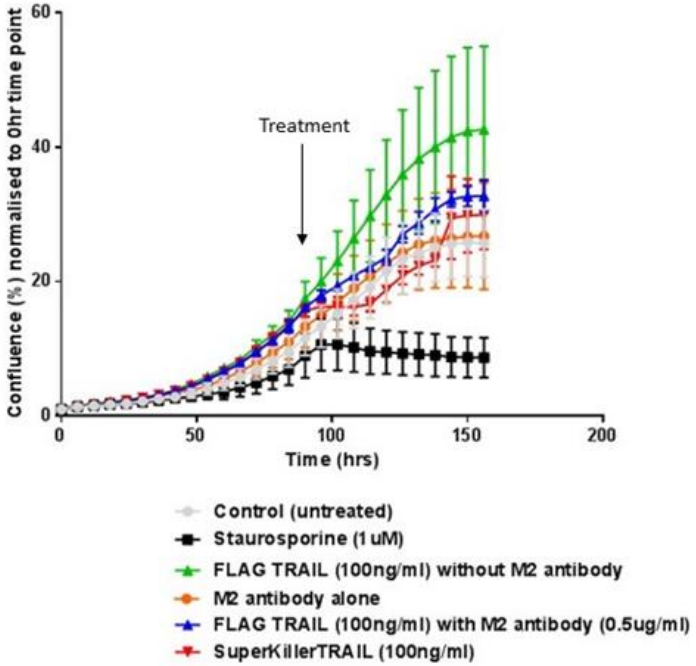

a

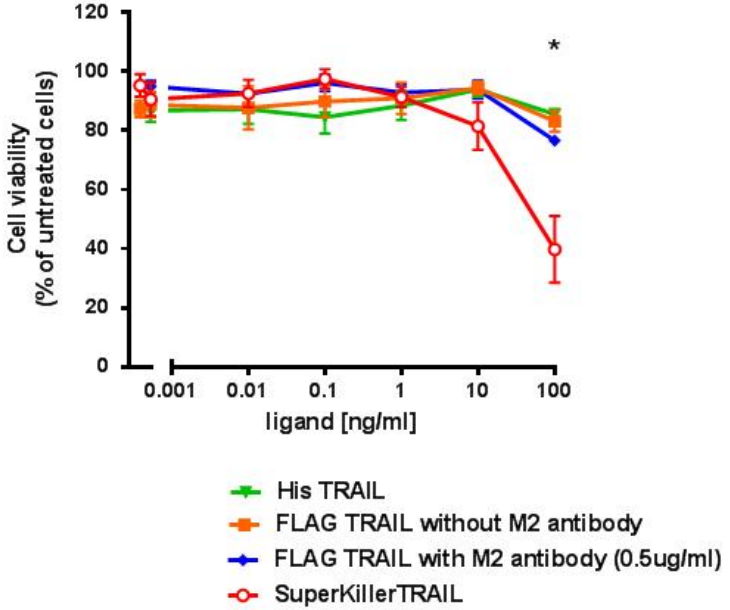

b

Figure 70 – U2OS IncuCyte® live-cell analysis tracking confluency normalised to seeding confluency following exposure of U2OS cells to non-crosslinked and crosslinked forms of TRAIL (treatment during exponential growth phase at about 72 hours) (mean +/- SEM, n = 3). (a) There is an initial decrease in confluency after SuperKillerTRAIL (SKT) (100 ng/ml) or FLAG TRAIL (100 ng/ml) with M2 antibody (0.5 µg/ml) treatment. FLAG TRAIL alone (100 ng/ml) appears to have a stimulatory effect. (b) Wst-8 cytotoxic assay used to compare used to compare the cytotoxic effects of crosslinked and non-crosslinked forms of TRAIL on U2OS cells. SKT has a greater effect compared to tagged forms of TRAIL such as FLAG TRAIL or His TRAIL (p<0.05, Student's unpaired t-test).

TC71 Ewing’s sarcoma cell line

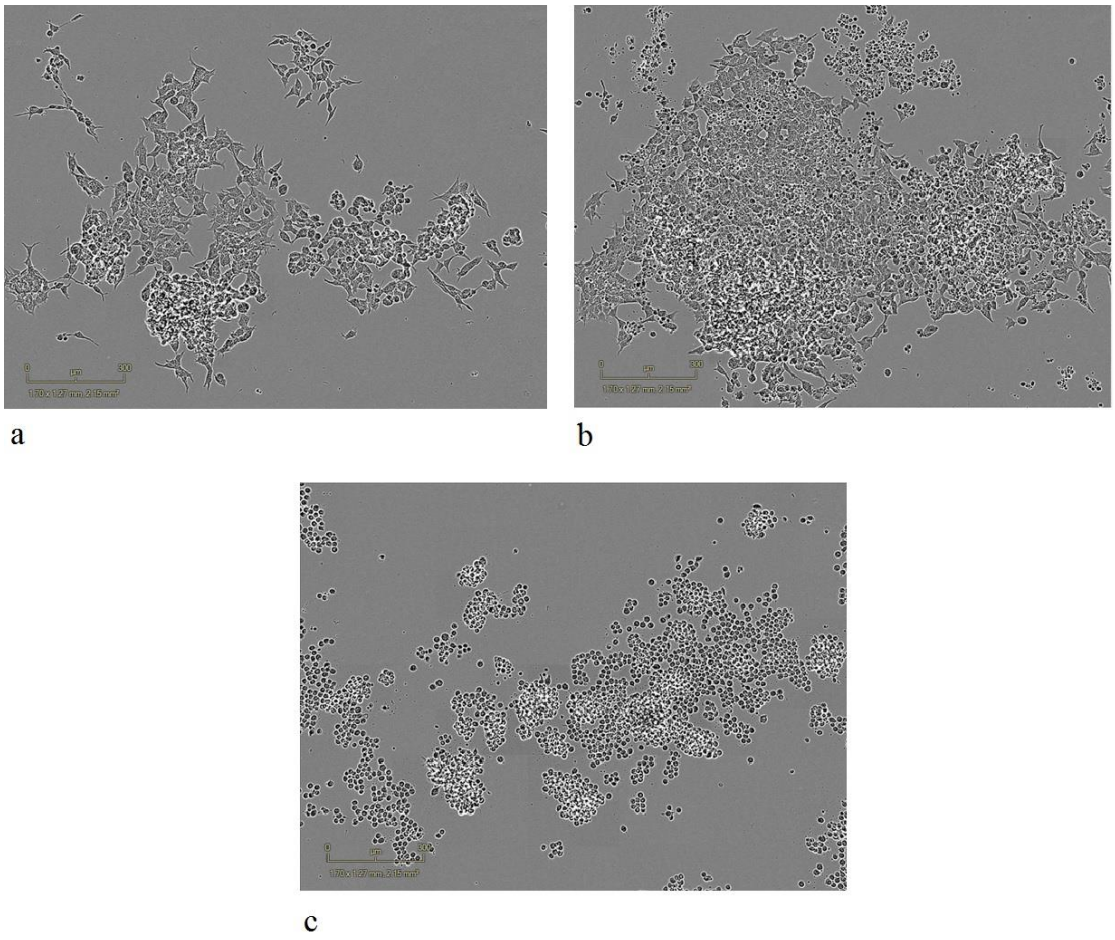

Figure 71 – IncuCyte® live-cell analysis images for TC71 cell line before and at 24 hours after treatment with 100 ng/ml SuperKillerTRAIL. (a) TC71 cells before treatment with 100 ng/ml SKT. (b) After 24 hours of treatment with 100 ng/ml SKT rounded body apoptotic cells are visible along with intact cells. (c) After 24 hours of treatment with staurosporine all the cells are dead.

TC71 Ewing's sarcoma cell line (n=3)

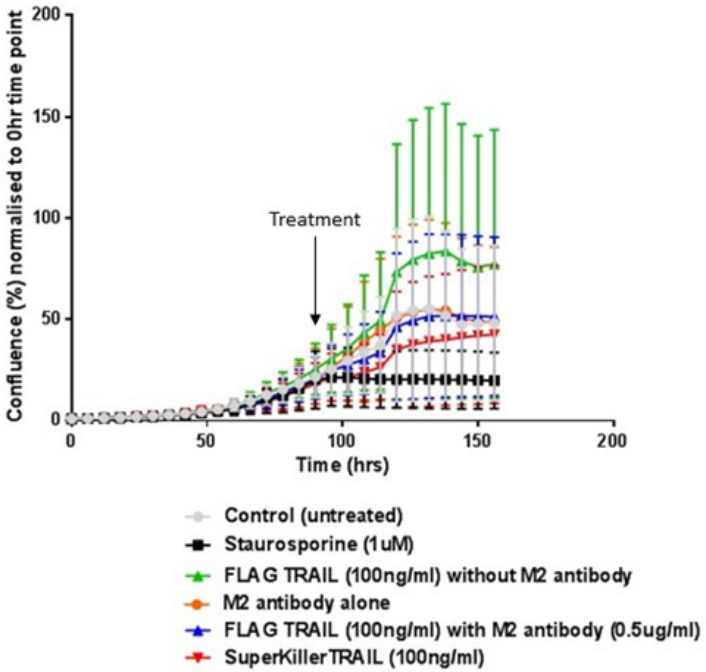

a

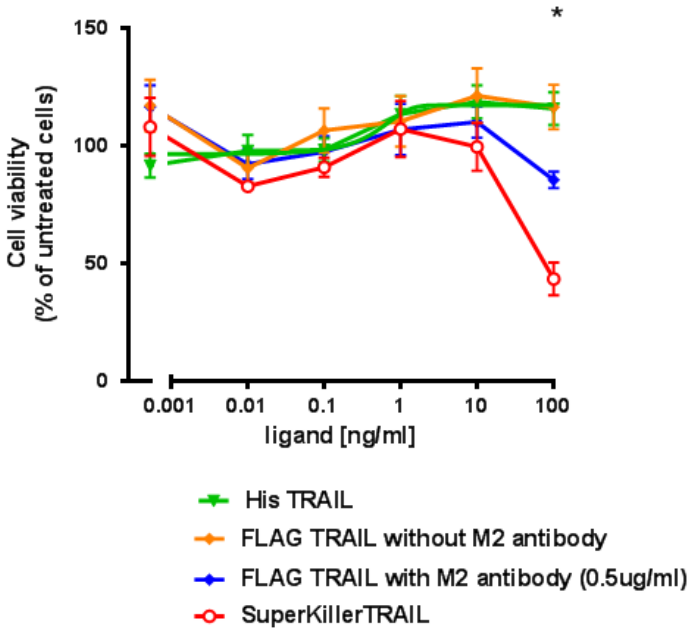

b

Figure 72 - TC71 IncuCyte® live-cell analysis tracking confluency normalised to seeding confluency following exposure of TC71 cells to non-crosslinked and crosslinked forms of TRAIL (treatment during exponential growth phase at about 72 hours) (mean +/- SEM, n = 3). (a) There is an initial decrease in confluency after SuperKillerTRAIL (100 ng/ml) treatment. FLAG TRAIL alone (100 ng/ml) appears to have a stimulatory effect. (b) Wst-8 cytotoxic assay used to compare used to compare the cytotoxic effects of crosslinked and non-crosslinked forms of TRAIL on U2OS cells. At the highest concentration, the crosslinked forms (SuperKillerTRAIL and FLAG TRAIL with M2 antibody) have a greater effect compared to non-crosslinked tagged forms of TRAIL such as FLAG TRAIL or His TRAIL ($p<0.05$, Student's unpaired *t*-test).

SW1353 chondrosarcoma cell line

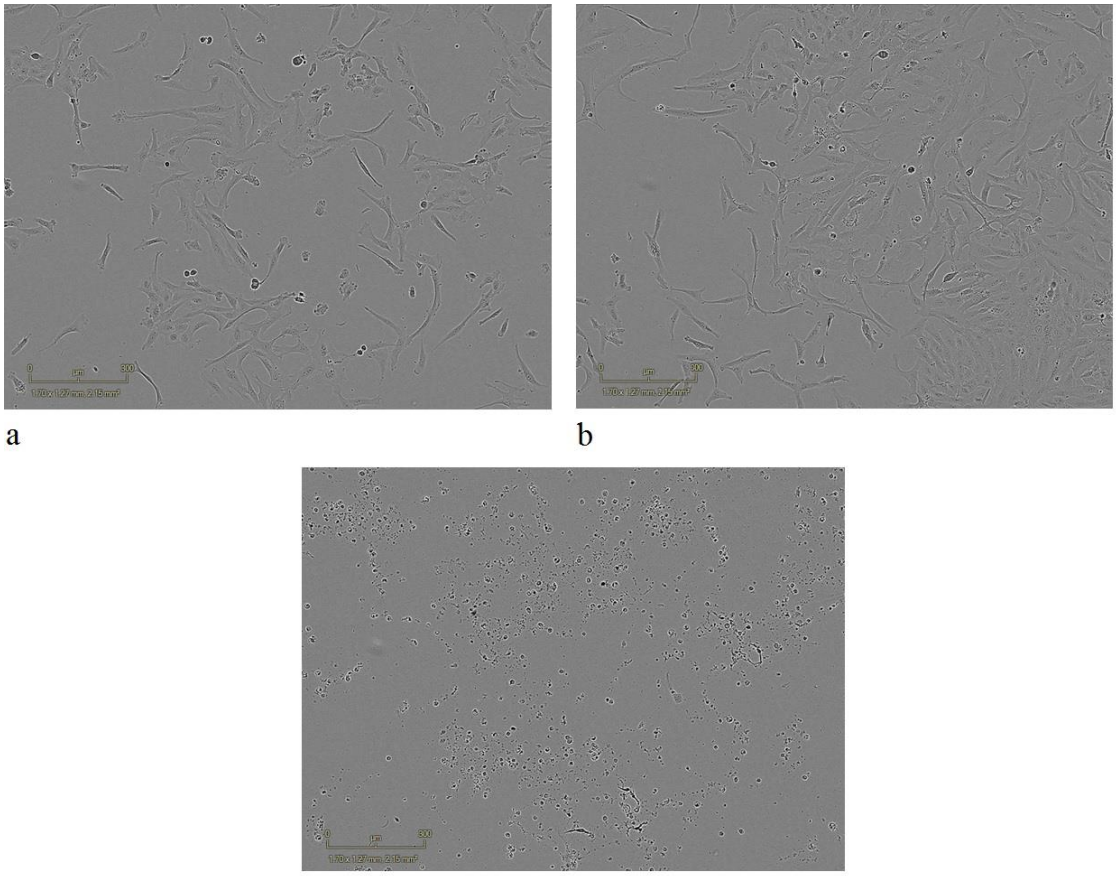

Figure 73 – IncuCyte® live-cell analysis images for SW1353 cell line before and at 24 hours after treatment with 100 ng/ml SuperKillerTRAIL. (a) SW1353 cells before treatment with 100 ng/ml SKT. (b) After 24 hours of treatment with 100 ng/ml SKT appearance of cells is similar to untreated with limited rounded body apoptotic cells visible. (c) After 24 hours of treatment with staurosporine all the cells are dead.

SW1353 chondrosarcoma cell line (n=3)

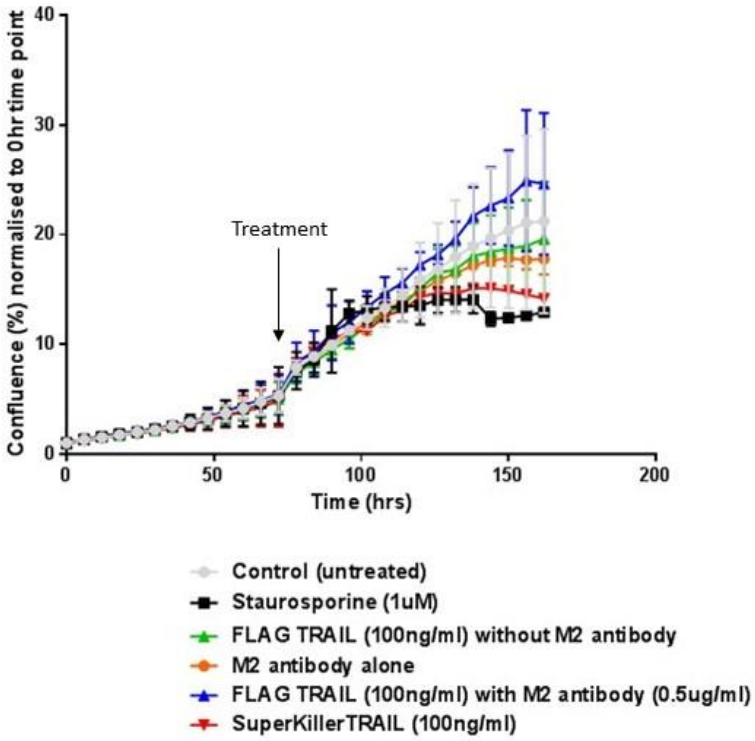

a

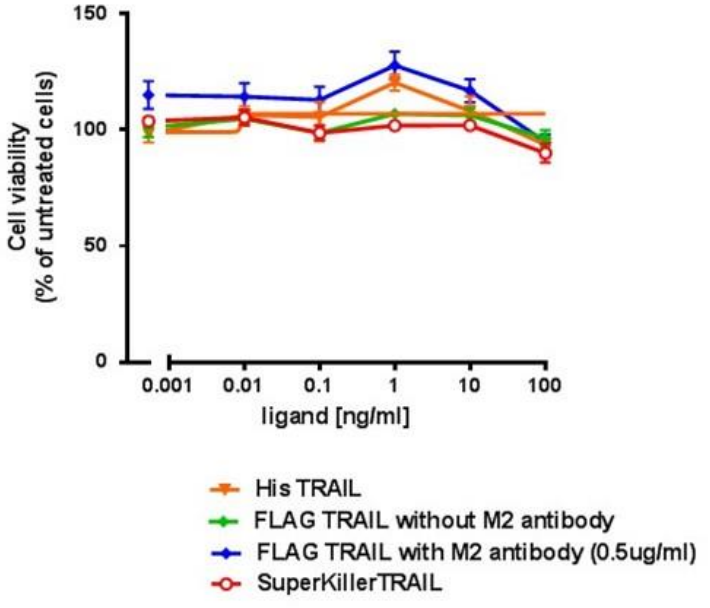

b

Figure 74 – SW1353 IncuCyte® live-cell analysis tracking confluency normalised to seeding confluency following exposure of SW1353 cells to non-crosslinked and crosslinked forms of TRAIL (treatment during exponential growth phase at about 72 hours) (mean +/- SEM, n = 3). (a) Evidence of cytotoxic effect with SuperKillerTRAIL could be observed at 100 ng/ml after 100 hours. (b) Wst-8 cytotoxic assay (n = 3, mean +/-SEM) used to compare used to compare the cytotoxic effects of crosslinked and non-crosslinked forms of TRAIL on SW1353 cells. At the highest concentration, the crosslinked forms (SuperKillerTRAIL and FLAG TRAIL with M2 antibody) have a similar effect compared to non-crosslinked tagged forms of TRAIL such as FLAG TRAIL. Nearly 100 % of the cells remain viable at the highest concentrations.

HT1080 dedifferentiated chondrosarcoma cell line

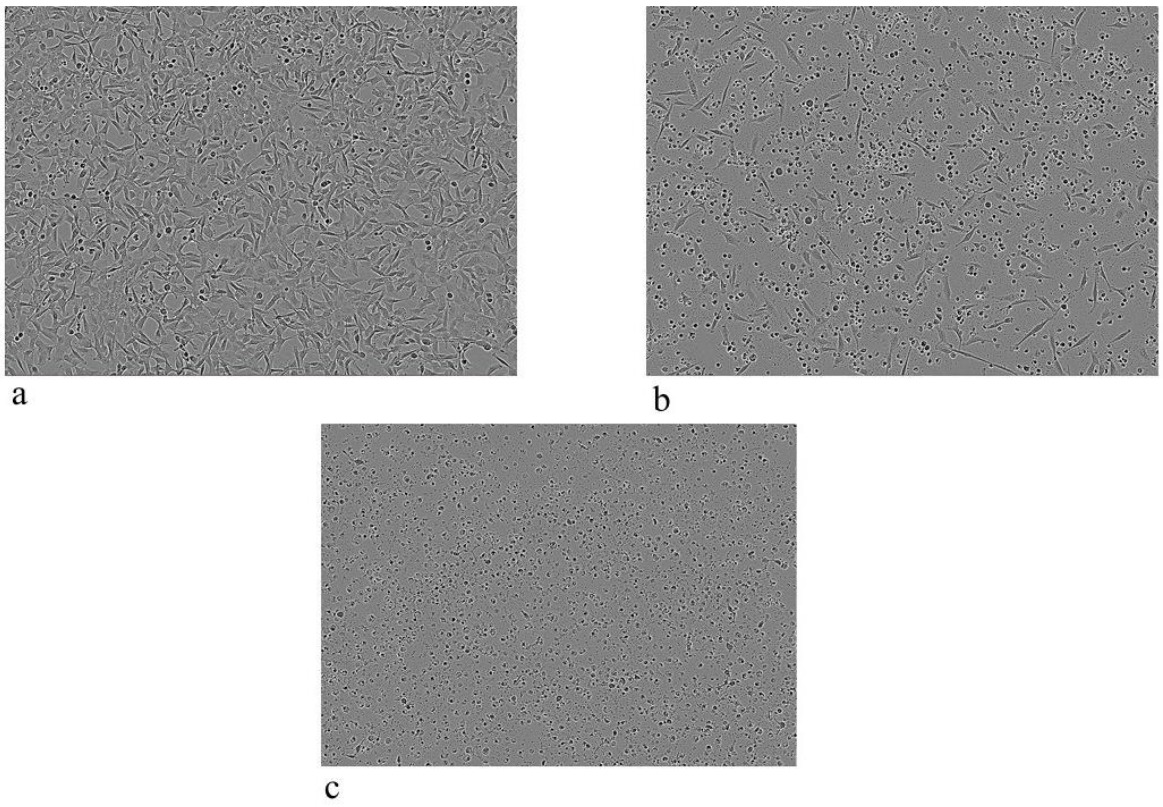

Figure 75 – IncuCyte® live-cell analysis images for HT1080 cell line before and at 24 hours after treatment with 100 ng/ml SuperKillerTRAIL. (a) View of the cells in a well using the IncuCyte® live-cell imaging system before treatment with 100 ng/ml SKT. (b) After 24 hours of treatment with 100 ng/ml SKT rounded body apoptotic cells are visible along with intact cells. (c) After 24 hours of treatment with staurosporine all the cells are dead.

HT1080 dedifferentiated chondrosarcoma cell line (n=3)

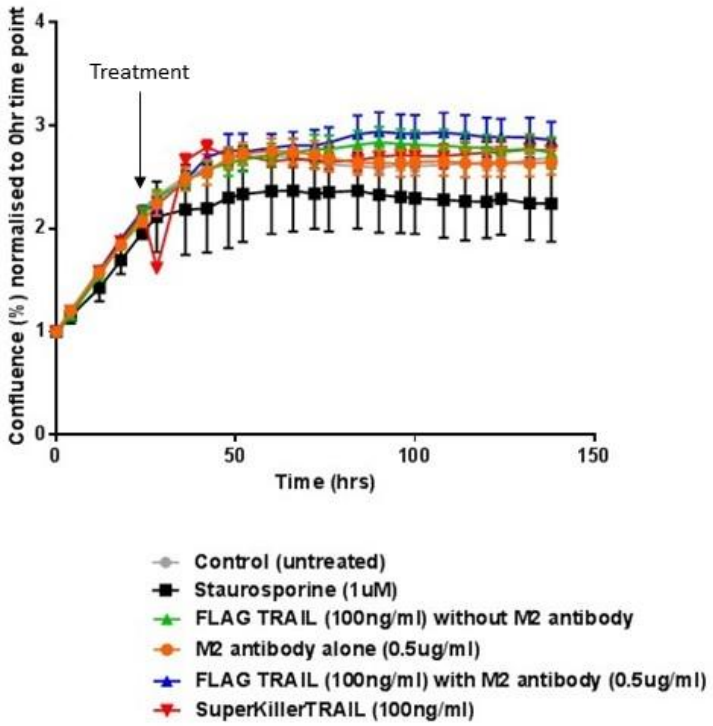

a

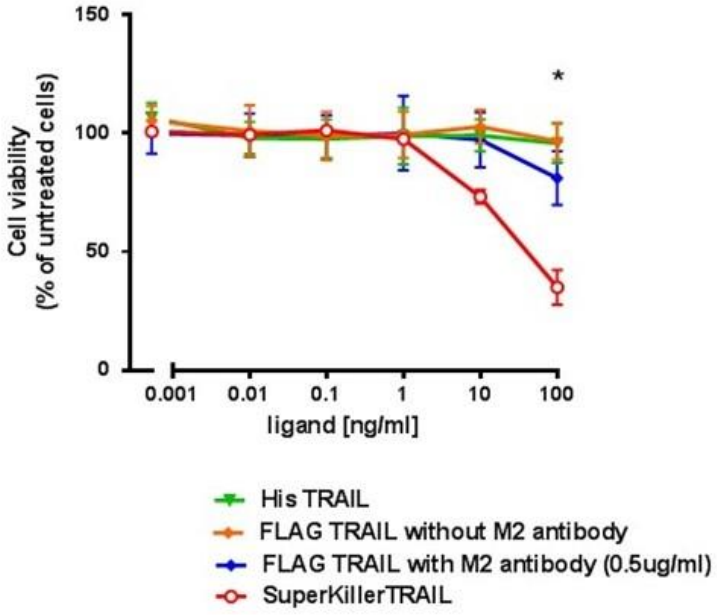

b

Figure 76 - HT1080 IncuCyte® live-cell analysis tracking confluency normalised to seeding confluency following exposure of HT1080 cells to non-crosslinked and crosslinked forms of TRAIL (treatment during exponential growth phase at about 24 hours) (mean +/- SEM, n = 3). (a) SuperKillerTRAIL (SKT) reduces rate of proliferation temporarily greater than FLAG TRAIL with M2 antibody (mean +/-SEM, n = 3). (b) Wst-8 cytotoxic assay (n = 4; mean +/-SEM) used to compare used the cytotoxic effects of crosslinked and non-crosslinked forms of TRAIL on HT1080 cells. SKT has a greater effect compared to tagged forms of TRAIL such as FLAG TRAIL or His TRAIL ($p<0.05$, unpaired *t*-test). Crosslinked forms of TRAIL (SuperKillerTRAIL) are more effective than non-crosslinked forms (His TRAIL and FLAG TRAIL) in the HT1080 dedifferentiated chondrosarcoma cell line similar to findings of previous reports [251].

Normal human dermal fibroblast (NHDF) cell line

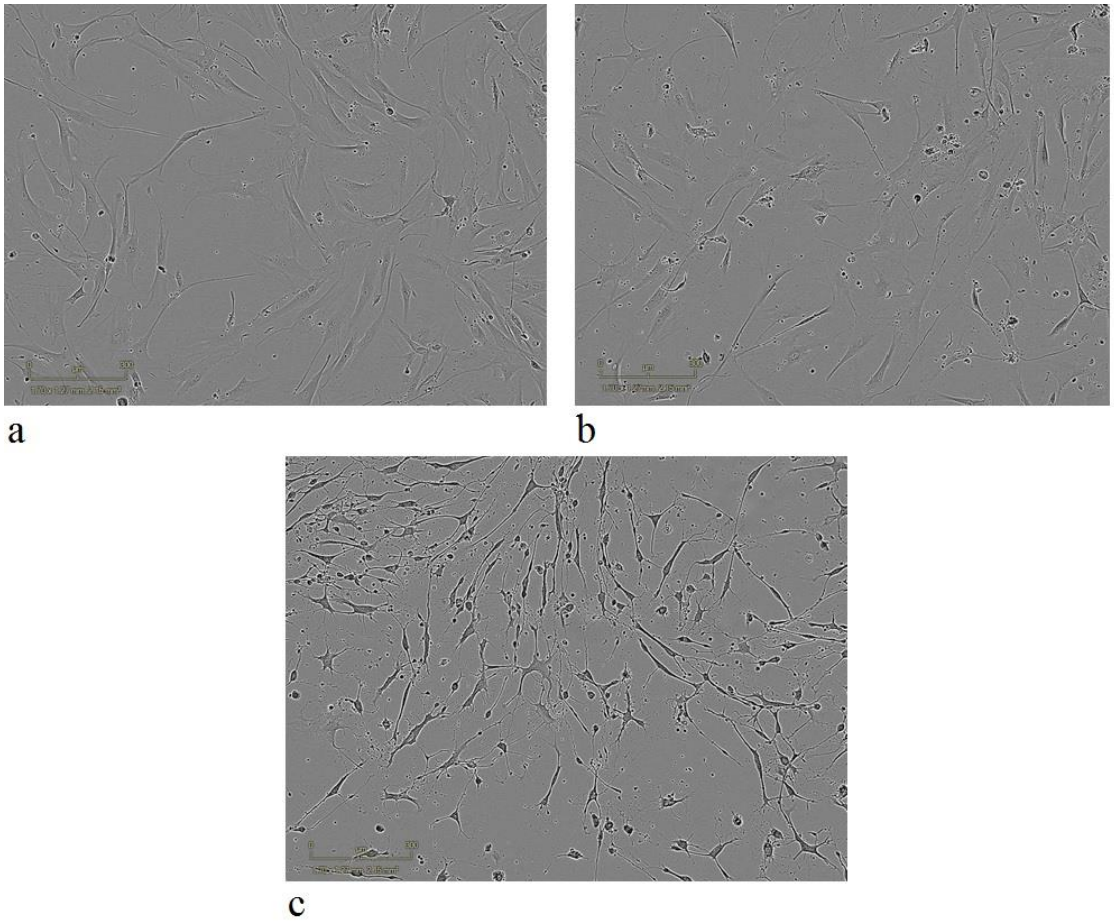

Figure 77 – IncuCyte® live-cell analysis images for NHDF cell line before and at 24 hours after treatment with 100 ng/ml SuperKillerTRAIL. (a) NHDF cells before treatment with 100 ng/ml SKT. (b) After 24 hours of treatment with 100 ng/ml SKT; appearance of cells is similar to untreated with limited rounded body apoptotic cells visible. (c) After 24 hours of treatment with staurosporine, cells appear to be dying and detaching from the surface.

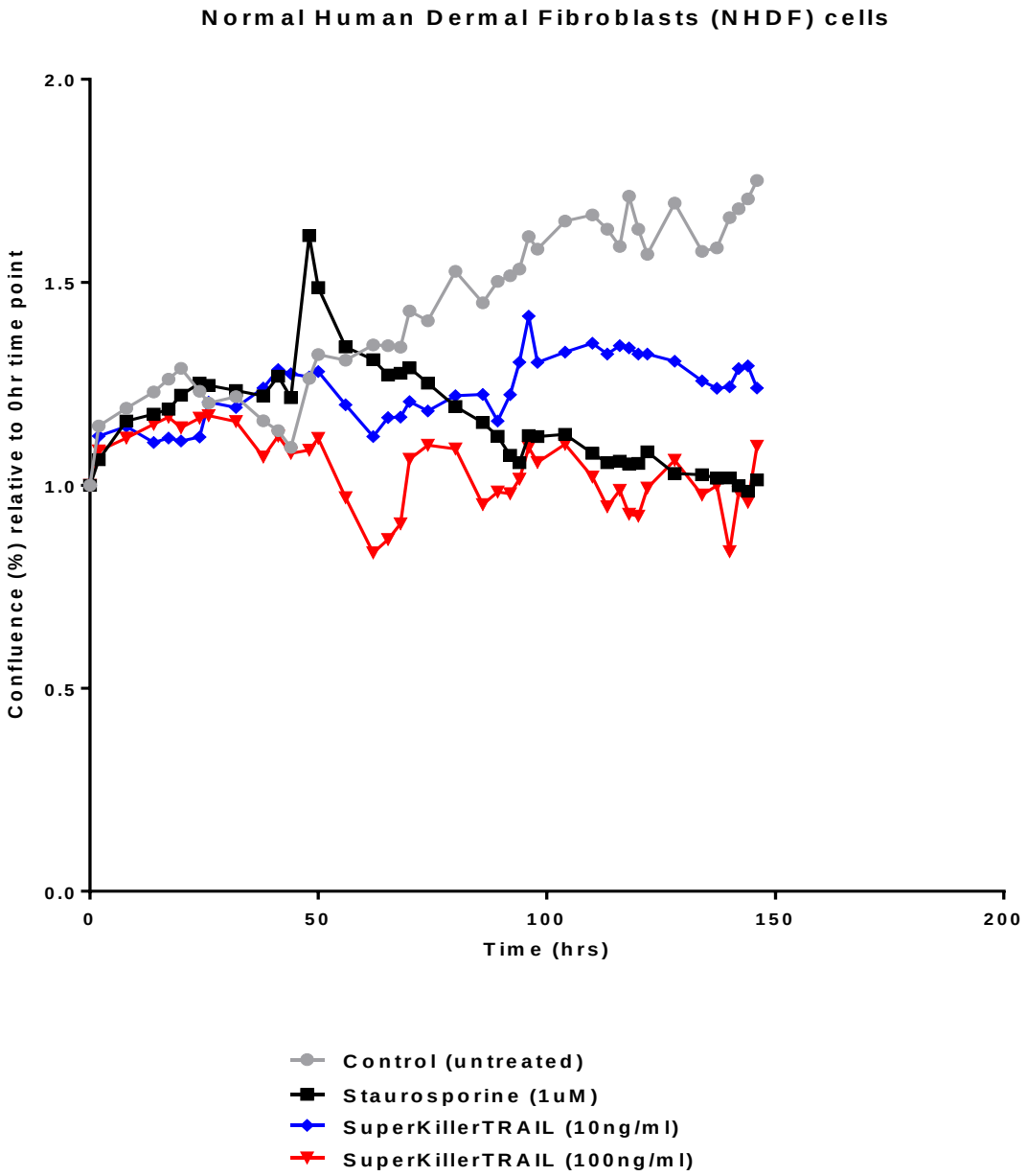

Figure 78 - IncuCyte® live-cell analysis images for NHDF cell line. The effects of SuperKillerTRAIL (SKT) on NHDF cell proliferation (seeded at 1200 cells, treatment at 48 hours). SuperKillerTRAIL (SKT) has a greater effect at reducing cell proliferation at 100 ng/ml than 10 ng/ml.

Table 18 - Summary table for the % change in confluency over 24 hours using IncuCyte® live-cell analysis system. R = no change/resistant. Reduction in confluence compared to control was observed with crosslinked SuperKillerTRAIL (100 ng/ml = 4 nM) in the U2OS, TC71 and HT1080 cell lines. There was a greater reduction compared to the non-malignant normal human dermal fibroblast (NHDF) cell line. FLAG TRAIL alone was observed to have stimulatory effects. No significant sensitivity was found in the SW1353 chondrosarcoma cell line over the first 24 hours.

Sarcoma type	Cell line	% change of confluency over 24 hours after treatment normalised to untreated (mean +/- SEM, n = 3)		
		FLAG TRAIL (100 ng/ml)	FLAG TRAIL (100 ng/ml) with M2 antibody	SuperKillerTRAIL (100 ng/ml)
Osteosarcoma	U2OS	3 % (+/-15 %)	-25 % (+/-4 %)	-56 % (+/-4 %)
Ewing's sarcoma	TC71	12 % (+/-8 %)	-1 % (+/-8 %)	-23 % (+/-12 %)
Chondrosarcoma	HT1080	2 % (+/-2 %)	-3 % (+/-1 %)	-31 % (+/-1.2 %)
	SW1353	R	R	R
Normal human dermal fibroblasts	NHDF	-	-	-10 %

5.1.3 Crosslinked SuperKillerTRAIL has cytotoxic effects on bone sarcoma cell lines and this can be correlated to the degree of DR5 expression

Wst-8 (cck-8) assays were performed to assess the degree of cytotoxicity of crosslinked SuperKillerTRAIL on the available bone sarcoma cell lines and the majority were sensitive. The most resistant were the SJSA-1 osteosarcoma cell line and the SW1353 chondrosarcoma cell line (Figure 79 to Figure 81, Table 19). It was found that when excluding the SJSA-1 and SW1353 cell lines, the degree of cytotoxicity was proportional to the degree of expression of DR5 on the cell surface (R^2 = 0.94, p<0.05 at 10 ng/ml, 0.4 nM Pearson's correlation coefficient) (Table 19, Figure 82).

Osteosarcoma

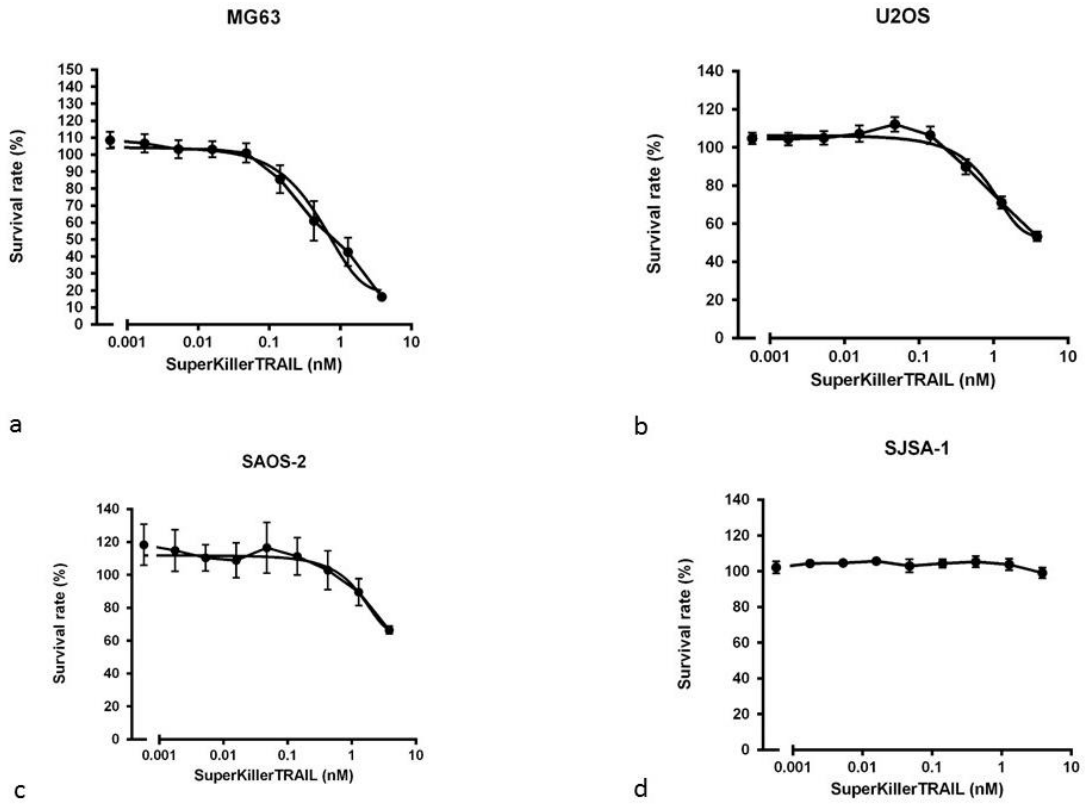

Figure 79 – SuperKillerTRAIL cytotoxicity assays in osteosarcoma cell lines: (a) MG63, (b) U2OS, (c) SAOS-2, (d) SJSA-1, from increasing to decreasing sensitivity (mean +/- SEM, n = 3).

Chondrosarcoma

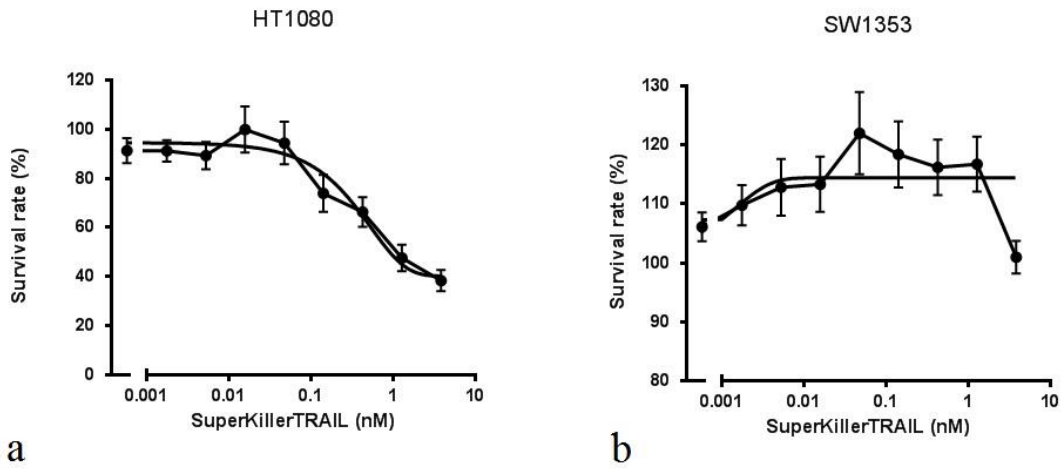

Figure 80 – SuperKillerTRAIL cytotoxicity assays in chondrosarcoma cell lines (a) HT1080, (b) SW1353 from increasing to decreasing sensitivity (mean +/- SEM, n = 3).

Ewing's sarcoma

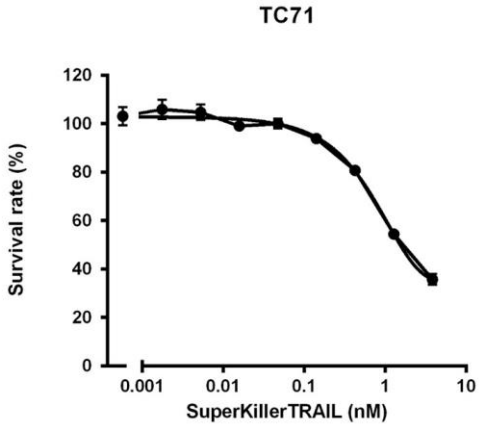

Figure 81 – SuperKillerTRAIL cytotoxicity assay in Ewing's sarcoma cell line (TC71). (mean +/- SEM, n = 3).

Table 19 – DR5 median fluorescence intensity (MFI) (S, Stained – ITC, Isotype Control) and response to crosslinked SuperKillerTRAIL (SKT), FLAG TRAIL + M2 antibody and non-crosslinked FLAG TRAIL and His TRAIL. Summary with DR5 MFI and SuperKillerTRAIL IC50 values (mean +/- SEM, n = 3). NC = Not Converged with doses up to 100 ng/ml. NA = Not Available.

Sarcoma type	Cell line	DR5 [MFI(S)-MFI(ITC)] (mean +/-SEM, n = 3)	SKT IC50 (nM), % dead at highest dose (100 ng/ml, 4 nM)	FLAG TRAIL + M2 antibody (0.5 µg/ml) IC50 (nM) % dead at highest dose (100 ng/ml, 5 nM)	FLAG TRAIL IC50 (nM) % dead at highest dose (100 ng/ml, 5 nM)	His TRAIL IC50 (nM) %dead at highest dose (100 ng/ml, 4 nM)
Osteosarcoma	SAOS-2	156 (+/- 47)	3.1, 34 %	NA	NA	NA
	U2OS	289 (+/- 85)	0.9, 47 %	NC, 23 %	NC, 17 %	NC, 14 %
	SJSA-1	592 (+/- 8) (DcR2-87+/-6)	NC, 1 %	NA	NA	NA
	MG63	793 (+/- 111)	0.8, 84 %	NA	NA	NA
Chondrosarcoma	SW1353	324 (+/- 47)	3.2, 0 %	NC, 5 %	NC, 3 %	NC, 6 %
	HT1080	815 (+/-131)	1.0, 62 %	NC, 19 %	NC, 3 %	NC, 4 %
Ewing's sarcoma	TC71	285 (+/-20) (DR4-138+/-22, DcR2-91+/-6)	1.0, 64 %	NC, 15 %	NC, 0 %	NC, 0 %
DR5 Control	MF DR5-Fas	1140 (DR4 = 9)	0.002 nM, 40 %	NA	0.03 nM, 45 %	NA
DR4 Control	MF DR4-Fas	10 (DR4 = 808)	0.01 nM, 63 %	NA	0.2 nM, 6 %	NA

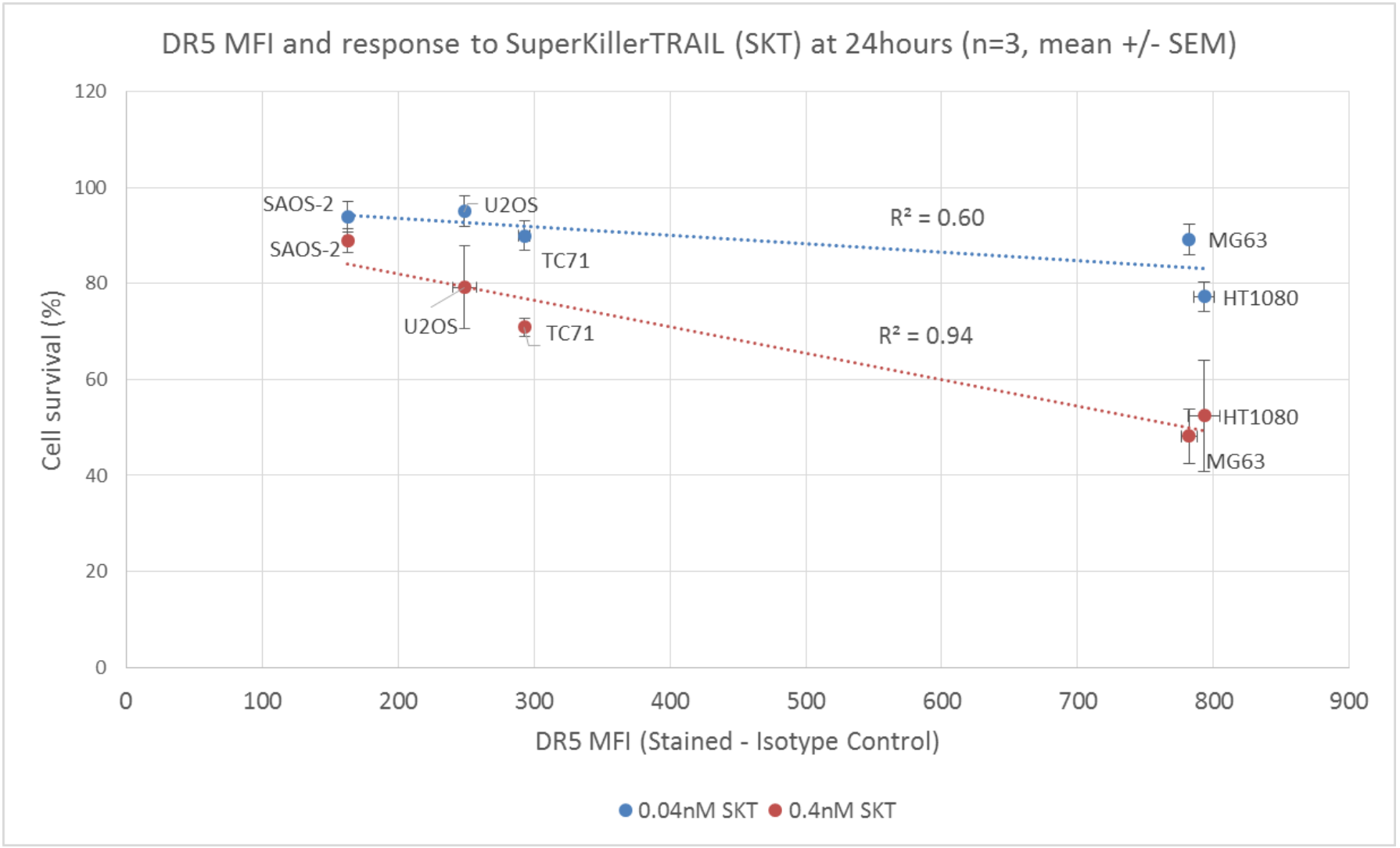

Figure 82 - Surface DR5 levels and responses to SuperKillerTRAIL (1 ng/ml, 0.04 nM and 10 ng/ml, 0.4 nM) (excluding more resistant SW1353 and SJSA-1) (strong correlation R^2 = 0.94, $p<0.05$ at 10 ng/ml, 0.4 nM Pearson's correlation coefficient).

5.1.4 Crosslinked SuperKillerTRAIL has limited cytotoxic effects on non-malignant cells except for human hepatocyte cell line (HHL5)

The majority of the non-malignant cell lines available were resistant to the effects of SuperKillerTRAIL. The most sensitive non-malignant cell line was the HHL5 hepatocyte cell line (Figure 83 and Figure 84).

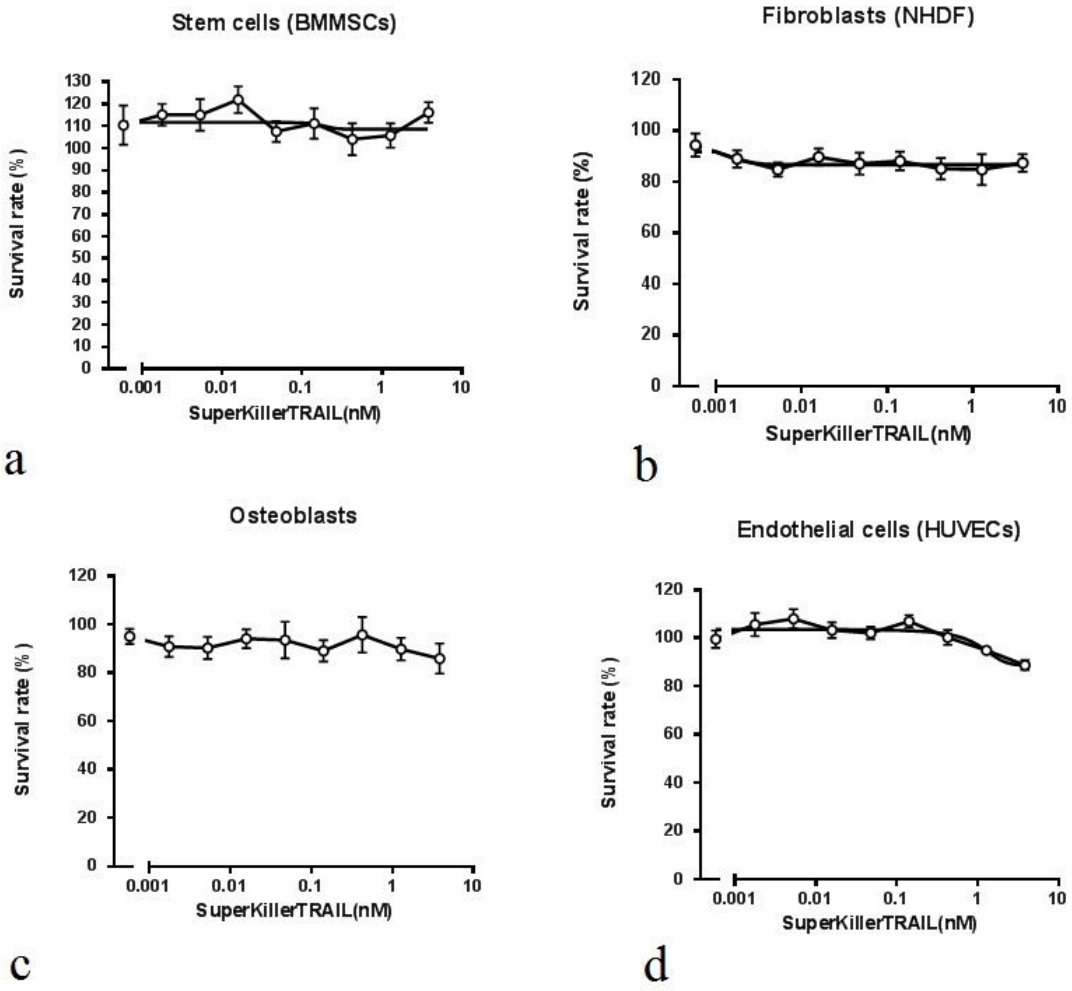

Figure 83 – Effects of SuperKillerTRAIL on: (a) Stem cells (BMMSCs), (b) Fibroblasts (NHDF), (c) Osteoblasts and (d) Endothelial cells (HUVECs).

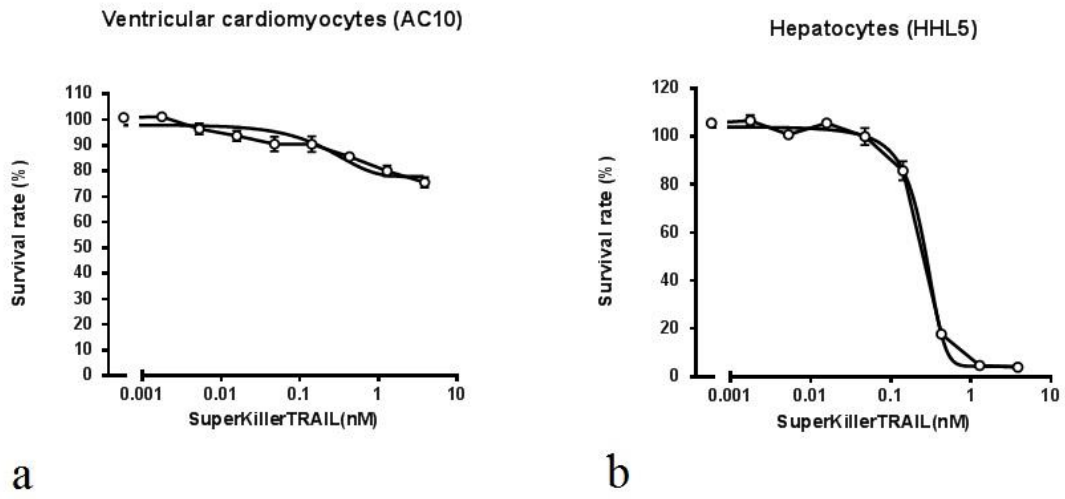

Figure 84 – Effect of SuperKillerTRAIL on: (a) Ventricular cardiomyocyte cell line (AC10) and (b) hepatocyte cell line (HHL5) (IC50 = 0.2 nM).

5.1.5 Anti-DR5 agonist monoclonal antibody (TRA-8) has limited cytotoxicity on bone sarcoma cell lines compared to SuperKillerTRAIL

Background: DR5 agonists are currently used in clinical trials for advanced cancers such as sarcoma, breast, colorectal and malignant melanoma [206]. Clinical trial NCT01327612 results, which includes sarcoma are expected in November 2019 (Table 20). DS-8273a has been found to be well tolerated in the first in-human study of patients with advanced solid tumours, including sarcoma at 24 mg/kg [260]. I have tested a similar antibody, the humanised anti-DR5 agonist monoclonal antibody (TRA-8, absolute antibody, UK) in the bone sarcoma cell lines and compared its effectiveness to crosslinked SuperKillerTRAIL (SKT) and generally found it to be less potent (Figure 85 to Figure 87, Table 21).

Table 20 - Active TRAIL and TRAIL-R based therapies in clinical trials [adapted from [206]].

TRAIL-R agonistic antibodies	In combination with	Cancer	Clinical trial identifier	Estimated completion date
Mapatumumab (HGS-ETR1) (DR4 agonist)	Sorafenib (multikinase inhibitor)	Advanced hepatocellular carcinoma	NCT01258608	December 2018
Conatumumab (AMG-655) (DR5 agonist)	FOLFOX6, ganitumab (anti-IGF1R) and/or bevacizumab (anti-VEGF)	Advanced solid tumours (includes sarcoma)	NCT01327612	November 2019
Tigatuzumab (CS-1008) (DR5 agonist)	Abraxane	Patients with metastatic, triple-negative breast cancer	NCT01307891	September 2017
DS-8273a (DR5 agonist)	Nivolumab (anti-PD1)	Advanced colorectal cancer	NCT02991196	September 2017
		Unresectable stage III or stage IV melanoma	NCT02983006	December 2019

1.FOLFOX, oxaliplatin–leucovorin–fluorouracil chemotherapy; IGF1R, insulin-like growth factor 1 receptor; PD1, programmed cell death protein 1;
2.TRAIL, tumour necrosis factor-related apoptosis-inducing ligand; TRAIL-R, TRAIL receptor; VEGF, vascular endothelial growth factor.

Osteosarcoma

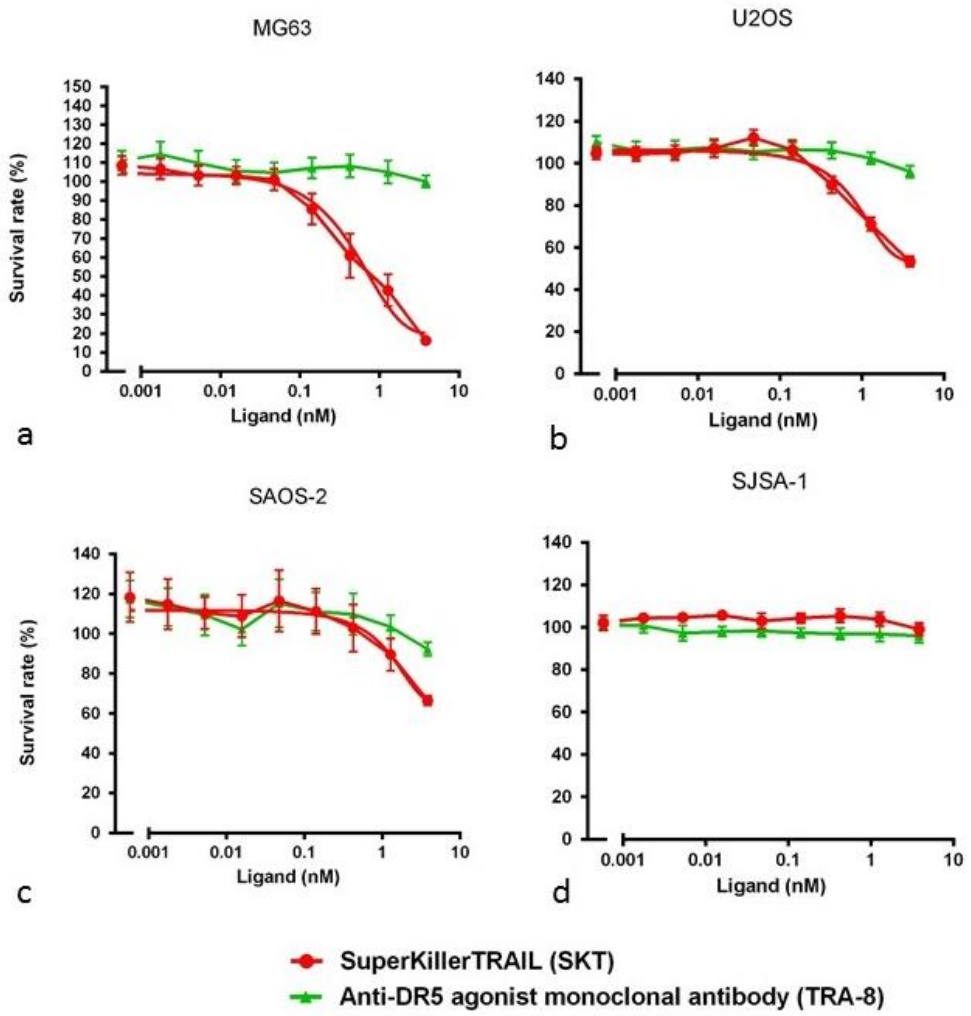

Figure 85 - Anti-DR5 agonist monoclonal antibody (TRA-8) vs SuperKillerTRAIL cytotoxicity assays in osteosarcoma cell lines (a) MG63, (b) U2OS, (c) SAOS-2, (d) SJSA-1 (mean +/- SEM, n = 3).

Chondrosarcoma

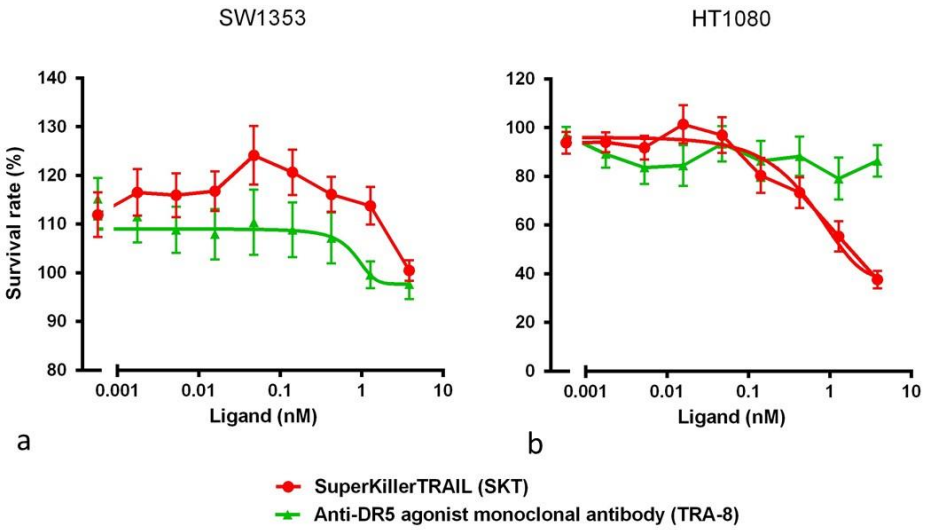

Figure 86 - Anti-DR5 agonist monoclonal antibody (TRA-8) vs SuperKillerTRAIL cytotoxicity assays in chondrosarcoma cell lines (a) SW1353, (b) HT1080 (mean +/- SEM, n = 3).

Ewing's sarcoma

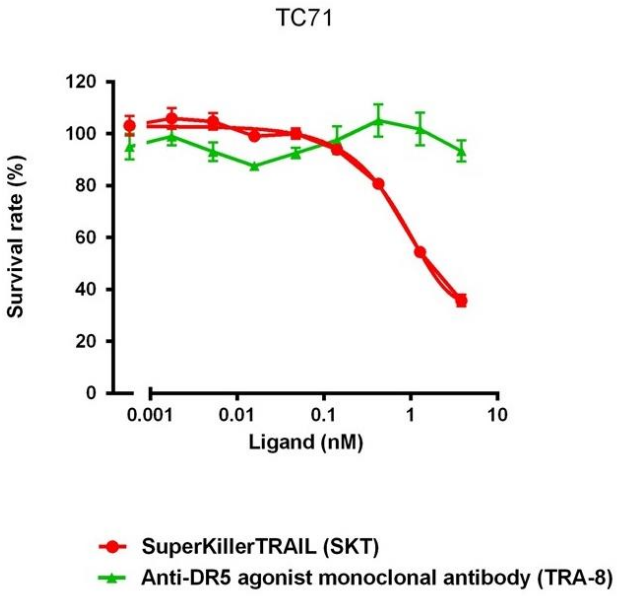

Figure 87 - Anti-DR5 agonist monoclonal antibody (TRA-8) vs SuperKillerTRAIL cytotoxicity assays in Ewing's sarcoma cell line (a) TC71 (mean +/- SEM, n = 3).

Table 21 - SuperKillerTRAIL (SKT) was generally found to have a more cytotoxic effect than TRA-8 on bone sarcoma cell lines (mean +/- SEM, n = 3). NC = Not Converged.

Sarcoma type	Cell line	DR5 [MFI(S)-MFI(US)] Mean +/- SEM (n = 3)	TRA-8 IC50 (nM), % dead at highest dose	SKT IC50 (nM), % dead at highest dose
Osteosarcoma	SAOS-2	156 (+/- 47)	1.9, 8 %	3.1, 34 %
	U2OS	289 (+/- 85)	NC	0.9, 47 %
	SJSA-1	592 (+/- 8) (DcR2-94)	NC	NC, 1 %
	MG63	793 (+/- 111)	1.9	0.8, 84 %
Chondrosarcoma	SW1353	324 (+/- 47)	NC	3.2, 0 %
	HT1080	815 (+/-131)	NC	1.0, 62 %

Ewing's sarcoma	TC71	285 (+/-20) (DR4-105, DcR2-86)	NC	1.0, 64 %

*5.1.6 Mode of cell death by Super*Killer*TRAIL is predominantly via apoptosis*

In order to investigate the mode of cell death (apoptosis or necroptosis) in response to SuperKillerTRAIL (SKT) treatment, agents were used to inhibit caspase activity (reversible, Ac-DEVD-CHO or irreversible, Z-VAD-FMK; to investigate for apoptosis) or inhibit receptor-interacting protein 1 (RIP1) kinase domain (necrostatin; to investigate for necroptosis) in the HT1080 and U2OS bone sarcoma cell lines. Cells were treated with the agent for 30 minutes before the application of SuperKillerTRAIL for 24 hours. It was found in the HT1080 and U2OS cell line that the application of the caspase inhibitors significantly reduced the effectiveness of SKT. Necrostatin did not have a significant effect on these cell lines (Figure 88 to Figure 92).

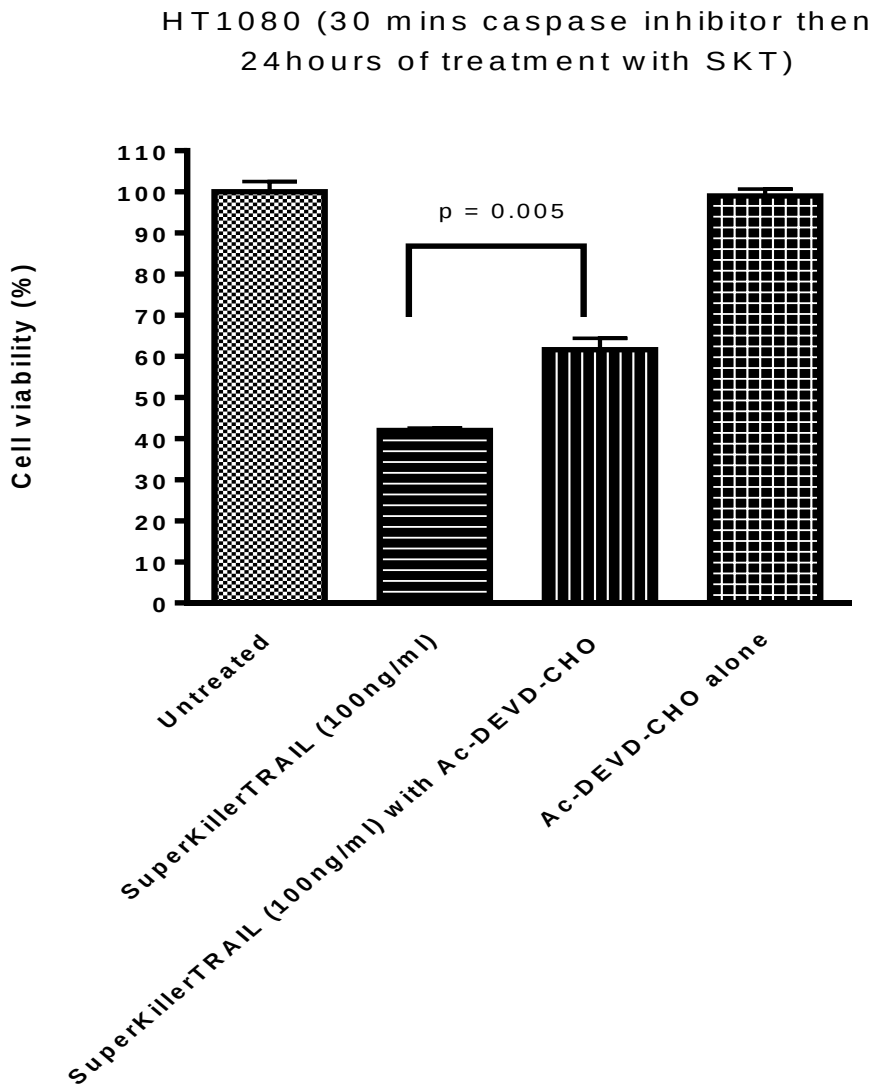

Figure 88 – Reversible caspase inhibition and response to SuperKillerTRAIL (SKT) in HT1080 cell line. 20 % less cell death was observed when applying reversible caspase inhibitor AC-DEVD-CHO (20 µM) compared to SuperKillerTRAIL (SKT) alone in the HT1080 cell line (p = 0.005, Mann-Whitney U test).

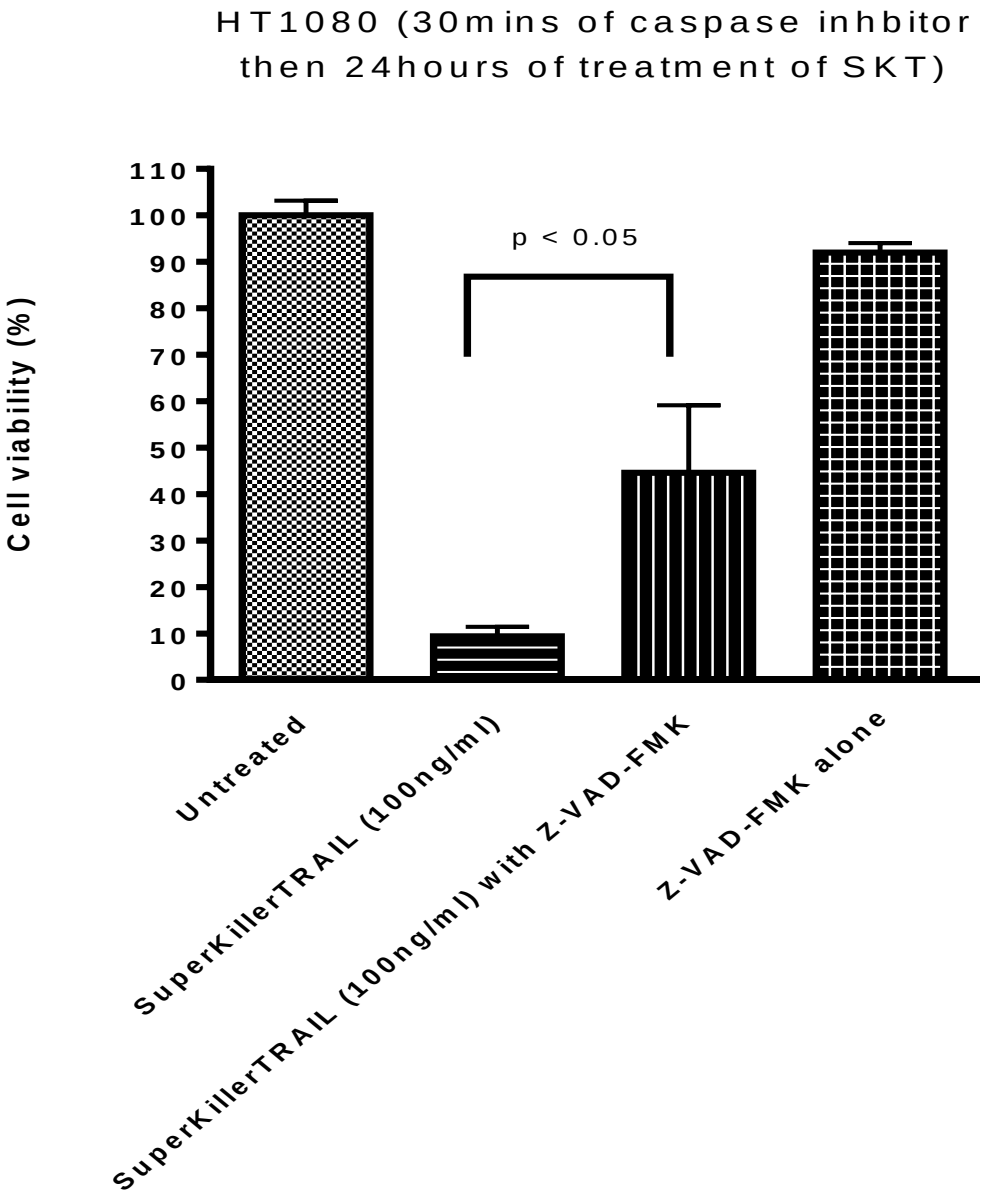

Figure 89 – Irreversible caspase inhibition and response to SuperKillerTRAIL (SKT) in HT1080 cell line. 35 % less cell death was observed when applying irreversible caspase inhibitor Z-VAD-FMK (20 µM) compared to SuperKillerTRAIL (SKT) alone in the HT1080 cell line ($p < 0.05$, Mann-Whitney *U* test).

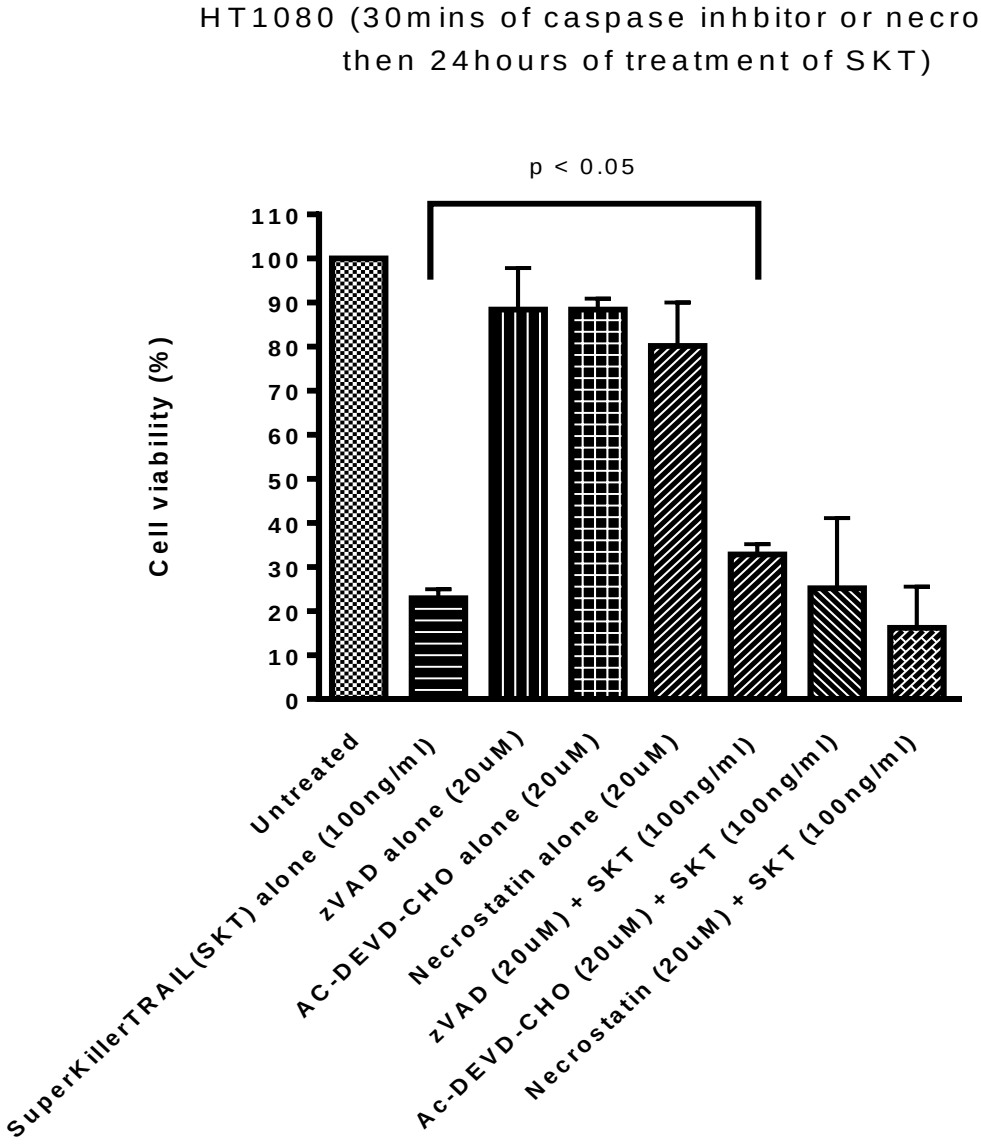

Figure 90 – Comparison of caspase inhibition (reversible, Ac-DEVD-CHO or irreversible, Z-VAD-FMK) or inhibition of receptor-interacting protein 1 (RIP1) kinase domain (necrostatin) and response to SuperKillerTRAIL (SKT) in the HT1080 cell line. Significance was observed when applying zVAD-FMK (20 µM), about 10 % less cell death when compared to SuperKillerTRAIL (SKT) alone ($p < 0.05$, Mann-Whitney *U* test). However, no significant difference was observed when applying the necrostatin (20 µM).

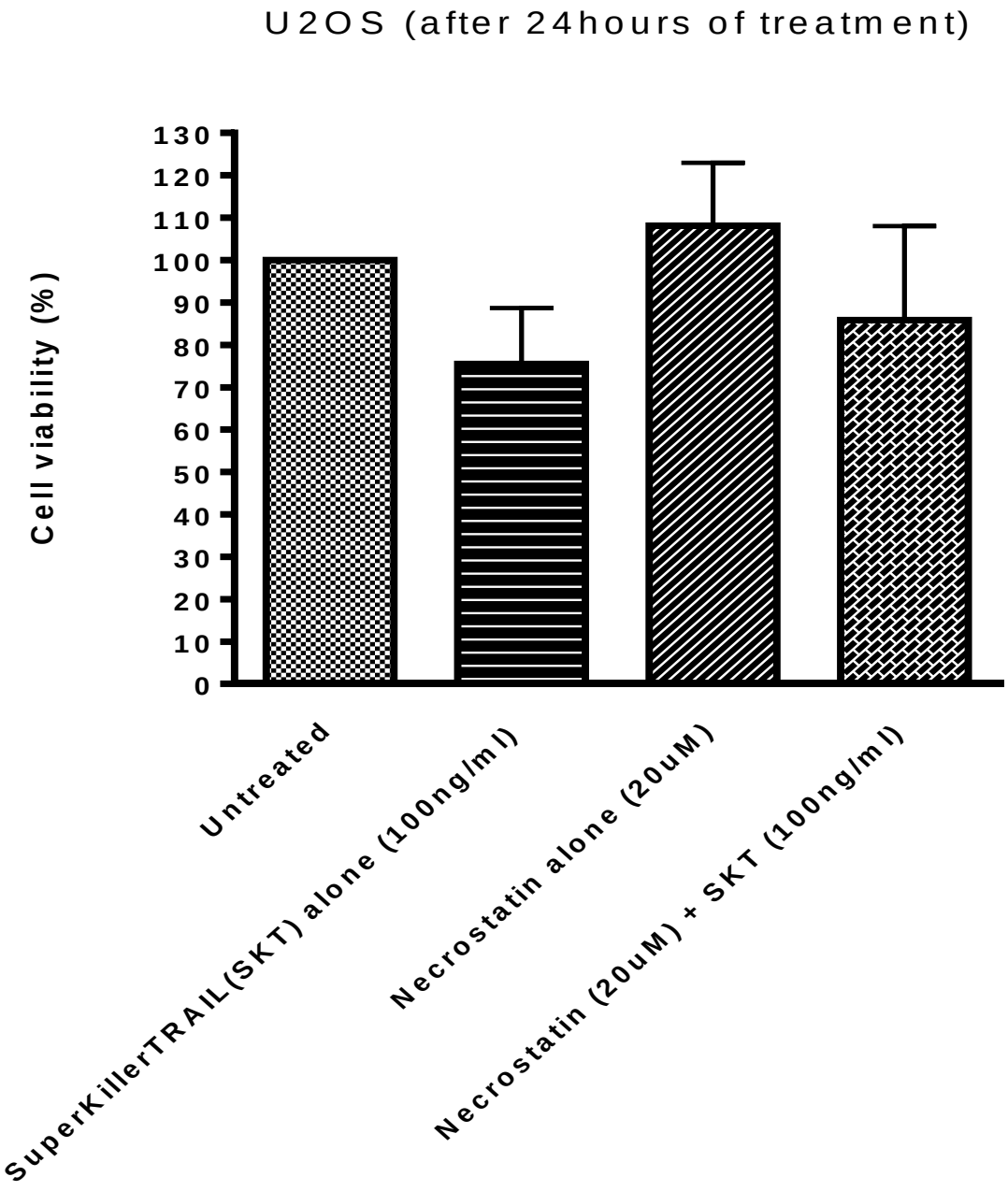

Figure 91 - Inhibition of receptor-interacting protein 1 (RIP1) kinase domain (using necrostatin) and response to SuperKillerTRAIL (SKT) in the U2OS cell line. No significant difference was observed when applying the necrostatin (20 µM).

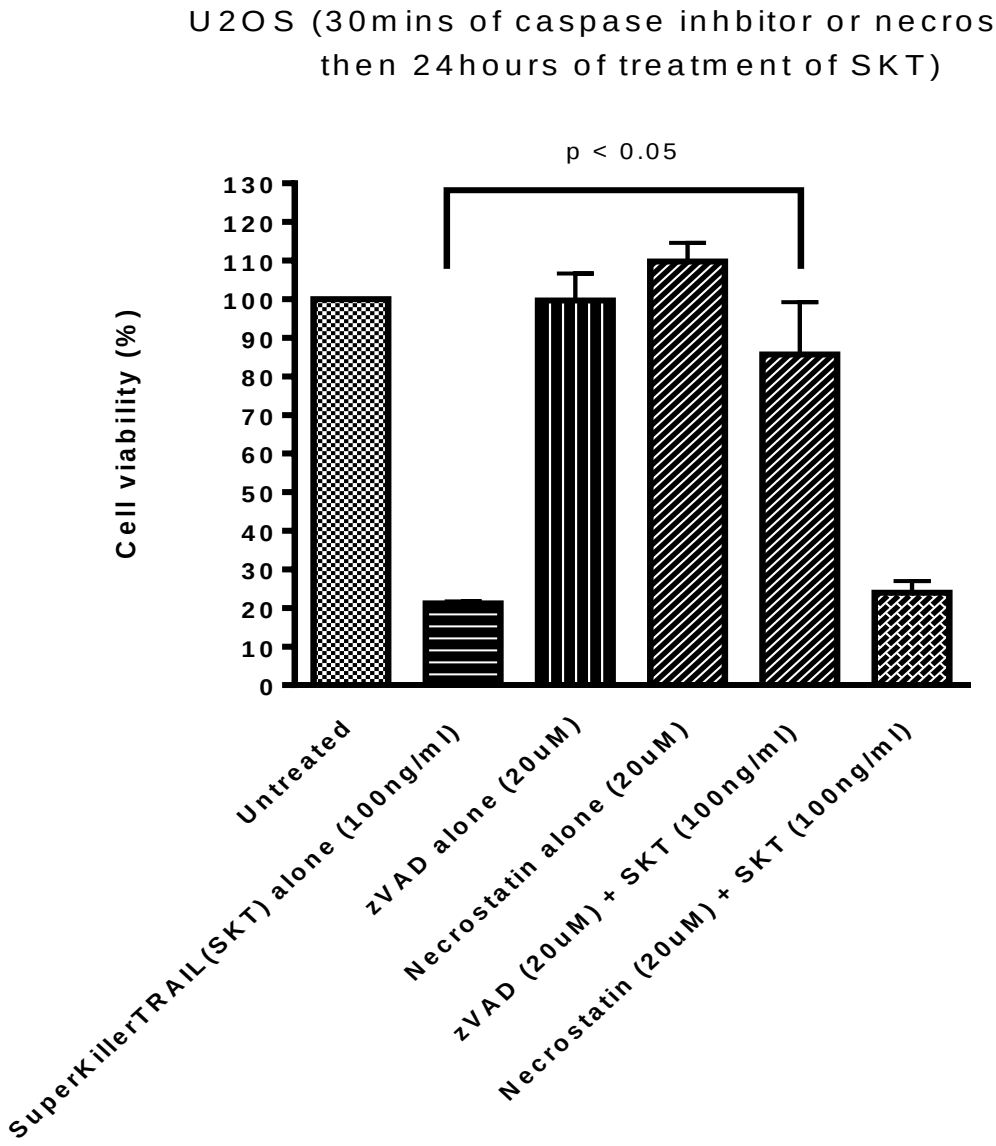

Figure 92 - Comparison of caspase inhibition (reversible, Ac-DEVD-CHO or irreversible, Z-VAD-FMK) or inhibition of receptor-interacting protein 1 (RIP1) kinase domain (necrostatin) and response to SuperKillerTRAIL (SKT) in the U2OS cell line. For the U2OS cell line, significance was observed when applying zVAD-FMK (20 µM), about 65 % less cell death when compared to SuperKillerTRAIL (SKT) alone ($p < 0.005$, Mann-Whitney *U* test). However, no significant difference was observed when applying the necrostatin (20 µM).

5.2 siRNA knockdown and response to TRAIL experiments

5.2.1 Overview

siRNA knockdown of DR5 and DR4

siRNA was used to knockdown DR5 in the SJSA-1 and U2OS cell lines in order to assess the requirement for DR5 to SKT to induce apoptosis in these cells and not from off target effects. From the flow cytometry data obtained, I found high and moderate levels of surface DR5 expression in the SJSA-1 and U2OS cell lines respectively. RT-PCR confirmed knockdown with the sequences, concentrations and the 72-hour time point chosen. A good degree of surface knockdown (>80 % in these cell lines) was also confirmed using flow cytometry. The SJSA-1 and U2OS cell lines were then treated with DR5 siRNA and monitored using the IncuCyte® live-cell analysis system for cell proliferation and response to SuperKillerTRAIL (SKT). Generally, I found that knockdown of DR5 conferred resistance to SKT in the U2OS and SJSA-1 cell lines (Section 4.2.2). DR4 was also successfully knocked down in the TC71 cell line. The application of SKT after a degree of knockdown did not appear to have a significant effect compared to non-targeting/scrambled siRNA.

siRNA knockdown of DcR2

From the flow cytometry data obtained I found high levels of surface DcR2 expression in the SJSA-1 osteosarcoma cell line. DcR2 siRNA was used to knockdown DcR2 in the SJSA-1 cell line (>80 % knockdown achieved). The SJSA-1 cell line treated with siRNA was monitored using the IncuCyte® live-cell analysis system for cell proliferation and response to SuperKillerTRAIL (SKT). There was no significant evidence to suggest increased sensitivity from the knockdown using 3.5 nM of SKT (Section 4.2.4).

5.2.2 DR5 knockdown using siRNA reduces the response to SuperKillerTRAIL (SKT)

DR5 knockdown was achieved in the U2OS and SJSA-1 cell lines using DR5 siRNA (Figure 93) and responses to SuperKillerTRAIL (SKT) was monitored using the IncuCyte® live-cell analysis system.

siRNA design and RT-PCR analysis

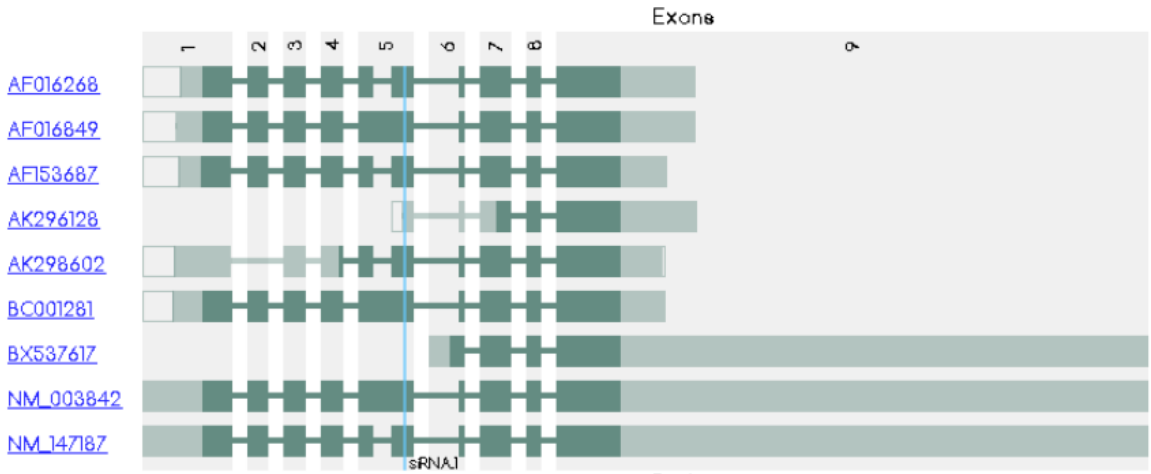

Figure 93 - DR5-1 siRNA target sequence location. DR5 is also known as 'TNFRSF10B CD262, DR5, KILLER, KILLER/DR5, TRAIL-R2, TRAILR2, TRICK2, TRICK2A, TRICK2B, TRICKB, ZTNFR9', chromosome 8, total exons = 9, 9 splice variants [261]. http://projects.insilico.us/SpliceCenter/PrimerCheck

5.2.2.1 DR5 siRNA knockdown in U2OS osteosarcoma cell line and response to SuperKillerTRAIL (SKT)

RT-PCR analysis of DR5 knockdown in U2OS cell line

Adequate knockdown was observed in U2OS cell line using RT-PCR (Figure 94).

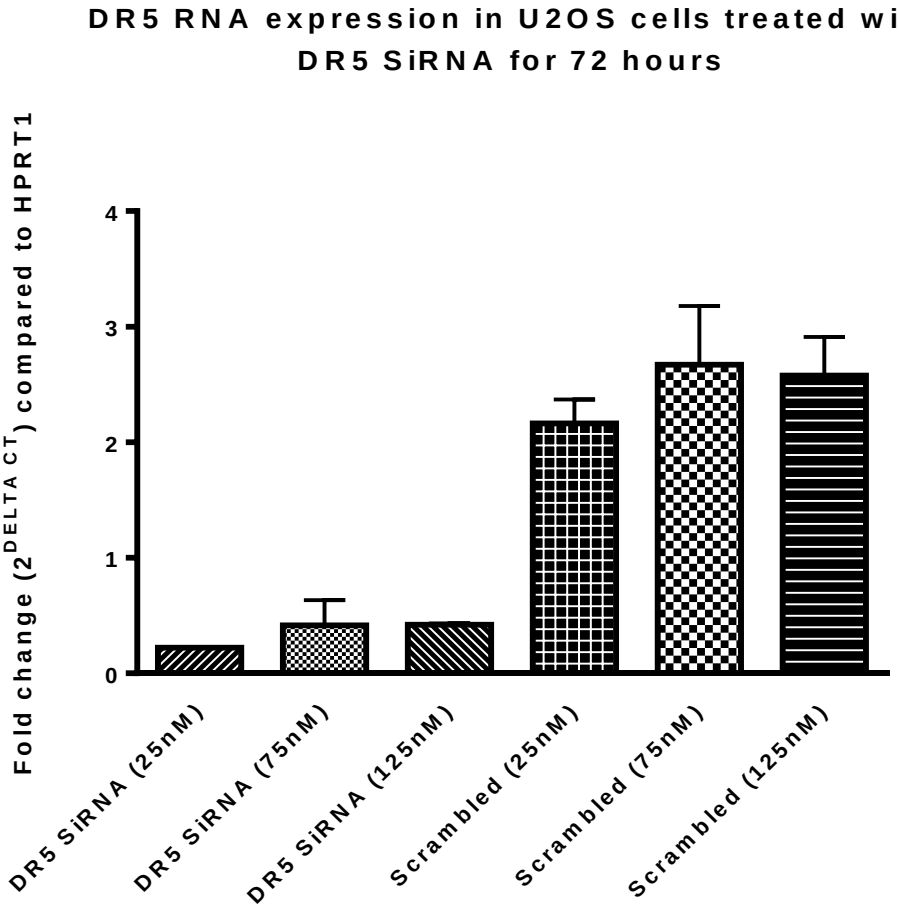

Figure 94 - U2OS cells were transfected with DR5 siRNA from sequences obtained from the following paper [258] and RNA was extracted at 72 hours. A reduction in DR5 transcript levels were found using RT-PCR compared to non-targeted/scrambled siRNA (mean +/- SEM, n = 1).

Flow cytometry analysis of DR5 surface level knockdown in U2OS cell line

Flow cytometry analysis demonstrated adequate knockdown of DR5 at the surface protein level in the U2OS cell line (Figure 95).

(a)

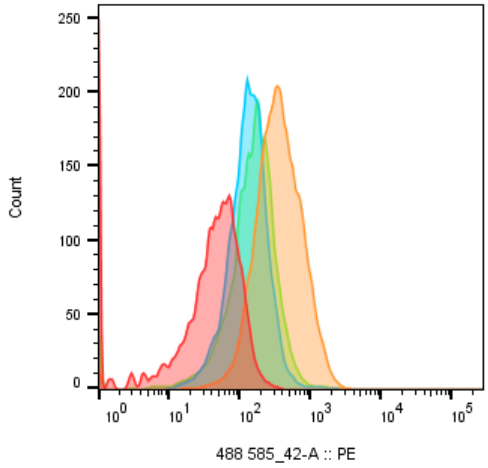

Sample Name	Subset Name	Count	Median : 488 585_42-A
345787.fcs	Unstained	5457	43.6
345790.fcs	U2OS Scrambled	7641	340
345788.fcs	U2OS ITC	6229	130
345791.fcs	U2OS DR5 SIRNA	6166	157

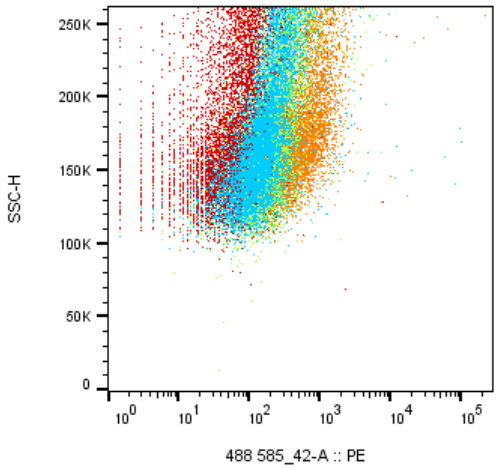

Sample Name	Subset Name	Count	Median : 488 585_42-A
345788.fcs	Ungated	10000	193
345787.fcs	Ungated	10000	69.6
345791.fcs	Ungated	10000	228
345790.fcs	Ungated	10000	434

(b)

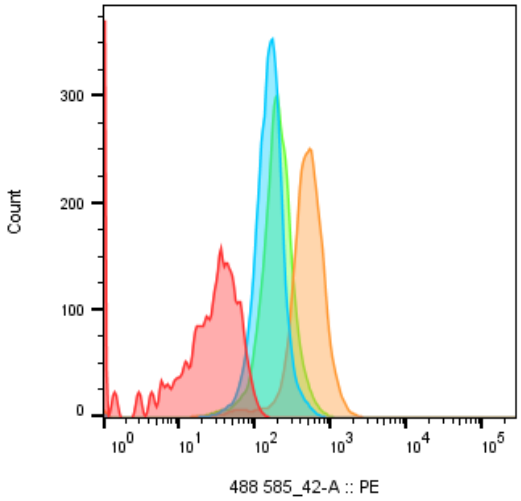

	Sample Name	Subset Name	Count	Median : 488 585_42-A
	381749.fcs	U2OS Unstained	7078	21.4
	381750.fcs	U2OS ITC	7117	153
	381771.fcs	U2OS DR5 Scrambled	6040	485
	381751.fcs	U2OS DR5 SiRNA at 72hours	6492	191

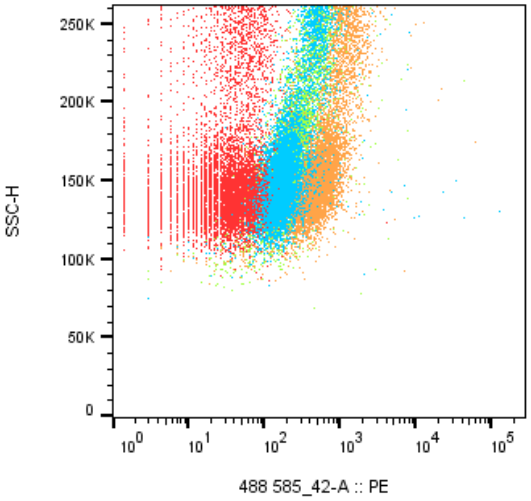

	Sample Name	Subset Name	Count	Median : 488 585_42-A
	381749.fcs	Ungated	10000	27.2
	381750.fcs	Ungated	10000	182
	381771.fcs	Ungated	10000	657
	381751.fcs	Ungated	10000	247

Figure 95 – U2OS cells were transfected with DR5 siRNA (50 nM) and surface level DR5 was analysed using flow cytometry at 72 hours. A reduction in DR5 surface expression was found in DR5 siRNA treated cells compared to non-targeted/scrambled U2OS treated cells [(MFI scrambled - MFI DR5 siRNA)/MFI scrambled x100 = 54 % knockdown could be achieved (a) and 61 % (b)].

Response to SuperKillerTRAIL

DR5 siRNA and scrambled siRNA treated U2OS cells were exposed to IC50 of SuperKillerTRAIL (SKT) and 100 ng/ml (4 nM) (SKT) and the effect on proliferation was measured using the IncuCyte® live-cell analysis system. DR5 siRNA was found to reduce proliferation and increase resistance to SKT (Figure 96). More apoptotic cells were observed in scrambled siRNA treated cells (Figure 97).

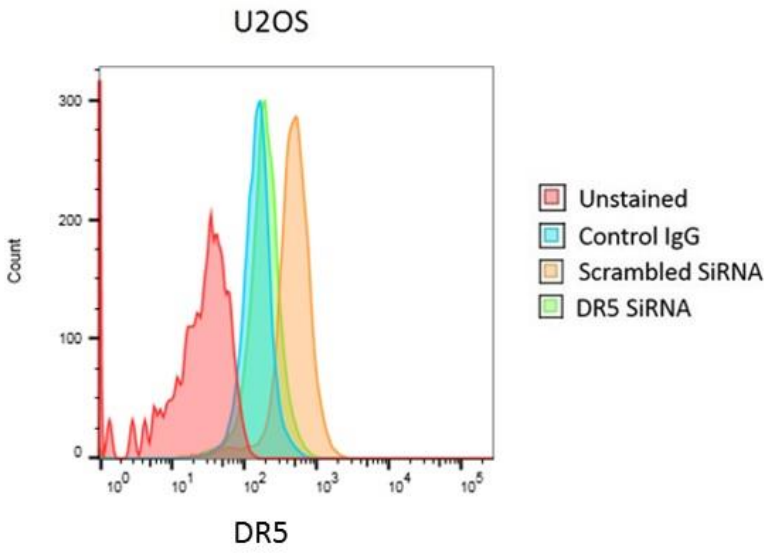
U2OS
Count
300
200
100
0
10^0
10^1
10^2
10^3
10^4
10^5
DR5
Unstained
Control IgG
Scrambled SiRNA
DR5 SiRNA

a

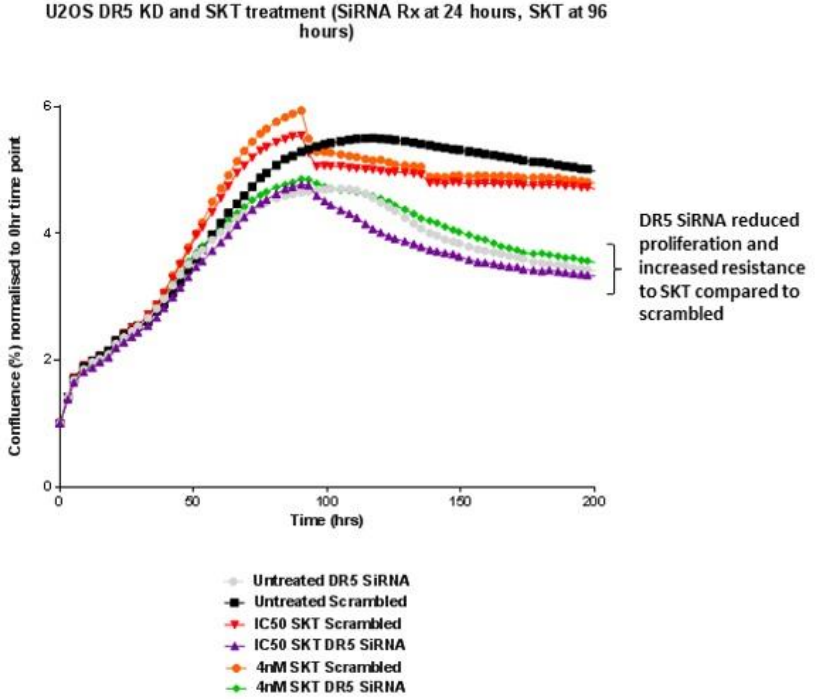
U2OS DR5 KD and SKT treatment (SiRNA Rx at 24 hours, SKT at 96 hours)
Confluence (%) normalised to 0hr time point
6
4
2
0
0
50
100
150
200
Time (hrs)
DR5 SiRNA reduced proliferation and increased resistance to SKT compared to scrambled
Untreated DR5 SiRNA
Untreated Scrambled
IC50 SKT Scrambled
IC50 SKT DR5 SiRNA
4nM SKT Scrambled
4nM SKT DR5 SiRNA

b

Figure 96– (a) 61% DR5 Knockdown was achieved using DR5 siRNA. (b) Knockdown reduces U2OS cell proliferation and confers resistance to SuperKillerTRAIL (SKT). DR5 siRNA was applied at 24 hours and SKT was applied at 72 hours at the IC50 for the U2OS osteosarcoma cell line or at 100 ng/ml (4 nM).

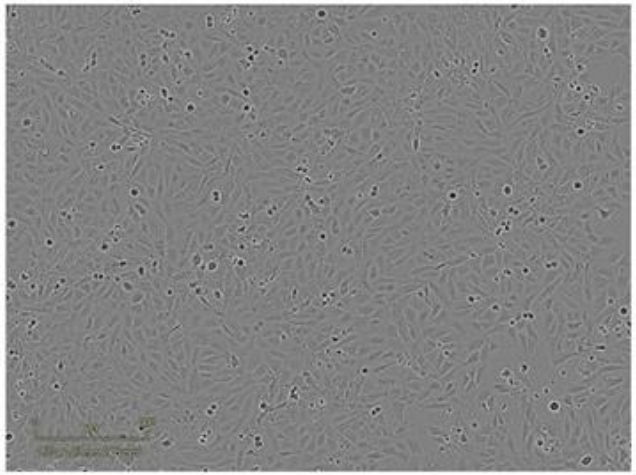

(a) Control scrambled siRNA treated U2OS cells

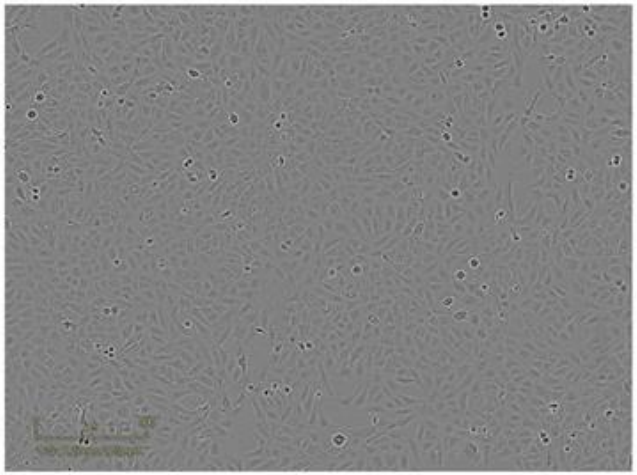

(c) Control DR5 siRNA treated U2OS cells

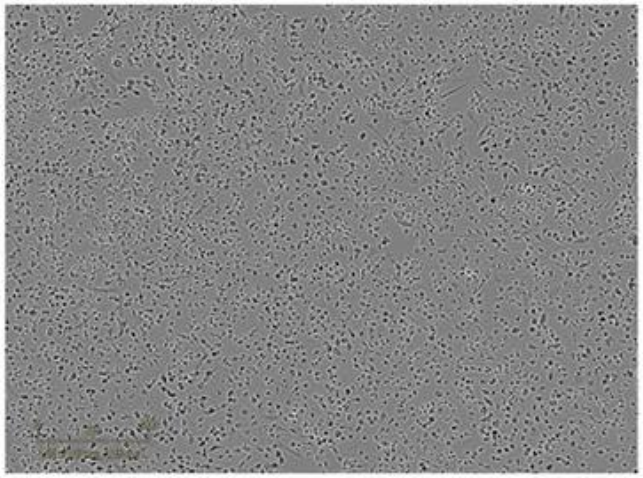

(b) Scrambled siRNA treated U2OS cells
5 hours after SKT (IC50) applied

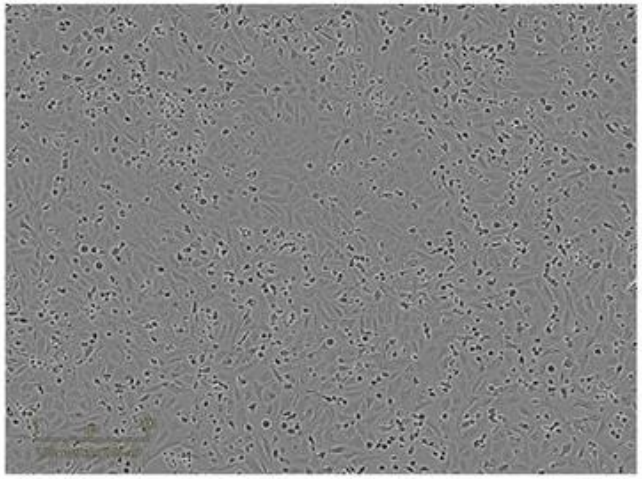

(d) DR5 siRNA treated U2OS cells
5 hours after SKT (IC50) applied

Figure 97 - IncuCyte® live-cell analysis system image following SuperKillerTRAIL (100 ng/ml, 4 nM) treatment. (a) Before SuperKillerTRAIL (100 ng/ml) treatment in scrambled siRNA treated U2OS cells. (b) 24 hours after SuperKillerTRAIL (100 ng/ml) treatment in scrambled siRNA treated U2OS cells. (c) Before SuperKillerTRAIL (100 ng/ml) treatment in DR5 KD U2OS cells. (d) After SuperKillerTRAIL (100 ng/ml) treatment in DR5 KD U2OS cells.

5.2.2.2 DR5 surface level knockdown in SJSA-1 osteosarcoma cell line and response to SuperKillerTRAIL

Flow cytometry analysis demonstrated adequate knockdown of DR5 at the surface protein level in the SJSA-1 cell line (Figure 98). More apoptotic cells were observed in scrambled siRNA treated cells (Figure 99).

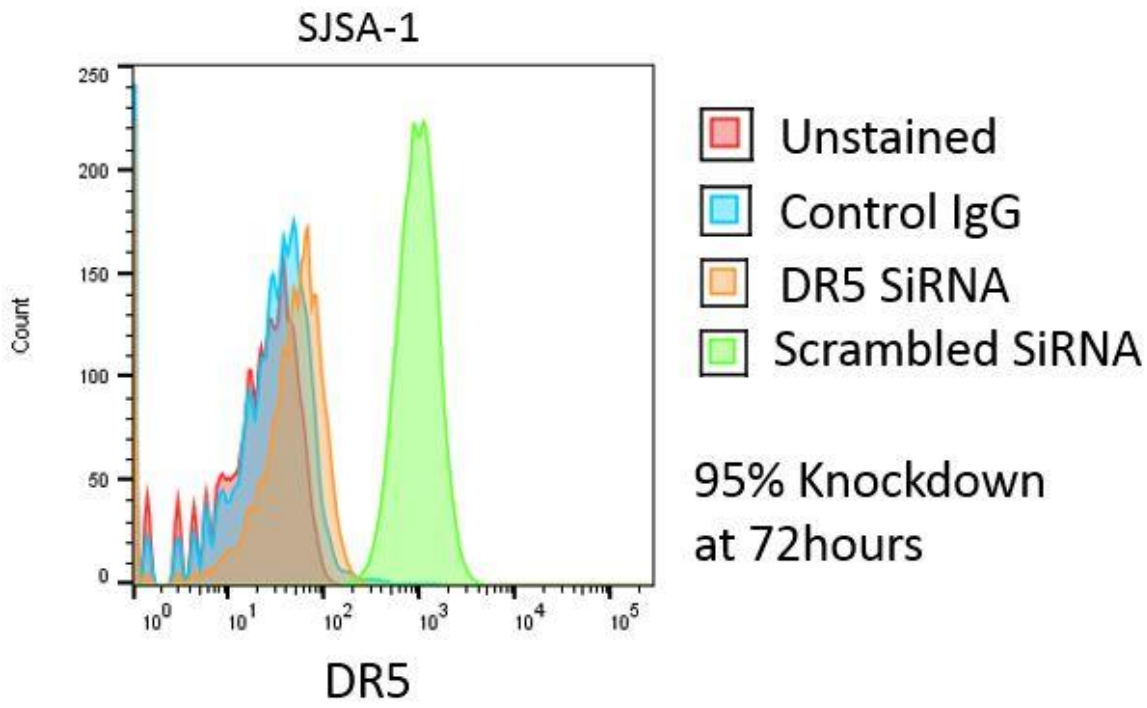

Figure 98 – SJSA-1 cells were transfected with DR5 siRNA (50 nM) and surface level DR5 was analysed using flow cytometry at 72 hours. A reduction in DR5 surface levels were found in DR5 siRNA treated cells compared to non-targeted/scrambled SJSA-1 treated cells. 95 % knockdown could be achieved using DR5 siRNA in the SJSA-1 cell line.

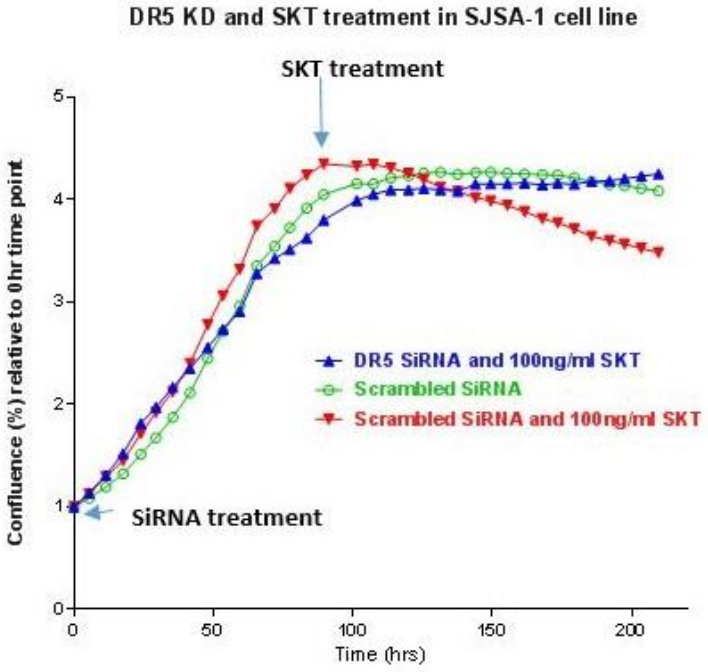
DR5 KD and SKT treatment in SJSA-1 cell line
SKT treatment
Confluence (%) relative to 0hr time point
DR5 SiRNA and 100ng/ml SKT
Scrambled SiRNA
Scrambled SiRNA and 100ng/ml SKT
SiRNA treatment
Time (hrs)
0
50
100
150
200
1
2
3
4
5

a

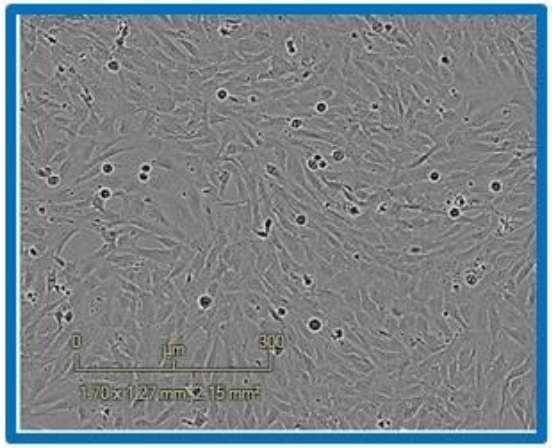

b

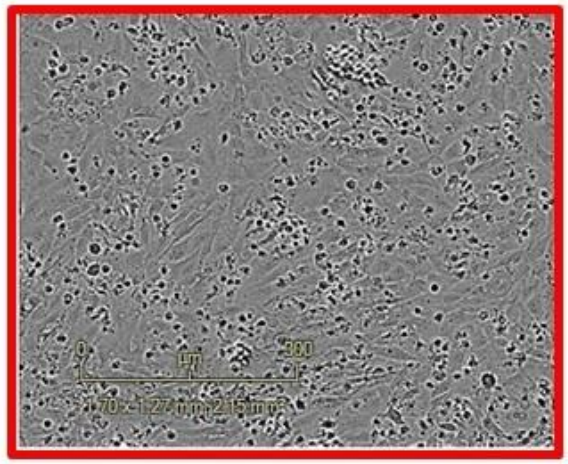

c

Figure 99 – DR5 siRNA treated SJSA-1 cells were more resistant to 100 ng/ml, 4 nM SuperKillerTRAIL (SKT) (a and b) than scrambled treated SJSA-1 cells (a and c).

5.2.3 DR4 knockdown using siRNA and response to SuperKillerTRAIL (SKT)

DR4 was knockdown was adequately achieved in the TC71 Ewing's sarcoma cell line using DR4 siRNA (Figure 100 and Figure 101) and response to SuperKillerTRAIL (SKT) was monitored using the IncuCyte® live-cell analysis system. DR4 siRNA and scrambled siRNA treated TC71 cells were exposed to IC50 of SuperKillerTRAIL (SKT) and IC50 + 1/3rd and the effect on proliferation was measured using the IncuCyte. Knockdown achieved was only 39 % and no obvious differences between DR4 siRNA and scrambled siRNA treated TC71 cells was observed (Figure 102 and Figure 103).

SIRNA design

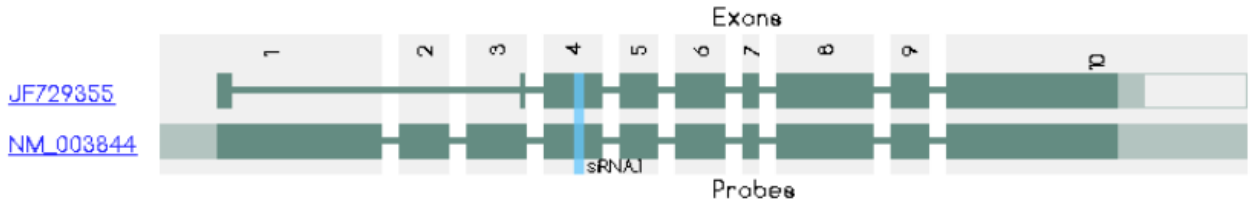

Figure 100 - DR4-1 siRNA target sequence location. DR4 is also known as TNFRSF10A, APO2, CD261, DR4, TRAILR-1, TRAILR1, chromosome 8, total exons = 10, 2 splice variants (http://projects.insilico.us/SpliceCenter/PrimerCheck).

Flow cytometry analysis of DR4 surface level knockdown in TC71 cell line

(a)

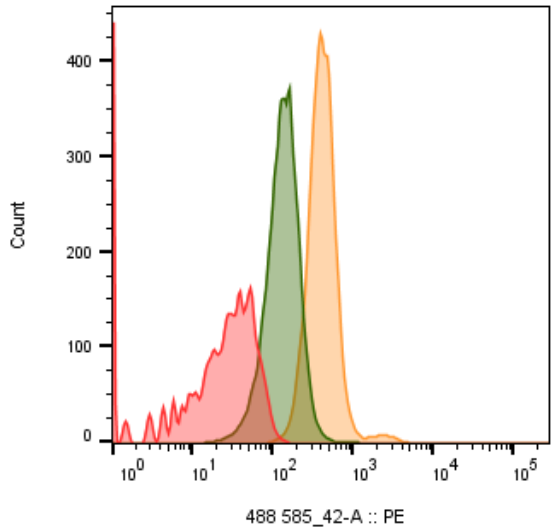

	Sample Name	Subset Name	Count	Median : 488 585_42-A
	349584.fcs	Unstained	8150	19.0
	350211.fcs	DR4 SiRNA (1) 48hours	8528	133
	349592.fcs	DR4 Scrambled	8436	400

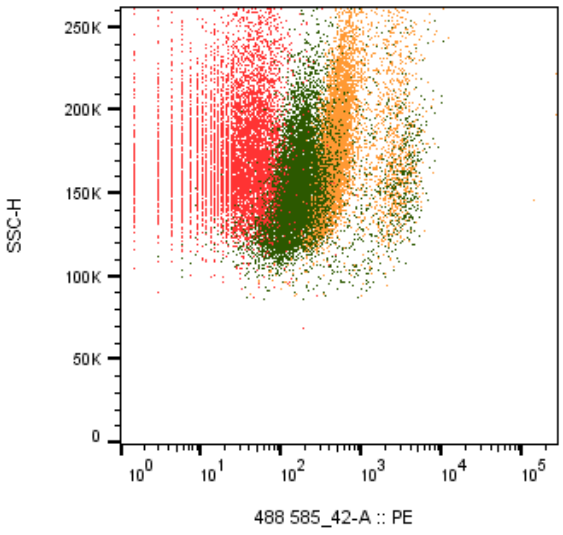

	Sample Name	Subset Name	Count	Median : 488 585_42-A
	349584.fcs	Ungated	10000	21.9
	350211.fcs	Ungated	10000	145
	349592.fcs	Ungated	10000	432

(b)

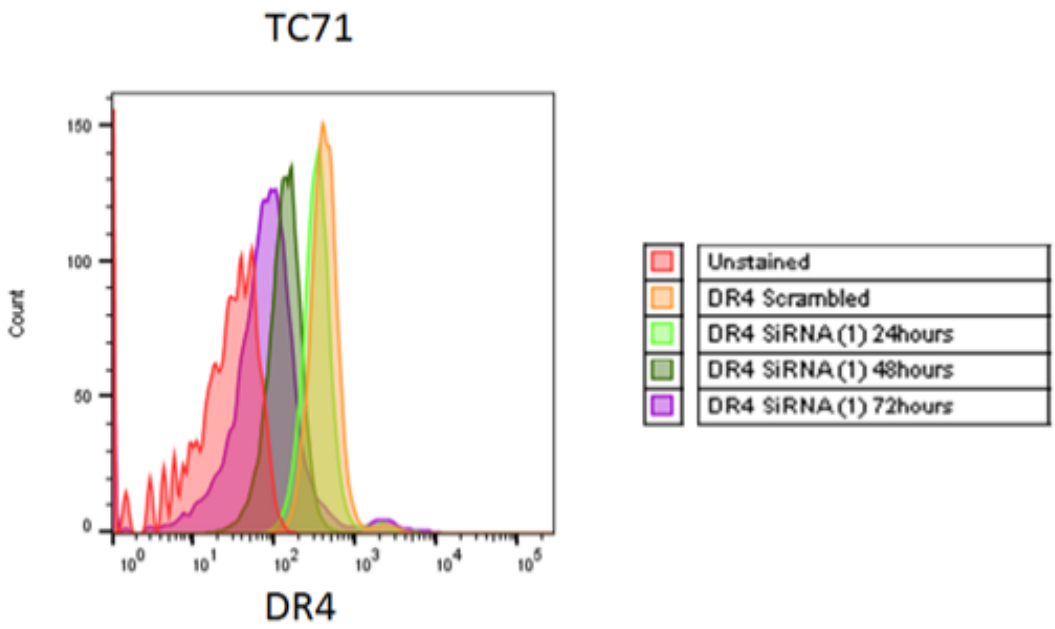

Figure 101 – TC71 cells were transfected with DR4 siRNA (50 nM) and surface level DR4 was analysed using flow cytometry at 24, 48 and 72 hours. A reduction in DR4 surface levels were found in DR4 siRNA treated cells compared to non-targeted/scrambled TC71 treated cells (67 % at 48 hours and 81 % knockdown at 72 hours) (a and b).

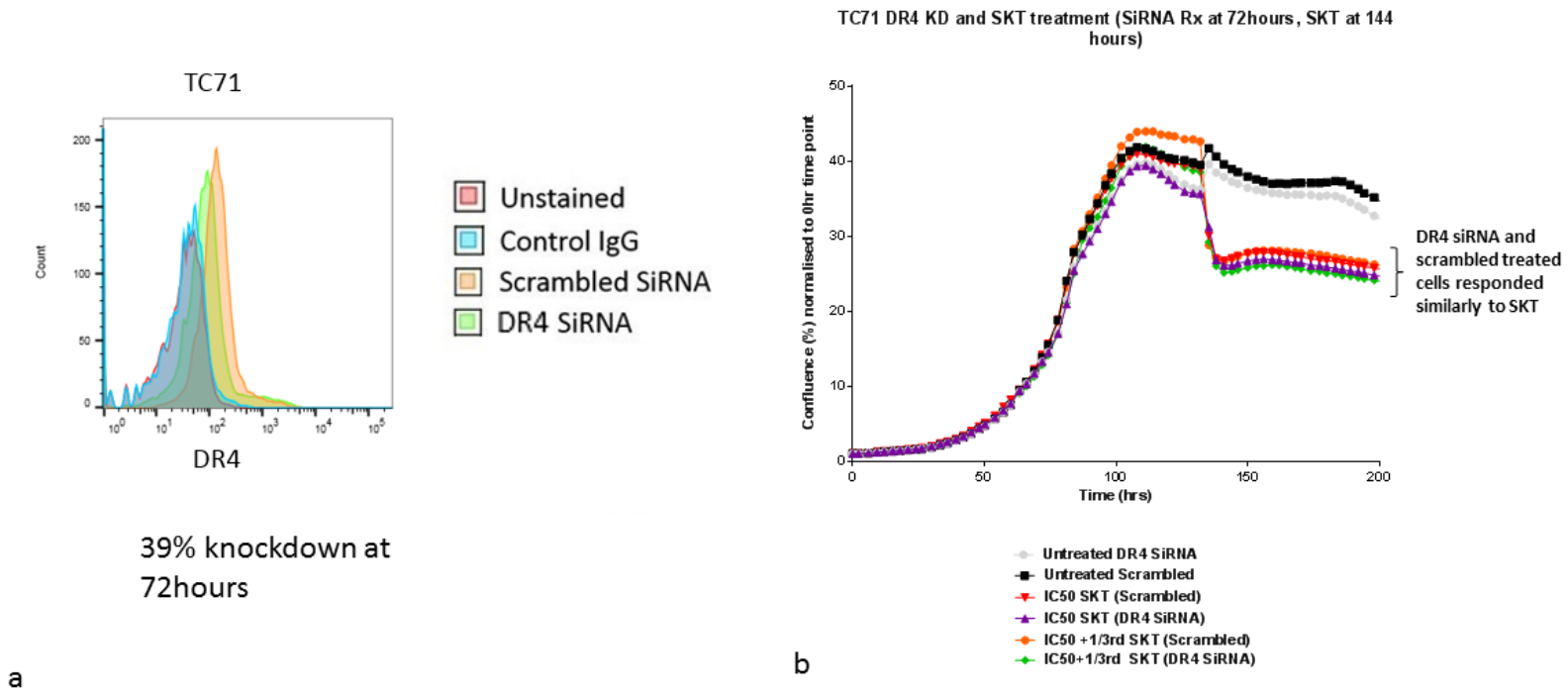

Figure 102 – (a) 39 % DR4 knockdown was achieved using DR4 siRNA. (b) Knockdown at this level did not significantly affect proliferation or confer resistance to SuperKillerTRAIL (SKT). DR4 siRNA was applied at 72 hours and SKT was applied at 144 hours.

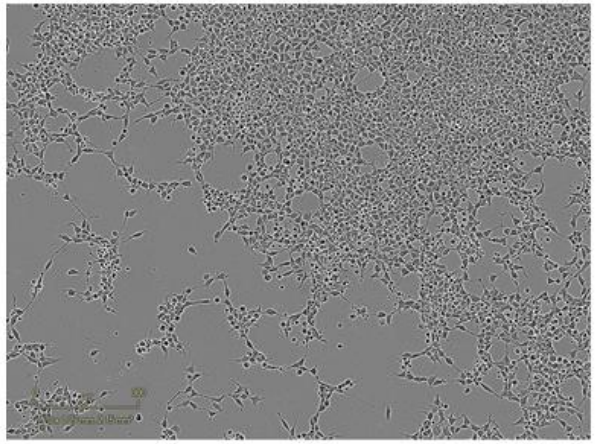

(a) Control scrambled siRNA treated TC71 cells

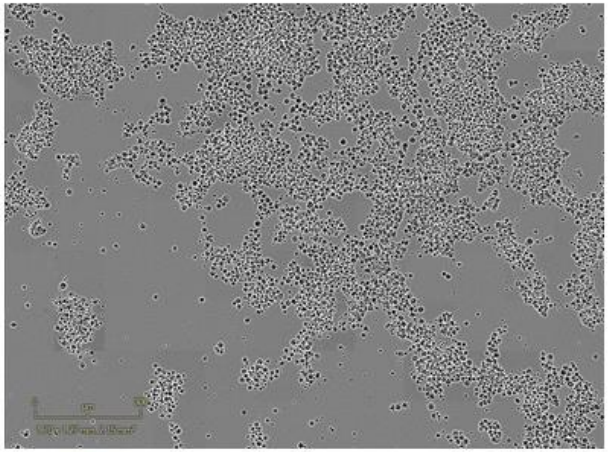

(b) Scrambled siRNA treated TC71 cells
6 hours after SKT (IC50) applied

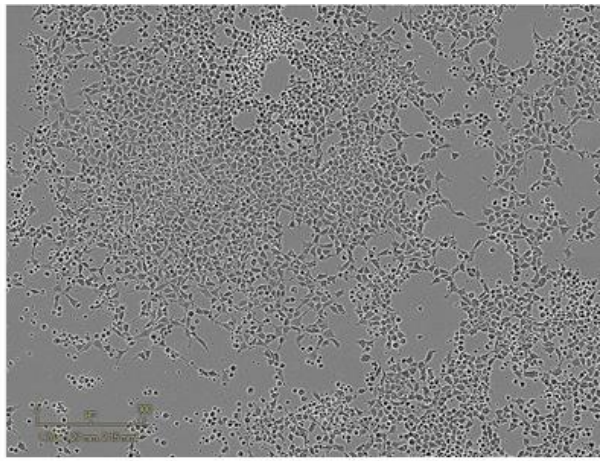

(c) Control DR4 siRNA treated TC71 cells

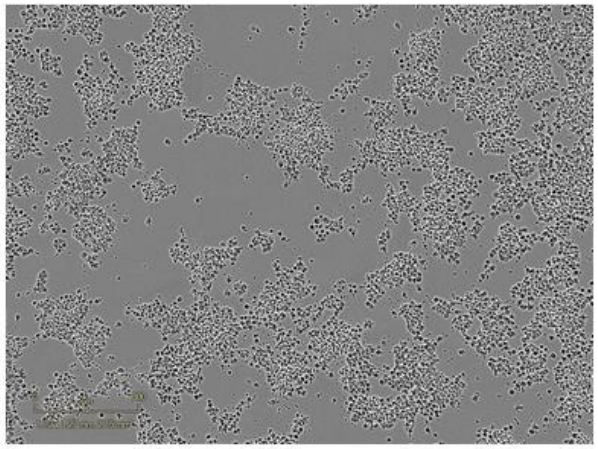

(d) DR4 siRNA treated TC71 cells
6 hours after SKT (IC50) applied

Figure 103 - IncuCyte® live-cell analysis system images following SuperKillerTRAIL (SKT) (IC50 for TC71) treatment. (a) Before SKT treatment in scrambled siRNA treated TC71 cells. (b) 24 hours after SKT treatment in scrambled siRNA treated TC71 cells. (c) Before SKT treatment in DR4 KD TC71 cells. (d) 24 hours after SKT treatment in DR4 KD TC71 cells.

5.2.4 DcR2 knockdown and response to SuperKillerTRAIL (SKT)

Adequate level of DcR2 knockdown was achieved in the SJSA-1 cells line (Figure 104 and Figure 105).

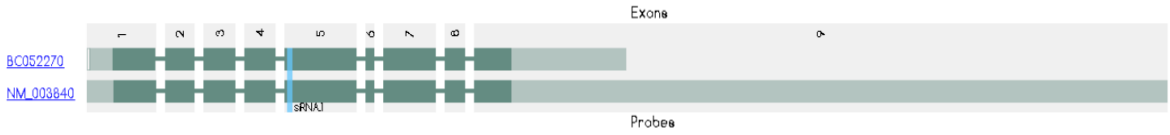

Figure 104 - DcR2 siRNA target sequence location. DcR2 also known as TNFRSF10D, CD264, DCR2, TRAIL-R4, TRAILR4, TRUNDD, ENSG00000173530, chromosome 8, total exons = 9, 2 splice variants. http://projects.insilico.us/SpliceCenter/PrimerCheck.

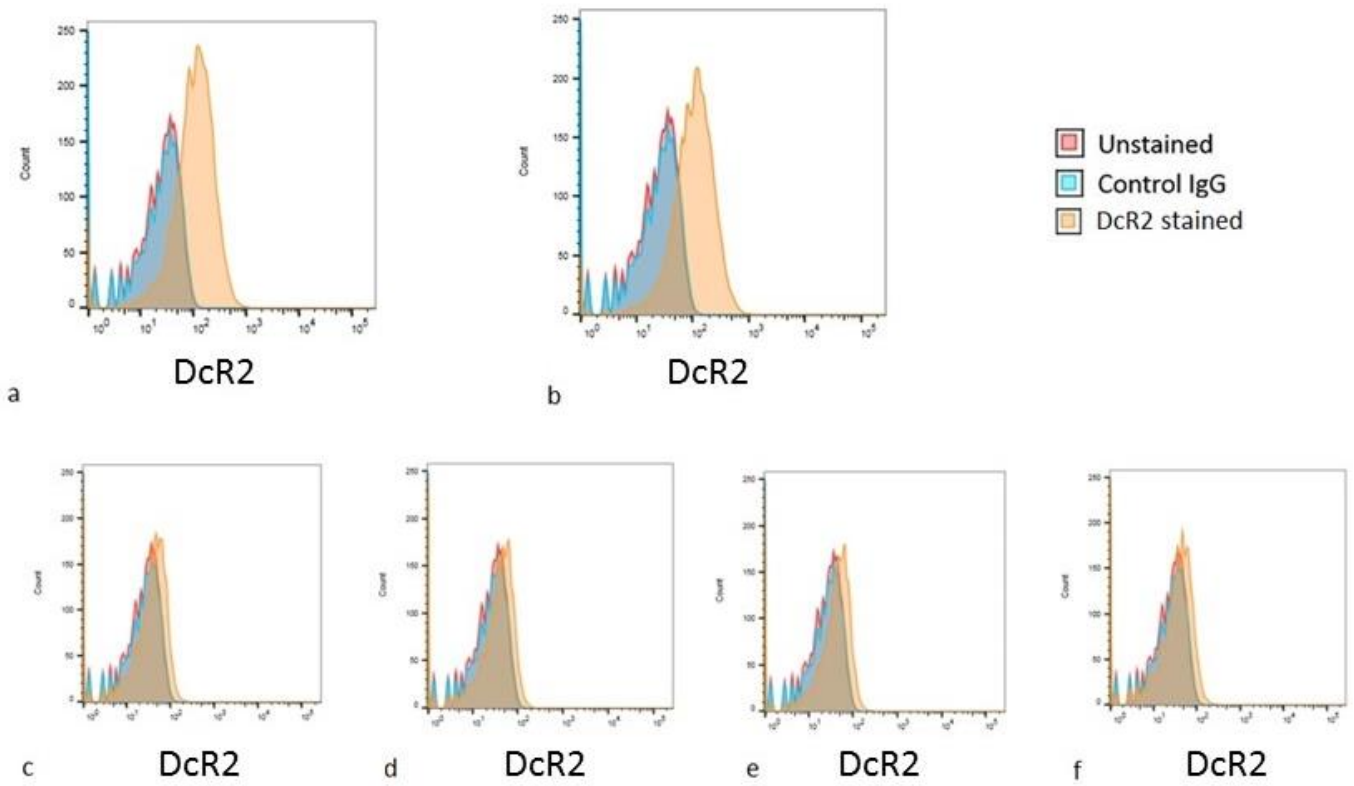

Figure 105 – Flow cytometry analysis for DcR2 expression after siRNA treatment. (a) SJSA-1 cells staining positive for DcR2, (b) same degree of shift with scrambled siRNA, nearly complete knockdown with (c) sequence A, (d) sequence B, (e) sequence C and (f) pooled.

5.2.4.1 IncuCyte monitoring of DcR2 KD and sensitivity to SuperKillerTRAIL

Following successful DcR2 KD in the SJSA-1 osteosarcoma cell line, response to SKT treatment was observed using the IncuCyte® live-cell analysis system. Despite nearly complete knockdown of DcR2, the rate of decline of confluency following treatment with SuperKillerTRAIL (3.5 nM) is similar in DcR2 siRNA treated cells compared to SJSA-1 cells treated with scrambled siRNA (Figure 106).

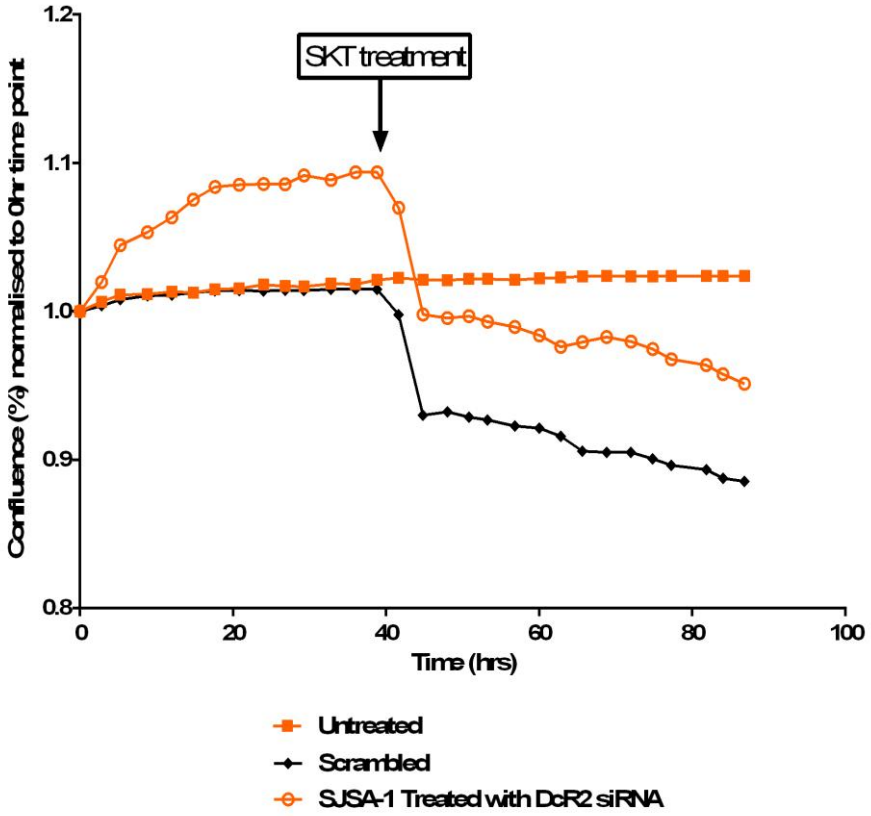

Figure 106 - Despite nearly complete knockdown of DcR2, the rate of decline of confluency following treatment with SuperKillerTRAIL (3.5 nM) is similar in DcR2 siRNA treated cells compared to SJSA-1 cells treated with scrambled siRNA.

5.3 Clustered regularly interspaced short palindromic repeats (CRISPR) knockout of DR5

CRISPR was used to knockout DR5 in the SW1353 and HT1080 cell lines. Flow cytometry was used to select the cells negative for DR5. After confirmation of knockout of DR5 on the cell surface, the cells were seeded into a 6-well plate and the proliferation of those cells was monitored using the IncuCyte. This was of interest as the receptor is thought to promote invasion and metastases [262]. Furthermore, I assessed their response to crosslinked forms of TRAIL. Genome cleavage detection (GCD) assay indicated adequate DR5 gRNA editing efficiency (Figure 107).

Genome cleavage detection (GCD) assay assessment of DR5 gRNA editing efficiency

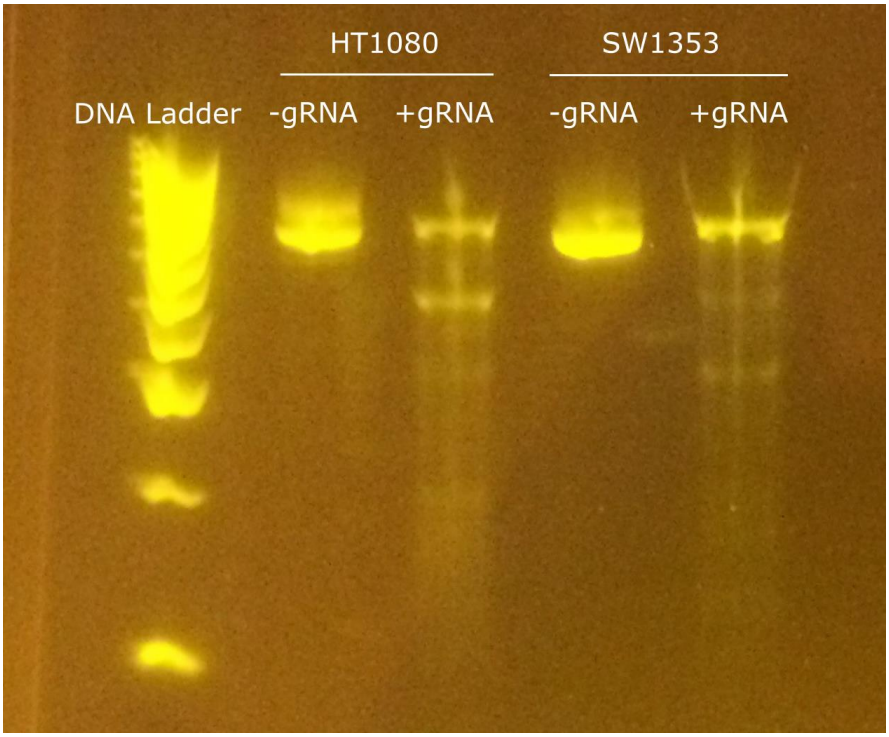

Figure 107 – GCD assay and DNA electrophoresis to confirm presence of cleaved DNA products and degree of efficiency of editing in cell lines with an indel created by CRISPR Cas9. (a) DNA ladder, (b) HT1080 unedited (-gRNA), (b) HT1080 edited (+gRNA), (c) SW1353 unedited (-gRNA), (d) SW1353 edited (+gRNA). There is about 50 % efficiency indicated by the top band in lanes (c) and (e) in relation to the bands in (b) and (d) respectively.

Flow cytometry and FACS analysis to confirm DR5 knockout

SW1353 and HT1080 confirmation of DR5 knockout at protein level and surface protein level was carried out using western blotting (Figure 108 and Figure 109) and flow cytometry respectively. Two populations (one DR5 positive and the other DR5 negative) for the HT1080 and SW1353 cell lines were visible using flow cytometry. The negative population was sorted into a 6-well plate for further expansion and later single cell sorting (presented in general materials and methods).

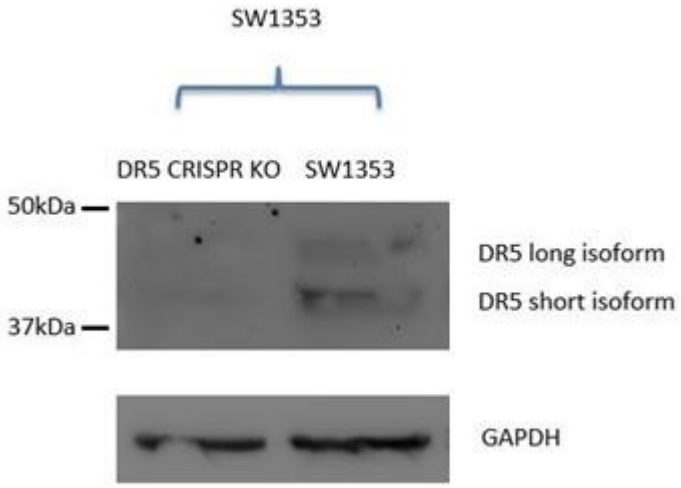

Figure 108 - DR5 isoforms in the SW1353 cell line, which are not as visible following DR5 CRISPR Knockout following treatment of the cells with CRISPR mRNA, lipofectamine and DR5 gRNA.

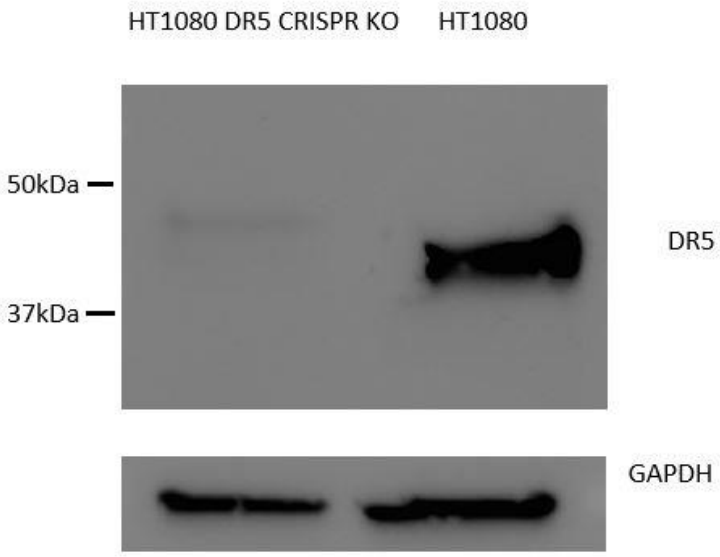

Figure 109 - Strong DR5 band in the HT1080 cell line, which is no longer strongly visible following DR5 CRISPR Knockout following treatment of the cells with CRISPR mRNA, lipofectamine and DR5 gRNA.

5.3.1 HT1080 DR5 CRISPR KO abolishes cytotoxic effect of crosslinked TRAIL

HT1080 DR5-ve CRISPR KO cell line proliferation and growth in culture was not impaired on inspection and demonstrated significant resistance to SuperKillerTRAIL (SKT), Fc containing crosslinked TRAIL (Fc-scTRAIL) and an NG2 targeted crosslinked form of TRAIL (ScFv(MCSP)-Fc-scTRAIL) compared to the non CRISPR treated DR5+ve HT1080 cells (Figure 110).

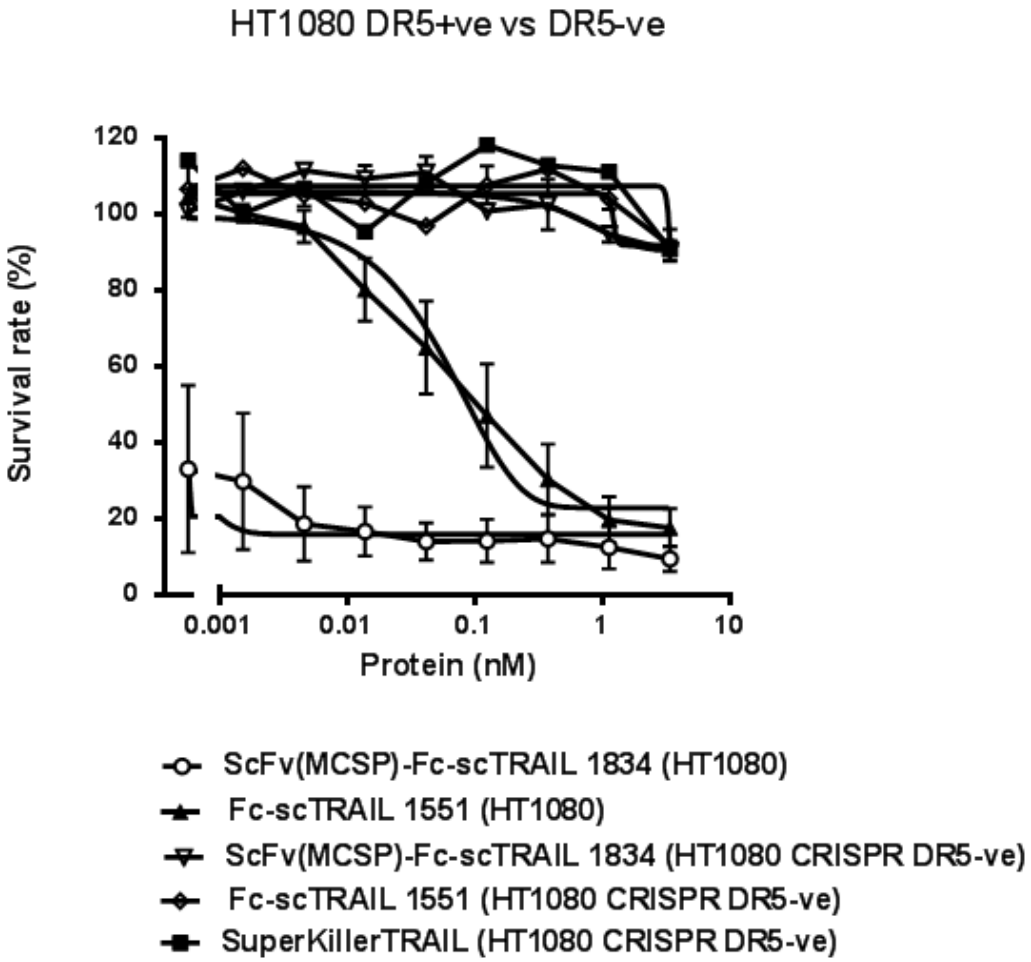

Figure 110 – DR5 negative CRIPSR KO HT1080 cell response to crosslinked forms of TRAIL and SuperKillerTRAIL (SKT) vs control DR5+ve HT1080 cells. The HT1080 DR5

CRISPR KO cell line demonstrated significant resistance to a crosslinked form of TRAIL (Fc-scTRAIL) and NG2/MCSP targeted crosslinked from of TRAIL scFv(MCSP)-Fc-scTRAIL compared to the non CRISPR treated HT1080 cells (n = 3, mean+/-SEM).

5.4 Discussion and future direction

Death receptor/TRAIL-R agonists

The ability of TRAIL to induce apoptosis selectively in cancer cells has resulted in clinical trials using rhTRAIL and several trail agonistic antibodies, which has included mapatumumab (DR4 agonist), conatumumab (DR5 agonist), tigatuzumab [CS-1008] and DS-8273A, which are DR5 agonists and humanised versions of murine TRA-8 (DR5 agonist). There are ongoing clinical trials using these DR5 agonists; however, to date DR5 and DR4 agonists have not produced a clinical benefit in cancer patients. There appears to be three main contributors to the failure of these clinical trials such as: (1) insufficient agonistic activity of the drug candidate in question, (2) resistance of the primary cells to the monotherapy with the DR agonists, and (3) lack of a suitable biomarker to identify patients who are likely to respond to DR agonist therapy.

Recombinant human TRAIL (rhTRAIL)

There is a move towards using recombinant forms of TRAIL that mimics the natural form of TRAIL, which has a trimeric structure and several recombinant TRAIL formulations have been developed with the aim of increasing stability or tumour specific delivery of the TRAIL. Stabilisation of the trimer has been attempted by addition of FLAG epitope, LZ and isoleucine zipper motifs and polyhistidine as an end terminal tag.

Further modifications have been fusion of the TRAIL to Fc portion of human immunoglobulin IgG and fusion of TRAIL to human serum albumin. Thus far for the clinical application in bone sarcoma patients, the recombinant form of TRAIL developed known as APO2L (dulanermin), which is dual apoptotic receptor DR4 and DR5 agonist also known as AMG-951 has been used for chondrosarcoma. Subbiah *et al.,* in 2012 [263] found regression in lung metastases three years after APO2L/TRAIL was administered. The patient achieved a sustained partial response and ultimately a

complete response. Dulanermin treatment was given as 8 mg/kg IV on days 1-5 in a 21-day cycle with cycle one, day one commencing in August 2005. The patient achieved a sustained partial response by response evaluation criteria in solid tumours (RECIST) [264], with only residual sub-centimeter nodules remaining which were not positive on positron emission tomography (PET) scan. RECIST is tumour response determination using response evaluation criteria in solid tumours by repeated tomography CT scans or PET [264]. The patient had tolerated the treatment without significant side effects and maintained a performance status of 100 %. After five months of treatment, however, the patient was noted to have progressive lung disease and underwent a resection that confirmed chondrosarcoma. He continued therapy at the same dosage for an additional 16 months. Eighteen months after starting the treatment and at restaging in October 2011, 6 years after commencement of therapy, CT scans showed no evidence of disease. The resistant tumour was analysed using immunohistochemistry and morphoproteomic analysis to evaluate the mechanisms of response and resistance.

The study found activation of pro-survival proteins such as pSTAT3, pERK1/2, NFkB-p65, p-mTOR with nuclear translocation (mTORC2) and also antiapoptotic Bcl-2 was present in resistant tumour tissue. Wider studies using these DR agonists in other solid tumours, which have included bone and soft-tissue sarcoma have failed to show any significant anti-cancer activity [257]. It is thought that the culprit for failure is short half-life of approximately 30 minutes *in vivo* and its weak capacity to induce high order clustering of TRAIL receptors. It is also thought to possibly engage the decoy receptors, DcR1 also known as TRAIL-R3, and DcR2 (TRAIL-R4), and OPG as discussed before, which reduces effectiveness. In a review, Von Karstedt *et al.,* (2017) discussed ongoing clinical trials and suggested that for enhanced apoptosis there should be optimised multimeric variants of TRAIL or other DR4, DR5 agonists in combination with potent sensitisers to overcome cancer cell resistance to current TRAIL-based therapeutics [206].

In my investigations *in vitro*, I found evidence that multimeric structures of TRAIL, e.g. Crosslinked SuperKillerTRAIL (SKT) were more potent than the tagged human recombinant forms of TRAIL (His-TRAIL and FLAG-TRAIL). I also investigated TRA-8 (human IgG1 Fc Silent™) a humanised version of the standard TRA-8 murine DR5

agonist and found that crosslinked SKT had the most potent effects on bone sarcoma cell lines. The most sensitive non-malignant cell line was the HHL5 hepatocyte cell line. Human osteoblasts (OBs), bone-marrow-derived mesenchymal stem cells (BMMSCs), human umbilical vascular endothelial cells (HUVECs) and human neonatal dermal fibroblasts (NHDFs) had reduced sensitivity to SKT and the AC10 cardiac ventricular cardiomyocyte cell line demonstrated some sensitivity at the higher doses. Further investigation should focus on other hepatocyte and cardiomyocyte cell lines or primary cells.

I have also tested SKT with sensitisers, current chemotherapeutics such as doxorubicin and etoposide (VP16), sensitisers such as Smac mimetic and ABT-737 which is a Bcl antiapoptotic protein inhibitor and also I have tested proteasome inhibitors such as bortezomib and HDAC inhibitors which is discussed in Chapter 6. This is of importance as I have found some of the bone sarcoma cell lines to be less sensitive to the crosslinked form of TRAIL. This is the chondrosarcoma SW1353 cell line, the SAOS-2 osteosarcoma cell line and the SJSA-1 osteosarcoma cell line. The SJSA-1 and the SW1353 have proved to be the most resistant cell lines; however, they can be sensitised using doxorubicin. The SW1353 cell line could also be sensitised using Smac mimetic. This is discussed in Chapter 6.

Of note, when recombinant human TRAIL (dulanermin) was administered to cynomolgous monkeys, this induced production of anti-drug antibodies (ADAs), which is an anti-drug antibody response. This was directed against only four amino acids in which humans and cynomolgous monkey TRAIL differ and was shown to be responsible for observed liver toxicity [265]. There should be caution with regards to considering the immunogenic potential of novel bio-therapeutic agents. However, administration of these agents in humans has not been reported in the literature to cause significant side effects to date.

Mode of cell death

There is a general understanding in the literature that TRAIL induces apoptosis through caspase activation. There are two pathways involved, depending on whether the cell is a type 1 cell or type 2 cell. In type 2 cells there is additional involvement of the intrinsic pathway of apoptosis. Both pathways converge on the executioner caspase, known as

caspase 3. TRAIL can also induce necroptosis via RIPK1 (receptor interacting protein kinase 1) and RIPK3, which can be PARP-1 dependent [266] or independent [267]. The mode of cell death can be dependent on extracellular pH conditions, with acidic pH stimulating necroptosis [266]. More recently, TNF-dependent necroptosis can be stimulated with agents that activate mitochondrial outer membrane permeabilisation (MOMP) in caspase deficient conditions as a form of caspase independent cell death [268]. There is an interest in the induction of necroptosis or caspase independent cell death as a method of cell cancer killing as this may stimulate immune cells to the malignant cell site and induce further cancer cell death. Recent reports by Giampazolias *et al.,* support that caspase independent cell death displays potent anti-tumourigenic effects promoting complete tumour regression in a manner dependent on intact immunity [268,269].

In my investigation, I found that using inhibitors of necroptosis did not significantly affect degree of HT1080 and U2OS bone sarcoma cell survival when exposed to SuperKillerTRAIL (SKT). However, I did find that when exposing sarcoma cells to caspase inhibitors that there was a significant reduction in cytotoxicity with SKT treatment. My results suggest, that in these sarcoma cells lines the mode of cell death when exposed to TRAIL is predominately apoptosis through the caspases. Further investigation is required in sarcoma cells to deduce the degree of activation of necroptosis upon TRAIL exposure with and without caspase inhibition as studies so far have either investigated this in carcinoma or epithelial cells [266,268].

DR4 and DR5 perturbation studies

A study in 2019 by Staniek J *et al*., [270] further investigated the specific contribution of each DR to apoptosis known to be dependent upon relative level of surface expression in B cell lymphoma cells [271]. They used DR4 blocking antibody in a primary human B cell line with DR5 present and absent in a CRISPR KO B cell lymphoma line. Anti-DR4 completely inhibited apoptosis in the DR5 KO cell line (BJAB TRAIL R2 KO). In primary human B cells there was an increase from 26% to 45% survival in DR4 blocked cells by pre-incubating with DR4 blocking antibody then treating with TRAIL. Blocked and TRAIL untreated cells had 57% survival; the authors attributed this

to the contribution of DR5. They concluded overall that ligand crosslinking of both DR4 and DR5 contribute to apoptosis in primary human B cells [270].

In comparison to studies in Ewing's sarcoma cell lines, which can express DR5 but varying levels of DR4, the use of short hairpin RNA (shRNA) to reduce DR4 levels in the TC71 cell line (shDR4TC-71 cells with 50% decrease in surface level) can reduce sensitivity to TRAIL despite presence of DR5. Overexpression of DR4 in resistant cell lines restored sensitivity [202]. It has also been claimed that more sensitive Ewing's sarcoma cell lines contain both DR4 and DR5 and those that are more resistant lack DR5, which when reintroduced sensitises the cells to TRAIL [81].

Further study is required in a range of bone sarcoma cell lines, initially addressing again the TC71 Ewing's sarcoma cell line, knockdown of DR4 using siRNA and TRAIL treatment of cells with greater levels of KD, and reduction in surface protein level. Also, use of anti-DR4 antibody or CRIPSR knockout models would add further information about roles of DR4 and DR5 in TRAIL induced apoptosis in this Ewing's sarcoma cell line and other bone sarcoma cell lines that express both DR4 and DR5 as to the best of my knowledge there is no published data regarding this. This is clinically important as targeting DR5 alone using Lexatumumab in Phase I study showed rare objective response in an Ewing's sarcoma population [272]. These DR KD/KO investigations, therefore, would add further strength to the argument that development of TRAIL to crosslink both DR4 and DR5 should be used in future clinical studies and potentially introducing a receptor if it is lacking.

For the current PhD project, CRISPR was used to knockout the DR5 gene in the HT1080 dedifferentiated chondrosarcoma cell line and the pool of cells was used for experiments. A clonal cell line could have provided cells sharing the same loss of function mutation with more consistent and reproducible results, preferably with 2 clones to account for any variability during the single-cell clonal expansion. I attempted single-cell isolation using Fluorescence-activated cell sorting (FACS); however, growth of the cells was unsuccessful. I proceeded to work with the pool of cells, which may have risked experimenting on cells with protein expression due to unedited or heterozygous cells (limitation when using siRNA). Western blotting studies and flow cytometry data in this project, however, demonstrated appearances consistent with

full knockout and the desired phenotype when testing the pool of cells (all DR5 negative sorted using FACS) and I was able to progress the project. There is also the potential for off-target effects from the gRNA in CRISPR treated cells [273]. Predicted off-target effects using the company design tool demonstrates 2 off-target effects from a gRNA sequence targeting TNFRSF10B/DR5 (GACAACGAGCACAAGGGTCT): location chr12[46841983] affecting human gene SLC38A4 (Solute Carrier Family 38 Member 4) and location chr9[122002349] affecting human gene TTLL11 coding for polyglutamase, with no obvious relation to apoptotic pathways. There have also been tools developed that can be used such as the CRISPR/Cas9 target online predictor (CCTop, http://crispr.cos.uni-heidelberg.de) [274]. This is achieved by aligning the gRNA sequence with reference genome sequence on a homology basis. Further validation would involve CRISPR gene editing confirmation of on-target and off-target genes using Sanger sequencing.

Overall summary and future direction

In summary, activation of TRAIL receptors requires the corresponding TRAIL ligand as agonist antibodies are unable to effectively activate signalling alone. Effective activation requires a stable trimeric ligand with cross-linking antibodies. The alternative is a ligand analogue, which mimics the membrane form of TRAIL. These strategies take advantage of the described hexagonal model of activation [275]. A better understanding of the arrangement of the receptors on the membrane and the function of the membrane has increased the interest in the development of more stable TRAIL ligand analogues, with improved half-life, increased activity and lower immunogenicity. This should form the basis for future investigations and has been studied *in vitro* and *in vivo* in Chapters 7 and 8, respectively as part of this thesis for chondrosarcoma.

Other considerations are FDA approved drugs that can induce tumour cell death via engagement of the endogenous TRAIL, TRAIL-R system and blocking of TRAIL and TRAIL receptor to neutralise the autocrine and paracrine tumour supportive roles in KRAS mutant cancers and the concept of combining with immune checkpoint blockade could provide efficacious [206]. Determining which patients will benefit and deciphering more the underlying biology will be important feats for the future.

Chapter 6. Investigating the effect of TRAIL in combination with current chemotherapeutic agents and other novel sensitisers on bone sarcoma cell lines

6.1 Introduction

Increased sensitivity to TRAIL has been found when used in combination with chemotherapeutic agents [71,89,242,276]. This has been commonly associated with increased caspase-8 expression but also upregulation of the death receptors (DRs) and downregulation of c-FLIP and has been discussed extensively in the introduction Chapter 1.

Doxorubicin is one of the main chemotherapeutic agents currently used in clinical practice for bone sarcoma. More resistant bone sarcomas, such as chondrosarcoma can show some sensitivity to doxorubicin, which is included in most regimens [277] and the chondroid matrix does not significantly reduce doxorubicin entering the nucleus [278]. Response rates can be poor, particularly for chondrosarcoma: mesenchymal (31 % response), dedifferentiated chondrosarcoma (20.5 %), conventional chondrosarcoma (11.5 %) and clear cell chondrosarcoma (0 %) [277].

The aims of this chapter are to:

1. Investigate the cytotoxic effects of crosslinked TRAIL in combination with chemotherapeutic agents currently used for the treatment of bone sarcoma in the bone sarcoma cell lines and determine IC50 values.

2. Investigate cytotoxic effects of crosslinked TRAIL with chemotherapeutics in non-malignant cells.

3. Explore the efficacy of using novel sensitisers such as Smac mimetics, HDAC inhibition, inhibitors of the Bcl-2 family (ABT-737) in combination with crosslinked TRAIL on the bone sarcoma cell lines, with a focus on the more resistant lines.

6.2 Combining doxorubicin with SuperKillerTRAIL on bone sarcoma cell lines

Doxorubicin

Doxorubicin produces a range of cytotoxic effects by binding to DNA associated enzyme, intercalating with DNA base pairs. It activates AMPK (AMP-activated protein kinase inducing apoptosis) and alters the Bcl-2/Bax ratio resulting in downstream activation of different caspases [279]. In cancer cell lines such as PC3, doxorubicin has been found to decrease c-FLIP levels. This decrease has been found to correlate with caspase-8 activation and PARP cleavage [280,281]. In breast and renal cancer cell lines, doxorubicin also enhances the effect of TRAIL [282,283].

The concentration of doxorubicin in circulation is 6.73 µmol/l according to a recent paper; 75 % is protein bound [284] (Equation 6).

$$\text{Doxorubicin Cmax} = 6.73\text{umol/l} - 75\% \text{ protein bound}$$

Equation 6 - Concentration of doxorubicin in circulation – 75 % is protein bound [284]. Therefore, approximately 1.7 µM is considered free depending on patient condition.

Materials and Methods

Doxorubicin was applied to the bone sarcoma cell lines in combination with SuperKillerTRAIL (SKT) to assess for enhanced cytotoxic effects. Doxorubicin (10 mg, Sigma Aldrich, UK) was dissolved in sterile distilled water to a concentration of 10 mM. Serial dilutions by factors of 3 in a master plate was applied to the cells in a 96-well plate (5000 cells per well).

The plate setup was such that there were three technical repeats for each doxorubicin concentration (titrated) and fixed dose of (SKT). Three wells were treated with SKT alone and three wells were left untreated. This was carried out in combination with 0.1 ng/ml SKT, 1 ng/ml SKT and 10 ng/ml SKT. The results are presented and summarised below.

IncuCyte® live-cell imaging analysis

Preliminary data using the IncuCyte® live-cell analysis revealed that combining doxorubicin with SuperKillerTRAIL (SKT) is more effective at reducing confluency than doxorubicin or SKT alone (Figure 111).

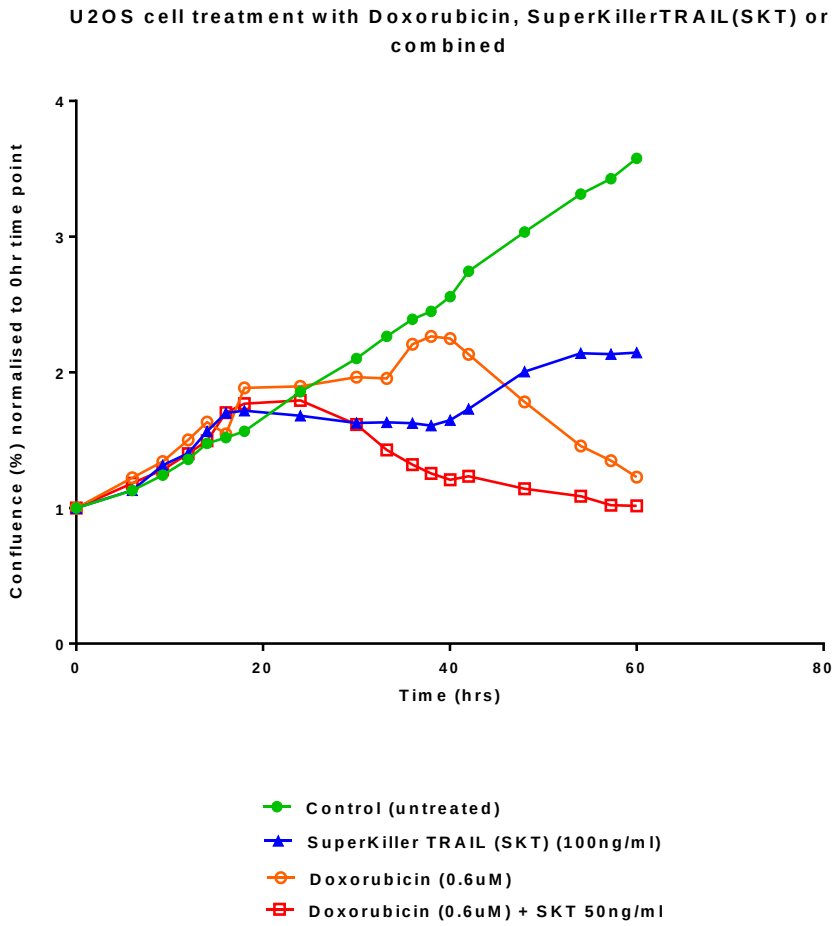

Figure 111 - U2OS cells were treated at 16-hour timepoint at exponential growth phase. Combination of SuperKillerTRAIL with doxorubicin can be seen to have enhanced cytotoxic effects. There is regrowth after administration of SuperKillerTRAIL alone (100 ng/ml; 4 nM) as demonstrated in previous IncuCyte® live-cell analysis data. However, regrowth is not seen, when doxorubicin is combined with SuperKillerTRAIL (50 ng/ml; 2 nM) and is more effective than administration of doxorubicin alone.

Doxorubicin combined with SuperKillerTRAIL (SKT) on bone sarcoma cell lines

The combination of doxorubicin and SuperKillerTRAIL increased the cytotoxic effects on osteosarcoma, Ewing's sarcoma and chondrosarcoma cell lines (Figure 112 to Figure 114, summarised in Table 22).

Osteosarcoma

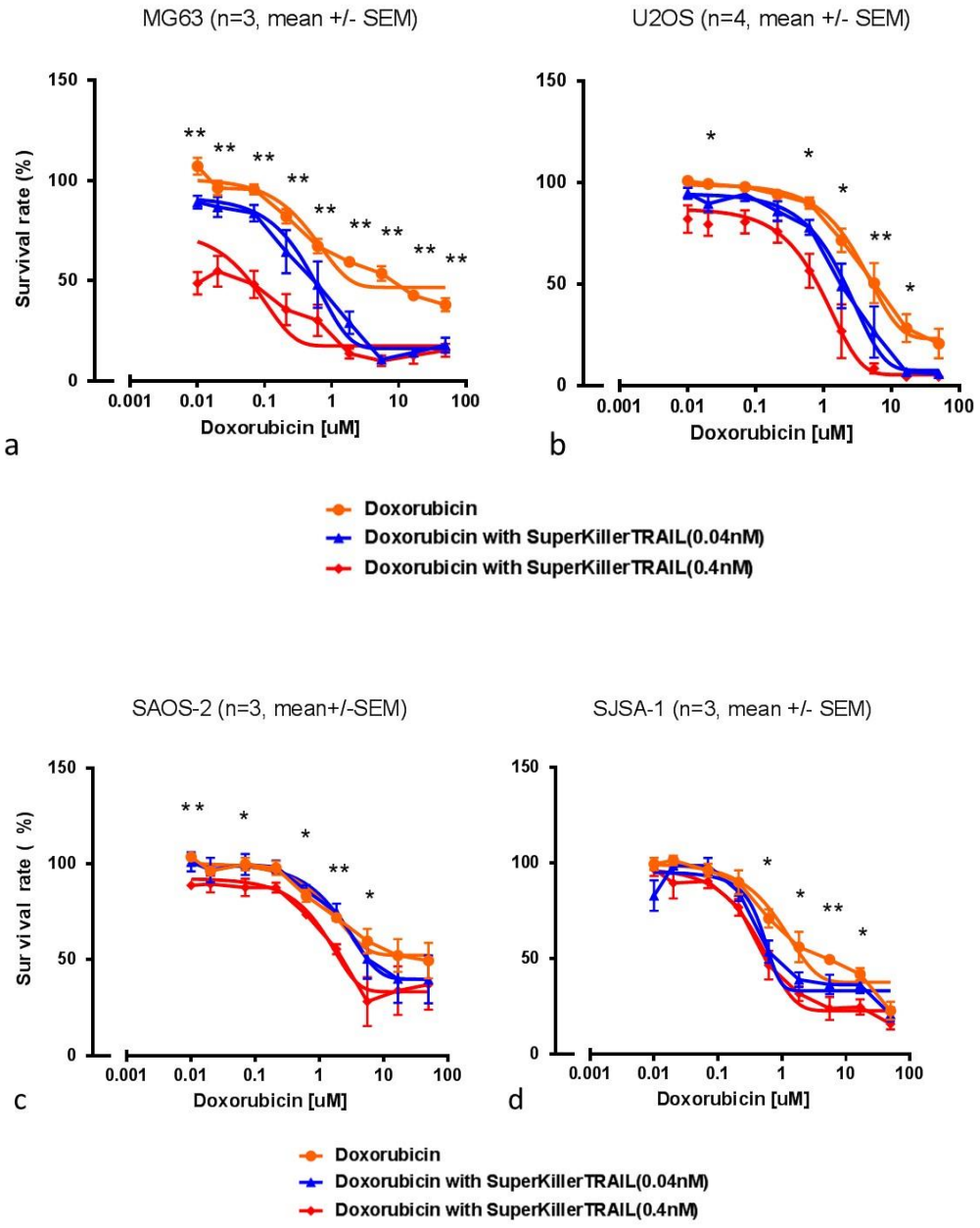

Figure 112 - Doxorubicin combined with SuperKillerTRAIL (SKT) on osteosarcoma cell lines: (a) MG63, (b) U2OS, (c) SAOS-2 and (d) SJSA-1 (n = 3, mean +/- SEM * = p<0.05, ** = p<0.001, Student's t-test Doxorubicin vs Doxorubicin with 0.4 nM SKT.

Ewing's sarcoma

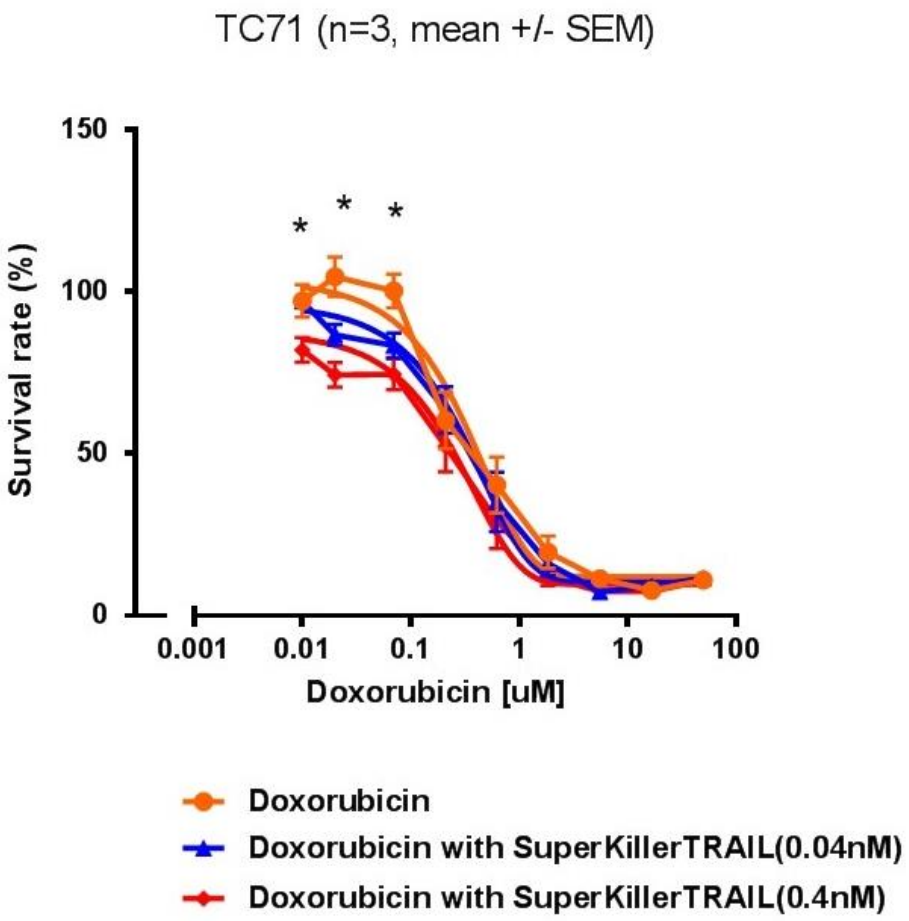

Figure 113 - Doxorubicin combined with SuperKillerTRAIL on TC71 Ewing's sarcoma cell line (n = 3, mean +/- SEM * = p<0.05, Student's t-test, Doxorubicin vs Doxorubicin with 0.4 nM SKT).

Chondrosarcoma

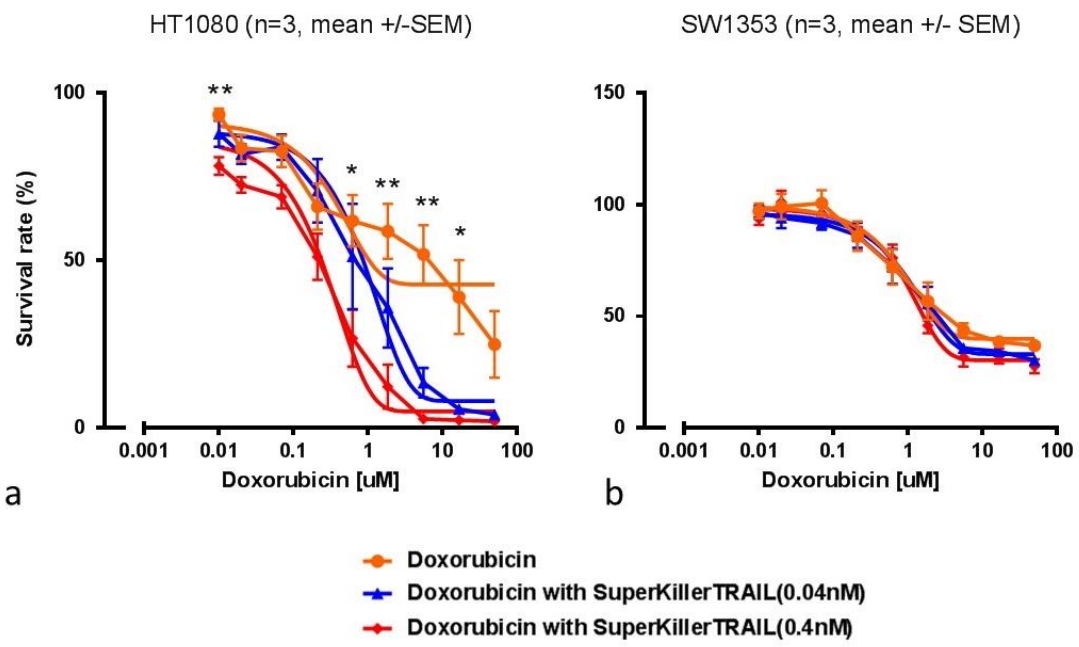

Figure 114 - Doxorubicin combined with SuperKillerTRAIL on chondrosarcoma cell lines: (a) HT1080 dedifferentiated chondrosarcoma cell line. (b) SW1353 chondrosarcoma cell line (n = 3, mean +/- SEM * = p<0.05, Student's t-test Doxorubicin vs Doxorubicin with 0.4 nM SKT).

Table 22 - Summary of the IC50 values and efficacy of combining doxorubicin (Dox) with SuperKillerTRAIL (SKT) (n = 3). Enhanced toxicity was observed for all cell lines except for the SW1353 chondrosarcoma cell line. Etoposide (VP16) values for TC71 are included for comparison and the fold change was similar to doxorubicin (also see Section 5.3).

Sarcoma type	Cell line	(1)Dox IC50 (µM), %dead at highest dose	(2)Dox IC50 (µM) + 0.04 nM SKT	(3)Dox IC50 (µM) + 0.4 nM SKT, % dead at highest dose	IC50 Fold change (1) vs (3)
Osteosarcoma	SAOS-2	1.4 µM,50 %	2.2 µM	1.3 µM,63 %	1
	U2OS	3.9 µM,79 %	2.1 µM	1.0 µM,96 %	4
	SJSA-1	2.1 µM,77 %	0.5 µM	0.4 µM,84 %	5
	MG63	0.5 µM,62 %	0.5 µM	0.4 µM,85 %	1
Chondrosarcoma	SW1353	0.8 µM,63 %	1.1 µM	1.0 µM,72 %	1
	HT1080	5.6 µM,75 %	1.0 µM	0.4 µM,98 %	14
Ewing's sarcoma	TC71	0.3 µM,89 % VP16 = 0.8 µM, 94 %	0.3 µM VP16 = 0.5 µM	0.3 µM,89 % VP16 = 0.6 µM, 95 %	1

6.3 Combining doxorubicin with SuperKillerTRAIL (0.04 nM vs 0.4 nM) on non-malignant cell lines compared to HT1080 dedifferentiated chondrosarcoma cell line

Combining doxorubicin with SuperKillerTRAIL (SKT) was more toxic to the HT1080 dedifferentiated chondrosarcoma and U2OS osteosarcoma cell line compared to non-

malignant cells, except for the AC10 ventricular cardiomyocyte and HHL5 hepatocyte cell line (Figure 115 to Figure 120). Data for the U2OS osteosarcoma cell line is included in the Appendix (11.6).

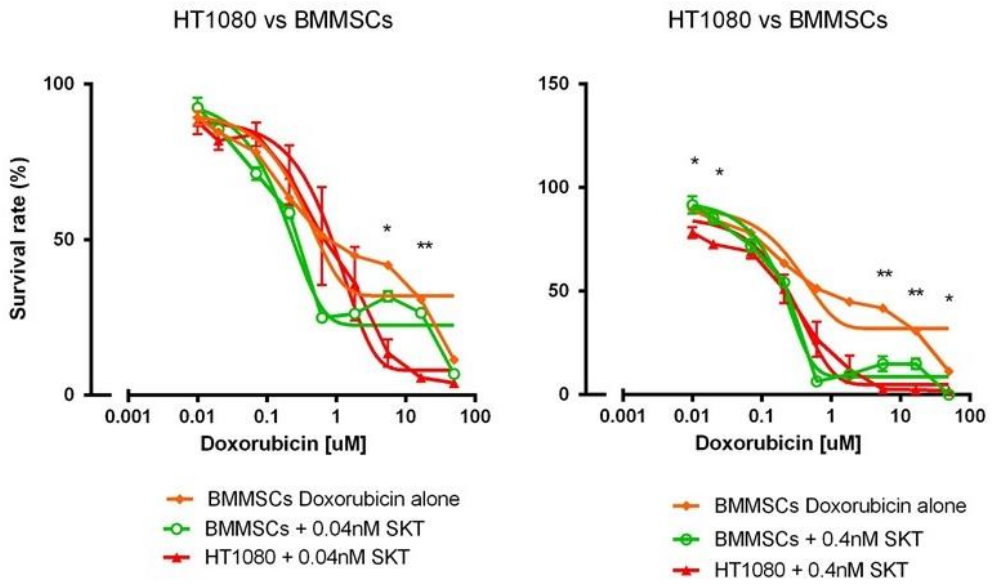

Figure 115 – HT1080 vs bone marrow-derived mesenchymal stem cells (BMMSCs), doxorubicin with (a) 0.04 nM SKT and (b) 0.4 nM SKT. * = p<0.05, ** = p<0.001, Student's t-test.

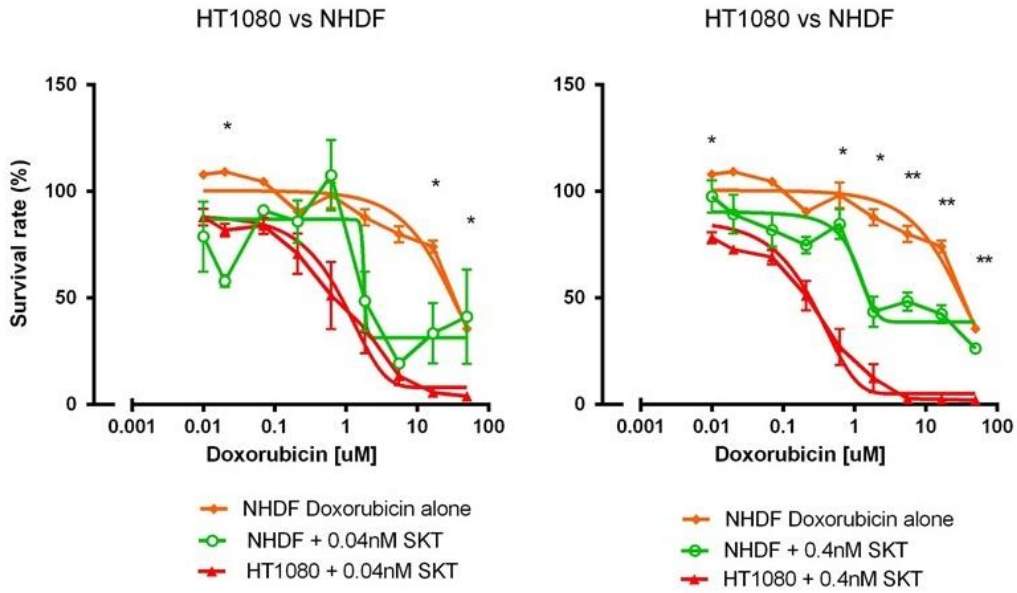

Figure 116 – HT1080 vs normal human dermal fibroblast (NHDF), doxorubicin with (a) 0.04 nM SKT and (b) 0.4 nM SKT. * = $p<0.05$, ** = $p<0.001$, Student's *t*-test.

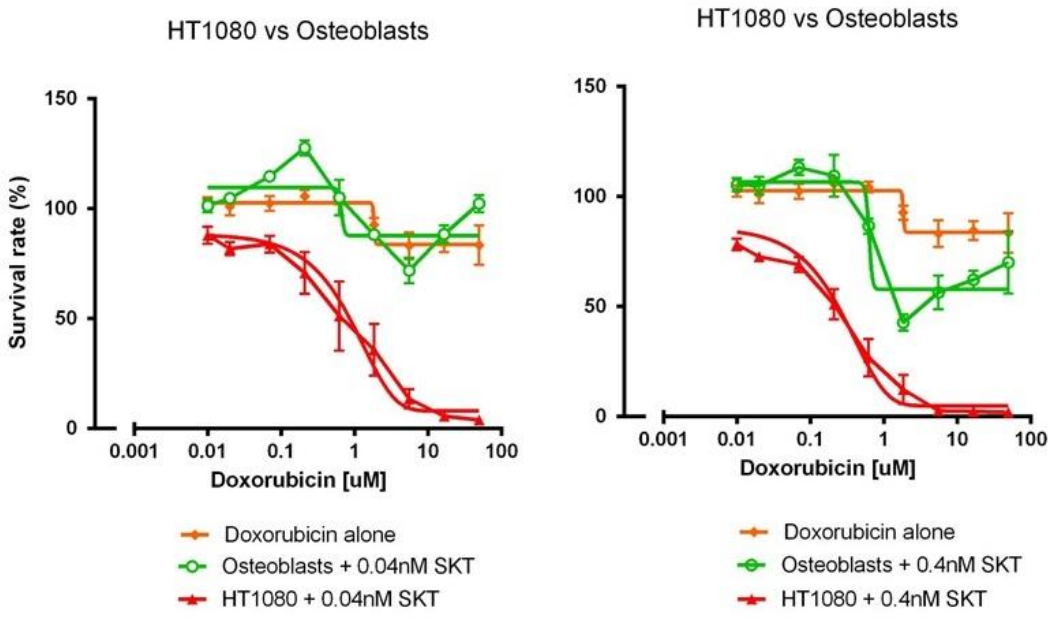

Figure 117 – HT1080 vs osteoblasts (OBs), doxorubicin with (a) 0.04 nM SKT and (b) 0.4 nM SKT.

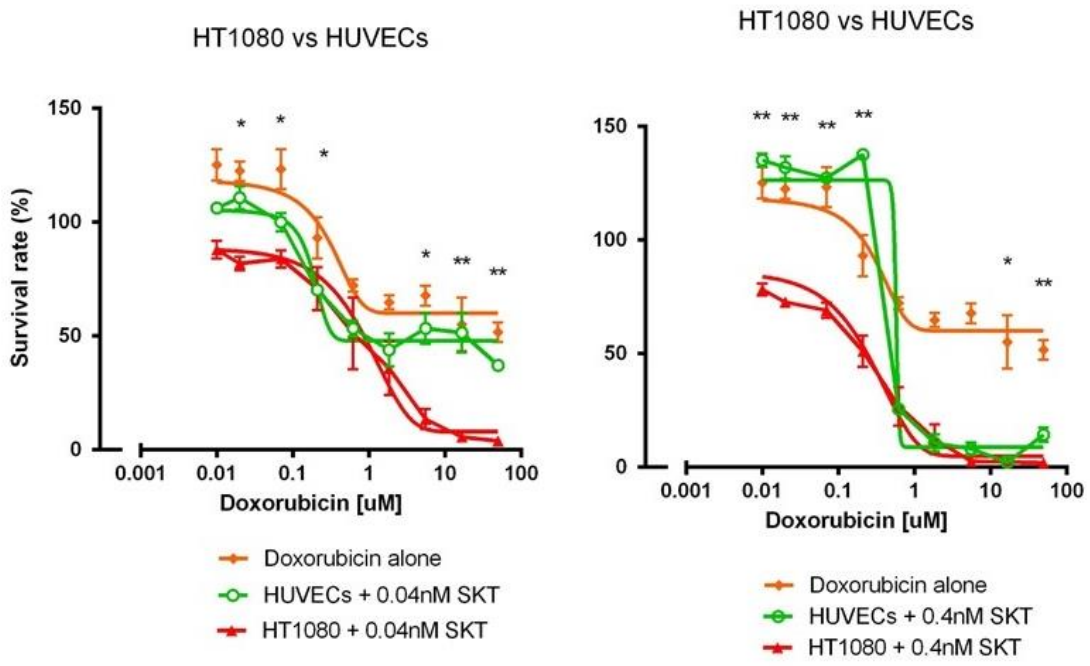

Figure 118 – HT1080 vs human umbilical vein endothelial cells (HUVECs), doxorubicin with (a) 0.04 nM SKT and (b) 0.4 nM SKT. * = $p<0.05$, ** = $p<0.001$, Student's *t*-test.

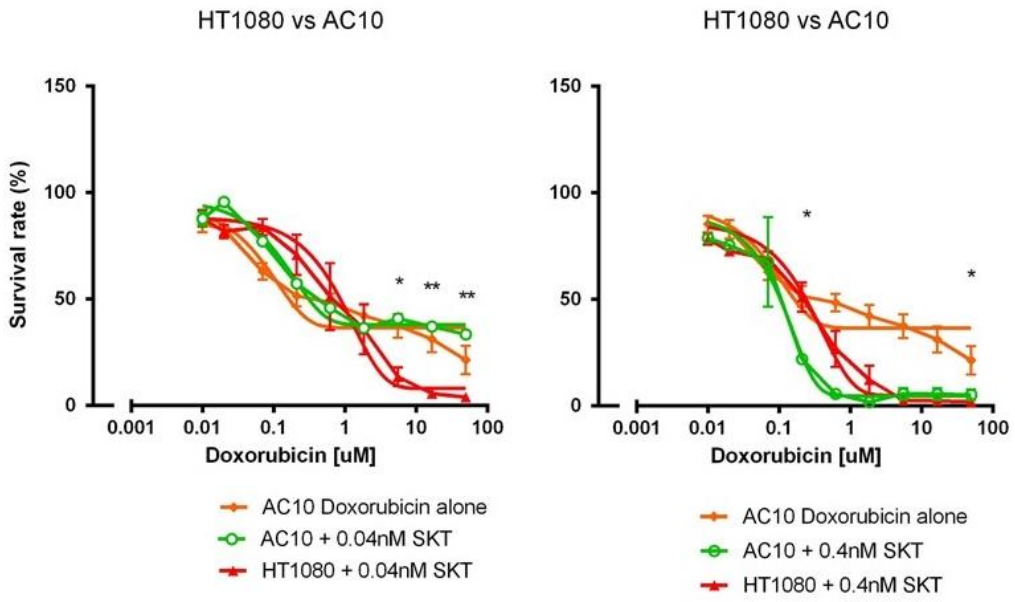

Figure 119 – HT1080 vs AC10 ventricular cardiomyocyte cell line, doxorubicin with (a) 0.04 nM SKT and (b) 0.4 nM SKT. * = p<0.05, ** = p<0.001, Student's t-test.

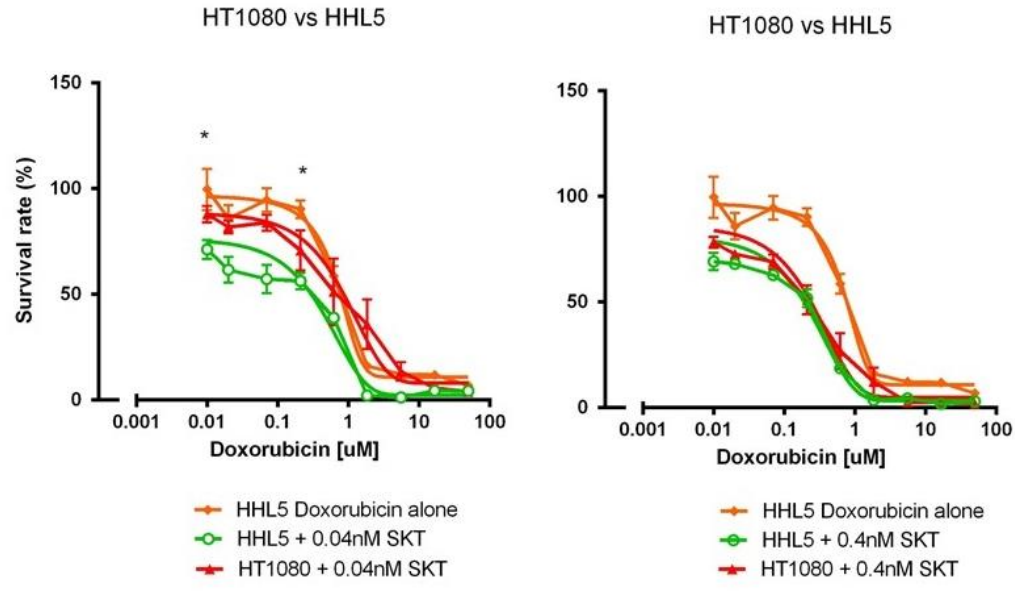

Figure 120 – HT1080 vs HHL5 human hepatocyte cell line, doxorubicin with (a) 0.04 nM SKT and (b) 0.4 nM SKT. * = p<0.05, ** = p<0.001, Student's t-test.

6.4 Doxorubicin and DR5 levels

Surface HT1080 DR5 level was assessed using flow cytometry in response to 24 hours of doxorubicin treatment. Increased expression levels were found when assessing at 0.5 µg/ml doxorubicin (Figure 121).

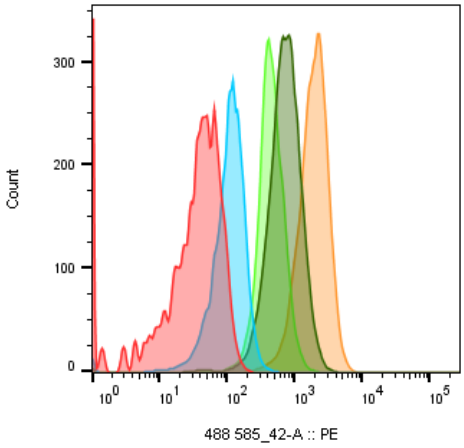

	Sample Name	Subset Name	Count	Median : 488 585_42-A
	391153.fcs	Unstained	8377	34.3
	391154.fcs	ITC PE	8922	110
	391187.fcs	Untreated (No Dox)	8225	699
	391169.fcs	Dox 0.5ug only	8297	428
	391155.fcs	DR5 Dox 0.5ug	7992	1880

Figure 121 – Flow cytometry analysis of HT1080 surface DR5 levels in response to 24 hours of treatment with 0.5 µg/ml of doxorubicin. Increased surface levels (orange) was found in relation to basal expression level (dark green) taking into account the background doxorubicin fluorescence (light green).

6.5 Combining etoposide (VP16) with SuperKillerTRAIL on TC71 Ewing's sarcoma cell line

Etoposide (VP16)

Etoposide acts by targeting DNA topoisomerase II and results in a number of DNA breaks and triggers apoptotic pathways [285]. It has been reported to increase DR4 and DR5 levels, thereby, enhancing the effect of TRAIL [286]. It is one of the chemotherapeutic agents together with doxorubicin used currently in clinical practice for Ewing's sarcoma [287]. Etoposide (VP16) (Sigma Aldrich, UK) was made up as per instructions to a concentration of 10 mM and its effects in combination with SuperKillerTRAIL on the TC71 Ewing's sarcoma cell line were assessed. DMSO was used to dissolve the VP16 and this had no noticeable cytotoxic effect on the TC71 cell line or NHDF cell line at increasing concentrations (data for effects of DMSO on cell lines is

presented in the Appendix 11.5). VP16 in combination with SuperKillerTRAIL on TC71 cells does not significantly enhance the effects compared to VP16 alone (Figure 122). VP16 with or without SKT is more toxic to TC71 Ewing's sarcoma cells in comparison to NHDF cells (Figure 123).

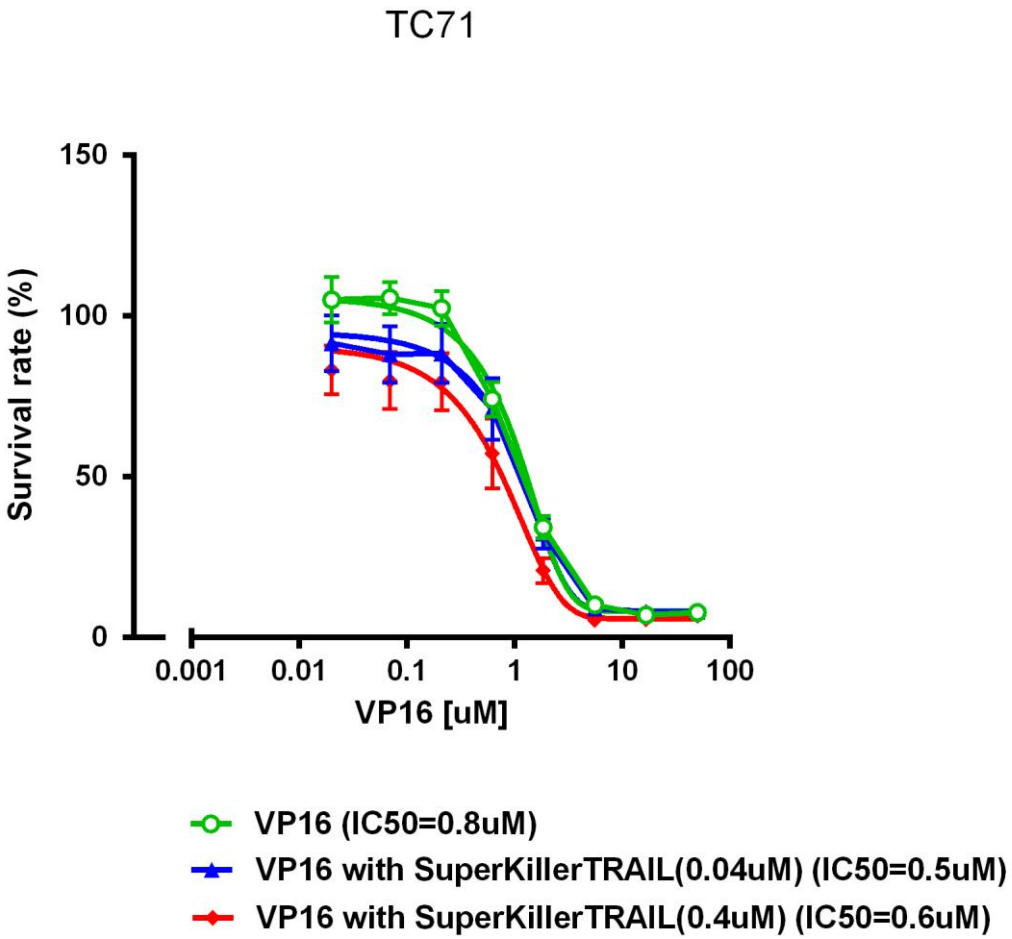

Figure 122 – VP16 in combination with SuperKillerTRAIL on TC71 cells does not significantly enhance the effects compared to VP16 alone.

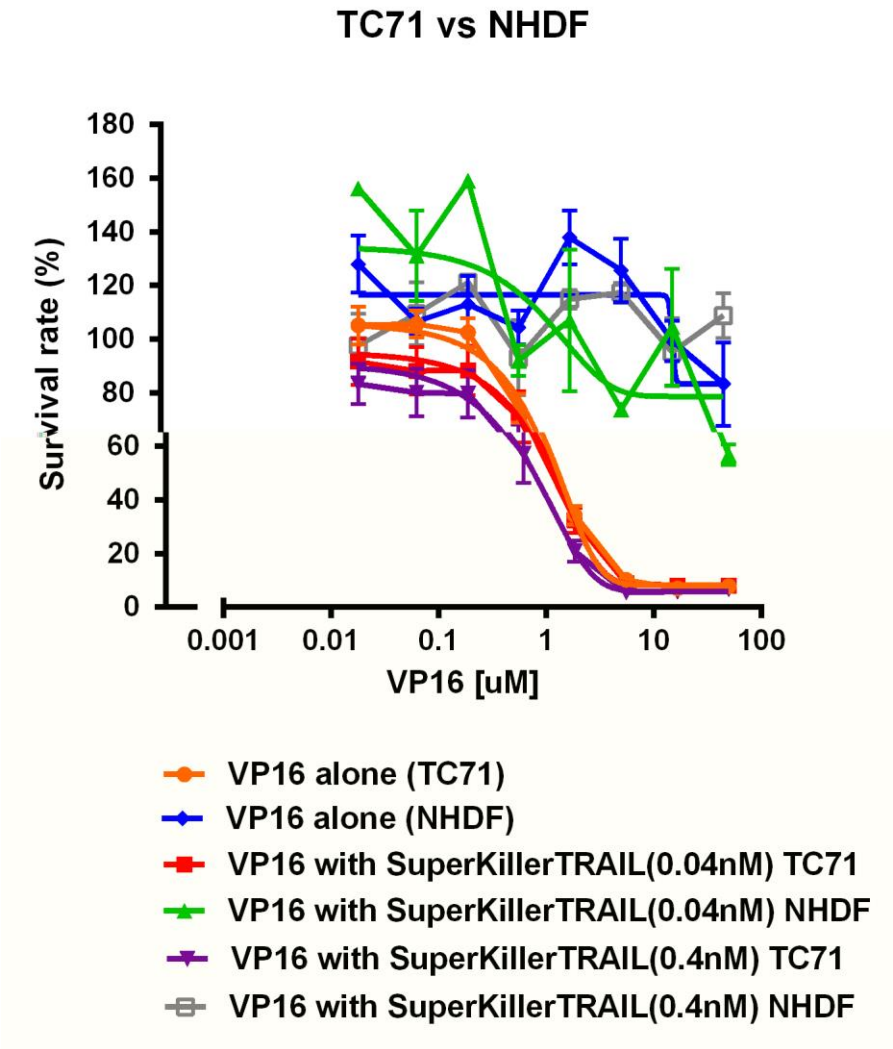

Figure 123 – VP16 with or without SKT is more toxic to TC71 Ewing's sarcoma cells in comparison to NHDF cells.

6.5.1 VP16 has similar toxicity to Ewing's sarcoma TC71 cell line as doxorubicin when combined with SuperKillerTRAIL (SKT)

The TC71 Ewing's sarcoma cell line was treated with VP16 in combination with SuperKillerTRAIL (SKT). The combination was not significantly different to VP16 alone or the combination with doxorubicin (Figure 124).

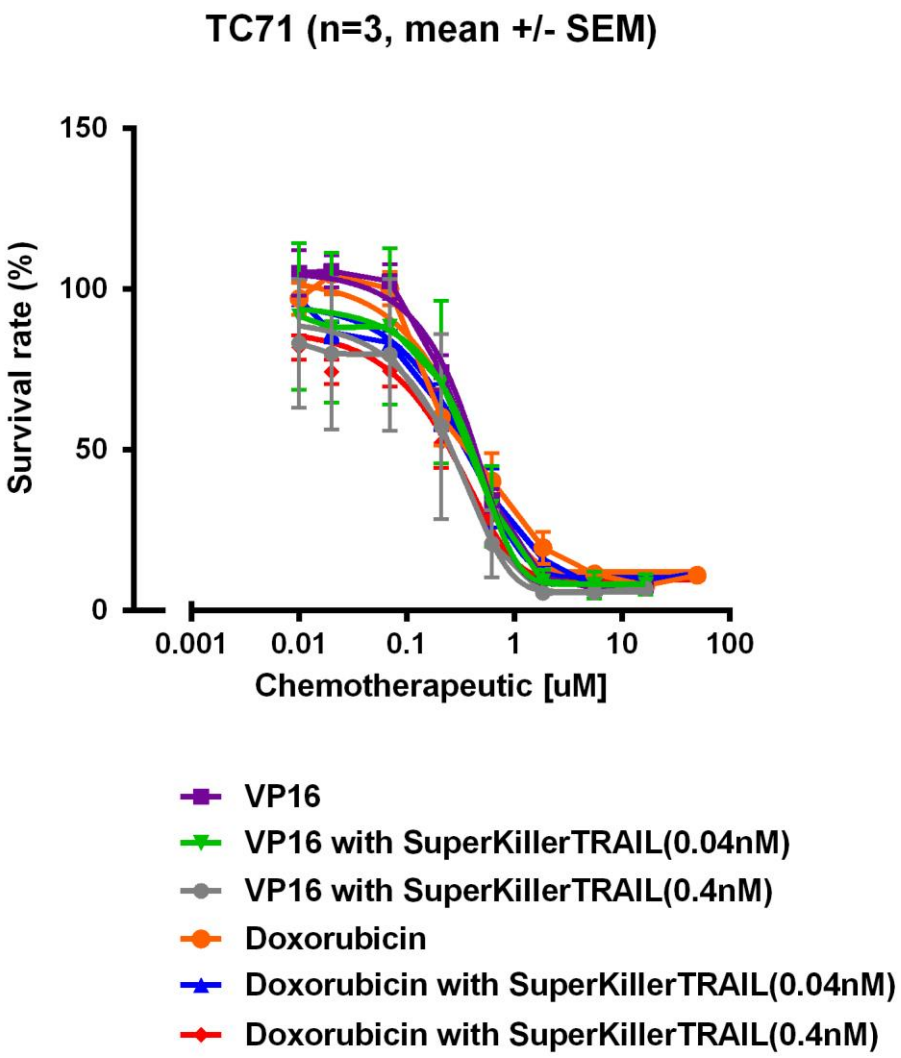

Figure 124 - The TC71 Ewing's sarcoma cell line was treated with VP16 in combination with SuperKillerTRAIL (SKT). The combination was not significantly different to VP16 alone or the combination with doxorubicin.

6.5.2 VP16 with SuperKillerTRAIL (SKT) is less toxic to NHDF cells than doxorubicin with SKT

Combining VP16 with SuperKillerTRAIL (SKT) was less toxic to the NHDF cell line than the doxorubicin/SKT combination (Figure 125).

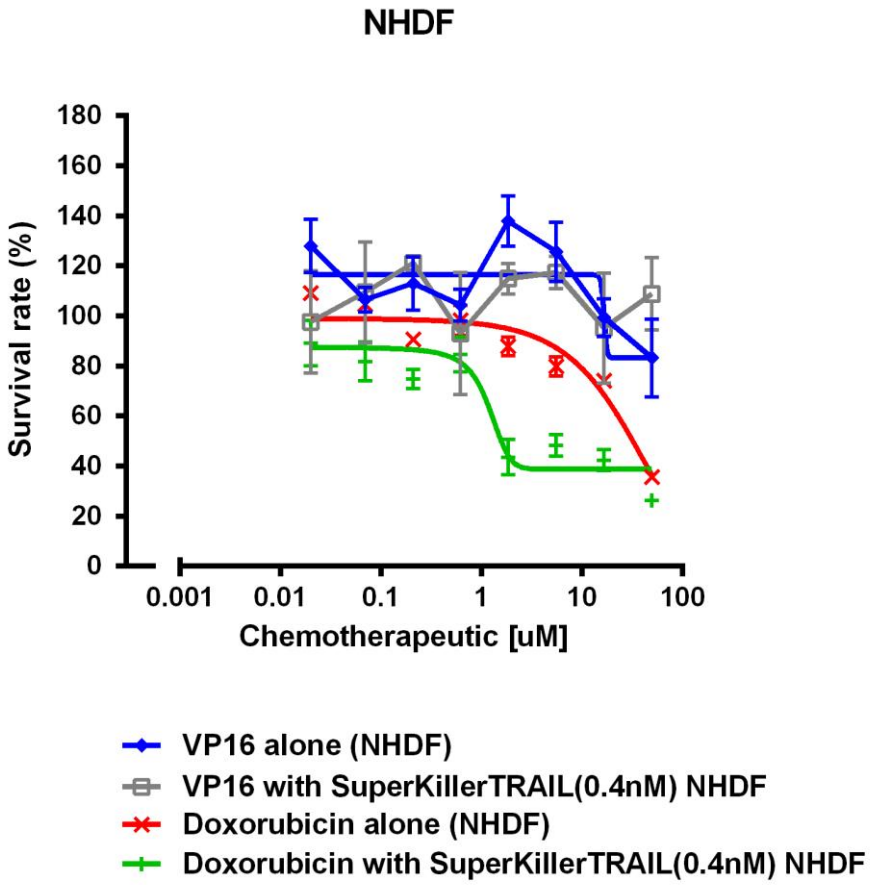

Figure 125 - Combining VP16 with SuperKillerTRAIL (SKT) was less toxic to the NHDF cell line than the doxorubicin/SKT combination.

6.6 Combining TRAIL with novel sensitisers on bone sarcoma cell lines

The use of inhibitor of apoptosis protein (IAP) inhibitors or reducing IAP levels has been considered an effective approach for the sensitisation of malignant cells to TRAIL. Smac/Diablo is an endogenous antagonist of X-linked inhibitor of apoptosis (XIAP), cIAP1 and cIAP2 [242]. The potency of the use of Smac mimetics together with TRAIL has been documented in several preclinical studies [288,289]. Synergistic interaction

has been reported for Smac mimetic AT-406 and the DR5 antibody TRA-8 [290]. For pancreatic cancer silencing XIAP or use of KD using RNAi significantly increased apoptosis when combined with stem cell delivery of solubleTRAIL (sTRAIL) [291].

Smac mimetics have been used in clinical studies of head and neck cancer and metastatic colorectal cancer with promising findings. There is currently a phase 1 clinical trial combining the DR5 agonist conatumumab (AMG 655) and birinapant in patients with relapsed ovarian cancer (clinicalTrials.gov Identifier: NCT01940172) [292]. I used the Smac mimetic birinapant (CT-BIRI ChemieTek, Indianapolis, USA) in combination with SuperKillerTRAIL in the bone sarcoma and non-malignant cell lines.

Through collaboration with Pieczykolan *et al.,* I obtained a novel recombinant fusion protein known as AD-O53.2. The activities of TRAIL/Apo2L and Smac/Diablo are combined in AD-O53.2 (mode of action is presented in Figure 126) and I tested it on the resistant SW1353 cell line [293].

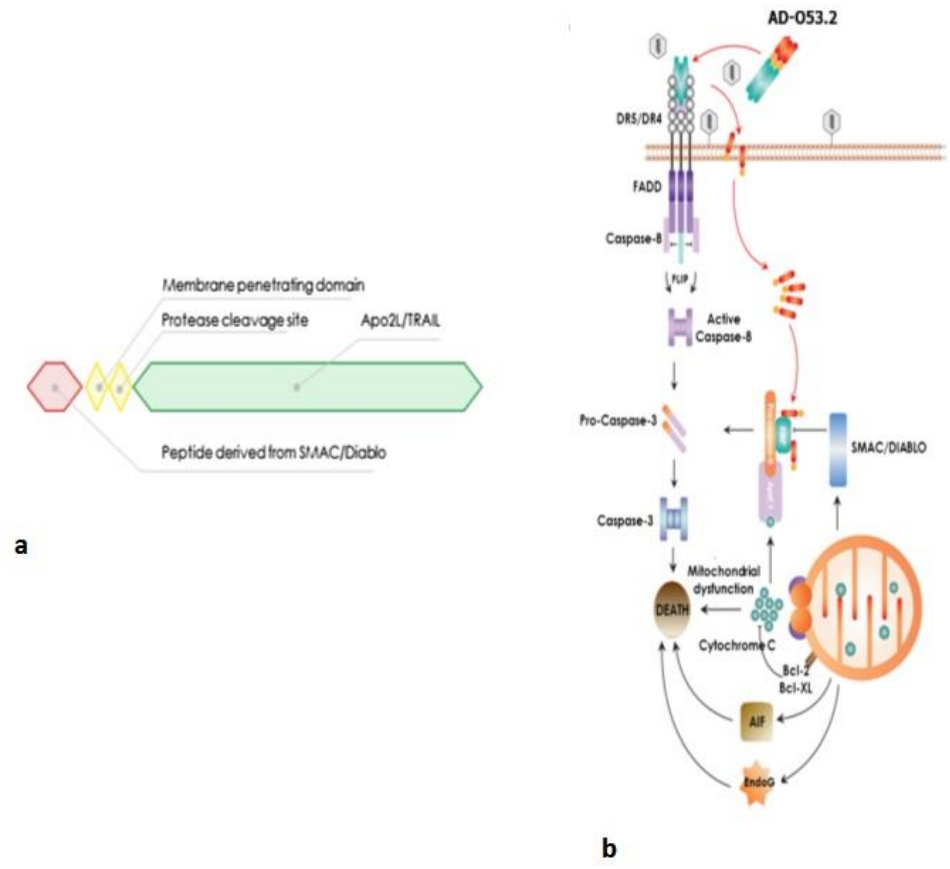

Figure 126 – Schematic representation of (a) AD-O53.2 and (b) its mode of action. Adapted from [293].

The combination of HDAC inhibition (HDACi) and TRAIL has also been shown to enhance apoptosis *in vitro* and *in vivo* in haematological and solid tumours [254,255]. The HDAC inhibitor Trichostatin A (TSA), was obtained from Sigma-Aldrich® and applied alone and with SuperKillerTRAIL on bone sarcoma cell lines.

ABT-737 was obtained from Adooq BioSciences LLC (ABT-737 5 mg A10255-5) and is an inhibitor of the Bcl-2 family of proteins (known to inhibit TRAIL signalling) and can induce expression of DR5 [294,295]. There are findings from clinical studies to suggest the upregulation of the Bcl-2 proteins as a mechanism for resistance in TRAIL therapy for chondrosarcoma [263]. Previous studies have suggested doses of 100 nM or higher to see a synergistic effect with TRAIL [294,295].

6.6.1 Smac mimetics

U2OS osteosarcoma cell line

Increasing the concentrations of Smac mimetic was found to have a positive effect at sensitising U2OS cells to SuperKillerTRAIL (SKT) (Figure 127) and was also found to have a sensitising effect on SW1353 cells (Figure 128).

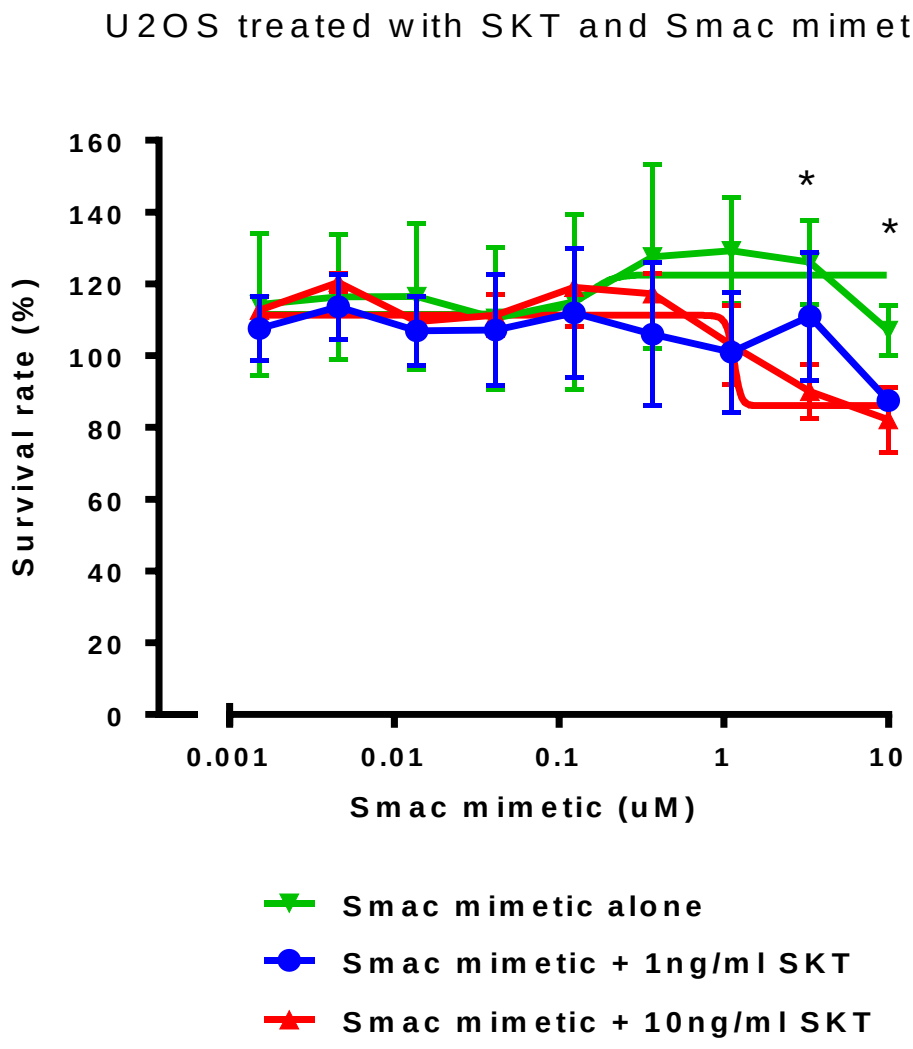

Figure 127 – For the U2OS cell line, when titrating Smac mimetic combined with fixed amount of SuperKillerTRAIL (SKT) (either 1 ng/ml, 0.04 nM or 10 ng/ml, 0.4 nM of SKT) significance was found at 1 or above of Smac mimetic in combination with 1 ng/ml (0.04 nM) SKT or 10 ng/ml (0.4 nM) SKT, when compared to Smac mimetic alone, which did not appear to be toxic at those doses (Student's *t*-test, $p < 0.05$).

SW1353 chondrosarcoma cell line

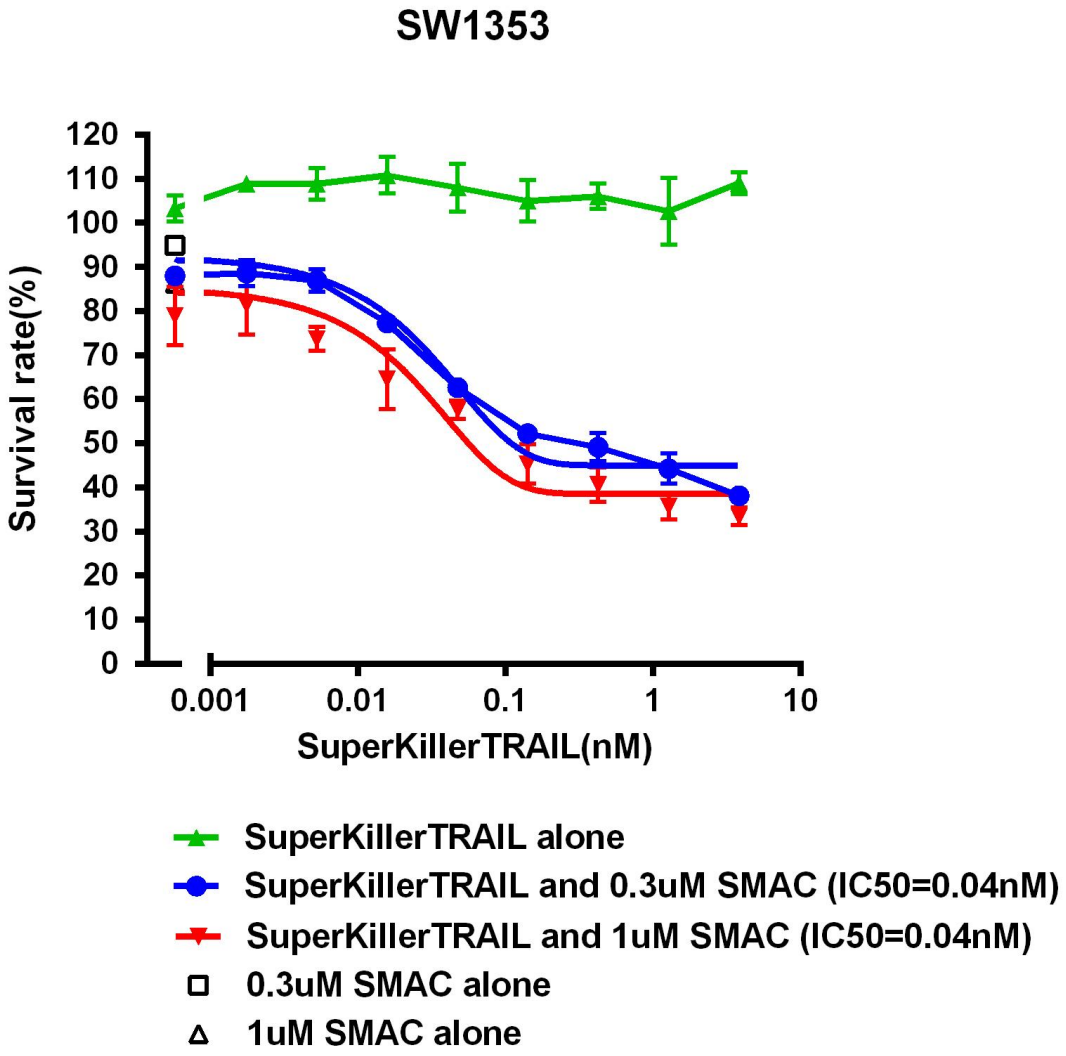

Figure 128 – The SW1353 chondrosarcoma cell line was sensitised significantly to effects of SKT when combined with 0.3 µM or 1 µM Smac mimetic.

Effect of Smac mimetic on DR4 and DR5 levels in the SW1353 cell line

In order to gain an understanding of the potential mechanism of action for the sensitisation of the SW1353 to TRAIL when cotreating with Smac mimetic, the degree of surface expression of DR4 and DR5 after 24 hours of treatment with Smac mimetic at two different doses (0.3 µM and 1 µM) was assessed. No obvious shift was evident compared to the untreated control (Figure 129).

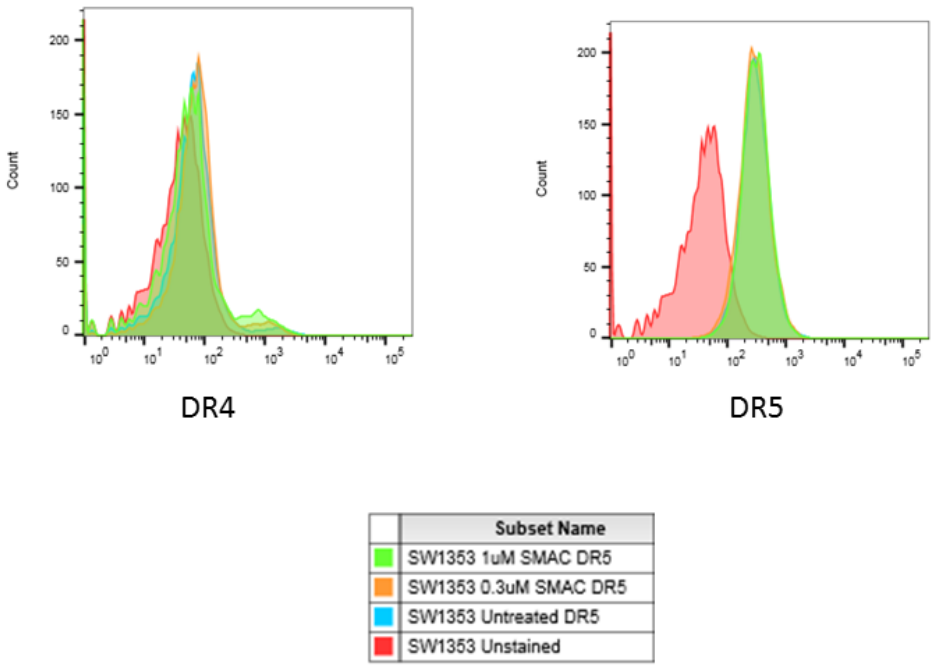

Figure 129 – Assessment of DR4 and DR5 expression after 24 hours of Smac treatment. No obvious change was observed with addition of Smac mimetic.

Effect of Smac mimetic on SAOS-2 and SJSA-1 osteosarcoma cell lines

No significant sensitising effect was observed on the SAOS-2 or SJSA-1 cell lines when combining Smac mimetic with SuperKillerTRAIL (SKT) (Figure 130).

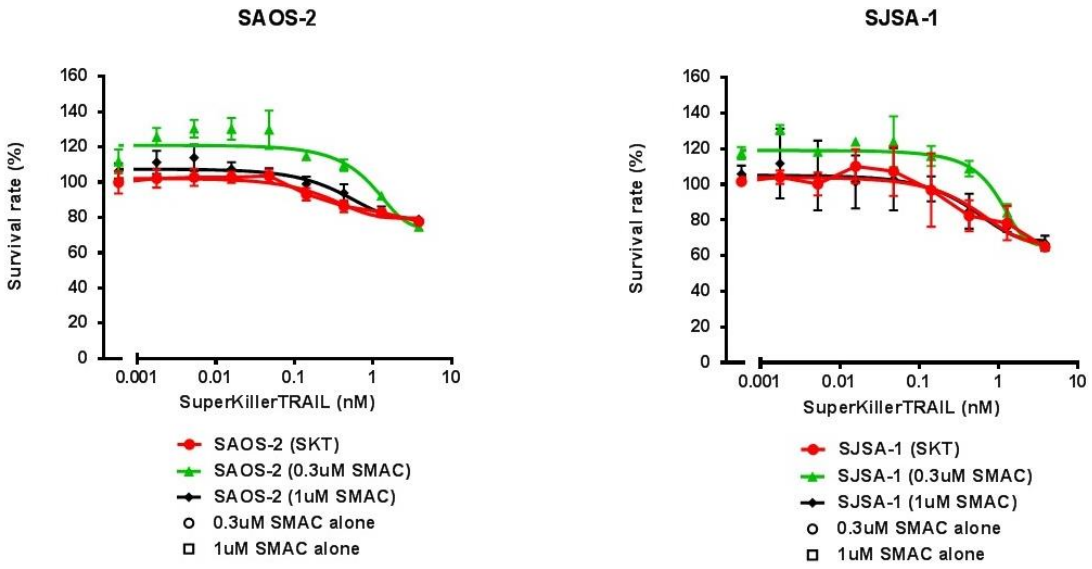

Figure 130 – SAOS-2 and SJSA-1 treatment with Smac mimetic and SKT combination. SAOS-2 (IC50 = 0.3 nM, 1.1 nM, 0.5 nM; SKT alone, with 0.3 µM Smac mimetic and with 1 µM Smac mimetic respectively). SJSA-1 (IC50 = 0.5 nM, 1.0 nM, 0.7 nM; SKT alone, with 0.3 µM Smac mimetic and with 1 µM Smac mimetic respectively).

Effect of Smac mimetic on HT1080 dedifferentiated chondrosarcoma cell line

A sensitising effect was observed on the HT1080 cell line when combining Smac mimetic with SuperKillerTRAIL (SKT) (Figure 131).

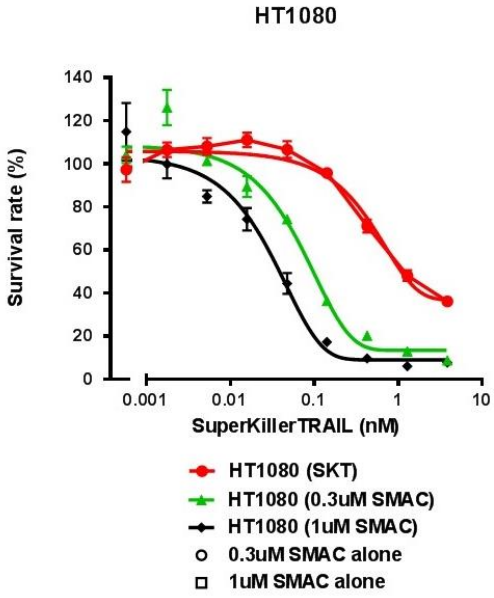

Figure 131 - HT1080 treatment with Smac mimetic and SKT combination. SKT IC50 = 0.5 nM, 0.06 nM (with 0.3 µM Smac mimetic), 0.02 nM (with 1 µM Smac mimetic).

6.6.2 Antibody drug-like conjugates (SMACTRAIL fusion protein, AD-O53.2) has limited effect compared to crosslinked SuperKillerTRAIL and Smac mimetic Birinapant administered in combination

AD-O53.2 (SMACTRAIL) was found to have a greater cytotoxic effect on the U2OS osteosarcoma cell line compared to SuperKillerTRAIL at lower concentrations (Figure 132).

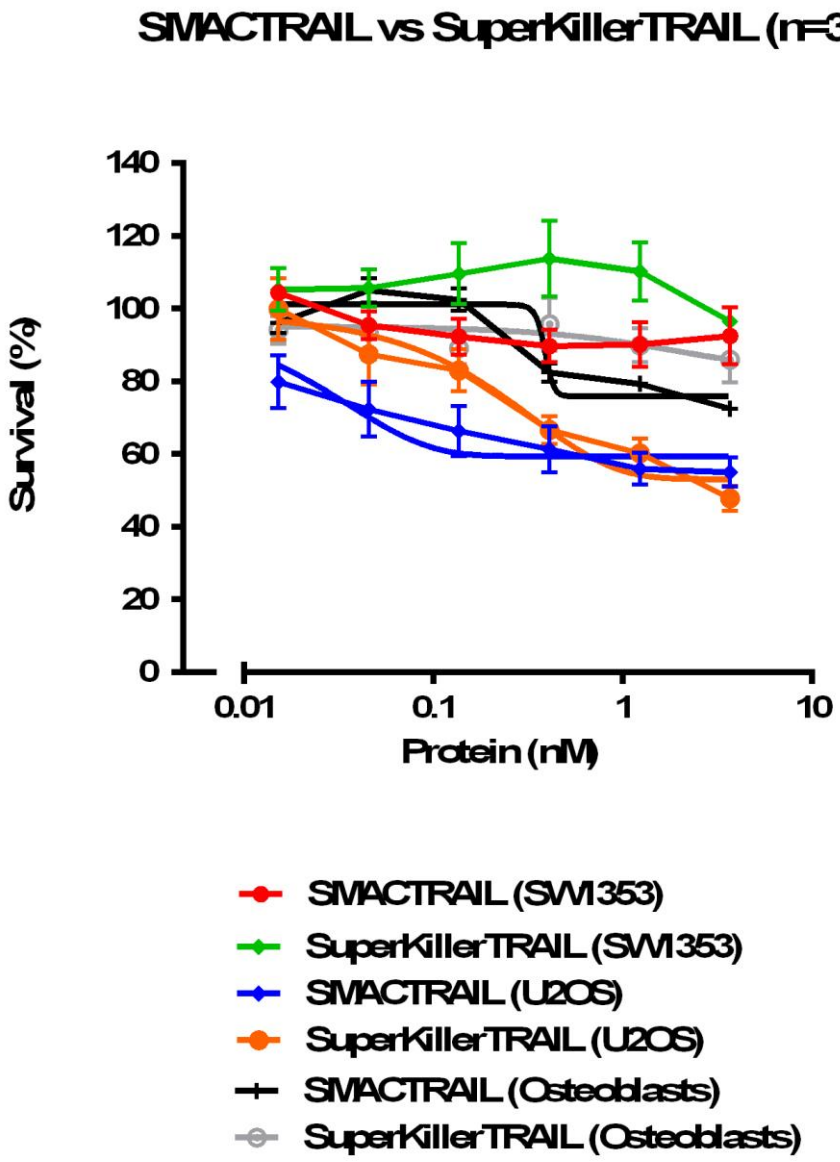

Figure 132 – AD-O53.2 (SMACTRAIL) was most cytotoxic to the U2OS osteosarcoma cell line at the lower dosages when compared to the SuperKillerTRAIL (SKT) treated U2OS cells, the SW1353 chondrosarcoma cell line and osteoblasts.

6.6.3 Combining TRAIL with HDAC inhibition on bone sarcoma cell lines

HDAC inhibition alone was not significantly toxic to the HT1080 cell line (Figure 133). Its combination with SuperKillerTRAIL (SKT) significantly enhanced cytotoxicity in the HT1080, SW1353, SAOS-2, SJSA-1 and U2OS cell lines (Figure 134).

Effect of HDAC inhibition alone on HT1080 pSLIEW cell line

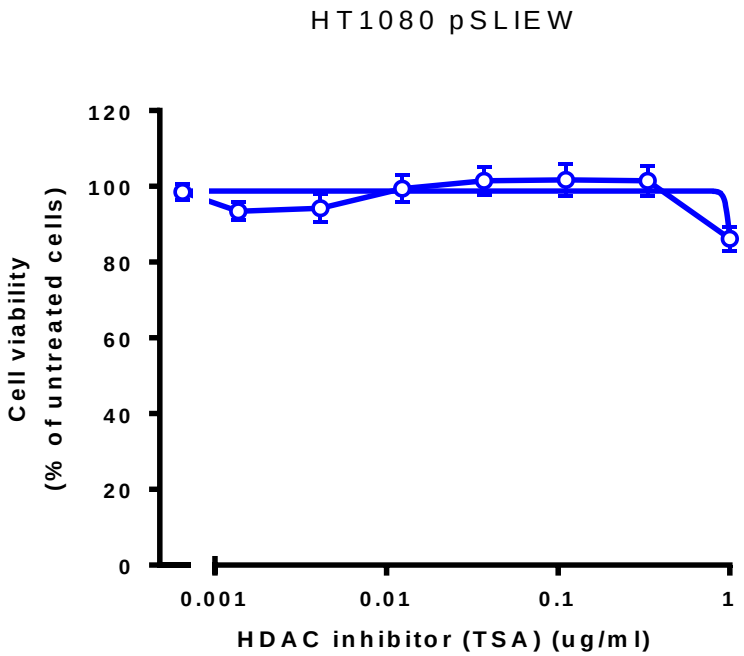

Figure 133 - HDAC inhibition alone using TSA, was not significantly toxic to the HT1080 cell line.

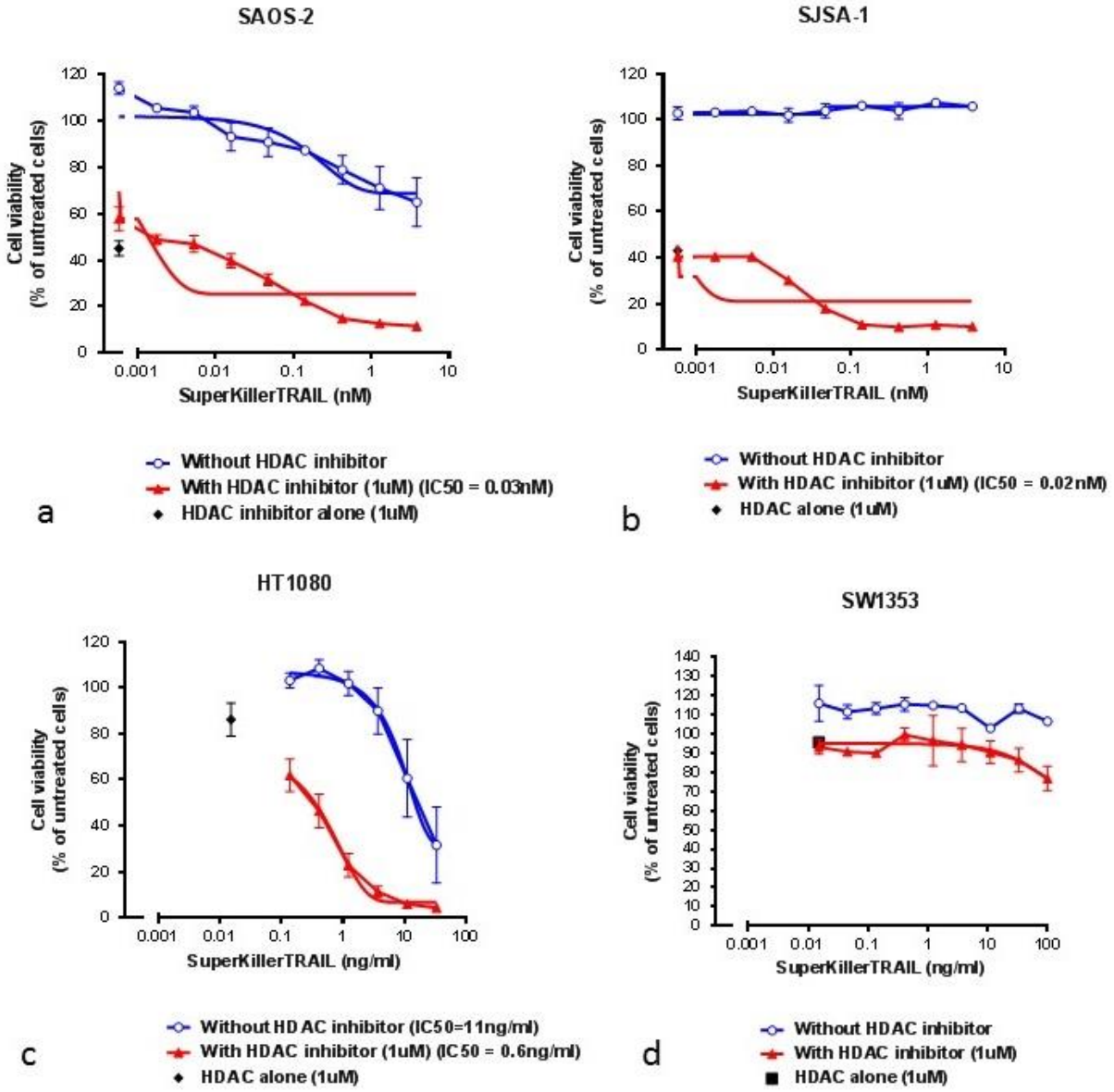
SAOS-2
Cell viability (% of untreated cells)
SuperKillerTRAIL (nM)
Without HDAC inhibitor
With HDAC inhibitor (1uM) (IC50 = 0.03nM)
HDAC inhibitor alone (1uM)
a
SJSA-1
Cell viability (% of untreated cells)
SuperKillerTRAIL (nM)
Without HDAC inhibitor
With HDAC inhibitor (1uM) (IC50 = 0.02nM)
HDAC alone (1uM)
b
HT1080
Cell viability (% of untreated cells)
SuperKillerTRAIL (ng/ml)
Without HDAC inhibitor (IC50=11ng/ml)
With HDAC inhibitor (1uM) (IC50 = 0.6ng/ml)
HDAC alone (1uM)
c
SW1353
Cell viability (% of untreated cells)
SuperKillerTRAIL (ng/ml)
Without HDAC inhibitor
With HDAC inhibitor (1uM)
HDAC alone (1uM)
d

Figure 134 - SuperKillerTRAIL combined with pan-HDAC inhibitor (TSA) (1 µM) on (a) SAOS-2 and (b) SJSA-1 osteosarcoma cell lines. (c) HT1080 dedifferentiated chondrosarcoma cell line. (d) SW1353 chondrosarcoma cell line. HDACi (TSA) alone was found to have a cytotoxic effect. Combining (TSA) with SuperKillerTRAIL (SKT) increased the cytotoxic effects in all bone sarcoma cell lines.

Effect of HDAC inhibition on osteosarcoma cell lines

HDAC inhibitor (HDACi) was found to have a cytotoxic effect on osteosarcoma cell lines (U2OS, SAOS-2). The effect was more pronounced when combined with SuperKillerTRAIL (SKT) (Figure 135).

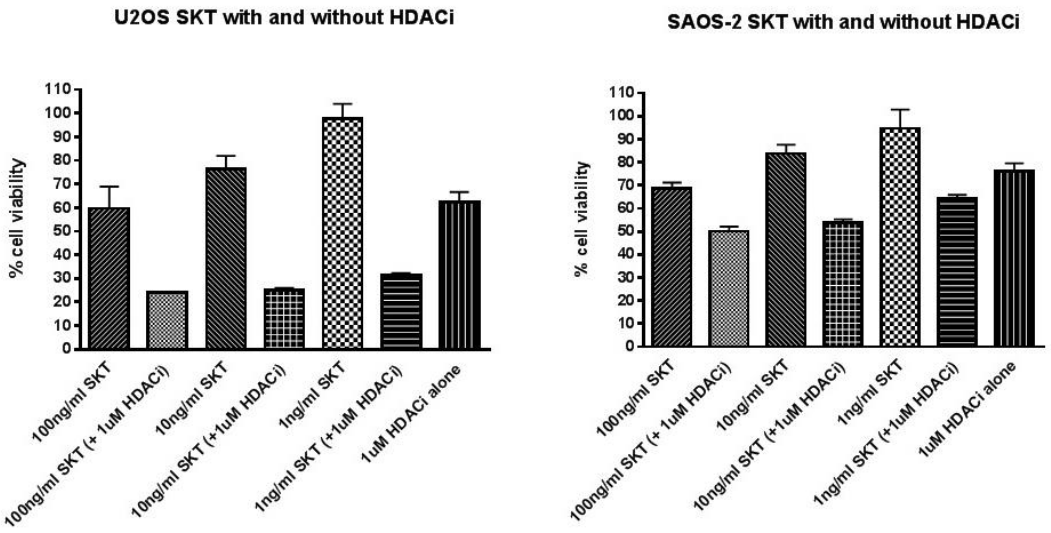

Figure 135 – Combining HDAC inhibitor (TSA) enhanced the effects of SuperKillerTRAIL (SKT) on U2OS and SAOS-2 osteosarcoma cell lines when compared to untreated cells. HDACi alone was also found to have a cytotoxic effect. Significance was found between SKT alone and SKT+HDACi for all does of SKT tested ($p < 0.05$, Student's unpaired *t*-test).

6.6.4 Combining TRAIL with ABT-737 on bone sarcoma cell lines

Doses of ABT-737 above 100 nM were found to be toxic to the more resistant SJSA-1, SAOS-2 and SW1353 bone sarcoma cell lines (Figure 136). The more resistant sarcoma cells were treated with combination of SuperKillerTRAIL and ABT-737 to assess for any enhanced cytotoxic effects. No significant effect was observed when using the 10 nM dose (Figure 137). However, at 100 nM significant effects were visible for the SW1353 chondrosarcoma cell line (Figure 138).

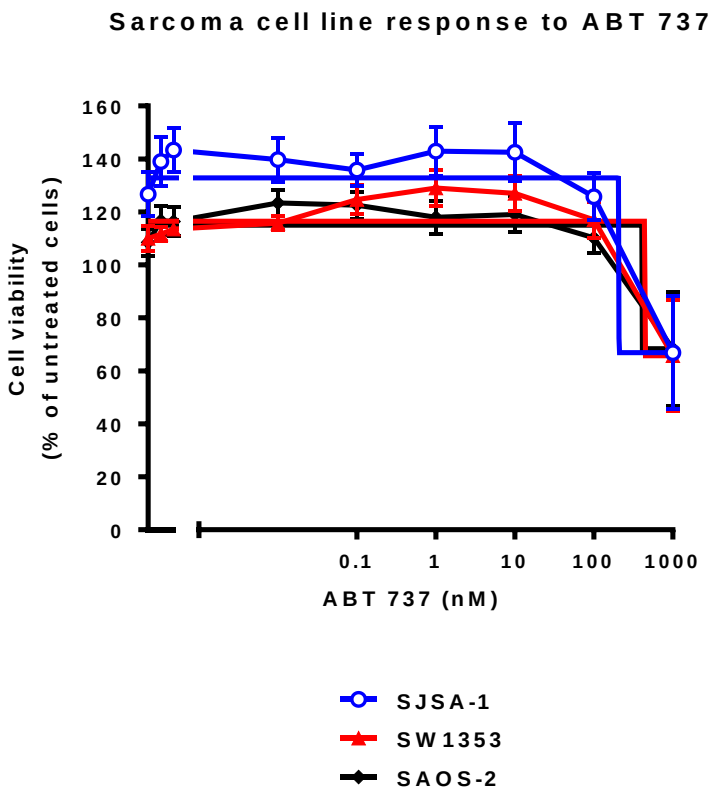

Figure 136 – Doses of Bcl-2 inhibitor (ABT-737) above 100 nM were found to be toxic to the more resistant SJSA-1, SAOS-2 and SW1353 bone sarcoma cell lines

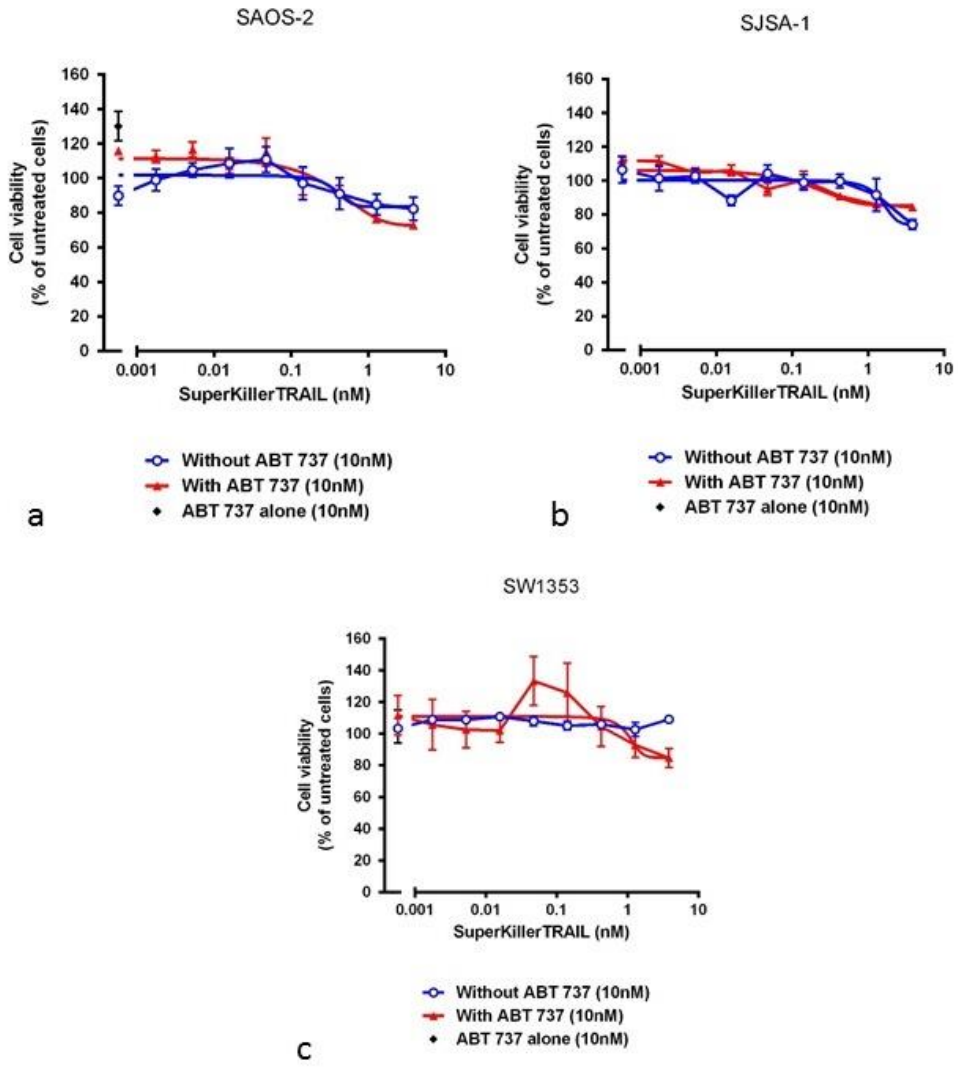

Figure 137 – Combination of 10 nM of ABT-737 with SuperKillerTRAIL (SKT) was not found to have significant additional effects compared to SKT alone.

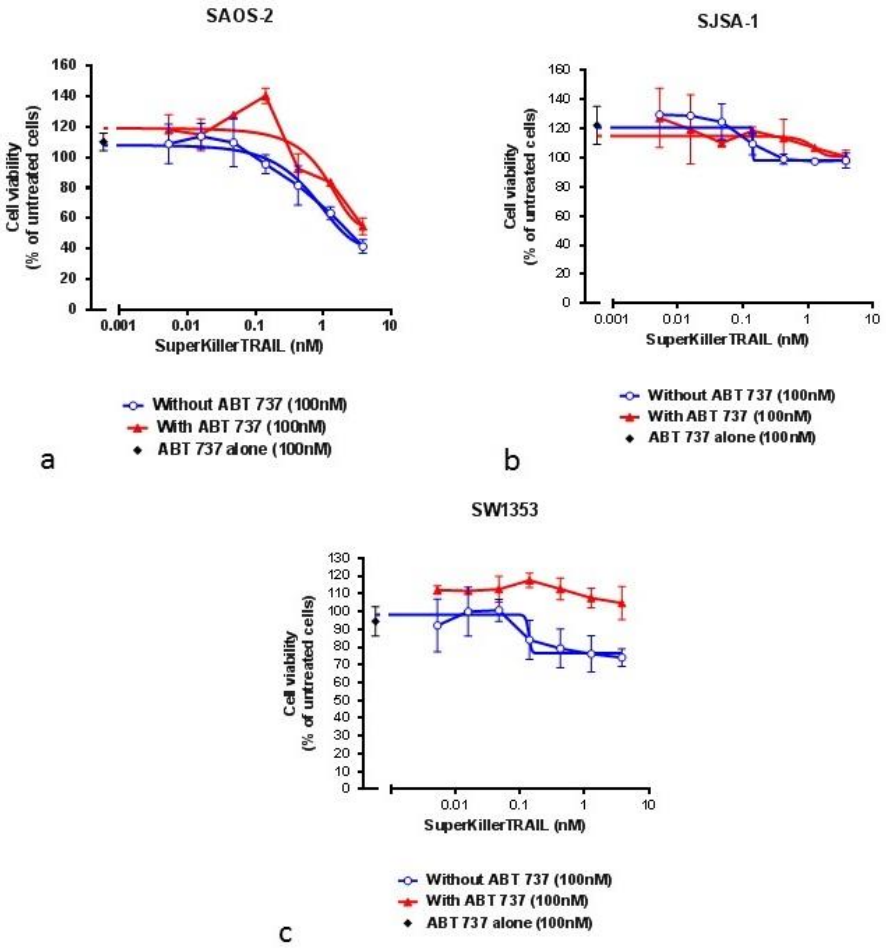

Figure 138 - Combination of 100 nM of ABT-737 with SuperKillerTRAIL (SKT) was found to have significant additional effects compared to SKT alone on SW1353 chondrosarcoma cell line.

6.7 Discussion and future direction

Current chemotherapeutics doxorubicin and etoposide

Doxorubicin

In this study, I found that doxorubicin can sensitise the bone sarcoma cells to SuperKillerTRAIL. This supports data from a previous publication by Van Valen *et al.,* 2003, which confirmed that the chemotherapeutic agents such as doxorubicin sensitises a range of sarcoma cells lines such as U2OS, SAOS-2, SJSA-1, and other

osteosarcoma cell lines [296]. They also found that doxorubicin when combined with TRAIL is significantly toxic to human osteoblast cells obtained commercially. The human osteoblasts, however, were insensitive to TRAIL alone. They used a recombinant form of TRAIL/APO2L. When used alone in this study, they found that 300 ng/ml of the agent was significantly toxic to U2OS cells when treated for 96 hours; however, human osteosarcoma (HOS) cells, SAOS-2, SJSA-1, and human osteoblasts HOBs were not significantly different from controls. However, the 96-hour values for U2OS and OST were significantly different $p<0.05$. The 24-hour value for the VH64 Ewing's sarcoma cell line was also significantly different from control. The findings in my study was that crosslinked TRAIL did not have significant cytotoxic effect on SAOS-2 and SJSA-1 osteosarcoma cell lines. However, upon addition of doxorubicin there was a sensitisation to SuperKillerTRAIL found in both these cell lines which reflects the findings of Van Valen *et al.,*. Interestingly, there is some debate in the literature as to the concentration of the recombinant human TRAIL that is as toxic to U2OS cells. In the Van Valen *et al.,* 2003 study, they found that 300 ng/ml was toxic. However in a more recent investigation, it is thought that up to 1 µg/ml is required to induce cell death in the U2OS cell line [258]. I have found that 100 ng/ml (0.1 µg/ml, 4 nM) of SuperKillerTRAIL (26 kDa) can induce up to 50 % cell death in the U2OS cell line. The Van Valen study reports up to about 75 % of viable cells, i.e., 25 % cell death with the 300 ng/ml rhTRAIL (19.6 kDa) (0.3 µg/ml, 15 nM) and further confirms that the crosslinked form of TRAIL is more toxic to this cell line. In combination with doxorubicin, I found more significant toxicity to the bone sarcoma cell lines when compared to normal non-malignant cells such as patient-derived human osteoblasts (OBs), neonatal human dermal fibroblast cells (NHDFs), human vascular endothelial cells (HUVECs) and human bone marrow-derived mesenchymal stem cells (BMMSCs).

Etoposide/ VP16

In my study, I found that the TC71 Ewing's sarcoma cell line is sensitive to the crosslinked form of TRAIL, SuperKillerTRAIL, and the effect is enhanced when combined with VP16. This, again, supports the finding from Van Valen *et al.,* 2003 who investigated Ewing's sarcoma cell lines, which did not include TC71, but included a range such as ES-3, ES-3, RD-ES, SK-ES-1, and STA-ET-2.1 and found significantly enhanced toxicity when TRAIL was combined with VP16 when compared to VP16 alone

[296]. However, there was a greater amount of cell death when TRAIL was combined with doxorubicin when compared to doxorubicin alone. Interestingly, the study found selective toxicity when VP16 was combined with TRAIL and was toxic to osteosarcoma cells, U2OS, SJSA-1, SAOS-2, OST, HOS, however when the combination was tested in the human osteoblasts it was not toxic. This is in contrast to the findings when doxorubicin is combined with TRAIL. However, in my study I found that when SuperKillerTRAIL was combined with VP16, the effect is similar to VP16 alone. When comparing VP16 with TRAIL and doxorubicin with TRAIL, the combination with VP16 was less toxic to the NHDF cell line but had similar efficacy in the TC71 cell line.

The Van Valen *et al.,* 2003 study [296] found increasing cytotoxicity with an increasing concentration of TRAIL in a range of osteosarcoma cell lines. However there did appear to be a slight plateau after 50 ng/ml. The more sensitive cell lines being the U2OS and the OST cell line. The less sensitive cell lines were SJSA-1 and the HOS cells and the human osteoblasts. The reduced sensitivity of the SJSA-1 to TRAIL also reflects the findings of my study. The study by Van Valen *et al.,* (2003) found that with an increased incubation time, there was increased toxicity and reduced cell viability in the SAOS-2 cell line. This was significant at 48 hours, 72 hours, and 96 hours; however, was not significant at 24 hours. For the majority of my cytotoxicity assays, I investigated up to 24 hours of exposure to the cytotoxic agent and was able to find significant toxicity using this time point. It was noted, however, that in cell lines such as the more resistant SJSA-1 osteosarcoma cell line that beyond 24 hours of TRAIL exposure there was evidence of decreased cell viability/confluence using the IncuCyte® live-cell analysis system (Section 5.2.2.2).

A general finding by Van Valen *et al.,* (2003) is that the chemotherapeutic agents down regulated the c-FLIP protein in the bone sarcoma cell lines. c-FLIP confers resistance to TRAIL. In Section 4.8, upregulated transcript levels have been found in the TC71 Ewing's sarcoma, U2OS osteosarcoma and HT1080 dedifferentiated chondrosarcoma cell lines. However, interestingly, c-FLIP has been found to be upregulated in the human osteoblast cell line by VP16. Furthermore, it appeared that P21 (a potent cyclin dependent kinase inhibitor) was also upregulated in the human osteoblast cell line when treated with VP16. The P21 protein has been demonstrated to be critical for the resistance of osteoblastic cells to apoptosis triggered by FasL/CD95 activation. The

findings suggest that normal human osteoblasts die through a mitochondrial dependent pathway according to Van Valen *et al.,* 2003. In contrast to the HOS cells, which mainly undergo apoptosis through the mitochondrial independent pathway in response to TRAIL. Furthermore, the selective effect of VP16 may be related to its ability to reduce c-FLIP expression in bone tumour cells.

In terms of further study, it would appear that VP16 has a more selective effect. I have found that VP16 was more toxic to the bone sarcoma cell lines compared to non-malignant NHDF cell lines. This was similar to the effects of doxorubicin and not significantly different. I have observed evidence of this selective effect as the NHDF cell line was more sensitive to doxorubicin particularly when combined with SuperKillerTRAIL compared to the VP16 and SuperKillerTRAIL combination. This is maybe due to the induction of c-FLIP and P21 expression and requires confirmation. Further study may include investigating the effects over time as it has been reported that there is more pronounced cell death after the 24-hour time point. My IncuCyte data demonstrates that cell death can reduce cell confluency over time when the chemotherapeutic agent is combined with SuperKillerTRAIL when compared to each agent alone.

Smac mimetics

The mammalian IAP family consists of eight members:

Neuronal IAP (NIAP), cellular IAP one (cIAP1), cellular IAP two (cIAP2), X-chromosome IAP (XIAP), survivin, ubiquitin-conjugating BIR domain enzyme Apollon, melanoma IAP and IAP-like protein two. Playing a direct role in apoptosis regulation are the following proteins, XIAP, cIAP1, cIAP2 and ML-IAP. High levels of XIAP and cIAP proteins have been correlated to chemoresistance and poor prognosis [297]. Smac mimetics function as effective cellular antagonists of XIAP, cIAP1 and cIAP2 proteins and have, therefore, been used clinically to try and induce apoptosis or facilitate the induction of apoptosis [242].

Smac mimetics have been investigated in clinical studies as a cancer therapeutic. The bivalent Smac mimetic birinapant (TL-32711) has been studied as weekly intravenous infusions on a three week on, one week off schedule in a study by Amaravadi *et al.,*

(2015). Patients included those with advanced solid tumours for the evaluation of the safety and the pharmacokinetics. The dose ranged from 0.18-26 mg/m^2 in 27 patients and there was no reported toxicity; however, there was some adverse events such as lymphopenia and rash. Prolonged stable disease was observed in three patients: liposarcoma (9 months), small cell lung cancer and colorectal cancer (5 months). There was evidence of tumour regression following administration of birinapant in two patients with colorectal cancer [298].

There has been concerns raised, however, about Smac mimetics use in *vivo* in Smac mimetic sensitive and resistant human and murine breast tumours. Smac mimetics can cause a high bone turnover, osteoporosis, increase NK mediated osteoclastogenesis, enhanced tumour associated osteolysis and metastases which is of concern [299].

There has been a number of Smac mimetics in development; however, the one I chose for *in vitro* experiments as part of the PhD is birinapant, which has shown promise clinically. I did not observe any significant toxicity to the sarcoma cell lines when administered alone and when administered in combination with SuperKillerTRAIL (SKT). Smac was found to enhance the cytotoxic effect of SKT on the resistant SW1353 chondrosarcoma cell line.

I utilised a dose of SKT ranging from 0.3 µM to 1 µM. The difference between 0.3 µM and the 1 µM was not significant for the SW1353 chondrosarcoma cell line. I did test the agent on other bone sarcoma cell lines but there did not appear to be a significant effect.

Smac TRAIL fusion protein (AD-053.2)

Fusion proteins have been developed, which attempt to combine the activities of TRAIL and Smac and try to overcome the resistance of human cancer cells. A study by Pieczykolan *et al.,* (2014) demonstrated that fusion protein AD-053.2 had more of an enhanced effect compared to soluble TRAIL alone [293]. This was demonstrated in a SCID mice engrafted with COLO205 and NCI-H460 cell lines to produce a xenograft model. The agent was given at 30 mg/kg and compared to the control six times every second day for a period of 10 days and they found a regression in the tumour size which was maintained for about two weeks post-implantation. The molecule combines

the intracellular activity of Smac derived elements and involves a membrane penetrating domain. The inclusion of the cleavable link between Smac and TRAIL not only enables a functional separation of these two effectors, but also increases the specificity on cells with elevated expression of MMPs. It is well documented that collagenases MMP2 and MMP9 secretion is up-regulated in several types of human cancers and over-expression has been associated with a poor prognosis. AD-053.2 demonstrated efficacy against non-transformed normal human epithelial cells or isolated normal rat or human hepatocytes [293]. I have found that this agent is more effective at lower concentrations than SuperKillerTRAIL in the U2OS osteosarcoma cell line and not significantly more toxic to osteoblasts.

HDAC inhibitors

Histone deacetylase inhibitors (HDAC Inhibitors or HDACi), have been investigated for sarcoma as a monotherapy reviewed recently by Tang *et al.,* 2017 [300]. They summarise that these epigenetic modifying agents can inhibit sarcoma cell growth *in vitro* and *in vivo* through a variety of pathways including induction of apoptosis, cell cycle arrest and prevention of invasion and metastasis. There are several phase 1 and phase 2 clinical trials assessing HDACi in combination with chemotherapeutic agents or alone and they have been shown to sensitise sarcomas to chemotherapy and radiotherapy in pre-clinical studies [300].

To date, 18 distinct histone deacetylases have been identified and they are classified into four groups based on the structural diversions, class 1, class 2, class 3 and class 4 HDACs. These HDACs are located within the nucleus and cytoplasm, some are exclusively in the nucleus such as, HDAC 1, 2 and 8 and they function as histone deacetylases.

In sarcoma cases, a high level of HDACs has been associated with an advanced disease and poor clinical outcomes. For example, HDACs 1, 4, 6, 7 and 8 exhibit high frequency and strong immunoreactivity with lower disease-free survival trend and has represented a potential therapeutic target for endometrial stroma sarcoma. In osteosarcoma, over expression of HDAC 5 could promote proliferation of cancer cells and upregulating and expression of twist 1 which has been reported as an oncogene. Beta-catenin is also an oncogene and subsidiary of HDAC 6. They have also been of

interest for the treatment of chordomas as they express HDACs 2-6, with the strongest expression of HDAC 6 [300].

HDACi enhance the susceptibility of the sarcoma cells to apoptosis as shown when HDAC inhibitors vorinostat (also known as suberoylanilide hydroxamic acid, SAHA) and sodium butyrate enhanced TRAIL apoptosis induced activity in SK-ES-1 and WE-68 Ewing's sarcoma cell lines [301]. A variety of mechanisms have been proposed for the induction of apoptosis in osteosarcoma cells or the enhancement of the induction of apoptosis in osteosarcoma cells. Valproic acid is an HDAC inhibitor and in a study by Yamanegi *et al*. was shown to 'enhance the susceptibility of osteosarcoma cells to Fas-induced cell death'. This is because the level of soluble Fas secretion decreased and overall Fas-induced cell death is enhanced [302]. cFLIP is a master anti-apoptotic regulator and sarcoma cells can exhibit resistance to DR mediated apoptosis with increased cFLIP. However, HDAC inhibitors can sensitise the resistant sarcoma cells by downregulating cFLIP mRNA expression [303]. Oral HDACi (MS-275, etinostat) administered to nu/nu-mice with osteosarcoma and established lung metastases mice can result in decreased cFLIP and decreased tumour nodules and tumour regression, with no significant toxicity observed [304].

There is a variety of HDAC inhibitors that are available. These include vorinostat and Tricostatin A (TSA), also known to be pan HDAC inhibitors. Vorinostat inhibits HDACs class 1 and 2. TSA is also an inhibitor of class 1 and 2. Sodium butyrate is a pan-HDAC inhibitor of class 1, 2A and also 4.

I have performed *in vitro* analysis of the HDACi Trichostatin A (TSA). It was found to have toxic effects at a concentration of 1 μM on the bone sarcoma cell lines. In combination with SuperKillerTRAIL (SKT), it did appear to sensitise the majority of the cell lines compared to SuperKillerTRAIL alone. HDAC inhibitors are also known to induce cell cycle arrest sarcomas and decrease invasion and metastases; however, for the PhD, I focused on investigating the sensitisation of the cells to induction of apoptosis through TRAIL and found a synergistic effect. The investigation of the other enhancement of the modes of cell death, or induction of cell cycle arrest was beyond the scope of the project. Future studies should also try to elucidate the effectiveness of the different types of HDAC inhibitors for specific sarcomas.

ABT-737

Other sensitisers that have been of interest are inhibitors of the anti-apoptotic Bcl family of proteins. The Bcl-2 inhibitor ABT-737 is reported to induce expression of DR5 and sensitise human cancer cells to TRAIL induced apoptosis. This is of interest as one common mechanism for the resistance of TRAIL induced apoptosis is the over expression of Bcl-2 or its family members that block the mitochondrial intrinsic pathway, which limit apoptosis following the binding of TRAIL to its DRs.

In a study by Song *et al.,* (2008), the administration of ABT-737 induced conformational changes in bax and bak proteins in the PV10 renal carcinoma cell line. They also describe in detail the upregulation of TRAIL receptor DR5 by using ABT-737 in renal and prostate cancer cell lines. ABT-737 can transcriptionally activate the DR5 promoter and stimulate an increase in DR5 mRNA. It has also been suggested that the ability of ABT-737 to induce apoptosis is dependent on the levels of Bcl-2 and the amount of Bim bound to Bcl-2 [294].

I found that when the sarcoma cell lines were exposed to high levels of ABT-737 (1000 nM), it can be toxic and at lower levels does not appear to sensitise the cells significantly to SuperKillerTRAIL (SKT) when the cells are treated in combination with ABT-737 at either 10 nM or 100 nM of ABT-737.

With regards to sarcoma, it has been found that the inhibition of the Bcl-2 family members sensitises soft tissue leiomyosarcoma to chemotherapy. In a report published by Degraaff *et al.* (2016), leiomyosarcoma is an aggressive soft tissue sarcoma with a five-year survival rate of 15 to 16 % and the treatment options are limited. However, when combination treatment was given, doxorubicin with ABT-737 and leiomyosarcoma cells revealed a synergism in the cell lines. It was concluded that the Bcl-2 family of proteins contribute to soft tissue leiomyosarcoma chemoresistance [305].

Studies reviewed by de Graff *et al.,* (2016) have demonstrated that when ABT-737 is used as a monotherapy in chondrosarcoma and small cell lung cancer it has limited activity. Interestingly, it has been discussed that cells can be resistant to apoptosis and administration of doxorubicin can decrease cell viability but actually have no impact on

apoptosis. They may stop proliferating and lose their viability, but they fail to activate the apoptotic pathway at the doses tested, most probably due to expression of the Bcl-2 family members. However, when the ABT-737 is given in combination with doxorubicin in high grade sarcomas, there is a synergistic effect seen with decreased cell viability and apoptosis demonstrated. The combination may not downregulate Bcl-2 family members but block their inhibitory effect on pro-apoptotic bak/bax [305].

With regards to P53 status, it is found that ABT-737 renders sarcoma cell lines, such as leiomyosarcoma cell, are more sensitive to doxorubicin especially in the presence of wild type TP53 and is potentially a new therapeutic option for soft tissue sarcomas with metastatic inoperable disease [305].

Further *in vitro* investigation is required for bone sarcoma, such as osteosarcoma and Ewing's sarcoma. However, there has been some studies in chondrosarcoma. Also, future experiments would involve using ABT-737, with doxorubicin, for the bone sarcoma cell lines with or without crosslinked forms of TRAIL.

MDM2 inhibition

At our institute, a group has found evidence of upregulation of DR5 transcript levels with administration of MDM2 inhibitor HDM201 in the SJSA-1 osteosarcoma cell line (Figure 139). Future investigation would involve investigation at the protein level and coadminstration of these agents with TRAIL, particularly in the more resistant cell lines such as the SAOS-2 and SJSA-1 osteosarcoma cell lines and the SW1353 chondrosarcoma cell lines.

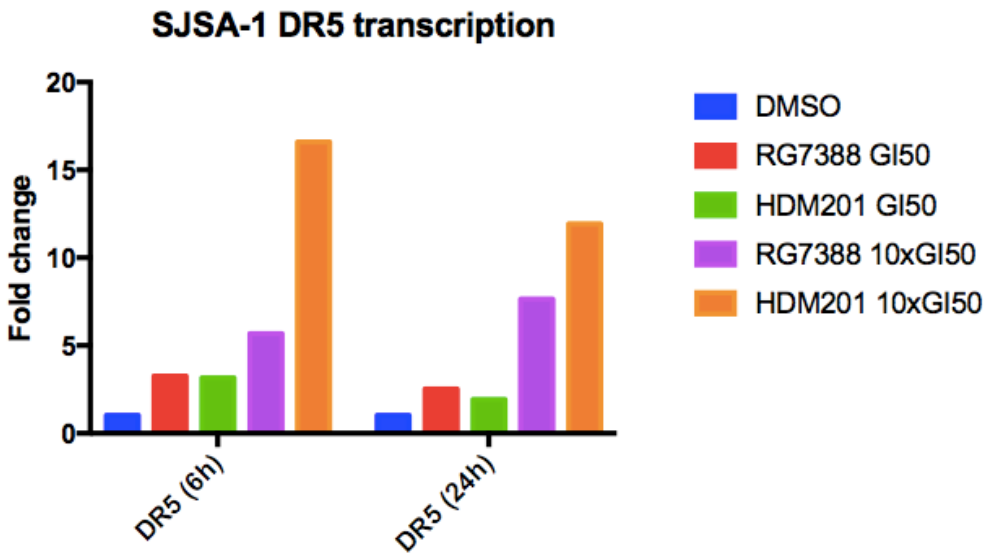

Figure 139 – Increase in DR5 transcript levels in SJSA-1 osteosarcoma cell line with exposure to MDM2 inhibitors. Greatest increases were seen with RG7388 and HDM201 (courtesy of Corey Tweedle of Professor John Lunec's group, NICR, Newcastle University).

Overall summary and future direction

TRAIL-induced bone sarcoma cell death can be enhanced when combined with agents such as current chemotherapeutics (doxorubicin) and more novel agents such as Smac mimetics, HDAC inhibitors and inhibition of Bcl-2 family members. This type of combination therapy (particularly with the targeted forms of TRAIL) holds great promise for the more resistant sarcomas and to help personalise therapy depending on types of pro and anti-apoptotic factors that may be expressed in the malignant tissue. There should be a focus on how the novel sensitisers compare with conventional chemotherapeutics and the degree to which effective combinations also affect non-malignant cells.

Chapter 7. *In vitro* investigation of NG2 targeted TRAIL construct

7.1 Targeted forms of TRAIL

Background and principle: A number of strategies have been devised to increase the half-life of TRAIL. An approach is to use single-chain TRAIL (scTRAIL) expressed as a single protein chain consisting of three TRAIL monomers joined by short peptide linkers [189].

Although there is convincing data for the successful *in vitro* use of TRAIL, and responses in patients with resistant bone sarcomas such as chondrosarcoma, results from a few clinical trials show that the efficacy of TRAIL in bone sarcoma treatment is only low or moderate [263]. This is most likely due to the use of agonistic DR4 or DR5-specific antibodies that do not achieve the same effect as pre-oligomerised TRAIL and the short half-life of TRAIL in the bloodstream. The latter is caused by (i) dissociation of bioactive homotrimeric TRAIL into non-functional TRAIL monomers and (ii) quick release from the bloodstream due to its low molecular weight. To overcome this difficulty, single-chain derivatives of TNF-ligands have previously been designed, including single-chain TRAIL (scTRAIL), resulting in a 10-fold increase of stability *in vitro* and 2-fold in the bloodstream [306]. This design was also incorporated in the design of scFvNG2(9.2.27)-IgG1Fc-scTRAIL, which will be assessed in this Chapter.

Soluble TRAIL can be genetically linked to a single-chain variable fragment of an antibody (scFv) and this is known as a fusion protein. This could enhance the efficacy of TRAIL and reduce potential toxic effects to normal cells by improving the selectivity of TRAIL at the bone sarcoma site. Designing the scFv portion to recognise a pre-selected tumour specific target antigen (such as EpCam, CD7 and CD19) has been demonstrated to induce the accumulation of TRAIL at the tumour site [66-68,259]. This not only kills the cell expressing the target antigen but neighbouring cells expressing the antigen (a 'bystander' effect). In a bone fibrosarcoma cell line (HT1080), our collaborator found that scFv:scTRAIL (engineered to recognise erb-b2) is more effective *in vitro* than KillerTRAIL, a pre-dimerised derivative of TRAIL [259]. Moreover, the larger molecular weight of scFv:scTRAIL reduced glomerulal excretion and extended circulation time [307]. In a recent study by our collaborator, an 8-fold increase in the half-life was found *in vivo* with scFv-IgG1Fc-scTRAIL compared to

scTRAIL (17.4 hours vs 2.2 hours) and a strong antitumour effect in a model of colon carcinoma [308].

Fc-containing targeted forms of TRAIL

ScFv:scTRAIL has been further fused with a Fc portion of human IgG to form a hexameric molecule with superior activity (Hutt et al., 2017). The Fc portion can potentially activate antibody dependent cytotoxicity and complement dependent cytotoxicity [309].

Targeting NG2

One protein of interest in bone sarcoma to target is NG2, or neural/glial antigen 2, which is expressed highly at the RNA level in chondrosarcoma [147]. This cell surface protein, which is found in a wide variety of tumours has been used for drug targeting in melanoma [310]. Studies in melanoma have found enhanced activity with anti-(9.2.27)MCSP/NG2-TRAIL *in vitro* and *in vivo* [311], or by using a bispecific antibody directed to DR5 (anti-(9.2.27)MCSP/NG2-DR5) [310]. NG2 increases cancer cell proliferation, invasion, angiogenesis and resistance and NG2-antagonistic scFv-fusion proteins have been demonstrated to reduce tumour growth and improve the survival in a melanoma cell derived lung metastases mouse model [147,312,313]. ScFvNG2(9.2.27)-IgG1Fc-scTRAIL combines all three strategies (stabilisation, pre-oligomerisation and targeting) including targeting NG2-positive bone sarcoma (Figure 140).

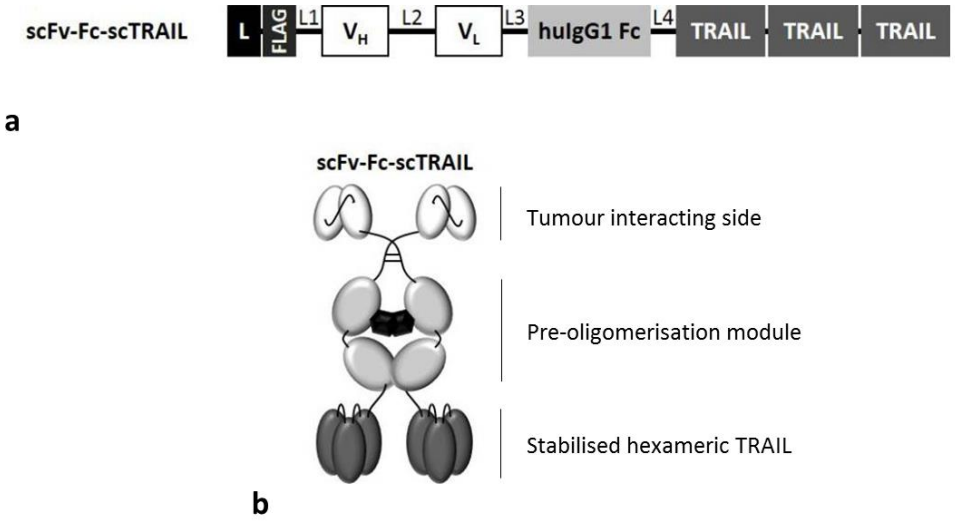

Figure 140 - Pictorial representation of the composition of (a) scFv-Fc-scTRAIL. I will use this construct fused to a fully humanised scFv-fragment specific for NG2 (clone 9.2.27), which is named scFvNG2(9.2.27)-IgG1Fc-scTRAIL. (b) Schematic assembly of scFv-Fc-scTRAIL [189].

The main aims of this chapter are to:

1. Investigate the levels of NG2 in the bone sarcoma cell lines.

1. Investigate the use of an NG2 targeted form of TRAIL and assess its efficacy in bone sarcoma cells expressing NG2 and cytotoxic effects in non-malignant cells.

2. To assess the NG2 targeted form of TRAIL in combination with doxorubicin on bone sarcoma cell lines and non-malignant cells.

7.1.1 NG2 expression in bone sarcoma cell lines

PCR

This is explored in Chapter 4.

Flow cytometry

Surface expression of NG2 in the available bone sarcoma cell lines was analysed using flow cytometry. The SW1353 chondrosarcoma cell line and the MG63 osteosarcoma cell line expressed the greatest surface levels (Figure 141).

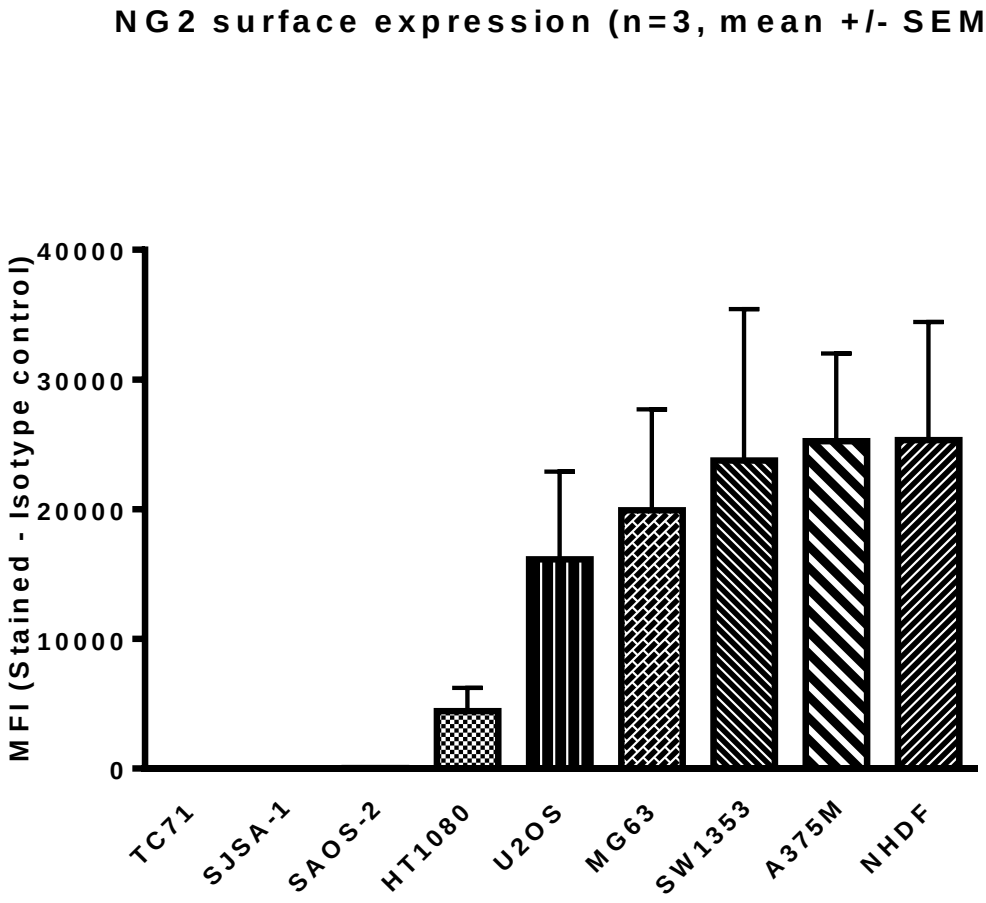

Figure 141 – Flow cytometry analysis of surface NG2 expression in bone sarcoma cell lines and NHDF. A375M melanoma cell line is the positive control.

Western blotting

High levels were demonstrated in the SW1353 chondrosarcoma cell line and MG63 osteosarcoma cell line (Figure 142).

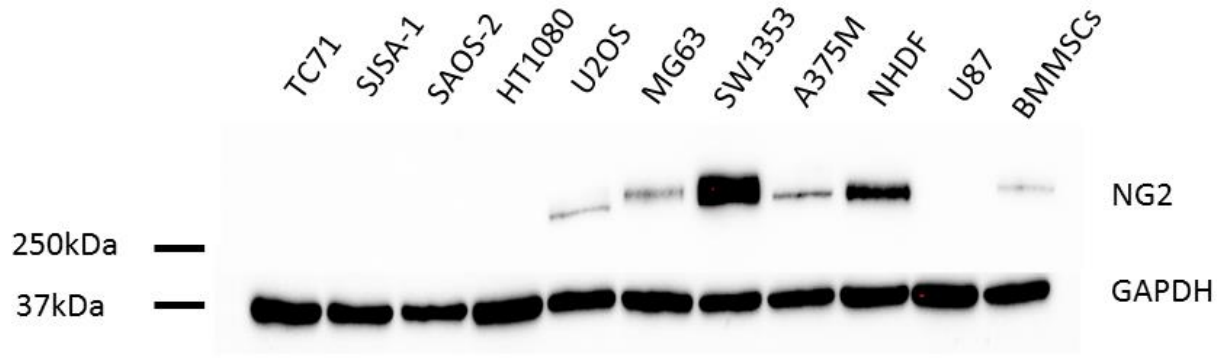

Figure 142 – Western blot analysis of NG2 expression in bone sarcoma cell lines. High NG2 expression levels in the SW1353 chondrosarcoma cell line and MG63 osteosarcoma cell line. A375M melanoma cell line was used as the positive control. NHDF = normal human dermal fibroblasts, U87 = human glioma cell line, BMMSCs = bone marrow-derived mesenchymal stem cells.

Immunohistochemistry (IHC)

A specific cell line block was manufactured (courtesy of histoCyte laboratories Ltd) to help optimise the antibody concentration for anti-NG2 (Abcam, ab139406 Anti-NG2 antibody [EPR9195] (also as described for DR5 in Section 2.6) (Figure 143). Antibody staining demonstrated at 1 in 100 concentration, which was optimal (Figure 144).

	Cell line
1	A375M
2	MG63
3	TC71
4	SW1353
5	U2OS
6	HT1080
	Total

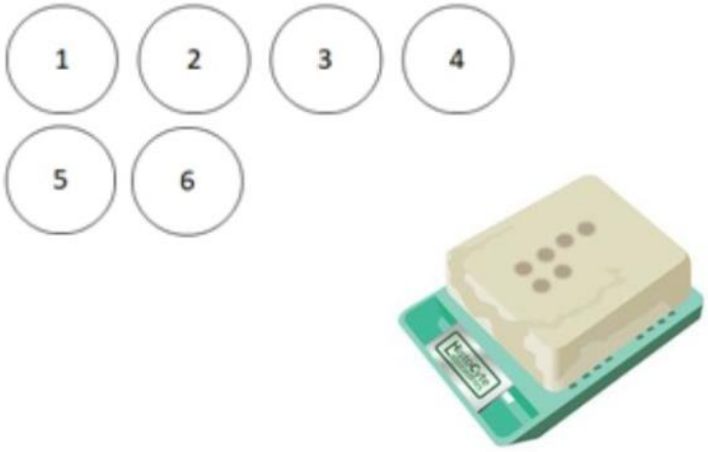

Figure 143 - Cell line block was manufactured (courtesy of histoCyte laboratories Ltd) to help optimise the antibody concentration for anti-NG2.

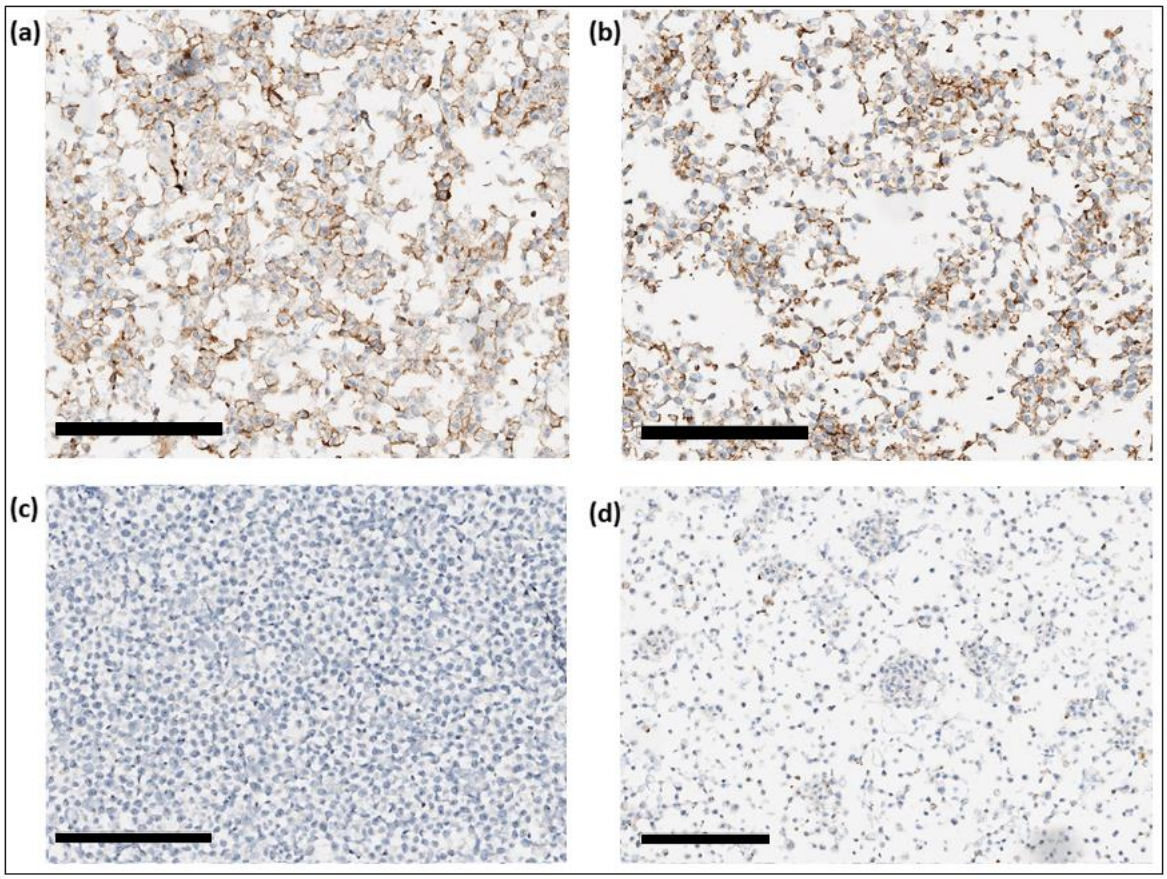

Figure 144 - Selected cell lines from a cell line block developed to optimise anti-NG2 antibody concentration for staining sarcoma cells at higher magnification. Antibody staining demonstrated at 1 in 100 concentration. Scale bars = 200 μM. There is strong staining in SW1353 chondrosarcoma (a) and MG63 osteosarcoma (b) cell lines. Weak/moderate staining is demonstrated in HT1080 dedifferentiated chondrosarcoma cell line (d). There is absent staining in TC71 Ewing's sarcoma cell line (c).

Bone sarcoma cell line death receptor 5 (DR5) and NG2 surface expression analysed using imagestream

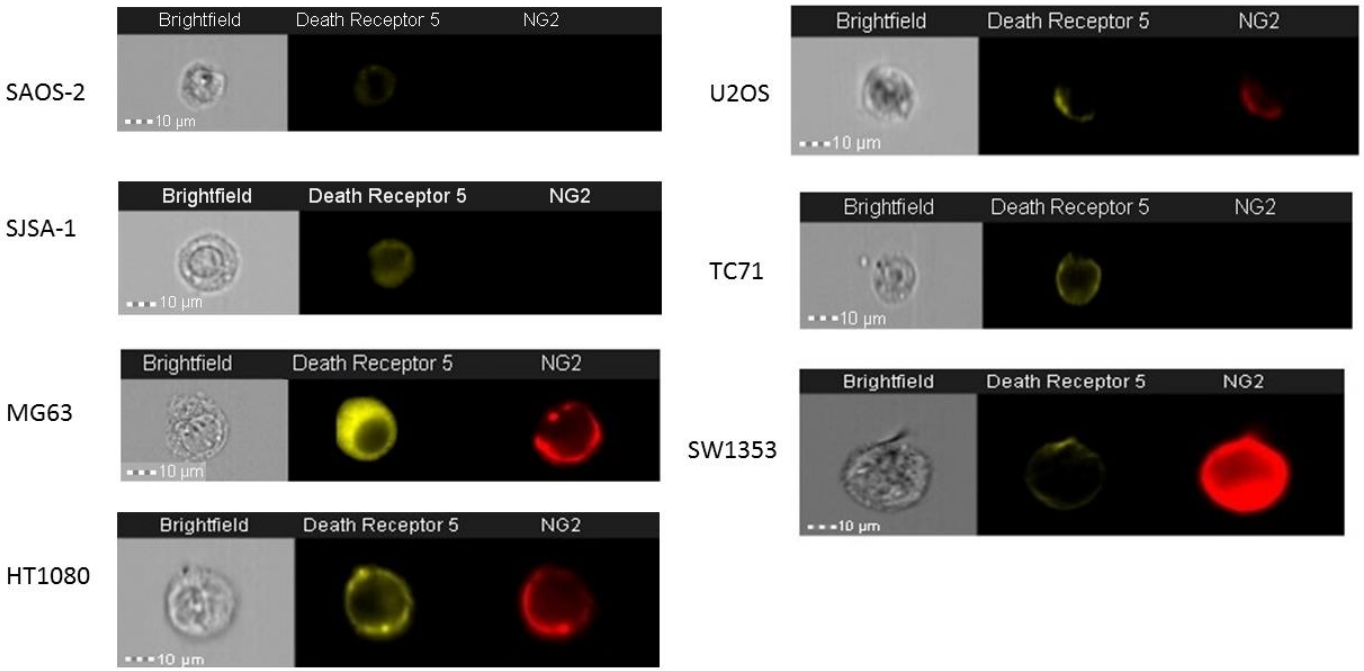

Figure 140 – NG2 is visible at the surface level in the U2OS and MG63 osteosarcoma cell lines and the SW1353 and HT1080 chondrosarcoma cell lines. It appears to be strongest in the SW1353 cell line. DR5 is visible in all of the bone sarcoma cell lines but strongest in the MG63 and HT1080 cell lines.

7.2 Cytotoxicity data using MCSP:DR5 bispecific antibody

Initial investigations involved collaborating with a team (Professor Wijanand Helfrich, University of Groningen), who have also demonstrated previously the superiority of targeted versions of TRAIL [66] and have developed an NG2/MCSP:DR5 bispecific antibody successfully used in animal models of melanoma [310,314]. It has not yet been used in human clinical trials. They kindly tested the bone sarcoma cells lines and found enhanced activity in the HT1080 dedifferentiated chondrosarcoma cell line, which they found to express high levels of surface NG2 and DR5 using flow cytometry (Figure 145).

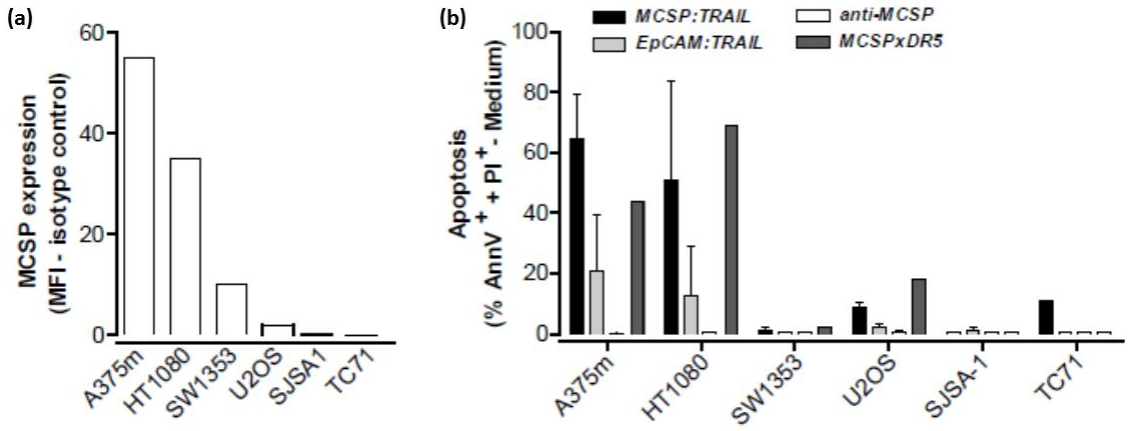

Figure 145 – (a) High surface expression of NG2 was found in the HT1080 dedifferentiated chondrosarcoma cell line. A375M was used as the positive control for NG2. (b) Bispecific antibody MCSP:TRAIL or MCSPxDR5 induced greater degree of apoptosis in cells expressing NG2 compared to control EpCAM:TRAIL and anti-MCSP alone (courtesy of Professor Wijanand Helfrich, University of Groningen).

7.3 NG2 targeted TRAIL (scFvNG2 (9.2.27)-IgG1Fc-scTRAIL) on bone sarcoma cell lines

ScFvNG2(9.2.27)-IgG1Fc-scTRAIL was more cytotoxic to bone sarcoma cell lines expressing both DR5 and NG2 (Figure 146). However, the SJSA-1 osteosarcoma cell line and the DR5 and NG2 expressing SW1353 chondrosarcoma cell line remained resistant (Figure 147). IC50 values have been summarised (Table 23).

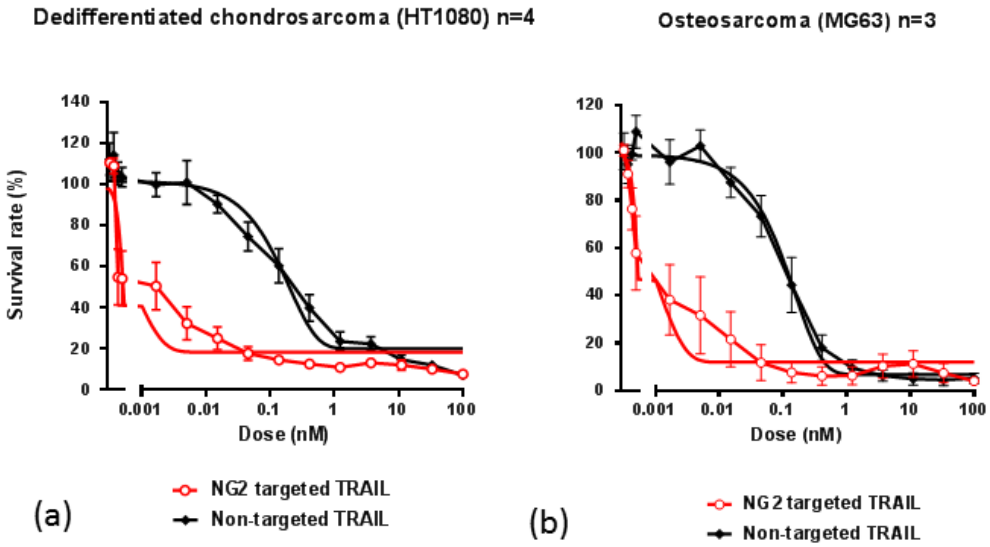
Dedifferentiated chondrosarcoma (HT1080) n=4
Survival rate (%)
Dose (nM)
NG2 targeted TRAIL
Non-targeted TRAIL
(a)
Osteosarcoma (MG63) n=3
Dose (nM)
NG2 targeted TRAIL
Non-targeted TRAIL
(b)

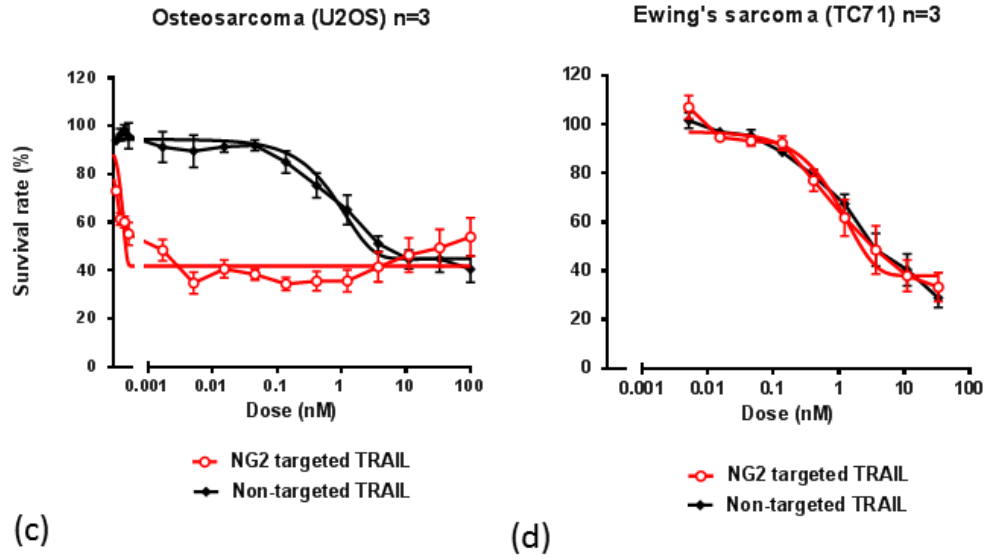
Osteosarcoma (U2OS) n=3
Survival rate (%)
Dose (nM)
NG2 targeted TRAIL
Non-targeted TRAIL
(c)
Ewing's sarcoma (TC71) n=3
Dose (nM)
NG2 targeted TRAIL
Non-targeted TRAIL
(d)

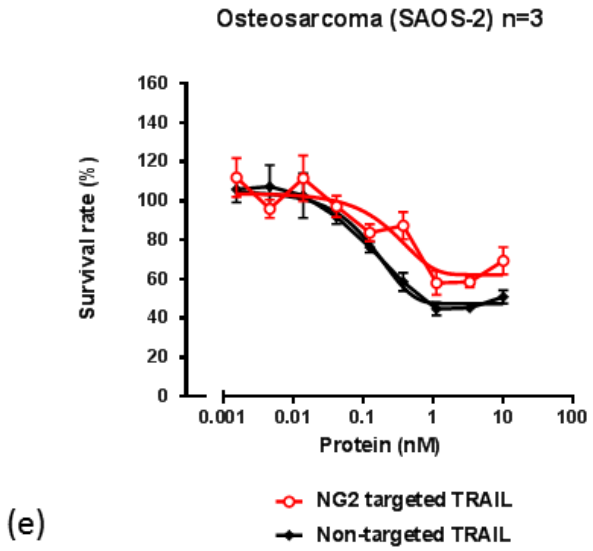
Osteosarcoma (SAOS-2) n=3
Survival rate (%)
Protein (nM)
NG2 targeted TRAIL
Non-targeted TRAIL
(e)

Figure 146 - Bone sarcoma cell lines that express both NG2 and DR5, (a) HT1080, (b) MG63 and (c) U2OS are sensitive to the NG2 targeted TRAIL (scFvNG2(9.2.27)-IgG1Fc-scTRAIL). The TC71 Ewing's sarcoma line (d) and SAOS-2 osteosarcoma cell line (e) are negative for NG2 and therefore has the same response to the targeted TRAIL as the non-targeted TRAIL (mean +/-SEM, n=3).

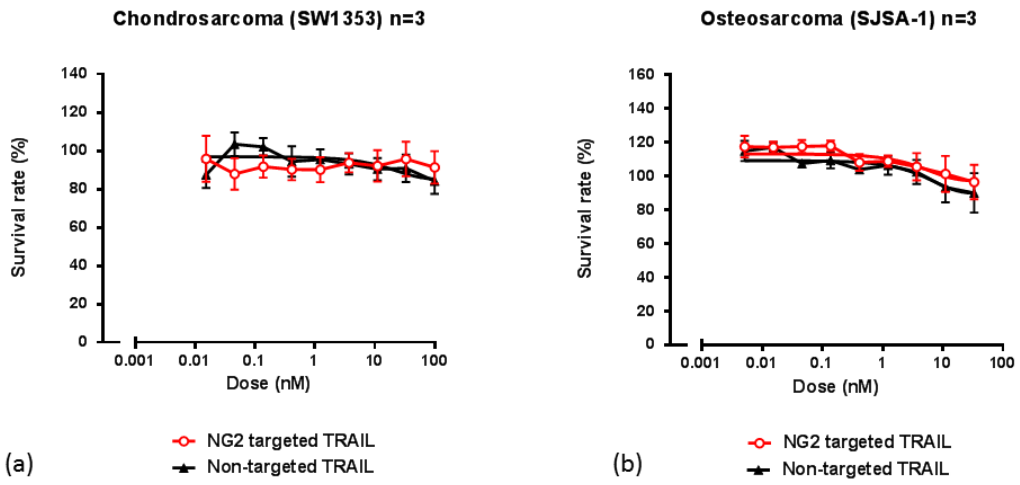

Figure 147 – (a) SW1353 chondrosarcoma cell line is resistant to both NG2 targeted TRAIL and non-targeted TRAIL; there still remains a large proportion of viable cells. (b) NG2 targeted TRAIL does not have an enhanced effect compared with non-targeted TRAIL on the SJSA-1 osteosarcoma cell line.

Incucyte® live-cell analysis

NG2 targeted TRAIL is more effective than non-targeted TRAIL at lower 0.01 nM dose at reducing HT1080 rate of proliferation (Figure 148) and low doses of NG2 targeted TRAIL are as effective as the higher doses at reducing the rate of HT1080 proliferation; however, regrowth is evident following treatment (Figure 149).

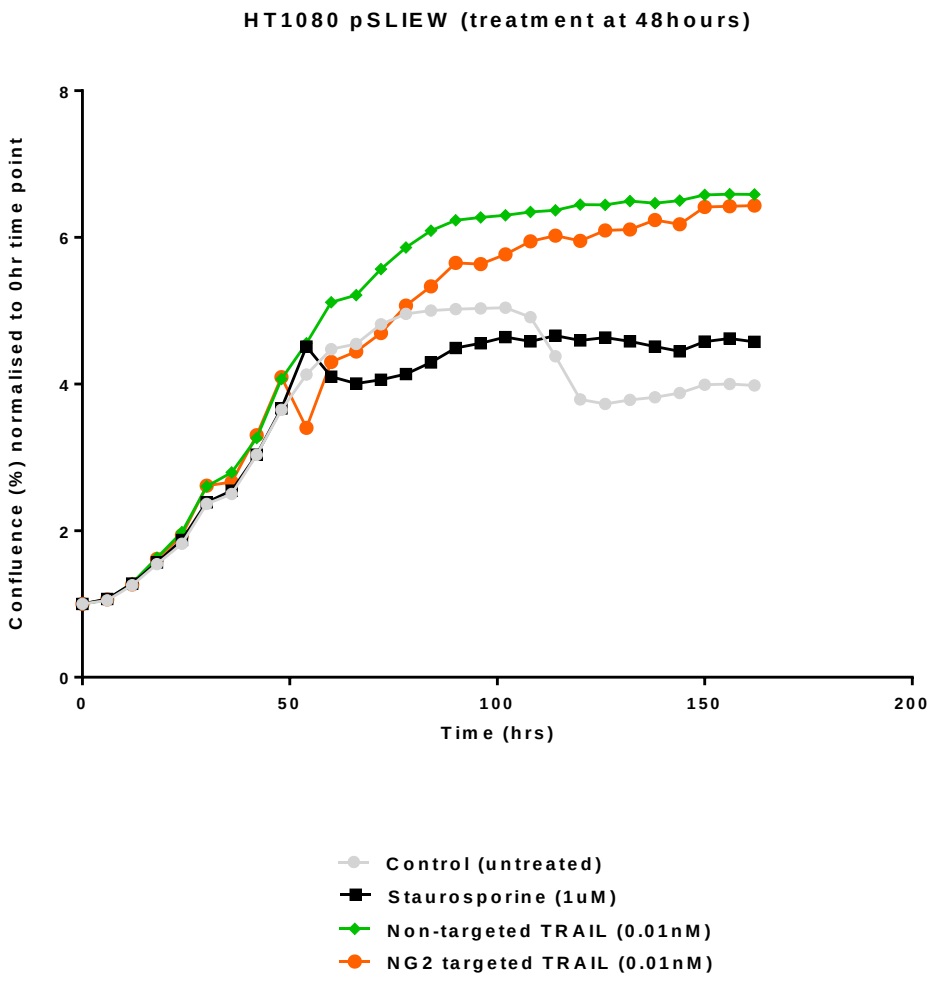

Figure 148 - NG2 targeted TRAIL is more effective than non-targeted TRAIL at low dose (0.01 nM) at reducing HT1080 rate of proliferation. Staurosporine (1 µM) was included as control for cell death and background signal.

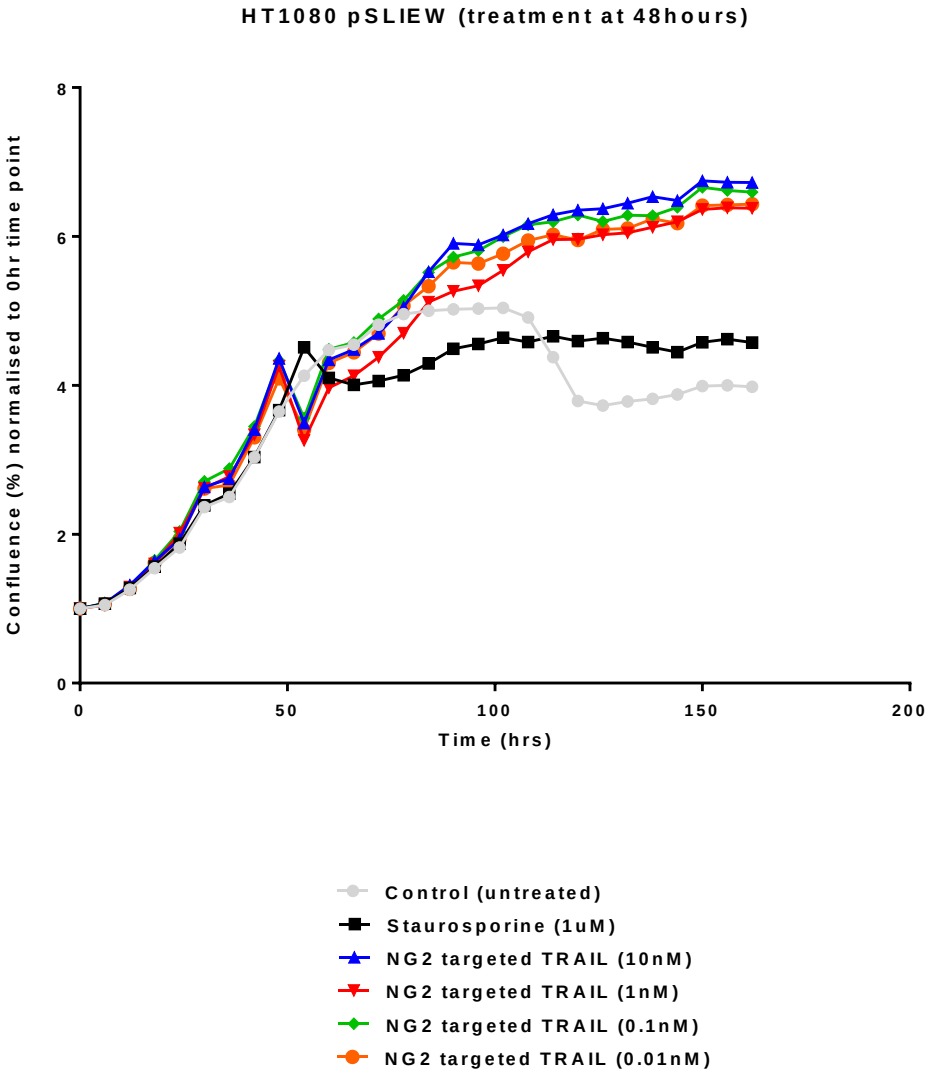

Figure 149 - Low dose of NG2 targeted TRAIL (0.01 nM) is as effective as the higher dose (10 nM) at reducing the rate of HT1080 proliferation; however, regrowth is visible following treatment. Staurosporine (1 µM) was included as control for cell death and background signal.

7.4 NG2 targeted TRAIL (scFvNG2 (9.2.27)-IgG1Fc-scTRAIL) on non-malignant cell lines

The HHL5 human hepatocyte cell line was the most sensitive to the NG2 targeted and non-targeted forms of TRAIL. Despite expressing both DR5 and NG2, all the other non-malignant cells tested (BMMSCs, AC10 and NHDF) did not show significant sensitivity to the NG2 targeted or non-targeted forms of TRAIL (Figure 150) (Table 23).

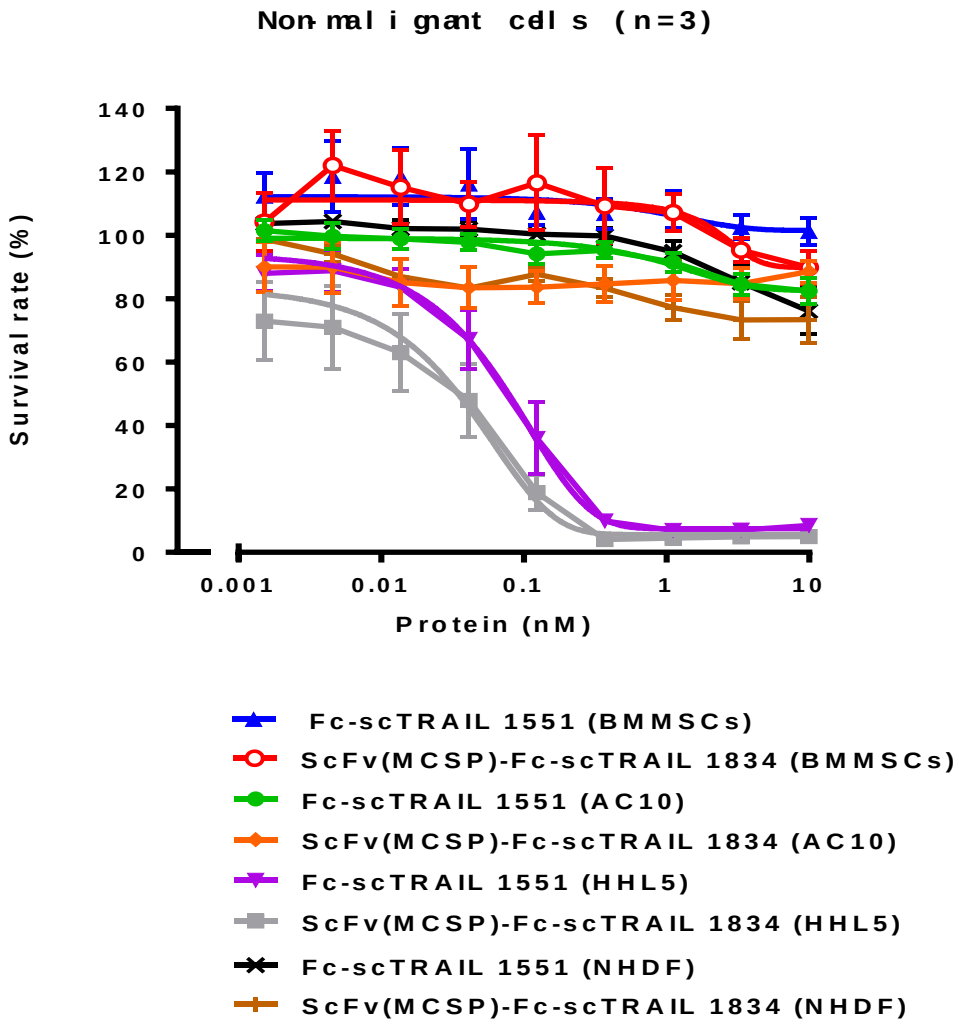

Figure 150 – NG2 targeted and non-targeted TRAIL on non-malignant cell lines. The HHL5 cell line is the most sensitive; however, the targeted form does not have significantly greater effect compared to non-targeted in this NG2 negative cell line (mean +/- SEM, n=3).

Table 23 - Summary table of IC50 values and fold change in all cell lines tested with NG2 targeted and non-targeted TRAIL.

Sarcoma type	Cell line	Non-targeted TRAIL (IC50)(nM)	NG2 targeted TRAIL (IC50)(nM)	Fold change
Osteosarcoma	SAOS-2	0.11	0.19	0.6
	U2OS	0.09	0.000005	18000
	SJSA-1	NC	NC	-
	MG63	0.01	0.00008	125
Chondrosarcoma	SW1353	NC	NC	-
	HT1080	0.01	0.00004	250
Ewing's sarcoma	TC71	0.1	0.1	1
Non-malignant cell type	**Cell line**	**Non-targeted TRAIL (IC50)(nM)**	**NG2 targeted TRAIL (IC50)(nM)**	**Fold change**
Stem cells	BMMSCs	0.009	2.04	0.004
Hepatocytes	HHL5	0.08	0.06	1
Ventricular cardiomyocytes	AC10	NC	NC	-
Fibroblasts	NHDF	4.97	NC	-

7.5 Combining doxorubicin with targeted forms of TRAIL on bone sarcoma cell lines

IncuCyte® live-cell analysis and cytotoxicity assays demonstrated that doxorubicin sensitised bone sarcoma cells to SuperKillerTRAIL (SKT) (Section 5.1). This was also observed when using NG2 targeted TRAIL, which had visible cytotoxic effects on the HT1080 dedifferentiated chondrosarcoma cell line, and these effects further increased when combined with doxorubicin (Figure 151).

NG2 expressing bone sarcoma cell lines were more susceptible than bone sarcoma cell lines with lower NG2 expression, when NG2 targeted TRAIL was used in combination with doxorubicin (Figure 152 to Figure 154). The resistant SW1353 cell line was sensitised when NG2 targeted TRAIL was used in combination with doxorubicin and this was to a greater extent than sensitive non-malignant cell lines (HHL5 hepatocyte cell line and AC10 ventricular cardiomyocyte cell line) (Section 7.5.1).

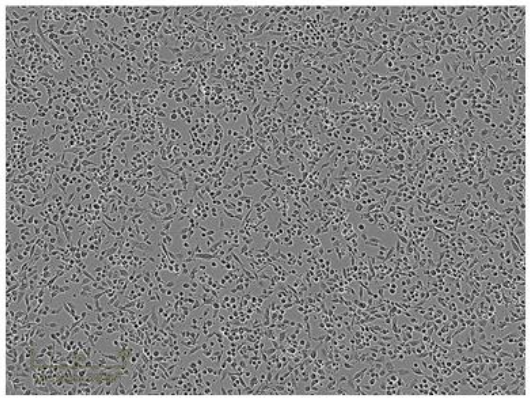

a Untreated HT1080 cells

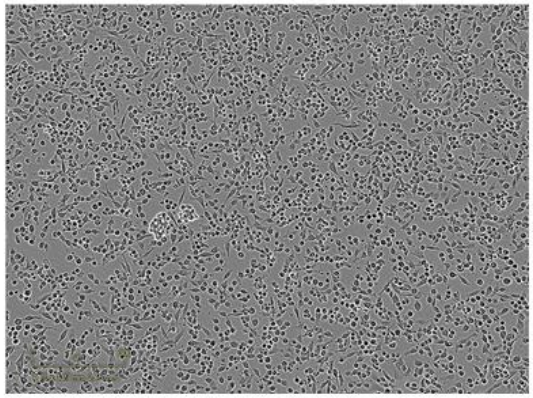

b 1.85uM Doxorubicin

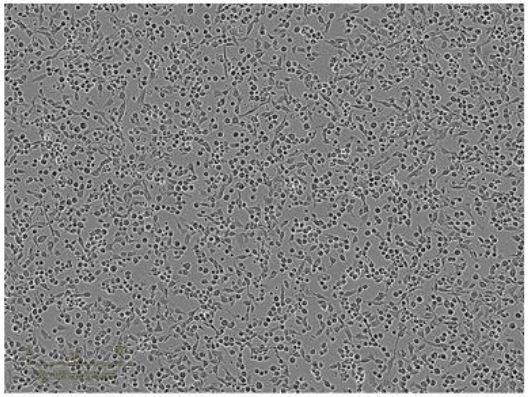

c 5.5uM Doxorubicin

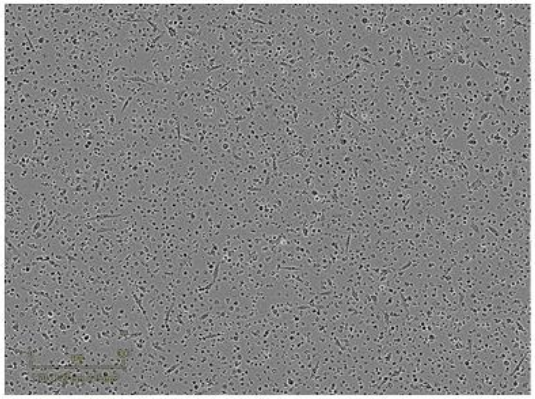

d 0.01nM NG2 TRAIL

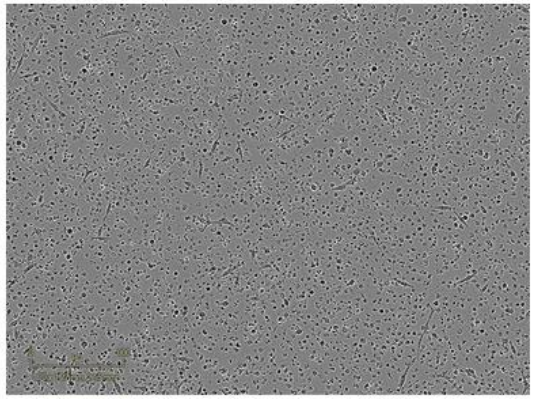

e 0.01nM NG2 TRAIL + 1.85uM Doxorubicin

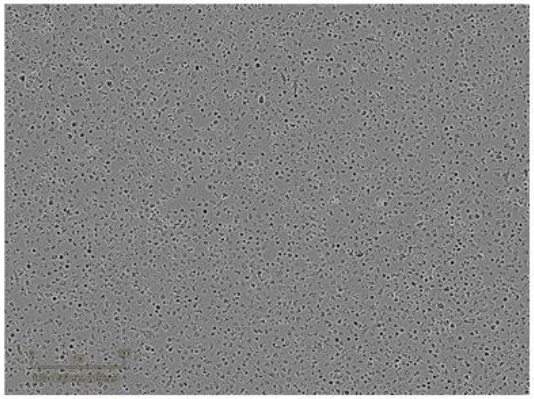

f 0.01nM NG2 TRAIL + 5.5uM Doxorubicin

Figure 151 – IncuCyte® live-cell analysis at 24 hours following treatment of HT1080 dedifferentiated chondrosarcoma cell line. (a) Untreated HT1080 cells. Targeted NG2 TRAIL (0.01 nM) has visible cytotoxic effect on majority of HT1080 cells (d) compared to doxorubicin alone at 1.85 µM and 5.5 µM (b and c); however, some remaining intact cells are visible. The remaining intact cells appear to decrease in number when increasing the concentration of the coadministered doxorubicin (e and f).

Low NG2

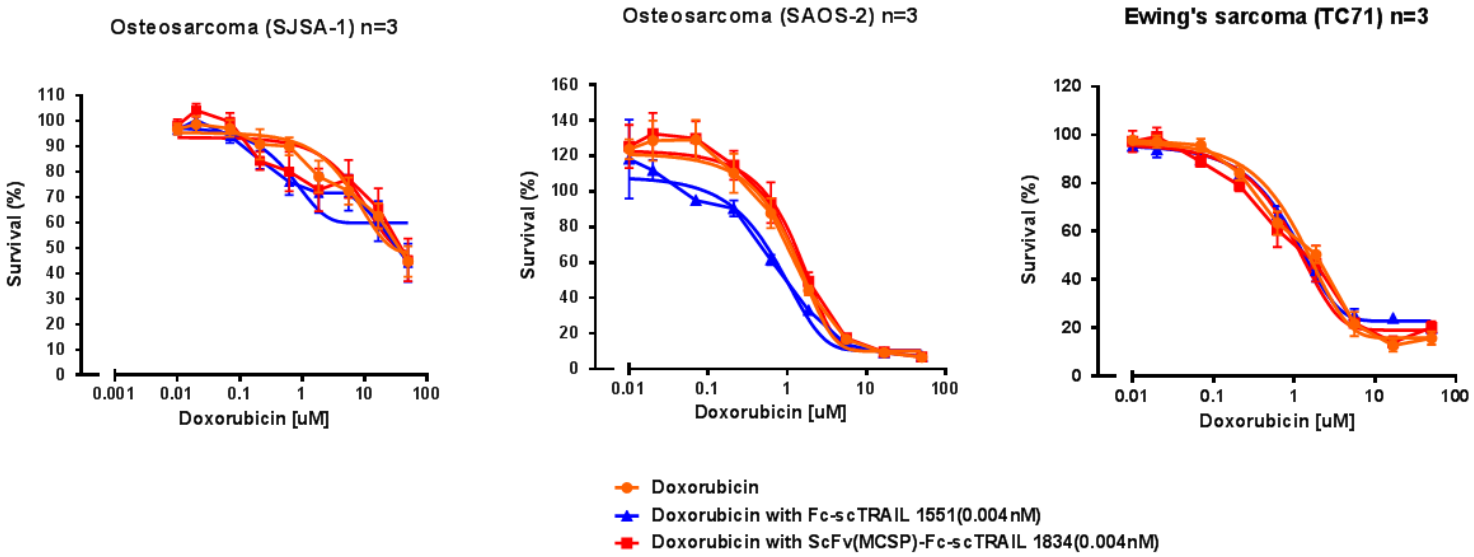

Figure 152– Low NG2 cell lines and response to targeted and non-targeted TRAIL. The SJSA-1 and SAOS-2 osteosarcoma cell lines are slightly sensitised to TRAIL with doxorubicin; however, NG2 targeted TRAIL has a similar effect to non-targeted TRAIL. This is also observed in the TC71 Ewing's sarcoma cell line.

Moderate NG2

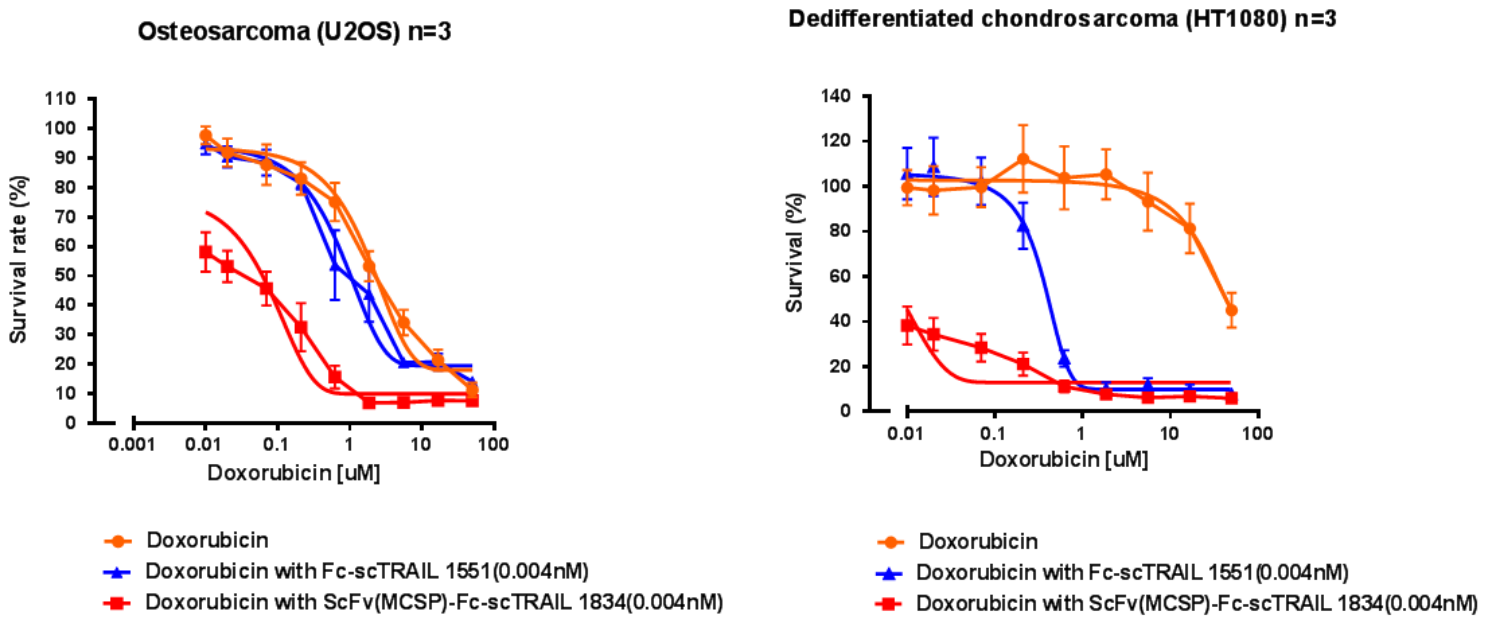

Figure 153 – Moderate NG2 cell lines and response to targeted and non-targeted TRAIL. The U2OS osteosarcoma and HT1080 dedifferentiated chondrosarcoma cell lines are sensitised to TRAIL with doxorubicin; and NG2 targeted TRAIL has greater effect compared to non-targeted TRAIL. A greater response is observed in the HT1080 cell line due to higher DR5 surface expression levels.

High NG2

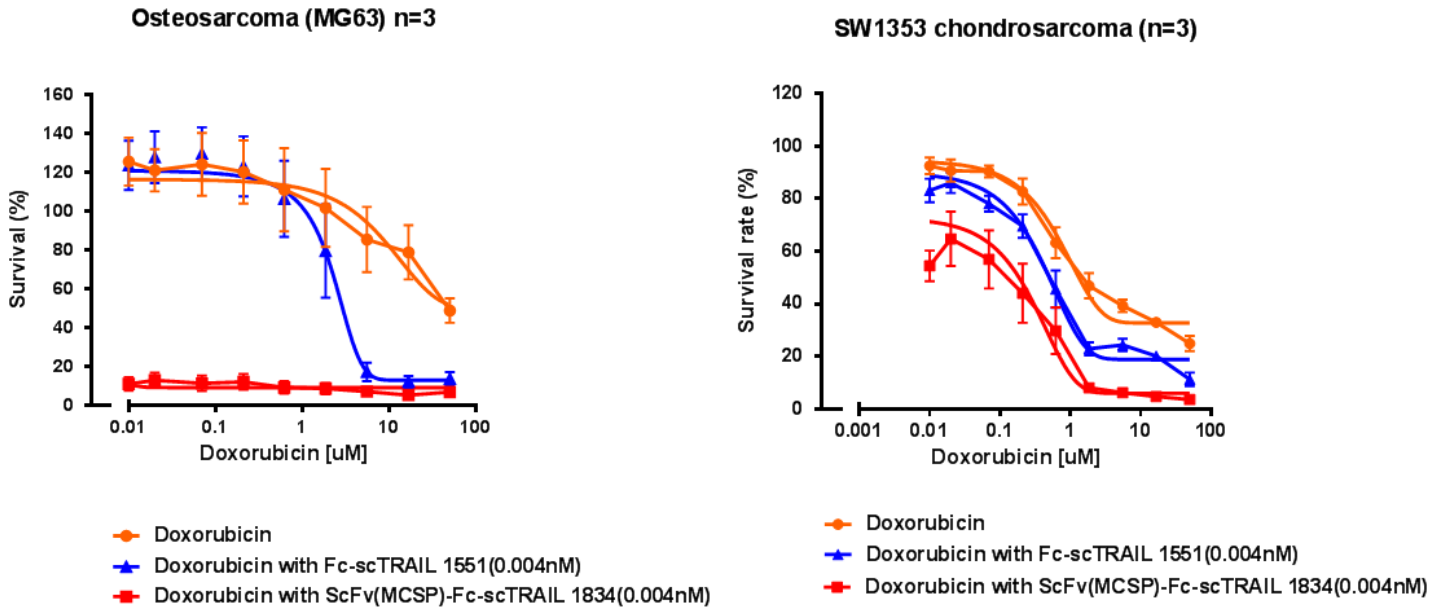

Figure 154 - Strong NG2 cell lines and response to targeted and non-targeted TRAIL The MG63 osteosarcoma and SW1353 chondrosarcoma cell lines are sensitised to TRAIL with doxorubicin; and NG2 targeted TRAIL has greater effect compared to non-targeted TRAIL. A greater response is observed in the HT1080 cell line due to higher DR5 surface expression levels.

7.5.1 Comparison of non-malignant TRAIL sensitive cells with bone sarcoma cell lines

The non-malignant cell lines were sensitive to the TRAIL and doxorubicin combination (greater when using NG2 targeted TRAIL) (Figure 155). However, the resistant SW1353 chondrosarcoma cell line, which was sensitised when NG2 targeted TRAIL was used in combination with doxorubicin and was sensitised to a greater extent than the non-malignant cell lines (HHL5 hepatocyte cell line and AC10 ventricular cardiomyocyte cell line are presented) (Figure 156) (Table 24).

Non-malignant cells

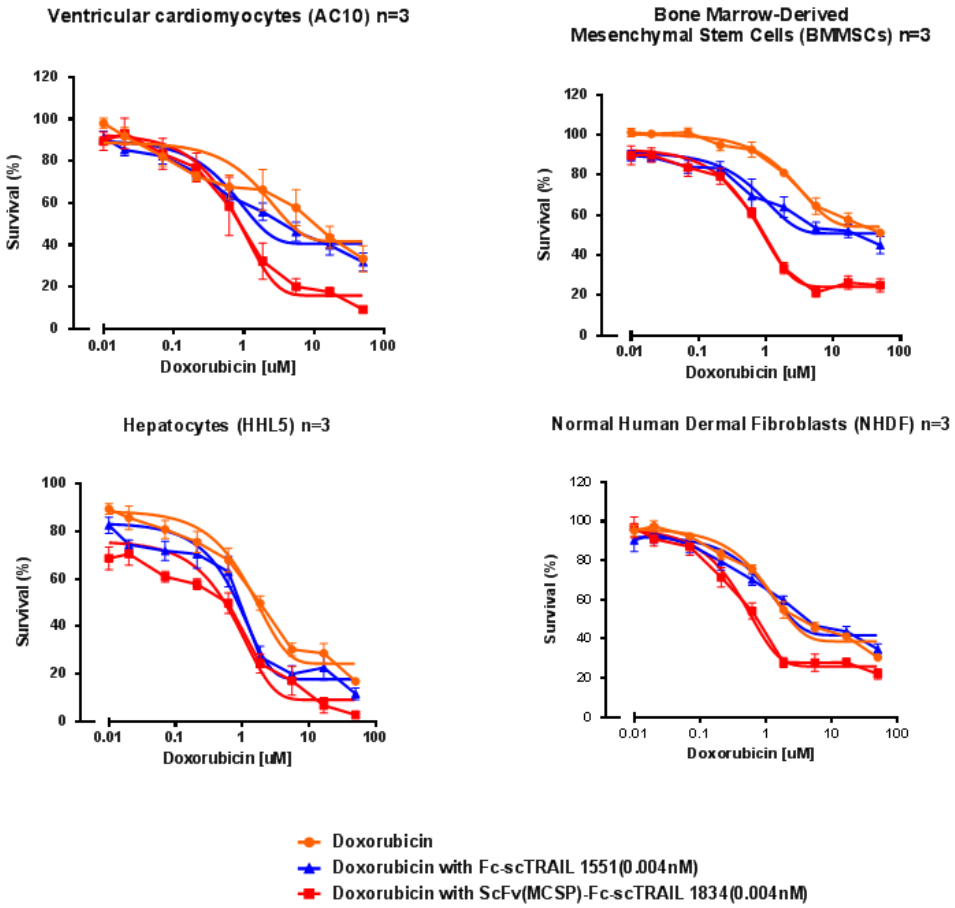

Figure 155 – Non-malignant cells were sensitive to the TRAIL and doxorubicin combination (greater when using NG2 targeted TRAIL).

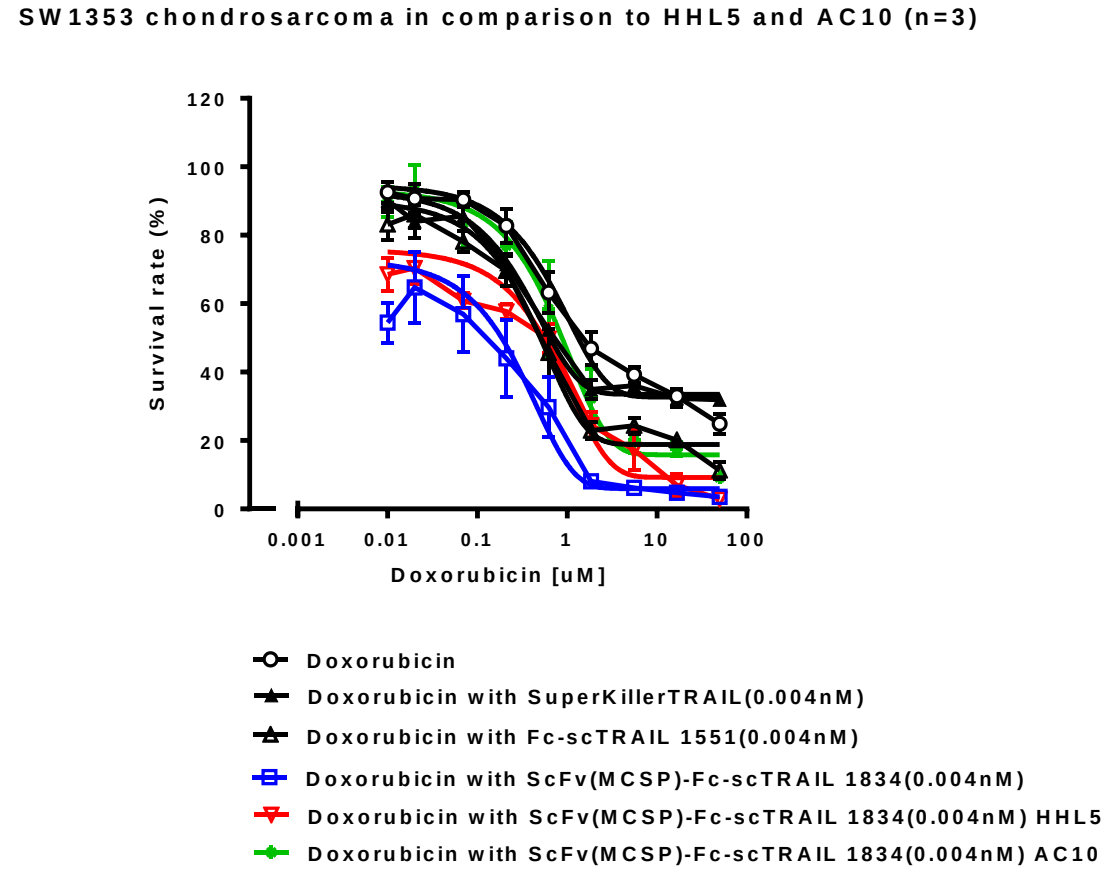

Figure 156 – The resistant SW1353 chondrosarcoma cell line (blue) was sensitised when NG2 targeted TRAIL was used in combination with doxorubicin and this was to a greater extent than sensitive non-malignant cell lines (HHL5 hepatocyte cell line (red) and AC10 ventricular cardiomyocyte cell line (green).

Table 24 - Summary table of IC50 values and fold change in all cell lines tested with NG2 targeted and non-targeted TRAIL in combination with doxorubicin. NC = Not Converged.

Sarcoma or type	Cell line	Doxorubicin (IC50)(µM) (1)	Non-targeted TRAIL (0.004 nM) + Doxorubicin (IC50)(µM) (2)	NG2 targeted TRAIL (0.004 nM) + Doxorubicin (IC50)(µM) (3)	IC50 Fold change (2)vs (3)
Osteosarcoma	SAOS-2	1.03	0.62	1.17	0.5
	U2OS	2.40	0.79	0.19	4
	SJSA-1	NC	NC	NC	-
	MG63	NC	2.07	1.11	2
Chondrosarcoma	SW1353	0.84	0.49	0.49	1
	HT1080	52.85	0.32	0.15	2
Ewing's sarcoma	TC71	1.13	0.96	0.82	1
Non-malignant cell					
Stem cells	BMMSCs	2.75	1.07	0.71	1.5
Hepatocytes	HHL5	1.64	1.01	1.23	0.8
Ventricular cardiomyocytes	AC10	NC	1.26	0.8	1.6
Fibroblasts	NHDF	1.21	1.24	0.4	3.1

Myxofibrosarcoma

Myxofibrosarcoma belongs to a group of malignant fibrous histiocytomas. It is an aggressive soft tissue sarcoma that exhibits high local recurrence and metastatic rates [315]. Our group obtained myxofibrosarcoma cell lines (*MUG-Myx2a* and *MUG-Myx2b*) generated and donated by Lohberger *et al.,* [316]. *MUG-Myx2a* is known to exhibit greater proliferation, migration and tumourigenicity [316]. Both cell lines were grown in DMEM supplemented with Gibco® Insulin-Transferrin-Selenium (ITS-G).

Flow cytometry revealed expression of surface DR5 in both cell lines (*MUG-Myx2b* > *MUG-Myx2a*) and high levels of surface NG2 expression (*MUG-Myx2a* > *MUG-Myx2b*) (Figure 157). Both cell lines showed limited response to NG2 targeted TRAIL alone (Figure 158); however, there was obvious sensitisation and greater response to NG2 targeted TRAIL with the addition of doxorubicin. *MUG-Myx2b* demonstrated greater doxorubicin sensitisation to targeted TRAIL to than *MUG-Myx2a* (Figure 159).

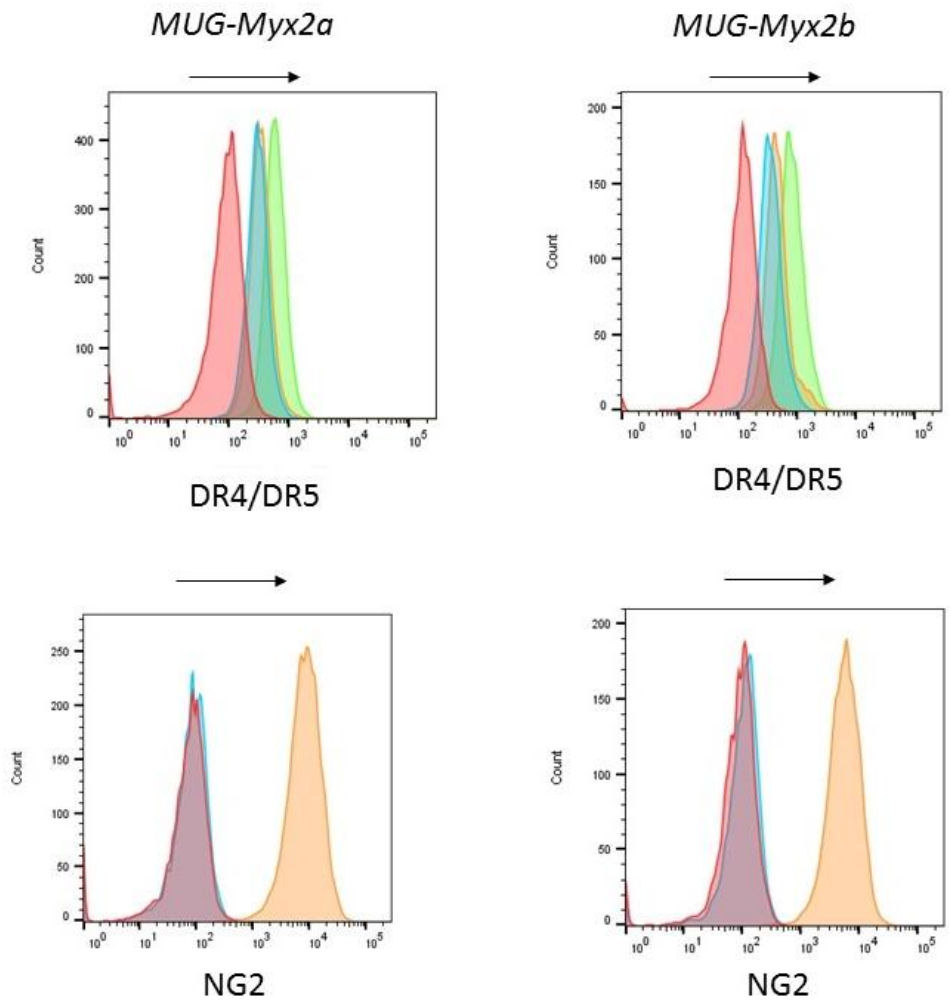

Figure 157 – DR5 and NG2 expression in myxofibrosarcoma cell lines (*MUG-Myx2a* and *MUG-Myx2b*). Red = unstained, blue = isotype control, orange = DR4 (histograms top row, NG2 (histograms bottom row, NG2 MFI = 7906 *MUG-Myx2a* vs 5221 *MUG-Myx2b*), green = DR5 (MFI = 275 *MUG-Myx2a* vs 420 *MUG-Myx2b*).

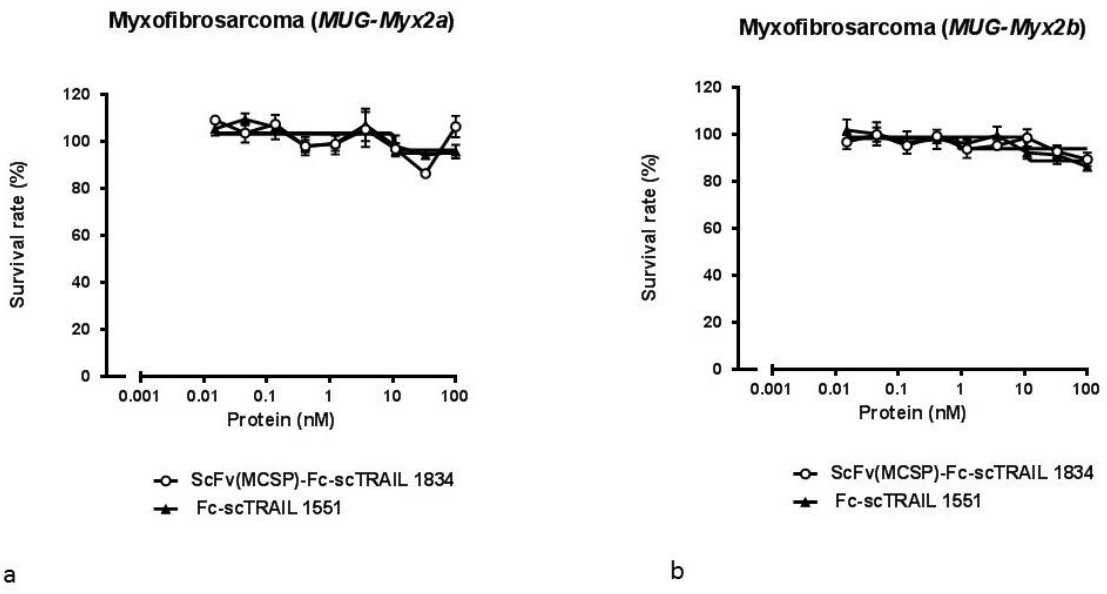

Figure 158 – Limited sensitivity of myxofibrosarcoma *MUG-Myx2a* (a) and *MUG-Myx2b* (b) cell lines to NG2 targeted TRAIL or non-targeted TRAIL.

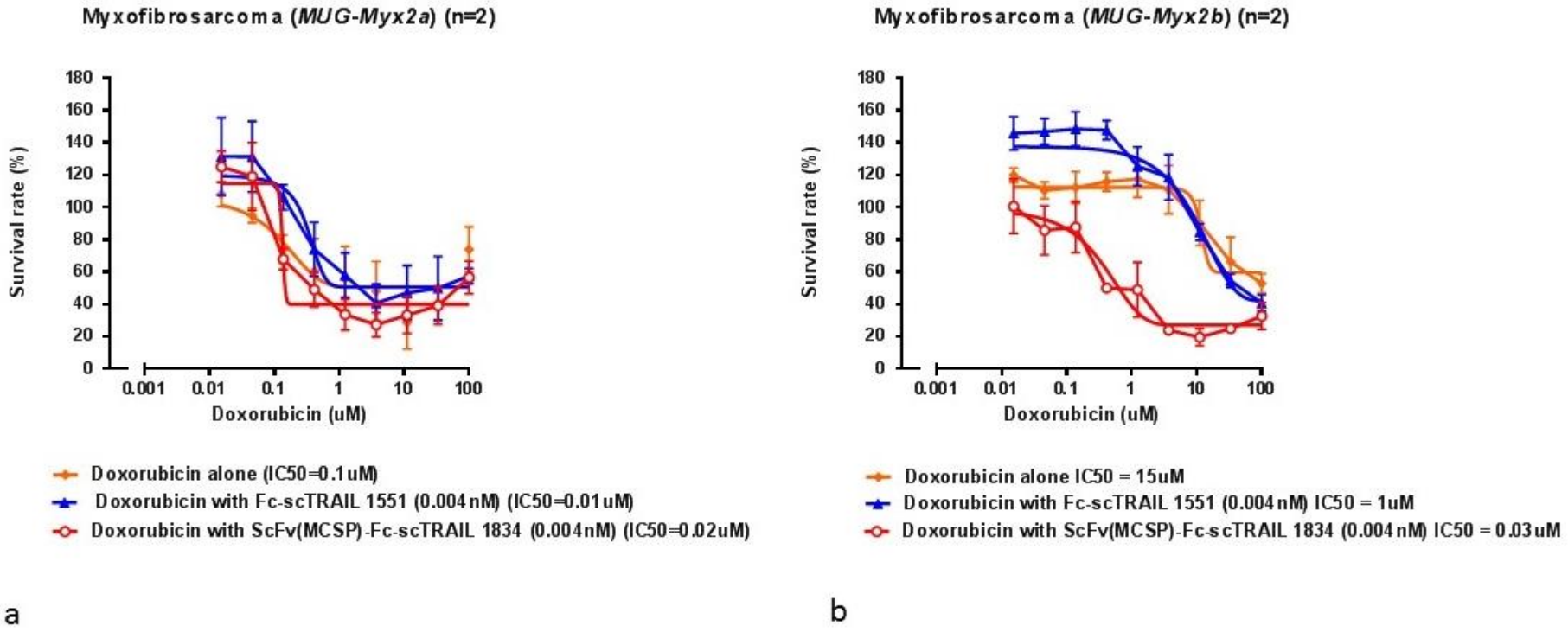

Figure 159 – Addition of doxorubicin sensitised the myxofibrosarcoma cell lines to TRAIL. There was a greater response to NG2 targeted TRAIL with the addition of doxorubicin. MUG-Myx2b demonstrated greater doxorubicin sensitisation to targeted TRAIL than MUG-Myx2a.

7.6 Use of novel sensitisers in combination with NG2 targeted TRAIL

Our collaborators Hutt *et al.,* tested novel sensitisers such as bortezomib (BZB), a proteasome inhibitor known to sensitise cells to TRAIL through upregulation of DR5 [317], and Smac mimetic (SM83) in combination with NG2 targeted TRAIL and found that the SW1353 chondrosarcoma cell line and U2OS osteosarcoma cell line could be sensitised with both agents. The SJSA-1 osteosarcoma cell line, however, remained resistant with SM83 in combination with TRAIL but could be sensitised with BZB; the targeted form did not have an enhanced effect, expected due to lack of NG2 expression in this cell line. Cells were treated for 24 hours and stained with crystal violet (Figure 160).

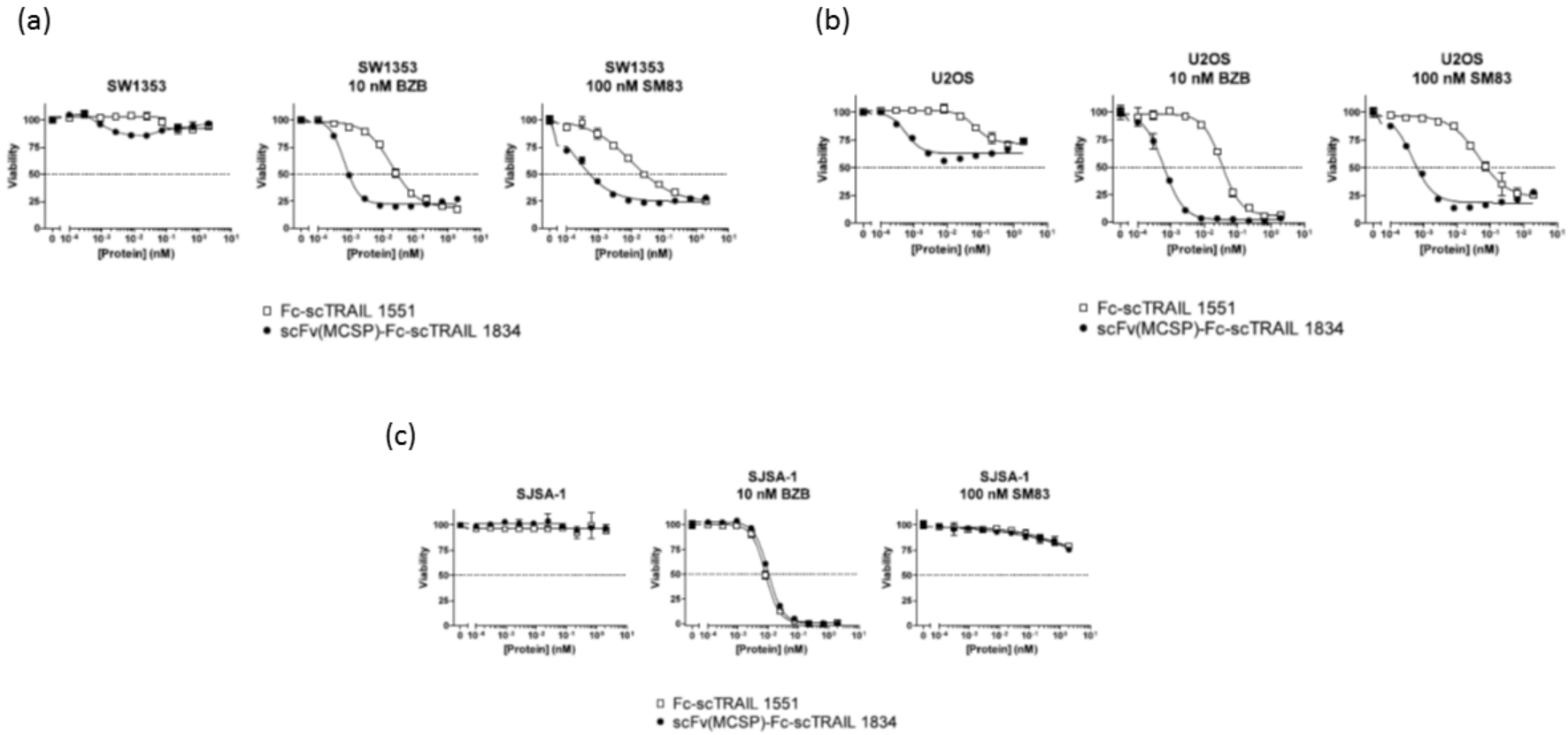
(a)
SW1353
SW1353
10 nM BZB
SW1353
100 nM SM83
Viability
[Protein] (nM)
Fc-scTRAIL 1551
scFv(MCSP)-Fc-scTRAIL 1834
(b)
U2OS
U2OS
10 nM BZB
U2OS
100 nM SM83
Viability
[Protein] (nM)
Fc-scTRAIL 1551
scFv(MCSP)-Fc-scTRAIL 1834
(c)
SJSA-1
SJSA-1
10 nM BZB
SJSA-1
100 nM SM83
Viability
[Protein] (nM)
Fc-scTRAIL 1551
scFv(MCSP)-Fc-scTRAIL 1834

Figure 160 – (a) SW1353 chondrosarcoma cell line is resistant to NG2 targeted scFv(MCSP)-Fc-scTRAIL 1834 and Fc-scTRAIL 1551; addition of 10 nM bortezomib/BZB or 100 nM Smac mimetic/SM83 sensitised the cells to both forms of TRAIL and to a greater extent the NG2 targeted form. (b) Sensitisation was also observed for the U2OS osteosarcoma cell line. (c) The SJSA-1 cell line was sensitised with the addition of BZB but no difference was observed between the targeted and non-targeted forms due to lack of NG2 expression (mean +/- SD, n = 1). Data courtesy of Hutt *et al*.

7.7 NG2 knockdown

Using siRNA, NG2 was knocked down in the SW1353 chondrosarcoma cell line (up to 72 %) and the U2OS osteosarcoma cell line (up to 58 %) at 72 hours (Figure 161). The proliferative rate was investigated in the U2OS cell line and decreased after knockdown when compared to scrambled treated cells (Figure 162a and b).

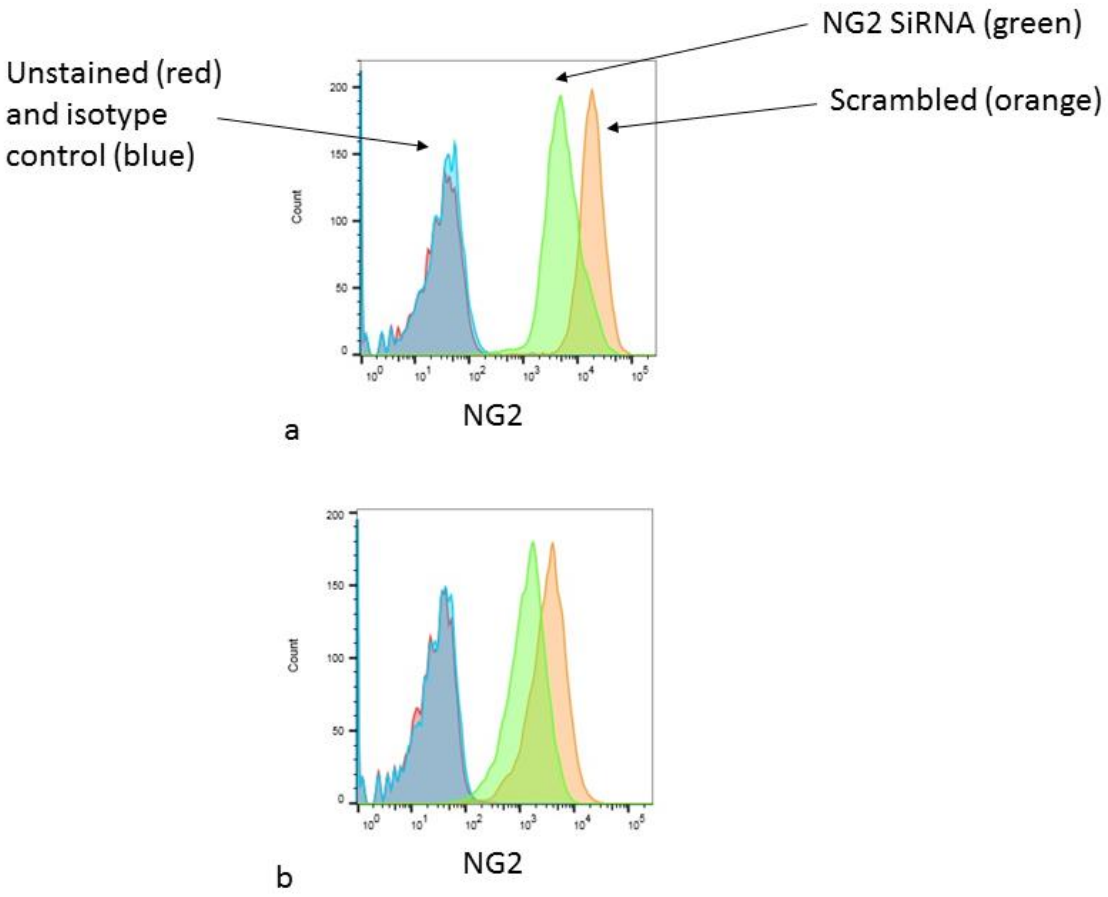

Figure 161 – NG2 knockdown (KD) using siRNA. 72 % NG2 KD achieved in SW1353 cell line (a) and 58 % KD in U2OS cell line (b).

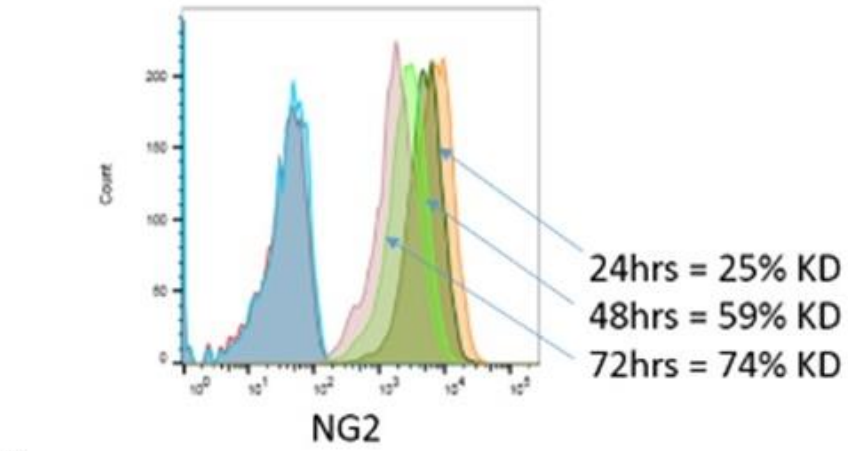

a

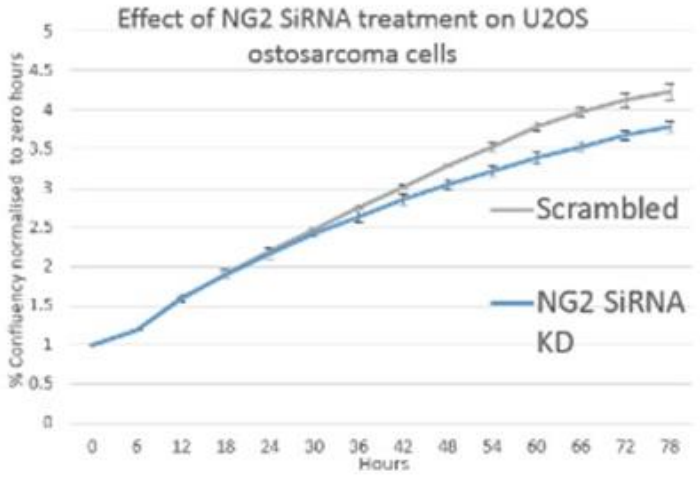

b

Figure 162 – (a) Up to 74 % NG2 knockdown could be achieved in U2OS osteosarcoma cell line at 72 hours. (b) IncuCyte® live-cell analysis monitoring revealed decreasing proliferation and confluency compared to scramble siRNA treated U2OS cells in time period measured.

7.8 Discussion and future direction

NG2/CSPG4/MCSP

Neuron glial antigen 2 (NG2), is also known as chondroitin sulphate proteoglycan 4, (CSPG4) or melanoma-associated chondroitin sulfate proteoglycan (MCSP). This protein is of interest because it is involved in pathological processes such as angiogenesis in many cancer types. For example, breast cancer, melanoma, squamous cell carcinoma and paediatric and adult sarcomas. NG2 has a role in the growth and survival, as well as, spreading and metastases of tumour cells. It is also thought to be restricted and have low expression in normal tissues. Immunohistochemistry has demonstrated that in the human tissues, fetal and adults, the distribution of NG2 is in the adrenal cortex, liver, small intestine, and also in the stem cell population. At the RNA level, it has been reported to be present in skin, lung, heart, muscle, but more importantly, it's at 6.6 times lower levels than found in tumours. This physiological function is not completely understood, but reports suggest specific roles in different tissues throughout development.

For my project, I was particularly interested in NG2 as it is expressed in soft tissue and bone sarcomas. NG2 expression is known to be increased in soft tissue sarcoma such as liposarcoma and synovial sarcoma and in chondrosarcoma [147,318] and is associated with increased invasion and metastases [318]. It was also shown to be expressed using immunohistochemistry in liposarcoma, leiomyosarcoma, fibrosarcoma, and MFH-like pleomorphic sarcoma. In a study carried out by Benassi *et al.,* 2009, they correlated the survival and metastases of the patients that had tissues stained for NG2, and they found that when enhanced NG2 expression in primary lesions was compared in a multivariate analysis, it emerged that the upregulation was independent prognostic parameter capable of defining an increased risk for a post-surgical metastatic event by 55 % [318].

Previous studies investigating the functional role of NG2, or CSPG4, in chondrosarcoma, and certain chondrosarcoma cell lines have been found to have high NG2 expression, such as the chondrosarcoma cell line JJ012 cell line. I have also found that the SW1353 cell line has high levels of NG2 expression. The SW1353 chondrosarcoma cell line has high levels of NG2 surface expression. In the study by

Jamil *et al.,* (2016) they performed a knockdown of NG2 and tried to gain more information about cell adhesion spreading and migration. They demonstrated that knockdown is associated with a decrease in sub-perforation and migration, while spreading on extra-cellular matrices increased. The knockdown of NG2 is also associated with change in expression of MMP3, MMP13 and ADAMT, ADAMTS4. They also discussed that NG2 is expressed by chondrocytes during cartilaginous bond formation in articular cartilage and by chondrosarcomas [147].

There has been interest in the expression of NG2 in soft tissue sarcomas. There was a detailed study carried out by Cattaruzza *et al.,* (2013), who investigated expression of NG2 in a number of different sarcoma cell lines [319]. The high expression was found in another SW872, which is a liposarcoma cell line, and also SKLMS1, which is a leiomyosarcoma cell line. They also found that the MG63 had high surface NG2 expression levels with flow cytometry, which is consistent with the findings found in this project. They also managed to engraft the MG63 and HT1080 cell lines in a mouse model. They demonstrated that NG2 positive HT1080, NT-LMS-1 and NT1-LMS-1 cell lines have greater engraftment levels and tumour volume compared to NG2 negative counterparts. The authors were particularly interested in direct NG2-collagen VI interaction because it was thought to have 'an important role in primary and secondary lesions local propagation, which is controlled by this interaction'. It was indeed found that cell adhesion to collagen VI decreased when NG2 siRNA was used to knockdown NG2 in the NG2 positive cell lines. This was significant for collagen VI however for collagen I, there was no significance between knockdown cells and non-knockdown cells [319].

NG2 may promote chemoresistance by activation of endocrine-dependent PI3K/AKT signalling described by Chekenya *et al.,*(2008). Interestingly, comparison of tumours revealed high levels of phospho-AKT in the NG2/MGP expressing tumours indicative of increased PI3K/AKT signalling [256]. They looked at the effect of TNF-alpha on U87 human primary glioblastoma tumours transfected with control or NG2 shRNAs and they demonstrate a protective effect on NG2 against TNF-alpha induced apoptosis. Comparison of these tumours reveal high levels of phospho-AKT in support of *in vitro* data. Downregulation of NG2 in the same cell line, U87, lead to marked reduction in tumour growth rates even in absence of TNF-alpha. This is likely due to the role of NG2

in functions unrelated to apoptosis. For example, NG2 promotes proliferation as a result of its participation in growth factor signalling. Also, NG2 is known to stimulate angiogenesis by sequestering angiostatin and affecting its inhibitory effects on neutralising its inhibitory effects on angiogenesis. U87 is a glioblastoma cell line, which was included in my PCR analysis of NG2 and not found to express NG2 to the same degree as some of the bone sarcoma cell lines such as the MG63 osteosarcoma and SW1353 chondrosarcoma cell lines.

Targeting NG2 has been carried out to try to inhibit tumour growth. A study carried out by Claire Hsu *et al.,* 2018, engrafted human undifferentiated pleomorphic sarcoma into NSG mice (xenografts) and were treated with 50 µg/ml per mouse of anti-NG2 antibody mAb 9.2.7 [Abcam] or isotype control IgG every other day for two weeks. This significantly reduced the average tumour volume as compared with the IgG controls and no signs of toxicity were detected [320]. The data suggested that NG2 CSPG4 monoclonal antibody-based immunotherapy could be developed as an approach for treatment of NG2 expressing soft tissue sarcomas. The antiviral knockdown of NG2 in the established human tumour xenografts delayed engraftment.

NG2 is expressed in precursor cells such as stem cells, which could play a role in regulating stem cell line properties and driving the oncogenic mutations in those cells and result in sarcoma formation. In summary, the NG2 immunotherapy decreased cell proliferation and increased apoptosis.

The study also explored how cells adapt to loss of NG2 in tumour initiation compared to loss of NG2 after the tumour is already formed. They found that deleting NG2 at the time of tumour initiation resulted in an opposite and increased effect on tumour growth. Activation of IGF signalling occurred as a result of NG2 deletion at initiation of the tumour. Insulin-like growth factor proteins are known to inhibit IGF signalling and regulate proliferation, and there was no loss of their normal regulation [320].

NG2 targeted delivery of DR5 agonists or TRAIL

Targeted forms of DR5 agonists/TRAIL have been developed with the aims of increasing local concentrations of TRAIL and reducing toxic effects to normal cells. There has been an interest in dual antibody therapy using anti-MCSP, which is anti-

NG2 TRAIL. Upon binding to MCSP positive melanoma cells and accumulation at the cell surface, results in inhibition of MCSP tumourigenic signalling and at the same time activate apoptotic TRAIL signalling [311,314,321]. A study carried out by Bruyn *et al.,* (2010) found that this mode of therapy can potently inhibit melanoma outgrowth *in vitro* and *in vivo*. The antibody was again a monoclonal antibody 9.2.7 [311]. Activation of apoptosis occurred in a dose-dependent manner (within 16 hours) upon anti-MCSP:TRAIL treatment of MCSP transfected M14 melanoma cells. Upon anti-MCP:TRAIL treatment, parental MCSP negative M14 cells were shown to be resistant. The advantage of targeting the TRAIL therapy is high levels of tumour cell surface bound TRAIL to activate apoptotic signalling via the TRAIL receptors DR4 and DR5 in a mono- and/or bi-multicellular manner.

Soluble TRAIL has no selective tumour binding and is considered not to be as effective at cross-linking and subsequent activation of DR5. DR5 is best activated by crosslinked forms of TRAIL. An *in vivo* study xenografted subcutaneously A375M melanoma cells in nude mice and allowed to form small tumours, approximately 50 mm^3. A low dose of ~0.14 mg/kg of anti-MCSP TRAIL was administered by an intraperitoneal injection daily. The mice treated with this fusion protein had 50 % reduction in tumour size at the end of experiment compared to the sham treated mice [311]. It is reported here that the anti-MCSP TRAIL does not cross react with mouse MCSP, this is anti-MCSP mAb 9.2.7, which has also been used as part of this PhD.

Of note, earlier animal studies utilising xenografts models with A375M and non-targeted recombinant human TRAIL required 300 times higher concentrations, 50 mg/kg for cell death, compared to more recent studies using targeted MCSP therapy [311]. Targeted therapy, thereby, enables low dose required for therapeutic activity and has potent *in vivo* anti-melanotic activity at a very low dose. Another benefit reported is that this fusion protein lacks apoptotic activity towards normal cells. No apoptosis was induced in melanocytes despite the treatment performed with 4 µg/ml of the anti-MCSP TRAIL. This was also extended up to 8 days and when comparing with the medium control, this did not result in a significant increase in apoptosis. Similarly, reported here, when treated with anti-MCSP TRAIL, MCSP negative hepatocytes were found to be resistant. The effects of TRAIL related toxicity have been shown with hepatocytes which are a highly susceptible normal cell type.

There was no deleterious effects on liver morphology, and morphology of the liver in the mice was comparable to the morphology of the liver sections of some treated mice [311]. To date, there are no serious adverse effects and no dose-limiting toxicity with regards to TRAIL therapy. Indeed, safety has been confirmed from ongoing clinical trials of recombinant TRAIL.

In data obtained as part of this project, I have found that the HHL5 hepatocyte cell line lacks NG2 surface expression, but does express DR5. Previous studies (described above) have utilised primary human hepatocytes and melanocytes and not found significant toxicity when using MCSP targeted TRAIL forms. I have found sensitivity of the HLL5 cell line to crosslinked forms of TRAIL and has been one of the most sensitive cell lines to this type of therapy. However, this may be due to a P53 aberration. The use of NG2 to target delivery of human proteins has been reviewed extensively recently by Jordan *et al.,* 2017. There has been an advancement in the creation of fusion proteins such as development of stable trimeric ScFv:scTRAIL such as alpha-MCSP:sTRAIL which contains three identical tumour targeting ScFv domains. The presence of a net surplus of soluble TRAIL domains allows agonistic TRAIL receptors to be subsequently activated on even neighbouring tumour cells. This is known as a by-stander effect which has the potential to also eliminate neighbouring tumour cells that lack the target antigen expression thus amplifying the effect [314].

It is also been of interest as to why NG2 is over-expressed and this has been associated with hypomethylation of CPG islands in the promoter region whilst others have postulated chromosomal translocations at 11Q23 encoding a transcription factor that regulates NG2 transcription that may result in NG2 over-expression. I have also found consistent with previous studies that in the A375M melanoma cell line there are high levels of NG2 expression.

Overall summary and future direction

In our bone sarcoma cell lines, we have found the SW1353 chondrosarcoma cell line and the MG63 osteosarcoma cell line to express the highest levels of NG2. The HT1080 dedifferentiated chondrosarcoma cell line expresses moderate levels of NG2 and also the U2OS osteosarcoma cell line. I have found no NG2 expression in the SJSA-1 and

SAOS2 osteosarcoma cell lines and the TC71 Ewing's sarcoma cell line. I have found that all of these bone sarcoma cell lines express DR5 and in the TC71 also DR4.

As a further development, on the theme of the human cytolytic fusion proteins, the inclusion of an Fc comprising single chain TRAIL fusion protein has been found to have more enhanced effects and this has been engineered to target tumour associated antigens such as the epidermal growth factor receptor, EGFR. In a study by Hutt et al., (2017), they demonstrated superior *in vitro* activity of EGFR targeted dimeric single chain TRAIL fusion proteins compared to single chain TRAIL alone and dimeric non-targeted formats; their *in vivo* studies demonstrated improved half-life and higher efficacy of the hexavalent single chain TRAIL fusion protein comprising an Fc portion [188].

Depending on the tumour studied, the non-targeted Fc ScTRAIL fusion protein may also induce equally effective complete tumour regressions as their targeted counterparts. I have developed this fusion protein to target NG2 in light of the findings. The hexavalent molecule is ideal for this as most of the bone sarcoma cell lines express a DR5, which requires higher order clustering for potent activation of apoptotic signalling. This can be achieved by using higher order hexavalent TRAIL fusion proteins with those based on the Fc region as a dimerisation module. Sensitising agents can also be employed in combination, such as those utilised by Hutt *et al.,* (2018) who found sensitisation when using bortezomib [188] and those described in Chapter 6.

Chapter 8. *In vivo* testing of NG2 targeted TRAIL construct

8.1 NG2 targeted TRAIL with or without doxorubicin

8.1.1 Toxicity pilot study

In vitro, synergistic effects were observed when NG2 targeted TRAIL was administered alongside doxorubicin. Doxorubicin has been formulated in PBS and used in sex-matched 7–8 week-old NSG mice without significant toxicity, when administered intravenously once weekly at 2 mg/kg in a previous study [322].

My aim was to assess for toxicity when NG2 targeted TRAIL was administered alongside doxorubicin, in a toxicity study, which I undertook for one month (schedule below in Figure 163). I did not find significant weight loss or toxic effects from the combined therapy and the signal from the engrafted tumour did not reach the levels found by four weeks in the untreated mice in the engraftment study described in Section 2.10. Results are presented in Section 8.1.1.1.

Day 0 – Cell transplant
Day 4 – IVIS
Day 7 – IVIS and treatment (NG2 TRAIL + Doxorubicin)
Day 12 – Treatment (NG2 TRAIL only)
Day 15 – IVIS and treatment (NG2 TRAIL + Doxorubicin)
Day 19 – Treatment (NG2 TRAIL only)
Day 22 – IVIS and treatment (NG2 TRAIL + Doxorubicin)
Day 26 – Treatment (NG2 TRAIL only)
Day 30 – IVIS

Figure 163 – Treatment and imaging schedule for toxicity study utilising three NSG mice engrafted with HT1080 pSLIEW cells into the femur.

8.1.1.1 Pilot study results

Rapid tumour growth was observed using IVIS from day 5 to day 7 after implantation of HT1080 pSLIEW cells into the femur in NSG mice. Day 15 after implantation (and day 8 following commencement of therapy), there was a noticeable decrease in the signal on IVIS after treatment with the schedule described in Figure 163. All mice survived to the end of the study without significant toxicity issues and in comparison with data

from the engraftment study (Section 2.10), had significantly less IVIS signal [total Flux (p/s)] in the right femur at the engraftment site.

Mice survived for about a further three weeks following cessation of therapy. A working model was established and the doxorubicin and NG2 targeted TRAIL combination demonstrated effectiveness and no significant toxicity (Figure 164).

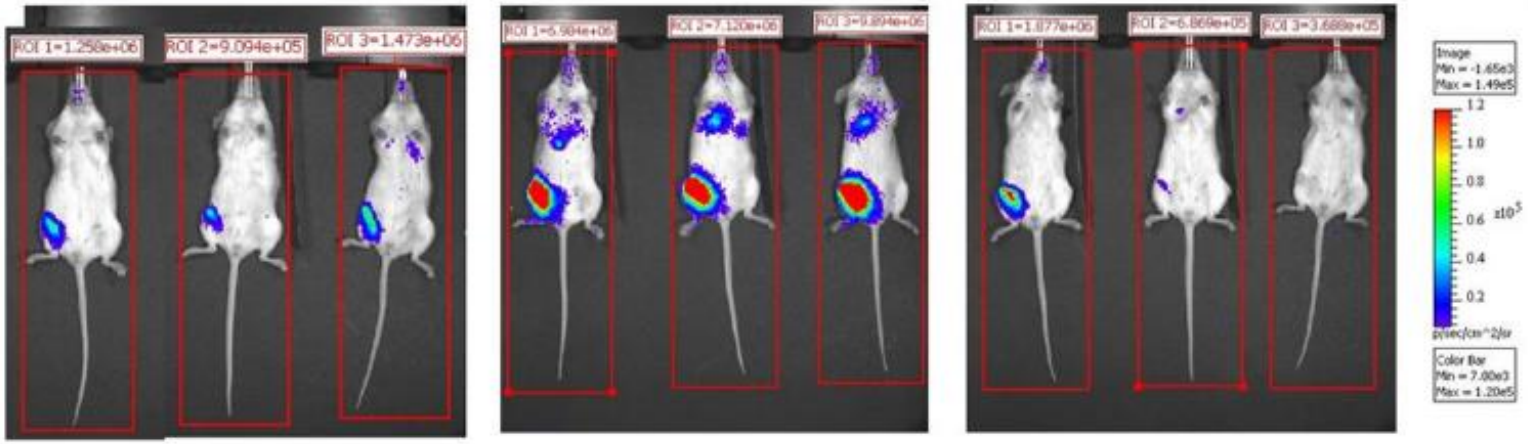

26/11/18
Day 5 after implantation

28/11/18
Day 7 after implantation

05/12/18
Day 15 after implantation and day 8 following commencement of therapy

Day 0 – cell transplant (21st)
Day 4 – IVIS (26th)
Day 7 – IVIS and treatment (NG2 TRAIL + Doxorubicin) (28th)
Day 12 – treatment (NG2 TRAIL only) (3rdDec)
Day 15 – IVIS (5th) and treatment (NG2 TRAIL + Doxorubicin) (6th)
Day 19 – treatment (NG2 TRAIL only) (10th)
Day 22 – IVIS (11th) and treatment (NG2 TRAIL + Doxorubicin) (13th)
Day 26 – treatment (NG2 TRAIL only) (17th)
Day 30 – cessation of therapy (21st)

Figure 164 – Pilot study investigating the engraftment of HT1080 Luc +ve cells in NSG mice and treatment with combined doxorubicin and NG2 targeted TRAIL therapy. Rapid tumour growth was observed using IVIS when day 5 after implantation was compared to day 7 after implantation. Day 15 after implantation and day 8 following commencement of therapy, there was a noticeable decrease. Mice survived for about a further three weeks following cessation of therapy. With this, a working model was established and the doxorubicin and NG2 targeted TRAIL combination demonstrated effectiveness and no significant toxicity.

8.1.2 Formal in vivo study

The main aim was to inject 0.2 nmol of TRAIL construct with or without doxorubicin and compare this to the control vehicle treated mice (summarised in Table 25). Results are presented in Section 8.1.2.1:

Statistical analysis plan

A power calculation has been made based on the reduction in size of the tumours in the mice treated with the NG2 targeted TRAIL. Using IVIS flux data from a pilot study of 3 mice, a 50 % reduction in IVIS signal compared to controls allowed for a minimum for 6 mice per treatment arm to power the study at a level greater than 90 %.

Group 1 (6 mice) - Doxorubicin alone (2 mg/kg) once a week

Group 2 (6 mice) – 42.1 µl #1834 NG2 targeted TRAIL (scFvNG2(9.2.27)-IgG1Fc-scTRAIL)

Group 3 (6 mice) – Doxorubicin 2 mg/kg once a week in combination with 42.1 µl #1834 NG2 targeted TRAIL (scFvNG2(9.2.27)-IgG1Fc-scTRAIL)

Control group 4 – (3 mice) - PBS only at largest volume used for mouse 1, 2 or 3.

Group 5 – (3 mice) – 23 µl of #1551 Non-targeted TRAIL

Treatment schedule -

Six injections of NG2 targeted TRAIL (2 injections/week for 3 weeks) and 3 injections of Doxorubicin at 2 mg/kg (1 injection per week). 6 injections of non-targeted TRAIL. PBS for control mice.

Mice with inadequate signal (too high or too low defined approx. outside of total flux (p/s - 2e6 to 2e7) at week 1, were treated with doxorubicin and NG2-targeted TRAIL and they were used for blood studies and immunohistochemistry (IHC) at 3 time points (to undergo schedule 1): 1 day, 3 days and 7 days (up to an additional 9 mice).

In this respect, immunohistochemistry (IHC) on paraffin embedded mice sections will be performed in future. I will assess for markers of cell death e.g., active caspase-3, cleaved

PARP or TUNEL staining as described in previous studies [323,324] and will compare these to control, i.e. PBS treated mice. Tumour cells will be detected by staining for MT1-MMP.

To assess the presence of targeted TRAIL at the tumour side, I will also attempt to detect NG2-targeted TRAIL the sections using anti-Flag antibodies (M2 clone) as used in previous studies [325] or anti-human IgG antibodies.

Table 25 - Experimental plan to assess the effect of targeted and non-targeted forms of TRAIL with and without doxorubicin on tumour volume of mice.

Cell line	**Randomisation**				**Minimum number of mice**
HT1080 pSLIEW (dedifferentiated chondrosarcoma)	Doxorubicin alone n = 6	NG2 targeted TRAIL (one group with and one group without doxorubicin) n = 12	Non-targeted TRAIL n = 3	PBS n = 3	24

8.1.2.1 Formal study results

NSG mice treated with non-targeted TRAIL or NG2 targeted TRAIL (with or without doxorubicin) showed much reduced signal intensity, after therapy when compared to control NSG mice and NSG mice treated with doxorubicin alone ($p<0.05$ at day 27; two-way ANOVA). CT reconstruction images demonstrated early evidence of bone destruction in the control group compared to those treated with the doxorubicin and NG2 targeted TRAIL therapy combination (Figure 165). Table of complete dataset and outcome metrics is presented in Appendix 11.8.

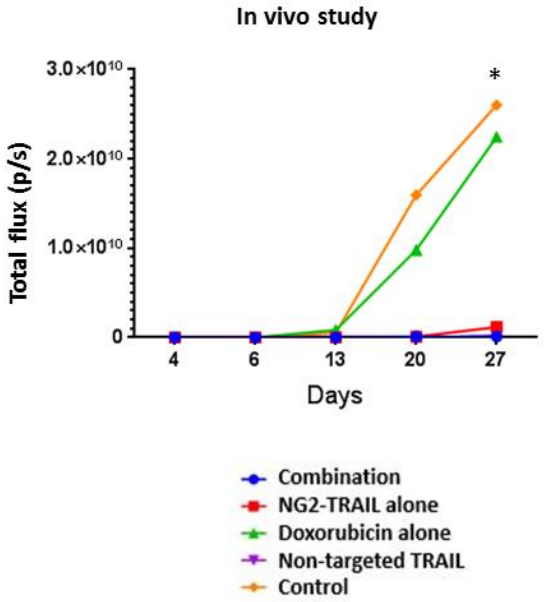

*= $p<0.05$ using Two-way ANOVA analysis between control and groups containing TRAIL

a

Control

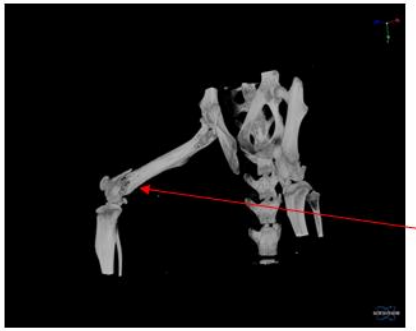

b

Fracture

NG2-TRAIL + Doxorubicin

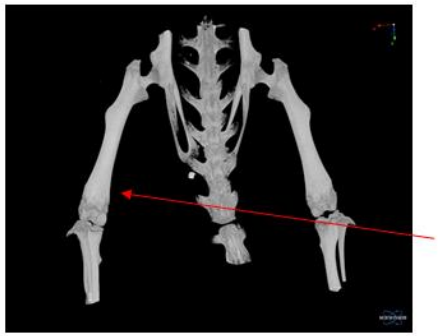

c

No evidence of fracture

Figure 165 – Randomised study comparing group 1 (6 mice) - Doxorubicin alone (2 mg/kg) once a week; Group 2 (6 mice) –NG2 targeted TRAIL (scFvNG2(9.2.27)-IgG1Fc-scTRAIL); Group 3 (6 mice) – Doxorubicin 2 mg/kg once a week in combination with NG2 targeted TRAIL (scFvNG2(9.2.27)-IgG1Fc-scTRAIL); Control group 4 – (3 mice) - PBS treated; Group 5 – (3 mice) - Non-targeted TRAIL. (a) NSG mice treated with non-targeted TRAIL or NG2 targeted TRAIL (with or without doxorubicin) showed much reduced intensity of signal, after therapy when compared to control NSG mice and NSG mice treated with doxorubicin alone ($p<0.05$ at day 27; two-way ANOVA). CT reconstruction images demonstrated early evidence of bone destruction in the control group (b) compared to those treated with the doxorubicin and NG2 targeted TRAIL therapy combination (c).

8.2 Discussion and future direction

In summary, I have produced an *in vivo* mouse orthotopic model of dedifferentiated chondrosarcoma. This has been achieved by intrafemoral engraftment of the HT1080 dedifferentiated chondrosarcoma cell line in NSG mice, using 5000 HT1080 luciferase positive cells. The latency of engraftment was about a week, and then there was a rapid proliferation and increasing signal in intensity on IVIS with metastases visible around week 2 to 3 and disseminated tumour around week 4. The humane end point was undergoing of schedule one killing if there were any signs of ill health or significant weight loss in the mouse. I observed in the pilot studies that there was a significant mass on examination of the NSG mice and significant IVIS signal intensity and metastases and bone destruction on CT scan reconstruction images by about 5 weeks, compared to the non-engrafted femur and this could be reduced by using the TRAIL construct with or without doxorubicin.

A recent review by Jacques *et al.,* (2018) has summarised current mouse models of bone sarcoma and the majority have been undertaken in hydrotropic sites by subcutaneous cell injections and also incorporating into a matrigel based matrix, to provide a scaffold and aid engraftment [326]. The other modes of implantation include the deep non-osseous environment, such as deep heterotopic sites, inoculated in the renal capsule, which has been achieved for the Ewing's sarcoma TC71 cell line and the human JJ012 chondrosarcoma cells. The other sites include paraosseous cell injections, such as in close proximity to the tibia [326].

I have undertaken the interosseous mode of injection, and among the currently available methods to generate models of bone sarcomas, the interosseous models are technically most difficult to achieve, and the operator needs to be specifically trained. However, I feel this best recapitulates the human disease. The strengths in my study is that in our institute, there are personnel that have been trained in this procedure and we have been able to achieve reproducible models.

Cell lines injected via the intraosseous route currently in the literature include osteosarcoma cells K7M2L2 with matrigel [325]. The model that I have undertaken using the HT1080 dedifferentiated chondrosarcoma cell line has not been reported

before, and rapid engraftment was observed without need for a matrix-based gel. I undertook a pilot study using doxorubicin and the NG2 targeted form of TRAIL, and I found that there was reduction in the cell signal day 15 after implantation and day 8 following the commencement of the therapy. The mice survived a further 3 weeks following the cessation of therapy, and there was no significant toxicity evident from the combination of the therapy. Following this, I undertook a formal study, and I randomised the mice to either doxorubicin alone, NG2 targeted TRAIL alone, a combination of doxorubicin and NG2 targeted trial, control, and non-targeted TRAIL, and the main finding was that arms utilising the NG2 targeted TRAIL and non-targeted TRAIL showed much reduced intensity of signal, after therapy.

It has been debated in the literature about the safe levels of doxorubicin to give NSG mice and reports have indicated up to 2 mg/kg doesn't have a significant toxic effect [322]. I decided to use 2 mg/kg of doxorubicin once weekly and did not witness significant toxic effects. Studies have also utilised intraperitoneal injections of doxorubicin at higher levels; however, there has been reported concerns with weight loss. I have also taken serum for analysis of doxorubicin and TRAIL, based on previous pK data and organ function tests. This is a separate study including nine mice, which were treated with a combination therapy, and I will analyse the blood samples for liver function and pancreatic function; furthermore, the femurs, with and without the tumour *in situ*, lung, liver, spleen and heart were also stored in formalin and will be assessed histologically for apoptosis, tumour burden and DR5 and NG2 levels pre and post treatment.

Future direction

It would be useful to explore using the NG2 targeted form of TRAIL with and without doxorubicin in orthotopic mouse models engrafted with other sarcoma cell lines, such as the osteosarcoma MG63 cell line, which has shown high NG2 and DR5 levels, to try help delineate the differences between the NG2 targeted and non-targeted forms of TRAIL *in vivo*. Furthermore, the doxorubicin levels may not have been sufficient to have a synergistic effect as there has been reports to suggest that the level is at its highest level in the serum 1 hour after administration (100 ng/ml when 1.24 mg/kg administrated) but then decreases in BALB/c mice [327]. The concentration present in

the bone is also unclear. Other possibilities of administering doxorubicin are utilising liposomal doxorubicin to maintain the level of doxorubicin in the blood and use of the Rag2 mouse strain that may tolerate a higher dose of doxorubicin. I plan to analyse the tissue histologically for NG2 and DR5 as the levels expressed may change after treatment. Serum levels of doxorubicin and TRAIL will be analysed as part of this *in vivo* investigation.

There have been several studies that report the use of osteosarcoma and Ewing's sarcoma PDX models for personalised therapeutic tests, however the models are limited by their availability of the samples, and also difficulties in achieving engraftment, and the cost of the immunodeficient mice, the constraining process, and the mandatory quality control. However, they have been achieved in NSG mice using original cell lines isolated from patient biopsies subsequently implanted in NSG mice [326], and, therefore, this is also a potential future avenue to pursue. Also, use of spheroids and more sophisticated 3D culture models better represent the bone sarcoma microenvironment and niche than 2D models and can reduce the use of animal based models [328].

Chapter 9. Use of ‘activated’ bone marrow-derived stem cells (BMMSCs) as cell vehicle expressing TRAIL on bone sarcoma cell death

9.1 Introduction

As discussed in the introductory chapter, studies have investigated the use of stem cells as a potential to be used for cancer therapy. They have promising properties such as homing to the tumour site and the ability to be activated to express anti-tumourigenic molecules such as TRAIL and DKK-3 in proximity to the tumour cells and potentially avoid systemic toxicity. Cocultures have found increased cell death when MSCs expressing TRAIL are cocultured with breast cancer cells and also reduction in metastases in a breast cancer mouse model [329].

MSCs have also been engineered to express TRAIL and have enhanced effects when also combined with chemotherapeutic agents. For the delivery of DR targeting therapies, MSCs are currently the preferred stem cell type. Other stem cells types require further investigation. Of particular interest are induced pluripotent stem cells (iPSCs) as they offer autologous cells and an inexhaustible source of MSCs. There has been a concern that when stem cells are used alone there is a potential for harmful effects such as an increase in sarcoma cell proliferation [330].

The aims of this chapter are to investigate:

1. If bone marrow-derived mesenchymal stem cells can be stimulated to express membrane bound TRAIL using TNF-alpha.

2. To set up/establish cocultures with MSCs and bone sarcoma cell lines and analyse for increased sarcoma cell death.

3. To assess for harmful effects such as increased proliferation of sarcoma cells when coculturing MSCs with bone sarcoma cells.

9.2 The effects of TNF-alpha on BMMSCs

9.2.1 TNF-alpha potency

TNF-alpha was used to 'activate' patient-derived bone-derived mesenchymal stem cells (BMMSCs) to enable them to express the membrane-bound form of TRAIL. The membrane-bound form of TRAIL is considered to be more potent compared to the soluble form of TRAIL. Before applying TNF-alpha onto the BMMSCs, the potency of my TNF-alpha was tested on murine fibroblasts engineered to express TNF receptor 1 (MF TNFR1-Fas cells) (Figure 166). A dose of 0.1 ng/ml was potent and could kill up to 80 % of these cells in culture. This is the minimum dose stated in the literature to be able to 'activate' BMMSCs [329]. TNF-alpha was not found to be significantly toxic to the BMMSCs consistent with the findings of previous studies suggesting intact cell proliferation/survival at concentrations ranging from 0.01 ng/ml to 100 ng/ml [331] (Figure 167).

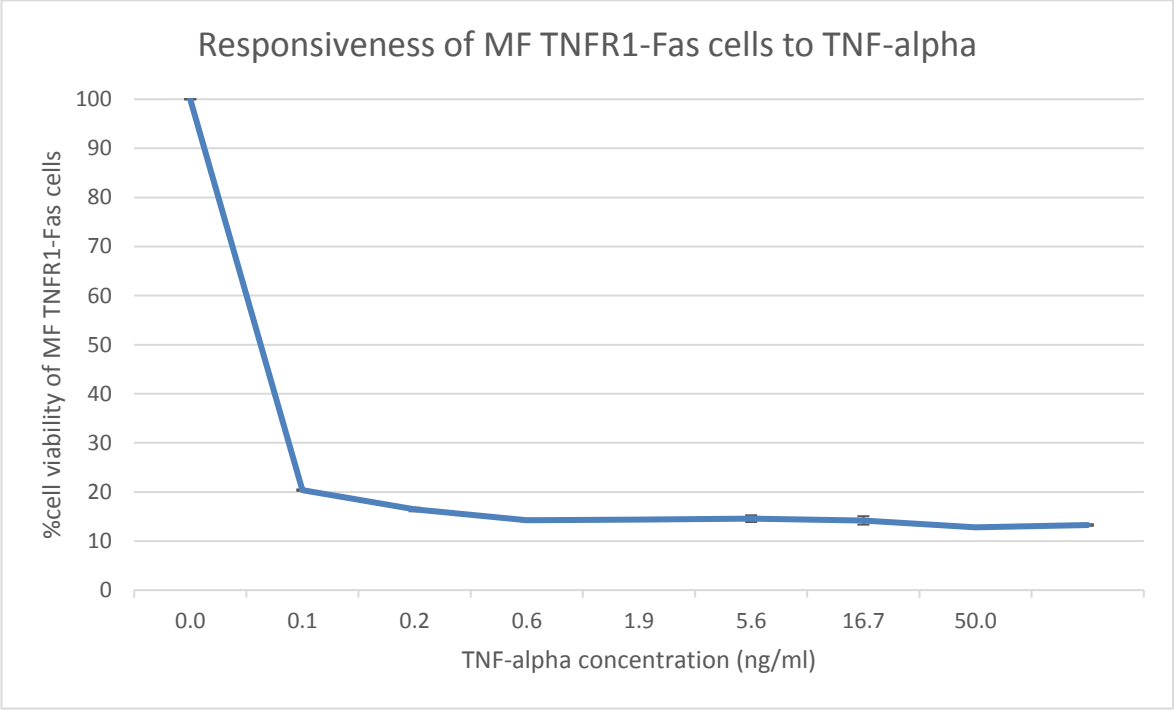

Figure 166 - MF TNFR1-Fas cells are responsive to the lab TNF-alpha, which has an effective concentration at 0.1 ng/ml. The cells were cultured in RPMI containing 10 % Fetal Bovine Serum (FBS). Treatment for 24 hours. Viability assessed using CKK-8 assay. (Mean +/- SEM, n = 3).

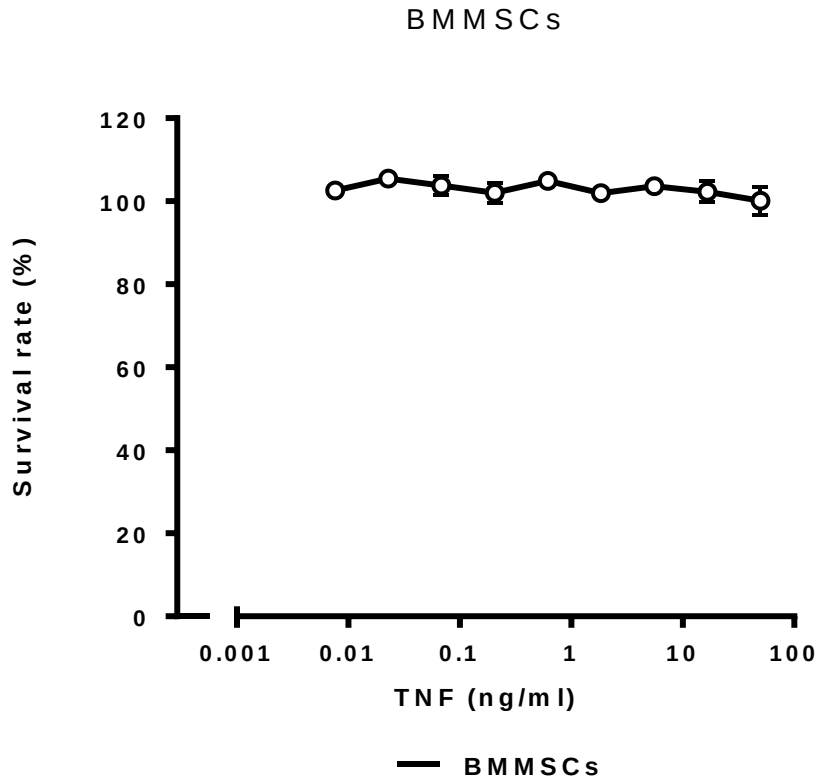

Figure 167 – TNF-alpha is not significantly toxic to BMMSCs at concentrations up to 100 ng/ml. Incubation time of 24 hours. (Mean +/- SEM, n = 3)

9.2.2 TNF-alpha preactivation of BMMSCs

9.2.2.1 The effect of TNF-alpha on BMMSC TRAIL mRNA expression

The passage number and BMMSC donor specificities are known to influence the degree of TRAIL expression when TNF-alpha is used to 'activate' them [329]. A concentration of 20 ng/ml of TNF-alpha was applied as previously described [332] to early passage number (passage 3) BMMSCs and there was evidence of increased TRAIL expression at the RNA level using PCR (at 72 hours when compared to untreated BMMSCs or NHDF cells treated with TNF-alpha) (Figure 168) and at the protein level using flow cytometry at days 2 and 5 (Figure 169). The 786-0 renal clear cell adenocarcinoma cell line was used as positive control for TRAIL expression.

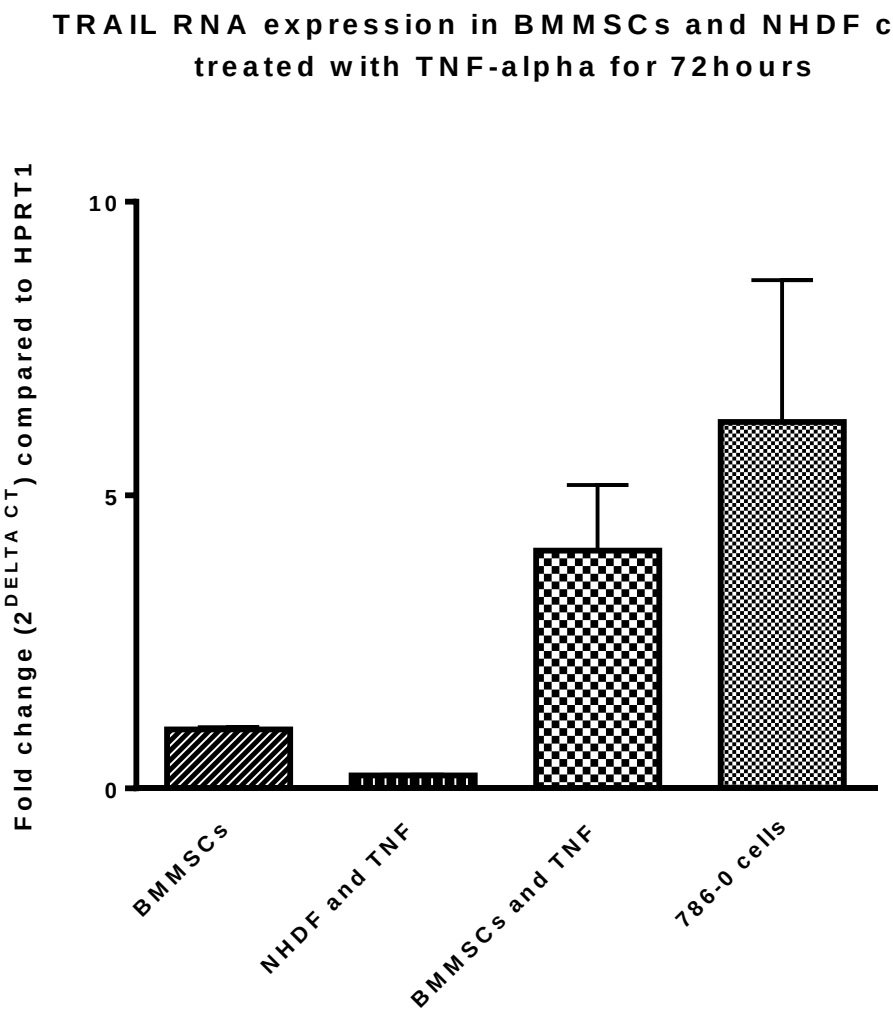

Figure 168 - RT-PCR results demonstrating elevated TRAIL RNA expression in BMMSCs treated with TNF-alpha (20 ng/ml) for 72 hours. This was significantly greater than BMMSCs alone or NHDF cells treated with TNF-alpha (20 ng/ml) $p<0.05$, Student's *t*-test (mean +/- SEM, n = 3). 786-0 renal adenocarcinoma cell line was included as the positive control.

9.2.2.2 The effect of TNF-alpha on BMMSC TRAIL protein surface expression

BMMSCs were treated with TNF-alpha (20 ng/ml) and increased surface levels of TRAIL were found compared to untreated cells ($p<0.05$, Student's *t*-test) at 48 hours (Figure 169).

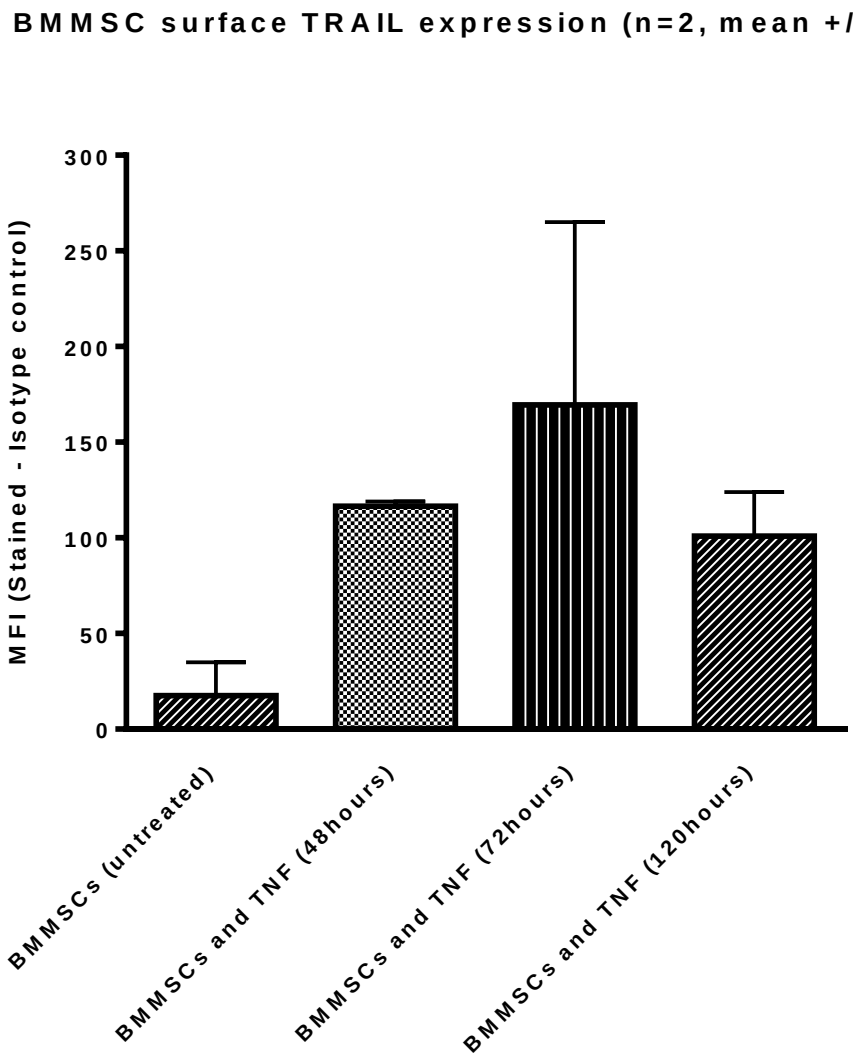

Figure 169 - Flow cytometry data demonstrating increased expression of TRAIL in bone marrow-derived mesenchymal stem cells (BMMSCs) when exposed to 20 ng/ml TNF-

alpha. Expression levels were found to be increased at 48 hours, 72 hours and 120 hours ($p<0.05$, Student's *t*-test at 48 hours (n = 2, mean +/- SEM).

9.2.2.3 Effect of TNF-alpha on BMMSC osteogenic differentiation

There is conflicting information regarding the role of TNF-alpha in osteogenic differentiation of MSCs. Recent data suggests that lower concentrations of TNF-alpha (1 ng/ml or lower) appear to be have a more prodifferentiatory effect stimulating them towards an osteoblastic phenotype. Markers of osteoblastic differentiation such as cbfa-1/Runx-2 and ALP can be upregulated after treatment with lower doses of TNF-alpha (0.01 ng/ml or 0.1 ng/ml) [331,333]. Other studies suggest increased Alizarin red staining and TNAP activity at higher concentrations of TNF-alpha (10 ng/ml) [334,335]. However, there has been concerns about an upper boundary that may have antiosteogenic effects [336].

It was confirmed that cbfa-1/Runx2 RNA levels are increased in patient-derived osteoblasts compared to normal human dermal fibroblasts (NHDF) cells (Figure 170). This is a transcription factor associated with osteogenic differentiation of BMMSCs into osteoblasts. When BMMSCs were treated with TNF-alpha (20 ng/ml) for 72 hours, cbfa-1/Runx2 mRNA levels were not found to be elevated or significantly decreased when compared to untreated BMMSCs and NHDF cells treated with TNF-alpha (20 ng/ml) (Figure 171).

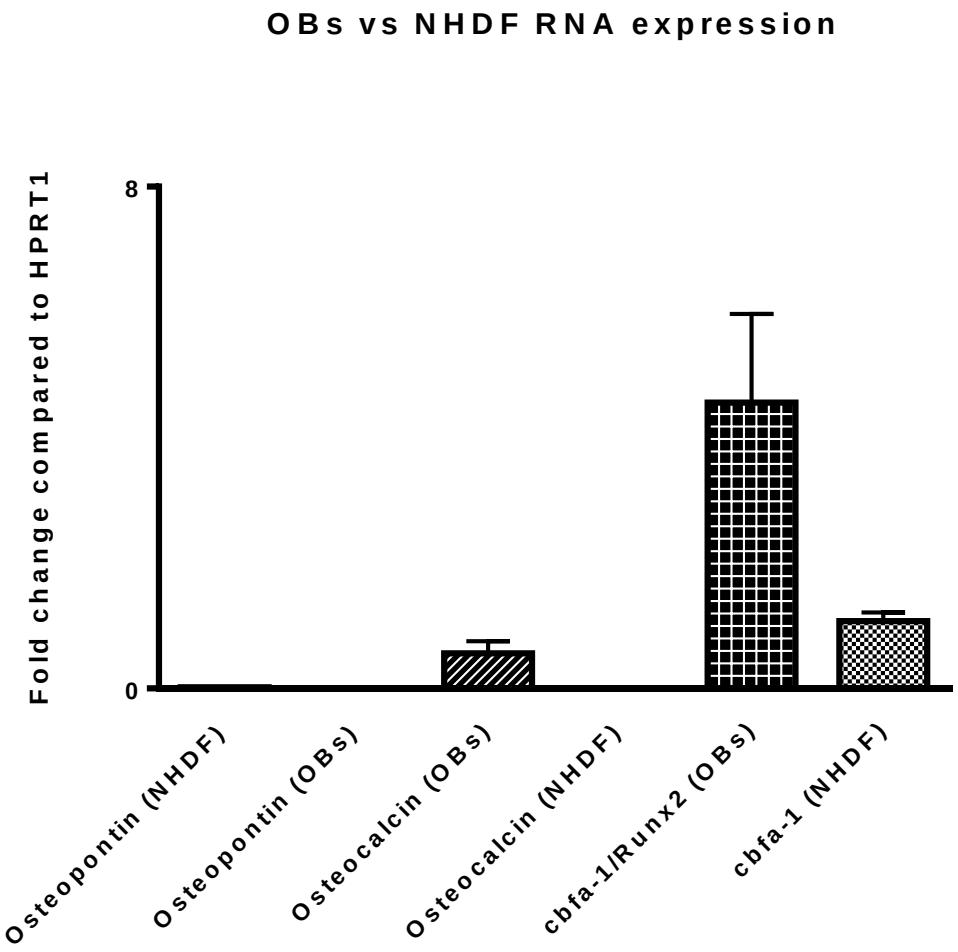

Figure 170 - Increased cbfa-1/Runx2 and osteocalcin RNA levels in patient-derived osteoblasts (OBs) compared to normal human dermal fibroblasts (NHDF).

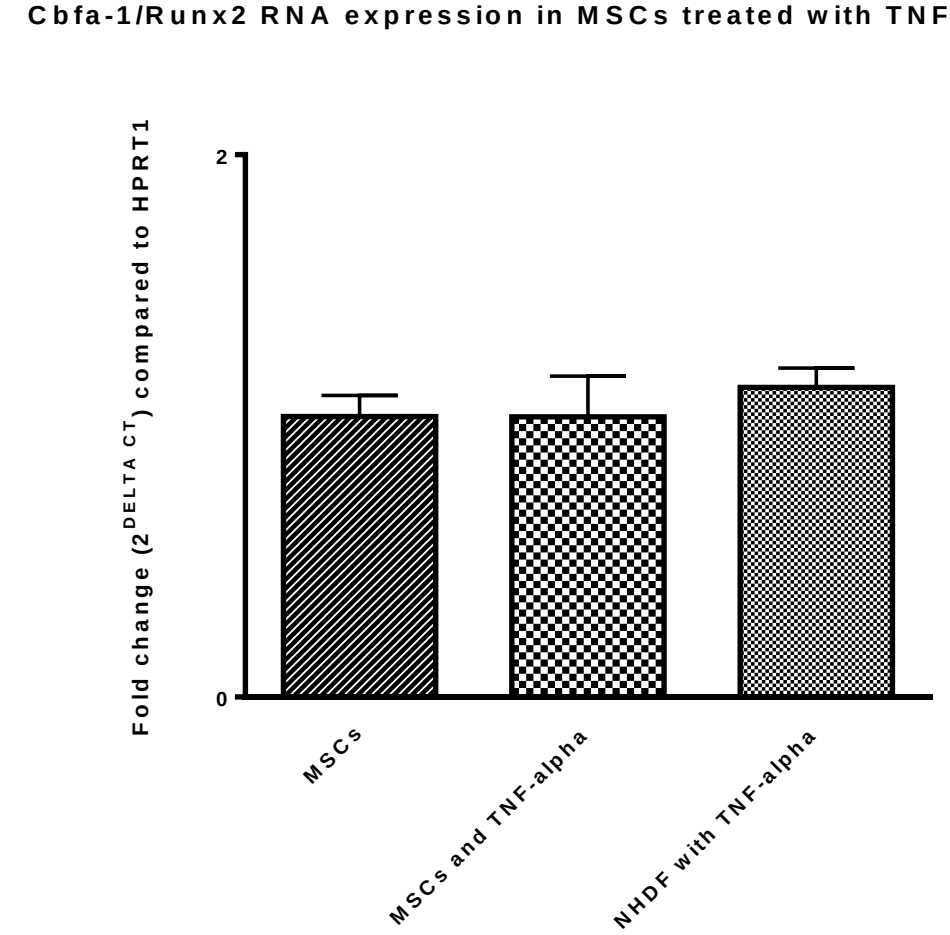

Figure 171 - No obvious differences in cbfa-1/Runx2 expression levels in MSCs treated with TNF-alpha (20 ng/ml) for 72 hours compared to untreated MSCs and NHDF cells treated with TNF-alpha (mean +/- SEM, n = 2).

9.3 Coculturing 'activated' TRAIL expressing BMMSCs with sarcoma cells

9.3.1 Preliminary coculture experiments and flow cytometry gating strategies

The focus of the experiment was to assess if surface expression of TRAIL during coculture facilitated the direct contact of TRAIL expressing BMMSCs to death receptor expressing sarcoma cells thereby inducing their apoptosis.

TNF-alpha treated or 'activated' BMMSCs, treated for either 48 or 72 hours were cocultured together with sarcoma cells (GFP+ve osteosarcoma U2OS pSLIEW cells) or Ewing's sarcoma TC71 cells in 1:1 ratio for at least 48 hours in DMEM culture media with 20 % FBS and analysed for cell death using flow cytometry. Data in the literature suggest that cell death can be observed at 24 hours for breast cancer cells [329]. GFP+ve U2OS pSLIEW cells were used to help separate the BMMSCs from the U2OS cells and BMMSCs were also labelled using CD90 to help separate them from the TC71 cells. DAPI staining was used to help label cells that are dead.

GFP expression was used to gate on the U2OS cells and assess percentage of cell death in that population when cultured with 'activated' BMMSCs (treated with TNF-alpha for 48 hours and cocultured for 72 hours). This was compared to non-activated BMMSCs. Tendencies towards increased cell death were noted. Repeats of five experiments revealed tendency towards greater U2OS cell death in coculture containing TNF preactivated BMMSCs; however, this was non-significant on Mann-Whitney *U* testing. Values for cocultures containing activated or non-activated BMMSCs were greater than cocultures containing activated or non-activated NHDF cells and was significant when comparing TNF preactivated BMMSCs + U2OS and NHDF + TNF + U2OS (Figure 172 to Figure 175). The experiment was repeated using a more sophisticated 3D printing strategy to enable more precise positioning of the cells in relation to one another (Section 7.3.2).

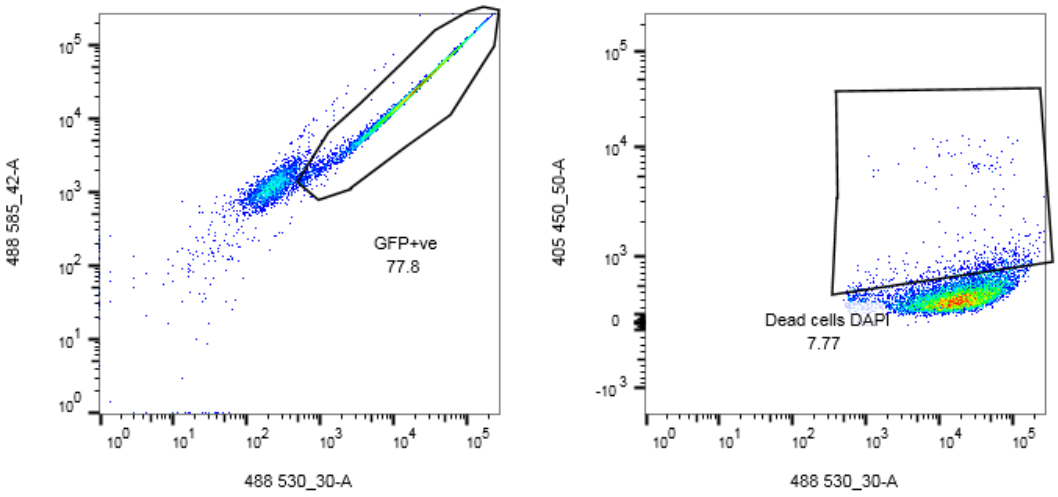

Figure 172 - Flow cytometry demonstrating 78 % of U2OS cells alone, which are GFP+ve cells. The uptake of DAPI occurs in 8 % of GFP+ve cells.

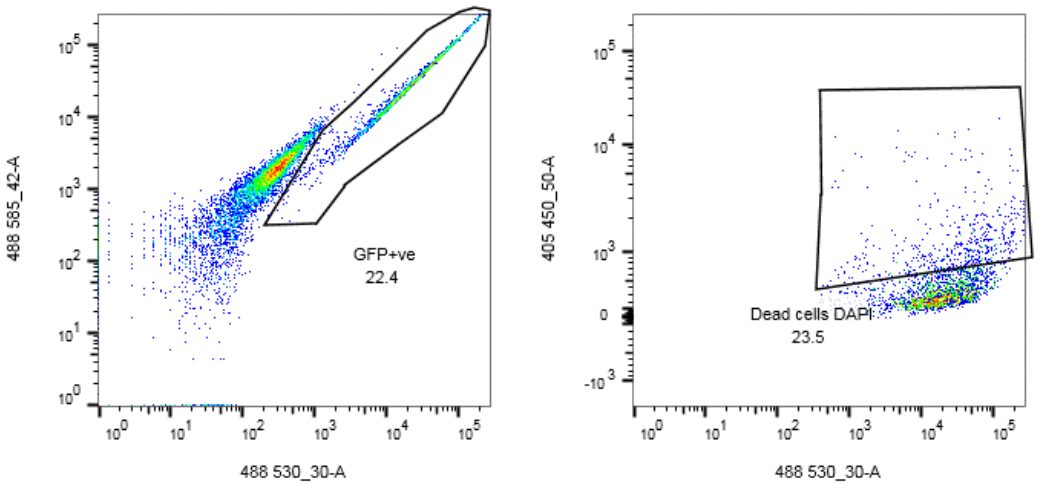

Figure 173 - Flow cytometry demonstrating 22 % of GFP+ve U2OS cells in the **'non-activated'** BMMSCs and U2OS coculture. The uptake of DAPI occurs in 24 % of the GFP+ve cells.

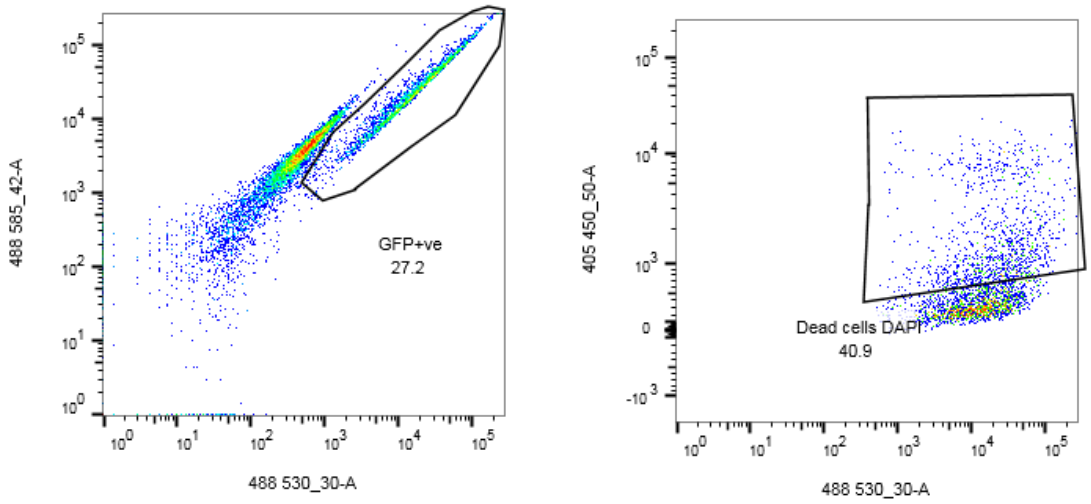

Figure 174 - Flow cytometry demonstrating 27 % of GFP+ve U2OS cells in the **'activated'** BMMSCs and U2OS coculture. The uptake of DAPI occurs in 41 % of the GFP+ve cells.

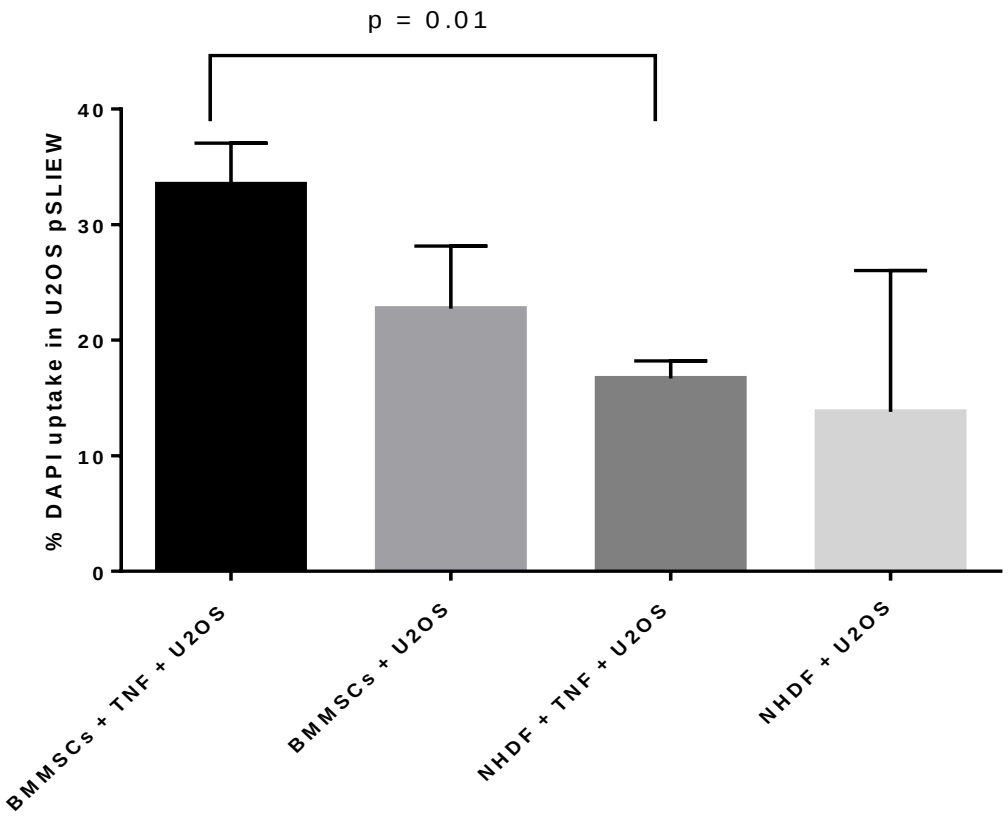

Figure 175 – There was significantly greater U2OS pSLIEW cell death when coculture with TNF-alpha treated BMMSCs compared to TNF-alpha treated NHDF cells. Results are presented as Mean +/- SEM, Mann Whitney *U* test.

BMMSCs cocultured with TC71 cells

Coculture experiments were also performed using 'activated' BMMSCs with TC71 cells (CD90 negative). BMMSCs could be separated from the TC71 cells based on BMMSC positive staining for CD90 [337]. There appeared to be an increase in TC71 cell death and uptake of DAPI in a population of the TC71 cells when coculturing with 'activated' BMMSCs, but not significantly more compared to coculturing with 'non-activated' BMMSCs (about 10 % vs 5 %) (Figure 176) and (Figure 177) respectively. TRAIL expression on the surface of the 'activated cells' in the coculture was evident when gating on the BMMSCs (Figure 176).

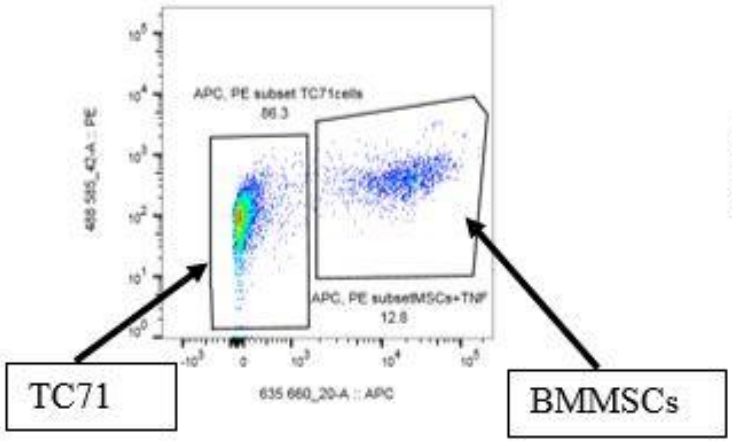
APC, PE subset TC71cells
86.3
APC, PE subsetMSCs+TNF
12.8
488 585_42-A :: PE
635 660_20-A :: APC
TC71
BMMSCs
324279.fcs
Ungated
10000

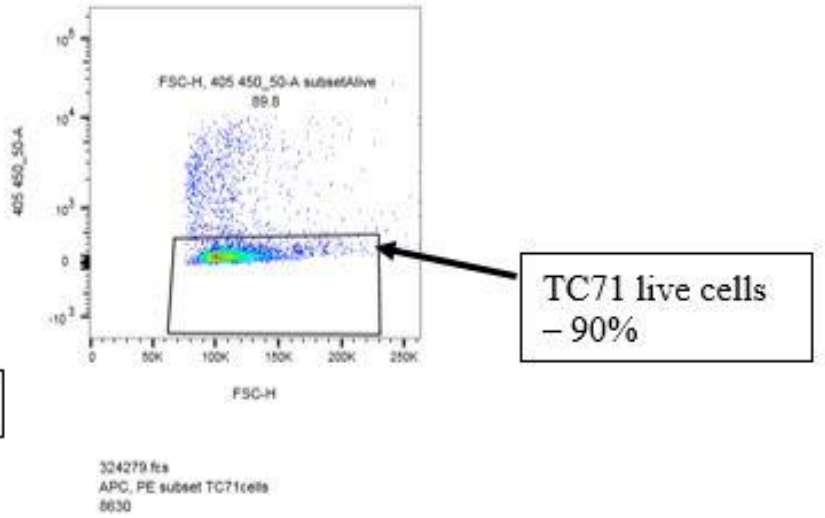
FSC-H, 405 450_50-A subsetAlive
89.8
405 450_50-A
FSC-H
TC71 live cells
– 90%
324279.fcs
APC, PE subset TC71cells
8630

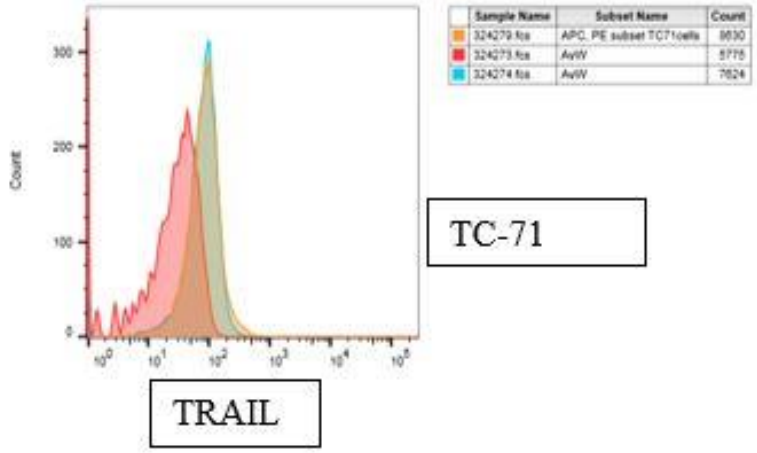
Sample Name | Subset Name | Count
324279.fcs | APC, PE subset TC71cells | 8630
324279.fcs | AnW | 5775
324274.fcs | AnW | 7624
Count
TC-71
TRAIL

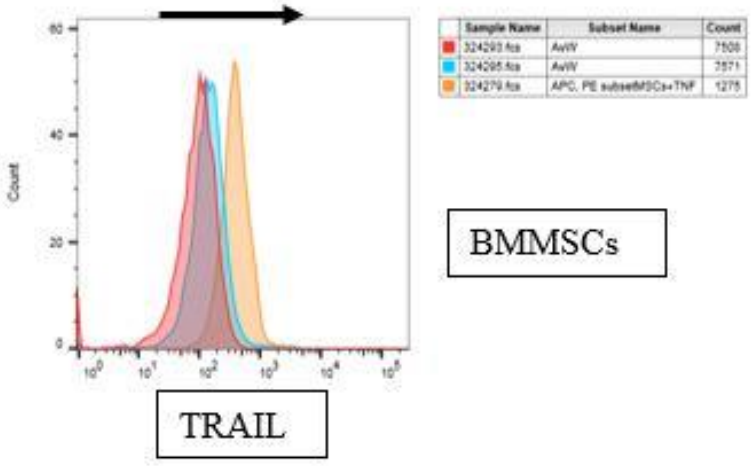
Sample Name | Subset Name | Count
324293.fcs | AnW | 7506
324295.fcs | AnW | 7571
324279.fcs | APC, PE subsetMSCs+TNF | 1275
Count
BMMSCs
TRAIL

Figure 176 - Coculture of ‘activated’ TRAIL expressing BMMSCs with Ewing’s sarcoma TC71 cells. BMMSCs were treated with TNF-alpha for 48 hours before coculture experiment with TC71 cells. Coculture was for 72 hours. TRAIL expression can be seen on the surface of BMMSCs (orange histogram peak = TRAIL surface expression, red histogram peak = unstained cells, blue histogram peak = isotype control); however, there does not appear to be a significant amount of cell death at 72 hours. BMMSCs could be separated from the TC71 cells based on BMMSCs staining positive for CD90.

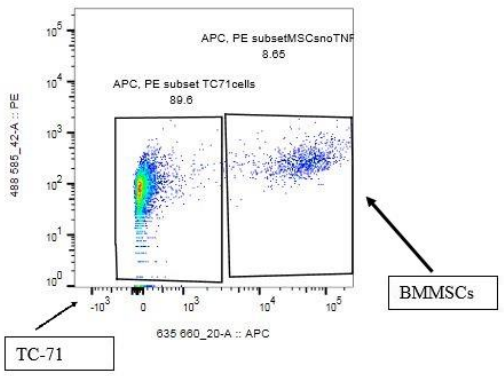

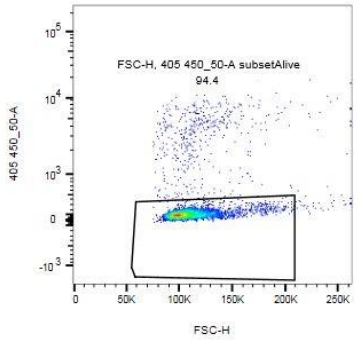

TC71 - live cells
94%

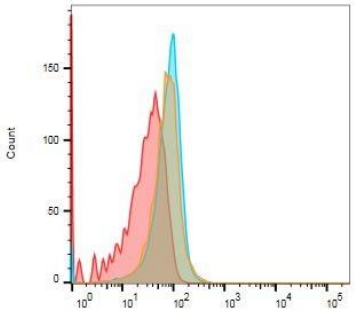

	Sample Name	Subset Name	Count
	324278.fcs	APC, PE subset TC71cells	8961
	324274.fcs	AvW	7624
	324273.fcs	AvW	5775

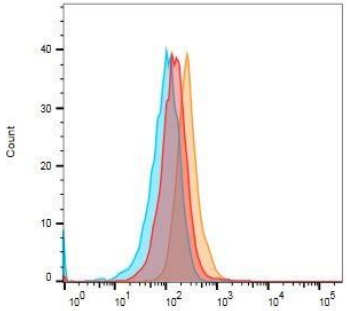

	Sample Name	Subset Name	Count
	324295.fcs	AvW	7571
	324293.fcs	AvW	7508
	324278.fcs	APC, PE subsetMSCsnoTNF	865

BMMSCs

Figure 177 - Coculture of ‘non-activated’ expressing BMMSCs with Ewing’s sarcoma TC71 cells. Coculture was for 72 hours. TRAIL expression cannot be seen on surface of BMMSCs; there does not appear to be significant amount of cell death at 72 hours. BMMSCs could be separated from the TC71 cells based on BMMSC positive staining for CD90.

9.3.2 3D printed cocultures

These were set-up to coculture MSCs (TRAIL expressing or non-TRAIL expressing) with sarcoma cells in the following sarcoma cell: MSC ratios – 1:1, 1:2, 1:3, 1:5, 1:10 and 1:20 (Table 26 and Figure 178 and Figure 179). Cocultures were extended for longer than 3 days in light of findings from initial non-3D printed coculture experiments. I performed the same experiments using the BMMSCs 'activated' for 72 hours (TNF-alpha applied for 72 hours) and conducted the coculture with GFP+ve U2OS cells for 5 days or longer.

Flow cytometry was used as the methodology to distinguish between the sarcoma cells and BMMSCs and to assess for cell death in the sarcoma cells. BMMSCs are known to be positive for CD73 [337] and staining for CD73 was used to enable gating on the sarcoma cells and the measurement of the degree of apoptosis occurring in the sarcoma cell population (Figure 181). U2OS cells expressing GFP (U2OS pSLIEW) were used for the coculture. Loss of GFP has been used as a measure of cell death in previous studies and has shown good correlation with Annexin V expression [338]. U2OS pSLIEW cells can be seen to lose GFP expression when treating them with staurosporine (Figure 180).

3D printed coculture experiment set-up

Coculture experiments were repeated exposing the cells [(activated or non-activated mesenchymal stem cells (MSCs)] with GFP expressing U2OS osteosarcoma cells (U2OS pSLIEW) together for longer (5 days). MSCs were treated with TNF-alpha for 3 days prior to the coculture. A 48-well plate was used to culture them together in monolayer using 3D bioprinting technology (courtesy of Ricardo Ribeiro, School of Mechanical and Systems Engineering) and helped produce more a sophisticated and accurate cocultures in terms of cell numbers and locations. The layout is shown in Table 26 and an example of the image under the microscope of cells printed in 1:1 and 1:10 ratios is shown in Figure 178 and Figure 179.

Table 26 – Layout for U2OS pSLIEW and MSC printing.

Ratio 1:1 U2OS pSLIEW: Activated MSCs	Ratio 1:2 U2OS pSLIEW: Activated MSCs	Ratio 1:3 U2OS pSLIEW: Activated MSCs:	Ratio 1:5 U2OS pSLIEW: Activated MSCs	Ratio 1:10 U2OS pSLIEW: Activated MSCs	Ratio 1:20 U2OS pSLIEW: Activated MSCs	Activated MSCs alone	U2OS pSLIEW alone
Ratio 1:1 U2OS pSLIEW: Activated MSCs	Ratio 1:2 U2OS pSLIEW: Activated MSCs	Ratio 1:3 U2OS pSLIEW: Activated MSCs:	Ratio 1:5 U2OS pSLIEW: Activated MSCs	Ratio 1:10 U2OS pSLIEW: Activated MSCs	Ratio 1:20 U2OS pSLIEW: Activated MSCs	Activated MSCs alone	U2OS pSLIEW alone
Ratio 1:1 U2OS pSLIEW: Non - Activated MSCs	Ratio 1:2 U2OS pSLIEW: Non-Activated MSCs	Ratio 1:3 U2OS pSLIEW: Non-Activated MSCs	Ratio 1:5 U2OS pSLIEW: Non-Activated MSCs	Ratio 1:10 U2OS pSLIEW: Non-Activated MSCs	Ratio 1:20 U2OS pSLIEW: Non-Activated MSCs	Non-Activated MSCs alone	U2OS pSLIEW alone
Ratio 1:1 U2OS pSLIEW: Non - Activated MSCs	Ratio 1:2 U2OS pSLIEW: Non-Activated MSCs	Ratio 1:3 U2OS pSLIEW: Non-Activated MSCs	Ratio 1:5 U2OS pSLIEW: Non-Activated MSCs	Ratio 1:10 U2OS pSLIEW: Non-Activated MSCs	Ratio 1:20 U2OS pSLIEW: Non-Activated MSCs	Non-Activated MSCs alone	U2OS pSLIEW alone

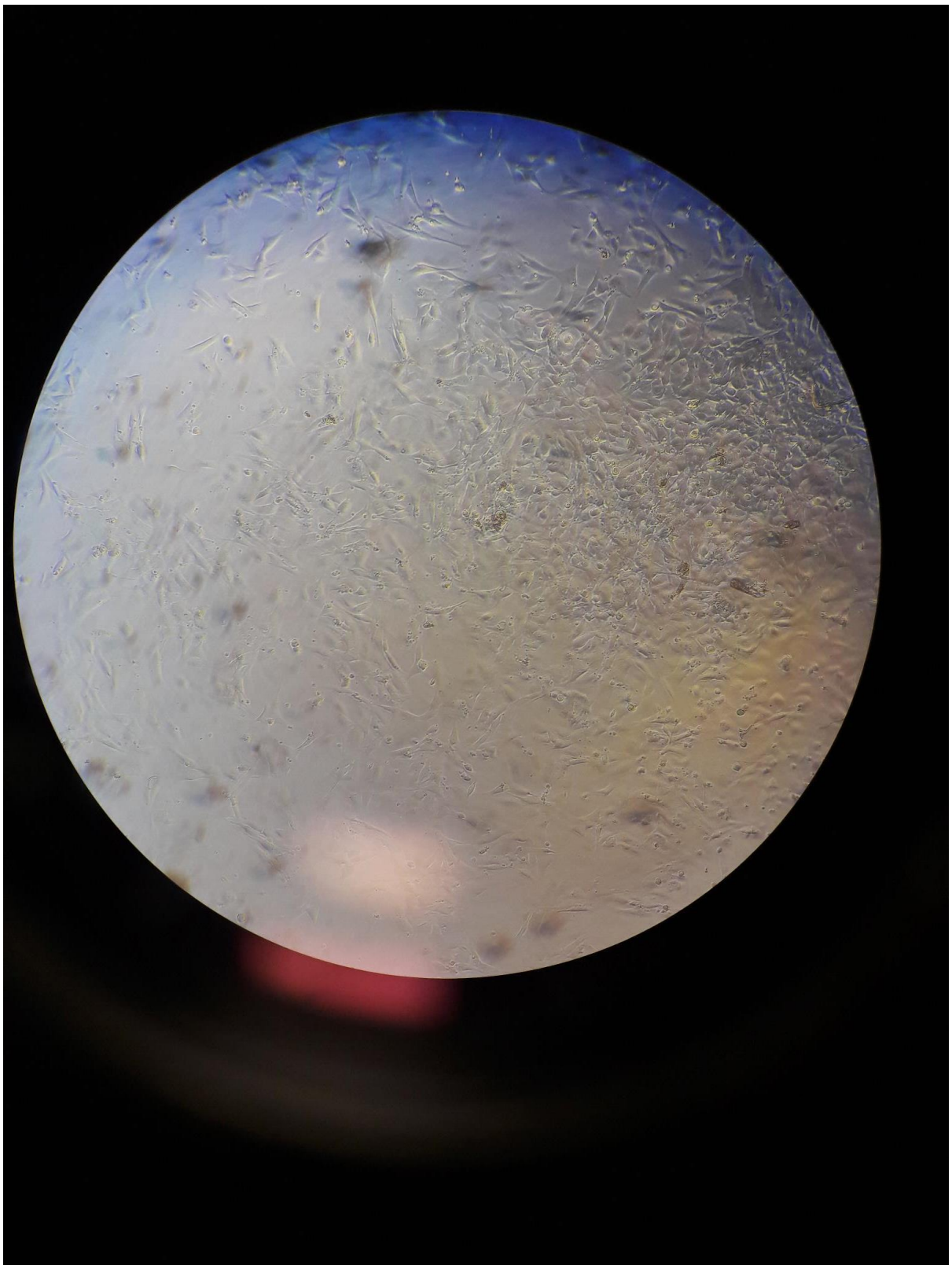

Figure 178 – Microscopic image of 1 to 1 ratio (U2OS pSLIEW: MSCs) in one well of a 48-well plate as per Table 26.

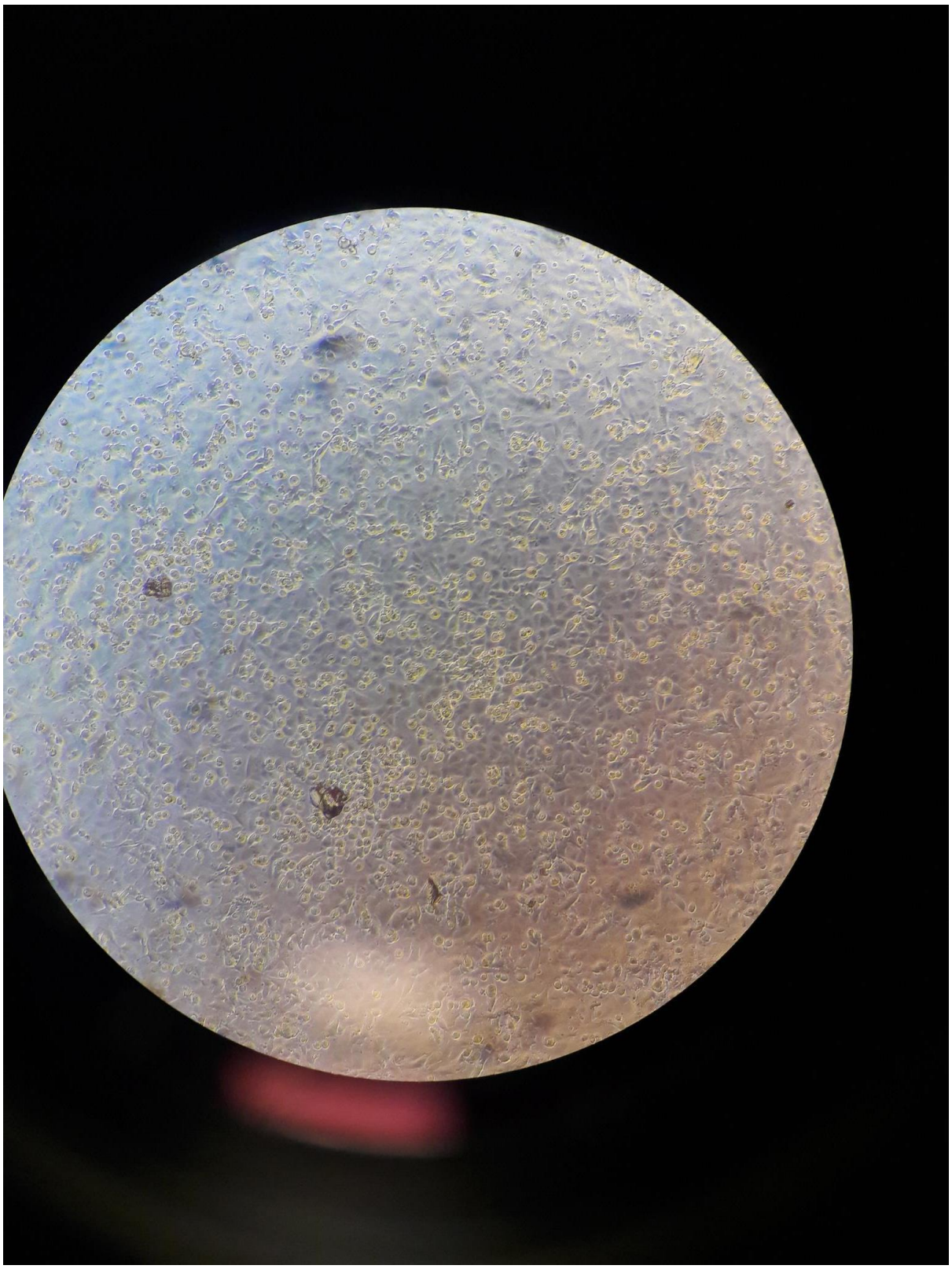

Figure 179 – Microscopic images of 1 to 10 ratio (U2OS pSLIEW: MSCs) in one well of a 48-well plate as per Table 26.

Loss of GFP signal in U2OS cells has been correlated to an increase in cell death in previous studies [338]. This has been observed in staurosporine (an agent used to cause cell death) treated U2OS pSLIEW cells (Figure 180).

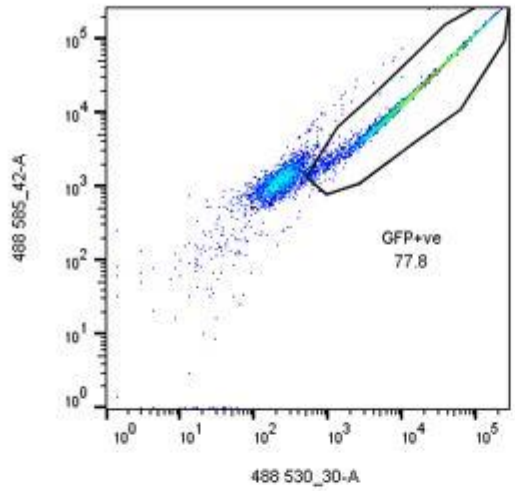

GFP +ve proportion is 78%

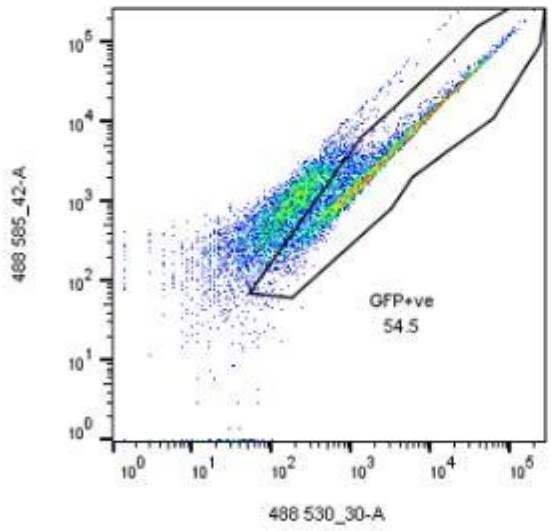

In staurosporine treated cells the GFP +ve proportion drops to 55%

Figure 180 – Proportion of GFP+ve U2OS pSLIEW cells drops from 78 % to 55 % when treated with 1 µM staurosporine.

Markers have been used in prior studies to gate out MSCs on flow cytometry such as CD90 used in previous studies to distinguish between the activated stem cells and breast cancer cells; however, this is expressed by both the MSCs and U2OS cells; therefore, I used another marker. The marker I used to separate MSCs from the U2OS was CD73. By using flow cytometry, I could separate the U2OS pSLIEW (GFP) population from the MSCs (APC-CD73) (gate out the APC positive MSCs) and then assess for loss of GFP signal in the U2OS pSLIEW cells. Examples of the gating strategies employed are shown below (Figure 182). Evidence of increased GFP negative cells (dead U2OS pSLIEW cells) in those wells with U2OS pSLIEW cells cultured with 'activated' MSCs. This appears to reach significance at the 1:2 U2OS:MSC ratio (Figure 183).

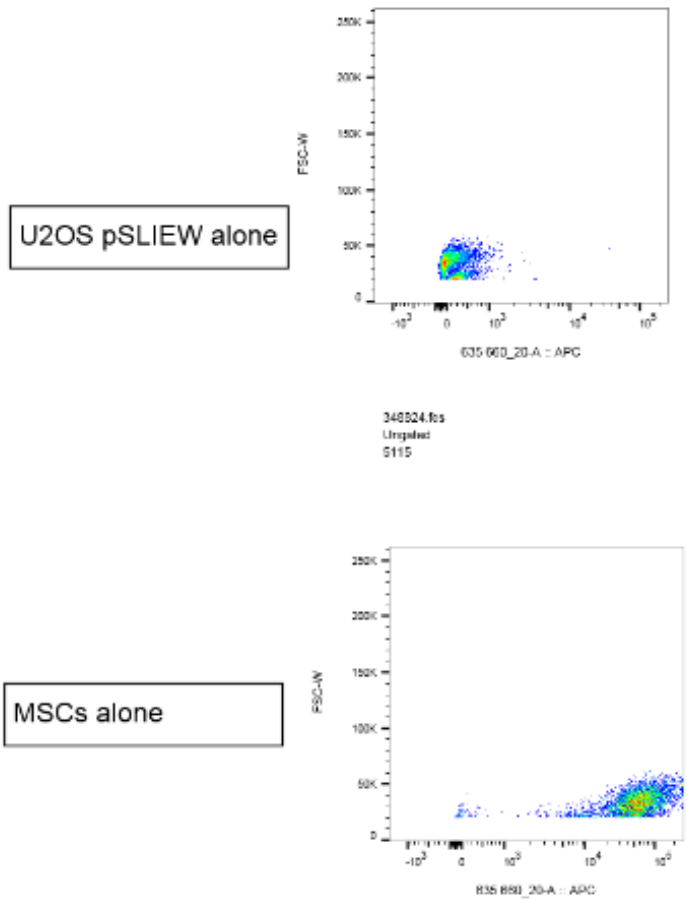

Figure 181 – MSCs stain positive for CD73 (APC channel).

1:1 activated

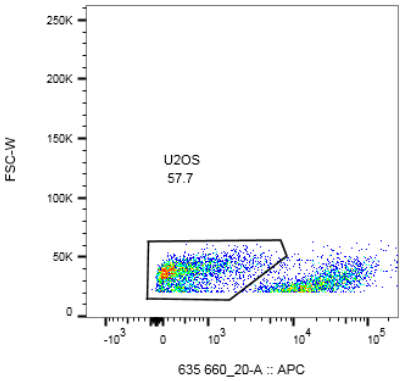

348773.fcs
Ungated
5000

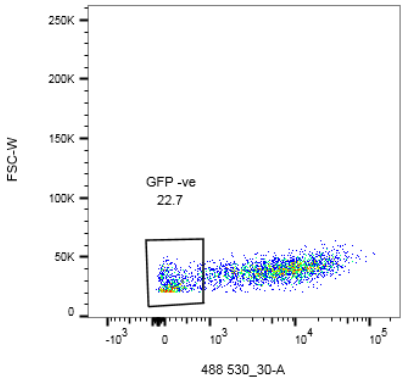

348773.fcs
U2OS
2886

1:1 non-activated

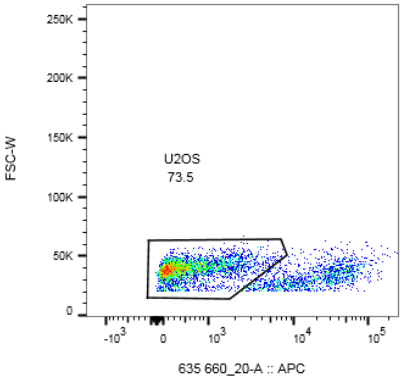

348774.fcs
Ungated
5000

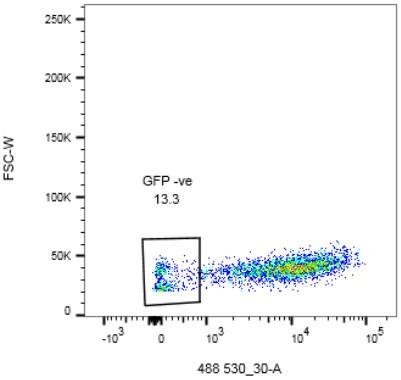

348774.fcs
U2OS
3677

1:2 activated

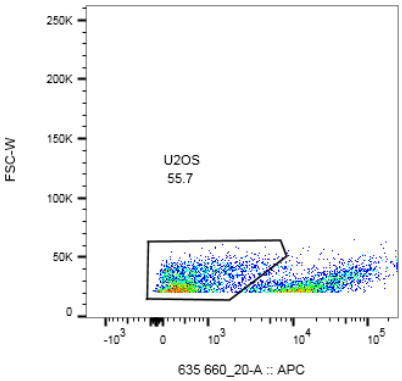

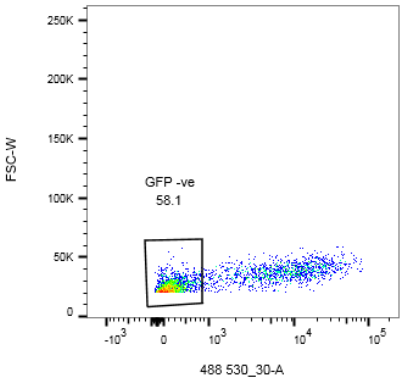

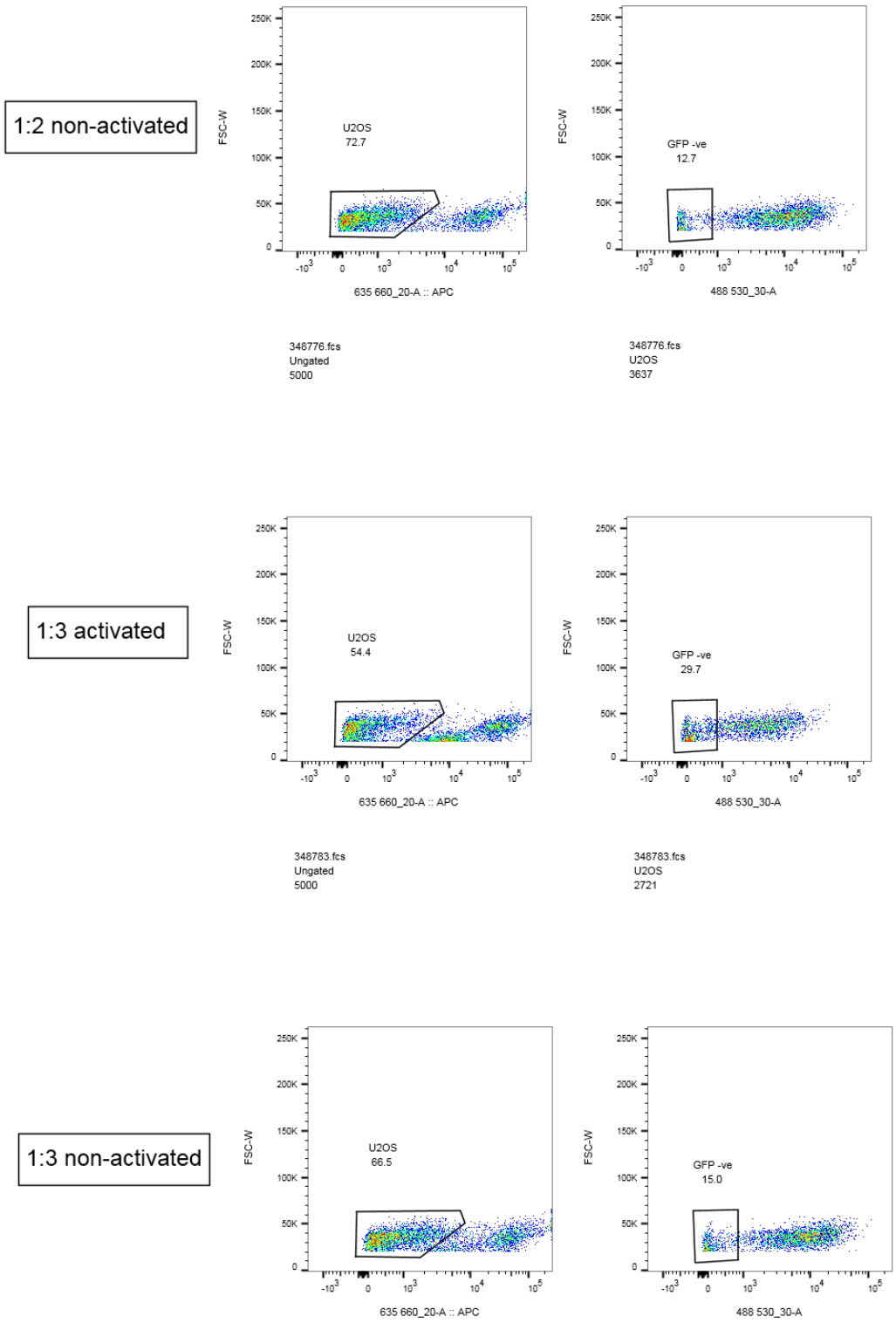

Figure 182 – Gating strategies employed to separate the CD73 APC positive MSCs from the U2OS pSLIEW cells. The degree of GFP-ve cells was then assessed in the U2OS pSLIEW cell population as a marker for cell death.

Using flow cytometry analysis, the degree of GFP loss in the U2OS pSLIEW cells was analysed (as a marker for cell death-therefore an increased percentage of GFP-ve cells equates to greater cell death) (mean + SEM from 3 rows of activated and 2 rows of non-activated). The points plotted for the 'activated' MSCs appear higher than the non-activated reaching significance at 1:2. The lower results at higher ratios are likely due to the reduced cell numbers used in those cocultures to be able to culture the cells in the wells of a 24-well plate at those ratios (Figure 183).

At the 1:2 ratio – on average of about 30 % were GFP negative (dead), which is close to that observed when using the highest SuperKillerTRAIL dose (100 ng/ml/ 3.9 nM), in which there was about 40 % of non-viable cells as shown below (Figure 184).

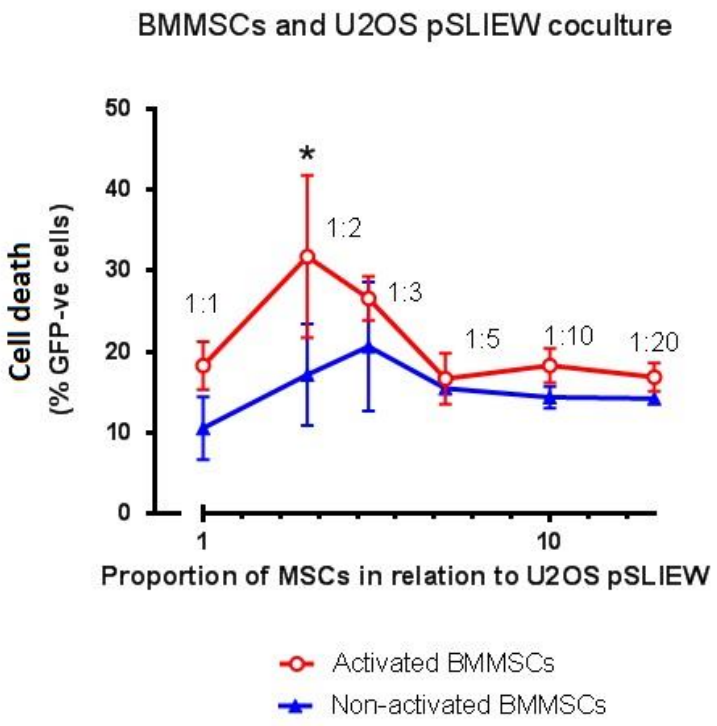

Figure 183 – Evidence of increased GFP negative cells (dead U2OS pSLIEW cells) in those wells with U2OS pSLIEW cells cultured with 'activated' MSCs. This appears to reach significance at the 1:2 U2OS:MSC ratio (* = $p<0.05$, Student's *t*-test, mean +/- SEM, n = 3).

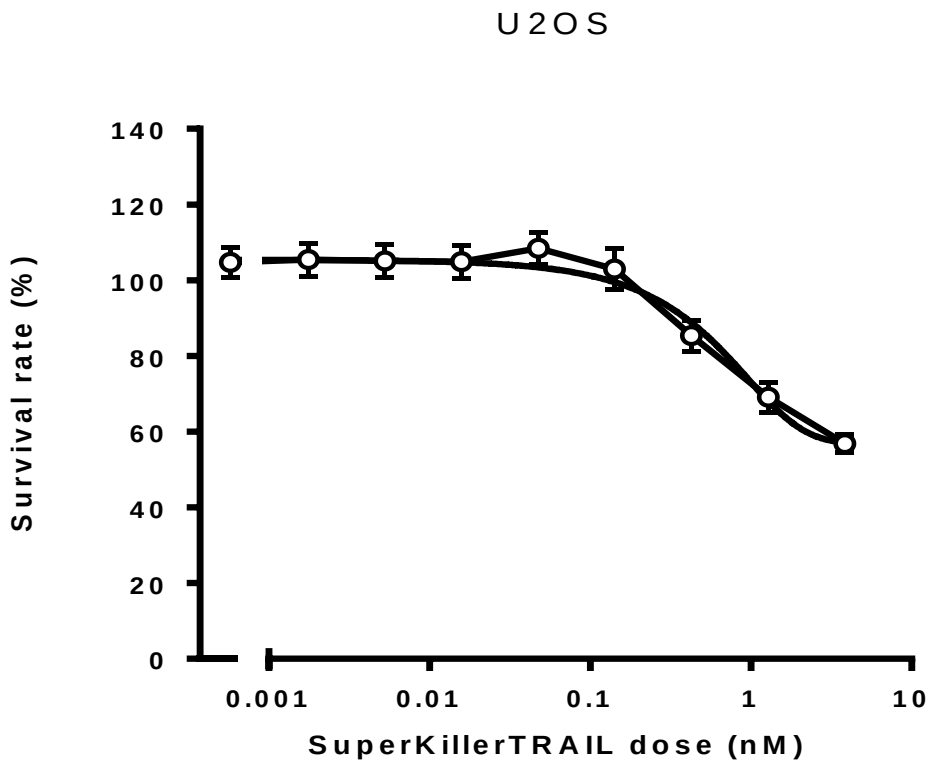

Figure 184 – U2OS cells treated with SuperKillerTRAIL (which mimics the membrane bound form of TRAIL) assessed using the Wst-8 cell proliferation assay. At the highest dose about 40 % of the cells are dead. (N = 3).

I have also transduced HT1080 cells (HT1080 pSLIEW) and my aim is to use this in the future. Theoretically, because HT1080 cells have also been sensitive to TRAIL therapy a response would be hypothesised when cocultured with 'activated MSCs'. HT1080 shows about 60 % cell death at maximum dose of 3.3 nM SuperKillerTRAIL, IC50 = 0.4 nM, compared to U2OS, which is about 40 % cell death at maximum dose of 3.3 nM; IC50 0.6 nM).

9.3.3 Assessment using Nikon® live cell fluorescence imaging

Following 3D printing of the coculture, after 24 hours of coculture, the 48-well plate was placed in an imaging system to assess the degree of loss of GFP in the U2OS pSLIEW cells. Data was recorded continuously for 8 hours after placement. It could be observed in the well with 'activated' MSCs that the GFP expression over the 8-hour time period that there was evidence of greater loss of GFP expression when MSCs were cultured in high ratio in relation to the U2OS pSLIEW cells.

Assessment using Nikon fluorescence imager

The Nikon TiE multi-modality system was used to take a snapshot of the cells at 24 hours after coculture (Figure 185) (courtesy of the Bioimaging, Newcastle University, Central Unit), which some papers have used as the timepoint for analysis. An assessment was then made of the degree of GFP positive cells present in each well (Figure 186). A graph was plotted to compare the degree of loss of GFP signal in each well.

I also monitored the cells over a 10-hour period. There was some evidence in the wells of reducing U2OS pSLIEW GFP fluorescence over time (in wells that containing both 'activated' MSCs and U2OS pSLIEW and 'non-activated' MSCs and U2OS pSLIEW and reduced overall fluorescence in the 1:1 U2OS pSLIEW and 'activated' MSC wells; however, this is an experiment that will require to be repeated to validate the findings (Figure 187 and Figure 188).

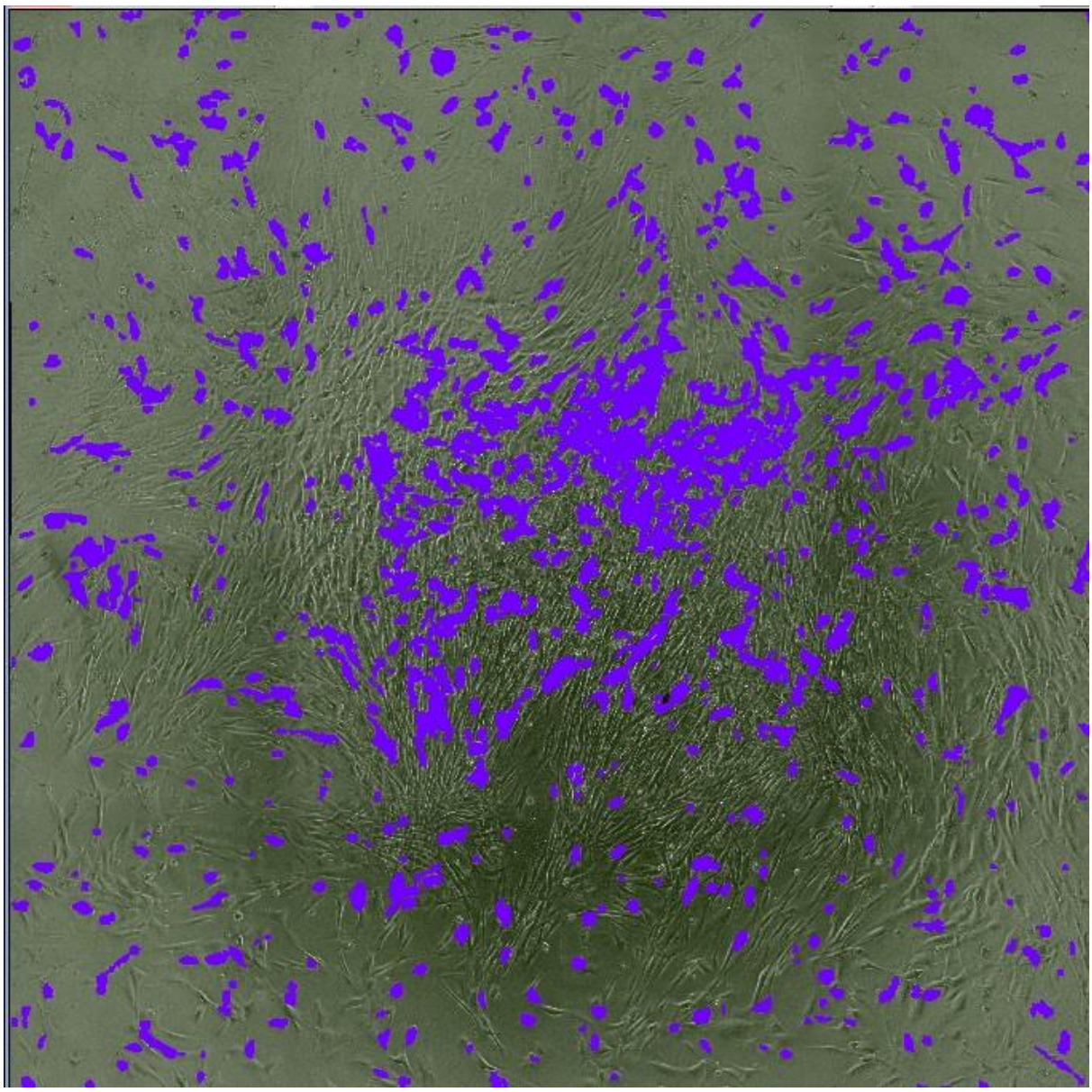

Figure 185 – Image taken using the Nikon TiE multi-modality system. The U2OS pSLIEW cells can be seen highlighted in purple among the MSCs.

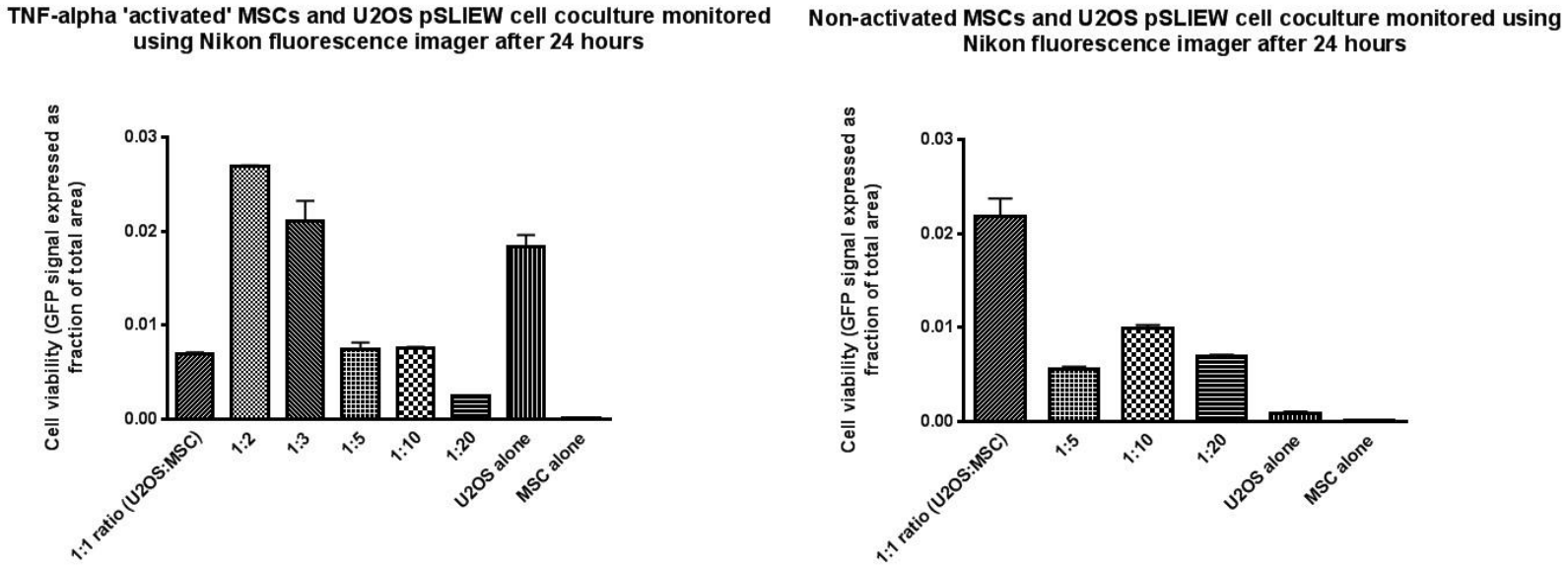

Figure 186 – Degree of GFP positive cells in each well after 24 hours of coculture ('activated' and non-activated MSCs with U2OS pSLIEW cells). (N = 1).

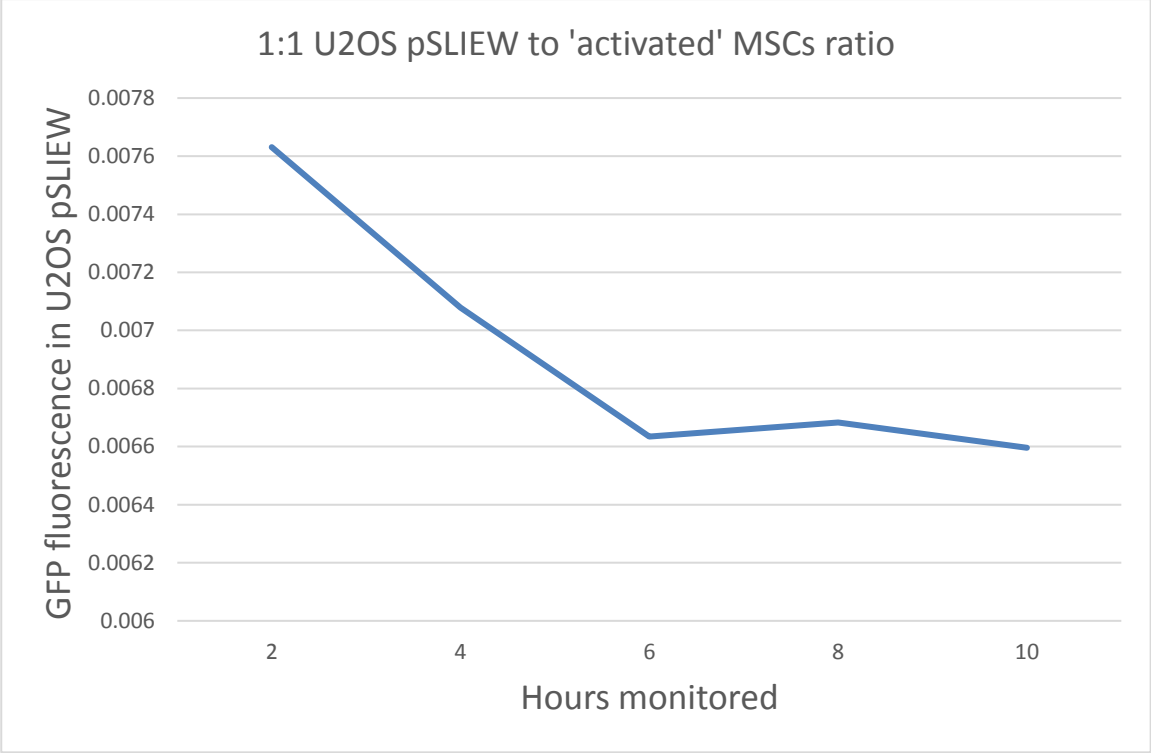

Figure 187 – Trend of reducing fluorescence over a 10-hour period in the U2OS pSLIEW cells cocultured with ‘activated’ MSCs.

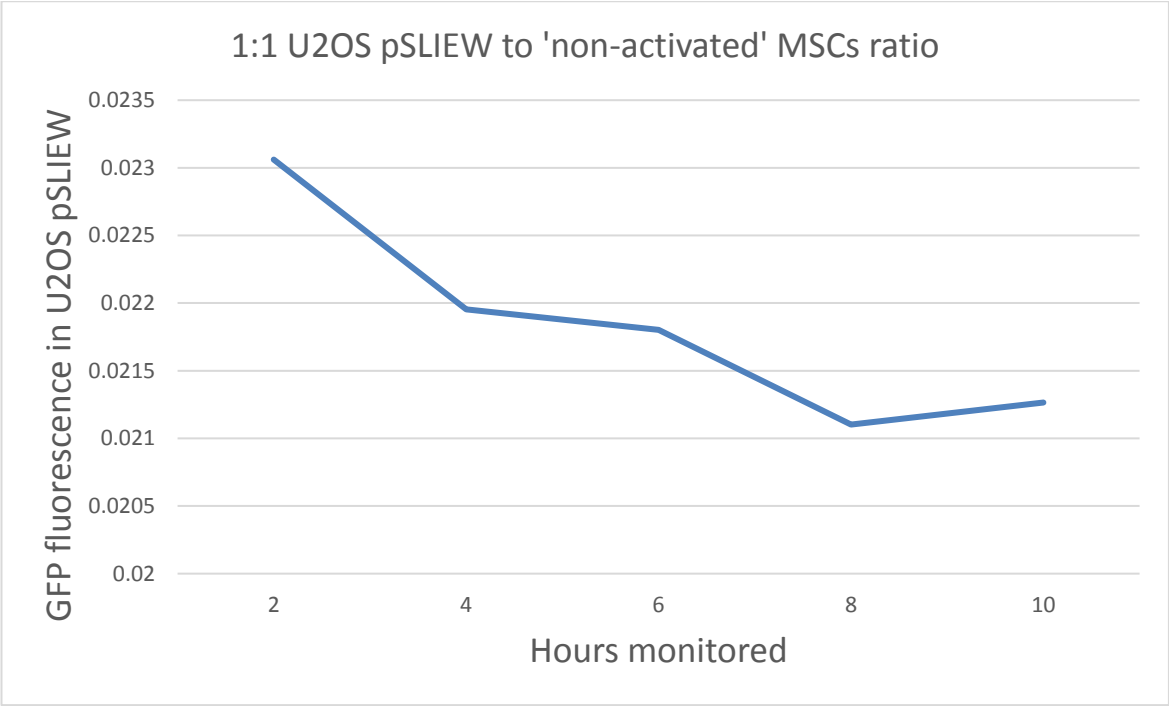

Figure 188 – Evidence of reducing florescence trend over a 10-hour period in the U2OS pSLIEW cells cocultured with 'non-activated' MSCs.

9.3.4 Cellular therapy in combination with doxorubicin

MSCs expressing TRAIL alone may be ineffective, and therefore, combination with other chemotherapeutics or irradiation has been shown to enhance efficacy and overcome resistance (Chapter 6). A number of chemotherapeutic agents such as doxorubicin, etoposide, 5-Flurouracil and irradiation have been found to increase levels of DR4 and DR5. Effect of chemotherapeutic agents on stem cell and sarcoma cell TRAIL expression has been less studied. Increased TRAIL expression in BMMSCs and cell death in MDA breast cancer cells has been found in cocultures with the addition of both doxorubicin and BMMSCs to the MDA cells (2 µM = 100 ng/ml) [329].

Effects of doxorubicin on BMMSCs and sarcoma cell surface TRAIL expression was assessed using flow cytometry. Treatment of TC71 Ewing's sarcoma cells with doxorubicin was found to increase surface levels of TRAIL (Figure 189). Enhanced TRAIL expression in both the BMMSCs and TC71 cells was observed with the addition of doxorubicin in a coculture and this resulted in greater cell death compared to the absence of doxorubicin in the coculture (Figure 190). About 80 % cell death was found previously with doxorubicin alone (2 µM) and greater when combined with

SuperKillerTRAIL (SKT) (Chapter 5) for the TC71 cell line versus about 40 % found in this experiment, which may reflect the sensitivity of the cell death assay (DAPI uptake vs cck-8) or actual degree of cell death and requires further investigation.

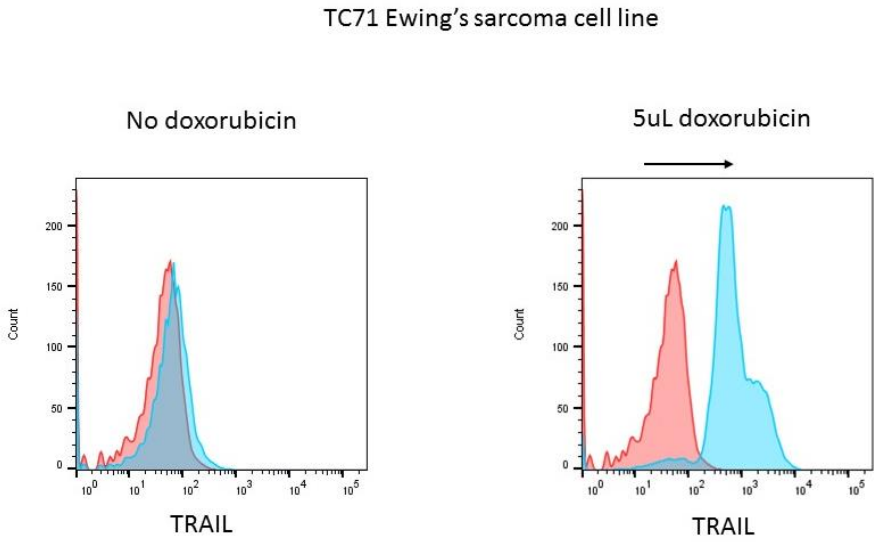

Figure 189 – Addition of doxorubicin to TC71 Ewing's cell line was found to increase the surface expression of TRAIL (red = unstained, blue = stained). Incubation time = 24 hours, doxorubicin concentration = 2 µM.

No Doxorubicin in coculture

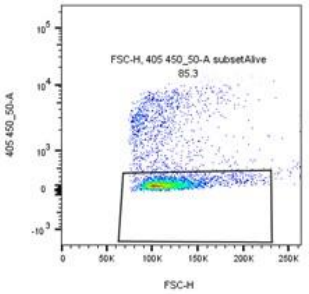

TC71

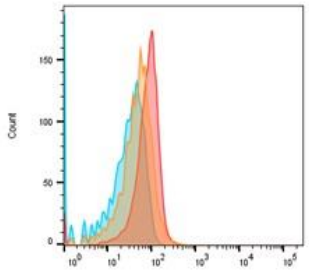

BMMSCs

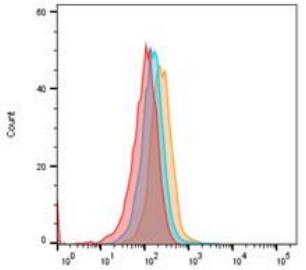

TC71 DAPI uptake - 15%

2uM Doxorubicin in coculture

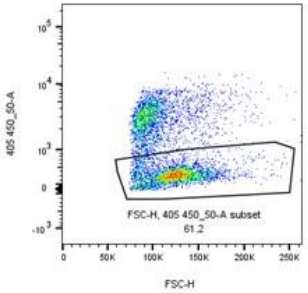

TC71

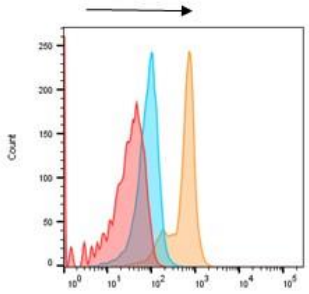

BMMSCs

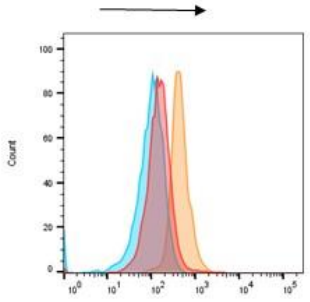

TC71 DAPI uptake - 39%

Red = unstained, blue = isotype control, orange=stained

Figure 190 – Addition of doxorubicin (2 μM) to BMMSCs then subsequent addition of TC71 Ewing's cell line after 48 hours in coculture was found to increase the surface expression of TRAIL in both cell lines at 120 hours (red = unstained, blue = isotype control, orange = stained). Surface TRAIL expression is not evident under normal conditions (absence of doxorubicin). Doxorubicin (2 μM) in TC71 and BMMSCs coculture increased surface TRAIL on both cell lines and increased TC71 cell death – 15 % alive (absence of doxorubicin) vs 39 % (with doxorubicin) as assessed by using DAPI uptake. Duration of coculture = 48 hours.

9.4 Discussion and future direction

In the current study, I investigated the preactivation of human mesenchymal stem cells (MSCs) with TNF-alpha following a report by Lee *et al.* 2012 [329]. The group treated MSCs derived from the bone marrow with TNF-alpha and found that with a dose of about as low as 0.1 ng/ml of TNF-alpha could stimulate the expression of TRAIL on the membrane of MSCs. They suggested that it was expressed on the membrane due to enhanced cytotoxic effects when directly co-cultured with breast cancer cell line MDA *in vitro*. They found increased protein levels of TRAIL using western blotting at 24- and 48-hours following exposure to 10 ng/ml TNF-alpha. They also found that there was evidence of increased expression of TRAIL using real-time PCR, in human MSCs (number of 1 x 10^5 cells) following 24-hour treatment with TNF-alpha or co-cultured with the MDA cells and TNF-alpha. They found that in an *in vivo* mouse model, administration of activated MSCs intravenously reduced the metastatic load in the lungs. The mice were treated for 11 weeks and the lung sections in the mice were analysed histologically. The evidence suggested that the TNF-alpha preactivated stem cells, suppressed tumour cell growth compared to control aided by a mechanism of homing of the stem cells to the tumour site.

I produced a similar model *in vitro* in which I exposed human bone marrow-derived mesenchymal stem cells to TNF-alpha up to 20 ng/ml and found that using flow cytometry there was a slight positive shift in membrane expression when compared to untreated stem cells and fibroblasts, which were untreated or treated. When I used a high concentration of FBS in the culture media, I found that there was no effect on the action of TNF-alpha when exposed to murine fibroblasts cell line expressing the TNF receptor one (MF TNF R1). Therefore, I treated the stem cells with a concentration of TNF-alpha that produced a shift on the flow cytometry and then exposed sarcoma cells to the activated stem cells and found evidence of increased cell death. This was significant when compared to fibroblasts exposed to TNF-alpha cultured with sarcoma cells. There was evidence that the ratio of stem cells two to one (twice as much stem cells compared to sarcoma cells) had significant effects.

It has been suggested by Lee *et al.,* (2012), that TNF-alpha can not only induce the expression of TRAIL, the mechanisms of which are unclear, but can also stimulate the expression of DKK3 from the MSCs, which can inhibit cell cycle progression in the MDA cells. They discussed that markers of cell cycle arrest, expression of cyclin D1, cyclin D3, were downregulated and upregulated P21. P21 is an inhibitor of the cyclin dependent kinases (CDKs). TNF-alpha had no significant effect on expression of cyclin D1, D3, and P21 in the MDA cells. These significant findings were found in the coculture. Also, to test whether the DKK3 up regulation in activated stem cells inhibited Wnt/beta-catenin-mediated cell cycle progression, in control MDA/ nonactivated stem cell cocultures, beta-catenin was present; however, in the co-cultures with activated stem cells, in the MDA cells, beta-catenin was markedly decreased [329].

The suggested mechanisms by which the stem cells expressed TRAIL after the exposure to TNF may be via Toll-like receptor 3 (TLR3), a specific receptor for RNA that increases NF-kB signalling and therefore triggers an essential step in the pathway for induction of TRAIL. Signalling via TNFR1 alone can increase NfkB-p65. There was an increase in the expression of TLR3 in the human MSCs in a previous study when incubated with TNF-alpha and this was further enhanced by coculture of the activated stem cells with the MDA cells. Increased expression of Toll-like receptor 3 was also observed when the stem cells were cultured with apoptotic MDA cells [329].

The majority of the literature, which has investigated the use of stem cells for cancer therapy have used viral transduction methods to enable the stem cells to express anti apoptotic proteins, such as TRAIL or OPG. However, the benefits of using pre-treatment of cells with TNF-alpha is that: (1) It avoids the complexities and dangers associated with viral transduction of the TRAIL gene and (2) delivery of the potent membrane tethered form of TRAIL, which I also found evidence for using flow cytometry and (3) production of the tumour suppressor protein DKK3 in high level of concentrations to cancers. They may also provide a therapy for metastatic cancers. In a separate experiment, the authors also discussed the benefits of using the chemotherapeutic agent doxorubicin along with the activated stem cells [329]. They discussed that a low dose of doxorubicin, backed up by their data, combined with the stem cells was enough to induce synergistic effects on apoptosis in the MDA cells

suggesting that this combination may be an effective therapy. I have also found this using crosslinked forms of TRAIL with doxorubicin in Chapter 6.

In a further study in 2015 [332], they demonstrated that the treatment of the human MSCs with a subtoxic dose of doxorubicin can help overcome TRAIL resistance. They treated stem cells with 20 ng/ml of TNF-alpha and found that the activated stem cells increased apoptosis in MDA cells when combined with a subtoxic dose of doxorubicin, which was mediated by upregulating TRAIL and Fas related pathways. They used the doxorubicin at a subtoxic dose of 100 ng/ml (0.2 nM). They again stressed the point that human MSCs not only express TRAIL to induce apoptosis, but also have a paracrine effect that triggers the cancer cells to undergo their own apoptosis.

The strengths of my study include using MSCs from a younger donor. The use of the stem cells was early-passage and early doubling time. This is of importance as it is thought that using stem cells beyond 20 population doublings in culture can reduce the ability of the biological properties of the stem cells, including their ability to express TRAIL upon TNF-alpha activation. The weaknesses of the investigation includes difficulty in finding a positive control cell line for TRAIL surface expression. Further study would require the use of more markers for cell death, as I only used DAPI uptake and loss of GFP expression and GFP transduced U2OS cells, which is more of a marker of late cell death; further study would use annexin V and PI as earlier markers of cell death. In future, I also wish to investigate the effect of activated stem cells on a different sarcoma cell line, HT1080 pSLIEW, GFP transduced, to see if I observe similar effects in this DR5 expressing cell line. It is interesting to note that from my data, a ratio greater than 1 to 1 of 'activated' stem cells to sarcoma cells, ideally 2 to 1 or 3 to 1 results in greater sarcoma cell killing and is preferred and supports the findings of a recent report by Guiho *et al.,* (2018) who used TRAIL transduced adipose stem cells in models of osteosarcoma at ratios higher than 1 to 1, which was found to be more effective [339].

Chapter 10. General discussion

10.1 General discussion

In the context of cancer therapy, the use of TNF-related apoptosis-inducing ligand (TRAIL) has been of great interest due to its ability to induce apoptosis in cancer cells while sparing non-malignant cells. Increasing investigation is taking place in areas such as discerning the significance and contribution of each death receptor (DR) to apoptosis in different cancers, resistance and mechanisms of toxicity in non-malignant cells. In my study, DR5 was expressed in all of the sarcoma cell lines and is preferentially activated by crosslinked TRAIL.

Both DR4 and DR5 receptors are often co-expressed in tumour cell lines and loss of DR4 can be found in many tumour cell lines. TRAIL receptor DR5 deficiency in DR4 expressing cells is rare but has been described in the human erythroleukemia cell line [340]. This is consistent with my findings as I did not find a bone sarcoma cell line that expresses DR4 and not DR5. Stimulation through DR5 can have pro-motile non-canonical effects such as in the colorectal cancer HCT116 cell line. DR4 may also induce tumour cell motility and contribute to metastases *in vivo* like DR5 [338]. Research has shown that like DR5, DR4 is always able to contribute to unresolved UPR-mediated apoptosis. In the course of ER stress, DR4 engages in the macromolecular complex including FADD, caspase 8, and contributes to apoptosis induced by ER stress inducers [338]. Of interest, is the lack of DR4 expression in the majority of the sarcoma cell lines in my study. Recent studies investigating this receptor suggest that it may be the more important receptor for the induction of apoptosis. This was investigated by DuFour *et al.,* 2017 and using a gene editing TALEN based method, the loss of the DR4 impairs caspase 8 activation within the TRAIL DISC in the colorectal cancer HCT116 and SW480 cell lines and the breast cancer MDA-MB-231 cell line after stimulation with his-TRAIL [341]. Further investigation is required in the mesenchymal in origin sarcoma cell lines.

However, DR5 in general has attracted more attention than DR4, this is evident as only one anti-DR4 antibody known as mapatumumab has been assessed in clinical trials whereas five distinct anti-DR5 antibodies have been tested. This is likely due to the fact that it is increased in more cancer cell lines and also owing to the fact that its expression is more prone to transcriptional regulation by genotoxic or non-genotoxic compounds and that its increase in expression is associated with an increased

sensitivity to TRAIL-induced cell death [341]. Also, TRAIL binding affinity to DR5 can be slightly stronger than DR4 in the following cell lines: The H1703 cell line, which is derived from stage 1 lung squamous cell carcinoma; HCT-116, from a human colon cancer cell line; and the MDA-MB-231 cell line, which is a human breast adenocarcinoma cell line [341]. An avenue for further investigation is confirming this degree of binding affinity to DR5 in sarcoma cell lines.

Resistance in non-malignant cells

Possible explanations for the increased resistance of the fibroblasts include the slower cell division time and through the incomplete activation of initiator caspase 8. In a study using an agent to inhibit the ubiquitination of caspase 8, it was found that normal human fibroblast cell line could be sensitised to TRAIL-induced apoptosis by using PR-619, a deubiquitinase inhibitor [342]. This increases the normal fibroblast caspase 8 ubiquitination and thereby susceptibility to TRAIL-induced cell death. It was found that there is decreased basal caspase 8 ubiquitination in the fibroblasts compared to colon cancer cells SW480 and DLD-1 [340].

Poor prognosis in head and neck squamous cell carcinoma is linked to decreased caspase 8 expression which is also present in a variety of malignancies [343]. Treatment with HDAC, deubiquitinase inhibitors or DNA methyltransferase inhibitors has been shown to increase the caspase 8 expression and improve TRAIL sensitivity in a variety of tumour cells. Also, these agents have been proposed to inhibit tumour progression in several solid tumour models. Normal fibroblasts can have a reduced caspase 8 protein and mRNA expression; however, deubiquitinase inhibitor combination with TRAIL may cause normal cell toxicity and should be examined carefully [344].

Summary of *in vitro* and *in vivo* data and future direction

In conclusion, the NG2 targeted TRAIL therapeutic, ScFv(NG2)-Fc-TRAIL, is potent *in vitro*, particularly in bone sarcoma cell lines expressing both DR5 and NG2 such as the HT1080 dedifferentiated chondrosarcoma cell line and the MG63 osteosarcoma cell line. This was also evident *in vivo* in what I have described as the first developed xenograft model of dedifferentiated chondrosarcoma. This model will not only be

useful for further analysis of this agent but also studies looking to enhance imaging for sarcoma surgery. TRAIL-induced bone sarcoma cell death might be able to be enhanced when combined with agents such as current chemotherapeutics (doxorubicin) and more novel agents such as Smac mimetics. This type of combination therapy (particularly with the targeted forms of TRAIL) holds great promise for the more resistant sarcomas and to help personalise therapy depending on types of pro and anti-apoptotic factors that may be expressed in the malignant tissue. There should be a focus on how the novel sensitisers compare with conventional chemotherapeutics and the degree to which effective combinations also affect non-malignant cells.

While, no significant toxicity was observed in the mouse model used in my study, supporting previous investigations using TRAIL in humans, further assessment of particularly liver and heart toxicity, drug targeting, dosing and drug stability needs to be undertaken in further animal models and humans. There is a requirement for the assessment and immunophenotyping of DR5 and NG2 expression in primary cells and patient tissue to assess the potential suitability of these patients for targeted TRAIL therapy, and its effectiveness which can be explored by utilising ScFvNG2-Fc-scTRAIL in a PDX derived bone sarcoma mouse model.

I have demonstrated that a novel TRAIL therapeutic tested, ScFvNG2-Fc-scTRAIL has a significant cytotoxic effect on cell lines expressing both DR5 and the TAA of interest (NG2) when tested *in vitro* and *in vivo* in the first developed xenograft model of dedifferentiated chondrosarcoma. These cytotoxic effects can be enhanced further with doxorubicin as demonstrated. Such combinations would minimise the risk of treatment failure due to drug resistance, a commonly observed problem of single agent approaches. Furthermore, these findings provide a framework for the clinical development of ScFvNG2-Fc-scTRAIL and could potentially be used in the neoadjuvant setting, which would be a shift from the usual convention of prioritising excision of the sarcoma.

Chapter 11. Appendix

The following data has been included to give the reader a full account of results presented in Chapters 3 to 9.

11.1 Flow cytometry

11.1.1 Using fixed or unfixed cells for flow cytometry

A decision was made to use unfixed live cells kept on ice and analyse on the same day, or stain then fix the cells if the analysis was going to be delayed. The strategies demonstrated a similar degree of histogram shift when gating on the live cells (Figure 191 and Figure 192).

a. Stained but not fixed

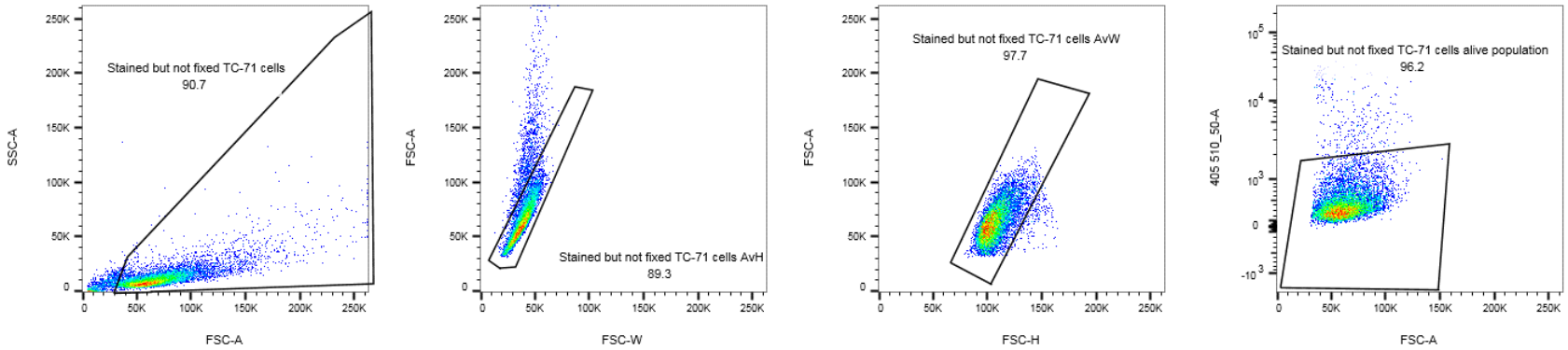

b. Stained then fixed with 4 % paraformaldehyde (PF)

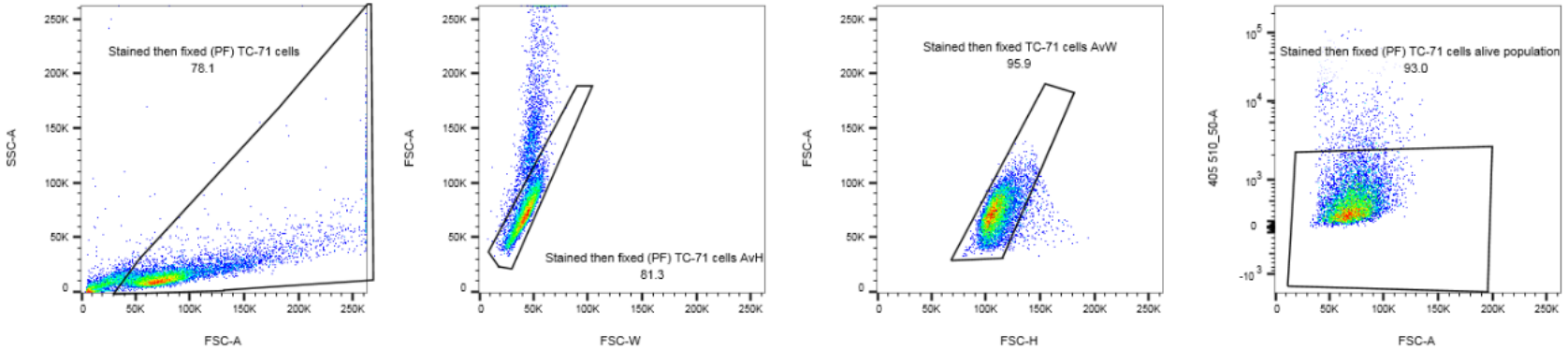

Figure 191 - Cells were either (a) stained but not fixed before analysis or (b) stained then fixed before analysis. Fixation of the cells with 4 % paraformaldehyde (PF). The aqua fluorescent live/dead stain (bandpass filter 405 510_50-A) was used to select for the live cells.

(a)

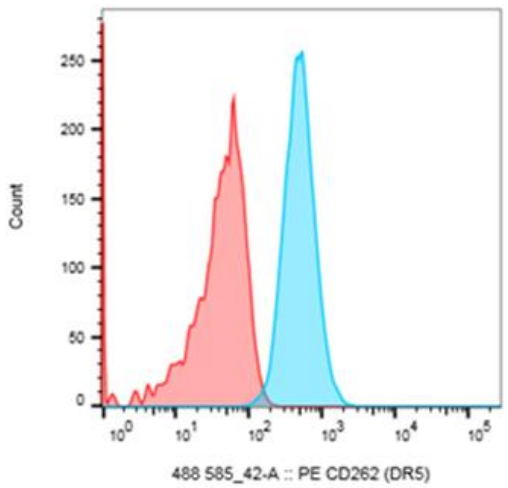

	Sample Name	Subset Name	Count	Median : 488 585_42-A
	245974.fcs	Stained but not fixed TC-71 cells alive population	8182	489
	245970.fcs	Unstained and fixed (FB) TC-71 cells AvW	7829	40.0

(b)

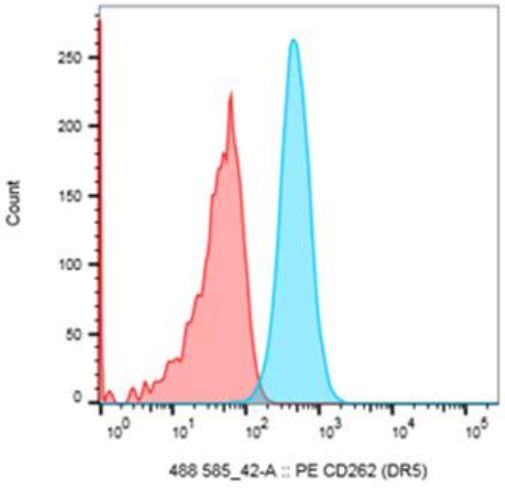

	Sample Name	Subset Name	Count	Median : 488 585_42-A
	245976.fcs	Stained then fixed (PF) TC-71 cells alive population	6788	462
	245970.fcs	Unstained and fixed (FB) TC-71 cells AvW	7829	40.0

Figure 192 - There was similar degrees of histogram shift in DR5 staining of the live TC71 Ewing's sarcoma cells whether: (a) unfixed (MFI = 489) (b) stained then fixed (MFI = 452). Unstained MFI = 40. Decision was made to use unfixed cells. MFI = median fluorescence intensity.

11.1.2 Example flow cytometry gating strategy for measuring surface expression of DR4 and DR4 in MG63 osteosarcoma cell line

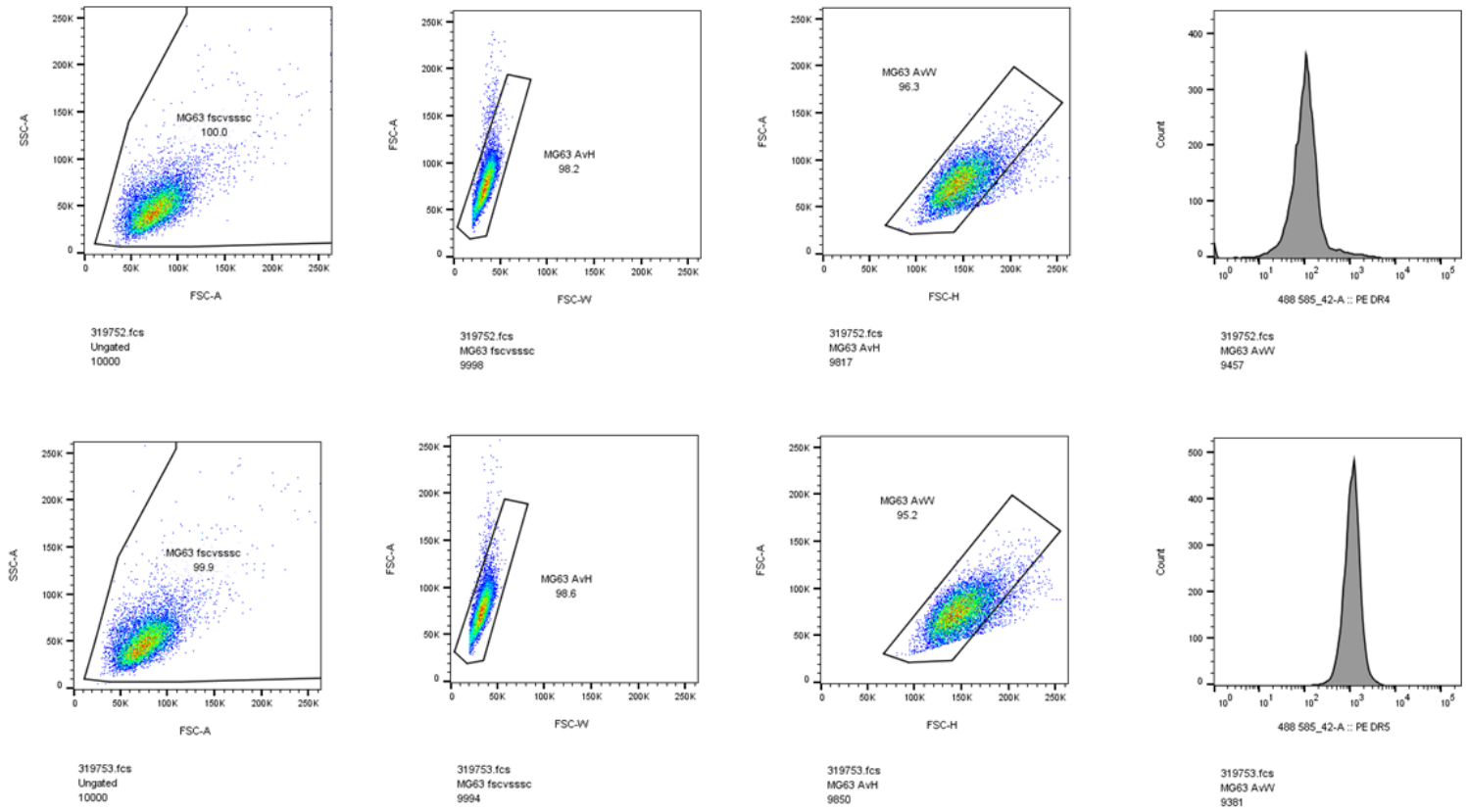

Figure 193 – Flow cytometry gating strategy for analysis of DR4 and DR5 surface expression in MG63 osteosarcoma cell line.

11.2 Protein analyses

11.2.1 BCA standard curve

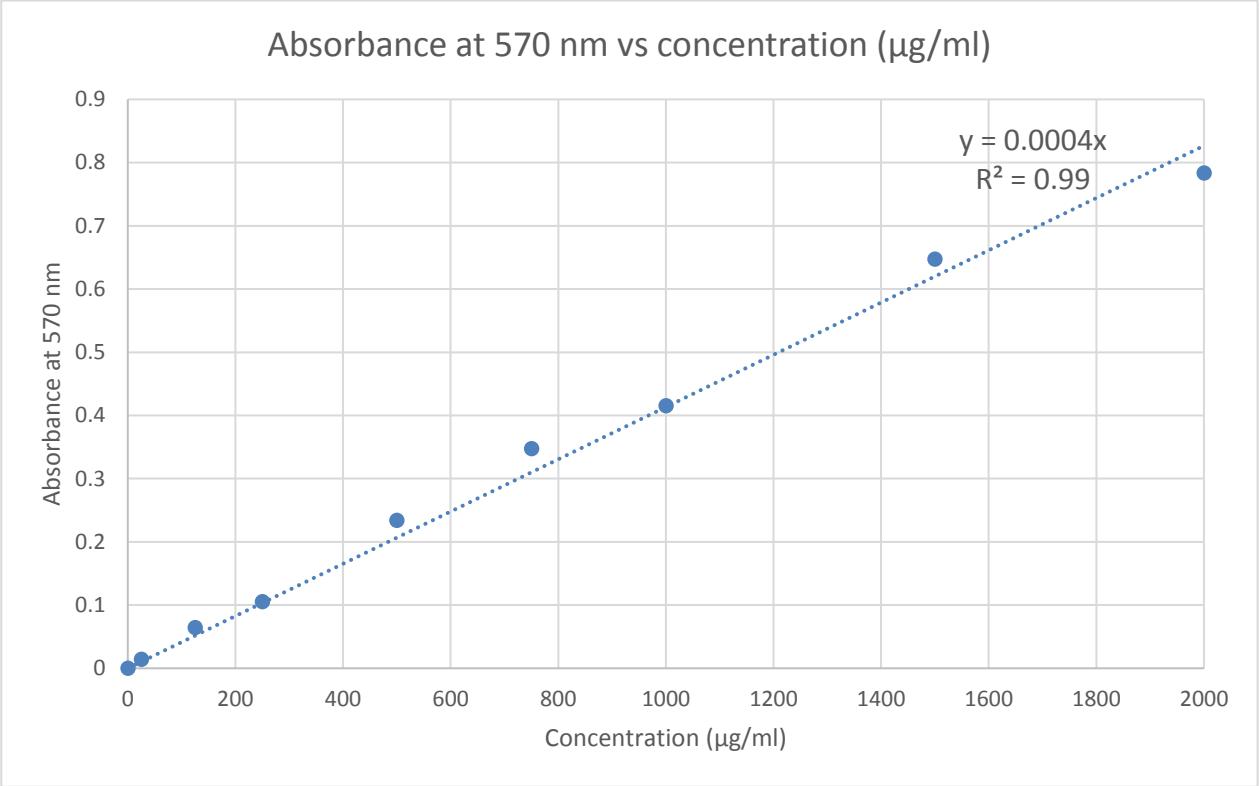

Figure 194 - An example of a standard curve formulated using BSA standards to estimate the protein concentrations of unknown samples (R^2 = 0.99).

11.2.2 Rationale for antibodies used in western blotting

Both monoclonal and polyclonal antibodies were used. Preference was given to monoclonal antibodies due to the few advantages they have in comparison to polyclonal antibodies in the following aspects:

•Due to their high specificity, monoclonal antibodies will often give significantly less background.

•Homogeneity of monoclonal antibodies is very high relative to polyclonals. If experimental conditions are kept constant, results from monoclonal antibodies will be highly reproducible between experiments.

•High specificity makes them extremely efficient for the binding of an antigen within a mixture of related molecules, such as during affinity purification.

Death receptor 5 (DR5)

(1) DR5 monoclonal antibody from Abcam® Recombinant Antibodies. The immunogen used to raise the anti-DR5 antibody [EPR1659(2)] (ab181846) is at amino acids 426 to 440 expected to recognise the precursor and the mature form of both long and short isoform [345].
(2) DR5 monoclonal antibody from Cell Signaling Technology (CST)(D4E9) XP® Rabbit mAb, was created using a synthetic peptide corresponding to residues surrounding Arg260 within the cytoplasmic region of human DR5 protein. Therefore, this antibody detects both the short (apparent MW of 40 kDa) and long (apparent molecular weight of 48 kDa) isoforms of DR5. Any additional bands are most likely due to glycosylation of the long and short isoforms of DR5.

Death receptor 4 (DR4)

(1) Monoclonal mouse anti-DR4 antibody from Abcam [32A242] (ab13890). This was raised against an immunogen at amino acids 1-20. A newly described bDR4 isoform [202] corresponds to amino acids 169-236 of the DR4 and, therefore, it was noted that the antibody would not be able to detect this bDR4.
(2) Monoclonal rabbit anti-DR4 antibody (D9S1R, Cell Signaling Technology)

Polyclonal antibodies for DR4 and DR5

DR5 (ab8416)/DR4 (ab8414) antibody (abcam polyclonal), were also utilised for IHC and western blotting applications respectively.

Ab8416 is a synthetic peptide corresponding to human DR5 aa388-407. This DR5 antibody was raised against a peptide corresponding to 20 amino acids near the carboxy terminus of human DR5 precursor. The immunogen is located within the last 50 amino acids of DR5. Based on the immunogen information, both ab181846 (above) and ab8416 are expected to recognise the precursor and the mature form of both long

and short isoform. Thus, they should produce the same outcome with respect to the protein target. Ab8414 is a synthetic peptide corresponding to human DR4 aa450-468.

Tumour necrosis factor-related apoptosis-inducing ligand (TRAIL)

(1) TRAIL (C92B9) rabbit monoclonal antibody was obtained from Cell Signaling Technology (CST) for western blotting applications.

Glyceraldehyde 3-phosphate dehydrogenase (GAPDH)

(1) GAPDH rabbit monoclonal antibody XP® (D16H11, Cell Signaling Technology) was used as the housekeeping protein for western blotting applications.
(2) GAPDH mouse monoclonal antibody (D4C6R, Cell Signaling Technology)

Lamin A/C

(1) As part of subfractionation experiments, for the nuclear fraction, an antibody was used to detect Lamin A/C (4C11, Cell Signaling Technology), which was used as the housekeeping protein for this fraction.

11.3 Cell proliferation assay optimisation

11.3.1 Quant-iT™ PicoGreen™ dsDNA Assay Kit

Principle and purpose: This is a sensitive fluorescent nucleic acid stain for quantifying double-stranded DNA (dsDNA) in solution. The kit accurately measures DNA from many sources including genomic DNA and from PCR amplification products. For the Quant-iT™ PicoGreen™ dsDNA Assay Kit (Thermo Fisher Scientific), the fluorescence reading was taken at an excitation wavelength of 480 nm and an emission wavelength of 520 nm.

Cell proliferation assay optimisation

Cell proliferation assays measure the number of metabolically active cells, but the assays may not reflect this accurately due to non-linearity and miscorrelating changes in activity and cell number over time in culture [346]. An experiment initially carried out using the PrestoBlue® Cell Viability Reagent and the Quant-iT™ PicoGreen™ dsDNA Assay Kit revealed that in the HT1080 cell line at the higher cell number (15000 cells per well of a 96-well plate), there was a reduction in the signal obtained when incubated for 1.5 hours; however, when measuring total DNA content in the wells it remained in correlation with the number of cells seeded (Figure 195 and Figure 196). For the main cell lines and assay to be used, it was ideal to carry this out to determine the appropriate cell numbers to seed and incubation time to be used to define a working range when assessing the activity of a drug.

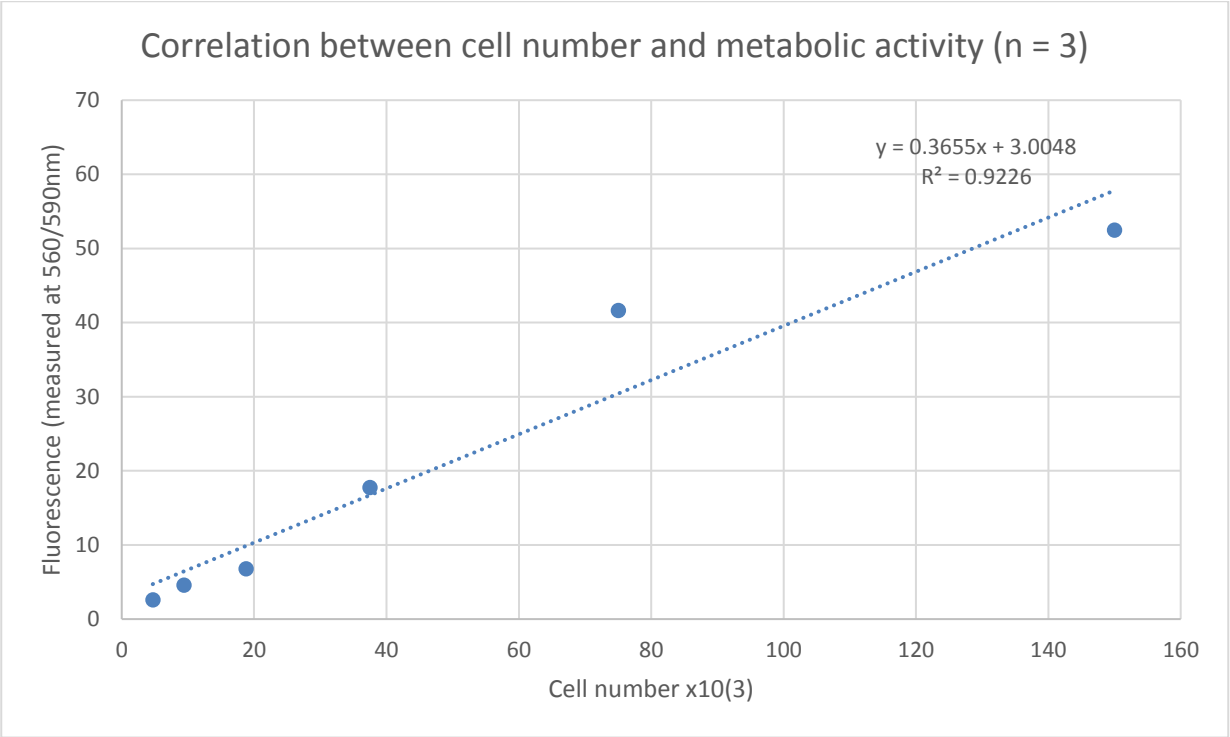

Figure 195 – HT1080 metabolic activity measured using the PrestoBlue® Cell Viability Reagent. Positive correlation is observed between cell number and proliferative activity; however, above 1.4x10^5 cells/well a reduction in HT1080 fluorescence absorbance is observed potentially due to high confluency and/or insufficient substrate.

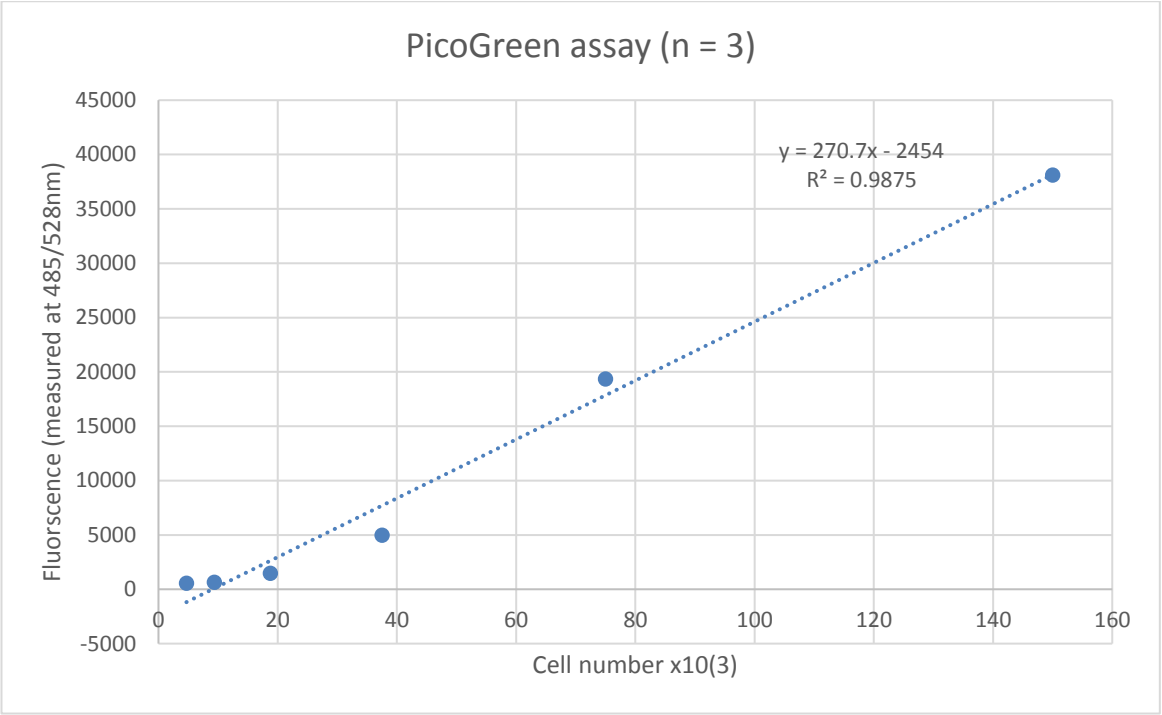

Figure 196 - Using the same plate as in Figure 29, it can be seen that at the higher HT1080 cell number the DNA content is in correlation as measured by using the Quant-iT™ PicoGreen™ dsDNA Assay Kit.

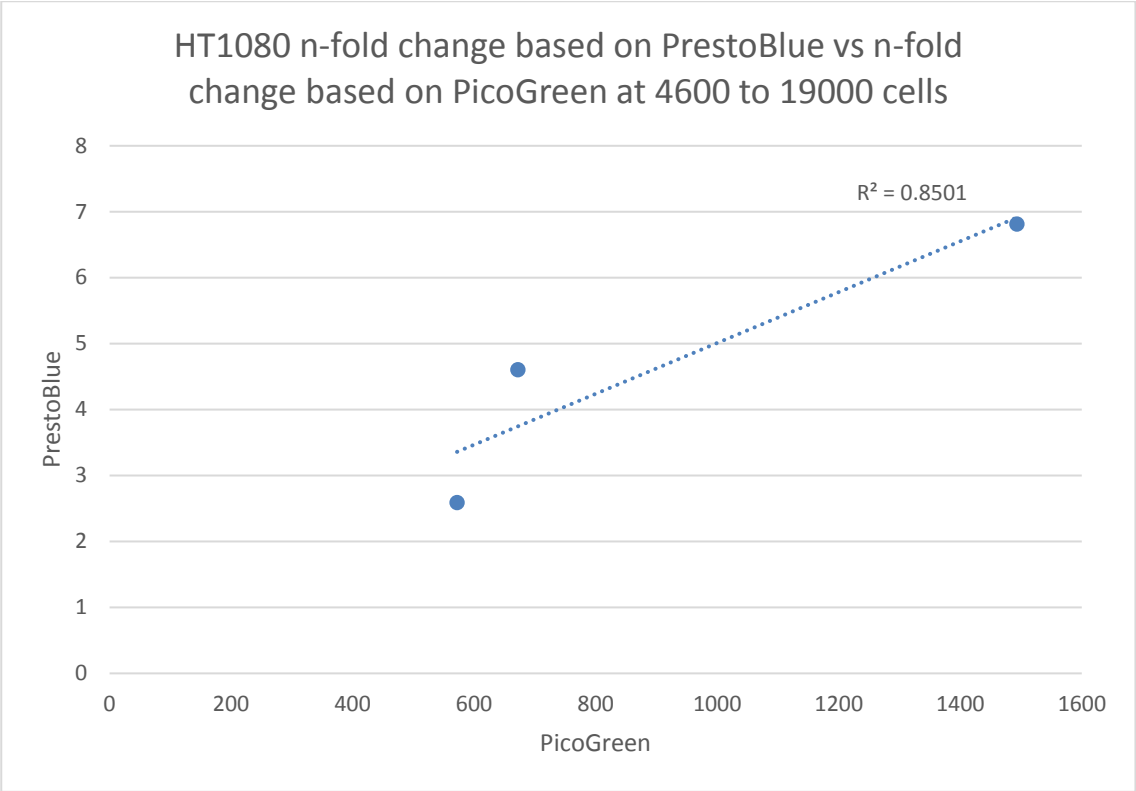

Figure 197 - HT1080 n-fold change based on PrestoBlue vs n-fold change based on PicoGreen at 4600 to 19000 cells.

Standard curves were plotted using osteosarcoma (U2OS), Ewing's sarcoma (TC71), chondrosarcoma (SW1353) and dedifferentiated chondrosarcoma (HT1080) cell lines in 96-well plates titrating from low to high cell numbers. There was a correlation between proliferative activity [using the CCK-8/Wst-8 assay (1:10 substrate to media ratio) incubated for 3 hours] and cell number and the linear range was found to be around 1000 to 20000 cells for all cell lines. Assay sensitivity was low at cell numbers below 1000; however, there was better correlation between Wst-8 and Quant-iT™ PicoGreen™ dsDNA Assay Kit results for cell numbers lower than 20000 when compared to PrestoBlue and PicoGreen. Therefore, the 5000 cell number was chosen as the seeding density for all cytotoxicity experiments and the tetrazolium based Wst-8 assay was used.

U2OS osteosarcoma cell line

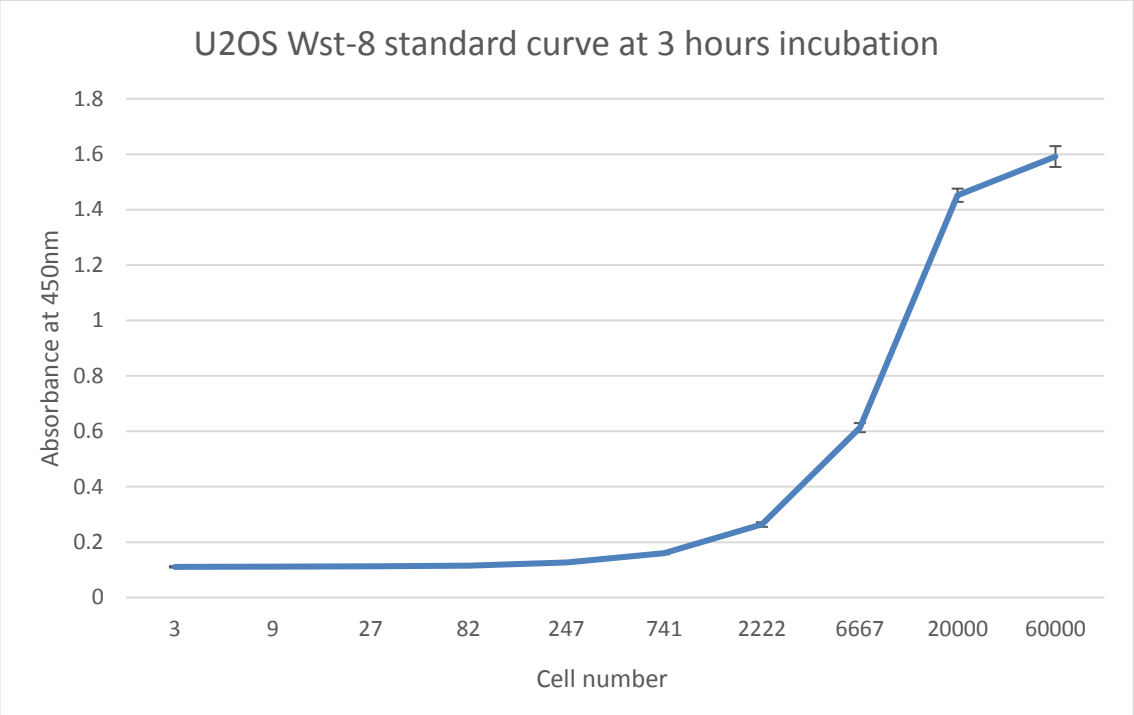

Figure 198 - U2OS standard curve demonstrating linear range from about 2000-20000 cells (mean+/-SEM, n = 3).

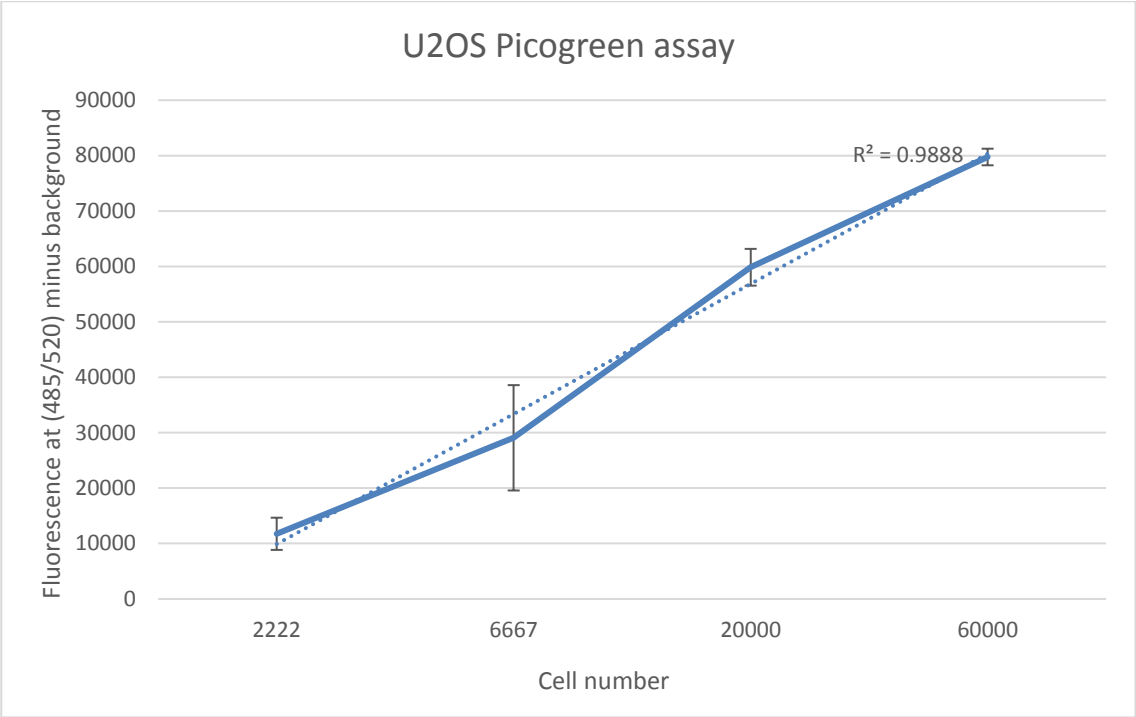

Figure 199 - Correlation between calculated cell number and DNA content in the linear range quoted above is R^2 = 0.99 (mean +/-SEM, n = 3).

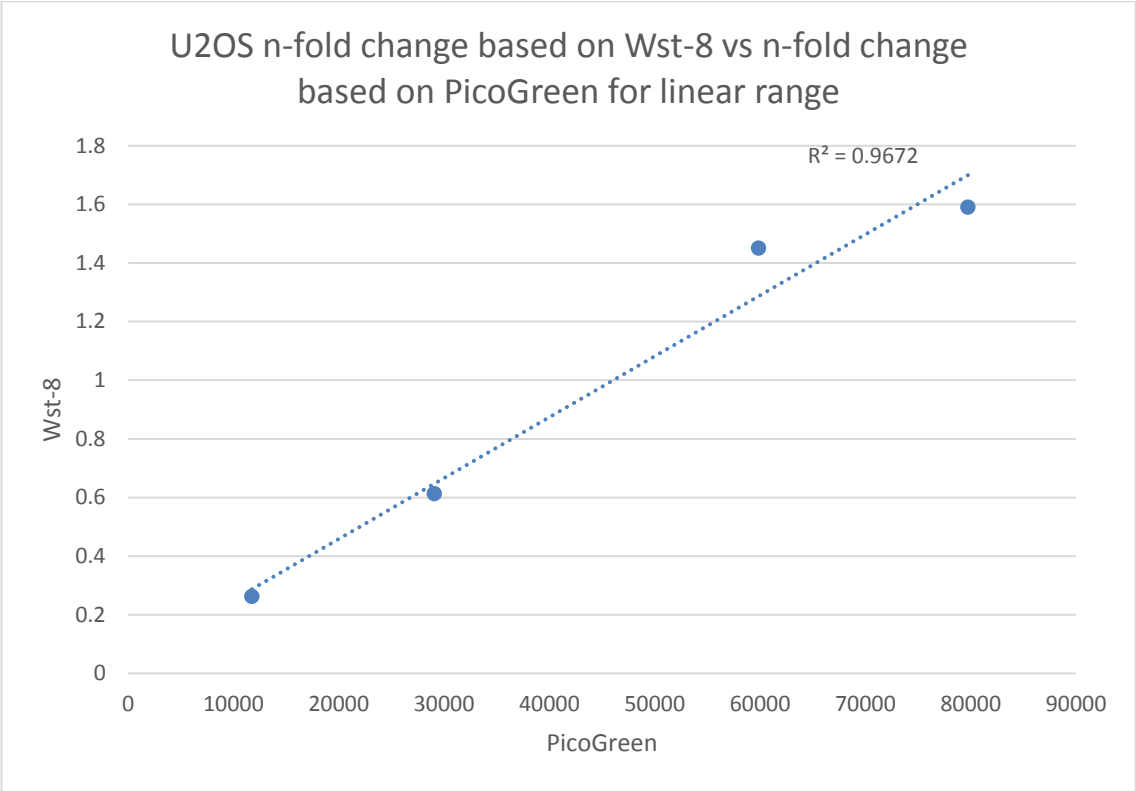

Figure 200 – U2OS n-fold change based on Wst-8 vs n-fold change based on PicoGreen for linear range.

TC71 Ewing's sarcoma cell line

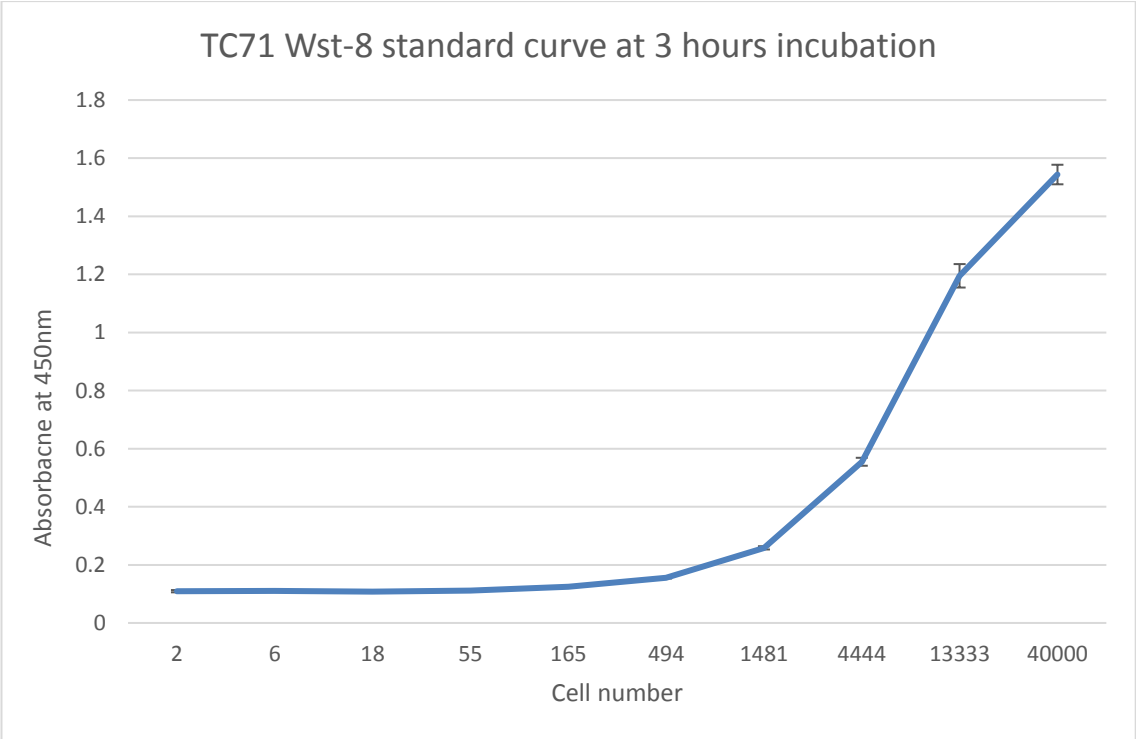

Figure 201 - TC71 standard curve demonstrating linear range from about 1000-20000 cells (mean+/-SEM, n = 3).

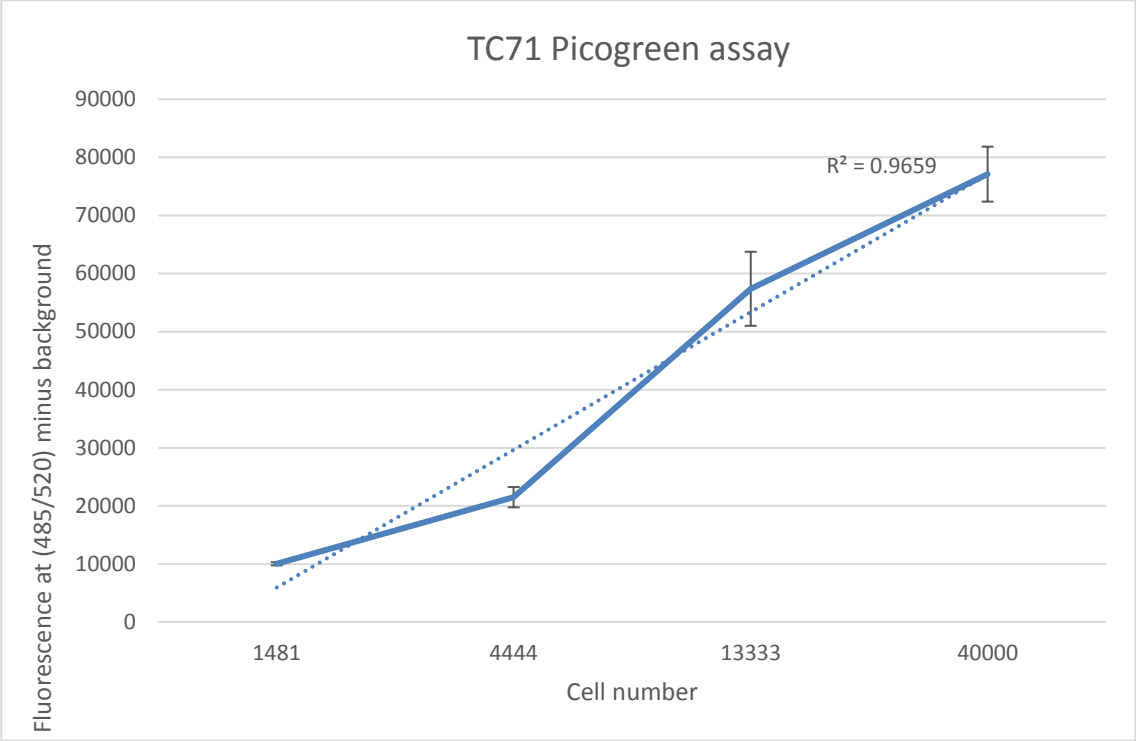

Figure 202 - Correlation between calculated cell number and DNA content in the linear range quoted above is R^2 = 0.97 (mean+/-SEM, n = 3).

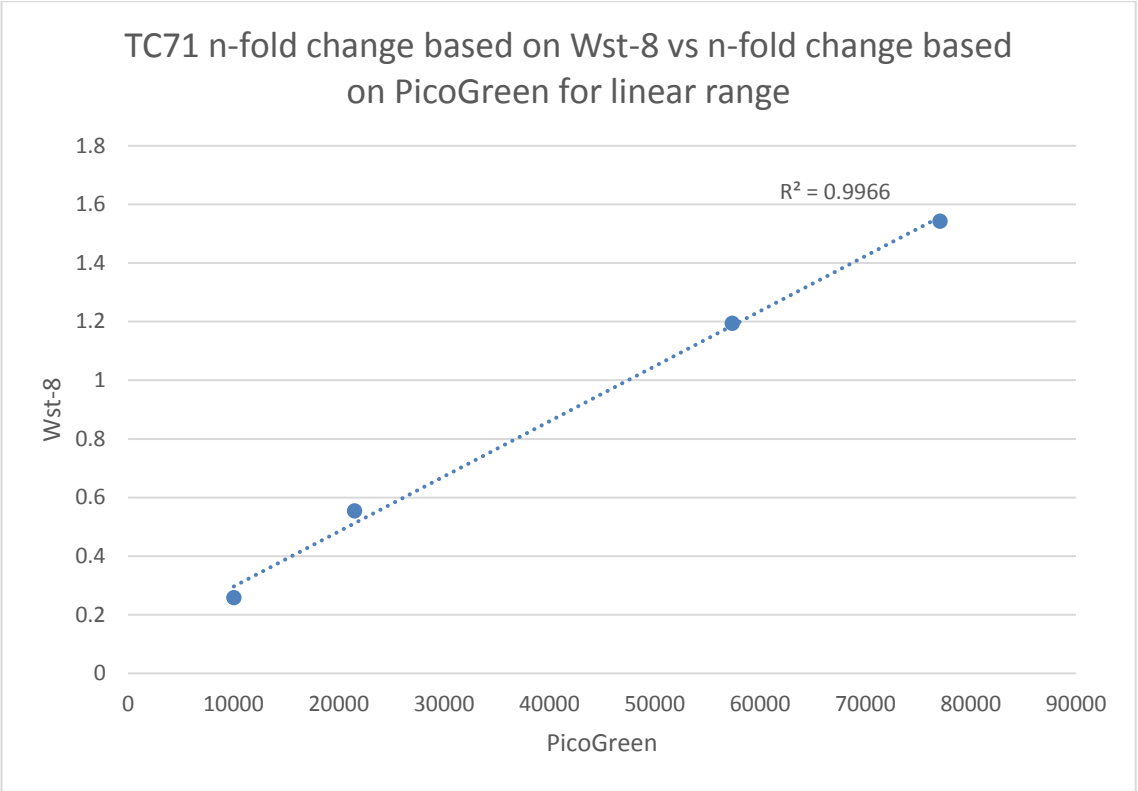

Figure 203 – TC71 n-fold change based on Wst-8 vs n-fold change based on PicoGreen for linear range.

SW1353 chondrosarcoma cell line

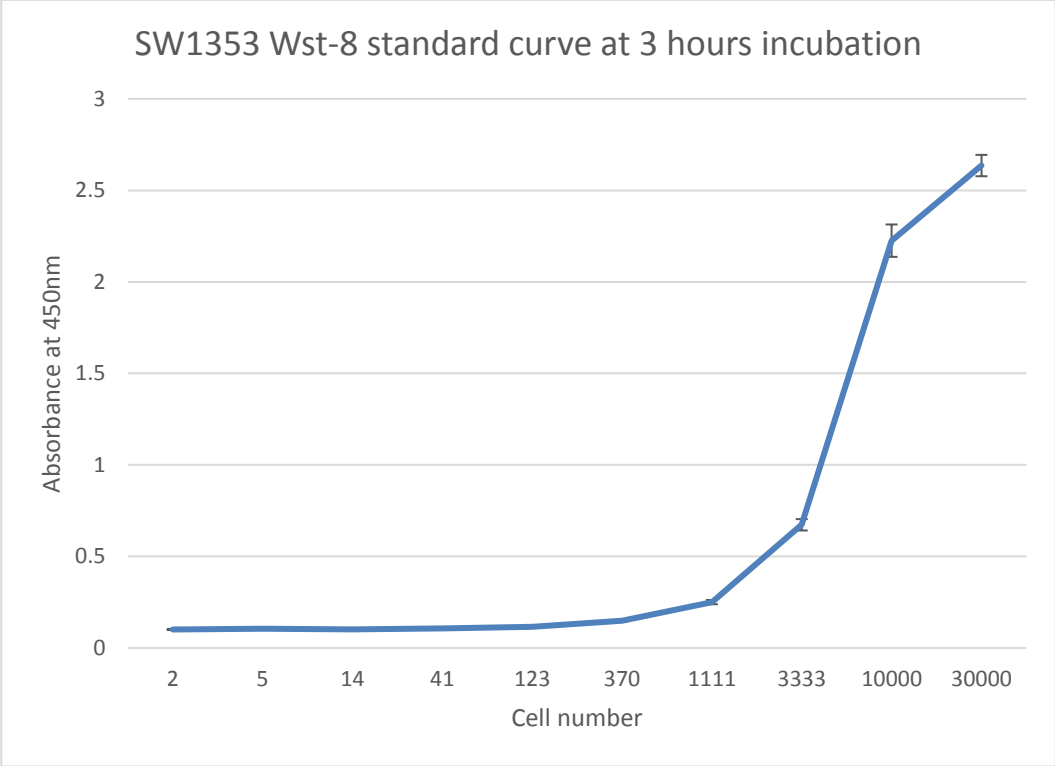

Figure 204 - SW1353 standard curve demonstrating linear range from about 1000-10000 cells (mean+/-SEM, n = 3).

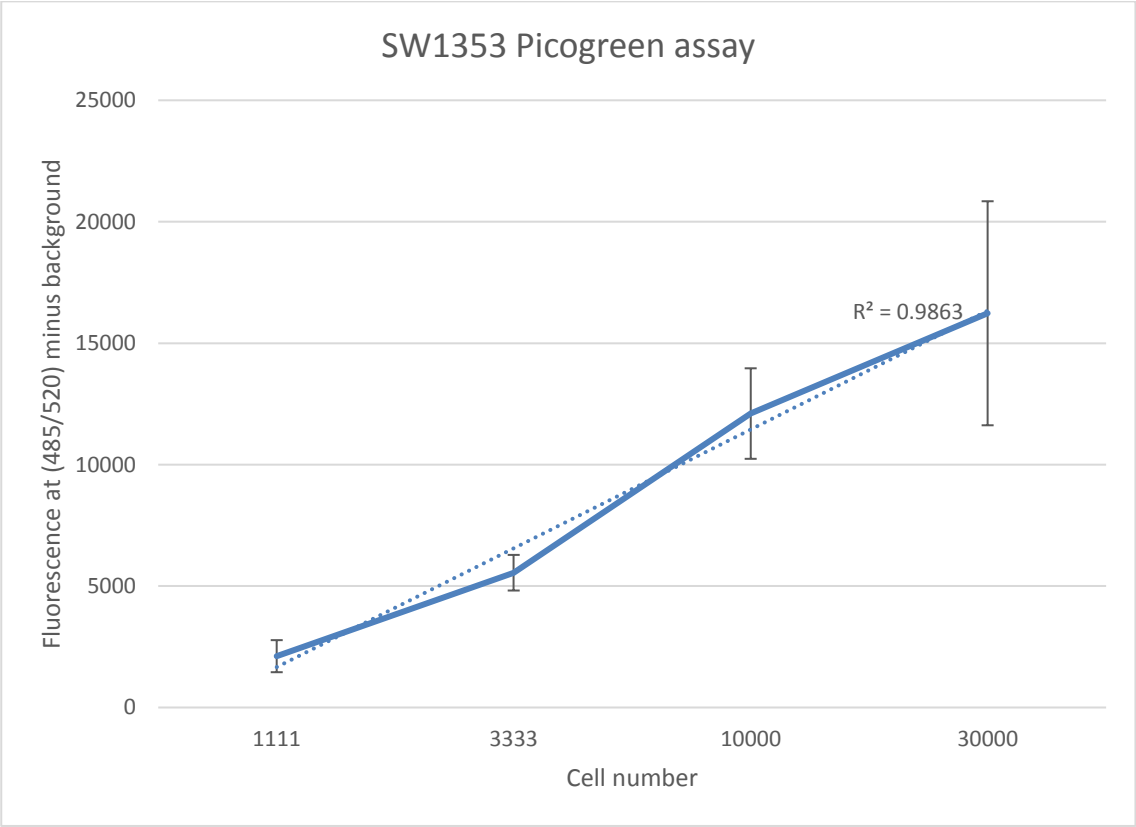

Figure 205 - Correlation between calculated cell number and DNA content in the linear range quoted above is R^2 = 0.99 (mean+/-SEM, n = 3).

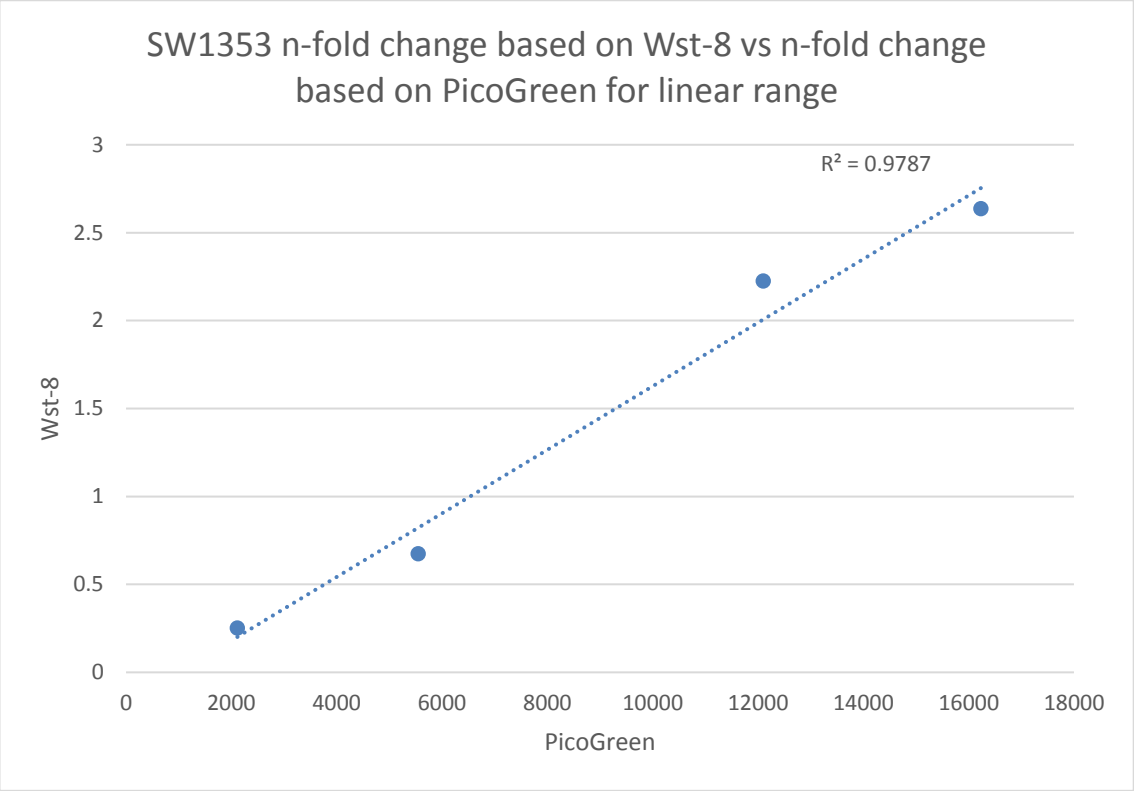

Figure 206 – SW1353 n-fold change based on Wst-8 vs n-fold change based on PicoGreen for linear range.

HT1080 dedifferentiated chondrosarcoma cell line

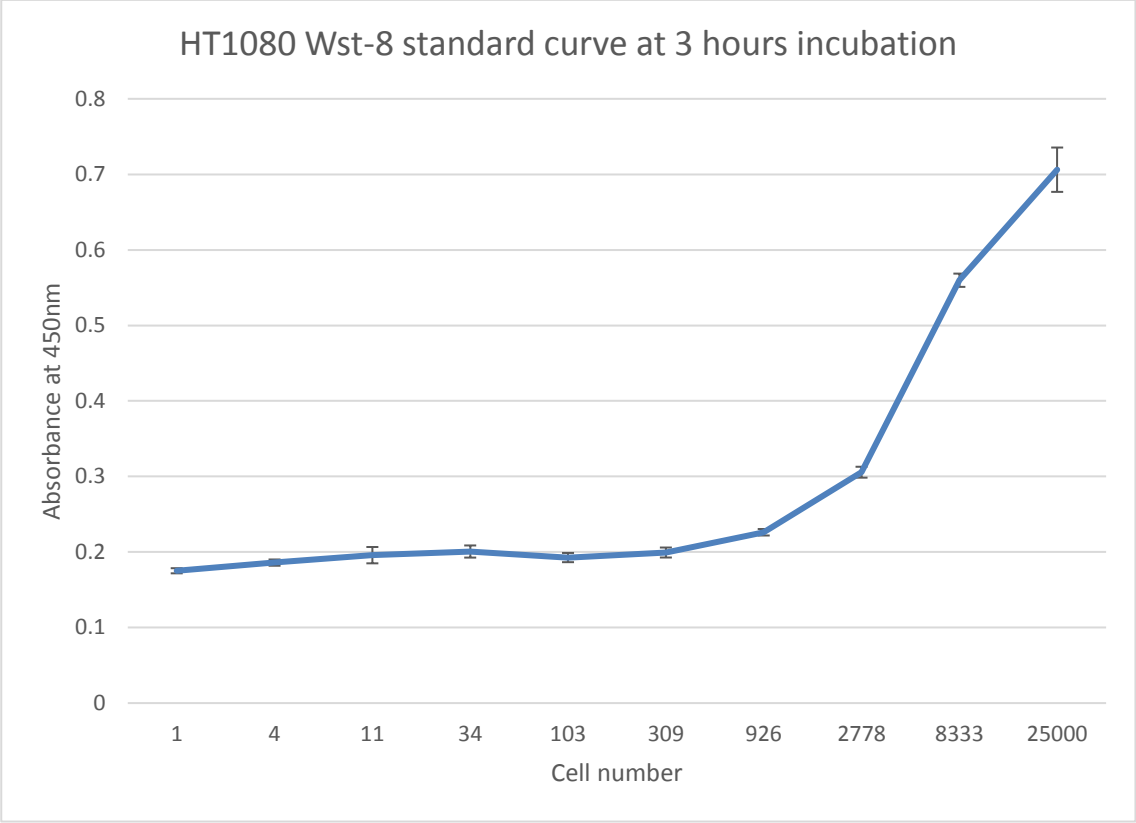

Figure 207 - HT1080 standard curve demonstrating linear range from about 1000-20000 cells (mean+/-SEM, n = 3).

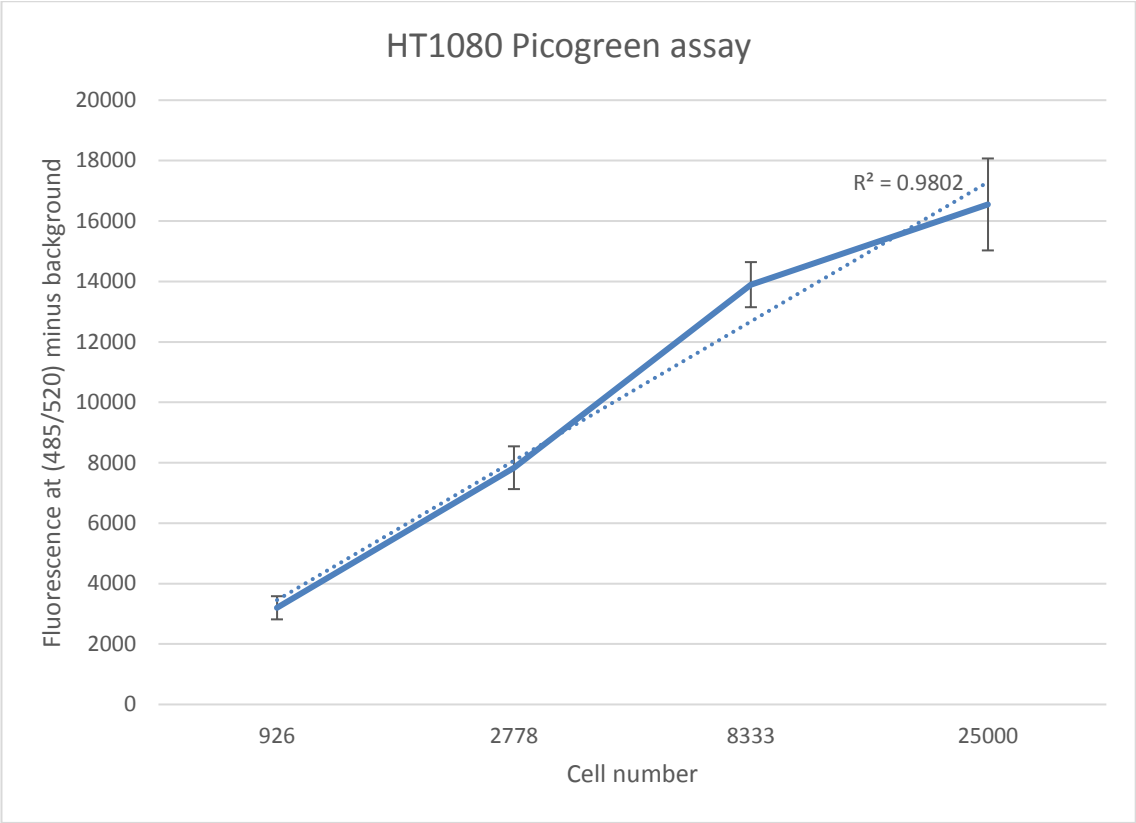

Figure 208 – Correlation between calculated cell number and DNA content in the linear range quoted above is R^2 = 0.98 (mean +/-SEM, n = 3).

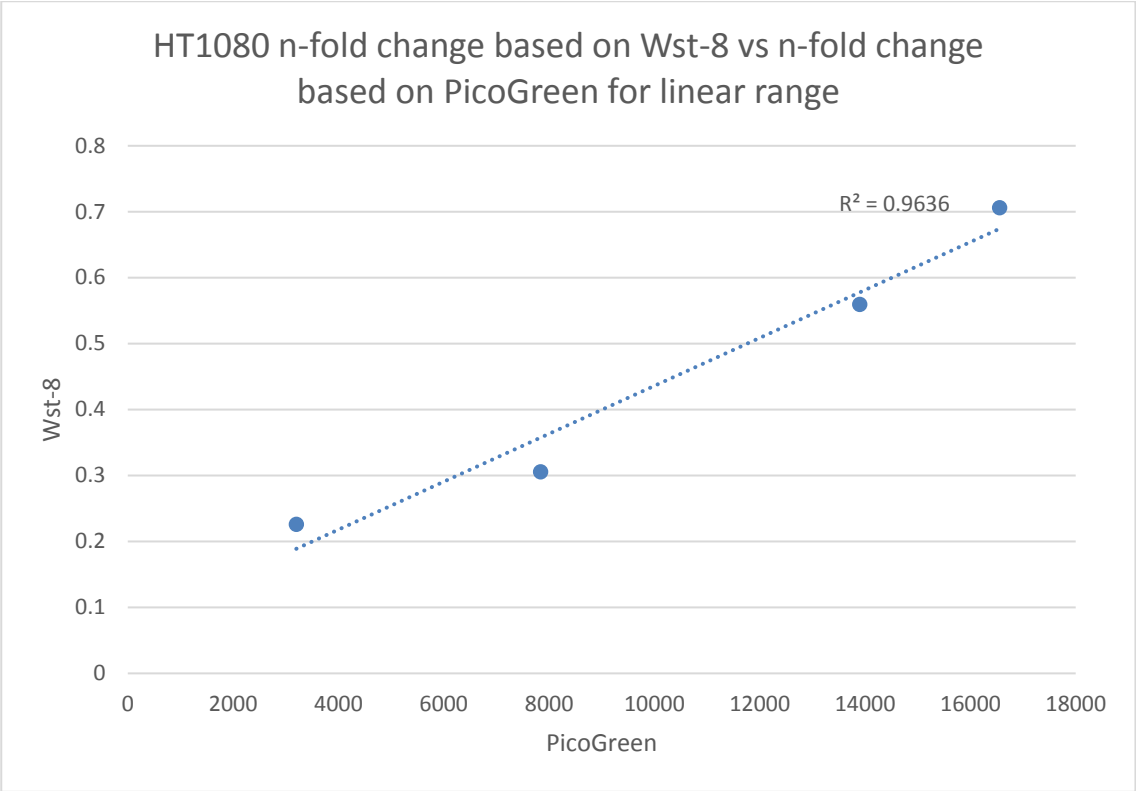

Figure 209 – HT1080 n-fold change based on Wst-8 vs n-fold change based on PicoGreen for linear range.

11.4 IncuCyte® live-cell imaging system cell seeding optimisation

U2OS osteosarcoma cell line

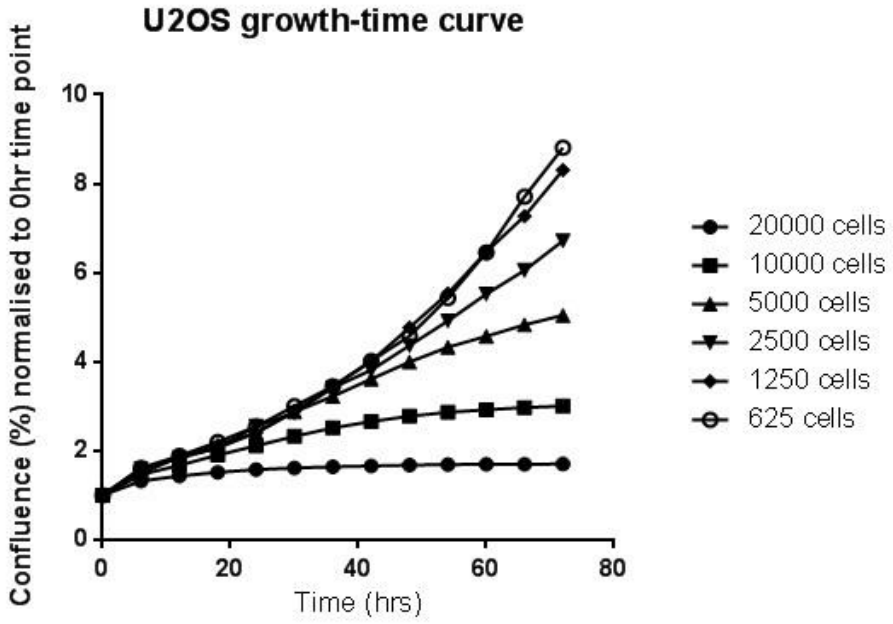

Figure 210 - Growth-time curves of U2OS cell line seeded at different cell numbers in a 96-well plate. Exceeding 5000 cells seeded would not be recommended to detect a change after treatment.

TC71 Ewing's sarcoma cell line

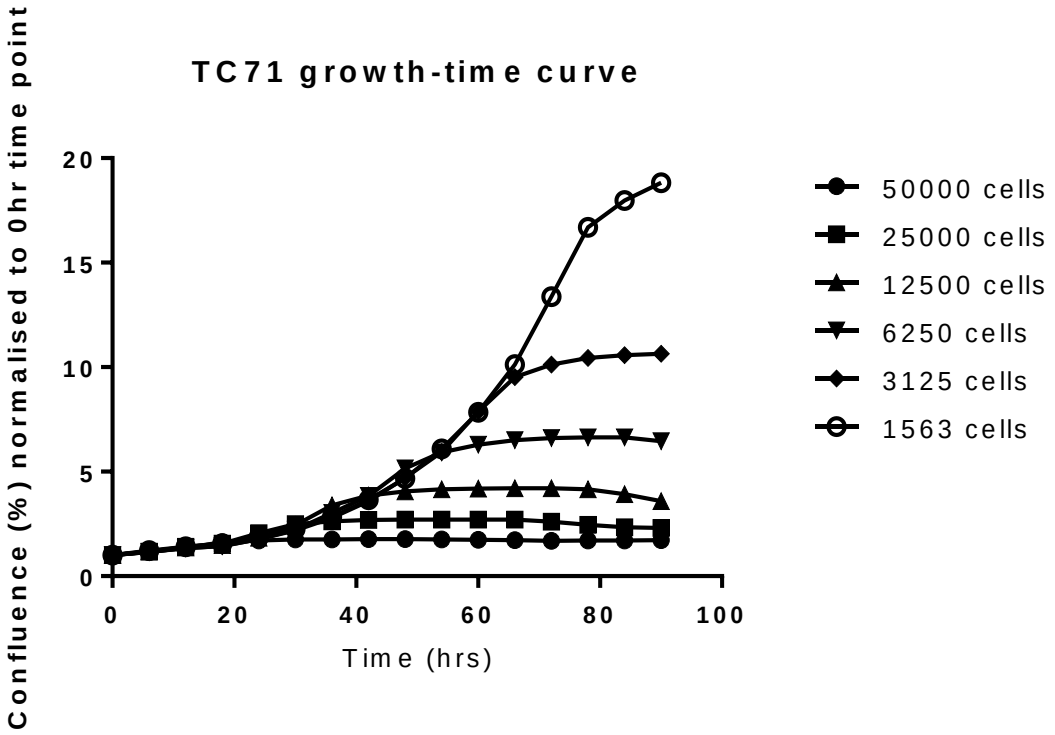

Figure 211 - Growth-time curves of TC71 cell line seeded at different cell numbers in a 96-well plate. Exceeding about 3000 cells seeded would not be recommended to detect a change after treatment.

SW1353 chondrosarcoma cell line

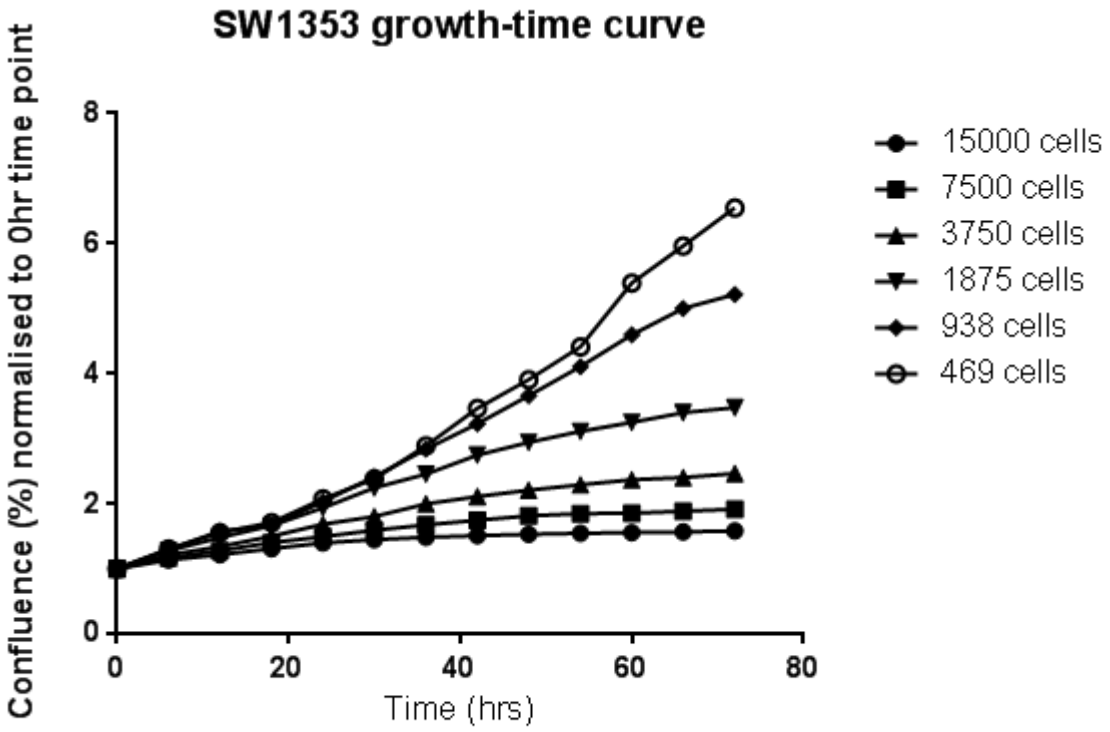

Figure 212 - Growth-time curves of SW1353 cell line seeded at different cell numbers in a 96-well plate. Exceeding about 2000 cells seeded would not be recommended to detect a change after treatment.

HT1080 dedifferentiated chondrosarcoma cell line

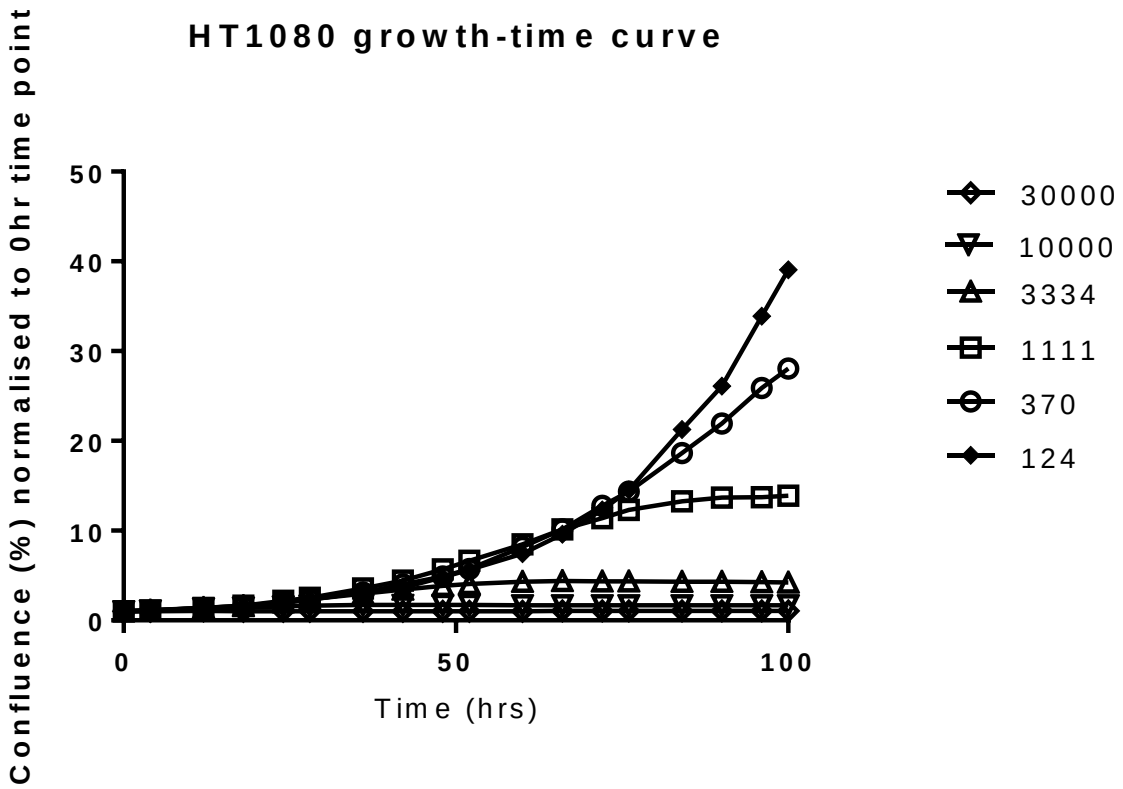

Figure 213 - Growth-time curves of HT1080 cell line seeded at different cell numbers in a 96-well plate. Exceeding about 1000 cells seeded would not be recommended to detect a change after treatment.

11.5 Cell exposure to DMSO

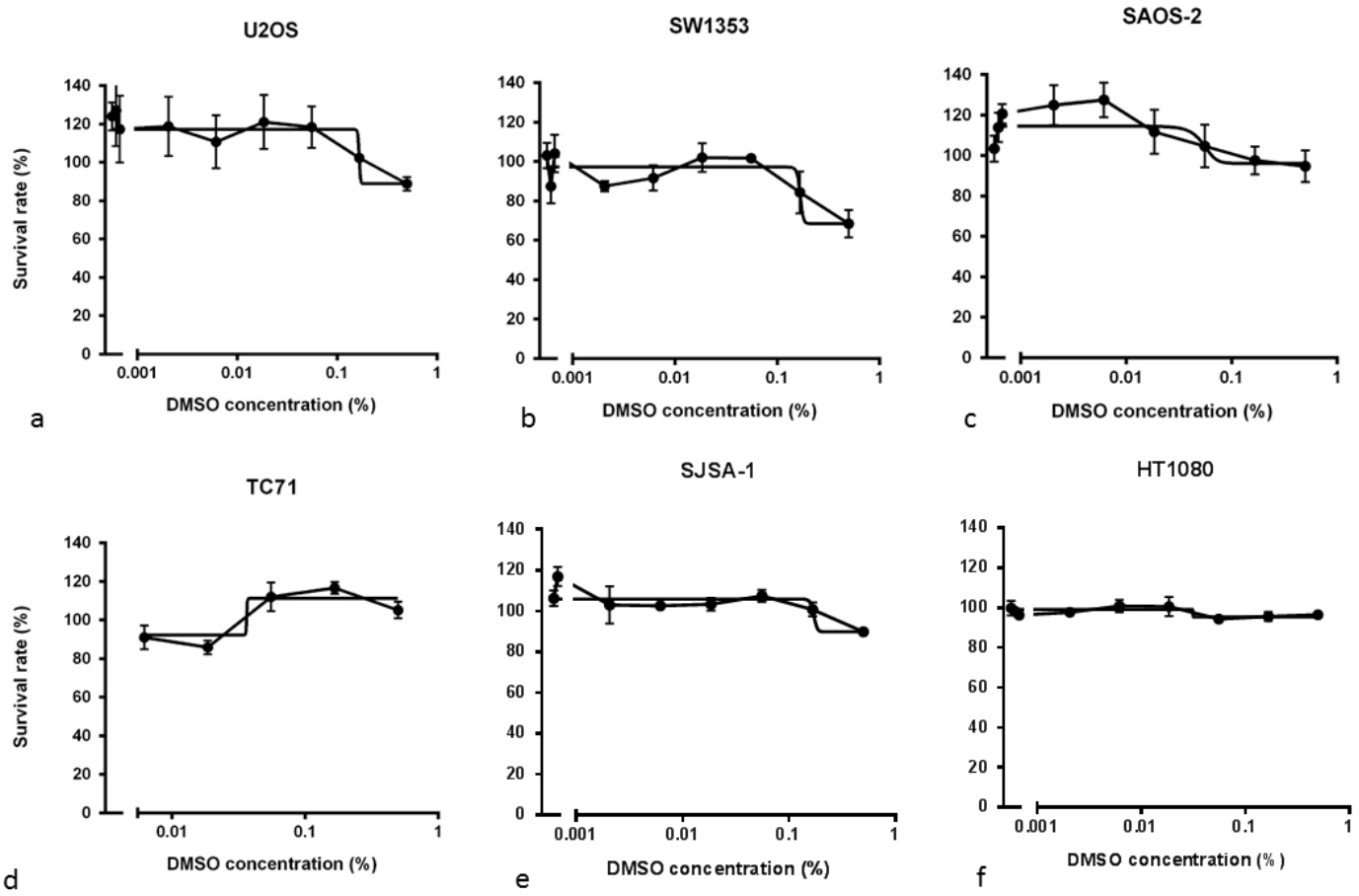

Figure 214 – Cell line exposure to DMSO. Toxic effects were evident above 0.1 % in U2OS, SW1353 cell lines.

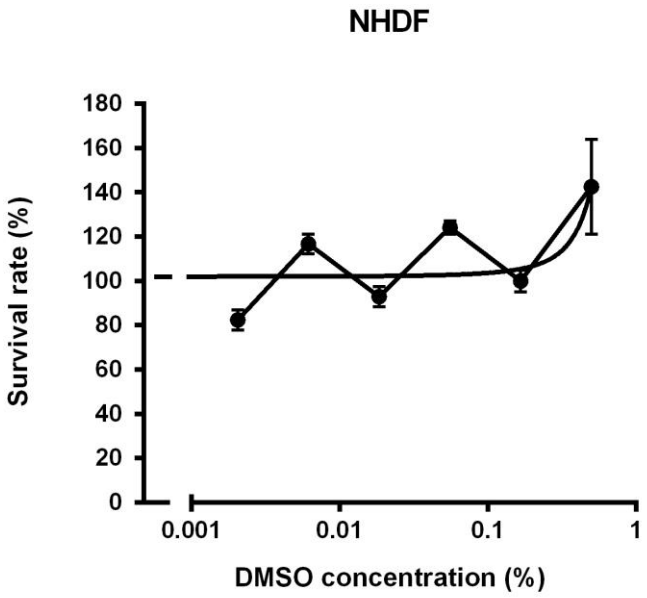

Figure 215 – Effect of DMSO exposure on NHDF cells.

11.6 Combining doxorubicin with SuperKillerTRAIL (0.04 nM vs 0.4 nM) on non-malignant cell lines compared to U2OS osteosarcoma cell line

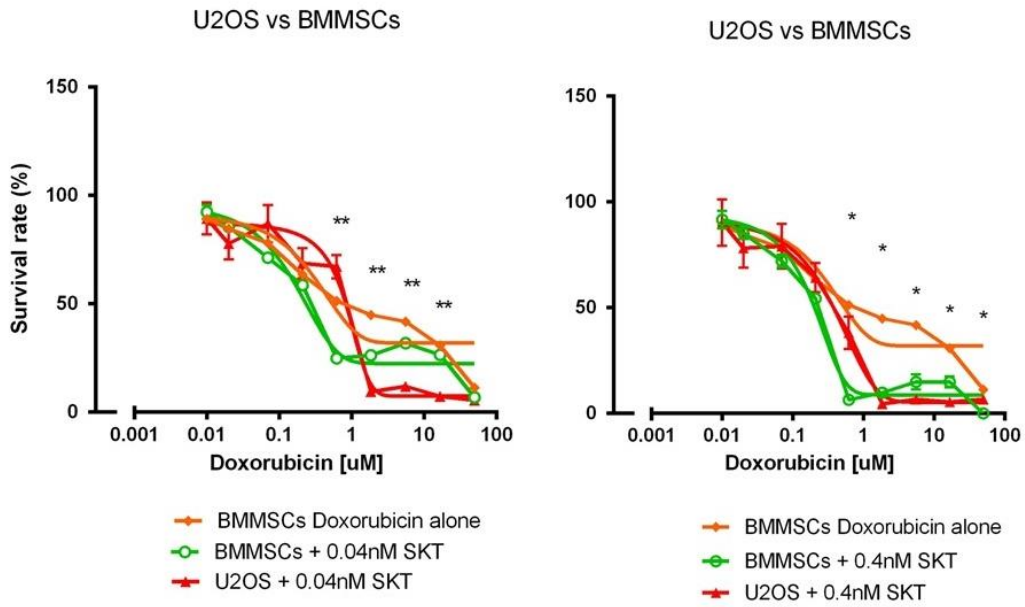

Figure 216 – U2OS vs BMMSCs, doxorubicin with (a) 0.04 nM SKT and (b) 0.4 nM SKT. * = $p<0.05$, ** = $p<0.001$, Student's *t*-test.

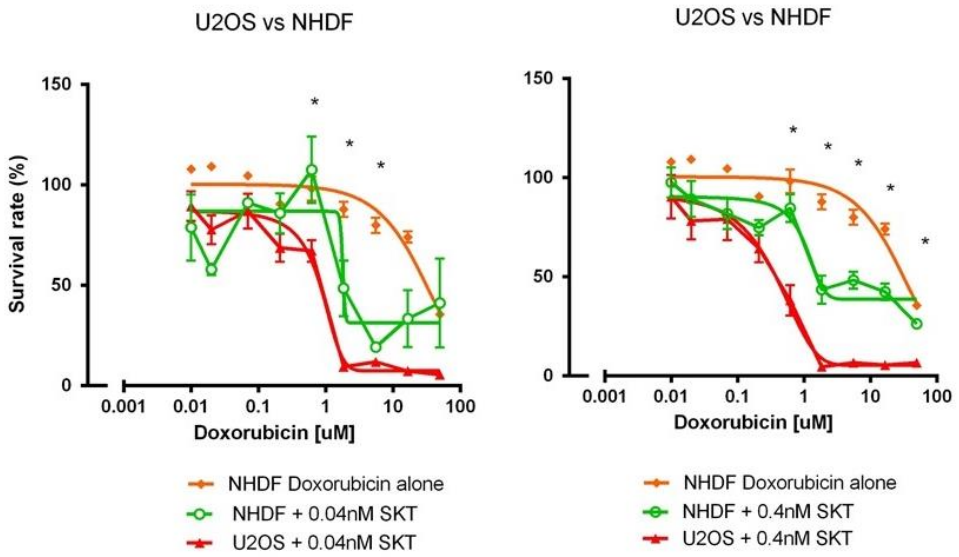

Figure 217 – U2OS vs NHDF, doxorubicin with (a) 0.04 nM SKT and (b) 0.4 nM SKT. * = $p<0.05$, ** = $p<0.001$, Student's *t*-test.

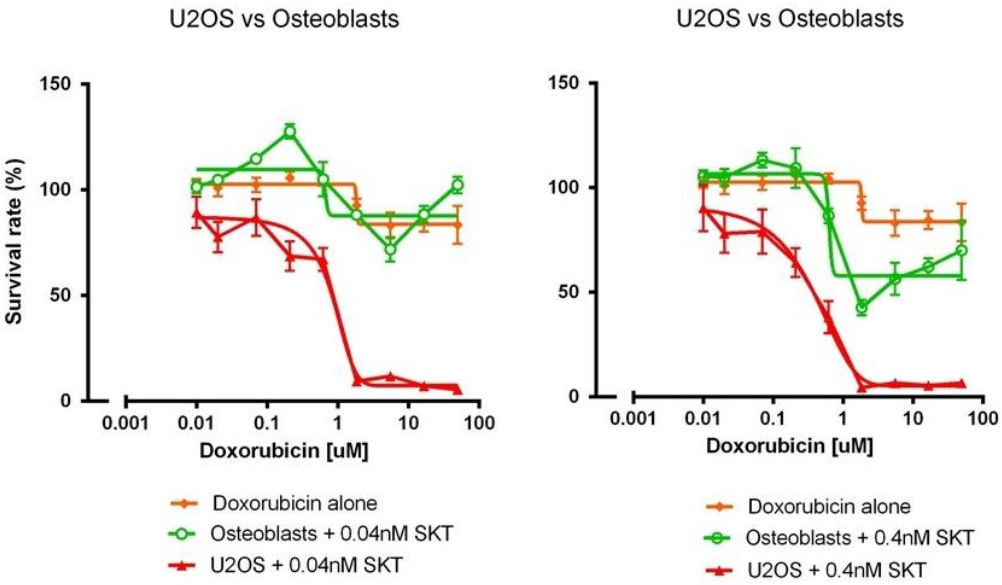

Figure 218 – U2OS vs osteoblasts (OBs), doxorubicin with (a) 0.04 nM SKT and (b) 0.4 nM SKT.

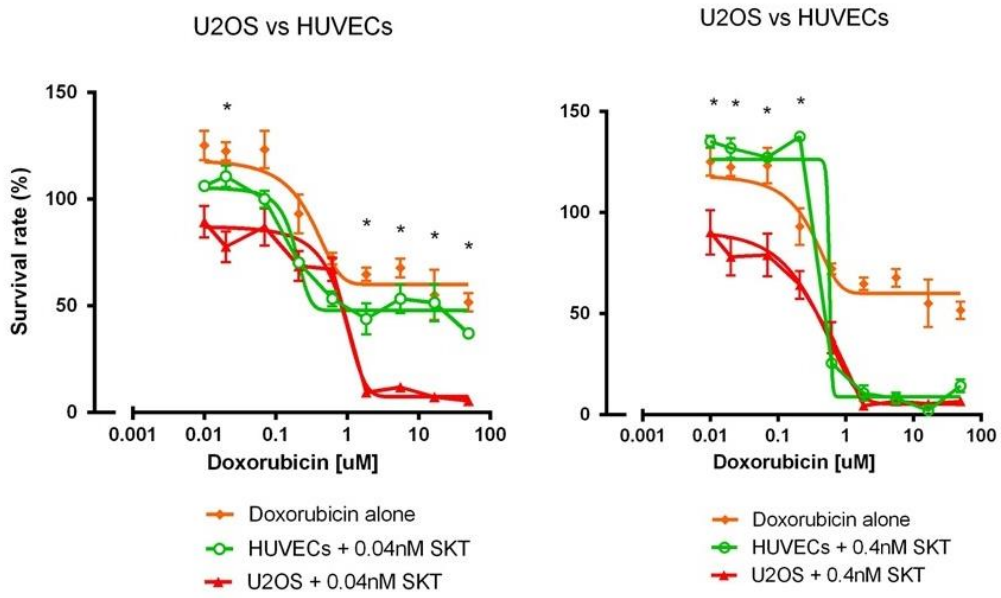

Figure 219 – U2OS vs human umbilical vein endothelial cells (HUVECs), doxorubicin with (a) 0.04 nM SKT and (b) 0.4 nM SKT. * = $p<0.05$, ** = $p<0.001$, Student's *t*-test.

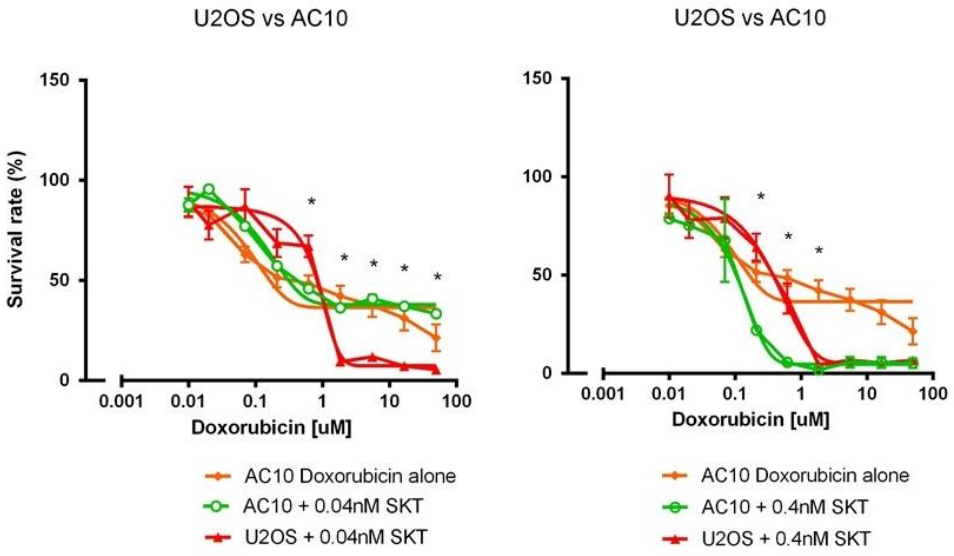

Figure 220 – U2OS vs AC10, doxorubicin with (a) 0.04 nM SKT and (b) 0.4 nM SKT. * = $p<0.05$, ** = $p<0.001$, Student's *t*-test.

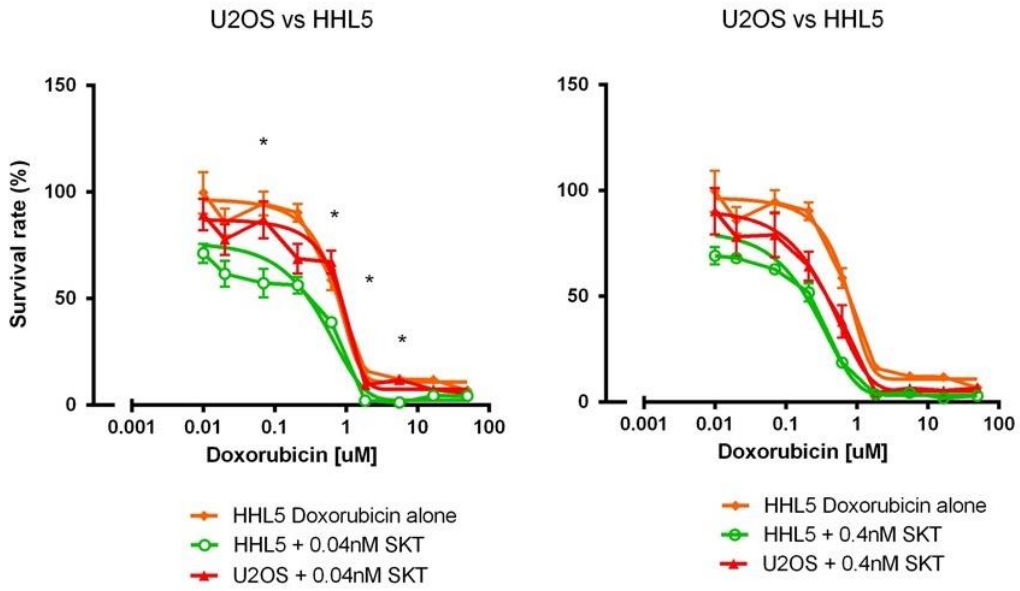

Figure 221 – U2OS vs HHL5, doxorubicin with (a) 0.04 nM SKT and (b) 0.4 nM SKT. * = $p<0.05$, ** = $p<0.001$, Student's *t*-test.

11.7 Quantification of transcript levels using Real-Time PCR (RT-PCR) analysis

11.7.1 Examples of melt curve plots

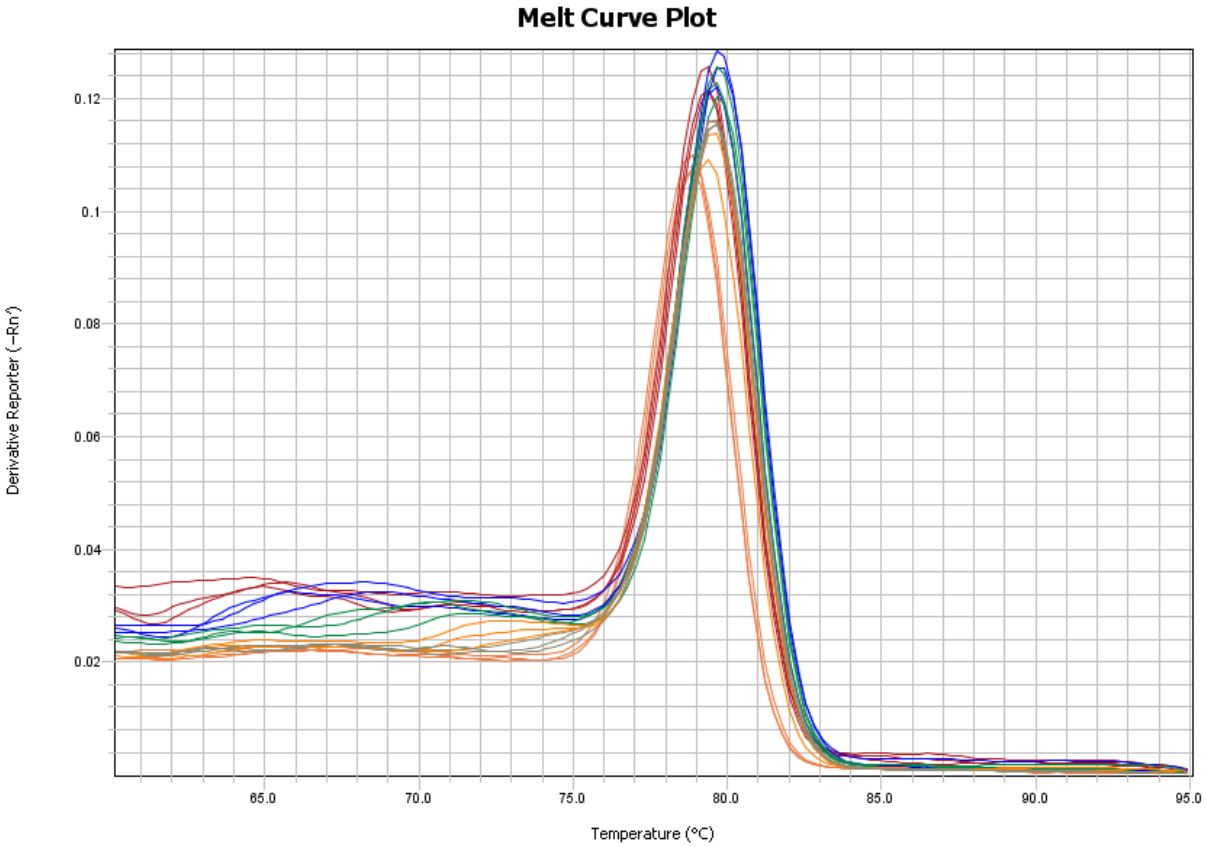

Figure 222 – Death receptor 5 (DR5) melt curve plot.

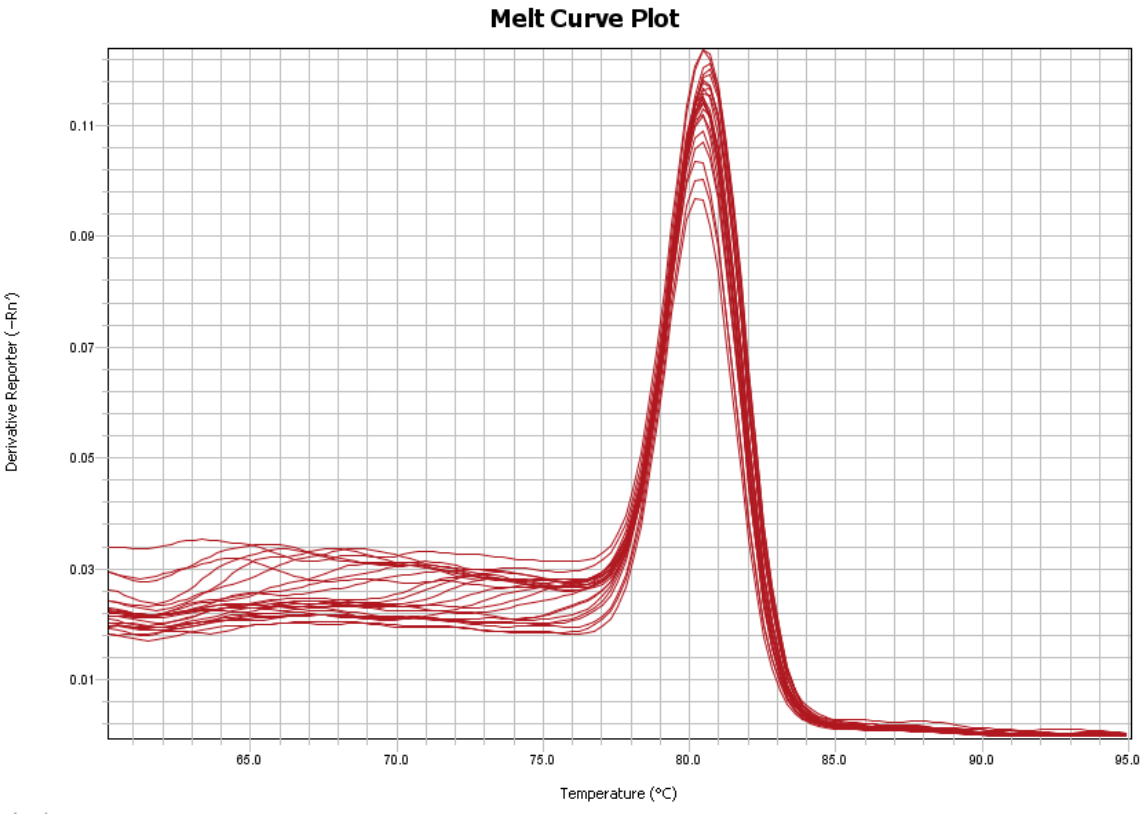

Figure 223 – Death receptor 4 (DR4) melt curve plot.

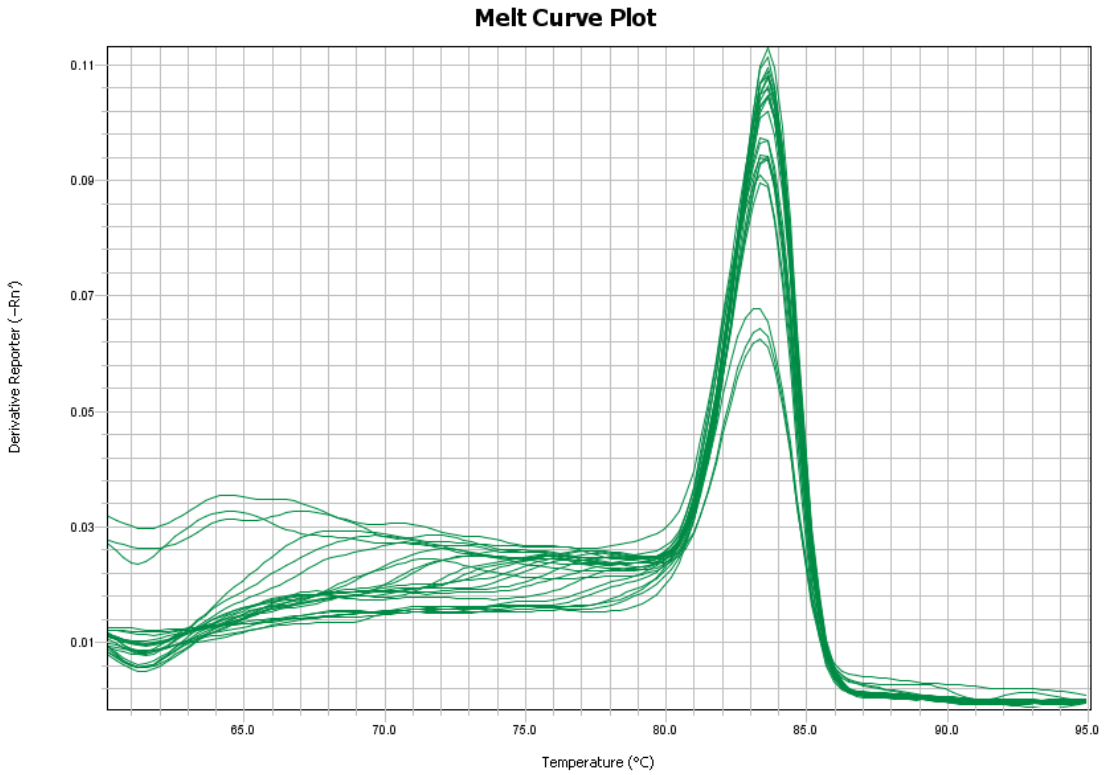

Figure 224 – Osteoprotegerin (OPG) melt curve plot.

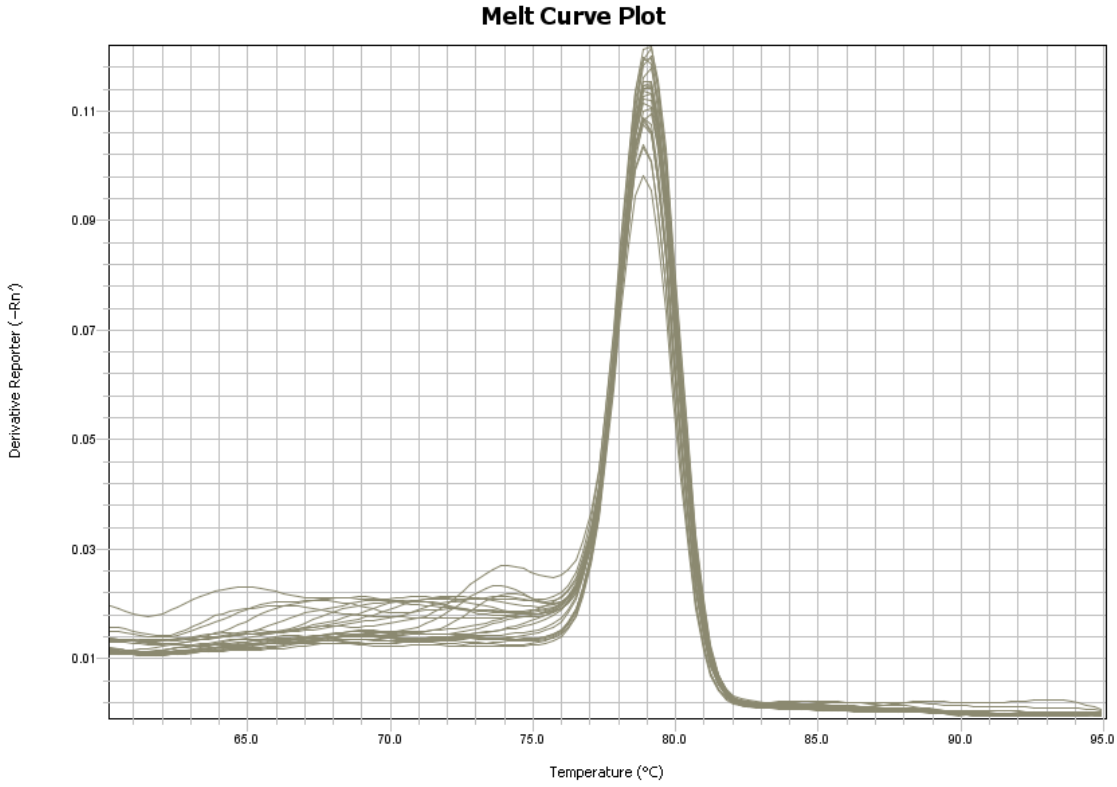

Figure 225 – X-linked inhibitor of apoptosis (XIAP) melt curve plot.

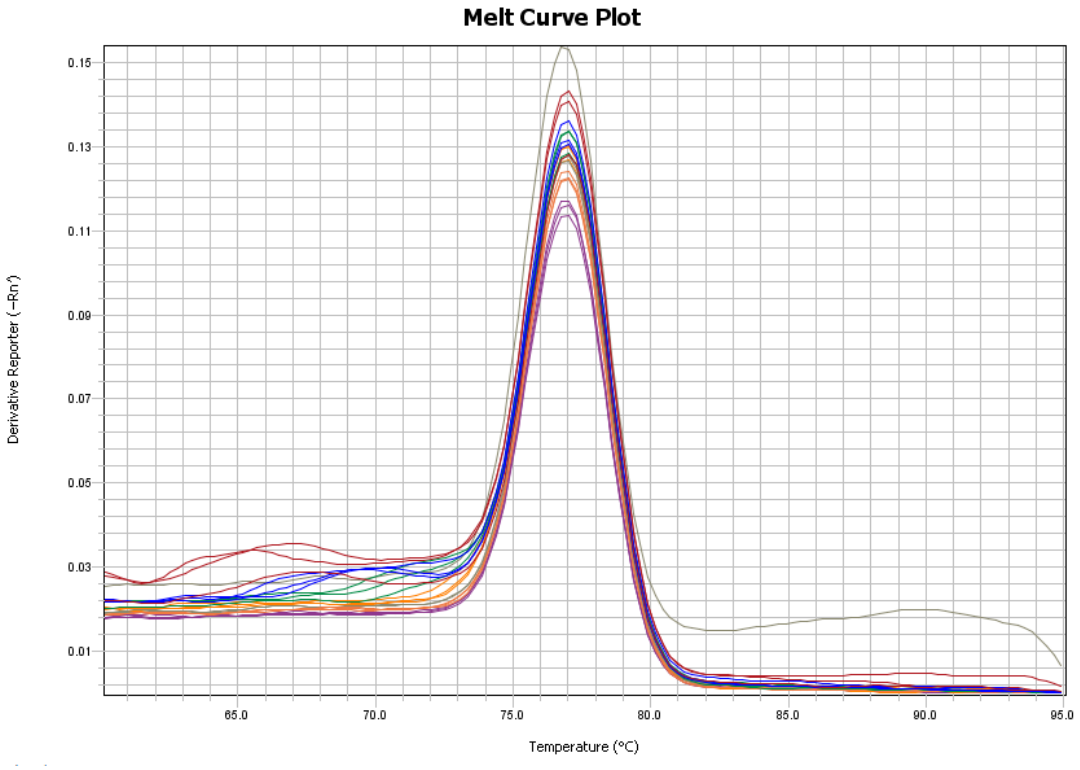

Figure 226 – Decoy receptor 1 (DcR1) melt curve plot.

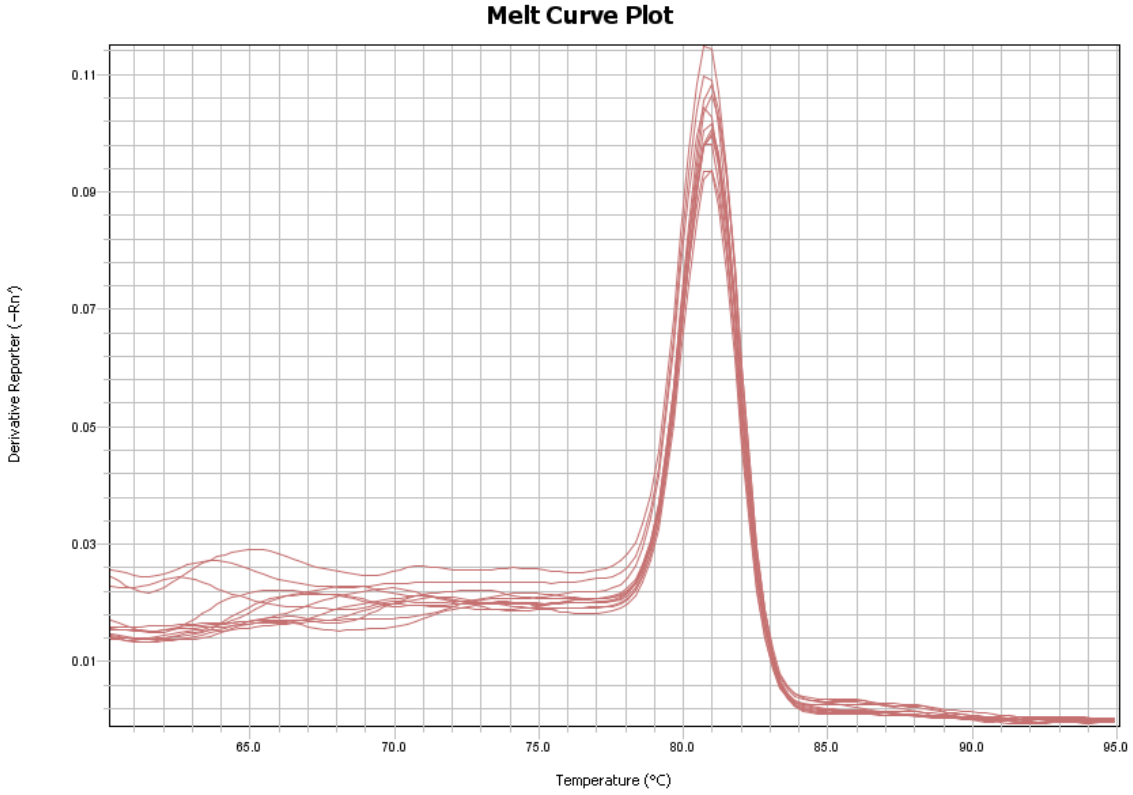

Figure 227 – Decoy receptor 2 (DcR2) melt curve plot.

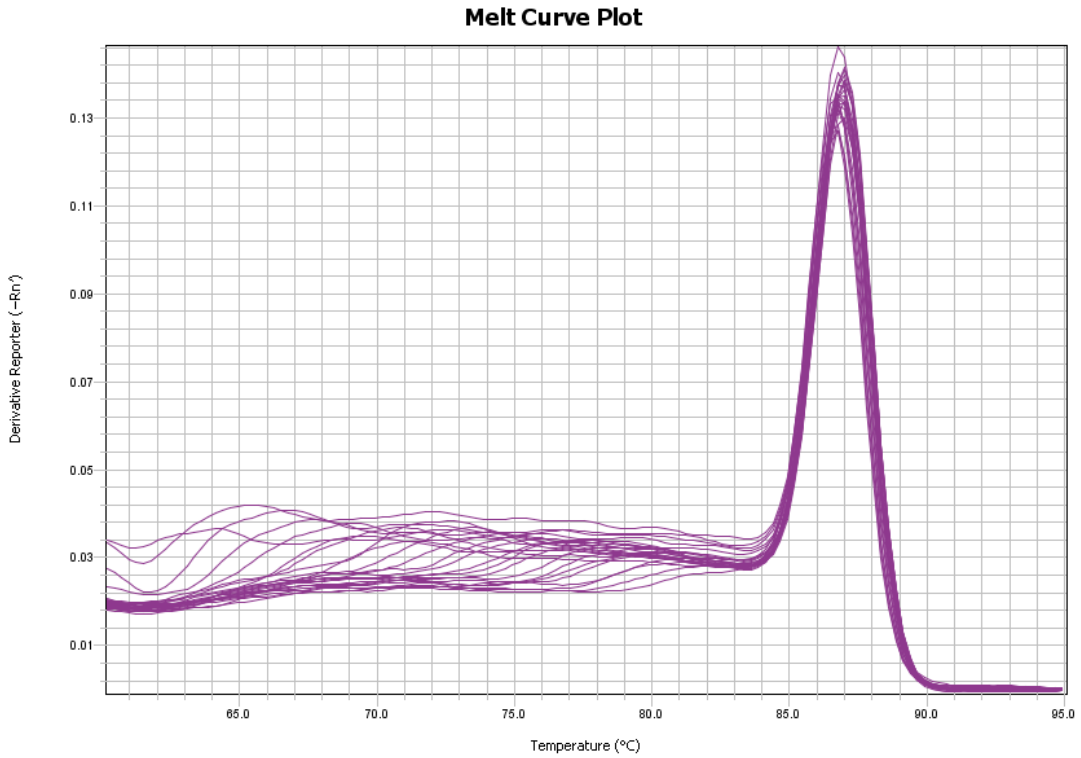

Figure 228 – Akt melt curve plot.

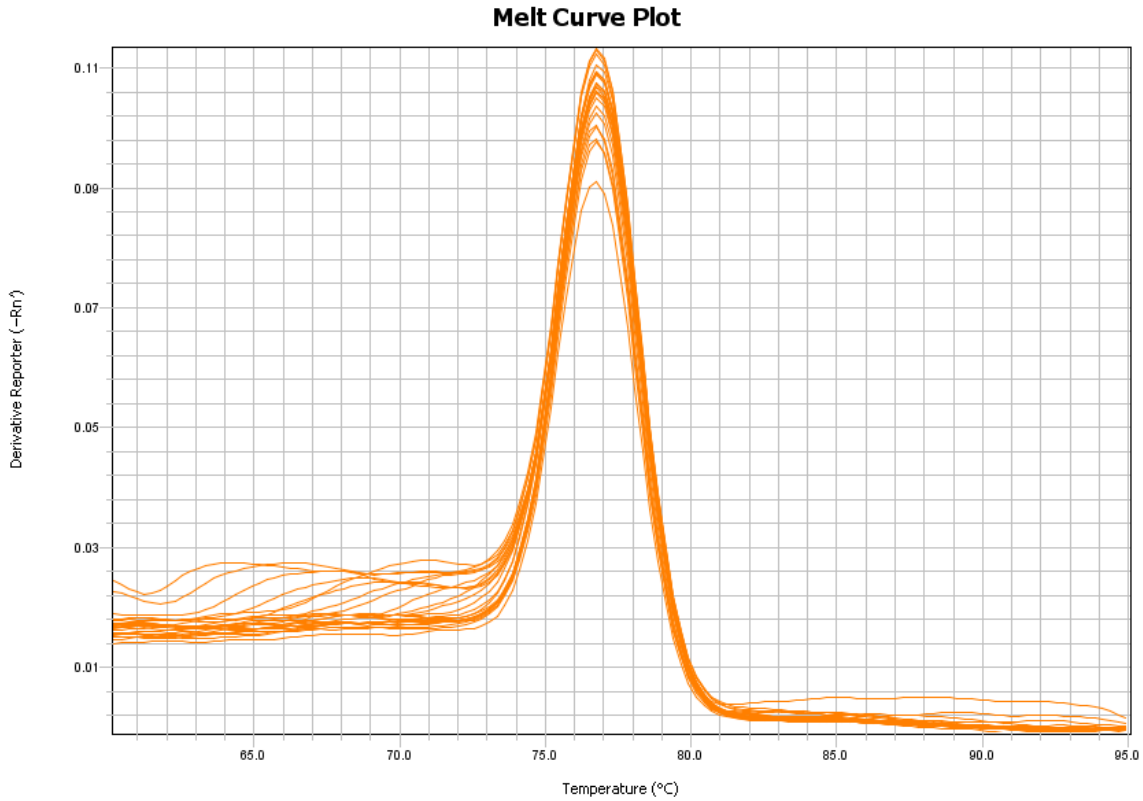

Figure 229 - Hypoxanthine phosphoribosyltransferase 1 (HPRT1) melt curve plot.

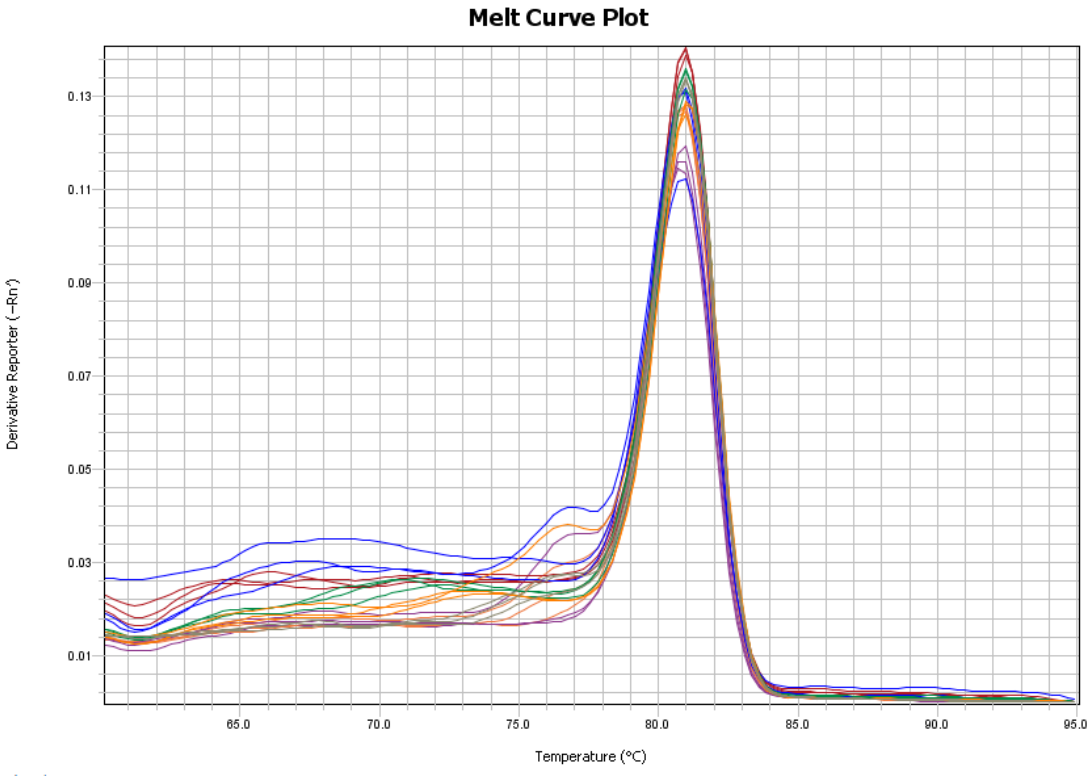

Figure 230 - Tumour necrosis factor (TNF)-related apoptosis-inducing ligand (TRAIL) melt curve plot.

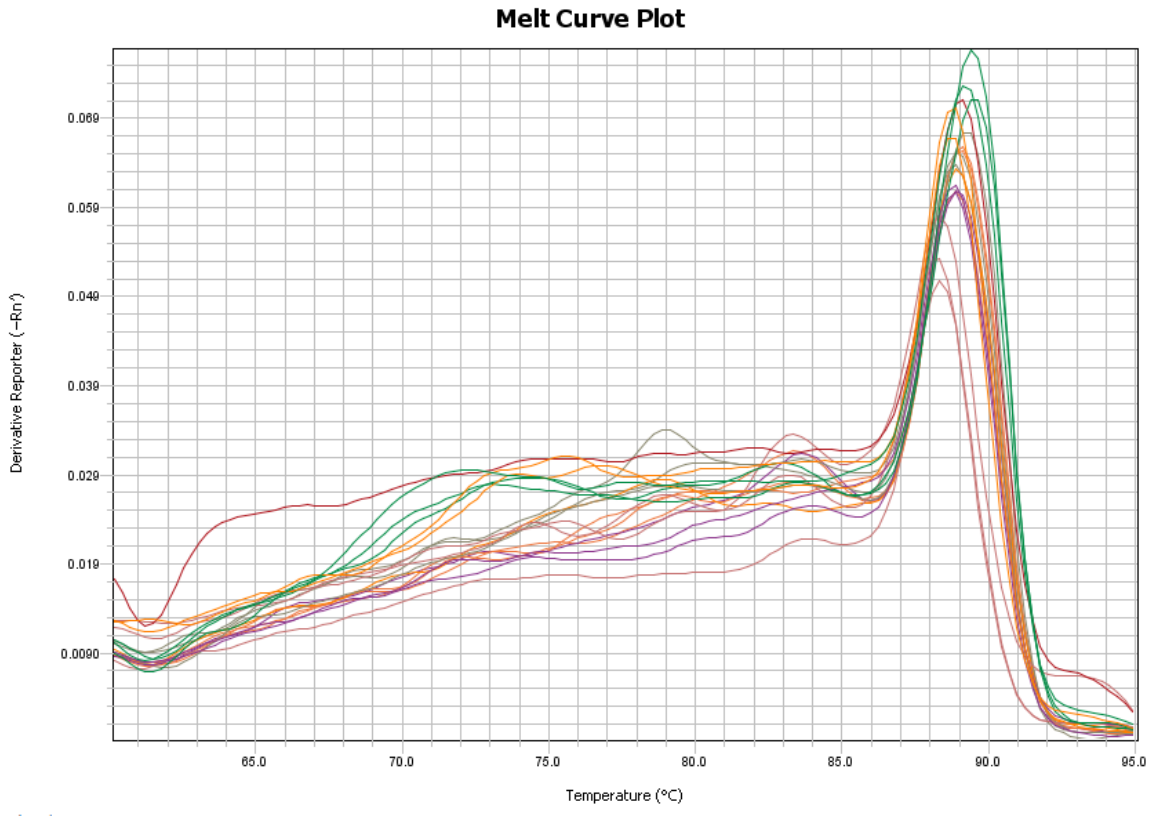

Figure 231 - H-Ras melt curve plot.

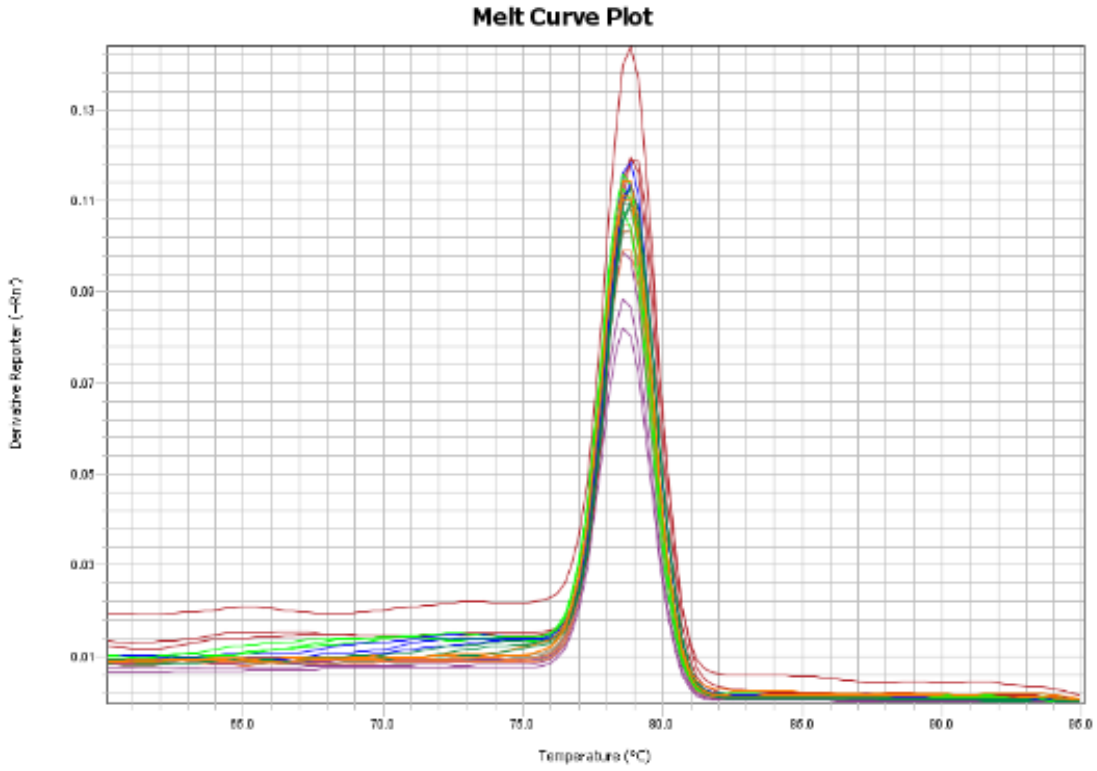

Figure 232 - Phosphatase and tensin homolog (PTEN) melt curve plot.

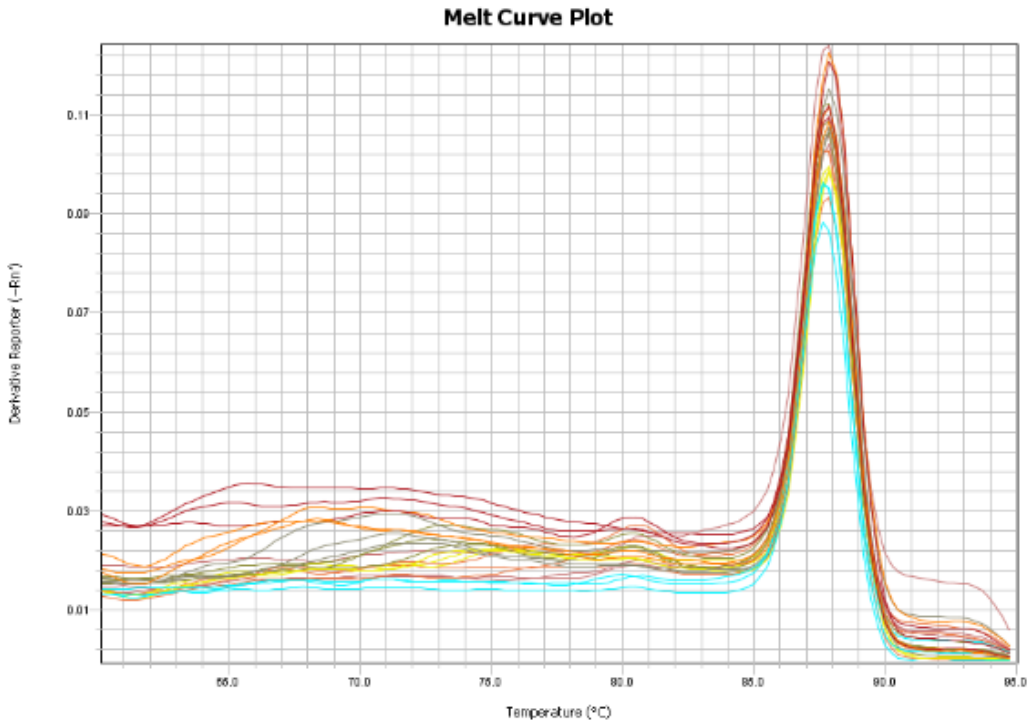

Figure 233 – NG2 melt curve plot.

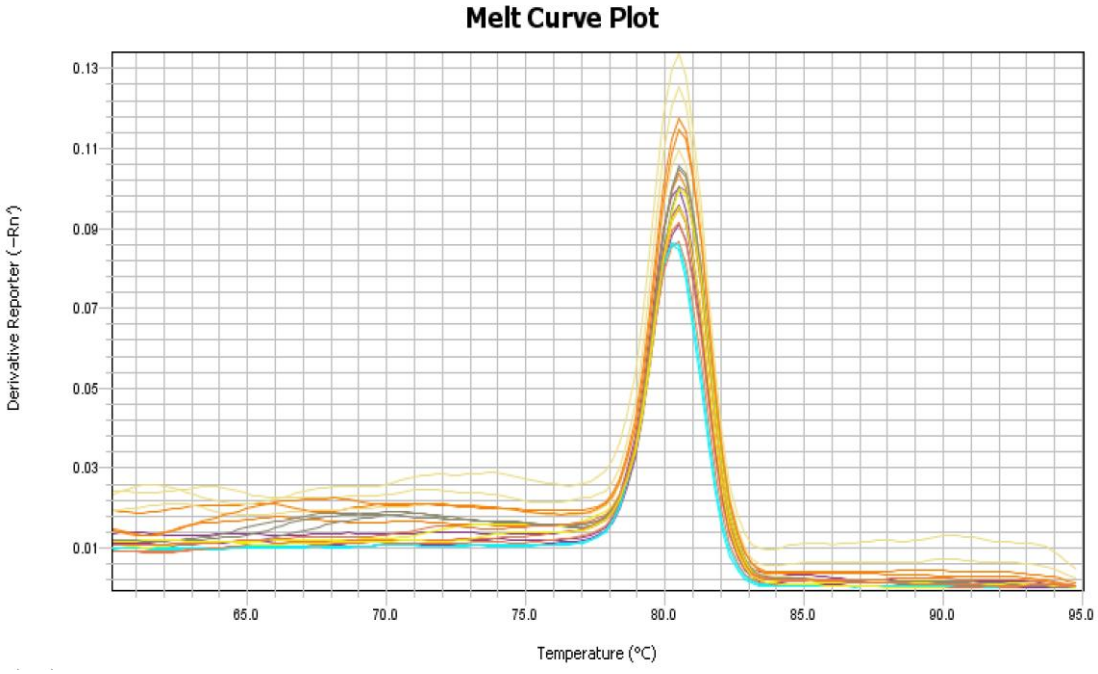

Figure 234 – cFLIP$_L$ melt curve plot.

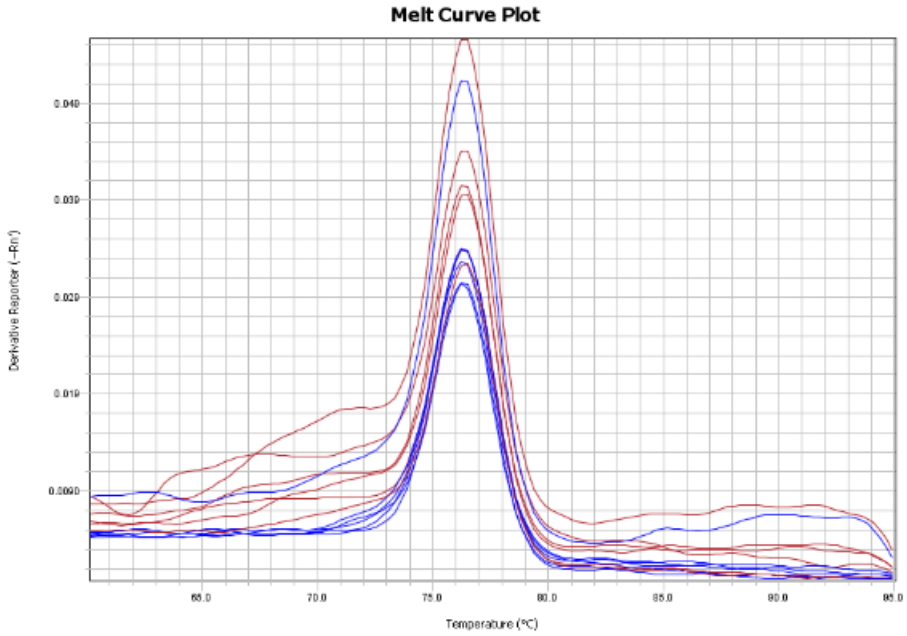

Figure 235 – cbfa-1/Runx2 melt curve plot.

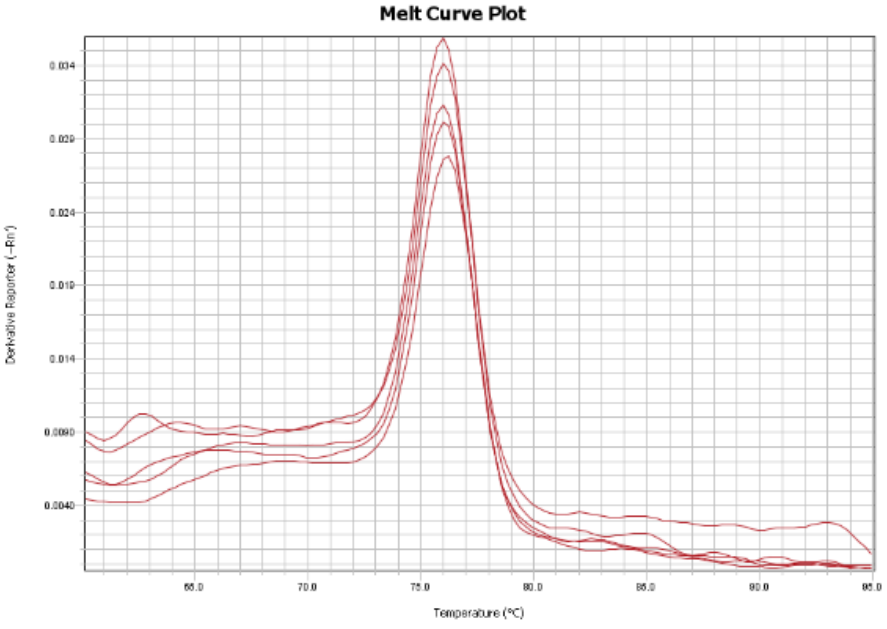

Figure 236 – Osteopontin melt curve plot.

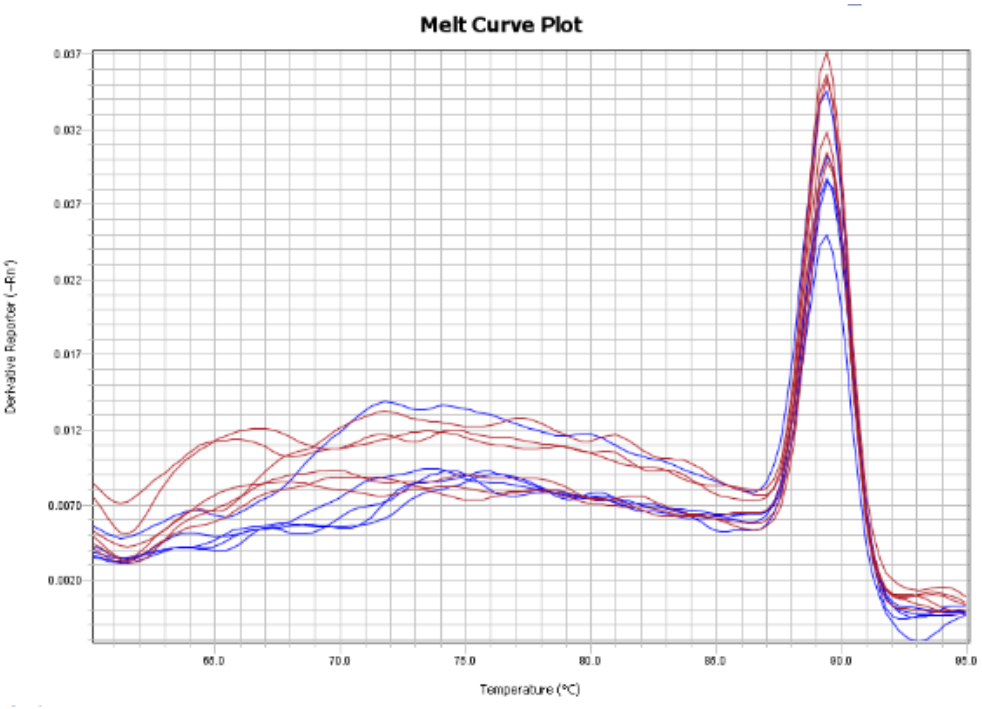

Figure 237 – Osteocalcin melt curve plot.

11.7.2 Example amplification plot

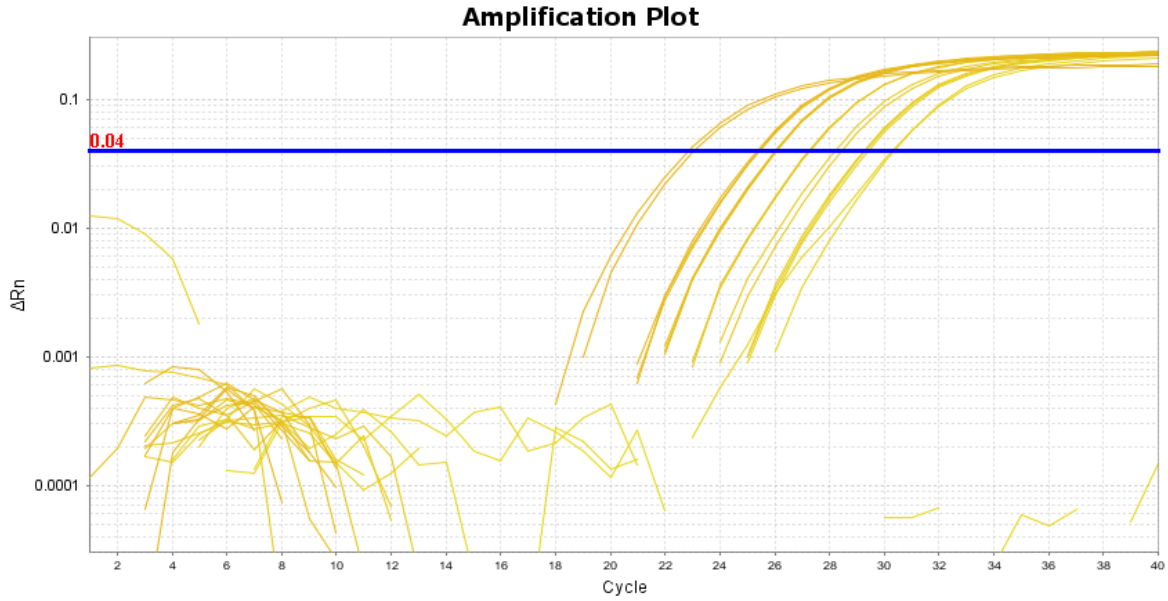

Figure 238 - Amplification plot for DR5 demonstrating increasing Ct values for the more dilute samples used for creating the standard curve. Water samples did not reveal amplification/contamination.

11.7.3 Examples of standard curve plots

11.7.3.1 Death receptor 4 (DR4)

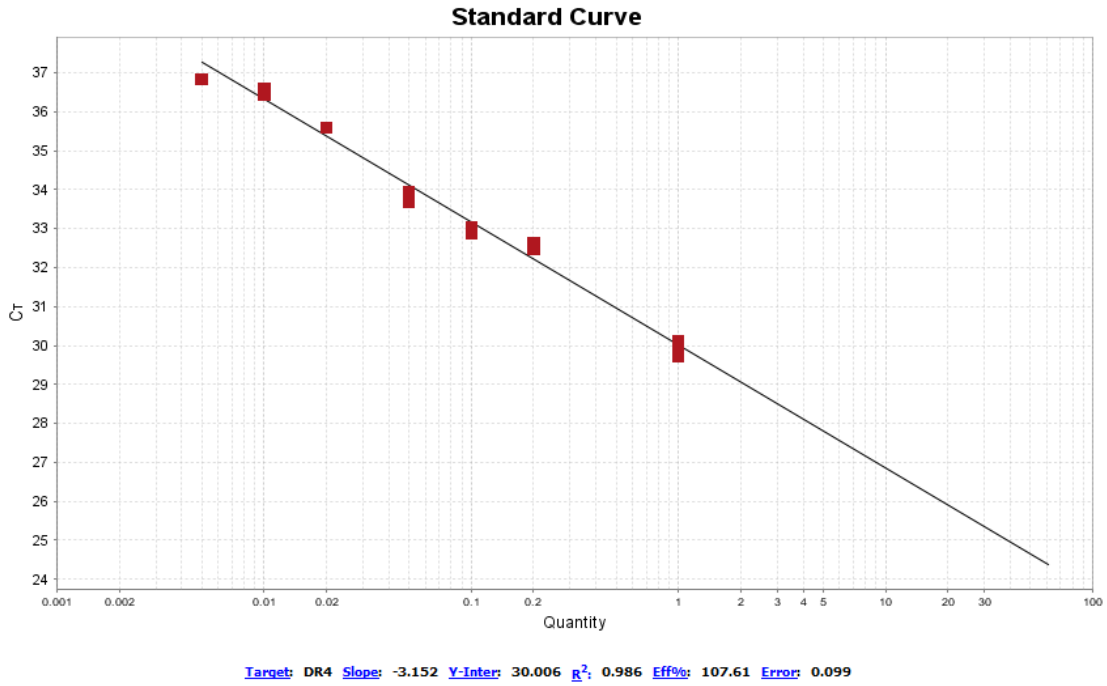

Figure 239 - Example standard curve plot for DR4. R^2 = 0.99 (recommended is >0.97). PCR efficiency = 108 % (90 % - 110 % is considered acceptable). Slope is -3.2 (acceptable is about -3.3) [347].

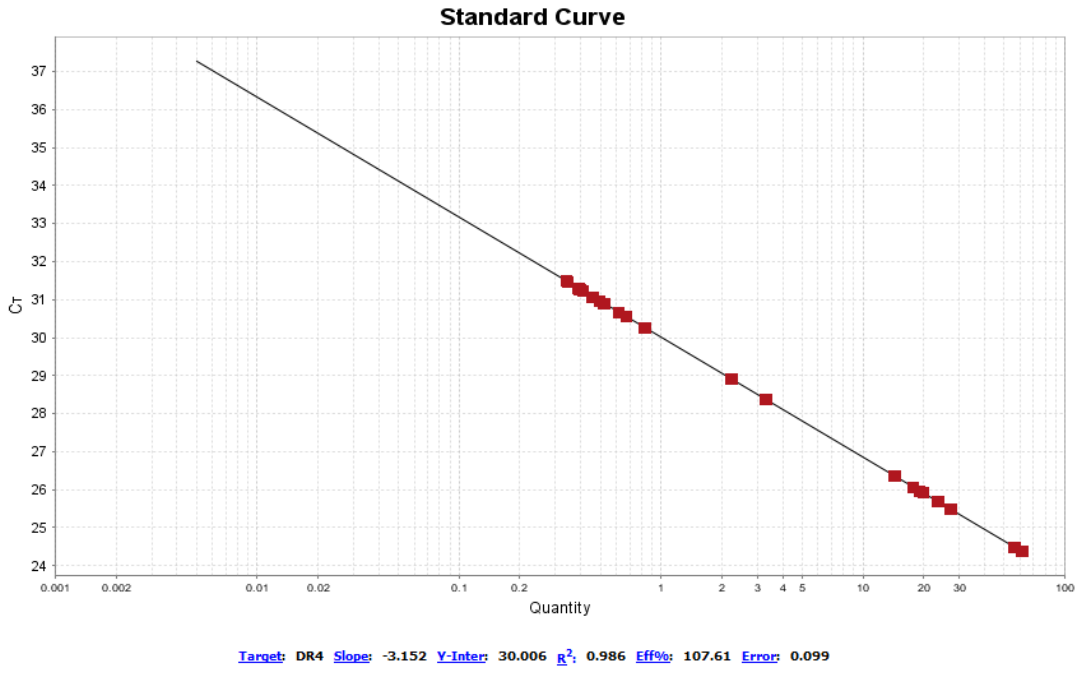

Figure 240 - The unknown bone sarcoma cell line samples are within the central region of the standard curve plot some with greater Ct values for DR4 than others [347].

11.7.3.2 Death receptor 5 (DR5)

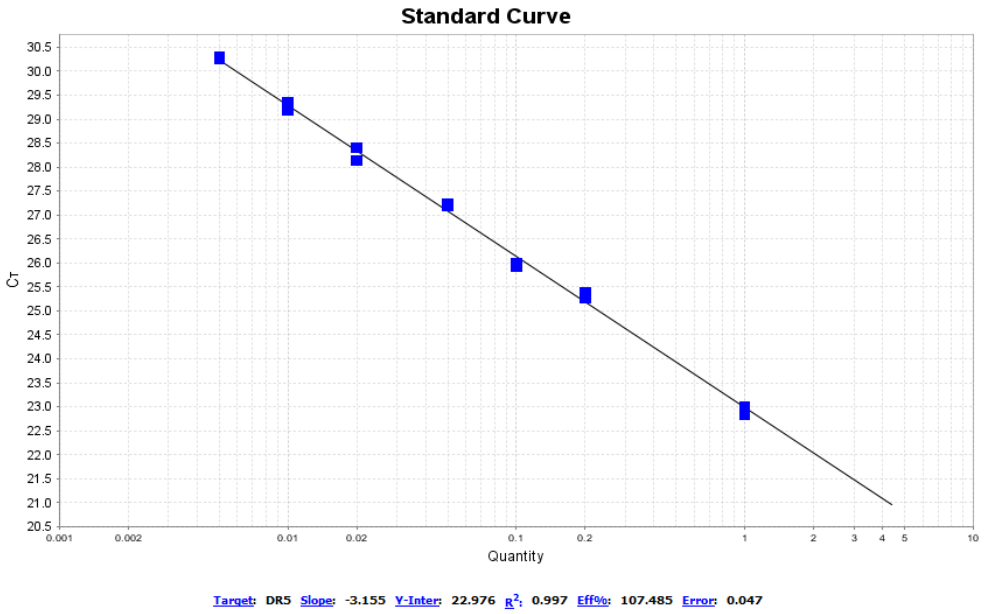

Figure 241 - Example standard curve plot for DR5. R^2 = 0.99 (recommended is >0.97). PCR efficiency = 108 % (90 % - 110 % is considered acceptable). Slope is -3.2 (acceptable is about -3.3) [347].

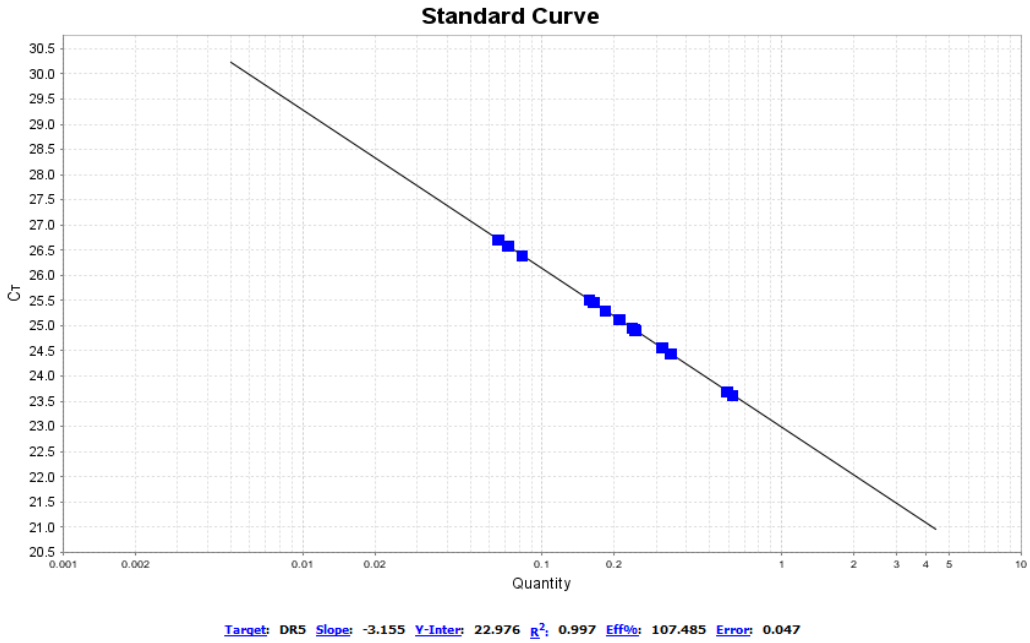

Figure 242 - The unknown bone sarcoma cell line samples are within the central region of the standard curve plot some with greater Ct values for DR5 than others [347].

11.7.3.3 Decoy receptor 1 (DcR1)

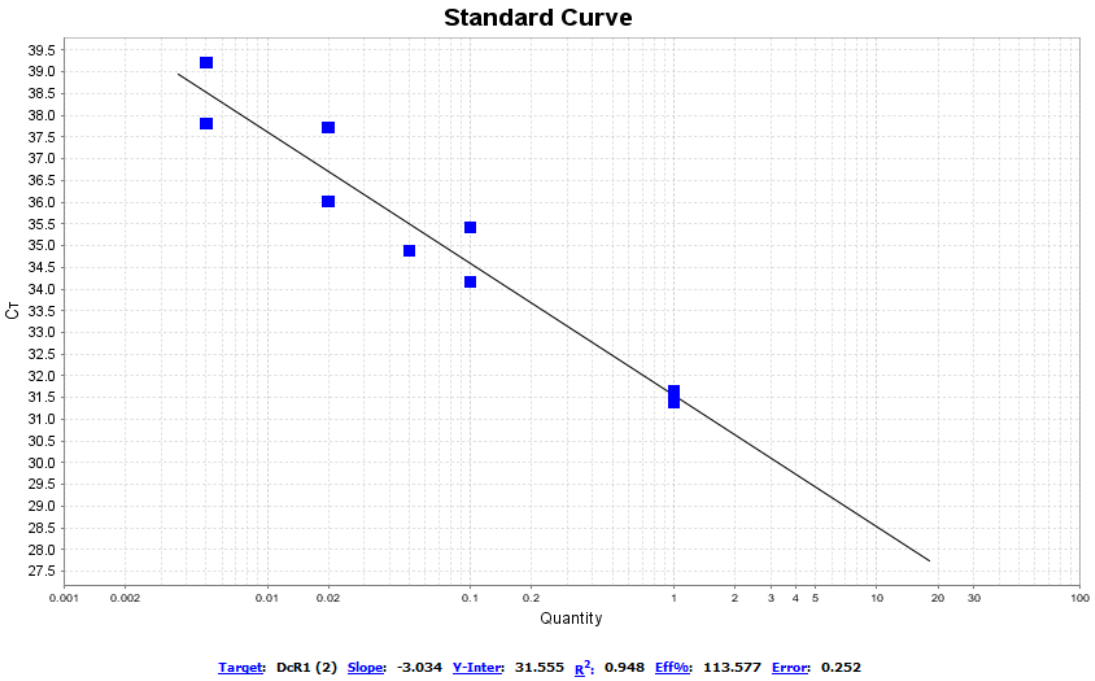

Figure 243 - Example standard curve plot for DcR1. R^2 = 0.95 (recommended is >0.97). PCR efficiency = 114 % (90 % - 110 % is considered acceptable). Slope is -3.0 (acceptable is about -3.3) [347].

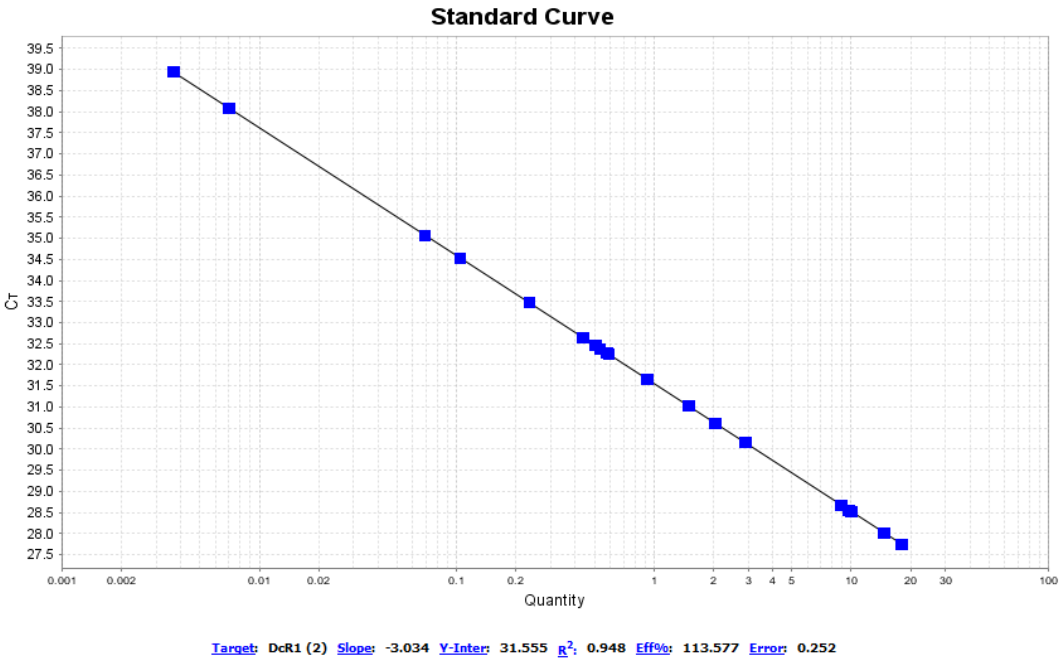

Figure 244 - The unknown bone sarcoma cell line samples are within the central region of the standard curve plot some with greater Ct values for DcR1 than others [347].

11.7.3.4 Decoy receptor 2 (DcR2)

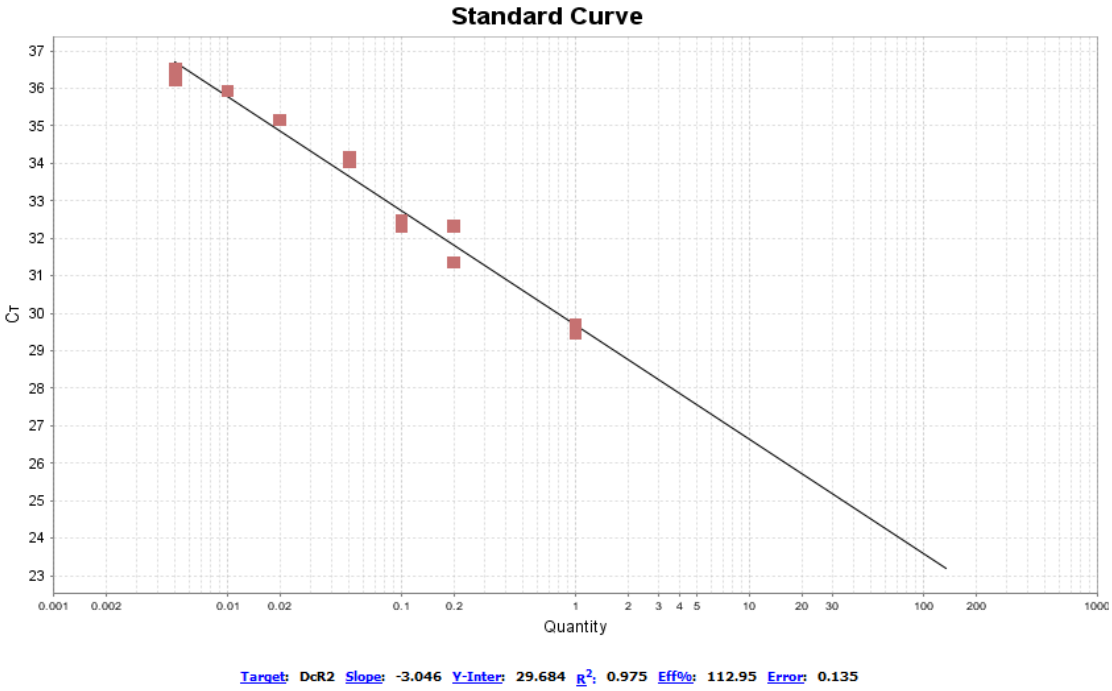

Figure 245 - Example standard curve plot for DcR2. R^2 = 0.98 (recommended is >0.97). PCR efficiency = 113 % (90 % - 110 % is considered acceptable). Slope is -3.1 (acceptable is about -3.3) [347].

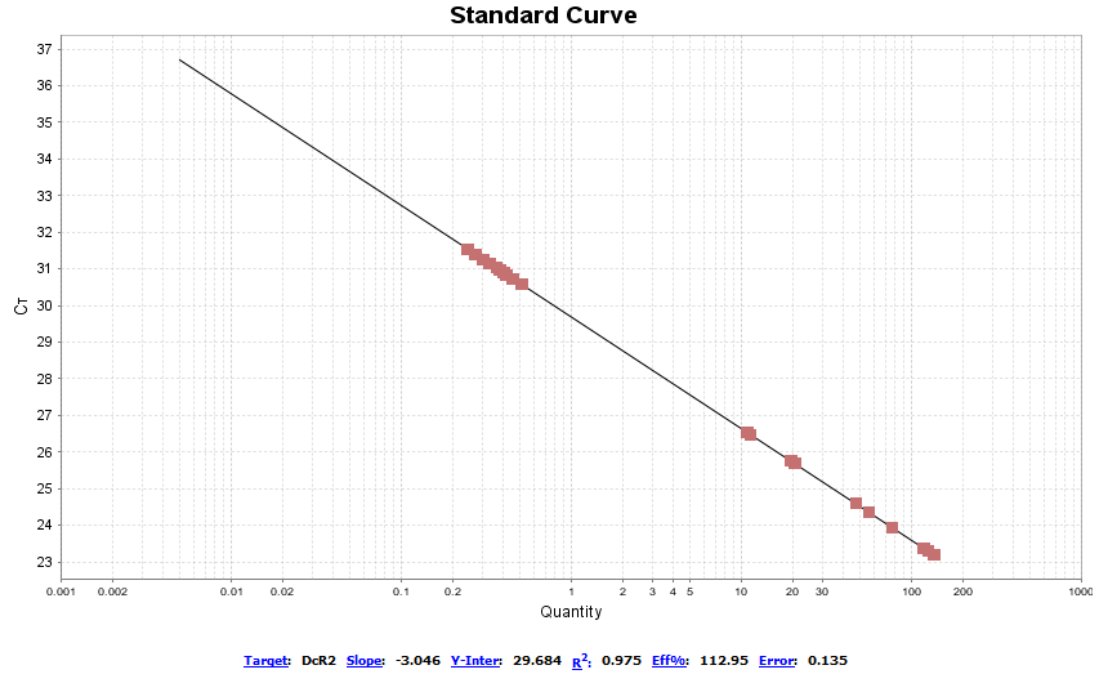

Figure 246 - The unknown bone sarcoma cell line samples are within the region of the standard curve plot some with greater Ct values for DcR2 than others [347].

11.7.3.5 Osteoprotegerin (OPG)

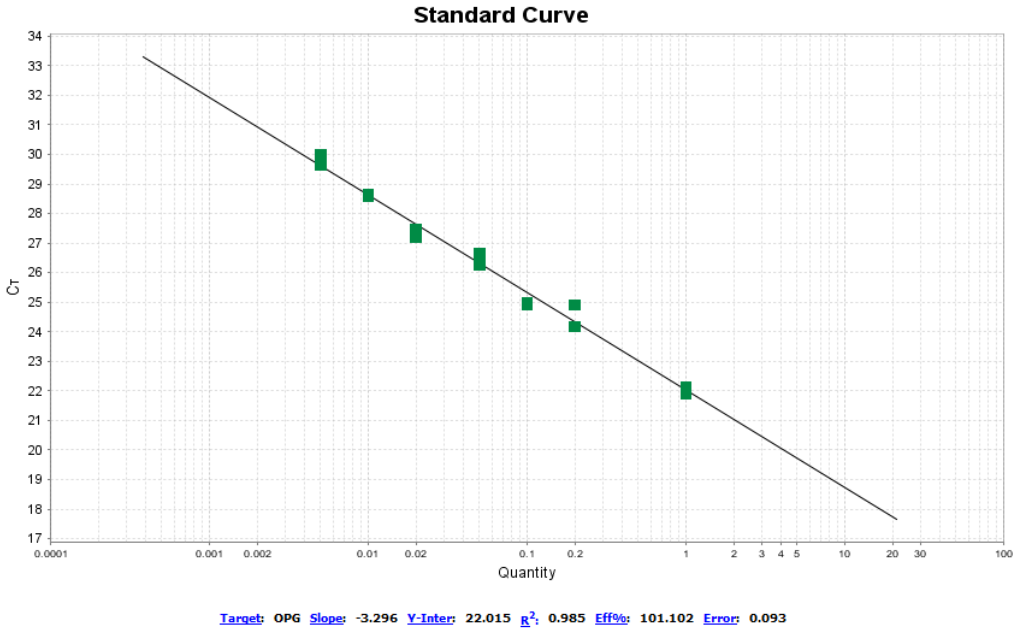

Figure 247 - Example standard curve plot for OPG. R^2 = 0.99 (recommended is >0.97). PCR efficiency = 101 % (90 % - 110 % is considered acceptable). Slope is -3.3 (acceptable is about -3.3) [347].

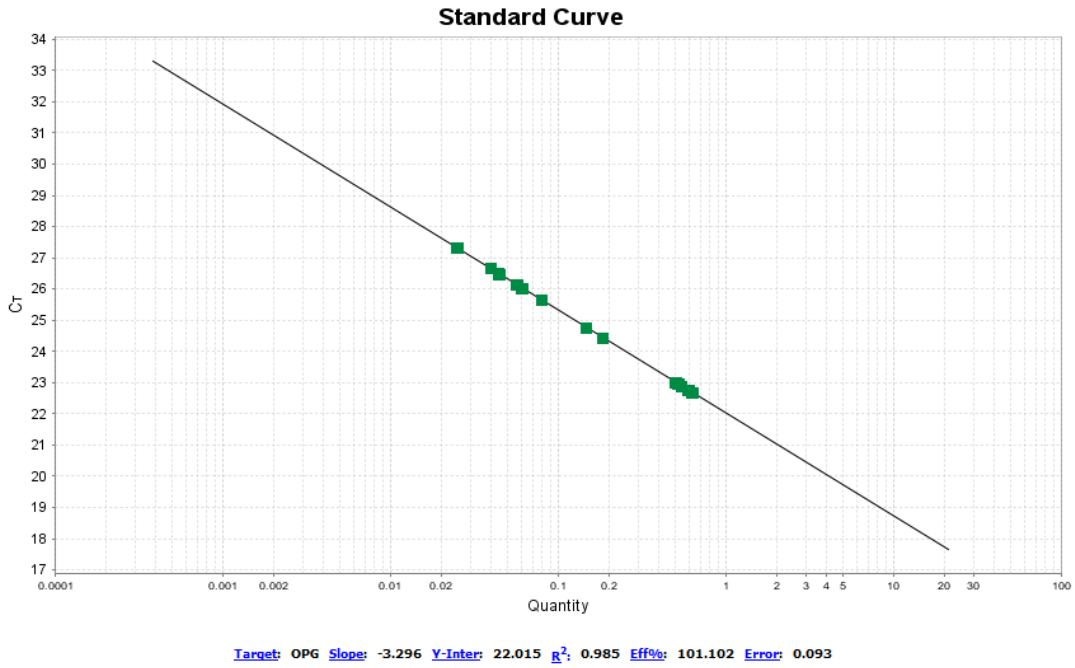

Figure 248 - The unknown bone sarcoma cell line samples are within the central region of the standard curve plot some with greater Ct values for OPG than others [347].

11.7.3.6 X-linked inhibitor of apoptosis protein (XIAP)

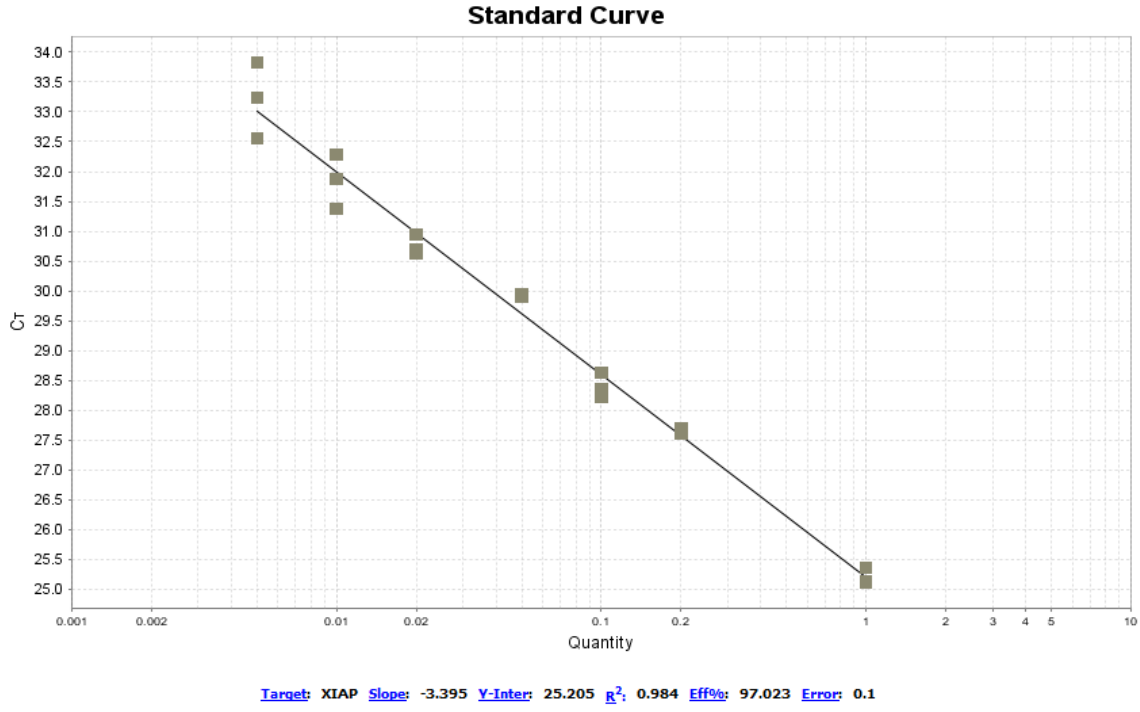

Figure 249 - Example standard curve plot for XIAP. R^2 = 0.99 (recommended is >0.97). PCR efficiency = 97 % (90 % - 110 % is considered acceptable). Slope is -3.4 (acceptable is about -3.3) [347].

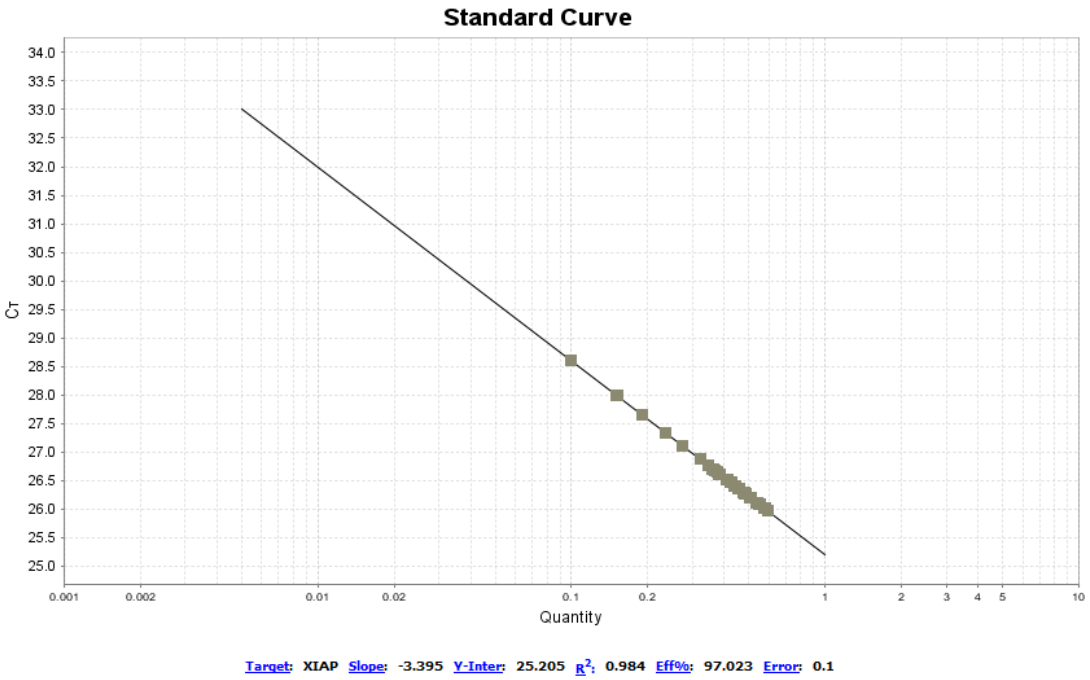

Figure 250 - The unknown bone sarcoma cell line samples are within the central region of the standard curve plot some with greater Ct values for XIAP than others [347].

11.7.3.7 Akt

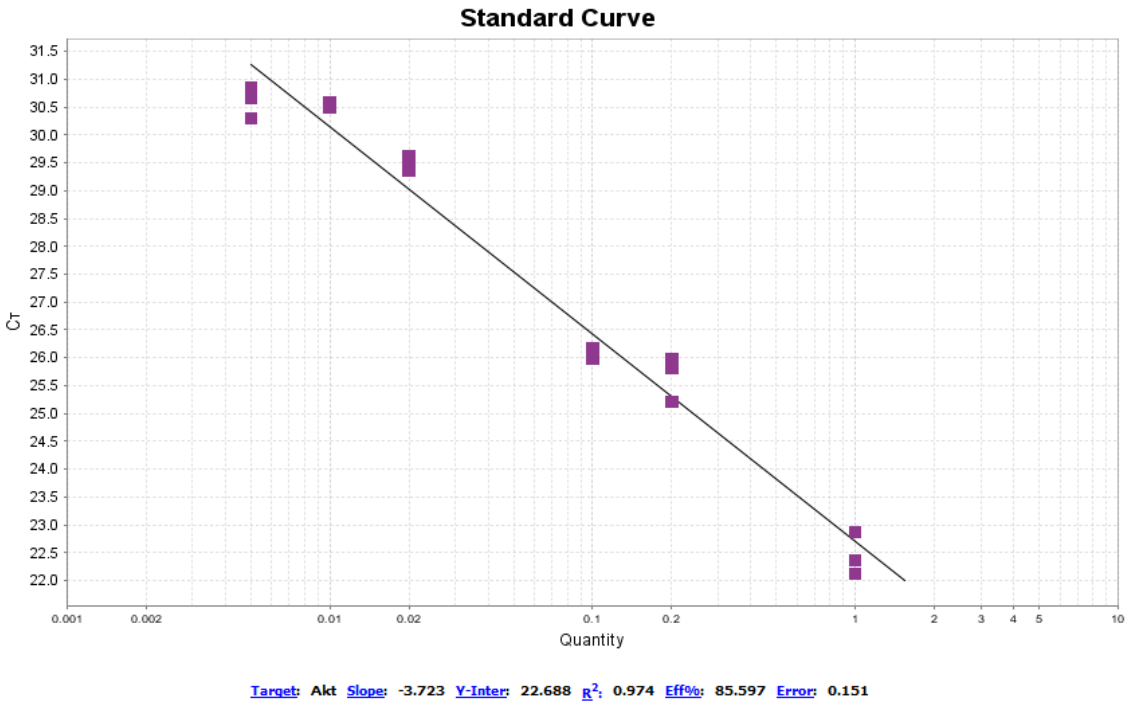

Figure 251 - Example standard curve plot for Akt. R^2 = 0.98 (recommended is >0.97).

PCR efficiency = 86 % (90 % - 110 % is considered acceptable). Slope is -3.7 (acceptable is about -3.3) [347].

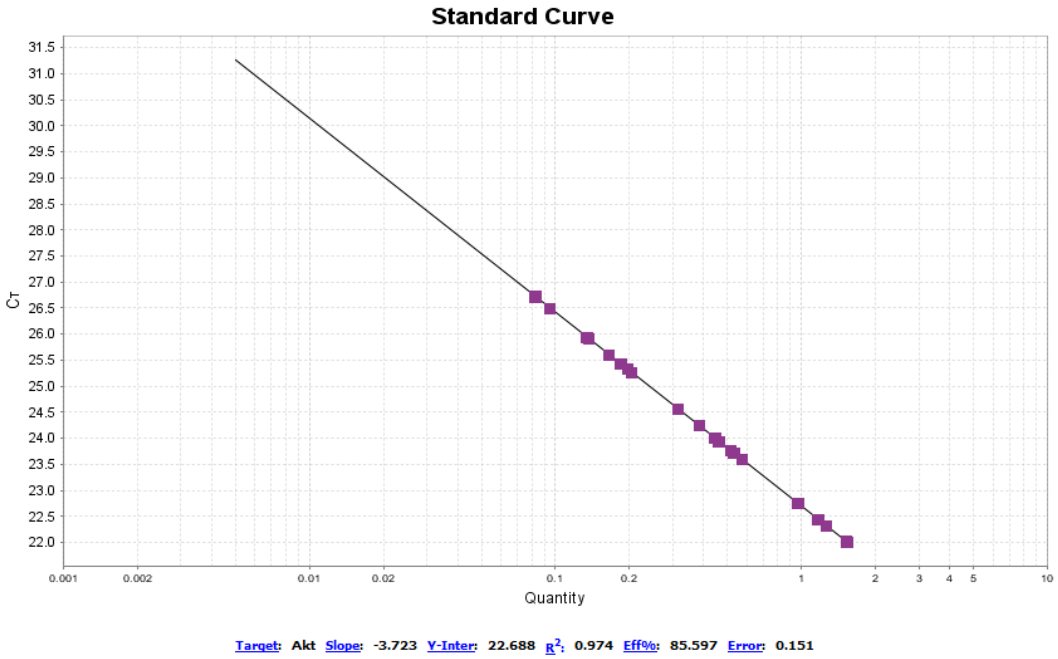

Figure 252 - The unknown bone sarcoma cell line samples are within the region of the standard curve plot some with greater Ct values for Akt than others [347].

11.7.3.8 Phosphatase and tensin homolog (PTEN)

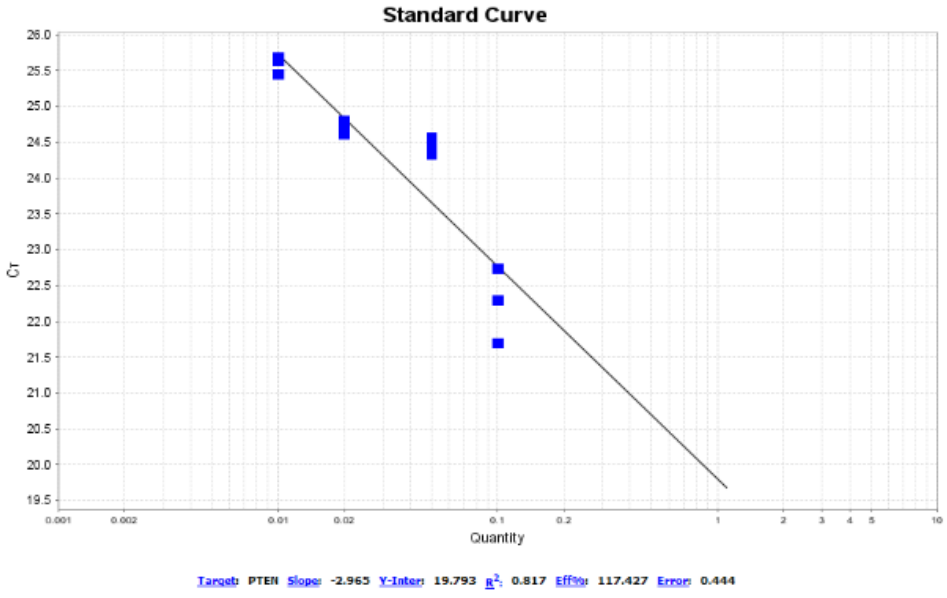

Figure 253 - Example standard curve plot for PTEN. R^2 = 0.82 (recommended is >0.97). PCR efficiency = 117 % (90 % - 110 % is considered acceptable). Slope is -3 (acceptable is about -3.3) [347].

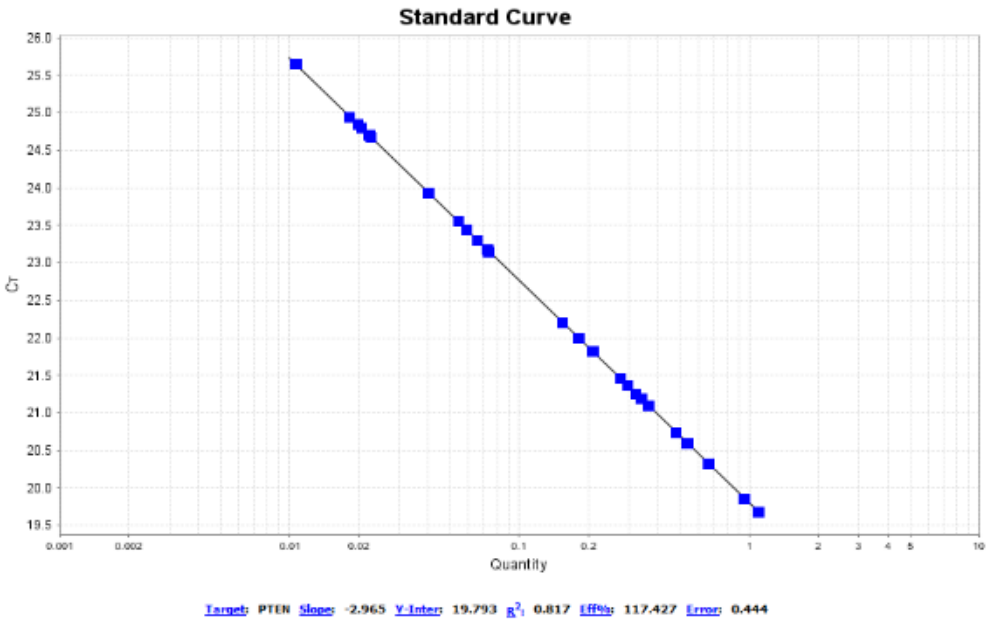

Figure 254 - The unknown samples are within the region of the standard curve plot some with greater Ct values for PTEN than others [347].

11.7.3.9 Hypoxanthine-guanine phosphoribosyltransferase 1 (HPRT1)

(a)

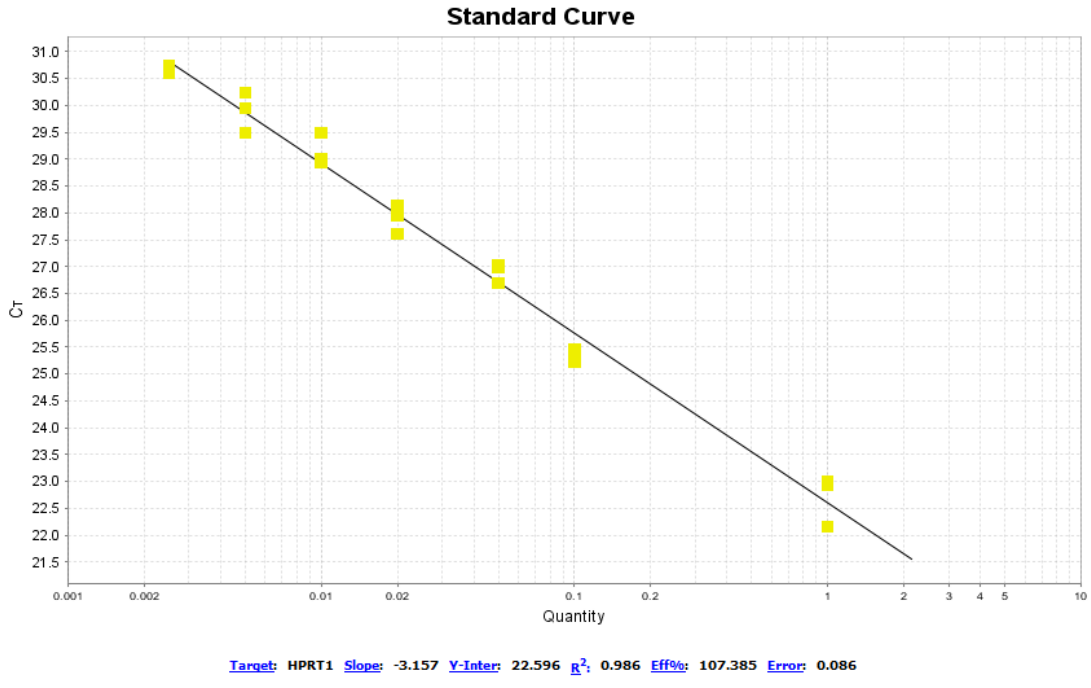

(b)

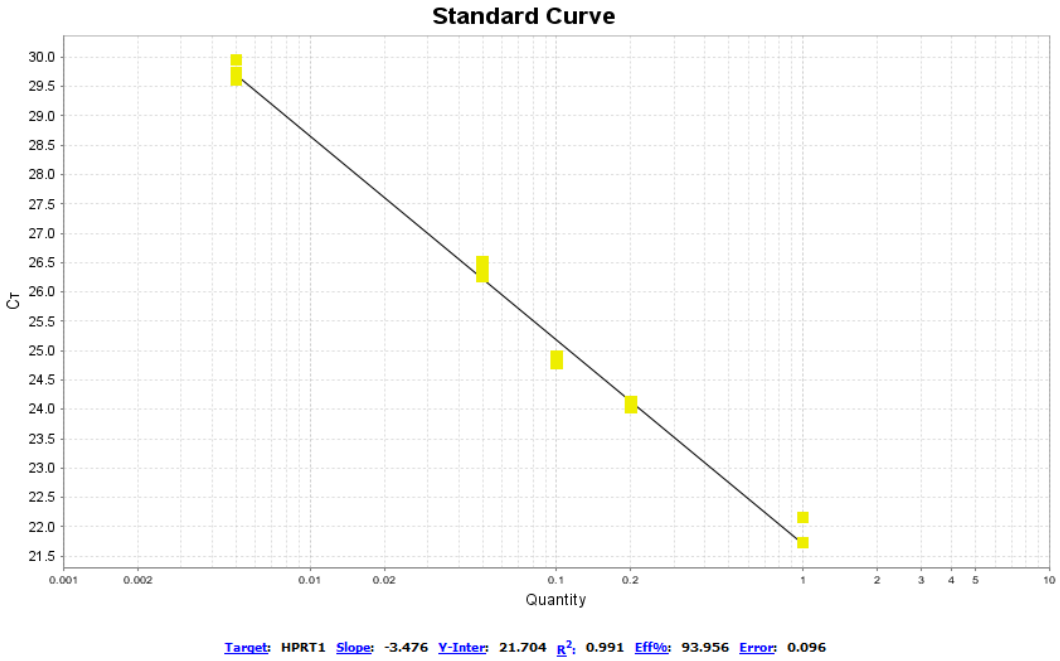

Figure 255 - Example standard curve plots for HPRT1. R^2 = 0.99 (recommended is

>0.97). PCR efficiency = 107 % in (a) and 94 % in (b) (90 % - 110 % is considered acceptable). Slope is -3.2 (a) and -3.5 (b) (acceptable is about -3.3) [347].

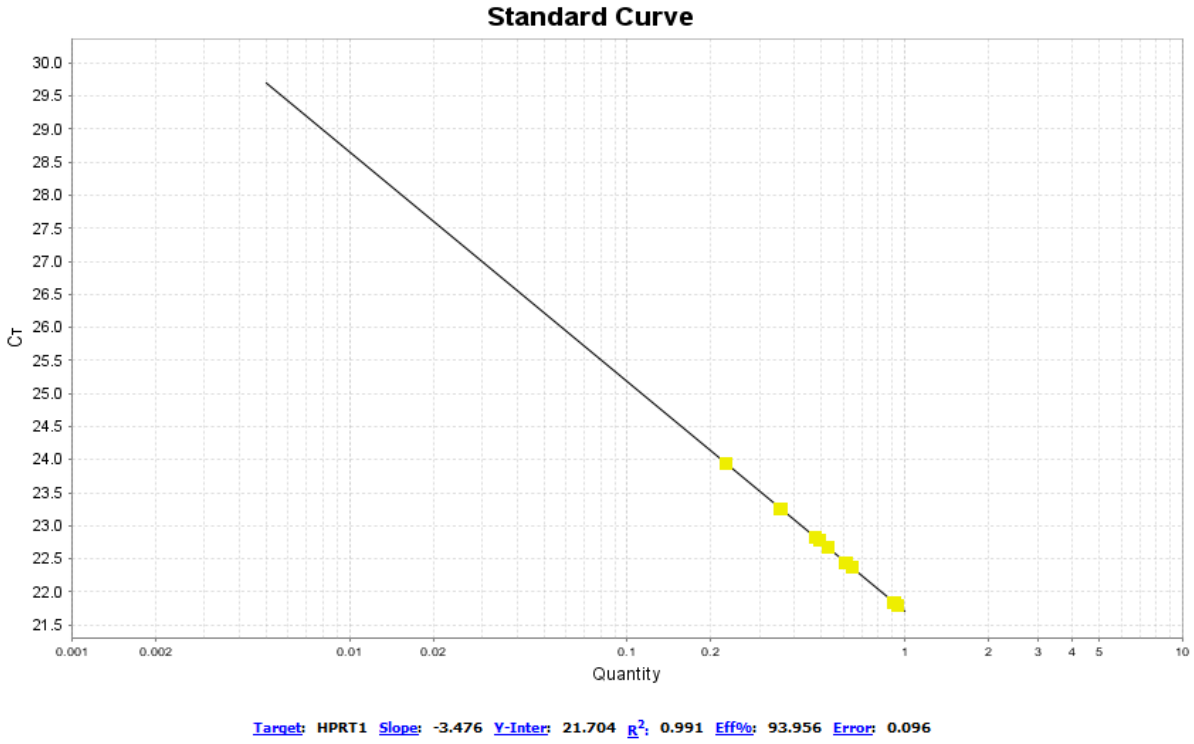

Figure 256 - The unknown bone sarcoma cell line samples are at the lower region of the standard curve plot some with greater Ct values for HPRT1 than others [347].

11.8 *In vivo* table of full dataset and outcome metrics

		21/01/2019	23/01/2019	30/01/2019	06/02/2019	13/02/2019	20/02/2019	
Treatment	Sex	Day 4	Day 6	Day 13	Day 20	Day 27	Day 34	
		Fluorescence	Fluorescence	Fluorescence	Fluorescence	Fluorescence		
Combination therapy	F	1.05E+06	1.25E+06	1.31E+06	1.62E+06	1.55E+06		
	M	9.83E+05	1.33E+06	5.91E+05	4.61E+05	6.36E+08		
	M	9.53E+05	1.34E+06	1.15E+06	2.95E+08	1.61E+06		
	M	9.45E+05	2.00E+06	3.48E+06	2.29E+07	3.70E+07		
	F	1.18E+06	3.77E+06	3.01E+06	1.52E+08	7.01E+06		
	F	3.60E+05	3.35E+06	2.75E+06	6.18E+07	1.83E+07		
M:F 3:3	**Mean**	**9.10E+05**	**2.17E+06**	**2.05E+06**	**8.90E+07**	**1.17E+08**		
	SD	**2.83E+05**	**1.12E+06**	**1.18E+06**	**1.16E+08**	**2.55E+08**		
	SEM	**1.16E+05**	**4.55E+05**	**4.80E+05**	**4.73E+07**	**1.04E+08**		
NG2TRAIL only	F	1.03E+06	1.75E+06	1.36E+06	1.24E+08	7.99E+08		
	F	2.21E+06	1.05E+06	3.67E+06	2.30E+08	5.73E+09		
	M	4.03E+05	1.35E+06	9.54E+06	3.08E+07	1.01E+08		
	M	9.06E+05	1.04E+06	1.69E+06	3.58E+06	8.65E+06		
	F	1.07E+06	2.92E+06	1.74E+06	2.29E+06	5.37E+06		
	F	4.29E+05	3.06E+06	1.63E+07	1.07E+08	3.30E+08		
M:F 2:4	**Mean**	**1.01E+06**	**1.86E+06**	**5.72E+06**	**8.29E+07**	**1.16E+09**		
	SD	**6.58E+05**	**9.12E+05**	**6.04E+06**	**8.86E+07**	**2.26E+09**		
	SEM	**2.69E+05**	**3.72E+05**	**2.47E+06**	**3.62E+07**	**9.21E+08**		
Doxorubicin only	M	7.11E+05	7.73E+05	1.21E+07	7.14E+07	2.78E+07	1.28E+09	1 week delayed dosing
	M	6.18E+05	1.48E+06	1.78E+08	1.94E+09	1.45E+10		
	M	8.17E+06	3.22E+07	3.51E+09	4.50E+10	euthanised 8/02/19		
	M	9.47E+05	3.10E+06	4.20E+08	1.61E+09	7.24E+10		
	F	4.44E+05	1.25E+06	9.00E+07	4.68E+08	2.96E+09		
M:F 4:1	**Mean**	**2.18E+06**	**7.76E+06**	**8.41E+08**	**9.81E+09**	**2.25E+10**		
	SD	**3353641.187**	**13680947.46**	**1497951126**	**19664720098**	**30998677828**		
	SEM	**1499793.933**	**6118305.705**	**669904108.8**	**8794330179**	**13863030167**		
Non-targeted TRAIL only	M	7.79E+05	1.16E+06	2.55E+06	1.91E+07	5.75E+07		
	F	1.47E+06	3.24E+06	1.92E+07	1.17E+08	4.26E+08		
	F	1.08E+06	1.66E+06	4.24E+06	1.37E+07	2.66E+07		
M:F 1:2	**Mean**	**1.11E+06**	**2.02E+06**	**8.68E+06**	**4.99E+07**	**1.70E+08**		
	SD	**348721.3979**	**1089723.054**	**9186425.874**	**58078535.62**	**222143670.9**		
	SEM	**201334.3929**	**629151.8983**	**5303785.451**	**33531658.18**	**128254708.2**		
Control	M	5.15E+05	1.66E+06	1.33E+08	7.94E+06	5.50E+09		
	M	1.75E+06	2.56E+06	1.53E+07	3.19E+10	7.24E+10		
	F	3.16E+06	4.37E+06	1.95E+09	2.09E+10	euthanised 12/02/19		
	F	4.36E+05	1.85E+07	6.67E+07	3.73E+09	2.42E+08		
M:F 2:2	**Mean**	**1.47E+06**	**6.77E+06**	**5.42E+08**	**1.41E+10**	**2.60E+10**		
	SD	**1281540.077**	**7889238.979**	**941948635.7**	**14932248171**	**35328801007**		
	SEM	**640770.0385**	**3944619.489**	**470974317.8**	**7466124085**	**17664400503**		

(a)

(b)

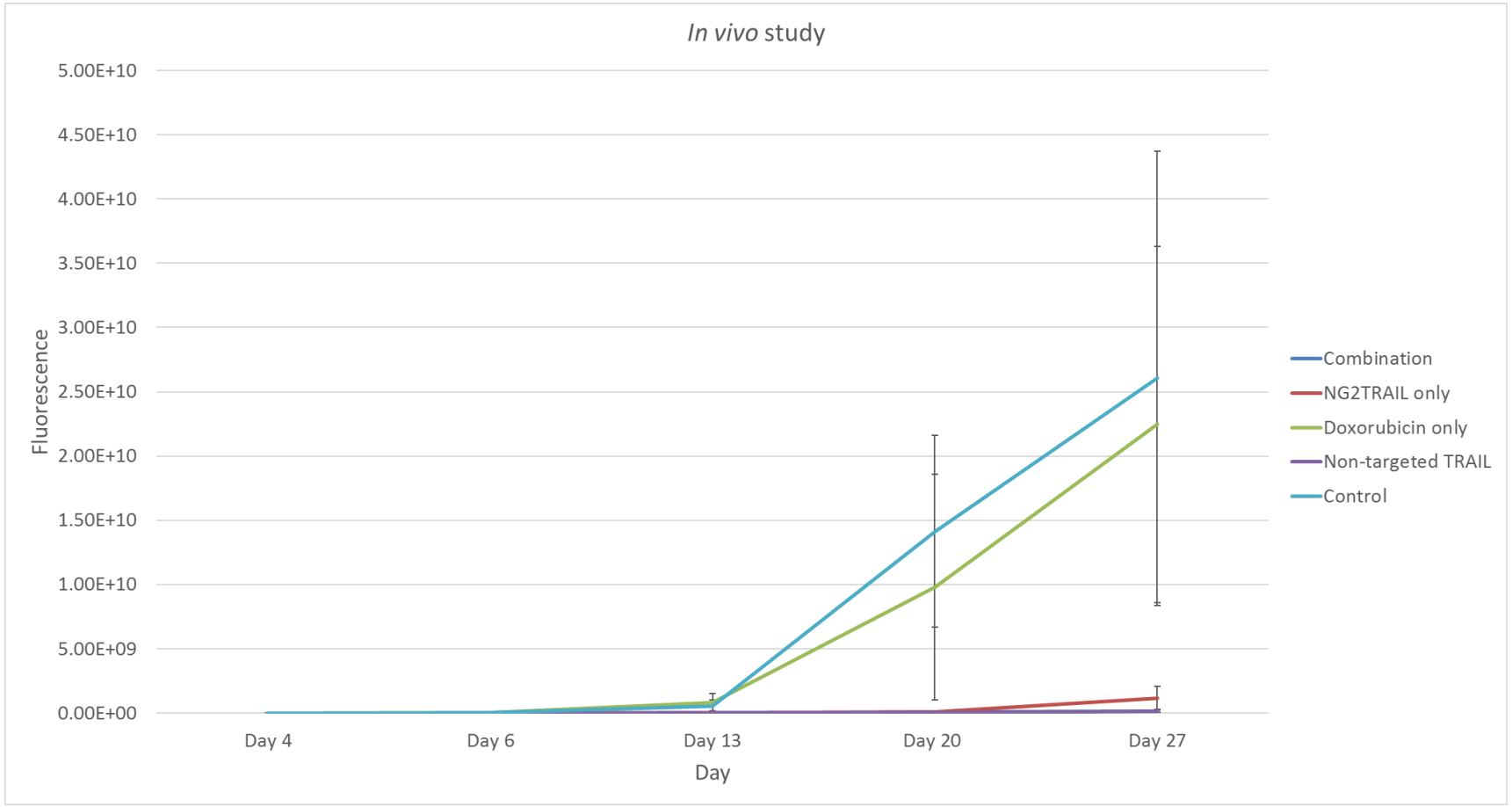
In vivo study
5.00E+10
4.50E+10
4.00E+10
3.50E+10
3.00E+10
2.50E+10
2.00E+10
1.50E+10
1.00E+10
5.00E+09
0.00E+00
Fluorescence
Day 4
Day 6
Day 13
Day 20
Day 27
Day
Combination
NG2TRAIL only
Doxorubicin only
Non-targeted TRAIL
Control

(c)

			21/01/2019	23/01/2019	30/01/2019	06/02/2019	13/02/2019
			Day 4	Day 6	Day 13	Day 20	Day 27
PK study	Day 1 harvest	M	1.50E+06	7.32E+05	1.62E+08	kd 05/02/19	N/A
		M	4.66E+05	5.74E+05	7.28E+08	kd 05/02/19	N/A
		M	4.77E+05	5.34E+05	1.39E+09	kd 05/02/19	N/A
	Day 3 Harvest	M	8.20E+05	7.39E+05	1.79E+08		kd 07/02/2019
		F	6.49E+05	1.61E+06	2.36E+08		kd 07/02/2019
		M	3.84E+05	4.24E+05	1.29E+08		kd 07/02/2019
	Day 7 Harvest	M	6.46E+05	8.40E+05	3.61E+07		kd 11/02/19
		M	4.86E+05	7.00E+05	2.97E+06		kd 11/02/19
		M	8.62E+05	1.64E+06	1.62E+08		kd 11/02/19
	PK study	F	1.01E+06	1.64E+06	2.07E+08	Kd 04/02/2019	N/A
	C	M	7.35E+05	1.10E+06	died 28/01/19	N/A	N/A
	C	F	7.17E+05	2.68E+06	1.67E+09	7.06E+08	died 07/02/19

Figure 257 – (a) Full dataset, summary statistics (M:F ratio; mean, SD and SEM) and outcome measures (Fluorescence) from the formal *in vivo* study, (b) graph of results, (c) summary table of schedule of blood and organ harvesting from TRAIL treated mice for future pharmacokinetic (PK) studies. M = male, F = female, SD = standard deviation, SEM = standard error of the mean, PK = pharmacokinetic.

Chapter 12. Research outputs

1. Presentations

Regional

- *Annual Kreibich meeting, June 2019, Durham*
  Podium presentation: Preclinical testing of TRAIL therapeutics for bone sarcoma

- *Northern Institute for Cancer Research, Research In Progress (RIP) meetings, 2017-2019, University of Newcastle*
  Podium presentation: Preclinical testing of TRAIL therapeutics for bone sarcoma

- *North East Surgical Training Academy (NESTAC), May 2018, Newcastle*
  Podium presentation: Preclinical testing of TRAIL therapeutics for bone sarcoma

- *Postgraduate Cancer conference, March 2018, The Great North Museum: Hancock, Newcastle*
  Podium and poster presentations: Preclinical testing of TRAIL therapeutics for bone sarcoma

National

- *British Orthopaedic Oncology Society (BOOS) Annual Meeting, June 2018, Edinburgh*
  Podium presentation: Preclinical testing of a novel targeted TRAIL therapeutic for dedifferentiated chondrosarcoma

- *Cancer and Bone Society Meeting, June 2018, St Catherine's College, Oxford*
  Poster presentation: Preclinical testing of TRAIL therapeutics for bone sarcoma

- *Workshop on Translational Research of Bone Sarcoma, June 2017, Sheffield*
  Podium presentation: Preclinical testing of TRAIL therapeutics for bone sarcoma

International

- *Connective Tissue Oncology Society (CTOS), November 2019, Tokyo, Japan*
  Poster presentation: Preclinical testing of TRAIL therapeutics for sarcoma

- *British Orthopaedic Oncology Society (BOOS), April 2019, Leiden, Netherlands*
  Podium presentation: Preclinical testing of a novel targeted TRAIL therapeutic for dedifferentiated chondrosarcoma – winner of Dr Takeshi Kashima basic science award

- *European Federation of National Associations of Orthopaedics and Traumatology (EFORT), May 2018, Barcelona, Spain*
  Oral presentation: Basic Science, Assessment and Strategy (Musculoskeletal Tumors) session- Preclinical testing of TRAIL therapeutics for bone sarcoma

2. Publications

- Stamatopoulos A, Stamatopoulos T, **Gamie Z**, Kenanidis E, Ribeiro RDC, Rankin KS, Gerrand C, Dalgarno K, Tsiridis E. Mesenchymal stromal cells for bone sarcoma treatment: Roadmap to clinical practice. Journal of bone oncology. 2019;16:100231.

- **Gamie Z**, Kapriniotis K, Papanikolaou D, Haagensen E, Da Conceicao Ribeiro R, Dalgarno K, Krippner-Heidenreich A, Gerrand C, Tsiridis E, Rankin KS. TNF-related apoptosis-inducing ligand (TRAIL) for bone sarcoma treatment: Pre-clinical and clinical data. Cancer letters. 2017;409:66-80.

3. Research Grants

- 2018: £75,000- Funding to complete PhD work. Newcastle Healthcare Charity and Other Related Charities. Charity Reg No: 502 473.

- 2018: Funding to complete PhD work. The JGW Patterson Foundation. Charity Reg No: 109 4086

- 2014: £74,000- William Edmund Harker Studentship, Newcastle University, 3D Bioprinting for bone sarcoma

- 2014: £75,000- Orthopaedic Research UK. Pre-conditioning of MSCs for use in 3D Bioprinting of bone cancers. Interim reports submitted on: (1) 19 June 2016, (2) 29 September 2016, (3) 1 February 2017, (4) 2 June 2017, (5) 2 October 2017, (6) 6 March 2018, (7) 24 May 2018, (8) 27 September 2018, (9) 1 February 2019.

Chapter 13. References

1. Burningham Z, Hashibe M, Spector L, Schiffman JD: **The epidemiology of sarcoma.** *Clin Sarcoma Res* (2012) **2**(1):14.

2. Hui J: **Epidemiology and etiology of sarcomas.** *Surg Clin North Am* (2016) **96.**(5):901-914.

3. Amankwah E, Conley A, Reed D: **Epidemiology and therapies for metastatic sarcoma.** *Clin Epidemiol* (2013) 5):147-162.

4. Whelan J, McTiernan A, Cooper N, Wong YK, Francis M, Vernon S, Strauss SJ: **Incidence and survival of malignant bone sarcomas in england 1979-2007.** *Int J Cancer* (2012) **131**(4):E508-517.

5. Seibel NL, Krailo M, Chen Z, Healey J, Breitfeld PP, Drachtman R, Greffe B, Nachman J, Nadel H, Sato JK, Meyers PA *et al*: **Upfront window trial of topotecan in previously untreated children and adolescents with poor prognosis metastatic osteosarcoma: Children's cancer group (ccg) 7943.** *Cancer* (2007) **109**(8):1646-1653.

6. Bernstein M, Kovar H, Paulussen M, Randall RL, Schuck A, Teot LA, Juergens H: **Ewing's sarcoma family of tumors: Current management.** *Oncologist* (2006) **11**(5):503-519.

7. Martins-Neves SR, Paiva-Oliveira DI, Wijers-Koster PM, Abrunhosa AJ, Fontes-Ribeiro C, Bovée JV, Cleton-Jansen AM, Gomes CM: **Chemotherapy induces stemness in osteosarcoma cells through activation of wnt/β-catenin signaling.** *Cancer Lett* (2016) **370**(2):286-295.

8. Schwarz R, Bruland O, Cassoni A, Schomberg P, Bielack S: **The role of radiotherapy in oseosarcoma.** *Cancer Treat Res* (2009) **152**(147-164).

9. Rickel K, Fang F, Tao J: **Molecular genetics of osteosarcoma.** *Bone* (2016).

10. Morrow JJ, Khanna C: **Osteosarcoma genetics and epigenetics: Emerging biology and candidate therapies.** *Crit Rev Oncog* (2015) **20**(3-4):173-197.

11. Chou AJ, Gorlick R: **Chemotherapy resistance in osteosarcoma: Current challenges and future directions.** *Expert Review of Anticancer Therapy* (2006) **6**(7):1075-1085.

12. Lessnick SL, Ladanyi M: **Molecular pathogenesis of ewing sarcoma: New therapeutic and transcriptional targets.** *Annu Rev Pathol* (2012) **7**(145-159.

13. Toomey EC, Schiffman JD, Lessnick SL: **Recent advances in the molecular pathogenesis of ewing's sarcoma.** *Oncogene* (2010) **29**(32):4504-4516.

14. Subbiah V, Anderson P, Lazar AJ, Burdett E, Raymond K, Ludwig JA: **Ewing's sarcoma: Standard and experimental treatment options.** *Curr Treat Options Oncol* (2009) **10**(1-2):126-140.

15. Yabe H, Fukuma M, Urano F, Yoshida K, Kato S, Toyama Y, Hata J, Umezawa A: **Lack of matrix metalloproteinase (mmp)-1 and -3 expression in ewing sarcoma may be due to loss of accessibility of the mmp regulatory element to the specific fusion protein in vivo.** *Biochem Biophys Res Commun* (2002) **293**(1):61-71.

16. Naing A, LoRusso P, Fu S, Hong DS, Anderson P, Benjamin RS, Ludwig JA, Chen HX, Doyle LA, Kurzrock R: **Insulin growth factor-receptor (igf-1r) antibody cixutumumab combined with the mtor inhibitor temsirolimus in patients with refractory ewing's sarcoma family tumors.** *Clin Cancer Res* (2012) **18**(9):2625-2631.

17. Sandberg A: **Genetics of chondrosarcoma and related tumors.** *Curr Opin Oncol* (2004) **16**(4):342-354.

18. Amary MF, Bacsi K, Maggiani F, Damato S, Halai D, Berisha F, Pollock R, O'Donnell P, Grigoriadis A, Diss T, Eskandarpour M *et al*: **Idh1 and idh2 mutations are frequent events in central chondrosarcoma and central and periosteal chondromas but not in other mesenchymal tumours.** *J Pathol* (2011) **224**(3):334-343.

19. Kim MJ, Cho KJ, Ayala AG, Ro JY: **Chondrosarcoma: With updates on molecular genetics.** *Sarcoma* (2011) **2011**(405437.

20. Bovée JV, Cleton-Jansen AM, Kuipers-Dijkshoorn NJ, van den Broek LJ, Taminiau AH, Cornelisse CJ, Hogendoorn PC: **Loss of heterozygosity and DNA ploidy point to a diverging genetic mechanism in the origin of peripheral and central chondrosarcoma.** *Genes Chromosomes Cancer* (1999) **26**(3):237-246.

21. Debatin KM, Krammer PH: **Death receptors in chemotherapy and cancer.** *Oncogene* (2004) **23**(16):2950-2966.

22. Ashkenazi A, Herbst RS: **To kill a tumor cell: The potential of proapoptotic receptor agonists.** *J Clin Invest* (2008 Jun) **118**(6):1979-1990.

23. Walczak H: **Death receptor-ligand systems in cancer, cell death, and inflammation.** *Cold Spring Harb Perspect Biol* (2013) **5**(5).

24. Spierings D, McStay G, Saleh M, Bender C, Chipuk J, Maurer U, Green DR: **Connected to death: The (unexpurgated) mitochondrial pathway of apoptosis.** *Science* (2005) **310**(5745):66-67.

25. Fridman JS, Lowe SW: **Control of apoptosis by p53.** *Oncogene* (2003) **22**(56):9030-9040.

26. Wang X: **The expanding role of mitochondria in apoptosis.** *Genes Dev* (2001) **15**(22):2922-2933.

27. Slee EA, O'Connor DJ, Lu X: **To die or not to die: How does p53 decide?** *Oncogene* (2004) **23**(16):2809-2818.

28. Yang JZ, Ma SR, Rong XL, Zhu MJ, Ji QY, Meng LJ, Gao YY, Yang YD, Wang Y: **Characterization of multidrugresistant osteosarcoma sublines and the molecular mechanisms of resistance.** *Mol Med Rep* (2016) **14**(4):3269-3276.

29. Debatin KM, Poncet D, Kroemer G: **Chemotherapy: Targeting the mitochondrial cell death pathway.** *Oncogene* (2002) **21**(57):8786-8803.

30. Knappskog S, Berge EO, Chrisanthar R, Geisler S, Staalesen V, Leirvaag B, Yndestad S, de Faveri E, Karlsen BO, Wedge DC, Akslen LA *et al*: **Concomitant inactivation of the p53- and prb- functional pathways predicts resistance to DNA damaging drugs in breast cancer in vivo.** *Mol Oncol* (2015) **9**(8):1553-1564.

31. Kelley SK, Ashkenazi A: **Targeting death receptors in cancer with apo2l/trail.** *Curr Opin Pharmacol* (2004) **4**(4):333-339.

32. Gonzalvez F, Ashkenazi A: **New insights into apoptosis signaling by apo2l/trail.** *Oncogene* (2010) **29**(34):4752-4765.

33. Maduro JH, de Vries EG, Meersma GJ, Hougardy BM, van der Zee AG, de Jong S: **Targeting pro-apoptotic trail receptors sensitizes hela cervical cancer cells to irradiation-induced apoptosis.** *Int J Radiat Oncol Biol Phys* (2008) **72**(2):543-552.

34. Surget S, Chiron D, Gomez-Bougie P, Descamps G, Ménoret E, Bataille R, Moreau P, Le Gouill S, Amiot M, Pellat-Deceunynck C: **Cell death via dr5, but not dr4, is regulated by p53 in myeloma cells.** *Cancer Res* (2012) **72**(17):4562-4573.

35. Koksal IT, Sanlioglu AD, Kutlu O, Sanlioglu S: **Effects of androgen ablation therapy in trail death ligand and its receptors expression in advanced prostate cancer.** *Urol Int* (2010) **84**(4):445-451.

36. Picarda G, Trichet V, Téletchéa S, Heymann D, Rédini F: **Trail receptor signalling and chemotherapeutic option in bone tumors: The trap of the bone microenvironment.** *Am J Cancer Res* (2012) **2**(1):45-64.

37. Dufour F, Rattier T, Shirley S, Picarda G, Constantinescu AA, Morlé A, Zakaria AB, Marcion G, Causse S, Szegezdi E, Zajonc DM *et al*: **N-glycosylation of mouse trail-r and human trail-r1 enhances trail-induced death.** *Cell Death Differ* (2017) **24**(3):500-510.

38. Wagner KW, Punnoose EA, Januario T, Lawrence DA, Pitti RM, Lancaster K, Lee D, von Goetz M, Yee SF, Totpal K, Huw L *et al*: **Death-receptor o-glycosylation controls tumor-cell sensitivity to the proapoptotic ligand apo2l/trail.** *Nat Med* (2007) **13**(9):1070-1077.

39. Holland PM: **Targeting apo2l/trail receptors by soluble apo2l/trail.** *Cancer Lett* (2013) **332**(2):156-162.

40. Wang S, El-Deiry WS: **Trail and apoptosis induction by tnf-family death receptors.** *Oncogene* (2003) **22**(53):8628-8633.

41. Mahalingam D, Szegezdi E, Keane M, de Jong S, Samali A: **Trail receptor signalling and modulation: Are we on the right trail?** *Cancer Treat Rev* (2009) **35**(3):280-288.

42. Bosman MC, Reis CR, Schuringa JJ, Vellenga E, Quax WJ: **Decreased affinity of recombinant human tumor necrosis factor-related apoptosis-inducing ligand (rhtrail) d269h/e195r to osteoprotegerin (opg) overcomes trail resistance mediated by the bone microenvironment** *J Biol Chem* (2014) **289**(2):1071–1078.

43. Shipman CM, Croucher PI: **Osteoprotegerin is a soluble decoy receptor for tumor necrosis factor-related apoptosis-inducing ligand/apo2 ligand and can function as a paracrine survival factor for human myeloma cells.** *Cancer Res* (2003) **63**(5):912-916.

44. Lamhamedi-Cherradi SE, Zheng SJ, Maguschak KA, Peschon J, Chen YH: **Defective thymocyte apoptosis and accelerated autoimmune diseases in trail(-/-) mice.** *Nat Immunol* (2003) **4**(3):255-260.

45. Martínez-Lorenzo MJ, Alava MA, Gamen S, Kim KJ, Chuntharapai A, Piñeiro A, Naval J, Anel A: **Involvement of apo2 ligand/trail in activation-induced death of jurkat and human peripheral blood t cells.** *Eur J Immunol* (1998) **28**(9):2714-2725.

46. Cretney E, Uldrich AP, Berzins SP, Strasser A, Godfrey DI, Smyth MJ: **Normal thymocyte negative selection in trail-deficient mice.** *The Journal of Experimental Medicine* (2003) **198**(3):491-496.

47. Simon AK, Williams O, Mongkolsapaya J, Jin B, Xu XN, Walczak H, Screaton GR: **Tumor necrosis factor-related apoptosis-inducing ligand in t cell development: Sensitivity of human thymocytes.** *Proceedings of the National Academy of Sciences* (2001) **98**(9):5158-5163.

48. Song K, Chen Y, Göke R, Wilmen A, Seidel C, Göke A, Hilliard B, Chen Y: **Tumor necrosis factor–related apoptosis-inducing ligand (trail) is an inhibitor of autoimmune inflammation and cell cycle progression.** *The Journal of Experimental Medicine* (2000) **191**(7):1095-1104.

49. Hilliard B, Wilmen A, Seidel C, Liu T-ST, Göke R, Chen Y: **Roles of tnf-related apoptosis-inducing ligand in experimental autoimmune encephalomyelitis.** *The Journal of Immunology* (2001) **166**(2):1314-1319.

50. Lub-de Hooge MN, de Vries EGE, de Jong S, Bijl M: **Soluble trail concentrations are raised in patients with systemic lupus erythematosus.** *Annals of the Rheumatic Diseases* (2005) **64**(6):854-858.

51. Robertson NM, Zangrilli JG, Steplewski A, Hastie A, Lindemeyer RG, Planeta MA, Smith MK, Innocent N, Musani A, Pascual R, Peters S *et al*: **Differential expression of trail and trail receptors in allergic asthmatics following segmental antigen challenge: Evidence for a role of trail in eosinophil survival.** *The Journal of Immunology* (2002) **169**(10):5986-5996.

52. Schneider B, Münkel S, Krippner-Heidenreich A, Grunwald I, Wels WS, Wajant H, Pfizenmaier K, Gerspach J: **Potent antitumoral activity of trail through generation of tumor-targeted single-chain fusion proteins.** *Cell Death Dis* (2010) **1**(e68.

53. Bos PD, Zhang XH, Nadal C, Shu W, Gomis RR, Nguyen DX, Minn AJ, van de Vijver MJ, Gerald WL, Foekens JA, Massagué J: **Genes that mediate breast cancer metastasis to the brain. .** *Nature* (2009) **459**(7249):1005-1009.

54. Ashkenazi A: **Targeting death and decoy receptors of the tumour-necrosis factor superfamily.** *Nat Rev Cancer* (2002) **2**(6):220-230.

55. Bouralexis S, Findlay DM, Atkins GJ, Labrinidis A, Hay S, Evdokiou A: **Progressive resistance of btk-143 osteosarcoma cells to apo2l/trail-induced apoptosis is mediated by acquisition of dcr2/trail-r4 expression: Resensitisation with chemotherapy.** *Br J Cancer* (2003) **89**(1):206-214.

56. Koschny R, Walczak H, Ganten TM: **The promise of trail--potential and risks of a novel anticancer therapy.** *J Mol Med (Berl)* (2007) **85**(9):923-935.

57. Ashkenazi A, Pai RC, Fong S, Leung S, Lawrence DA, Marsters SA, Blackie C, Chang L, McMurtrey AE, Hebert A, DeForge L *et al*: **Safety and antitumor activity of recombinant soluble apo2 ligand.** *J Clin Invest* (1999) **104**(2):155-162.

58. Fesik SW: **Promoting apoptosis as a strategy for cancer drug discovery.** *Nat Rev Cancer* (2005) **5**(11):876-885.

59. Zhao K, Wang Y, Wang X, Wang Y, Ma Y: **Tagged and untagged trail show different activity against tumor cells.** *Oncol Lett* (2012) **4**(6):1301-1304.

60. Lawrence DA, Shahrokh Z, Marsters SA, Achilles K, Shih D, Mounho B, Hillan K, Totpal K, DeForge L, Schow P, Hooley J *et al*: **Differential hepatocyte toxicity of recombinant apo2l/trail versions.** *Nat Med* (2001) **7**(4):383-385.

61. Hao C, Song JH, Hsi B, Lewis J, Song DK, Petruk KC, Tyrrell DL, Kneteman NM: **Trail inhibits tumor growth but is nontoxic to human hepatocytes in chimeric mice.** *Cancer Res* (2004) **64**(23):8502-8506.

62. Fulda S: **Safety and tolerability of trail receptor agonists in cancer treatment.** *Eur J Clin Pharmacol* (2015) **71**(5):525-527.

63. Mundt B, Wirth T, Zender L, Waltemathe M, Trautwein C, Manns MP, Kühnel F, Kubicka S: **Tumour necrosis factor related apoptosis inducing ligand (trail) induces hepatic steatosis in viral hepatitis and after alcohol intake.** *Gut* (2005) **54**(11):1590-1596.

64. Liang X, Liu Y, Zhang Q, Gao L, Han L, Ma C, Zhang L, Chen YH, Sun W: **Hepatitis b virus sensitizes hepatocytes to trail-induced apoptosis through bax.** *J Immunol* (2007) **178**(1):503-510.

65. Koschny R, Ganten TM, Sykora J, Haas TL, Sprick MR, Kolb A, Stremmel W, Walczak H: **Trail/bortezomib cotreatment is potentially hepatotoxic but induces cancer-specific apoptosis within a therapeutic window.** *Hepatology* (2007) **45**(3):649-658.

66. Bremer E, de Bruyn M, Samplonius DF, Bijma T, ten Cate B, de Leij LF, Helfrich W: **Targeted delivery of a designed strail mutant results in superior apoptotic activity towards egfr-positive tumor cells.** *J Mol Med (Berl)* (2008) **86**(8):909-924.

67. Bremer E, Samplonius D, Kroesen BJ, van Genne L, de Leij L, Helfrich W: **Exceptionally potent anti-tumor bystander activity of an scfv:Strail fusion protein with specificity for egp2 toward target antigen-negative tumor cells.** *Neoplasia* (2004) **6**(5):636-645.

68. Bremer E, Samplonius DF, Peipp M, van Genne L, Kroesen BJ, Fey GH, Gramatzki M, de Leij LF, Helfrich W: **Target cell-restricted apoptosis induction of acute leukemic t cells by a recombinant tumor necrosis factor-related apoptosis-inducing ligand fusion protein with specificity for human cd7.** *Cancer Res* (2005) **65**(8):3380-3388.

69. Staudacher AH, Brown MP: **Antibody drug conjugates and bystander killing: Is antigen-dependent internalisation required?** *Br J Cancer* (2017) **117**(12):1736-1742.

70. Hendriks D, He Y, Koopmans I, Wiersma VR, van Ginkel RJ, Samplonius DF, Helfrich W, Bremer E: **Programmed death ligand 1 (pd-l1)-targeted trail combines pd-l1-mediated checkpoint inhibition with trail-mediated apoptosis induction.** *Oncoimmunology* (2016) **5**(8):e1202390.

71. Hotta T, Suzuki H, Nagai S, Yamamoto K, Imakiire A, Takada E, Itoh M, Mizuguchi J: **Chemotherapeutic agents sensitise sarcoma cell lines to tumor necrosis factor-related apoptosis-inducing ligand-induced caspase-8 activation, apoptosis and loss of mitochondrial membrane potential.** *J Orthop Res* (2003) **21**(5):949-957.

72. Evdokiou A, Bouralexis S, Atkins GJ, Chai F, Hay S, Clayer M, Findlay DM: **Chemotherapeutic agents sensitize osteogenic sarcoma cells, but not normal human bone cells, to apo2l/trail-induced apoptosis.** *Int J Cancer* (2002) **99**(4):491-504.

73. Picarda G, Lamoureux F, Geffroy L, Delepine P, Montier T, Laud K, Tirode F, Delattre O, Heymann D, Rédini F: **Preclinical evidence that use of trail in ewing's sarcoma and osteosarcoma therapy inhibits tumor growth, prevents osteolysis, and increases animal survival.** *Clin Cancer Res* (2010) 16):2363-2374.

74. Takeda S, Iwai A, Nakashima M, Fujikura D, Chiba S, Li HM, Uehara J, Kawaguchi S, Kaya M, Nagoya S, Wada T *et al*: **Lkb1 is crucial for trail-mediated apoptosis induction in osteosarcoma.** *Anticancer Res* (2007) **27**(2):761-768.

75. Locklin RM, Federici E, Espina B, Hulley PA, Russell RG, Edwards CM: **Selective targeting of death receptor 5 circumvents resistance of mg-63 osteosarcoma cells to trail-induced apoptosis.** *Mol Cancer Ther* (2007) **6**(12 Pt 1):3219-3228.

76. Sun J, Fu ZM, Fang CQ, Li JH: **Induction of apoptosis in osteogenic sarcoma cells by combination of tumor necrosis factor-related apoptosis inducing ligand and chemotherapeutic agents.** *Chin Med J (Engl)* (2007) **120**(5):400-404.

77. Hanikoglu F, Cort A, Ozben H, Hanikoglu A, Ozben T: **Epoxomicin sensitizes resistant osteosarcoma cells to trail induced apoptosis.** *Anticancer Agents Med Chem* (2015) **15**(4):527-533.

78. Liu G, Yu MY, Huang X, Zhu D, Cheng S, Ma R, Gu G: **Synergistic effect of celecoxib in tumor necrosis factorrelated apoptosisinducing ligand treatment in osteosarcoma cells.** *Mol Med Rep* (2014) **10**(4):2198-2202.

79. Moon MH, Jeong JK, Seo JS, Seol JW, Lee YJ, Xue M, Jackson CJ, Park SY: **Bisphosphonate enhances trail sensitivity to human osteosarcoma cells via death receptor 5 upregulation.** *Exp Mol Med* (2011) **43**(3):138-145.

80. Van Valen F, Fulda S, Truckenbrod B, Eckervogt V, Sonnemann J, Hillmann A, Rödl R, Hoffmann C, Winkelmann W, Schäfer L, Dockhorn-Dworniczak B *et al*: **Apoptotic responsiveness of the ewing's sarcoma family of tumours to tumour necrosis factor-related apoptosis-inducing ligand (trail).** *Int J Cancer* (2000) **88**(2):252-259.

81. Mitsiades N, Poulaki V, Mitsiades C, Tsokos M: **Ewing's sarcoma family tumors are sensitive to tumor necrosis factor-related apoptosis-inducing ligand and express death receptor 4 and death receptor 5.** *Cancer Res* (2001) **15**(61):2704-2712.

82. Kontny HU, Hämmerle K, Klein R, Shayan P, Mackall CL, Niemeyer CM: **Sensitivity of ewing's sarcoma to trail-induced apoptosis.** *Cell Death Differ* (2001 May) **8**(5):506-514.

83. Kumar A, Jasmin A, Eby MT, Chaudhary PM: **Cytotoxicity of tumor necrosis factor related apoptosis-inducing ligand towards ewing's sarcoma cell lines.** *Oncogene* (2001) **20**(8):1010-1014.

84. Picarda G, Surget S, Guiho R, Téletchéa S, Berreur M, Tirode F, Pellat-Deceunynck C, Heymann D, Trichet V, Rédini F: **A functional, new short isoform of death receptor 4 in ewing's sarcoma cell lines may be involved in trail sensitivity/resistance mechanisms.** *Mol Cancer Res* (2010) **10**(3):336-346.

85. Merchant MS, Yang X, Melchionda F, Romero ME, Klein R, Thiele CJ, Tsokos M, Kontny HU, Mackall CL: **Interferon gamma enhances the effectiveness of tumor necrosis factor-related apoptosis-inducing ligand receptor agonists in a xenograft model of ewing's sarcoma.** *Cancer Res* (2004) **64**(22):8349-8356.

86. Lissat A, Vraetz T, Tsokos M, Klein R, Braun M, Koutelia N, Fisch P, Romero ME, Long L, Noellke P, Mackall CL *et al*: **Interferon-gamma sensitizes resistant ewing's sarcoma cells to tumor necrosis factor apoptosis-inducing ligand-induced apoptosis by up-regulation of caspase-8 without altering chemosensitivity.** *Am J Pathol* (2007) **170**(6):1917-1930.

87. Sonnemann J, Dreyer L, Hartwig M, Palani CD, Hong le TT, Klier U, Bröker B, Völker U, Beck JF: **Histone deacetylase inhibitors induce cell death and enhance the apoptosis-inducing activity of trail in ewing's sarcoma cells.** *J Cancer Res Clin Oncol* (2007) **133**(11):847-858.

88. Lu G, Punj V, Chaudhary PM: **Proteasome inhibitor bortezomib induces cell cycle arrest and apoptosis in cell lines derived from ewing's sarcoma family of tumors and synergizes with trail.** *Cancer Biol Ther* (2008) **7**(4):603-608.

89. Cheong HJ, Lee KS, Woo IS, Won JH, Byun JH: **Up-regulation of the dr5 expression by proteasome inhibitor mg132 augments trail-induced apoptosis in soft tissue sarcoma cell lines.** *Cancer Res Treat* (2011) **43**(2):124-130.

90. Tomek S, Koestler W, Horak P, Grunt T, Brodowicz T, Pribill I, Halaschek J, Haller G, Wiltschke C, Zielinski CC, Krainer M: **Trail-induced apoptosis and interaction with cytotoxic agents in soft tissue sarcoma cell lines.** *Eur J Cancer* (2003) **39**(9):1318-1329.

91. Tabernero J, Chawla SP, Kindler H, Reckamp K, Chiorean EG, Azad NS, Lockhart AC, Hsu CP, Baker NF, Galimi F, Beltran P *et al*: **Anticancer activity of the type i insulin-like growth factor receptor antagonist, ganitumab, in combination with the death receptor 5 agonist, conatumumab.** *Target Oncol* (2015) **10**(1):65-76.

92. Demetri GD, Le Cesne A, Chawla SP, Brodowicz T, Maki RG, Bach BA, Smethurst DP, Bray S, Hei YJ, Blay JY: **First-line treatment of metastatic or locally advanced unresectable soft tissue sarcomas with conatumumab in combination with doxorubicin or doxorubicin alone: A phase i/ii open-label and double-blind study.** *Eur J Cancer* (2012) **48**(4):547-563.

93. Merchant MS, Geller JI, Baird K, Chou AJ, Galli S, Charles A, Amaoko M, Rhee EH, Price A, Wexler LH, Meyers PA *et al*: **Phase i trial and pharmacokinetic study of lexatumumab in pediatric patients with solid tumors.** *J Clin Oncol* (2012) **30**(33):4141-4147.

94. Subbiah V, Brown RE, Buryanek J, Trent J, Ashkenazi A, Herbst RS, Kurzrock R: **Targeting the apoptotic pathway in chondrosarcoma using recombinant human apo2l/trail (dulanermin), a dual proapoptotic receptor (dr4/dr5) agonist.** *Mol Cancer Ther* (2012) **11**(11):2541-2546.

95. Herbst RS, Eckhardt SG, Kurzrock R, Ebbinghaus S, O'Dwyer PJ, Gordon MS, Novotny W, Goldwasser MA, Tohnya TM, Lum BL, Ashkenazi A *et al*: **Phase i dose-escalation study of recombinant human apo2l/trail, a dual proapoptotic receptor agonist, in patients with advanced cancer.** *J Clin Oncol* (2010) **28**(17):2839-2846.

96. Camidge DR, Herbst RS, Gordon MS, Eckhardt SG, Kurzrock R, Durbin B, Ing J, Tohnya TM, Sager J, Ashkenazi A, Bray G *et al*: **A phase i safety and pharmacokinetic study of the death receptor 5 agonistic antibody pro95780 in patients with advanced malignancies.** *Clin Cancer Res* (2010) **16**(4):1256-1263.

97. Belch A, Sharma A, Spencer A, Tarantolo S, Bahlis NJ, Doval D, Gallant G, Kumm E, Klein J, Chanan-Khan AA: **A multicenter randomized phase ii trial of mapatumumab, a trail-r1 agonist monoclonal antibody, in combination with bortezomib in patients with relapsed/refractory multiple myeloma (mm).** *Blood* (2010) **16**(21):5031.

98. Tschopp J, Irmler M, Thome M: **Inhibition of fas death signals by flips.** *Current Opinion in Immunology* (1998) **10**(5):552-558.

99. Chang DW, Xing Z, Pan Y, Algeciras-Schimnich A, Barnhart BC, Yaish-Ohad S, Peter ME, Yang X: **C-flip(l) is a dual function regulator for caspase-8 activation and cd95-mediated apoptosis.** *The EMBO Journal* (2002) **21**(14):3704-3714.

100. Poulaki V, Mitsiades N, Romero ME, Tsokos M: **Fas-mediated apoptosis in neuroblastoma requires mitochondrial activation and is inhibited by flice inhibitor protein and bcl-2.** *Cancer Research* (2001) **61**(12):4864-4872.

101. Adida C, Berrebi D, Peuchmaur M, Reyes-Mugica M, Altieri D: **Anti-apoptosis gene, survivin, and prognosis of neuroblastoma.** *Lancet* (1998) **351**(9106):882-883.

102. Ravi R, Bedi GC, Engstrom LW, Zeng Q, Mookerjee B, Gelinas C, Fuchs EJ, Bedi A: **Regulation of death receptor expression and trail/apo2l-induced apoptosis by nf-[kappa]b.** *Nat Cell Biol* (2001) **3**(4):409-416.

103. Harper N, Hughes MA, Farrow SN, Cohen GM, MacFarlane M: **Protein kinase c modulates tumor necrosis factor-related apoptosis-inducing ligand-induced apoptosis by targeting the apical events of death receptor signaling.** *Journal of Biological Chemistry* (2003) **278**(45):44338-44347.

104. El-Zawahry A, McKillop J, Voelkel-Johnson C: **Doxorubicin increases the effectiveness of apo2l/trail for tumor growth inhibition of prostate cancer xenografts. .** *BMC Cancer* (2005) 5):2.

105. Wen J, Ramadevi N, Nguyen D, Perkins C, Worthington E, Bhalla K: **Antileukemic drugs increase death receptor 5 levels and enhance apo-2l-induced apoptosis of human acute leukemia cells. .** *Blood* (2000) **96**(12):3900-3906.

106. Oh Y, Swierczewska M, Kim TH, Lim SM, Eom HN, Park JH, Na DH, Kim K, Lee KC, Pomper MG, Lee S: **Delivery of tumor-homing trail sensitizer with long-acting trail as a therapy for trail-resistant tumors.** *J Control Release* (2015) **220**(Pt B):671-681.

107. Deng C, Shao Z, Xiong X, Liu Z, Zhang Z: **The expression of trail and its receptors in osteosarcoma cells and the apoptosis effect of a combination of trail, adriamycin and ifnγ on mg-63 cells.** *Journal of Nanjing Medical University* (2009) **23**(4):251-256.

108. von Karstedt S, Montinaro A, Walczak H: **Exploring the trails less travelled: Trail in cancer biology and therapy.** *Nat Rev Cancer* (2017) **17**(6):352-366.

109. Guo F, Nimmanapalli R, Paranawithana S, Wittman S, Griffin D, Bali P, O'Bryan E, Fumero C, Wang HG, Bhalla K: **Ectopic overexpression of second mitochondria-derived activator of caspases (smac/diablo) or cotreatment with n-terminus of smac/diablo peptide potentiates epothilone b derivative-(bms 247550) and apo-2l/trail-induced apoptosis.** *Blood* (2002) **99**(9):3419-3426.

110. Dai Y, Liu M, Tang W, Li Y, Lian J, Lawrence TS, Xu L: **A smac-mimetic sensitizes prostate cancer cells to trail-induced apoptosis via modulating both iaps and nf-kappab.** *BMC Cancer* (2009) **9**(392.

111. Ray S, Bucur O, Almasan A: **Sensitization of prostate carcinoma cells to apo2l/trail by a bcl-2 family protein inhibitor.** *10* (2005) **6**(1411-8).

112. Belz K, Schoeneberger H, Wehner S, Weigert A, Bönig H, Klingebiel T, Fichtner I, Fulda S: **Smac mimetic and glucocorticoids synergize to induce apoptosis in childhood all by promoting ripoptosome assembly.** *Blood* (2014) **124**(2):240-250.

113. Kelley RF, Totpal K, Lindstrom SH, Mathieu M, Billeci K, DeForge L, Pai R, Hymowitz SG, Ashkenazi A: **Receptor-selective mutants of apoptosis-inducing ligand 2/tumor necrosis factor-related apoptosis-inducing ligand reveal a greater contribution of death receptor (dr) 5 than dr4 to apoptosis signaling.** *Journal of Biological Chemistry* (2005) **280**(3):2205-2212.

114. Ashkenazi A, Holland P, Eckhardt SG: **Ligand-based targeting of apoptosis in cancer: The potential of recombinant human apoptosis ligand 2/tumor necrosis factor-related apoptosis-inducing ligand (rhapo2l/trail).** *J Clin Oncol* (2008) **26**(21):3621-3630.

115. de Bruyn M, Bremer E, Helfrich W: **Antibody-based fusion proteins to target death receptors in cancer.** *Cancer Letters* **332**(2):175-183.

116. Müller N, Schneider B, Pfizenmaier K, Wajant H: **Superior serum half life of albumin tagged tnf ligands.** *Biochemical and Biophysical Research Communications* (2010) **396**(4):793-799.

117. Kim TH, Youn YS, Jiang HH, Lee S, Chen X, Lee KC: **Pegylated tnf-related apoptosis-inducing ligand (trail) analogues: Pharmacokinetics and antitumor effects.** *Bioconjugate Chemistry* (2011) **22**(8):1631-1637.

118. Jiang HH, Kim TH, Lee S, Chen X, Youn YS, Lee KC: **Pegylated tnf-related apoptosis-inducing ligand (trail) for effective tumor combination therapy.** *Biomaterials* (2011) **32**(33):8529-8537.

119. Kim TH, Jo YG, Jiang HH, Lim SM, Youn YS, Lee S, Chen X, Byun Y, Lee KC: **Peg-transferrin conjugated trail (tnf-related apoptosis-inducing ligand) for therapeutic tumor targeting.** *Journal of Controlled Release* (2012) **162**(2):422-428.

120. Kim TH, Jiang HH, Park CW, Youn YS, Lee S, Chen X, Lee KC: **Pegylated tnf-related apoptosis-inducing ligand (trail)-loaded sustained release plga microspheres for enhanced stability and antitumor activity.** *Journal of Controlled Release* (2011) **150**(1):63-69.

121. Lim SM, Kim TH, Jiang HH, Park CW, Lee S, Chen X, Lee KC: **Improved biological half-life and anti-tumor activity of tnf-related apoptosis-inducing ligand (trail) using peg-exposed nanoparticles.** *Biomaterials* (2011) **32**(13):3538-3546.

122. Kelley SK, Harris LA, Xie D, Deforge L, Totpal K, Bussiere J, Fox JA: **Preclinical studies to predict the disposition of apo2l/tumor necrosis factor-related apoptosis-inducing ligand in humans: Characterization of in vivo efficacy, pharmacokinetics, and safety.** *J Pharmacol Exp Ther* (2001) **299**(1):31-38.

123. Micheau O, Shirley S, Dufour F: **Death receptors as targets in cancer.** *Br J Pharmacol* (2013) **169**(8):1723-1744.

124. Guiho R, Biteau K, Grisendi G, Taurelle J, Chatelais M, Gantier M, Heymann D, Dominici M, Redini F: **Trail delivered by mesenchymal stromal/stem cells counteracts tumor development in orthotopic ewing sarcoma models.** *Int J Cancer* (2016) **139**(12):2802-2811.

125. Grisendi G, Spano C, D'souza N, Rasini V, Veronesi E, Prapa M, Petrachi T, Piccinno S, Rossignoli F, Burns JS, Fiorcari S *et al*: **Mesenchymal progenitors expressing trail induce apoptosis in sarcomas.** *Stem Cells* (2015) **33**(3):859-869.

126. Yuan Z, Kolluri KK, Sage EK, Gowers KH, Janes SM: **Mesenchymal stromal cell delivery of full-length tumor necrosis factor-related apoptosis-inducing ligand is superior to soluble type for cancer therapy.** *Cytotherapy* (2015) **17**(7):885-896.

127. Yuan ZQ, Kolluri KK, Janes SM: **Mesenchymal stem cells expressing full length trail – a promising therapy for cancer.** *Thorax* (2014) **69**(A58).

128. Lee HJ, Yang HM, Choi YS, Park SH, Moon SH, Lee YS, Sung YC, Kim SJ: **A therapeutic strategy for metastatic malignant fibrous histiocytoma through mesenchymal stromal cell-mediated trail production.** *Ann Surg* (2013) **257**(5):952-960.

129. Ciavarella S, Grisendi G, Dominici M, Tucci M, Brunetti O, Dammacco F, Silvestris F: **In vitro anti-myeloma activity of trail-expressing adipose-derived mesenchymal stem cells.** *Br J Haematol* (2012) **157**(5):586-598.

130. Barti-Juhasz H, Mihalik R, Nagy K, Grisendi G, Dominici M, Petak I: **Bone marrow derived mesenchymal stem/stromal cells transduced with full length human trail repress the growth of rhabdomyosarcoma cells in vitro.** *Haematologica* (2011) 96):e21.

131. Mohr A, Albarenque SM, Deedigan L, Yu R, Reidy M, Fulda S, Zwacka RM: **Targeting of xiap combined with systemic mesenchymal stem cell-mediated delivery of strail ligand inhibits metastatic growth of pancreatic carcinoma cells.** *Stem Cells* (2010) **28**(11):2109-2120.

132. Mohr A, Lyons M, Deedigan L, Harte T, Shaw G, Howard L, Barry F, O'Brien T, Zwacka R: **Mesenchymal stem cells expressing trail lead to tumour growth inhibition in an experimental lung cancer model.** *J Cell Mol Med* (2008) **12**(6B):2628-2643.

133. Loebinger MR, Eddaoudi A, Davies D, Janes SM: **Mesenchymal stem cell delivery of trail can eliminate metastatic cancer.** *Cancer Res* (2009) **69**(10):4134-4142.

134. Studeny M, Marini FC, Dembinski JL, Zompetta C, Cabreira-Hansen M, Bekele BN, Champlin RE, Andreeff M: **Mesenchymal stem cells: Potential precursors for tumor stroma and targeted-delivery vehicles for anticancer agents.** *J Natl Cancer Inst* (2004) **96**(21):1593-1603.

135. Kucerova L, Altanerova V, Matuskova M, Tyciakova S, Altaner C: **Adipose tissue-derived human mesenchymal stem cells mediated prodrug cancer gene therapy.** *Cancer Res* (2007) **67**(13):6304-6313.

136. Lee K, Majumdar MK, Buyaner D, Hendricks JK, Pittenger MF, Mosca JD: **Human mesenchymal stem cells maintain transgene expression during expansion and differentiation.** *Mol Ther* (2001) **3**(6):857-866.

137. Van Damme A, Thorrez L, Ma L, Vandenburgh H, Eyckmans J, Dell'Accio F, De Bari C, Luyten F, Lillicrap D, Collen D, VandenDriessche T *et al*: **Efficient**

lentiviral transduction and improved engraftment of human bone marrow mesenchymal cells. *Stem Cells* (2006) **24**(4):896-907.

138. Javazon EH, Beggs KJ, Flake AW: **Mesenchymal stem cells: Paradoxes of passaging.** *Exp Hematol* (2004) **32**(5):414-425.

139. Majumdar MK, Keane-Moore M, Buyaner D, Hardy WB, Moorman MA, McIntosh KR, Mosca JD: **Characterization and functionality of cell surface molecules on human mesenchymal stem cells.** *J Biomed Sci* (2003) **10**(2):228-241.

140. Tse WT, Pendleton JD, Beyer WM, Egalka MC, Guinan EC: **Suppression of allogeneic t-cell proliferation by human marrow stromal cells: Implications in transplantation.** *Transplantation* (2003) **75**(3):389-397.

141. Yuan Z, Lourenco SS, Sage EK, Kolluri KK, Lowdell MW, Janes SM: **Cryopreservation of human mesenchymal stromal cells expressing trail for human anti-cancer therapy.** *Cytotherapy* (2016) **18**(7):860-869.

142. Yuan Z, Kolluri KK, Gowers KHC, Janes SM: **Trail delivery by msc-derived extracellular vesicles is an effective anticancer therapy.** *Journal of Extracellular Vesicles* (2017) **6**(1):1265291.

143. Zhang S, Danchuk SD, Imhof KM, Semon JA, Scruggs BA, Bonvillain RW, Strong AL, Gimble JM, Betancourt AM, Sullivan DE, Bunnell BA: **Comparison of the therapeutic effects of human and mouse adipose-derived stem cells in a murine model of lipopolysaccharide-induced acute lung injury.** *Stem Cell Res Ther* (2013) **4**(1):13.

144. Suzuki K, Sun R, Origuchi M, Kanehira M, Takahata T, Itoh J, Umezawa A, Kijima H, Fukuda S, Saijo Y: **Mesenchymal stromal cells promote tumor growth through the enhancement of neovascularization.** *Mol Med* (2011) **17**(7-8):579-587.

145. Zhu Y, Sun Z, Han Q, Liao L, Wang J, Bian C, Li J, Yan X, Liu Y, Shao C, Zhao RC: **Human mesenchymal stem cells inhibit cancer cell proliferation by secreting dkk-1.** *Leukemia* (2009) **23**(5):925-933.

146. Waterman RS, Henkle SL, Betancourt AM: **Mesenchymal stem cell 1 (msc1)-based therapy attenuates tumor growth whereas msc2-treatment promotes tumor growth and metastasis.** *PLoS One* (2012) **7**(9):e45590.

147. Jamil NS, Azfer A, Worrell H, Salter DM: **Functional roles of cspg4/ng2 in chondrosarcoma.** *Int J Exp Pathol* (2016) **97**(2):178-186.

148. de Bruyn M, Rybczynska AA, Wei Y, Schwenkert M, Fey GH, Dierckx RA, van Waarde A, Helfrich W, Bremer E: **Melanoma-associated chondroitin sulfate proteoglycan (mcsp)-targeted delivery of soluble trail potently inhibits melanoma outgrowth in vitro and in vivo.** *Mol Cancer* (2010) **9**(301).

149. He Y, Hendriks D, van Ginkel R, Samplonius D, Bremer E, Helfrich W: **Melanoma-directed activation of apoptosis using a bispecific antibody directed at mcsp and trail receptor-2/death receptor-5.** *J Invest Dermatol* (2016) **136**(2):541-544.

150. Zhao XD, Deng HB, Lu CL, Bao YX, Lu X, Deng LL: **Association of egfr and kras mutations with expression of p-akt, dr5 and dcr1 in non-small cell lung cancer.** *Neoplasma* (2017) **64**(2).

151. Oikonomou E, Pintzas A: **The trail of oncogenes to apoptosis.** *Biofactors* (2013) **39**(4):343-354.

152. Nimmanapalli R, Perkins CL, Orlando M, O'Bryan E, Nguyen D, Bhalla KN: **Pretreatment with paclitaxel enhances apo-2 ligand/tumor necrosis factor-related apoptosis-inducing ligand-induced apoptosis of prostate cancer cells by inducing death receptors 4 and 5 protein levels.** *Cancer Res* (2001) **61**(2):759-763.

153. Ishioka C, Shimodaira H, Englert C, Shimada A, Osada M, Jia LQ, Suzuki T, Gamo M, Kanamaru R: **Oligomerization is not essential for growth suppression by p53 in p53-deficient osteosarcoma saos-2 cells.** *Biochem Biophys Res Commun* (1997) **232**(1):54-60.

154. Li L, Paz AC, Wilky BA, Johnson B, Galoian K, Rosenberg A, Hu G, Tinoco G, Bodamer O, Trent JC: **Treatment with a small molecule mutant idh1 inhibitor suppresses tumorigenic activity and decreases production of the oncometabolite 2-hydroxyglutarate in human chondrosarcoma cells.** *PLoS One* (2015) **10**(9):e0133813.

155. Neumann S, Bidon T, Branschadel M, Krippner-Heidenreich A, Scheurich P, Doszczak M: **The transmembrane domains of tnf-related apoptosis-inducing ligand (trail) receptors 1 and 2 co-regulate apoptotic signaling capacity.** *PLoS One* (2012) **7**(8):e42526.

156. Bertsch U, Roder C, Kalthoff H, Trauzold A: **Compartmentalization of tnf-related apoptosis-inducing ligand (trail) death receptor functions: Emerging role of nuclear trail-r2.** *Cell Death Dis* (2014) **5**(e1390.

157. Zhang Y, Zhang B: **Trail resistance of breast cancer cells is associated with constitutive endocytosis of death receptors 4 and 5.** *Mol Cancer Res* (2008) **6**(12):1861-1871.

158. Sanlioglu AD, Dirice E, Aydin C, Erin N, Koksoy S, Sanlioglu S: **Surface trail decoy receptor-4 expression is correlated with trail resistance in mcf7 breast cancer cells.** *BMC Cancer* (2005) **5**(54).

159. Sakr RA, Barbashina V, Morrogh M, Chandarlapaty S, Andrade VP, Arroyo CD, Olvera N, King TA: **Protocol for pten expression by immunohistochemistry in formalin-fixed paraffin-embedded human breast carcinoma.** *Appl Immunohistochem Mol Morphol* (2010) **18**(4):371-374.

160. ten Cate B, Bremer E, de Bruyn M, Bijma T, Samplonius D, Schwemmlein M, Huls G, Fey G, Helfrich W: **A novel aml-selective trail fusion protein that is superior to gemtuzumab ozogamicin in terms of in vitro selectivity, activity and stability.** *Leukemia* (2009) **23**(8):1389-1397.

161. Kawata K, Iwai A, Muramatsu D, Aoki S, Uchiyama H, Okabe M, Hayakawa S, Takaoka A, Miyazaki T: **Stimulation of macrophages with the beta-glucan produced by aureobasidium pullulans promotes the secretion of tumor necrosis factor-related apoptosis inducing ligand (trail).** *PLoS One* (2015) **10**(4):e0124809.

162. Zhang XD, Nguyen T, Thomas WD, Sanders JE, Hersey P: **Mechanisms of resistance of normal cells to trail induced apoptosis vary between different cell types.** *FEBS Lett* (2000) **482**(3):193-199.

163. https://www.cellsignal.com.

164. Chen JJ, Bozza WP, Di X, Zhang Y, Hallett W, Zhang B: **H-ras regulation of trail death receptor mediated apoptosis.** *Oncotarget* (2014) **5**(13):5125-5137.

165. Tamm I, Kornblau SM, Segall H, Krajewski S, Welsh K, Kitada S, Scudiero DA, Tudor G, Qui YH, Monks A, Andreeff M *et al*: **Expression and prognostic significance of iap-family genes in human cancers and myeloid leukemias.** *Clin Cancer Res* (2000) **6**(5):1796-1803.

166. **Superkillertrail™, soluble (human) (rec.)** (2017). https://adipogen.com/ag-40t-0002-super-i-killer-i-trail-trade-soluble-human-rec.html/

167. Valley CC, Lewis AK, Mudaliar DJ, Perlmutter JD, Braun AR, Karim CB, Thomas DD, Brody JR, Sachs JN: **Tumor necrosis factor-related apoptosis-inducing ligand (trail) induces death receptor 5 networks that are highly organized.** *J Biol Chem* (2012) **287**(25):21265-21278.

168. Menke C, Bin L, Thorburn J, Behbakht K, Ford HL, Thorburn A: **Distinct trail resistance mechanisms can be overcome by proteasome inhibition but not generally by synergizing agents.** *Cancer Res* (2011) **71**(5):1883-1892.

169. Zijlstra A, Mellor R, Panzarella G, Aimes RT, Hooper JD, Marchenko ND, Quigley JP: **A quantitative analysis of rate-limiting steps in the metastatic cascade using human-specific real-time polymerase chain reaction.** *Cancer Res* (2002) **62**(23):7083-7092.

170. http://www.bea.ki.se/documents/EN-RNeasy%20handbook.pdf

171. Schipor S, Vladoiu, S., BACIU, A.E., Niculescu, A.M., Caragheorgheopol, A., Iancu, I., Plesa, A., Popescu, A.I., Manda, D. and Scientific, A., : **A comparative analysis of three methods used for rna quantitation.** *Romanian Reports in Physics* (2016) **68**(3):1178-1188.

172. Ryan MC, Zeeberg BR, Caplen NJ, Cleland JA, Kahn AB, Liu H, Weinstein JN: **Splicecenter: A suite of web-based bioinformatic applications for evaluating the impact of alternative splicing on rt-pcr, rnai, microarray, and peptide-based studies.** *BMC Bioinformatics* (2008) **9**(313.

173. Brown M, Wittwer C: **Flow cytometry: Principles and clinical applications in hematology.** *Clin Chem* (2000) **46**(8 Pt 2):1221-1229.

174. Jahan-Tigh RR, Ryan C, Obermoser G, Schwarzenberger K: **Flow cytometry.** *J Invest Dermatol* (2012) **132**(10):1-6.

175. Andersen MN, Al-Karradi SN, Kragstrup TW, Hokland M: **Elimination of erroneous results in flow cytometry caused by antibody binding to fc receptors on human monocytes and macrophages.** *Cytometry A* (2016) **89**(11):1001-1009.

176. Hulspas R, O'Gorman MR, Wood BL, Gratama JW, Sutherland DR: **Considerations for the control of background fluorescence in clinical flow cytometry.** *Cytometry B Clin Cytom* (2009) **76**(6):355-364.

177. van Vugt MJ, van den Herik-Oudijk IE, van de Winkle JG: **Binding of pe-cy5 conjugates to the human high-affinity receptor for igg (cd64).** *Blood* (1996) **88**(6):2358-2361.

178. Liu ZQ, Mahmood T, Yang PC: **Western blot: Technique, theory and trouble shooting.** *N Am J Med Sci* (2014) **6**(3):160.

179. Terry L Riss P, Richard A Moravec, BS, Andrew L Niles, MS, Sarah Duellman, PhD, Hélène A Benink, PhD, Tracy J Worzella, MS, and Lisa Minor.: *Cell viability assays.* (2013).

180. *https://www.dojindo.com/Protocol/Cell_Proliferation_Protocol_Colorimetric.pdf*

181. Iversen PW, Eastwood BJ, Sittampalam GS, Cox KL: **A comparison of assay performance measures in screening assays: Signal window, z' factor, and assay variability ratio.** *J Biomol Screen* (2006) **11**(3):247-252.

182. *https://support.collaborativedrug.com/hc/en-us/articles/214359383-Plate-Quality-Control#Z'factor*

183. Zhang JH, Chung TD, Oldenburg KR: **A simple statistical parameter for use in evaluation and validation of high throughput screening assays.** *J Biomol Screen* (1999) **4**(2):67-73.

184. Rao DD, Vorhies JS, Senzer N, Nemunaitis J: **Sirna vs. Shrna: Similarities and differences.** *Adv Drug Deliv Rev* (2009) **61**(9):746-759.

185. Nambudiri VE, Widlund HR: **Small interfering rna.** *J Invest Dermatol* (2013) **133**(12):1-4.

186. Ho HY, Cheng ML, Wang YH, Chiu DT: **Flow cytometry for assessment of the efficacy of sirna.** *Cytometry A* (2006) **69**(10):1054-1061.

187. Ran FA, Hsu PD, Wright J, Agarwala V, Scott DA, Zhang F: **Genome engineering using the crispr-cas9 system.** *Nat Protoc* (2013) **8**(11):2281-2308.

188. Hutt M, Marquardt L, Seifert O, Siegemund M, Muller I, Kulms D, Pfizenmaier K, Kontermann RE: **Superior properties of fc-comprising sctrail fusion proteins.** *Mol Cancer Ther* (2017) **16**(12):2792-2802.

189. Hutt M, Fellermeier-Kopf S, Seifert O, Schmitt LC, Pfizenmaier K, Kontermann RE: **Targeting scfv-fc-sctrail fusion proteins to tumor cells.** *Oncotarget* (2018) **9**(13):11322-11335.

190. Vormoor B, Knizia HK, Batey MA, Almeida GS, Wilson I, Dildey P, Sharma A, Blair H, Hide IG, Heidenreich O, Vormoor J *et al*: **Development of a preclinical orthotopic xenograft model of ewing sarcoma and other human malignant bone disease using advanced in vivo imaging.** *PLoS One* (2014) **9**(1):e85128.

191. Kilkenny C, Browne W, Cuthill IC, Emerson M, Altman DG, Group NCRRGW: **Animal research: Reporting in vivo experiments: The arrive guidelines.** *Br J Pharmacol* (2010) **160**(7):1577-1579.

192. Bomken S, Buechler L, Rehe K, Ponthan F, Elder A, Blair H, Bacon CM, Vormoor J, Heidenreich O: **Lentiviral marking of patient-derived acute lymphoblastic leukaemic cells allows in vivo tracking of disease progression.** *Leukemia* (2013) **27**(3):718-721.

193. Zhao XD, Deng HB, Lu CL, Bao YX, Lu X, Deng LL: **Association of egfr and kras mutations with expression of p-akt, dr5 and dcr1 in non-small cell lung cancer.** *Neoplasma* (2017) **64**(2):182-191.

194. Kojima Y, Nakayama M, Nishina T, Nakano H, Koyanagi M, Takeda K, Okumura K, Yagita H: **Importin beta1 protein-mediated nuclear localization of death receptor 5 (dr5) limits dr5/tumor necrosis factor (tnf)-related apoptosis-inducing ligand (trail)-induced cell death of human tumor cells.** *J Biol Chem* (2011) **286**(50):43383-43393.

195. Neville-Webbe HL, Cross NA, Eaton CL, Nyambo R, Evans CA, Coleman RE, Holen I: **Osteoprotegerin (opg) produced by bone marrow stromal cells protects breast cancer cells from trail-induced apoptosis.** *Breast Cancer Res Treat* (2004) **86**(3):269-279.

196. Clancy L, Mruk K, Archer K, Woelfel M, Mongkolsapaya J, Screaton G, Lenardo MJ, Chan FK: **Preligand assembly domain-mediated ligand-independent association between trail receptor 4 (tr4) and tr2 regulates trail-induced apoptosis.** *Proc Natl Acad Sci U S A* (2005) **102**(50):18099-18104.

197. Sprick MR, Weigand MA, Rieser E, Rauch CT, Juo P, Blenis J, Krammer PH, Walczak H: **Fadd/mort1 and caspase-8 are recruited to trail receptors 1 and 2 and are essential for apoptosis mediated by trail receptor 2.** *Immunity* (2000) **12**(6):599-609.

198. Bin L, Thorburn J, Thomas LR, Clark PE, Humphreys R, Thorburn A: **Tumor-derived mutations in the trail receptor dr5 inhibit trail signaling through the dr4 receptor by competing for ligand binding.** *J Biol Chem* (2007) **282**(38):28189-28194.

199. Thomas LR, Johnson RL, Reed JC, Thorburn A: **The c-terminal tails of tumor necrosis factor-related apoptosis-inducing ligand (trail) and fas receptors have opposing functions in fas-associated death domain (fadd) recruitment and can regulate agonist-specific mechanisms of receptor activation.** *J Biol Chem* (2004) **279**(50):52479-52486.

200. Screaton GR, Mongkolsapaya J, Xu XN, Cowper AE, McMichael AJ, Bell JI: **Trick2, a new alternatively spliced receptor that transduces the cytotoxic signal from trail.** *Curr Biol* (1997) **7**(9):693-696.

201. Vunnam N, Lo CH, Grant BD, Thomas DD, Sachs JN: **Soluble extracellular domain of death receptor 5 inhibits trail-induced apoptosis by disrupting receptor-receptor interactions.** *J Mol Biol* (2017) **429**(19):2943-2953.

202. Picarda G, Surget S, Guiho R, Teletchea S, Berreur M, Tirode F, Pellat-Deceunynck C, Heymann D, Trichet V, Redini F: **A functional, new short isoform of death receptor 4 in ewing's sarcoma cell lines may be involved in trail sensitivity/resistance mechanisms.** *Mol Cancer Res* (2012) **10**(3):336-346.

203. Kazhdan I, Marciniak RA: **Death receptor 4 (dr4) efficiently kills breast cancer cells irrespective of their sensitivity to tumor necrosis factor-related apoptosis-inducing ligand (trail).** *Cancer Gene Ther* (2004) **11**(10):691-698.

204. Lemke J, Noack A, Adam D, Tchikov V, Bertsch U, Roder C, Schutze S, Wajant H, Kalthoff H, Trauzold A: **Trail signaling is mediated by dr4 in pancreatic tumor cells despite the expression of functional dr5.** *J Mol Med (Berl)* (2010) **88**(7):729-740.

205. Yu R, Albarenque SM, Cool RH, Quax WJ, Mohr A, Zwacka RM: **Dr4 specific trail variants are more efficacious than wild-type trail in pancreatic cancer.** *Cancer Biol Ther* (2014) **15**(12):1658-1666.

206. von Karstedt S, Montinaro A, Walczak H: **Exploring the trails less travelled: Trail in cancer biology and therapy.** *Nat Rev Cancer* (2017) **17**(6):352-366.

207. Li Y, Jin X, Li J, Jin X, Yu J, Sun X, Chu Y, Xu C, Li X, Wang X, Kakehi Y *et al*: **Expression of trail, dr4, and dr5 in bladder cancer: Correlation with response**

to adjuvant therapy and implications of prognosis. *Urology* (2012) **79**(4):968 e967-915.

208. Haselmann V, Kurz A, Bertsch U, Hubner S, Olempska-Muller M, Fritsch J, Hasler R, Pickl A, Fritsche H, Annewanter F, Engler C *et al*: **Nuclear death receptor trail-r2 inhibits maturation of let-7 and promotes proliferation of pancreatic and other tumor cells.** *Gastroenterology* (2014) **146**(1):278-290.

209. Zhang XD, Franco AV, Nguyen T, Gray CP, Hersey P: **Differential localization and regulation of death and decoy receptors for tnf-related apoptosis-inducing ligand (trail) in human melanoma cells.** *J Immunol* (2000) **164**(8):3961-3970.

210. Sheridan JP, Marsters SA, Pitti RM, Gurney A, Skubatch M, Baldwin D, Ramakrishnan L, Gray CL, Baker K, Wood WI, Goddard AD *et al*: **Control of trail-induced apoptosis by a family of signaling and decoy receptors.** *Science* (1997) **277**(5327):818-821.

211. Jamshidi M, Fagerholm R, Khan S, Aittomaki K, Czene K, Darabi H, Li J, Andrulis IL, Chang-Claude J, Devilee P, Fasching PA *et al*: **Snp-snp interaction analysis of nf-kappab signaling pathway on breast cancer survival.** *Oncotarget* (2015) **6**(35):37979-37994.

212. Lalaoui N, Morle A, Merino D, Jacquemin G, Iessi E, Morizot A, Shirley S, Robert B, Solary E, Garrido C, Micheau O: **Trail-r4 promotes tumor growth and resistance to apoptosis in cervical carcinoma hela cells through akt.** *PLoS One* (2011) **6**(5):e19679.

213. Hesry V, Piquet-Pellorce C, Travert M, Donaghy L, Jegou B, Patard JJ, Guillaudeux T: **Sensitivity of prostate cells to trail-induced apoptosis increases with tumor progression: Dr5 and caspase 8 are key players.** *Prostate* (2006) **66**(9):987-995.

214. Chen JJ, Shen HC, Rivera Rosado LA, Zhang Y, Di X, Zhang B: **Mislocalization of death receptors correlates with cellular resistance to their cognate ligands in human breast cancer cells.** *Oncotarget* (2012) **3**(8):833-842.

215. Shivapurkar N, Toyooka S, Toyooka KO, Reddy J, Miyajima K, Suzuki M, Shigematsu H, Takahashi T, Parikh G, Pass HI, Chaudhary PM *et al*: **Aberrant methylation of trail decoy receptor genes is frequent in multiple tumor types.** *Int J Cancer* (2004) **109**(5):786-792.

216. Degli-Esposti MA, Smolak PJ, Walczak H, Waugh J, Huang CP, DuBose RF, Goodwin RG, Smith CA: **Cloning and characterization of trail-r3, a novel**

member of the emerging trail receptor family. *J Exp Med* (1997) **186**(7):1165-1170.

217. Picarda G, Trichet V, Teletchea S, Heymann D, Redini F: **Trail receptor signaling and therapeutic option in bone tumors: The trap of the bone microenvironment.** *Am J Cancer Res* (2012) **2**(1):45-64.

218. Corallini F, Celeghini C, Rimondi E, di Iasio MG, Gonelli A, Secchiero P, Zauli G: **Trail down-regulates the release of osteoprotegerin (opg) by primary stromal cells.** *J Cell Physiol* (2011) **226**(9):2279-2286.

219. Marsters SA, Sheridan JP, Pitti RM, Huang A, Skubatch M, Baldwin D, Yuan J, Gurney A, Goddard AD, Godowski P, Ashkenazi A: **A novel receptor for apo2l/trail contains a truncated death domain.** *Curr Biol* (1997) **7**(12):1003-1006.

220. Liu X, Yue P, Khuri FR, Sun SY: **Decoy receptor 2 (dcr2) is a p53 target gene and regulates chemosensitivity.** *Cancer Res* (2005) **65**(20):9169-9175.

221. Sanlioglu AD, Koksal IT, Ciftcioglu A, Baykara M, Luleci G, Sanlioglu S: **Differential expression of trail and its receptors in benign and malignant prostate tissues.** *J Urol* (2007) **177**(1):359-364.

222. Bolkun L, Lemancewicz D, Jablonska E, Szumowska A, Bolkun-Skornicka U, Moniuszko M, Dzieciol J, Kloczko J: **Prognostic significance of ligands belonging to tumour necrosis factor superfamily in acute lymphoblastic leukaemia.** *Leuk Res* (2015) **39**(3):290-295.

223. Bolkun L, Lemancewicz D, Jablonska E, Szumowska A, Bolkun-Skornicka U, Ratajczak-Wrona W, Dzieciol J, Kloczko J: **The impact of tnf superfamily molecules on overall survival in acute myeloid leukaemia: Correlation with biological and clinical features.** *Ann Hematol* (2015) **94**(1):35-43.

224. Duiker EW, van der Zee AG, de Graeff P, Boersma-van Ek W, Hollema H, de Bock GH, de Jong S, de Vries EG: **The extrinsic apoptosis pathway and its prognostic impact in ovarian cancer.** *Gynecol Oncol* (2010) **116**(3):549-555.

225. Toiyama D, Takaha N, Shinnoh M, Ueda T, Kimura Y, Nakamura T, Hongo F, Mikami K, Kamoi K, Kawauchi A, Miki T: **Significance of serum tumor necrosis factor-related apoptosis-inducing ligand as a prognostic biomarker for renal cell carcinoma.** *Mol Clin Oncol* (2013) **1**(1):69-74.

226. Vigneswaran N, Baucum DC, Wu J, Lou Y, Bouquot J, Muller S, Zacharias W: **Repression of tumor necrosis factor-related apoptosis-inducing ligand (trail) but not its receptors during oral cancer progression.** *BMC Cancer* (2007) **7**(108.

227. Yao Q, Du J, Lin J, Luo Y, Wang Y, Liu Y, Zhang B, Ren C, Liu C: **Prognostic significance of trail signalling molecules in cervical squamous cell carcinoma.** *J Clin Pathol* (2016) **69**(2):122-127.

228. Macher-Goeppinger S, Aulmann S, Tagscherer KE, Wagener N, Haferkamp A, Penzel R, Brauckhoff A, Hohenfellner M, Sykora J, Walczak H, Teh BT *et al*: **Prognostic value of tumor necrosis factor-related apoptosis-inducing ligand (trail) and trail receptors in renal cell cancer.** *Clin Cancer Res* (2009) **15**(2):650-659.

229. McLornan DP, Barrett HL, Cummins R, McDermott U, McDowell C, Conlon SJ, Coyle VM, Van Schaeybroeck S, Wilson R, Kay EW, Longley DB *et al*: **Prognostic significance of trail signaling molecules in stage ii and iii colorectal cancer.** *Clin Cancer Res* (2010) **16**(13):3442-3451.

230. Kuijlen JM, Mooij JJ, Platteel I, Hoving EW, van der Graaf WT, Span MM, Hollema H, den Dunnen WF: **Trail-receptor expression is an independent prognostic factor for survival in patients with a primary glioblastoma multiforme.** *J Neurooncol* (2006) **78**(2):161-171.

231. Strater J, Hinz U, Walczak H, Mechtersheimer G, Koretz K, Herfarth C, Moller P, Lehnert T: **Expression of trail and trail receptors in colon carcinoma: Trail-r1 is an independent prognostic parameter.** *Clin Cancer Res* (2002) **8**(12):3734-3740.

232. van Geelen CM, Westra JL, de Vries EG, Boersma-van Ek W, Zwart N, Hollema H, Boezen HM, Mulder NH, Plukker JT, de Jong S, Kleibeuker JH *et al*: **Prognostic significance of tumor necrosis factor-related apoptosis-inducing ligand and its receptors in adjuvantly treated stage iii colon cancer patients.** *J Clin Oncol* (2006) **24**(31):4998-5004.

233. van Dijk M, Halpin-McCormick A, Sessler T, Samali A, Szegezdi E: **Resistance to trail in non-transformed cells is due to multiple redundant pathways.** *Cell Death Dis* (2013) **4**(e702.

234. Demicco EG, Maki RG, Lev DC, Lazar AJ: **New therapeutic targets in soft tissue sarcoma.** *Adv Anat Pathol* (2012) **19**(3):170-180.

235. Wang H, Zhang P, Lin C, Yu Q, Wu J, Wang L, Cui Y, Wang K, Gao Z, Li H: **Relevance and therapeutic possibility of pten-long in renal cell carcinoma.** *PLoS One* (2015) **10**(2):e114250.

236. Ewald F, Ueffing N, Brockmann L, Hader C, Telieps T, Schuster M, Schulz WA, Schmitz I: **The role of c-flip splice variants in urothelial tumours.** *Cell Death Dis* (2011) **2**(e245.

237. Bagnoli M, Canevari S, Mezzanzanica D: **Cellular flice-inhibitory protein (c-flip) signalling: A key regulator of receptor-mediated apoptosis in physiologic context and in cancer.** *Int J Biochem Cell Biol* (2010) **42**(2):210-213.

238. Borrelli S, Candi E, Alotto D, Castagnoli C, Melino G, Vigano MA, Mantovani R: **P63 regulates the caspase-8-flip apoptotic pathway in epidermis.** *Cell Death Differ* (2009) **16**(2):253-263.

239. Zhang YP, Kong QH, Huang Y, Wang GL, Chang KJ: **Inhibition of c-flip by rnai enhances sensitivity of the human osteogenic sarcoma cell line u2os to trail-induced apoptosis.** *Asian Pac J Cancer Prev* (2015) **16**(6):2251-2256.

240. de Hooge AS, Berghuis D, Santos SJ, Mooiman E, Romeo S, Kummer JA, Egeler RM, van Tol MJ, Melief CJ, Hogendoorn PC, Lankester AC: **Expression of cellular flice inhibitory protein, caspase-8, and protease inhibitor-9 in ewing sarcoma and implications for susceptibility to cytotoxic pathways.** *Clin Cancer Res* (2007) **13**(1):206-214.

241. Safa AR, Day TW, Wu CH: **Cellular flice-like inhibitory protein (c-flip): A novel target for cancer therapy.** *Curr Cancer Drug Targets* (2008) **8**(1):37-46.

242. Bai L, Smith DC, Wang S: **Small-molecule smac mimetics as new cancer therapeutics.** *Pharmacol Ther* (2014) **144**(1):82-95.

243. Vogler M, Walczak H, Stadel D, Haas TL, Genze F, Jovanovic M, Gschwend JE, Simmet T, Debatin KM, Fulda S: **Targeting xiap bypasses bcl-2-mediated resistance to trail and cooperates with trail to suppress pancreatic cancer growth in vitro and in vivo.** *Cancer Res* (2008) **68**(19):7956-7965.

244. Fakler M, Loeder S, Vogler M, Schneider K, Jeremias I, Debatin KM, Fulda S: **Small molecule xiap inhibitors cooperate with trail to induce apoptosis in childhood acute leukemia cells and overcome bcl-2-mediated resistance.** *Blood* (2009) **113**(8):1710-1722.

245. Zinda MJ, Johnson MA, Paul JD, Horn C, Konicek BW, Lu ZH, Sandusky G, Thomas JE, Neubauer BL, Lai MT, Graff JR: **Akt-1, -2, and -3 are expressed in both normal and tumor tissues of the lung, breast, prostate, and colon.** *Clin Cancer Res* (2001) **7**(8):2475-2479.

246. Pan W, Gong S, Li Y, Zhang H, Li N, Tang B: **A dr4 capturer with akt sirna for the synergetic enhancement of death receptor-mediated apoptosis.** *Chem Commun (Camb)* (2018) **54**(95):13439-13442.

247. Gong T, Su X, Xia Q, Wang J, Kan S: **Expression of nf-kappab and pten in osteosarcoma and its clinical significance.** *Oncol Lett* (2017) **14**(6):6744-6748.

248. Kawano M, Tanaka K, Itonaga I, Iwasaki T, Tsumura H: **Microrna-301a promotes cell proliferation via pten targeting in ewing's sarcoma cells.** *Int J Oncol* (2016) **48**(4):1531-1540.

249. Tian K, Di R, Wang L: **Microrna-23a enhances migration and invasion through pten in osteosarcoma.** *Cancer Gene Ther* (2015) **22**(7):351-359.

250. Brandstadter JD, Yang Y: **Natural killer cell responses to viral infection.** *J Innate Immun* (2011) **3**(3):274-279.

251. Khanbolooki S, Nawrocki ST, Arumugam T, Andtbacka R, Pino MS, Kurzrock R, Logsdon CD, Abbruzzese JL, McConkey DJ: **Nuclear factor-kappab maintains trail resistance in human pancreatic cancer cells.** *Mol Cancer Ther* (2006) **5**(9):2251-2260.

252. Romagnoli M, Desplanques G, Maiga S, Legouill S, Dreano M, Bataille R, Barille-Nion S: **Canonical nuclear factor kappab pathway inhibition blocks myeloma cell growth and induces apoptosis in strong synergy with trail.** *Clin Cancer Res* (2007) **13**(20):6010-6018.

253. Shetty S, Graham BA, Brown JG, Hu X, Vegh-Yarema N, Harding G, Paul JT, Gibson SB: **Transcription factor nf-kappab differentially regulates death receptor 5 expression involving histone deacetylase 1.** *Mol Cell Biol* (2005) **25**(13):5404-5416.

254. Rosato RR, Almenara JA, Dai Y, Grant S: **Simultaneous activation of the intrinsic and extrinsic pathways by histone deacetylase (hdac) inhibitors and tumor necrosis factor-related apoptosis-inducing ligand (trail) synergistically induces mitochondrial damage and apoptosis in human leukemia cells.** *Mol Cancer Ther* (2003) **2**(12):1273-1284.

255. Zopf S, Neureiter D, Bouralexis S, Abt T, Glaser KB, Okamoto K, Ganslmayer M, Hahn EG, Herold C, Ocker M: **Differential response of p53 and p21 on hdac inhibitor-mediated apoptosis in hct116 colon cancer cells in vitro and in vivo.** *Int J Oncol* (2007) **31**(6):1391-1402.

256. Chekenya M, Krakstad C, Svendsen A, Netland IA, Staalesen V, Tysnes BB, Selheim F, Wang J, Sakariassen PO, Sandal T, Lonning PE *et al*: **The progenitor cell marker ng2/mpg promotes chemoresistance by activation of integrin-dependent pi3k/akt signaling.** *Oncogene* (2008) **27**(39):5182-5194.

257. Gamie Z, Kapriniotis K, Papanikolaou D, Haagensen E, Da Conceicao Ribeiro R, Dalgarno K, Krippner-Heidenreich A, Gerrand C, Tsiridis E, Rankin KS: **Tnf-related apoptosis-inducing ligand (trail) for bone sarcoma treatment: Pre-clinical and clinical data.** *Cancer Lett* (2017) **409**(66-80.

258. Wang G, Wang X, Yu H, Wei S, Williams N, Holmes DL, Halfmann R, Naidoo J, Wang L, Li L, Chen S *et al*: **Small-molecule activation of the trail receptor dr5 in human cancer cells.** *Nat Chem Biol* (2013) **9**(2):84-89.

259. Schneider B, Munkel S, Krippner-Heidenreich A, Grunwald I, Wels WS, Wajant H, Pfizenmaier K, Gerspach J: **Potent antitumoral activity of trail through generation of tumor-targeted single-chain fusion proteins.** *Cell Death Dis* (2010) **1**(e68.

260. Forero A, Bendell JC, Kumar P, Janisch L, Rosen M, Wang Q, Copigneaux C, Desai M, Senaldi G, Maitland ML: **First-in-human study of the antibody dr5 agonist ds-8273a in patients with advanced solid tumors.** *Invest New Drugs* (2017) **35**(3):298-306.

261. http://projects.insilico.us/.

262. Fritsche H, Heilmann T, Tower RJ, Hauser C, von Au A, El-Sheikh D, Campbell GM, Alp G, Schewe D, Hubner S, Tiwari S *et al*: **Trail-r2 promotes skeletal metastasis in a breast cancer xenograft mouse model.** *Oncotarget* (2015) **6**(11):9502-9516.

263. Subbiah V, Brown RE, Buryanek J, Trent J, Ashkenazi A, Herbst R, Kurzrock R: **Targeting the apoptotic pathway in chondrosarcoma using recombinant human apo2l/trail (dulanermin), a dual proapoptotic receptor (dr4/dr5) agonist.** *Mol Cancer Ther* (2012) **11**(11):2541-2546.

264. Schwartz LH, Litiere S, de Vries E, Ford R, Gwyther S, Mandrekar S, Shankar L, Bogaerts J, Chen A, Dancey J, Hayes W *et al*: **Recist 1.1-update and clarification: From the recist committee.** *Eur J Cancer* (2016) **62**(132-137.

265. Zuch de Zafra CL, Ashkenazi A, Darbonne WC, Cheu M, Totpal K, Ortega S, Flores H, Walker MD, Kabakoff B, Lum BL, Mounho-Zamora BJ *et al*: **Antitherapeutic antibody-mediated hepatotoxicity of recombinant human apo2l/trail in the cynomolgus monkey.** *Cell Death Dis* (2016) **7**(8):e2338.

266. Jouan-Lanhouet S, Arshad MI, Piquet-Pellorce C, Martin-Chouly C, Le Moigne-Muller G, Van Herreweghe F, Takahashi N, Sergent O, Lagadic-Gossmann D, Vandenabeele P, Samson M *et al*: **Trail induces necroptosis involving ripk1/ripk3-dependent parp-1 activation.** *Cell Death Differ* (2012) **19**(12):2003-2014.

267. Sosna J, Philipp S, Fuchslocher Chico J, Saggau C, Fritsch J, Foll A, Plenge J, Arenz C, Pinkert T, Kalthoff H, Trauzold A *et al*: **Differences and similarities in trail- and tumor necrosis factor-mediated necroptotic signaling in cancer cells.** *Mol Cell Biol* (2016) **36**(20):2626-2644.

268. Giampazolias E, Zunino B, Dhayade S, Bock F, Cloix C, Cao K, Roca A, Lopez J, Ichim G, Proics E, Rubio-Patino C *et al*: **Mitochondrial permeabilization engages nf-kappab-dependent anti-tumour activity under caspase deficiency.** *Nat Cell Biol* (2017) **19**(9):1116-1129.

269. Giampazolias E, Tait SWG: **Caspase-independent cell death: An anti-cancer double whammy.** *Cell Cycle* (2018) **17**(3):269-270.

270. Staniek J, Lorenzetti R, Heller B, Janowska I, Schneider P, Unger S, Warnatz K, Seidl M, Venhoff N, Thiel J, Smulski CR *et al*: **Trail-r1 and trail-r2 mediate trail-dependent apoptosis in activated primary human b lymphocytes.** *Front Immunol* (2019) **10**(951.

271. Rubio-Moscardo F, Blesa D, Mestre C, Siebert R, Balasas T, Benito A, Rosenwald A, Climent J, Martinez JI, Schilhabel M, Karran EL *et al*: **Characterization of 8p21.3 chromosomal deletions in b-cell lymphoma: Trail-r1 and trail-r2 as candidate dosage-dependent tumor suppressor genes.** *Blood* (2005) **106**(9):3214-3222.

272. Morales E, Olson M, Iglesias F, Dahiya S, Luetkens T, Atanackovic D: **Role of immunotherapy in ewing sarcoma.** *J Immunother Cancer* (2020) **8**(2).

273. Naeem M, Majeed S, Hoque MZ, Ahmad I: **Latest developed strategies to minimize the off-target effects in crispr-cas-mediated genome editing.** *Cells* (2020) **9**(7).

274. Stemmer M, Thumberger T, Del Sol Keyer M, Wittbrodt J, Mateo JL: **Cctop: An intuitive, flexible and reliable crispr/cas9 target prediction tool.** *PLoS One* (2015) **10**(4):e0124633.

275. Vanamee ES, Faustman DL: **Structural principles of tumor necrosis factor superfamily signaling.** *Sci Signal* (2018) **11**(511).

276. Lacour S, Hammann A, Wotawa A, Corcos L, Solary E, Dimanche-Boitrel MT: **Anticancer agents sensitize tumor cells to tumor necrosis factor-related apoptosis-inducing ligand-mediated caspase-8 activation and apoptosis.** *Cancer Res* (2001) **61**(4):1645-1651.

277. Italiano A, Mir O, Cioffi A, Palmerini E, Piperno-Neumann S, Perrin C, Chaigneau L, Penel N, Duffaud F, Kurtz JE, Collard O *et al*: **Advanced chondrosarcomas: Role of chemotherapy and survival.** *Ann Oncol* (2013) **24**(11):2916-2922.

278. Italiano A: **Advanced conventional chondrosarcomas: Time to revisit treatments and clinical research for what is not an indolent disease.** *Cancer* (2014) **120**(20):3103-3104.

279. Tacar O, Sriamornsak P, Dass CR: **Doxorubicin: An update on anticancer molecular action, toxicity and novel drug delivery systems.** *J Pharm Pharmacol* (2013) **65**(2):157-170.

280. Kang J, Bu J, Hao Y, Chen F: **Subtoxic concentration of doxorubicin enhances trail-induced apoptosis in human prostate cancer cell line lncap.** *Prostate Cancer Prostatic Dis* (2005) **8**(3):274-279.

281. Kelly MM, Hoel BD, Voelkel-Johnson C: **Doxorubicin pretreatment sensitizes prostate cancer cell lines to trail induced apoptosis which correlates with the loss of c-flip expression.** *Cancer Biol Ther* (2002) **1**(5):520-527.

282. Keane MM, Ettenberg SA, Nau MM, Russell EK, Lipkowitz S: **Chemotherapy augments trail-induced apoptosis in breast cell lines.** *Cancer Res* (1999) **59**(3):734-741.

283. Wu XX, Kakehi Y, Mizutani Y, Nishiyama H, Kamoto T, Megumi Y, Ito N, Ogawa O: **Enhancement of trail/apo2l-mediated apoptosis by adriamycin through**

inducing dr4 and dr5 in renal cell carcinoma cells. *Int J Cancer* (2003) **104**(4):409-417.

284. Liston DR, Davis M: **Clinically relevant concentrations of anticancer drugs: A guide for nonclinical studies.** *Clin Cancer Res* (2017) **23**(14):3489-3498.

285. Montecucco A, Zanetta F, Biamonti G: **Molecular mechanisms of etoposide.** *EXCLI J* (2015) **14**(95-108.

286. Gibson SB, Oyer R, Spalding AC, Anderson SM, Johnson GL: **Increased expression of death receptors 4 and 5 synergizes the apoptosis response to combined treatment with etoposide and trail.** *Mol Cell Biol* (2000) **20**(1):205-212.

287. Requile A, Clement PM, Bechter OE, Dumez H, Verbiest A, Sciot R, Hompes D, Sinnaeve F, Van Limbergen E, Schoffski P: **Single-centre experience of systemic treatment with vincristine, ifosfamide, and doxorubicin alternating with etoposide, ifosfamide, and cisplatin in adult patients with ewing sarcoma.** *Sarcoma* (2017) **2017**(1781087.

288. Lu J, McEachern D, Sun H, Bai L, Peng Y, Qiu S, Miller R, Liao J, Yi H, Liu M, Bellail A *et al*: **Therapeutic potential and molecular mechanism of a novel, potent, nonpeptide, smac mimetic sm-164 in combination with trail for cancer treatment.** *Mol Cancer Ther* (2011) **10**(5):902-914.

289. Varfolomeev E, Alicke B, Elliott JM, Zobel K, West K, Wong H, Scheer JM, Ashkenazi A, Gould SE, Fairbrother WJ, Vucic D: **X chromosome-linked inhibitor of apoptosis regulates cell death induction by proapoptotic receptor agonists.** *J Biol Chem* (2009) **284**(50):34553-34560.

290. Amm HM, Zhou T, Steg AD, Kuo H, Li Y, Buchsbaum DJ: **Mechanisms of drug sensitization to tra-8, an agonistic death receptor 5 antibody, involve modulation of the intrinsic apoptotic pathway in human breast cancer cells.** *Mol Cancer Res* (2011) **9**(4):403-417.

291. Mohr A, Albarenque SM, Deedigan L, Yu R, Reidy M, Fulda S, Zwacka RM: **Targeting of xiap combined with systemic mesenchymal stem cell-mediated delivery of strail ligand inhibits metastatic growth of pancreatic carcinoma cells.** *Stem Cells* (2010) **28**(11):2109-2120.

292. *https://clinicaltrials.gov/ct2/show/NCT01940172*

293. Pieczykolan JS, Kubinski K, Maslyk M, Pawlak SD, Pieczykolan A, Rozga PK, Szymanik M, Galazka M, Teska-Kaminska M, Zerek B, Bukato K *et al*: **Ad-o53.2--a novel recombinant fusion protein combining the activities of trail/apo2l and smac/diablo, overcomes resistance of human cancer cells to trail/apo2l.** *Invest New Drugs* (2014) **32**(6):1155-1166.

294. Song JH, Kandasamy K, Kraft AS: **Abt-737 induces expression of the death receptor 5 and sensitizes human cancer cells to trail-induced apoptosis.** *J Biol Chem* (2008) **283**(36):25003-25013.

295. Flusberg DA, Sorger PK: **Modulating cell-to-cell variability and sensitivity to death ligands by co-drugging.** *Phys Biol* (2013) **10**(3):035002.

296. Van Valen F, Fulda S, Schafer KL, Truckenbrod B, Hotfilder M, Poremba C, Debatin KM, Winkelmann W: **Selective and nonselective toxicity of trail/apo2l combined with chemotherapy in human bone tumour cells vs. Normal human cells.** *Int J Cancer* (2003) **107**(6):929-940.

297. Dubrez L, Berthelet J, Glorian V: **Iap proteins as targets for drug development in oncology.** *Onco Targets Ther* (2013) **9**(1285-1304.

298. Amaravadi RK, Schilder RJ, Martin LP, Levin M, Graham MA, Weng DE, Adjei AA: **A phase i study of the smac-mimetic birinapant in adults with refractory solid tumors or lymphoma.** *Mol Cancer Ther* (2015) **14**(11):2569-2575.

299. Yang C, Davis JL, Zeng R, Vora P, Su X, Collins LI, Vangveravong S, Mach RH, Piwnica-Worms D, Weilbaecher KN, Faccio R *et al*: **Antagonism of inhibitor of apoptosis proteins increases bone metastasis via unexpected osteoclast activation.** *Cancer Discov* (2013) **3**(2):212-223.

300. Tang F, Choy E, Tu C, Hornicek F, Duan Z: **Therapeutic applications of histone deacetylase inhibitors in sarcoma.** *Cancer Treat Rev* (2017) **59**(33-45.

301. Sonnemann J, Dreyer L, Hartwig M, Palani CD, Hong le TT, Klier U, Broker B, Volker U, Beck JF: **Histone deacetylase inhibitors induce cell death and enhance the apoptosis-inducing activity of trail in ewing's sarcoma cells.** *J Cancer Res Clin Oncol* (2007) **133**(11):847-858.

302. Yamanegi K, Yamane J, Hata M, Ohyama H, Yamada N, Kato-Kogoe N, Futani H, Nakasho K, Okamura H, Terada N: **Sodium valproate, a histone deacetylase inhibitor, decreases the secretion of soluble fas by human osteosarcoma cells and increases their sensitivity to fas-mediated cell death.** *J Cancer Res Clin Oncol* (2009) **135**(7):879-889.

303. Watanabe K, Okamoto K, Yonehara S: **Sensitization of osteosarcoma cells to death receptor-mediated apoptosis by hdac inhibitors through downregulation of cellular flip.** *Cell Death Differ* (2005) **12**(1):10-18.

304. Rao-Bindal K, Koshkina NV, Stewart J, Kleinerman ES: **The histone deacetylase inhibitor, ms-275 (entinostat), downregulates c-flip, sensitizes osteosarcoma cells to fasl, and induces the regression of osteosarcoma lung metastases.** *Curr Cancer Drug Targets* (2013) **13**(4):411-422.

305. de Graaff MA, de Rooij MA, van den Akker BE, Gelderblom H, Chibon F, Coindre JM, Marino-Enriquez A, Fletcher JA, Cleton-Jansen AM, Bovee JV: **Inhibition of bcl-2 family members sensitises soft tissue leiomyosarcomas to chemotherapy.** *Br J Cancer* (2016) **114**(11):1219-1226.

306. Krippner-Heidenreich A, Grunwald I, Zimmermann G, Kuhnle M, Gerspach J, Sterns T, Shnyder SD, Gill JH, Mannel DN, Pfizenmaier K, Scheurich P: **Single-chain tnf, a tnf derivative with enhanced stability and antitumoral activity.** *J Immunol* (2008) **180**(12):8176-8183.

307. de Bruyn M, Bremer E, Helfrich W: **Antibody-based fusion proteins to target death receptors in cancer.** *Cancer Lett* (2013) **332**(2):175-183.

308. Hutt M, Marquardt L, Seifert O, Siegemund M, Muller I, Kulms D, Pfizenmaier K, Kontermann RE: **Superior properties of fc-comprising sctrail fusion proteins.** *Mol Cancer Ther* (2017).

309. Kellner C, Otte A, Cappuzzello E, Klausz K, Peipp M: **Modulating cytotoxic effector functions by fc engineering to improve cancer therapy.** *Transfus Med Hemother* (2017) **44**(5):327-336.

310. He Y, Hendriks D, van Ginkel R, Samplonius D, Bremer E, Helfrich W: **Melanoma-directed activation of apoptosis using a bispecific antibody directed at mcsp and trail receptor-2/death receptor-5.** *J Invest Dermatol* (2016) **136**(2):541-544.

311. de Bruyn M, Rybczynska AA, Wei Y, Schwenkert M, Fey GH, Dierckx RA, van Waarde A, Helfrich W, Bremer E: **Melanoma-associated chondroitin sulfate proteoglycan (mcsp)-targeted delivery of soluble trail potently inhibits melanoma outgrowth in vitro and in vivo.** *Mol Cancer* (2010) **9**(301.

312. Yadavilli S, Hwang EI, Packer RJ, Nazarian J: **The role of ng2 proteoglycan in glioma.** *Transl Oncol* (2016) **9**(1):57-63.

313. Wang X, Katayama A, Wang Y, Yu L, Favoino E, Sakakura K, Favole A, Tsuchikawa T, Silver S, Watkins SC, Kageshita T *et al*: **Functional characterization of an scfv-fc antibody that immunotherapeutically targets the common cancer cell surface proteoglycan cspg4.** *Cancer Res* (2011) **71**(24):7410-7422.

314. Jordaan S, Chetty S, Mungra N, Koopmans I, van Bommel PE, Helfrich W, Barth S: **Cspg4: A target for selective delivery of human cytolytic fusion proteins and trail.** *Biomedicines* (2017) **5**(3).

315. Castronovo C, Arrese JE, Quatresooz P, Nikkels AF: **Myxofibrosarcoma: A diagnostic pitfall.** *Rare Tumors* (2013) **5**(2):60-61.

316. Lohberger B, Stuendl N, Leithner A, Rinner B, Sauer S, Kashofer K, Liegl-Atzwanger B: **Establishment of a novel cellular model for myxofibrosarcoma heterogeneity.** *Sci Rep* (2017) **7**(44700).

317. Cheong HJ, Lee KS, Woo IS, Won JH, Byun JH: **Up-regulation of the dr5 expression by proteasome inhibitor mg132 augments trail-induced apoptosis in soft tissue sarcoma cell lines.** *Cancer Res Treat* (2011) **43**(2):124-130.

318. Benassi MS, Pazzaglia L, Chiechi A, Alberghini M, Conti A, Cattaruzza S, Wassermann B, Picci P, Perris R: **Ng2 expression predicts the metastasis formation in soft-tissue sarcoma patients.** *J Orthop Res* (2009) **27**(1):135-140.

319. Cattaruzza S, Nicolosi PA, Braghetta P, Pazzaglia L, Benassi MS, Picci P, Lacrima K, Zanocco D, Rizzo E, Stallcup WB, Colombatti A *et al*: **Ng2/cspg4-collagen type vi interplays putatively involved in the microenvironmental control of tumour engraftment and local expansion.** *J Mol Cell Biol* (2013) **5**(3):176-193.

320. Hsu SC, Nadesan P, Puviindran V, Stallcup WB, Kirsch DG, Alman BA: **Effects of chondroitin sulfate proteoglycan 4 (ng2/cspg4) on soft-tissue sarcoma growth depend on tumor developmental stage.** *J Biol Chem* (2018) **293**(7):2466-2475.

321. He Y, Hendriks D, van Ginkel R, Samplonius D, Bremer E, Helfrich W: **Melanoma-directed activation of apoptosis using a bispecific antibody directed at mcsp and trail receptor-2/death receptor-5.** *J Invest Dermatol* (2016) **136**(2):541-544.

322. Inoue-Yamauchi A, Jeng PS, Kim K, Chen HC, Han S, Ganesan YT, Ishizawa K, Jebiwott S, Dong Y, Pietanza MC, Hellmann MD *et al*: **Targeting the differential addiction to anti-apoptotic bcl-2 family for cancer therapy.** *Nat Commun* (2017) **8**(16078).

323. Bressenot A, Marchal S, Bezdetnaya L, Garrier J, Guillemin F, Plenat F: **Assessment of apoptosis by immunohistochemistry to active caspase-3, active caspase-7, or cleaved parp in monolayer cells and spheroid and subcutaneous xenografts of human carcinoma.** *J Histochem Cytochem* (2009) **57**(4):289-300.

324. Taraborrelli L, Peltzer N, Montinaro A, Kupka S, Rieser E, Hartwig T, Sarr A, Darding M, Draber P, Haas TL, Akarca A *et al*: **Lubac prevents lethal dermatitis by inhibiting cell death induced by tnf, trail and cd95l.** *Nat Commun* (2018) **9**(1):3910.

325. Ferrando RE, Newton K, Chu F, Webster JD, French DM: **Immunohistochemical detection of flag-tagged endogenous proteins in knock-in mice.** *J Histochem Cytochem* (2015) **63**(4):244-255.

326. Jacques C, Renema N, Lezot F, Ory B, Walkley CR, Grigoriadis AE, Heymann D: **Small animal models for the study of bone sarcoma pathogenesis:Characteristics, therapeutic interests and limitations.** *J Bone Oncol* (2018) **12**(7-13.

327. Mazzucchelli S, Ravelli A, Gigli F, Minoli M, Corsi F, Ciuffreda P, Ottria R: **Lc-ms/ms method development for quantification of doxorubicin and its metabolite 13-hydroxy doxorubicin in mice biological matrices: Application to a pharmaco-delivery study.** *Biomed Chromatogr* (2017) **31**(4).

328. Cortini M, Baldini N, Avnet S: **New advances in the study of bone tumors: A lesson from the 3d environment.** *Front Physiol* (2019) **10**(814.

329. Lee RH, Yoon N, Reneau JC, Prockop DJ: **Preactivation of human mscs with tnf-alpha enhances tumor-suppressive activity.** *Cell Stem Cell* (2012) **11**(6):825-835.

330. Yu R, Deedigan L, Albarenque SM, Mohr A, Zwacka RM: **Delivery of strail variants by mscs in combination with cytotoxic drug treatment leads to p53-independent enhanced antitumor effects.** *Cell Death Dis* (2013) **4**(e503).

331. Huang H, Zhao N, Xu X, Xu Y, Li S, Zhang J, Yang P: **Dose-specific effects of tumor necrosis factor alpha on osteogenic differentiation of mesenchymal stem cells.** *Cell Prolif* (2011) **44**(5):420-427.

332. Yoon N, Park MS, Peltier GC, Lee RH: **Pre-activated human mesenchymal stromal cells in combination with doxorubicin synergistically enhance tumor-suppressive activity in mice.** *Cytotherapy* (2015) **17**(10):1332-1341.

333. Hess K, Ushmorov A, Fiedler J, Brenner RE, Wirth T: **Tnfalpha promotes osteogenic differentiation of human mesenchymal stem cells by triggering the nf-kappab signaling pathway.** *Bone* (2009) **45**(2):367-376.

334. Ding J, Ghali O, Lencel P, Broux O, Chauveau C, Devedjian JC, Hardouin P, Magne D: **Tnf-alpha and il-1beta inhibit runx2 and collagen expression but increase alkaline phosphatase activity and mineralization in human mesenchymal stem cells.** *Life Sci* (2009) **84**(15-16):499-504.

335. Daniele S, Natali L, Giacomelli C, Campiglia P, Novellino E, Martini C, Trincavelli ML: **Osteogenesis is improved by low tumor necrosis factor alpha concentration through the modulation of gs-coupled receptor signals.** *Mol Cell Biol* (2017) **37**(8).

336. Deshpande S, James AW, Blough J, Donneys A, Wang SC, Cederna PS, Buchman SR, Levi B: **Reconciling the effects of inflammatory cytokines on mesenchymal cell osteogenic differentiation.** *J Surg Res* (2013) **185**(1):278-285.

337. Dominici M, Le Blanc K, Mueller I, Slaper-Cortenbach I, Marini F, Krause D, Deans R, Keating A, Prockop D, Horwitz E: **Minimal criteria for defining multipotent mesenchymal stromal cells. The international society for cellular therapy position statement.** *Cytotherapy* (2006) **8**(4):315-317.

338. Strebel A, Harr T, Bachmann F, Wernli M, Erb P: **Green fluorescent protein as a novel tool to measure apoptosis and necrosis.** *Cytometry* (2001) **43**(2):126-133.

339. Guiho R, Biteau K, Grisendi G, Chatelais M, Brion R, Taurelle J, Renault S, Heymann D, Dominici M, Redini F: **In vitro and in vivo discrepancy in inducing apoptosis by mesenchymal stromal cells delivering membrane-bound tumor necrosis factor-related apoptosis inducing ligand in osteosarcoma pre-clinical models.** *Cytotherapy* (2018) **20**(8):1037-1045.

340. Di Pietro R, Secchiero P, Rana R, Gibellini D, Visani G, Bemis K, Zamai L, Miscia S, Zauli G: **Ionizing radiation sensitizes erythroleukemic cells but not normal erythroblasts to tumor necrosis factor-related apoptosis-inducing ligand (trail)--mediated cytotoxicity by selective up-regulation of trail-r1.** *Blood* (2001) **97**(9):2596-2603.

341. Dufour F, Rattier T, Constantinescu AA, Zischler L, Morle A, Ben Mabrouk H, Humblin E, Jacquemin G, Szegezdi E, Delacote F, Marrakchi N *et al*: **Trail receptor gene editing unveils trail-r1 as a master player of apoptosis induced by trail and er stress.** *Oncotarget* (2017) **8**(6):9974-9985.

342. Crowder RN, Dicker DT, El-Deiry WS: **The deubiquitinase inhibitor pr-619 sensitizes normal human fibroblasts to tumor necrosis factor-related apoptosis-inducing ligand (trail)-mediated cell death.** *J Biol Chem* (2016) **291**(11):5960-5970.

343. Elrod HA, Fan S, Muller S, Chen GZ, Pan L, Tighiouart M, Shin DM, Khuri FR, Sun SY: **Analysis of death receptor 5 and caspase-8 expression in primary and metastatic head and neck squamous cell carcinoma and their prognostic impact.** *PLoS One* (2010) **5**(8):e12178.

344. D'Arcy P, Brnjic S, Olofsson MH, Fryknas M, Lindsten K, De Cesare M, Perego P, Sadeghi B, Hassan M, Larsson R, Linder S: **Inhibition of proteasome deubiquitinating activity as a new cancer therapy.** *Nat Med* (2011) **17**(12):1636-1640.

345. *http://www.uniprot.org/uniprot/O14763#sequences*

346. Quent VM, Loessner D, Friis T, Reichert JC, Hutmacher DW: **Discrepancies between metabolic activity and DNA content as tool to assess cell proliferation in cancer research.** *J Cell Mol Med* (2010) **14**(4):1003-1013.

347. Hui K, Feng ZP: **Efficient experimental design and analysis of real-time pcr assays.** *Channels (Austin)* (2013) **7**(3):160-170.